Kinetic Control of Polyaryl Formation in a Pyrolysis Environment

by

Michael Christopher Masonjones

B.S. Chemical Engineering
California Institute of Technology (1990)

Submitted to the Department of Chemical Engineering
in partial fulfillment of the requirements for the degree of

Doctor of Philosophy

at the

Massachusetts Institute of Technology
February, 1995

Signature of Author _____
Department of Chemical Engineering
February 5, 1995

Certified by _____
Professor Adel F. Sarofim
Thesis Supervisor

Accepted by _____
Professor Robert E. Cohen, Chair
Department Committee for Graduate Students

Kinetic Control of Polyaryl Formation in a Pyrolysis Environment

by Michael Christopher Masonjones

Doctoral Thesis Submitted to the
Department of Chemical Engineering,
Massachusetts Institute of Technology, Cambridge, MA, 02139

January 23, 1995.

Abstract

Four solid fuels have been pyrolyzed in a flow of nitrogen for a residence time of 2 seconds in a drop-tube furnace at temperatures in the range 1200 K to 1500 K. The fuels were: 1) pure naphthalene, 2) pure anthracene, 3) a 1:1 mole ratio mixture of anthracene and naphthalene, and 4) ortho-terphenyl.

Experiments 1) and 2) were predicted to produce product spectra that are subsets of those for experiment 3), and they were performed as baseline preliminary studies to eliminate any confounding effects in experiment 3) and to establish consistency with previous investigations into biaryl formation.

Experiment 3) was performed at 5 different temperatures in the range 1200 K to 1500 K. Many of the 6 ring condensation products of the expected naphthyl-anthracenes in this experiment are known to be mutagenic in bioassay studies, and an investigation into the mechanism governing their formation is sought. Relative abundances of the six isomeric naphthyl-anthracenes, six isomeric bianthracenes, and 3 isomeric binaphthalenes, as well as aggregate concentrations for each of the three primary biaryl isomer series, were measured, and evidence was found for several polyaryl products in chains up to at least six units long, along with many of their corresponding condensation products. The total concentration (mole basis) of the 6 naphthyl-anthracenes was observed to be roughly twice that of both the total binaphthalene abundance and the total bianthracene abundance at all temperatures in this study, with a slight favoring of isomers containing anthracene components at the lower temperatures. This is exactly what one would predict for a probability of collision model given that anthracene is theorized to form radicals at lower temperatures that naphthalene. A thermodynamic model based on heats of formation and molecular conformations as calculated with the semi-empirical molecular orbital model Austin Model 1 available within the program MOPAC 6.0 is found to be insufficient to describe such a phenomenon. While the thermodynamic model predicts relative concentrations of isomers within a series rather well, a kinetic model based on very simple notions about activation energy and probability of collision does equally well, and it is thought that the correspondence between the two theories is due to the dominating effect of steric hindrance on biaryl formation.

Experiment 4) is performed at 5 different temperatures in the range 1250 K to 1350 K, the temperature range in which a fundamental shift in product types appears to occur. Evidence is found for all of the expected compounds in the benzene polymerization pathway up to at least molecular weight 700. Minimal evidence is found for the existence of acetylene addition products, demonstrating the importance of the polymerization pathway to soot growth, especially as the compounds become large. Less condensed, polymer-like species dominate the product spectrum at the lower temperatures. A shift to more condensed species, many of which are

total-resonant-sextet (TRS) compounds, is seen at the higher temperatures, in agreement with the previously established thermodynamic theory of Stein. However, the lack of abundance of the TRS compounds, overabundance of the dimer of the fuel, and an identifiable rate-limiting critical species as defined by that work suggest that the product spectrum is not at equilibrium and is thus kinetically controlled. In addition, relatively high energy ring rupture and rearrangement mechanisms (several of which lead to toxic products) are found to compete substantially with ring-closing reactions to the highly stable TRS compounds, even at the highest temperature where equilibration times might be expected to be shorter. TRS species are also found to fall off with molecular weight, counter to equilibrium calculations, and characteristic of kinetic control in which formation of larger molecular weight compounds is dependent on and limited by the rate at which lower molecular weight compounds can form in significant concentrations. These observations indicate that thermodynamic considerations are insufficient in describing biaryl product spectra under such conditions.

A detailed kinetic mechanism is used to test the proposed kinetic theory for molecular weight growth via polymerization against the experimental data from the naphthalene/anthracene study (experiment 3). A reaction set has been composed that takes into account: 1) 5 types of reactions (radical-radical interaction, hydrogen abstraction, polyaryl formation, polyaryl condensation, and hydrogen balance), 2) the most recent information available about the kinetic parameters governing those reactions (including the different bond dissociation energies associated with different radical site environments), 3) individual species up to biaryls and their condensation products, and 4) "lumped" species up to 700 molecular weight. The resulting mechanism contains 2146 reactions and 169 species representing almost 5.5 million compounds. A working definition of symmetry number is also postulated to correct back reaction rates for reactions involving lumped compounds. The computer model gives a reasonable prediction all of the general trends observed in experiment after taking into account systematic biases due to uncertainties in input reaction rates and steric hindrance parameters as predicted by MOPAC. Radical formation is found to be the dominant rate-limiting step, followed closely in importance by condensation reactions.

Identification of 8 previously uncharacterized biaryls (the six isomeric naphthyl-anthracenes and 2 isomeric phenyl-triphenylenes) critical to the investigation of the PAH product spectrum of these experiments has been accomplished. Because of the unavailability of standard reference compounds for many of the key biaryl products of interest, structural elucidation was achieved by correlating UV-Vis spectral features, mass spectral cracking patterns, and GCMS and HPLC elution order with those for bianthracenes, binaphthalenes, and other structurally similar molecules. In addition, steric hindrance to rotation at the linking bond, and thus the extent of non-planarity in the isomers, a factor that governs HPLC elution order and contributes to mass spectral differences, was estimated using the same heats of formation and conformation information derived from MOPAC for the thermodynamic calculations.

An oxygenated polymer contaminant of unknown origin has also been found and identified as poly(ethylene terephthalate). Understanding the nature of its presence in the sample was crucial to describing the pathway to soot growth via polymerization, as many of its properties mimicked those of a certain hypothetical series of fullerenes, molecules whose presence could greatly influence the conclusions drawn on this research.

The results presented in this thesis demonstrate the relevance and importance of reactive coagulation pathways to soot growth and mutagen formation, and they provide important insight into the mechanisms that control such schemes.

Thesis Supervisor: Prof. Adel F. Sarofim
Thesis Committee: Prof. Janos M. Beer
Prof. Jack B. Howard
Dr. Arthur L. Lafleur

Acknowledgments

Many people have made possible the work which extends beyond this page. It is an extension of myself, yet so many people go into making a person. Who should get the credit for a person's being?

Certainly, the most influential person in helping to realize my academic potential is Professor Adel F. Sarofim. He enabled me to find my own way around problems - the way it should be. Perspectives are not always easy to come by, but he could always manage to find a couple of extra ones he had lying around to give to me. Thank you for arming me with the knowledge to find some of my own.

Thanks also go to the members of my committee, Professors Janos Beer and Jack Howard, and Dr. Arthur Lafleur. Dr. Lafleur's reluctance to concede any new discovery made me work that much harder, and made me that much better of a scientist. If I could convince Art, it must be true. Likewise, Prof. Howard's and Prof. Beer's enthusiasm for exploring the consequences of new revelations enabled me to experience a couple of "eureka" moments, too, even if they were short-lived sometimes.

Nothing could have been done without the help of the analytical chemistry staff in the CORE lab. Elaine Plummer and Koli Taghizadeh were a tremendous help in analyzing my samples and exploring the inevitable conundrums that arise with every one that is injected. Their expertise and insight was invaluable, and I think that kind of work goes too often underacknowledged. Tony Modestino should be given the patience award of the century for all the questions he had to put up with regarding mechanical/electrical/plumbing/machining/computing/where's-this/where's-that/etc. His

help was very influential on the way I go about seeking the answers to life's little mysteries, and it was greatly appreciated. Steve McElvany and the Naval Research Institute are also thanked for their patience and for the use of their tandem mass spectrometer in chasing at least one of the wild geese that were let loose in this project. Gabrielle Joseph and Emmi Snyder should not be missed, either, in the support staff category. Their help and kindness were extraordinary. My UROP throughout the project, John Klepeis, deserves special mention for his hands-on help in setting up and running the experiments and in preparing samples for analysis. I'm especially appreciative of the fact that he didn't make any mistakes bigger than my own, even though he had ample opportunity considering the comparable amounts of time each of us spent with the equipment

On the technical side, conversations with Adel Sarofim, Jim Mulholland, Judy Wornat, Chris Pope, Jan Tjissen, Joe Marr, Jack Howard, Art Lafleur and Jaideep Mukherjee contained many of the seeds of thought that eventually made it into this thesis. More friendly conversations with fellow graduate students Hiroshi Saito, Peter Nelson, Tapesh Yadav, Jon Allen, Angelo Kandas, Shakti Goel and Christian Felderman just kept me sane.

Of course, many thank yous must be addressed to those who pay the bills. The support of the National Institute for Environmental Health Sciences and the Chemical Engineering Department, and the fellowship support of the National Science Foundation, are greatly appreciated.

If anything is to be credited for keeping me going, it was home life. Anything I say here would not credit it enough. My wife Heather was tremendously supportive, and my children, Sawyer and Kellerin, made everything seem worth it. Talk about perspective! Nothing gives you a larger dose than your kids. Thanks are also given to my parents, sisters and extended family for their undying support, whether I wanted it or not

For better or for worse,

"I took the road less traveled by, and that has made all the difference."
-Robert Frost

Table of Contents

Abstract 3

Acknowledgments 5

Contents 8

List of Figures and Tables 10

Chapter 1: Introduction and Objectives 18
1.1 Introduction 18
1.2 Thesis Objectives 21

Chapter 2: Background and Motivation 22
2.1 Polyaryls as Precursors to Soot and Environmental Toxins 22
2.2 Thermodynamic Predictions of Polyaryl Chemistry 29
2.3 Analytical Chemistry Methods 31

Chapter 3: General Experimental Methods 33
3.1 Experimental Apparatus 33
3.2 Computer Modeling 41
3.3 Analytical Chemistry Procedures 43

Chapter 4: Naphthalene/Anthracene Pyrolysis 47
4.1 Introduction 47
4.2 Specific Experimental Methods 48
4.3 Results and Discussion 50
4.4 Conclusions 67

Chapter 5: Ortho-terphenyl Pyrolysis 69
5.1 Introduction 69
5.2 Specific Experimental Methods 72
5.3 Results and Discussion 73
5.4 Conclusions 86

Chapter 6: Biaryl Isomer Identification 88
6.1 Introduction 88
6.2 Naphthyl-Anthracene Identification 89
6.3 Phenyl-Triphenylene Identification 112
6.4 Conclusions 118

Chapter 7: Identification of poly-(ehthylene terephthalate)
(or: The Fullerene Fiasco) 119

7.1 Introduction 119
7.2 The Mystery 119
7.3 The Solution 131
7.4 Conclusions 135

Chapter 8: Kinetic Model 136
8.1 Introduction 136
8.2 The Programs - THERM 136
8.3 The Programs - CHEMKIN 146
8.4 The Kinetic Model 148
8.5 Results 152
8.6 Sensitivity Analysis 188
8.7 Conclusions 193

Chapter 9: General Conclusions and Direction of Future Research 194

Appendix A: Sample MOPAC Input and Output 200

Appendix B: Selected Computer Programs 207

Appendix C: Kinetic Mechanism for Anthracene/Naphthalene Pyrolysis 214

Appendix D: List of Relevant Compounds 251

Appendix E: Some Graph Theory Calculations for Fullerene Search 261

Appendix F: NASA Formatted Thermodynamic Parameters Used By CHEMKIN 264

Appendix G: Selected Full Output from CHEMKIN Calculations 275

References 296

List of Figures and Tables

Fig. 2.1.1 - Polymerization/condensation mechanism to high molecular weight growth with naphthalene and anthracene as fuels. p. 23

Fig. 2.1.2 - Polymerization/condensation mechanism to high molecular weight growth and several toxic byproducts with o-terphenyl as a fuel. p. 24

Fig. 2.1.3 - A comparison of sequential small chain addition and polymerization/condensation mechanisms to molecular weight growth. p. 27

Fig. 2.1.4 - Comparison of typical hydrogen/carbon ratios for a condensed PAH and a polyaryl of similar molecular weights. p. 27

Fig. 2.1.5 - Examples of condensation/ring-rupture/rearrangement reactions that can lead to the highly toxic dibenzopyrenes. p. 28

Fig. 3.1.1 - General design of the furnace used in all experiments. p. 34

Fig. 3.1.2 - Schematic Diagram of Gas Flow System to Furnace. Adjustable Valves are indicated as circles, and fixed flow valves by the standard triangle design. p. 35

Fig. 3.1.3 - Temperature calibration from major furnace parameters. p. 37

Fig. 3.1.4 - A diagram of the feeder probe used in all experiments. p. 39

Fig. 3.1.5 - A diagram of the fluidized bed entrained flow solids feeder used in these eperiments. p. 39

Fig. 4.3.1 - Relative abundances of the 3 binaphthalene isomers resulting from the pyrolysis of a 1:1 mole ratio mixture of anthracene and naphthalene p. 51

Fig. 4.3.2 - Relative abundances of the 6 naphthyl-anthracene isomers resulting from the pyrolysis of a 1:1 mole ratio mixture of anthracene and naphthalene. p. 52

Fig. 4.3.3 - Relative abundances of 3 out of 6 of the bianthracene isomers resulting from the pyrolysis of a 1:1 mole ratio mixture of anthracene and naphthalene. p. 53

Fig. 4.3.4 - Relative abundance of the 6 bianthracene isomers resulting from the pyrolysis of pure anthracene. p. 54

Table 4.3.1 - Theoretical vs. Observed ratios and angle of internal rotor for major biaryl products, by isomer group, of the pyrolysis of a 1:1 mole ratio mixture of anthracene and naphthalene. A-A = bianthracene, A-N = naphthyl-anthracene, N-N = binaphthalene.

Also included are the ratios for the bianthracenes resulting from the pyrolysis of pure anthracene. p. 55

Fig. 4.3.5 - Total relative abundances of the three major groups of biaryls resulting from the 1:1 mole ratio pyrolysis. I-J = total of all isomers in family I-J. p. 57

Fig. 4.3.6 - Total Ion Mass Spectra of the products of pyrolysis of a 1:1 mole ratio mixture of naphthalene and anthracene at 1180K as measured on LCMS system. p. 61

Fig. 4.3.7 - Total Ion Mass Spectra of the products of pyrolysis of a 1:1 mole ratio mixture of naphthalene and anthracene at 1277K as measured on LCMS system. p. 62

Fig. 4.3.8 - Total Ion Mass Spectra of the products of pyrolysis of a 1:1 mole ratio mixture of naphthalene and anthracene at 1348K as measured on LCMS system. p. 63

Fig. 4.3.9 - Total Ion Mass Spectra of the products of pyrolysis of a 1:1 mole ratio mixture of naphthalene and anthracene at 1416K as measured on LCMS system. p. 64

Fig. 4.3.10 - Total Ion Mass Spectra of the products of pyrolysis of a 1:1 mole ratio mixture of naphthalene and anthracene at 1496K as measured on LCMS system. p. 65

Fig. 5.3.1 - Total Ion Mass Spectra of the products of pyrolysis of pure ortho-terphenyl at 1248K as measured on LCMS system. p. 74

Fig. 5.3.2 - Total Ion Mass Spectra of the products of pyrolysis of pure ortho-terphenyl at 1275K as measured on LCMS system. p. 75

Fig. 5.3.3 - Total Ion Mass Spectra of the products of pyrolysis of pure ortho-terphenyl at 1302K as measured on LCMS system. p. 76

Fig. 5.3.4 - Total Ion Mass Spectra of the products of pyrolysis of pure ortho-terphenyl at 1326K as measured on LCMS system. p. 77

Fig. 5.3.5 - Total Ion Mass Spectra of the products of pyrolysis of pure ortho-terphenyl at 1352K as measured on LCMS system. p. 78

Fig. 5.3.6 - GCMS chromatogram of the products of pyrolysis of pure ortho-terphenyl at 1352K. p. 79

Fig. 5.3.7 - Two examples of a ring-rupture/recombination mechanism that can lead to the unusual products (CPAP, BghiF, etc) observed in the ortho-terphenyl pyrolysis experiments. p. 84

Fig. 6.2.1 - Total absorbance (236-500nm) HPLC chromatogram showing the biaryl isomers. ijNN = i,j'-binaphthalene, ijAA = i,j'-bianthracene. Unknown naphthyl-

anthracenes are labeled **1-6**, according to their elution order. Unknowns are later identified as **1**=91NA; **2**=92NA; **3**=11NA; **4**=21NA; **5**=12NA; **6**=22NA, where ijNA = i-(j'-naphthyl)anthracene. p. 90

Figure 6.2.2 - Subtracted and splined UV spectra (in acetonitrile/water) and structure for naphthyl-anthracene unknown **1** (91NA). p. 91

Figure 6.2.3 - Subtracted and splined UV spectra (in acetonitrile/water) and structure for naphthyl-anthracene unknown **2**. (92NA). p. 92

Figure 6.2.4 - Subtracted and splined UV spectra (in acetonitrile/water) and structure for naphthyl-anthracene unknown **3**. (11NA). p. 93

Figure 6.2.5 - Subtracted and splined UV spectra (in acetonitrile/water) and structure for naphthyl-anthracene unknown **4**. (21NA). p. 94

Figure 6.2.6 - Subtracted and splined UV spectra (in acetonitrile/water) and structure for naphthyl-anthracene unknown **5**. (12NA). p. 95

Figure 6.2.7 - Subtracted and splined UV spectra (in acetonitrile/water) and structure for naphthyl-anthracene unknown **6**. (22NA). p. 96

Figure 6.2.8. - GCMS mass 304 ion chromatogram of the six naphthyl-anthracene unknowns (**a-f** isomers). p. 97

Table 6.2.1. - Dominant mass ions and their abundances, normalized to base peak = 100, for each of the naphthyl-anthracene isomers. Mass loss/charging assignments are indicated in the first column. Horizontal divisons in the chart separate different carbon numbers (24, 23 and 22 carbons) and doubly charged fragments. ijNA = i-(j'-naphthyl)anthracene. p. 99

Table 6.2.2. - Dominant mass ions and their abundances, normalized to base peak = 100, for the binaphthalene isomers. Mass loss/charging assignments are indicated in the first column. Horizontal divisions in the chart separate different carbon numbers (20, 19 and 18 carbons) and doubly charged fragments. ijNN = i,j'-binaphthalene. p. 100

Table 6.2.3. - Correlation of notations and relavant transitions that represent the various UV absorption bands for naphthalene and anthracene. p. 102

Table 6.2.4. - Results of computer modelling with the program MOPAC using the AM1 semi-empirical molecular orbital model. Included are the heats of formation (kcal/mole), angles between planes of aryl constituents (degrees), and lengths of the most stable configurations (in angstroms) of each of the i-(j'-napthyl)anthracenes (ijNA), i,j'-binaphthalenes (ijNN), and i,j'-bianthracenes (ijAA). p. 102

Fig. 6.3.1 - Subtracted mass spectrum of 1-phenyl-triphenylene from GCMS system. p. 113

Fig. 6.3.2 - Subtracted mass spectrum of 2-phenyl-triphenylene from GCMS system. p. 113

Fig. 6.3.3 - HPLC chromatogram of selected products from the pyrolysis of ortho-terphenyl at 1352K. p. 114

Fig. 6.3.4 - Subtracted UV-Vis spectrum of 1-phenyl-triphenylene in acetonitrile/water. p. 115

Fig. 6.3.5 - Subtracted UV-Vis spectrum of 2-phenyl-triphenylene in acetonitrile/water. p. 116

Fig. 7.2.1 - A comparison of mass ion pattern of a known standard of a fullerene (C_{60}) and the unknown of mass 576. p. 122

Fig. 7.2.2 - Subtracted UV-Vis Spectrum of unknown 576 molecule in acetonitrile and water. p. 125

Fig. 7.2.3 - Proposed structures for hypothetical fullerene series C_{48}, C_{64}, C_{80}, C_{96} whose expected properties match some of those of the unknown series at masses 576, 768, 960, 1152. p. 126

Fig. 7.2.4 - High molecular weight LCMS Total Ion Mass Spectra of contaminant series. p. 129

Fig. 7.3.1 - High resolution mass spectrum of 576 mass ion as obtained from tandem LCMS at the Naval Research Center. p. 132

Fig. 7.3.2 - Negative ion mass fracture pattern of 576 mass ion at 50 eV as obtained from tandem LCMS at the Naval Research Center. p. 133

Fig. 8.2.1 - Diagram indicating group types used for estimating thermodynamic properties based on Benson's group additivity method. p. 138

Table 8.2.1 - Table indicating actual Benson group additivity types used for each compound in the kinetic model. p. 139

Table 8.3.1 - A list of the input run parameters that were used for modeling with the CHEMKIN programs. p. 147

Table 8.4.1 - A list of radicals in the mechanism and the assumed numbers of "reachable" (by anything larger than hydrogen molecule) sites on each. p. 151

Fig. 8.5.1 - Calculated total ion mass spectrum for the products of pyrolysis of pure naphthalene at 1177K. p. 154

Fig. 8.5.2 - Calculated total ion mass spectrum for the products of pyrolysis of pure naphthalene at 1277K. p. 154

Fig. 8.5.3 - Calculated total ion mass spectrum for the products of pyrolysis of pure naphthalene at 1350K. p. 155

Fig. 8.5.4 - Calculated total ion mass spectrum for the products of pyrolysis of pure naphthalene at 1415K. p. 155

Fig. 8.5.5 - Calculated total ion mass spectrum for the products of pyrolysis of pure naphthalene at 1498K. p. 156

Fig. 8.5.6 - Calculated total ion mass spectrum for the products of pyrolysis of a 1:1 mixture of naphthalene and anthracene at 1180K. p. 156

Fig. 8.5.7 - Calculated total ion mass spectrum for the products of pyrolysis of a 1:1 mixture of naphthalene and anthracene at 1277K. p. 157

Fig. 8.5.8 - Calculated total ion mass spectrum for the products of pyrolysis of a 1:1 mixture of naphthalene and anthracene at 1348K. p. 157

Fig. 8.5.9 - Calculated total ion mass spectrum for the products of pyrolysis of a 1:1 mixture of naphthalene and anthracene at 1416K. p. 158

Fig. 8.5.10 - Calculated total ion mass spectrum for the products of pyrolysis of a 1:1 mixture of naphthalene and anthracene at 1496K. p. 158

Fig. 8.5.11 - Calculated total ion mass spectrum for the products of pyrolysis of pure anthracene at 1181K. p. 159

Fig. 8.5.12 - Calculated total ion mass spectrum for the products of pyrolysis of pure anthracene at 1278K. p. 159

Fig. 8.5.13 - Calculated total ion mass spectrum for the products of pyrolysis of pure anthracene at 1350K. p. 160

Fig. 8.5.14 - Calculated total ion mass spectrum for the products of pyrolysis of pure anthracene at 1415K. p. 160

Fig. 8.5.15 - Calculated total ion mass spectrum for the products of pyrolysis of pure anthracene at 1496K. p. 161

Fig. 8.5.16 - Calculated equilibrium total ion mass spectrum (as approximated by a 2000 second run time) for the products of pyrolysis of a 1:1 mole ratio mixture of anthracene and naphthalene at 1180K. p. 161

Fig. 8.5.17 - Calculated equilibrium total ion mass spectrum (as approximated by a 2000 second run time) for the products of pyrolysis of a 1:1 mole ratio mixture of anthracene and naphthalene at 1277K. p. 162

Fig. 8.5.18 - Calculated equilibrium total ion mass spectrum (as approximated by a 2000 second run time) for the products of pyrolysis of a 1:1 mole ratio mixture of anthracene and naphthalene at 1348K. p. 162

Fig. 8.5.19 - Calculated equilibrium total ion mass spectrum (as approximated by a 2000 second run time) for the products of pyrolysis of a 1:1 mole ratio mixture of anthracene and naphthalene at 1416K. p. 163

Fig. 8.5.20 - Calculated equilibrium total ion mass spectrum (as approximated by a 2000 second run time) for the products of pyrolysis of a 1:1 mole ratio mixture of anthracene and naphthalene at 1496K. p. 163

Fig. 8.5.21 - Observed total ion mass spectrum for the products of pyrolysis of pure naphthalene at 1177K. p. 164

Fig. 8.5.22 - Observed total ion mass spectrum for the products of pyrolysis of pure naphthalene at 1277K. p. 165

Fig. 8.5.23 - Observed total ion mass spectrum for the products of pyrolysis of pure naphthalene at 1350K. p. 166

Fig. 8.5.24 - Observed total ion mass spectrum for the products of pyrolysis of pure naphthalene at 1415K. p. 167

Fig. 8.5.25 - Observed total ion mass spectrum for the products of pyrolysis of pure naphthalene at 1498K. p. 168

Fig. 8.5.26 - Observed total ion mass spectrum for the products of pyrolysis of a 1:1 mole ratio mixture of naphthalene and anthracene at 1180K. p. 169

Fig. 8.5.27 - Observed total ion mass spectrum for the products of pyrolysis of a 1:1 mole ratio mixture of naphthalene and anthracene at 1277K. p. 170

Fig. 8.5.28 - Observed total ion mass spectrum for the products of pyrolysis of a 1:1 mole ratio mixture of naphthalene and anthracene at 1348K. p. 171

Fig. 8.5.29 - Observed total ion mass spectrum for the products of pyrolysis of a 1:1 mole ratio mixture of naphthalene and anthracene at 1416K. p. 172

Fig. 8.5.30 - Observed total ion mass spectrum for the products of pyrolysis of a 1:1 mole ratio mixture of naphthalene and anthracene at 1496K. p. 173

Fig. 8.5.31 - Observed total ion mass spectrum for the products of pyrolysis of pure anthracene at 1181K. p. 174

Fig. 8.5.32 - Observed total ion mass spectrum for the products of pyrolysis of pure anthracene at 1496K. p. 175

Fig. 8.5.33 - Calculated relative abundances of the 3 binaphthalene isomers resulting from the pyrolysis of a 1:1 mole ratio mixture of anthracene and naphthalene. p. 176

Fig. 8.5.34 - Calculated relative abundances of the 6 naphthyl-anthracene isomers resulting from the pyrolysis of a 1:1 mole ratio mixture of anthracene and naphthalene. p. 177

Fig. 8.5.35 - Calculated relative abundance of the 6 bianthracene isomers resulting from the pyrolysis of a 1:1 mole ratio mixture of anthracene and naphthalene. p. 178

Fig. 8.5.36 - Calculated total relative abundances of the three major groups of biaryls resulting from the 1:1 mole ratio pyrolysis. I-J = total of all isomers in family I-J. p. 179

Fig. 8.5.37 - Calculated total relative abundances of the three major groups of condensation products resulting from the 1:1 mole ratio pyrolysis. I-J = total of all products from the condensation of biaryl family I-J. p. 180

Fig. 8.5.38 - Observed relative abundances of the 3 binaphthalene isomers resulting from the pyrolysis of a 1:1 mole ratio mixture of anthracene and naphthalene. p. 181

Fig. 8.5.39 - Observed relative abundances of the 6 naphthyl-anthracene isomers resulting from the pyrolysis of a 1:1 mole ratio mixture of anthracene and naphthalene. p. 182

Fig. 8.5.40 - Observed relative abundance of the 6 bianthracene isomers resulting from the pyrolysis of pure anthracene. p. 183

Fig. 8.5.41 - Observed total relative abundances of the three major groups of biaryls resulting from the 1:1 mole ratio pyrolysis. I-J = total of all isomers in family I-J. p. 184

Fig. 8.5.42 - Observed total relative abundances of the three major groups of condensation products resulting from the 1:1 mole ratio pyrolysis. I-J = total of all products from the condensation of biaryl family I-J. p. 185

Table 8.6.1 - Sensitivity of certain key representative measures of the kinetic model to changes in major input parameters. Units are fraction change per kcal for energy perturbations, fraction change per second for time perturbation, fraction change per Kelvin for temperature perturbations, and fraction change per % perturbation for pre-exponential factors. p. 188

Chapter One - Introduction and Objectives

1.1 - Introduction

Combustion sources have been around since the beginning of time. Most of them are associated with a long record of messy, choke-inducing smoke. Only in the last 50 years has mankind even begun to whittle away at the complex nature of the flame system. It is quite ironic that such a complex chemical system could once have been thought of as an element, the simplest and most basic of nature's building blocks, an axiom upon which many 'scientific' theories were based.

Combustion products, some of which are just beginning to be recognized for their mutagenic potential to human cells, are ubiquitous. Since most combustion sources release their products unfiltered and unconverted into the global air current system, it is a problem that must be addressed for the health of the entire world. While it has not gotten to the point where global impact has become a critical situation, the effect near major centers of combustion sources (and population) is certainly noticable now in the levels of photocatalyzed combustion products that we can see and feel as smog. Granted, there are many other things out there that are more deadly than inhaling smoke byproducts for a lifetime, but medical science is catching up fast with biological disease without much corresponding progress with combatting the more irreversible damage of diseases caused by environmental toxins. Another approach is needed for long-term success on this front -

the chemicals must be controlled at their source. Without a better understanding of the nature of the formation of these toxic products, this objective can not be accomplished.

It is well known now that the particulate matter portion of a combustion source byproduct consists of a complex array of chemicals - from small, condensed phase polycyclic aromatic hydrocarbons (PAH) all the way up to the large, mostly carbon macromolecules known commonly as soot. People are also becoming aware of the toxic nature of some of those compounds, so it becomes a natural next step to want to know how and why this occurs, in the interest of better public health. The brute force approach to controlling PAH and soot - high temperatures, low fuel/air ratio, long residence times, better mixing - is unfortunately not very practical or even possible in many situations with the current technology. Only very costly materials can survive very long at the required temperatures, too much air will dilute the system and lower the temperature requiring external heating and thus money, long residence times = big machines = big expense, and better mixing is limited by the nature of the fluids involved. In the end, the brute force approach is just not economically feasible in too many situations. A more elegant approach is needed to lower toxic byproduct and soot formation.

Focus in flame chemistry in the past has been on the detailed mechanisms of the smallest components that contribute to the flame environment, primarily short chain radicals and oxidation products. But this approach entirely neglects the chemical processes that take place inside the fuel-rich pyrolysis zones that occur within the surrounding oxidative atmosphere. It is inside these pockets that the chemistry leading to large PAH and soot formation takes place. This is not to say that the field has not been

explored, however. To the contrary, the field of soot formation is perceived to be rather mature. However, some important progress has been made in recent years that has caused some questions to be reexamined that were once thought resolved. Most notable of those discoveries are those involving fullerene formation and the recognition that polyaryls and PAH that contain 5 membered rings may play significant roles in the soot production mechanism.

The focus in soot formation mechanisms have traditionally relied on sequential acetylene (or other similarly small component) addition route to explain the conversion of relatively low molecular weight PAH into the very large scale structure of soot. While it is well known now that PAHs are precursors to soot in some way, in the sense that there is no other place for all that carbon to go and all of the PAHs appear to be destroyed coincident with soot formation, a global mechanism has not been found that can satisfactorily describe all of the product chemistry trends that are observed experimentally in sooting environments. In the quest for this goal, some intermediate conclusions must be drawn about the nature of these reaction mechanisms.

First, does the mechanism primarily involve simple small-chain aliphatic additions, as is currently believed to be true, at least in the low molecular weight regime? If so, how can that series of reactions proceed all the way to soot with the rapid dropoff in concentrations with molecular weight that are observed. Second, can an alternate mechanism be taking over at the higher molecular weights that can better explain the observed spectrum of product chemical species. Third, are the mechanisms thermodynamically controlled or kinetically limited, and what are the corresponding

characteristic reactions and times, if the latter is true? Fourth, in an increasingly health conscious yet polluted world, what are the connections between soot production and mutagen formation? Many intermediate byproducts of soot formation mechanisms are mutagenic, but which ones, and by which routes do they form? Understanding the pathway to soot formation will provide insight and perhaps a predictive understanding into what fuels and what flame environments might produce the most dangerous chemicals.

1.2 - Thesis Objectives

This thesis attempts to resolve some of the key issues of the above questions. Specifically the objectives of this thesis are the following: 1) Establish whether or not polyaryl formation can compete with acetylene addition mechanisms to high molecular weight PAH growth in the case of small 1-3 ring PAH compounds used as a fuel. 2) Establish conditions of fuel pyrolysis under which this competition can occur. 3) Determine whether the process is kinetically or thermodynamically controlled, and make hypotheses about the nature of mechanisms by which the process is limited. 4) Outline processes whereby toxic compounds (especially the highly mutagenic dibenzopyrenes) might be produced as byproducts or as intermediates in the soot formation mechanism. 5) Enhance the library of acquired knowledge about analytical procedures by which selected compounds might be identified to aid in future studies.

Chapter Two - Background and Motivation

This chapter presents a review of the literature relevant to the objectives of this thesis, along with more detailed descriptions of factors within these sources that motivated the experimental design and analysis of this project. The first section gives a brief history of the reasoning behind studying polyaryls as precursors to soot, along with rationale for their suspected contribution to producing species that are suspected to be toxic to humans. The second section presents an overview of the limited thermodynamic and calculations that have been performed on selected series of polyaryl isomers and their associated condensation products. The last section presents some of the existing theory relevant to identifying trends in mass and UV-Vis spectra of biaryls.

2.1 - Polyaryls as Precursors to Soot and Environmental Toxins

The reactive coagulation of large PAH radical species is known to occur in flames, and it is also theorized to be a step in the soot formation mechanism (Howard (1990), Harris et al. (1988), Hepp et al. (1994), Miller et al. (1984), McKinnon and Howard (1990), Miller (1990), Frenklach and Wang (1990), Takatsu and Yamamoto (1993)) In addition, several investigators have also focused on reactive coagulation of several aromatic compounds in a pyrolysis environment (Stein et al. (1987), Lang et al. (1957,1961), Kinney (1956), Bermudez and Pfefferle (1991), Wornat et al. (1992), Mukherjee et al. (1993), Masonjones et al. (1994)) based on a mechanism proposed by

Postulated Molecular Growth Pathway via Dimerization and Subsequent Condensation

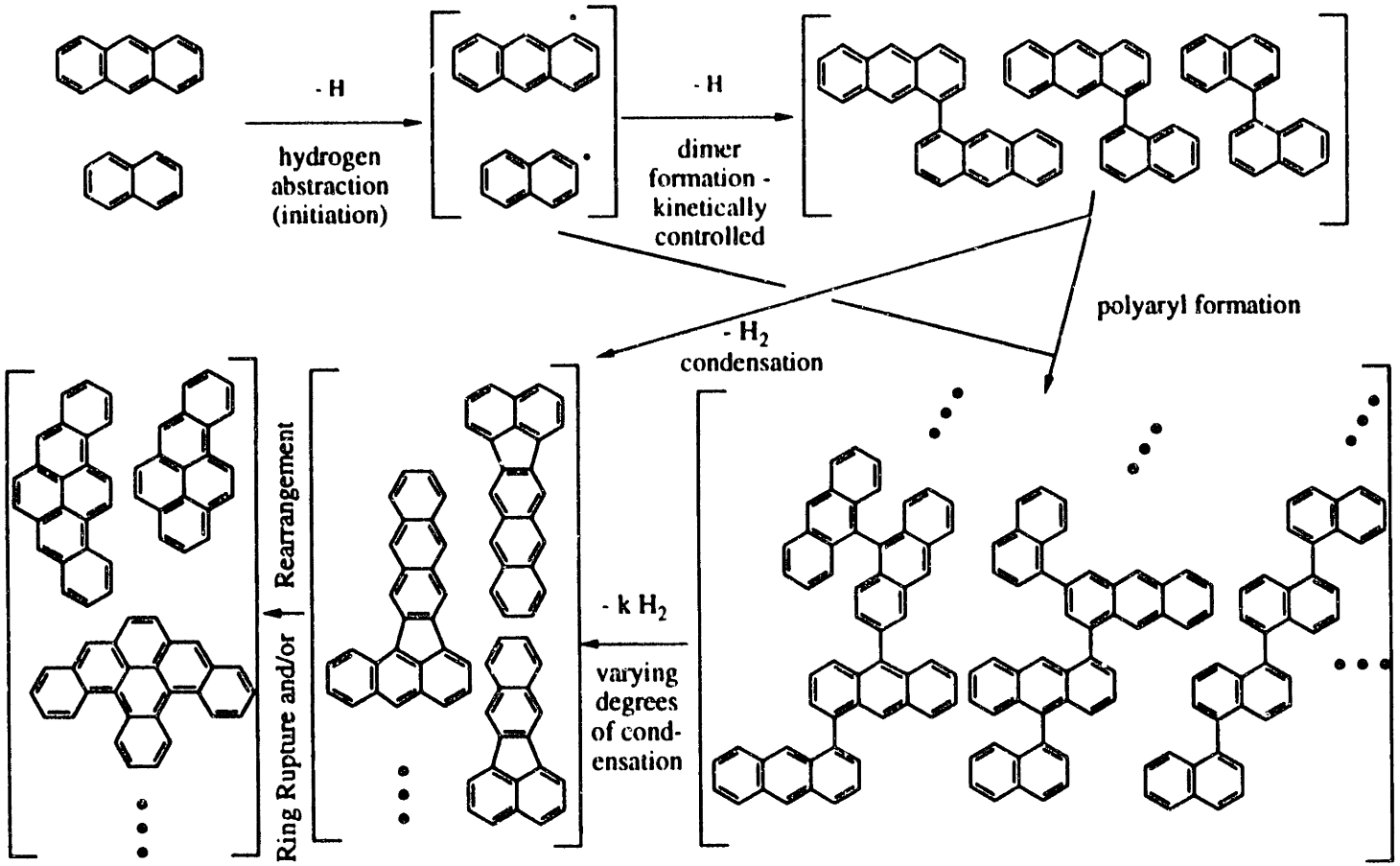

[ ] Brackets indicate all possible structural isomers of the types shown.

Fig. 2.1.1

Simplified Reaction Mechanism for the Benzene Polymerization Pathway

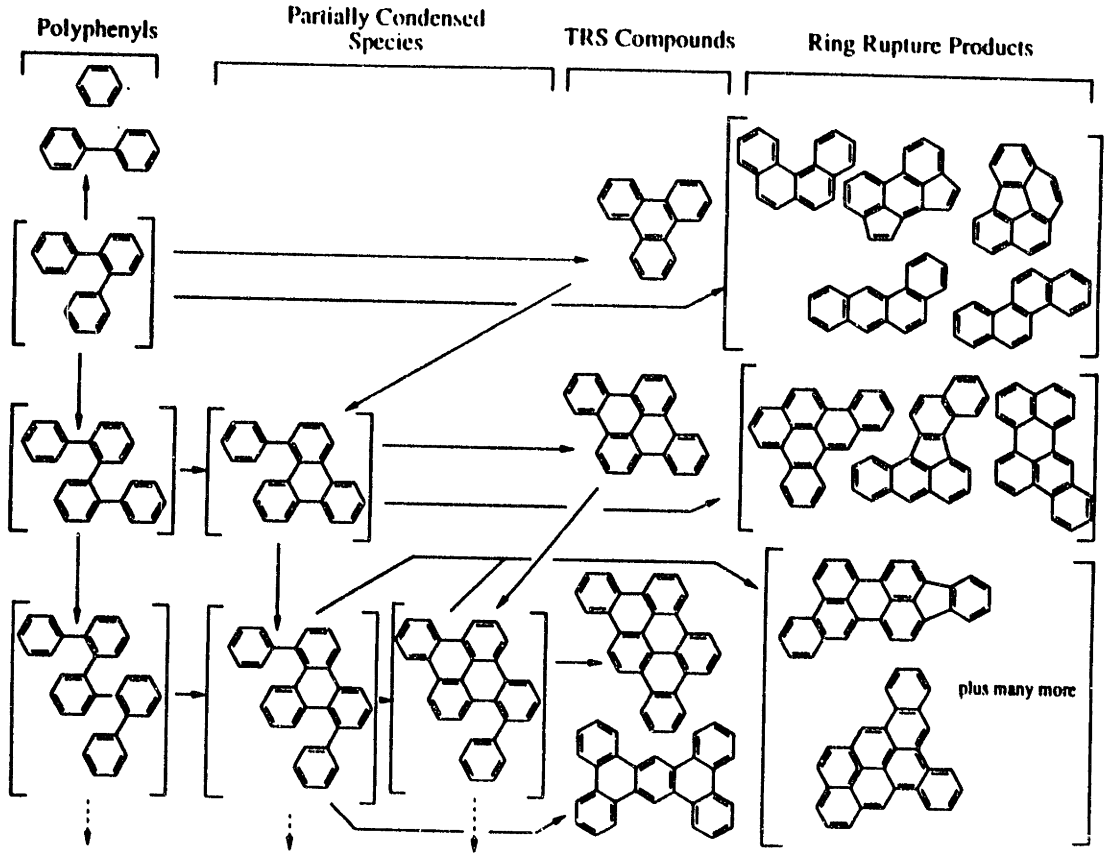

[ ] Brackets are used to indicate all related isomers in a group.

Fig. 2.1.2

Badger and coworkers (1964). Outlines for this type of mechanism for the species relevant to this research (the anthracene/naphthalene and benzene polymerization pathways) are shown in Figs. 2.1.1 and 2.1.2. These studies hint at the viability of a molecular weight growth pathway to soot via polymerization.

The competing (but perhaps complementary) theory to explain molecular weight growth to soot that has enjoyed the most attention is that of sequential addition of small chain aliphatics (Bittner and Howard, 1981, Frenklach et al., 1984, Homann and Wagner,1967, Graham.et al., 1975, Frenklach and Warnatz, 1987, Bauer and Jeffers, 1988). The aliphatics are either provided directly by the fuel (as acetylene, propene, allene, etc.) or are present in the flame/pyrolysis environment as a result of thermal decomposition of the fuel. One fuel that has been studied extensively for its ability to "crack" into two smaller constituent aliphatics (e.g. a C_3 and a C_4 species) is toluene (Smith, 1979, Kern et al., 1982, Robaugh and Tsang, 1986, Hippler et al., 1990). This growth process via small chain addition accounts for small molcular weight arenes and fragments quite well, but the mechanism is too slow (Calcote,1991) to account for the soot mass that is observed in flames. Furthermore, the H/C ratio of the soot particles created by such a mechanism are found to be too low to match the ratios that are observed in young soot particles (Wagner, 1981).

Polymerization of moderate molecular weight PAH's (2-10 rings) provides an alternative growth process to small chain addition that can account for both of the observed inconsistencies of speed and high H/C ratio. First, though comparable in rate to acetylene addition (the same types of reactions with similar energy barriers), the relevant

reactions need to occur far fewer times in sequence in order to generate high molecular weight compounds. A MW 300 PAH can dimerize to 600 MW, for example, with one step. The same magnitude of growth via small chain additions would require on the order of 10 steps to complete (see Fig. 2.1.3). Thus, by partially circumventing the slow serial nature of constructing large compounds from small ones, far less time is needed to create molecules the size of soot particles with the polymerization mechanism than with the acetylene addition mechanism.

The second advantage that the polymerization scheme has over that of the small chain addition mechanism in reproducing experimental observations is that the H/C ratio for polymeric arenes is much higher and comes much closer to matching experimentally observed H/C ratios than do compounds arising from sequential acetylene addition. An example of this concept is shown in Fig. 2.1.4. This observation, combined with the considerations in the preceding paragraph about proof for the existence of biaryls and the observed rate of molecular weight growth in flames, makes the case for the possibility that polymerization of arenes may be a dominant pathway to soot growth in high temperature environments.

Many unanswered questions remain, however, about the polymerization mechanism, and they form the basis of this thesis. A more detailed description of the types, variety, and concentrations of isomers involved in the mechanism is needed, for example, along with a detailed description of the mechanism itself. Chemical analysis methods and apparatus are also capable of much more now than they were even 5 years ago, and advantage has yet to be taken of the new information that is obtainable about high molecular weight PAH (>400 MW) from such techniques. Identifying isomers of

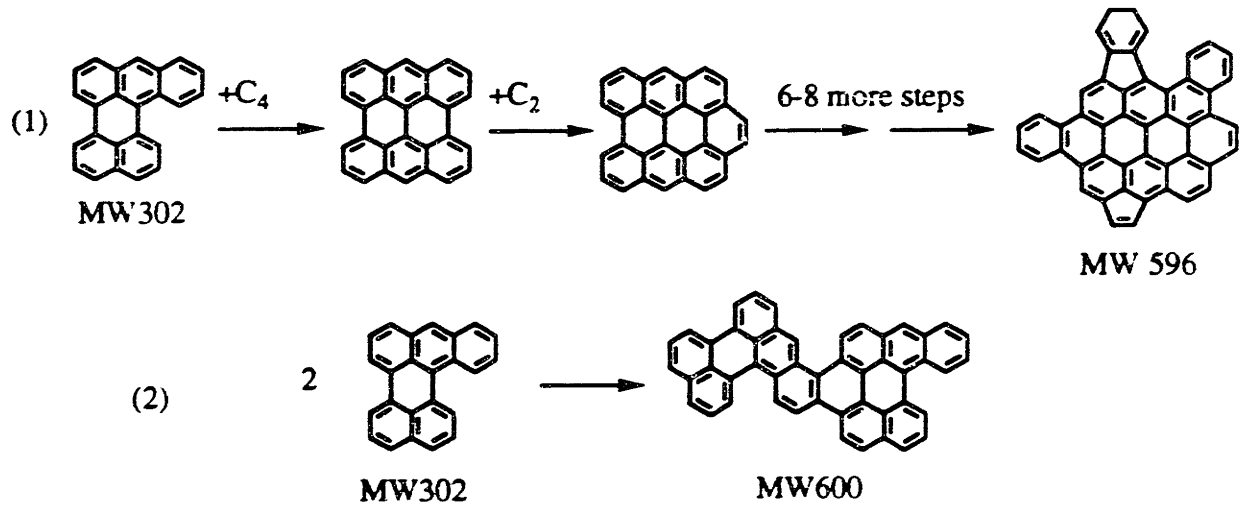

Fig. 2.1.3: A comparison of small chain addition (1) and polymerization/condensation (2) mechanisms.

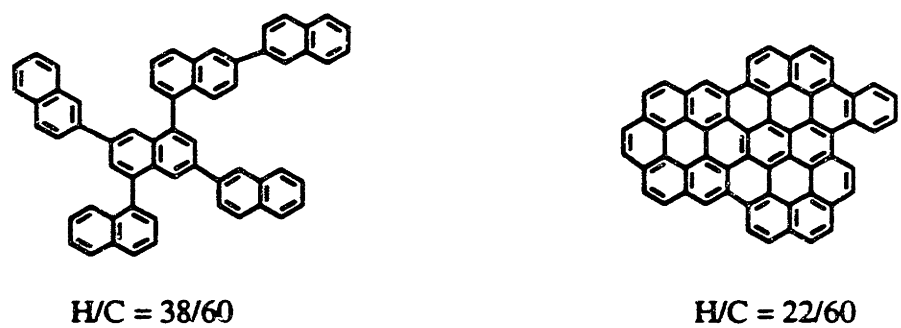

Fig. 2.1.4: A Comparison of hydrogen to carbon ratios for typical polyaryl and condensed species of similar molecular weights.

biaryls, for example, is a key step in checking the validity of the polymerization/condensation mechanism approach. Proving the existence of long polyaryl chains is also vital to establishing mecanisms to the formation of condensible soot precursors. Both techniques are just becoming available as analytical tools, and a better understanding of the theories governing these methods of compound identification are needed to fully exploit the potential insight into the mechanism that can be gained.

Another question related to the molecular weight growth through polymerization mechanism is whether the presence of polyaryl products in the reactant soup can explain some of the other chemsitry in a high temperature environment that had previously been attributed to small-chain addition reactions. Compounds that are toxic to humans are of particular interest, as the mechanisms to the formation of some of them are largely

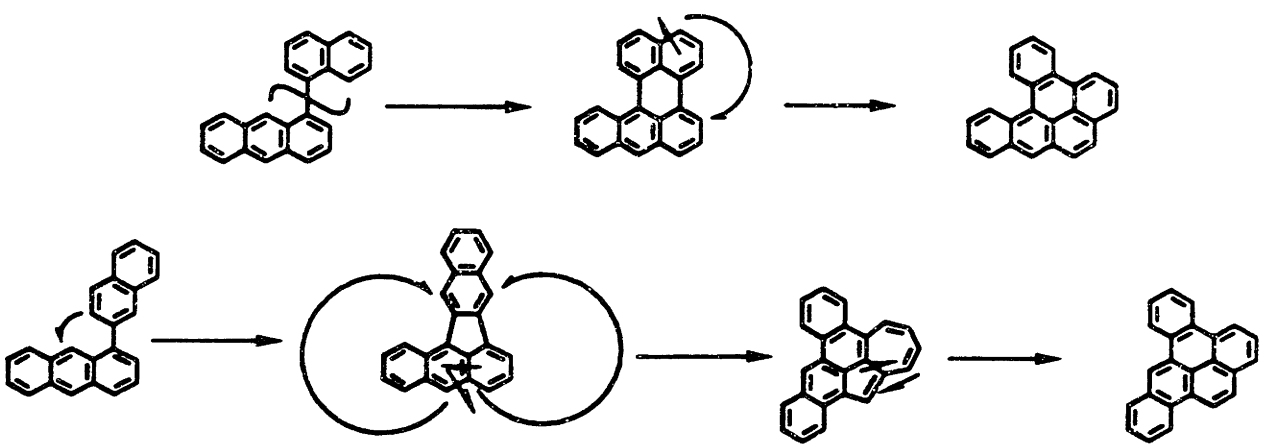

Fig. 2.1.5: Two examples of condensation/rearrangement mechanisms that can lead to dibenzopyrenes

unproven, but suspected. Some dibenzopyrenes, for example dibenzo(a,l)pyrene, are the most toxic PAH known (Cavalieri et al., 1991, Ralston et al., 1994, Higginbotham et al., 1993). They are six-ring PAHs which may be formed from the condensation of a 3-ring/2ring (or 4-ring/1-ring) biaryl, followed by ring rupture and/or four-centered structural rearrangements (see Fig. 2.1.5) similar to those employed by Scott and Roelofs (1987) to explain migration of five-membered rings around a PAH structure. A similar mechanism involving bianthracene condensation proceeding to 7-ring pyrene benzologues was postulated by Wornat (1992) to explain the presence of those compounds in a pure anthracene pyrolysis experiment. The possibility of mutagen formation via the pathway shown in Fig 2 1.5 will be investigated in this thesis as a natural next step in the ongoing examination in this laboratory of the role of PAH chemistry has in creating environmental toxins.

2.2 - Thermodynamic Predictions of Polyaryl Chemistry

The potential importance of at least biaryl formation has been recognized for some time (Badger and coworkers, 1961-1965, Stein et al., 1987, Wornat et al. (1992), Mukherjee et al. (1994), Masonjones et al. (1995)). In addition, several investigators have made some attempts at modeling the thermodynamic equilibrium of biaryl isomers (Mulholland et al., 1993 (both)) and of compounds relevant to the polymerization/condensation pathway (Stein,1978).

The investigations by Mulholland indicated that assumption of thermodynamic equilibrium was indeed a good enough approximation to describe experimental ratios of

biaryls within a particular group (e.g. bianthracenes). A semi-empirical molecular orbital model (Austin Model - 1) in the program MOPAC 6.0 was used to estimate steric hindrance effects on molecular conformation and heats of formation. Further attempts at verifying thermodynamic equilibrium based on this calculation method were limited by the unavailability of experimental data and the potential confounding effects of a heterogeneous fuel mixture. Differing propensities of the biaryls to condense were also left out of the calculations by Mulholland, although mention of this effect on the ratios of biaryl abundances was made. A model is thus sought to establish the effects of fuel mixture and condensation products on product spectrum, in an attempt to better understand the nature of the mechanism to biaryl formation.

The earlier work by Stein took the thermodynamic calculations a bit further than biaryls and assumed equilibrium for the entire sequence of compounds in the benzene polymerization pathway, among others, but his calculations were unsubstantiated by experiment. The main reason for this was the unavailability of analytical techniques and/or apparatus that could extract the kind of information about high molecular weight compounds needed to verify the calculations. The advent of several types of mass spectrometers that can detect (and at least roughly quantify) abundances of large PAH, however, has enabled the possibilty for experimental confirmation of such elaborate theories about PAH growth.

The main advantages of performing experiments to verify or refute Stein's calculations are that: 1) the calculations extend into a molecular weight range that is of interest in soot formation, and 2) *all* of the expected condensation products from the

benzene-polymerization pathway are total-resonant-sextet compounds (Clar, 1964, Knop et al., 1987), compounds noted for their exceptional stability due to their unique p - structure resonance. Indeed, evidence for them has been found in interstellar matter (Hendel et al., 1986). If equilibrium considerations are in effect, therefore, TRS compounds should be present in very large concentrations relative to their uncondensed precursors, a property not shared with condensation products of more complex polyarenes.

As better analytical techniques have become available to more thoroughly investigate the various biaryl isomers and high molecular weight compounds that are present in experimental samples, a test of the thermodynamic theories of Mulholland et al and Stein becomes possible. This thesis will thus focus on refining elements of these theories as a primary motivation for this research, along with proving the viability of a mechanism to soot growth that is alternative to the aliphatic small chain addition pathway.

2.3 - Analytical Chemistry Methods

Identifying as many isomers of compounds as one can in the soup of reactants is very desirable when trying to prove the validity of a model that takes their presence into account. At the very least, quantification of the primary biaryl products must be possible in order to test the performance differences of the competing models of polyaryl formation. Whereas biaryl formation at high temperatures has been well documented in the literature (see references in the preceding two sections), surprisingly little has been accomplished in the field of individual isomer identification. Several attempts were made

by Jones (1941-47) and House et al. (1972) to establish general rules for relating connectivity of arenes to the changes in their UV spectrum These identifications were based on theories about the contribution of p-structure conformation to different bands of UV-Vis absorption (Craig and Hobbins, 1955 (both), Grinter and Mason, 1964, Clar, 1972, Jones, 1941-7). Selected isomers of biarenes have also been isolated and identified when taken out of the context of the whole biarene series (Badger et al., 1964, Dworkin et al., 1979, Photoelectronic Spectroscopy Group, 1966, Thermodynamics Research Center, 1983, Heller, 1978, Bell and Waring, 1949). However, differing levels of certainty are claimed by the authors, and no definitive evidence has existed to establish rules for identifying an entire series of biarenes - a crucial step in the modeling portion of this research.

One biarene series, however, (besides the rather simple biphenyl, phenyl-naphthalene, and binaphthalene series) has been characterized in its entirety. Identification of all six isomers of bianthracene has been established by Wornat (1993) based on some preliminary identifications by Stein (1987), availability of some key reference standards, and the earlier established theories by Jones and others referenced in the preceding paragraph. In Wornat's paper, some rules about isomer identification were reiterated and new ones postulated that will aid in the identifications required for this work. These rules will be discussed further in the chapter on isomer identification.

Chapter Three - General Experimental Methods

Presented in this chapter are the experimental methods common to all sampling and analysis procedures used in this thesis. The first section describes the physical furnace setup used for acquiring samples in all the pyrolysis experiments. The second section is devoted to a description of the computer modeling used to test the various thermodynamic and kinetic models employed in this thesis. The last section gives a description of the analytical apparatus and methodology that were used to analyze the samples obtained by the methods described in section one of this chapter.

3.1 - Experimental Apparatus

All experiments described in this document used the same reactor - a drop-tube furnace equipped with a solid particle feeder. The general design of the reactor can be found in Fig. 3.1.1. The furnace is electrically heated and the temperature is held constant at the desired setting via process control circuitry with feedback from a boron-graphite thermocouple. Gases are individually metered, fed, and extracted from the furnace via the gas flow system shown in Fig. 3.1.2. In addition, pressures are controlled, and samples are taken and fed by appropriate manipulation of valves shown in the same figure.

The reaction zone consists of the center 32 cm section of a quartz tube that is 47mm in diameter. The quartz tube extends in both directions around the sampl probe and feeder tube insulation as shown. Mulholland (1992b) has already shown, with a

Fig. 3.1.1: Schematic of Furnace and Sampling Train

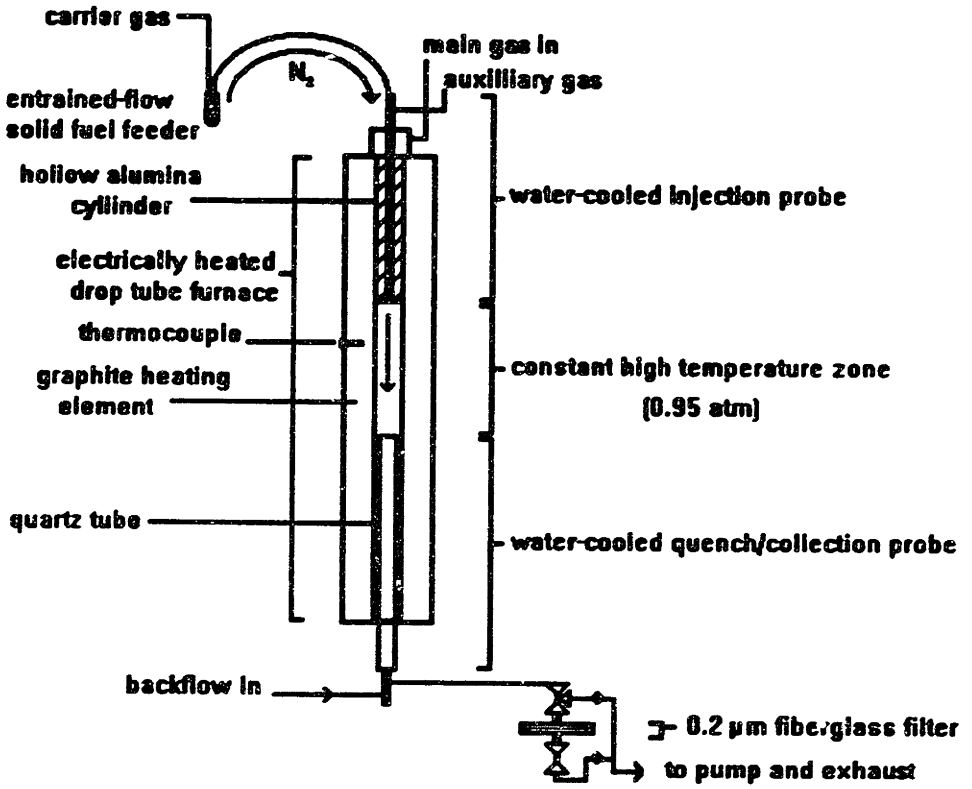

similar setup on the same furnace, that beyond the immediate vicinity (approx. 2-3 cm) of the initial and final temperature ramps to the water-cooled feeder and sample probe respectively, temperatures within the reaction zone are found to fluctuate with distance by less than 50K. The level temperature profile within the reaction zone for this setup has been verified by independent measurement of temperature via direct insertion of a chromel-alumel (type K) thermocouple into various postions in the furnace. It should be noted, however, that a smaller variation with axial distance (on the order of 10-20 K) was observed with this setup than with the setup employed by Mulholland, probably due to the

Fig. 3.1.2: Schematic of Gas Flow System

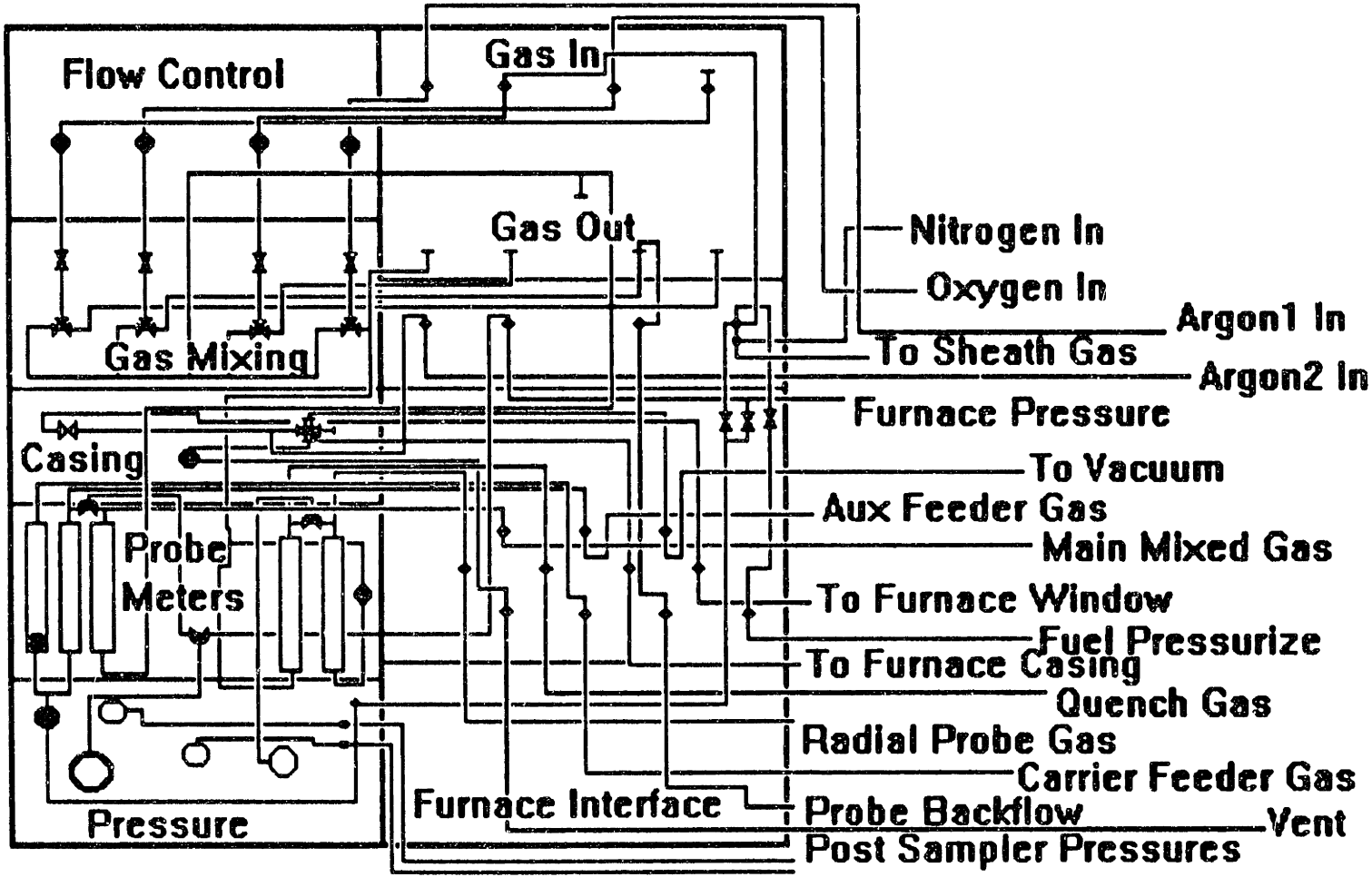

use of insulation within the reactor right up to the temperature controlled zone. Radial temperature gradients are also assumed to be small in these experiments, by analogy to Mulholland's experimental setup, and the temperature of the experiment is taken to be that of the furnace at the maximum temperature along the center line.

Calibration of temperature vs. response voltage of the boron-graphite thermocouple - the most direct measure of temperature available during experiments, is performed by the same method of inserting an independent thermocouple, but at a constant distance of 5 cm along the center line into the furnace, where the maximum temperature is closely approximated. Since the boron-graphite thermocouple is not in direct contact with the raction zone gases, but instead with the furnace casing gases, the temperature measured by it could not be relied on for an actual temperature of the reaction zone. However, a reasonable correlation of casing temperature vs reaction zone temperature could be made. Reproduction errors of less than 3 K could be achieved by taking into account the additional variable of casing gas pressure. A graph showing the correlation and the mathematical formula for calculating furnace temperature can be found in Fig. 3.1.3.

The sample collection probe has been previously described in detail (Mulholland, 1992b). The probe is water cooled, and its upper tip is taken to be the end of the reaction zone. The inner wall of the probe is composed of a porous sintered metal tube, approx 2 cm in diameter, to enable the flow of quench gas into the product stream. Inert quench gas (argon) is introduced radially in the first centimeter of the probe tip through the inner tube, and a radial gas flow (also argon) through the remainder of the sintered tube is employed to inhibit particle deposition on the probe walls. The combined flow rate of

Fig. 3.1.3: Temperature Calibration

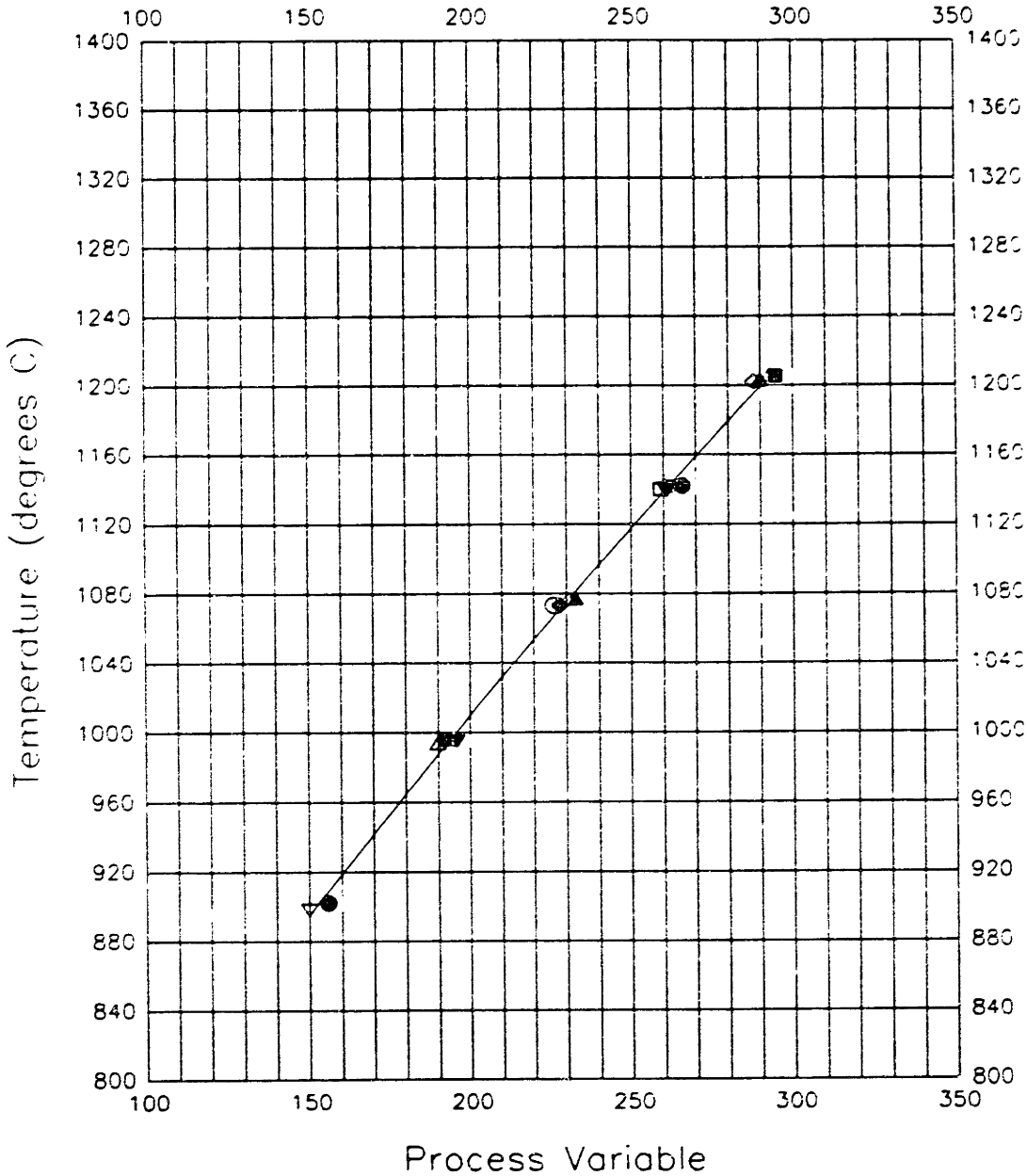

Temp = 481.4 + 2.882 PV − 0.00159 PV^2 + 3.38 Press.
Predicts within 2–3 degrees Celcius

quench (20 lpm) and radial (4 lpm) gases is enough to dilute the product stream fivefold, and the exit temperature of gases from the probe is less than 100 C in all experiments. At the bottom of the sample collection probe is a small (0.5 inch diameter) quartz window to allow line of sight laser access to the center of the furnace from below. Though the window was unused in these experiments, the 90 degree turn in the sample line required the use of a small amount of backflow of nitrogen (approx. 150cc/min) to prevent deposition of soot into the chamber above the window but below the 90 degree turn. A sheath gas of argon was also used to fill the space below the o-ring that seals off the furnace from the ambient air. This was done to neutralize the danger of oxygen leaking through a known but unfixable leak. This leak rate was isolated and measured to be 30 cc/min (as measured at 20 psig furnace pressurization), but was probably much less in actual experimental runs where furnace pressurization is less than 1 psi vacuum.

The sample collection apparatus consists of a pre-weighed 90 mm diameter fiberglass filter with pore size 0.2 μm (Millipore, Cat. no. FGLP 090) encased in a filter holder through which all of the product gas stream is pulled using an industrial vacuum pump. A pressure drop must be maintained accross the filter at all times before and during the sampling process to eliminate the possibility of backflow into the furnace, and gas lines are plumbed to meet this requirement. Samples are taken for 2 minutes, the approximate time at which the vacuum pump can no longer maintain a large enough pressure drop accross the filter due to heavy loading that occurs at the feed rates used. After weighing, the filter is placed inside a jar and the jar is placed into a freezer to await extraction.

The feeder probe (Fig. 3.1.4) is a water cooled probe equipped with two gas ports, one for the gas carrying entrained solid fuel particles and one for optional dilution gas

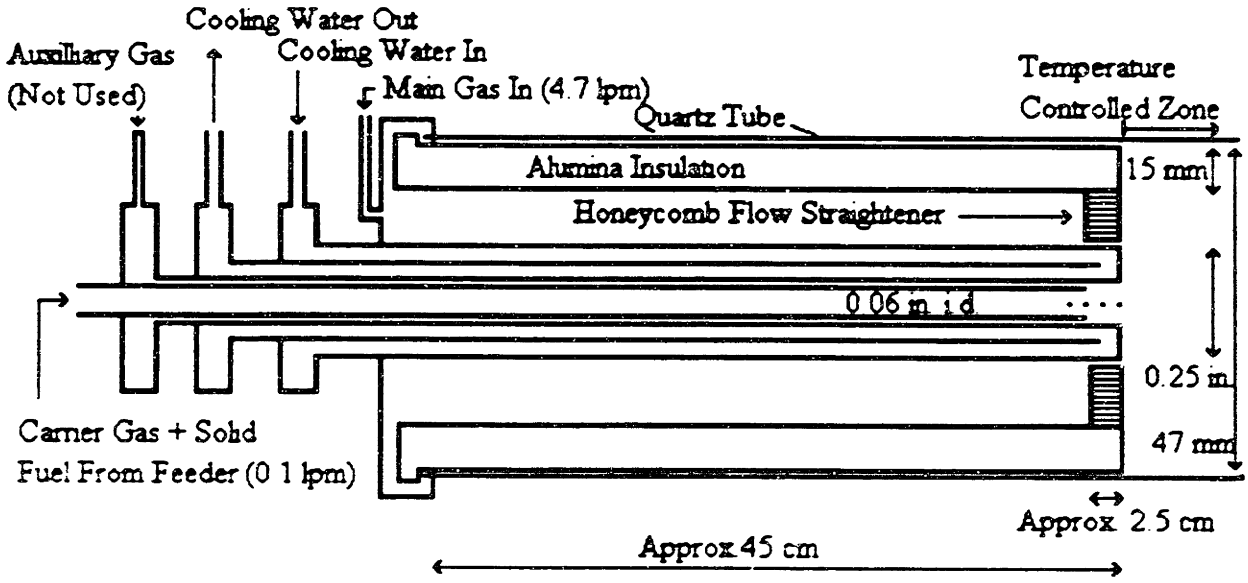

Fig.3.1.4 Schematic of Feeder Probe

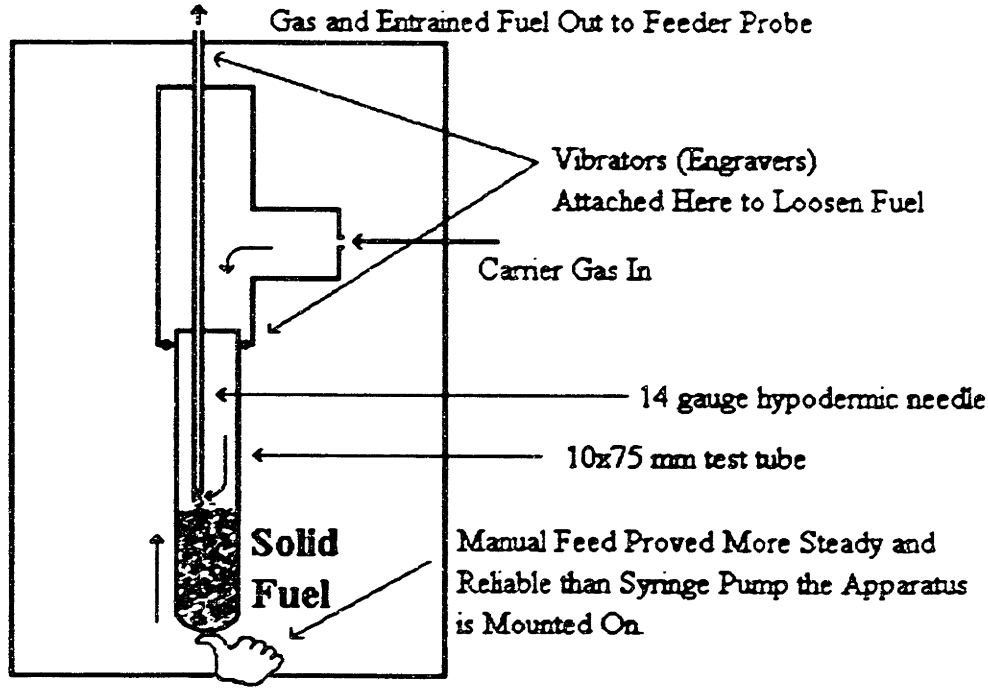

Fig. 3.1.5 Schematic of Entrained Flow Solids Feeder

requirements. The dilution gas flows through the outer cylinder, and the carrier gas flows through the inner. The other end of the inner tube was used to entrain particles in the fluidized bed feeder (Fig. 3.1.5). Trial and error produced the conclusion that the optimum fuel particle size to facilitate entrainment was found to be 150-200 μm, a compromise between static cling and weight. The corresponding i.d. of the hypodermic required is 0.06 inches (14 gage). Use of this size tubing, however, eliminates the possibility, and fortunately the need, for a dilution gas, so that feature of the probe is not utilized in these experiments. The feeder probe's tip, though small (0.1 inches) let in enough heat to melt the solid particles while they were still inside the tube, causing a tendency for them to stick to the walls of the narrow hypodermic tubing. By pulling the hypodermic tubing back approx. 3 cm from the probe tip, such clogging was eliminated. The carrier gas flow rate used in all experiments in this study was 0.1 standard lpm.

To help maintain a constant temperature profile in the reaction zone and to protect the small feeder probe from excessive heat damage, an inert alumina tube is used for insulation in the upper portion of the furnace. A 2.5 cm long honeycomb with a hole drilled into it for the feeder probe is cemented into the alumina tube for use as both a flow straightener and as a guide for the feeder probe to prevent the sample from being introduced at a postion or direction different from the axial centerline. The main gas flow (nitrogen) comes through the honeycomb at a rate of 4.8 standard lpm.

The fuel is crushed with a mortar and pestle and sieved with standardized screens to obtain the specified range of particle sizes All particles that pass through the 212 μm sieve but are trapped by the 150 μm sieve are assumed to be in the desired size range. The

solid fuel is place into a test tube and weighed, and the test tube is placed onto the feeder. Before introducing any fuel into the system, the test tube is evacuated once and purged with nitrogen for 30 minutes to remove any excess oxygen that may be in the sample. The gas lines are plumbed to minimize the amount of particles that are blown into the hypodermic tube accidently by this process. Weighings were performed directly after this procedure on some test samples to verify that loss was less than 2% of the total sample used in the experiment. Just before the sample is ready for injection into the furnace, a clean filter is placed in the sample collection device. Sampling takes place for 2 minutes at a steady feed rate that is controlled by pushing the test tube manually towards the hypodermic tube. After the sample is fed, the product stream continues to be pulled through the filter for another 10-15 seconds, at least triple the approximate residence time for the entire furnace, to insure collection of the entire sample. After changing the filter, the sampling sequence is repeated. The test tube is removed to be weighed and a clean test tube is put on while purging the furnace and sample lines for 30 minutes before the next experiment.

3.2 - Computer Modeling

Three main computer programs were employed in this research. The first, used to estimate molecular conformation and heats of formation of various biaryls and their condensation products, is the program MOPAC 6.0 (Coolidge and Stewart, 1990). The second is the set of programs supported by CHEMKIN (Kee et al., 1989), a program for analyzing kinetically controlled chemical pathways. The third is THERM (Ritter and

Bozelli, 1991), a program for calculating thermodynamic properties of molecules at a variety of temperatures based on Benson's group additivity approach. This section serves only to explain some of the logistics involved in operating these programs, and a more detailed treatment of the theoretical considerations involved with CHEMKIN and THERM can be found in Chapter 8.

The semi-empirical molecular orbital model used within the program MOPAC 6.0 is Austin Model 1 (Stewart, 1990). The model was chosen for its reliability in predicting realistic angles between the two arene planes in a biaryl molecule (Mulholland, 1992b). As very similar calculations were performed in the paper by Mulholland et al. (1993b), only the differences in technique are reported here. The standard heats of formation of the relevant biaryls, along with information on the angle associated with the internal rotors, are calulated with a slightly higher precision and efficiency (as allowed by the eigenvector following routine) using the same semiempirical model. Entropy differences due to internal rotation around the hindered internal rotor, as calculated by Mulholland, are confirmed, and the additional rigid body rotational entropy consideration of the entire molecule is included. The most stable molecular configuration is used for this calculation, and the cube of the reduced moment of inertia is taken as the determinant of the moment of inertia tensor, equivalent to the definition given by Benson (1976) and others. Most of the molecular simulations performed used less than 5 minutes of CPU time on the MIT Cray X-MP. A sample input, including the keywords used, and an abridged output are shown in Appendix A.

The chemical kinetics subroutine package CHEMKIN was used to examine the validity of the proposed mechanism to high molecular weight growth via polymerization

and condensation, and the plug-flow simulator SENKIN (Lutz et al., 1988) was used to approximate the conditions in the reaction zone of the furnace. Simulation of the reaction set required approximately 50 minutes of CPU time on a DEC 3000 model 300 computer.

The thermodynamic data required to perform the kinetic mechanism simulations were obtained using the program THERM on a desktop PC. Output from this program could be used directly as input for the CHEMKIN/SENKIN package.

Several other simple utility programs were written for translating one program's results to the input of another and for ease in data interpretation. All were written in qbasic (available in MSDOS 5.1 for IBM computers). These programs include: 1) a 3 dimensional display that takes the cartesian coordinate output from MOPAC and converts it into a rotatable picture for simple viewing, 2) a program that converts text output from lotus of the kinetic mechanism to the format required for SENKIN, 3) a program for converting SENKIN output into a graphical form interpretable as a mass spectrum, and 4) a program for extracting sensitivity analysis information from CHEMKIN results. The code for these programs can be found in Appendix B. Similar programs for related conversions and displays were also created, but their inclusion would be rather redundant.

3.3 - Analytical Chemistry Procedures

Dichloromethane (DCM) is used to extract PAH from the sample filters, the functional definition for soot being that material in flame/pyrolysis samples that does not dissolve in DCM. The filters are immersed in DCM and sonicated for 10 minutes while still in their jars. All glassware used in this process is rinsed three times each in water,

followed by methanol, followed by DCM, and teflon lids are used on all glassware from this point on to prevent dissolution and subsequent incorporation of lid material into the samples by DCM. The resulting DCM solution is placed into a syringe and filtered through a 0.2μm teflon filter into a graduated centrifuge cylinder. This process is repeated with fresh DCM until the solution being taken from the sample filter runs clear (twice more). The extracted solution is then concentrated by evaporation under a flow of nitrogen (typically to 20 ml from 50 ml), and 3 aliquots (100 μl each) are removed from each sample for weighing to ascertain the mass of the dissolved PAH.

A portion of each sample dissolved in DCM is concentrated almost to dryness for analysis on the GCMS system, which consists of a Hewlett-Packard Model 5890/II Gas Chromatograph with a DB-5 fused silica capillary column of length 30 m, film thickness 0.1 μm, and a diameter of 0.25 mm, and a Model 5971 Mass Selective Detector operating in electron-impact mode at an ionizing energy of 70 eV. The injector and detector were maintained at 320 C. The column temperature was ramped linearly from 100 to 320 C and 10 C/min., and then held at 320 C for 10 minutes.

Another portion of selected samples dissolved in DCM is concentrated and analyzed on the mass spectrometer portion of the LCMS system, which consists of a PE SCIEX API *I* mass spectrometer utilizing a single quadropole and atmospheric pressure chemical ion exchange which results in the transfer of a proton from the solvent in charging molecules for subsequent detection. This results in M/z ratios that are one unit higher than that of the neutral molecule, and this artifact should be kept in mind as the relevant spectra are interpreted. Discharge Needle Current is 3 μA, and the range of M/z

ratios that are programmed for detection is typically 200 to 900 amu, unless indicated otherwise. Approximately 20 μl of concentrated sample are injected into the sample loop of a Beckman System Gold programmable solvent module, and carried by a flow of 100% DCM through only a pre-filter into the mass spectrometer chamber, bypassing the available liquid chromatograph section of the apparatus. As minimal separation of compounds is achieved, the mass spectra of the integrated sample peak is taken as representative of the total of mass ions present in the entire sample.

A third portion of each sample is transferred into dimethyl-sulfoxide (DMSO) by transferring the desired amount of sample dissolved in DCM into a small vial, concentrating under a flow of nitrogen to 0.5 ml, adding 1.00 ml DMSO, and concentrating the resulting solution down to 1.0 ml (until only DMSO remains). The DMSO solution is then used for analysis by reverse phase HPLC, conducted on a Hewlett-Packard Model 1040 liquid chromatograph equipped with a model 1050 UV-Vis (190-600 nm) diode array detector. The column used is a Vydac model 201TP octadecylsilica column with a particle size 5 μm, i.d. 4.6 mm, and length 250mm. The mobile phase is initially 60% water and 40% acetonitrile. The mobile phase composition is ramped linearly to 100% acetonitrile in 40 min., followed by another 40 min. ramp to 100% DCM. Absorption spectra are taken every 640 ms with a resolution of 4 nm.

Dilution factors for the HPLC analysis are calculated for each sample based on the amount of fuel used in the experiment, the amount of sample collected, the dilution volumes of the resulting DCM solutions before weighing and before analyzing, and the HPLC area count of the peak representing DMSO. Application of only dilution factors

and molecular weights in obtaining relative molar abundances of compounds is assumed sufficient since the only comparisons in abundances that are being made in this thesis are for compounds that contain more than about 20 carbons, the approximate saturation cutoff in the calibration curves beyond which all PAH are known to have approximately the same response factor by mass for integrated total-spectrum UV-Vis absorbance. A linear calibration scale for area counts is also assumed since, for all compounds for which quantitative comparisons are made, area counts are below the value (2000) at which saturation of the detector sets in.

Chapter Four - Naphthalene/Anthracene Pyrolysis

4.1 - Introduction

Biaryl formation provides a pathway for molecular weight growth that is parallel to the addition of acetylene and its derivatives. The debate over which mechanism might dominate in various environments has been investigated by several researchers in both pyrolysis systems and a microreactor operated fuel rich (See Refs. in Chapter 2.1). These previous studies have shown the types of compounds that can be produced by aryl-aryl reactions. In addition, some of the studies on single aromatic compounds have quantified the biaryl isomers, and their subsequent cyclodehydrogenation, isomerization, and decomposition products. Simple rules were proposed for calculating the relative abundance of the biaryl isomers formed from single compounds from their thermodynamic properties (Mulholland et al., 1993). However, the rules for calculating the relative abundance of the biaryls in more complex mixtures have not been established, and this is a significant motivation for this experiment.

In addition to examining the factors that govern biaryl formation in mixtures, this experiment was designed to give some insight into the mechanism by which toxic byproducts of pyrolysis such as dibenzopyrenes can form. Some of the most toxic PAH known (via mouse and human skin studies) (Cavalieri et al., 1991, Ralston et al., 1994, Higginbotham et al., 1993) are the six ring dibenzopyrenes, especially dibenzo(a,l)pyrene. If such compounds are formed through the condensation of polyaryl species, one must start with either 1) a 2-ring and a 3-ring aromatic fuel, 2) a 1-ring and a 4-ring aromatic fuel, or 3) a 1-ring fuel (combining 3 times), as evidenced by graph theory laws governing the conservation of rings for such small aromatic

structures. Only the third pathway can be accomplished with a single starting fuel - the other two require an arene mixture for a fuel. Furthermore, if one wants to study only first generation products of pyrolysis in the interest of keeping complexity of the mechanism to a minimum, a fuel mixture must be employed. A fuel mixture of the first type using naphthalene and anthracene was chosen as the best candidate for the simplest product spectrum with components that possess properties that are as similar as possible.

Other critical tests of old questions become possible with the present mixed fuel experiment. Radicals are postulated to be key intermediates in the aryl-aryl reactions (Badger, 1964). Howard (1990) has shown that the number of radical sites on a PAH depends on the size of the PAH. In the case of sigma radicals, this is primarily a result of larger PAH having a higher percentage of hydrogens that are easier to abstract by virtue of the fact that they are bonded to carbons that are adjacent to fused ring carbons. As a natural consequence of the present study, it is possible to further justify, with indirect experimental evidence, the concept of larger PAH being able to support more radicals and doing so at lower temperatures than smaller PAH. The experiment outlined here allows examination of this effect by observing the relative abundances and temperature profiles of products resulting from the collisions of anthracene radical species and naphthalene radical species (two PAHs that differ slightly in their size, molecular topology and thus radical populations).

4.2 - Specific Experimental Methods

For the present experiment, solid anthracene (Aldrich 14,106-2, 99% pure) and solid naphthalene (Aldrich 18,450-0, 99+% pure) are each individually crushed and sieved to 150-

200 micron particle size. Three sets of experiments are performed - one using pure naphthalene, one using pure anthracene and one using a 1:1 mole ratio mixture of the solid particles. The first two experiments are performed merely as baseline studies for comparison against known literature results in the interest of eliminating the possibility of certain systemic sampling artifacts. The solids are fed into the drop-tube furnace and pyrolyzed in a flow of nitrogen for a residence time of approximately 2 seconds at 5 different temperatures: 1180, 1277, 1348, 1416, 1496 K.. All of the primary biaryl products have been identified on the basis of comparison with published trends in UV spectra for such compounds (see Chapter 6). Concentrations are calculated based on the integrated UV-Vis spectra of the compounds, and signals calculated from GCMS spectra, arising from an entirely different physical process, is used for corroboration. This is done to avoid the possibility of introducing an artifact into the calculations that is the result of an unquantified effect of heterogeneous biaryl coupling on the UV signal.

Three of the bianthracene peaks are obscured by other larger peaks on the LC spectra. These are the 9,9', 1,1' and 2,9' bianthracenes. The first has been observed in the present and previous studies of pure anthracene pyrolysis to be on the order of 5-10% of the largest bianthracene peaks. The second and third have also been shown in pure anthracene pyrolysis to be approximately 10% larger, on average, than the 1,9' bianthracene in magnitude, and this is shown to be approximately true here in at least the lowest temperature run, where the peaks separated enough to be quantifiable. These approximations contribute very little to the error in the total area counts, given that most of the calculated area (>80%) comes from directly observed peaks and the remaining 20% has an assumed expected error associated with it of less

than 30%. The overall error associated with the area counts is thus around 5%, which is within the experimental error typical of HPLC analysis. In a similar approximation, the benz(a)anthracene contribution to the 9-(2'-naphthyl)anthracene peak is assumed to be negligible.

For purposes of explaining the relative abundances of the different biaryl isomers, thermodynamic modeling follows the method used by Mulholland et al. (1993) using statistical mechanics considerations outlined by Benson (1976), with several modifications to improve the accuracy and efficiency of the calculations (see Chapter 8).

4.3 - Results and Discussion

The relative mole fractions of the i,j'-binaphthalenes, i-(j'-naphthyl)anthracenes and i,j'-bianthracenes resulting from the pyrolysis of a 1:1 mole ratio mixture of solid anthracene and naphthalene are reported vs. temperature in Fig.4.3.1, Fig.4.3.2 and Fig 4.3.3, respectively. A plot of bianthracenes resulting from the pyrolysis of pure anthracene under the same conditions is shown for comparison in Fig.4.3.4. Relative mole fractions on these graphs can be directly compared with one another.

Of immediate interest is an explanation of the relative abundances of each of the biaryls within its group of isomers. Following the suggestion of Mulholland et al. (1993) that biaryl isomer series might be governed by thermodynamic equilibrium, a simple thermodynamic model is pursued, and it appears to predict somewhat accurately the relative concentrations of all biaryl isomers within their respective groups. A summary of the results of the

Fig. 4.3.1

BINAPHTHALENES

ANTHRACENE/NAPHTHALENE PYROLYSIS

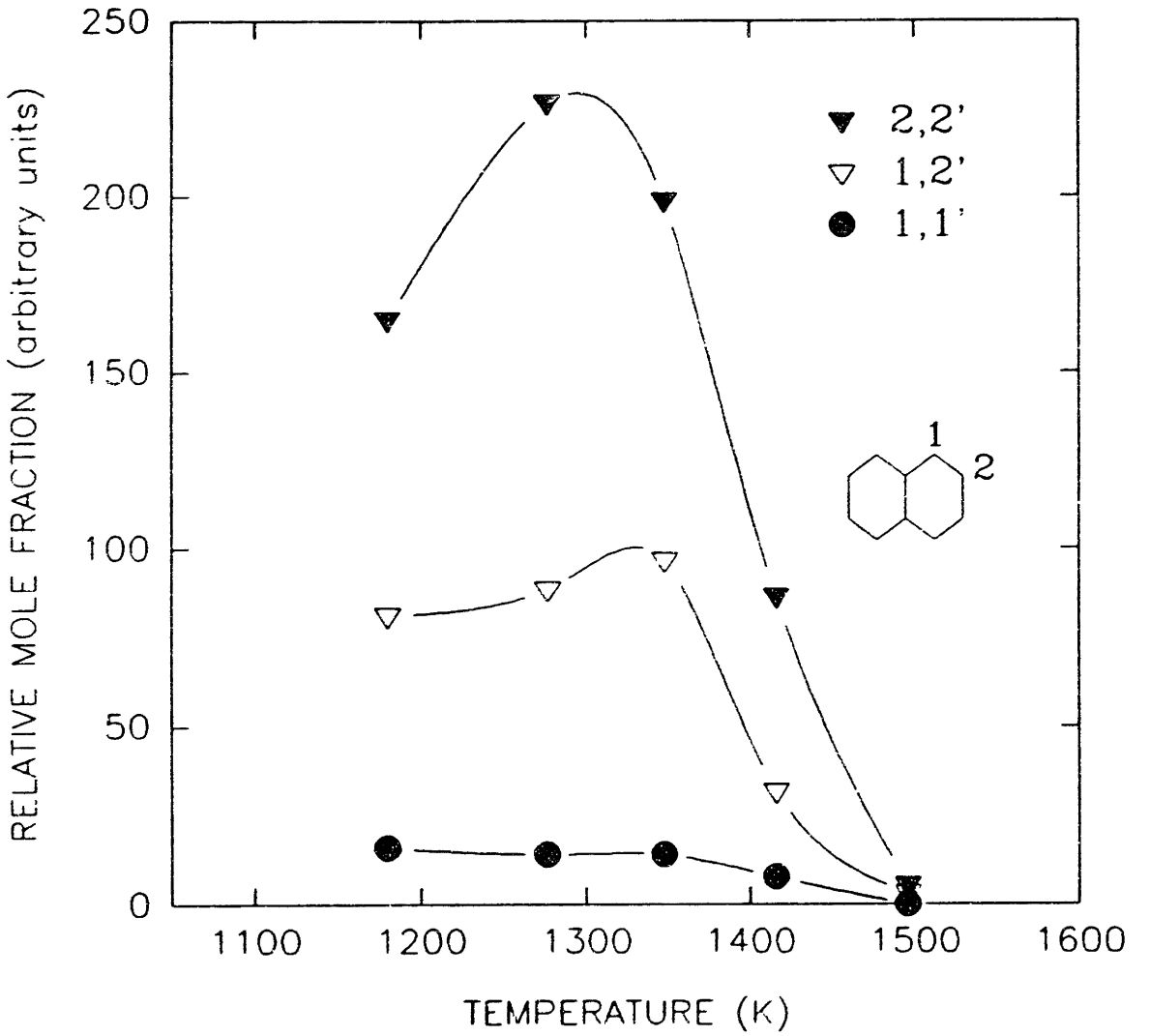

Fig. 4.3.2

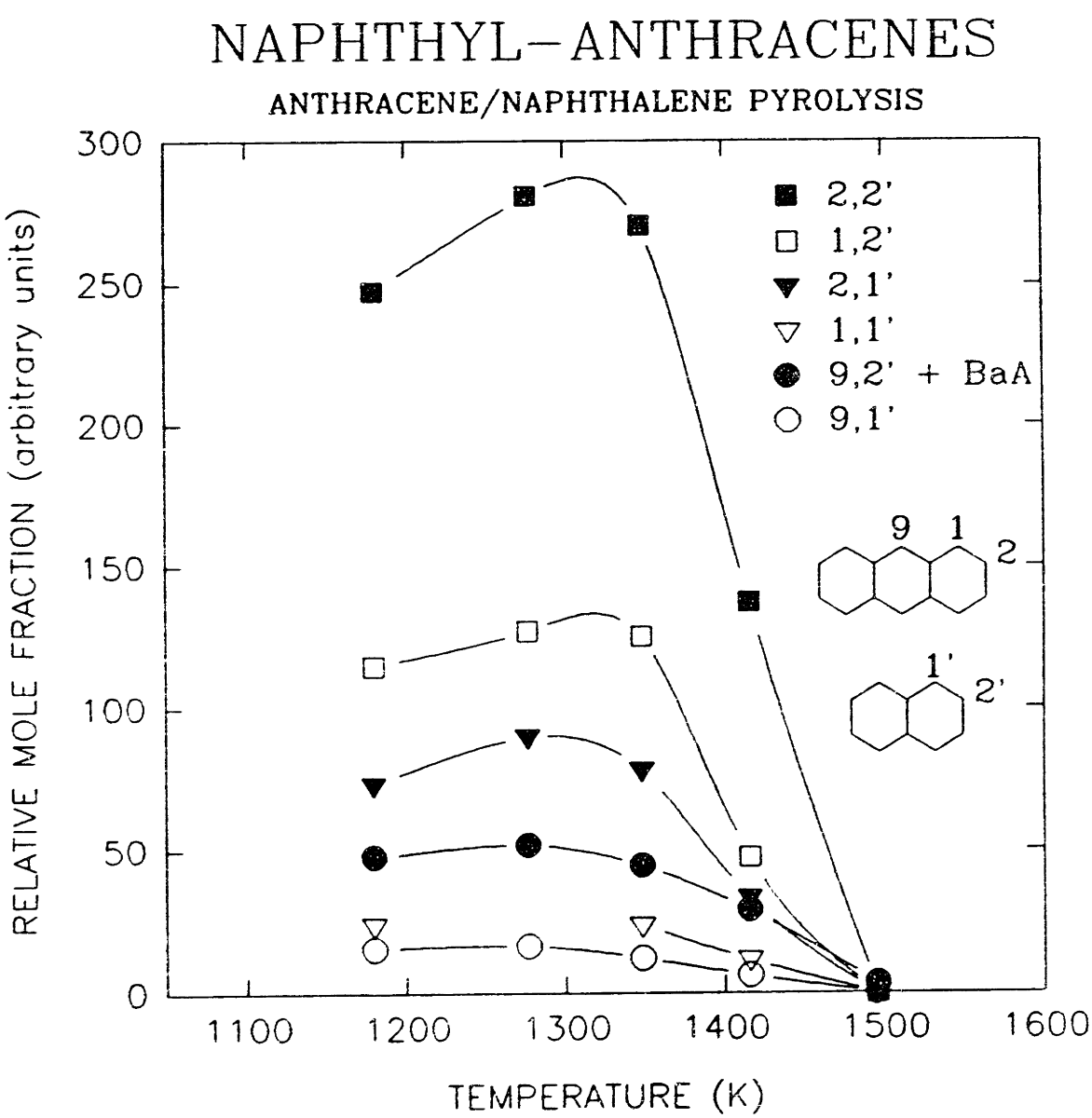
NAPHTHYL–ANTHRACENES
ANTHRACENE/NAPHTHALENE PYROLYSIS
RELATIVE MOLE FRACTION (arbitrary units)
300
250
200
150
100
50
0
1100
1200
1300
1400
1500
1600
TEMPERATURE (K)
2,2'
1,2'
2,1'
1,1'
9,2' + BaA
9,1'
9
1
2
1'
2'

Fig. 4.3.3

BIANTHRACENES

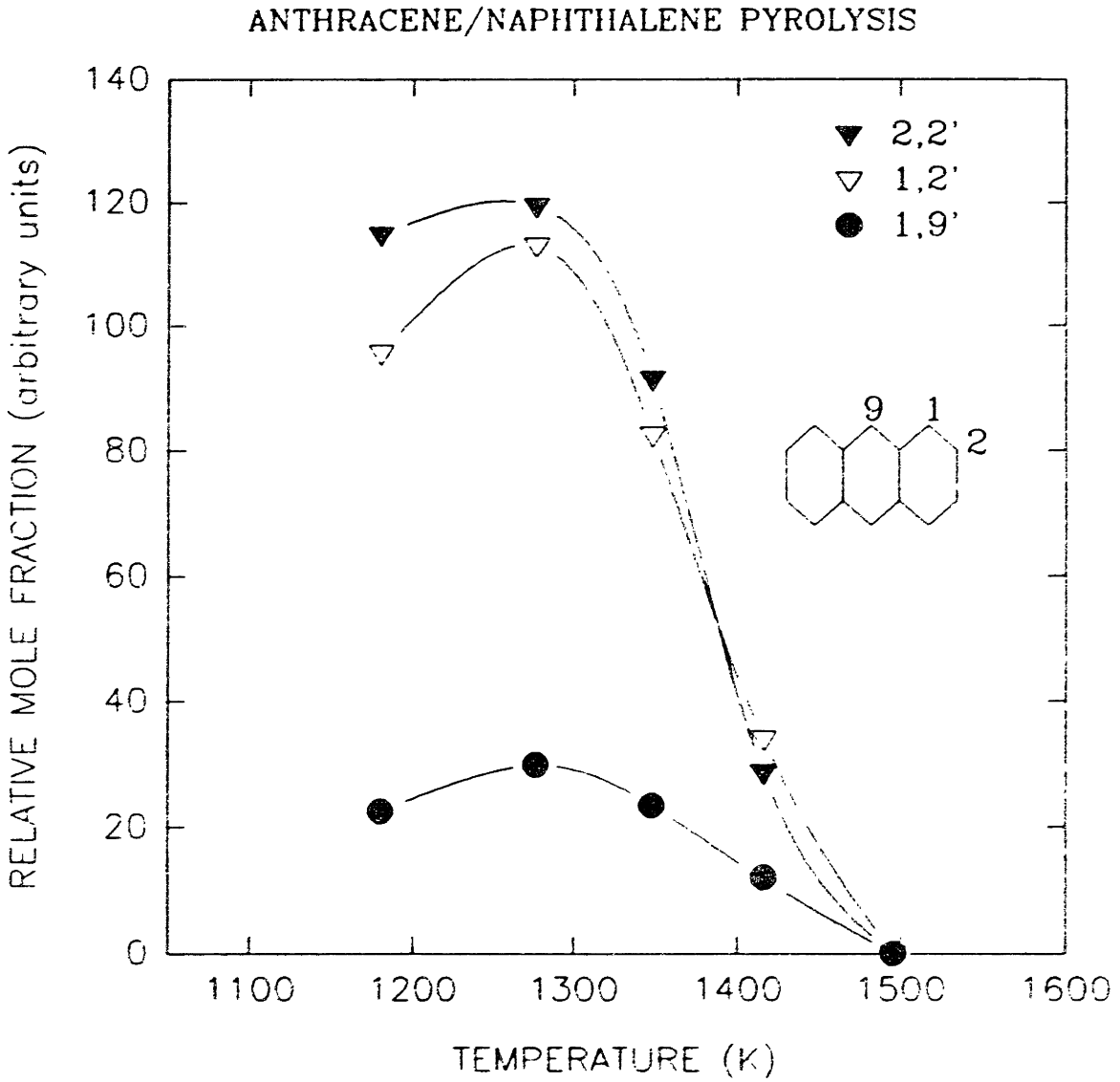

Fig. 4.3.4

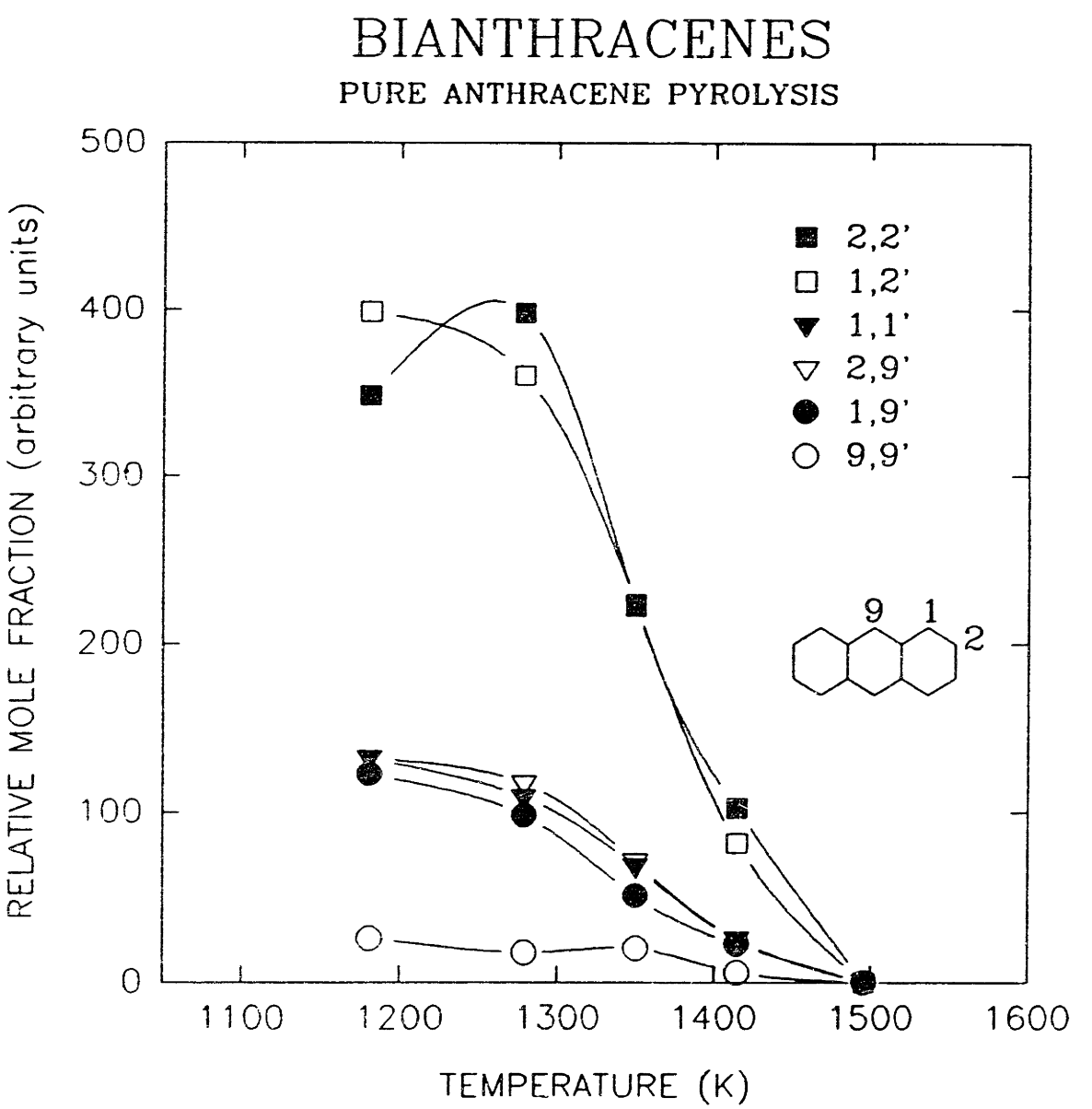
BIANTHRACENES
PURE ANTHRACENE PYROLYSIS
RELATIVE MOLE FRACTION (arbitrary units)
500
400
300
200
100
0
1100
1200
1300
1400
1500
1600
TEMPERATURE (K)
2,2'
1,2'
1,1'
2,9'
1,9'
9,9'
9
1
2

Table 4.3.1 Calculated vs. Observed Biaryl Abundances at 1280 and 1350K (naphthalene/anthracene pyrolysis)

	1280 K		1350 K		
BIARYL	Theoretical	Observed	Theoretical	Observed	Angle of Rotor
2,2' A-A	1	1	1	1	41.6
1,2' A-A	0.955	0.946	0.995	0.903	60.0
2,9' A-A	0.187	-	0.202	-	71.5
1,1' A-A	0.227	-	0.245	-	71.0
1,9' A-A	0.080	0.250	0.090	0.256	89.6
9,9' A-A	0.008	-	0.009	-	90.0
2,2' N-A	1	1	1	1	41.6
1,2' N-A	0.439	0.453	0.457	0.463	59.6
2,1' N-A	0.441	0.320	0.459	0.289	60.4
1,1' N-A	0.204	0.090	0.219	0.087	69.8
9,2' N-A	0.084	0.185	0.090	0.165	70.8
9,1' N-A	0.040	0.059	0.044	0.045	89.2
2,2' N-N	1	1	1	1	41.5
1,2' N-N	0.821	0.390	0.855	0.487	59.7
1,1' N-N	0.184	0.062	0.199	0.071	69.0
Bianthracenes from pure anthracene pyrolysis for comparison					
2,2' A-A	1	1	1	1	41.6
1,2' A-A	0.955	0.905	0.995	1.004	60.0
2,9' A-A	0.187	0.295	0.202	0.240	71.5
1,1' A-A	0.227	0.274	0.245	0.290	71.0
1,9' A-A	0.080	0.247	0.090	0.248	89.6
9,9' A-A	0.008	0.044	0.009	0.066	90.0

thermodynamic modeling and its predictions for the biaryl ratios at equilibrium and the experimental results at 1280 and 1350K is shown in Table 4.3.1. Included is the angle between the planes of the two aryl components in each case, as measured from the most stable planar configuration; this provides a measure of the steric hindrance (and indirectly, the relative heats of formation) relevant to that product's formation. The correct ordering of isomer concentrations is roughly achieved, and the predicted magnitudes of the ratios in concentrations are approximately correct. A few exceptions must be noted, however. The

1,2'-binaphthalene, 1,1'-binaphthalene, 2-(1'-naphthyl)anthracene and 1-(1'-naphthyl)anthracenes concentrations are significantly depleted from the expected values based on thermodynamic considerations. Likewise, the 9-(2'-naphthyl)anthracene, 1,9'-bianthracene and 9,9'-bianthracene concentrations appear enhanced.

Before placing weight on these discrepancies, the validity of the thermodynamic model should be assessed. The correct ranking provided by the thermodynamic model is likely due to the dominant change in enthalpy of formation term in the free energy calculation. This term is most influenced by steric factors, which would also be a major consideration in a kinetic model, where they would influence the enthalpy change to the transition state. Consequently, enhancement of a probability of collision model with a measure of steric hindrance provides an equally credible prediction of the biaryl isomer ratios. The bianthracene isomers, for example, are hindered sterically in the following order (based on the angle of the internal rotor (Table 4.3.1) as calculated by the thermodynamic modeling): 9,9'>1,9'>2,9'=1,1'>1,2'>2,2'. This model would predict an enhancement of the 2,2' isomer relative to all others; a slight enhancement, over the factor of two already accounted for in the probability portion of the model, of the 1,2' isomer relative to the 1,9', 2,9', 1,1' cluster; a depression of the 1,9' isomer concentration relative to the same cluster; and a depression of the 9,9' concentration, from the factor of 4 already considered by the probability portion of the model, relative to the 1,9' concentration. The plots of the bianthracene isomers (Figs. 4.3.3 and 4.3.4) show all of these trends to some extent. In addition, the naphthyl-anthracenes and binaphthalenes conform to similar trends, within a factor of two, when taking into account their steric hindrances. For the i-(j'-naphthyl)anthracenes, the ordering for the hindrances is: 9,1'>9,2'=1,1'>1,2'=2,1'>2,2', with probability of collision factors of 1,2'=2,1'=1,1'=2,2'=1.0 and 9,1'=9,2'=0.5. For the

Fig. 4.3.5

TOTAL BIARYLS

(ANTHRACENE/NAPHTHALENE PYROLYSIS)

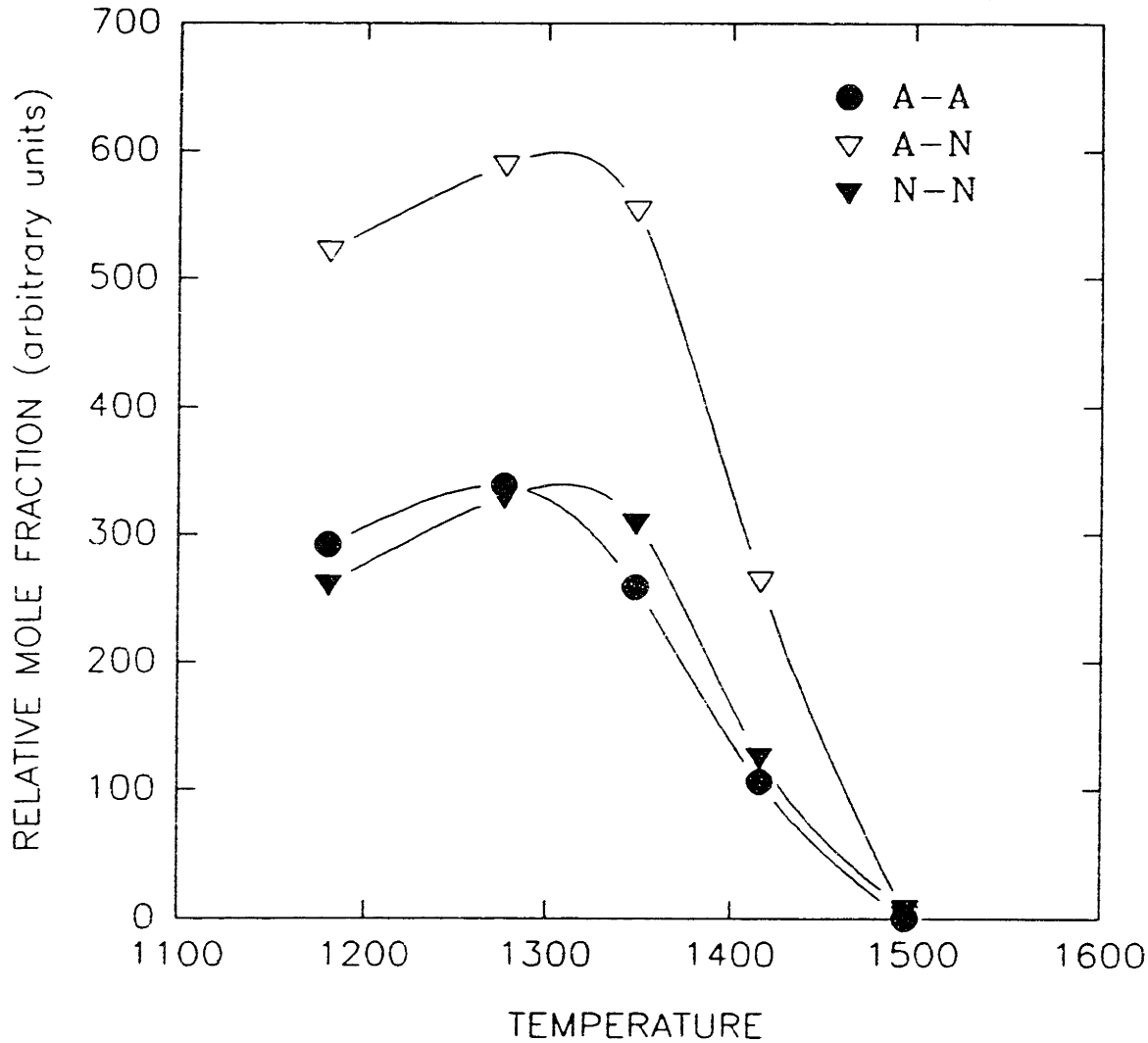

binapthalenes, the ordering is 1,1'>1,2'>2,2' with probability of collision factors of 1,2'=1.0 and 1,1'=2,2'=0.5. More quantitative attempts at explaining relative biaryl concentrations via a simplified kinetic model, using for example an Evans and Polanyi (1938) system of activation energies, did not fare any better. A lack of consideration of destruction routes to cyclodehydrogenation products is likely the cause of the discrepancy.

The above analysis does not show conclusively whether kinetics or thermodynamics controls biaryl formation. Up to now, both models have been adequately supported by the data available. However, consideration of the relative magnitude of the total bianthracenes, binaphthalenes and naphthyl-anthracenes (Fig.4.3.5) provides a more critical test of the kinetic vs. equilibrium models. According to the mechanism proposed by Badger (1964), biaryls form from the collision of an aryl radical and another aryl radical or its parent arene. Let x be the percentage of anthryl radicals among anthracenes, y be the percentage of naphthyl radicals among naphthalenes, and assume that aryl-aryl collisions are k times more reactive than an aryl-arene collision. It is easy to show that, in a kinetically controlled environment, considering only probablility of collisions and irreversible reactions, the ratios of bianthracenes to naphthyl-anthracenes to binaphthalenes resulting from the pyrolysis of a 1:1 mole-ratio mixture of anthracene and naphthalene should be $(x - x^2(1-k/2)) : (x + y - xy(1-k/2)) : (y - y^2(1-k/2))$. If x and y are similar, the ratios become close to 1:2:1. Thus, the relative concentration of total naphthyl-anthracene products should be twice that of both the bianthracene products and the binaphthalene products. This analysis assumes an equal abundance of naphthyl radicals and anthryl radicals relative to their respective parent arenes. If this assumption is violated by, for example, the anthryl radical being favored slightly relative to anthracene compared to the

naphthyl radical relative to naphthalene, the concentrations of the biaryls products will shift slightly to favor those compounds containing anthryl components. Furthermore, biaryls consisting of two anthryl halves will be favored relative to those containing only one anthryl component, which in turn will be favored relative to those containing no anthryl component.

The data from the 1:1 mole ratio pyrolysis experiments show exactly the above trends. Bianthracenes are favored at the lower temperatures relative to their predicted ratio, indicating an enhanced anthryl radical abundance. At all temperatures, the total naphthyl-anthracene concentrations are roughly double those of the binaphthalenes and the bianthracenes. That this factor is near 2.0 strongly supports the kinetic model for the formation of the biaryl concentrations.

By contrast, the equilibrium model cannot satisfactorily explain the results shown in Fig.4.3.5. The most likely equilibrium mechanism would be that of dissociation to parent aryls (all other mechanisms are considered too improbable, and none of the expected secondary evidence for them has been found). However, equilibration cannot occur by such a dissociation; if it does, one would expect the concentrations of all biaryl species to be at thermodynamic equilibrium with respect to each other. Exact calculations are unnecessary; as a group the naphthyl-anthracenes should be very close in free energy to the bianthracenes and the binaphthalenes, since enthalpy is the dominant term in most of the equilibrium reactions. At equilibrium, the total biaryl concentrations should be close to 1:1:1 if all compounds involved are asymmetric. If all of the bianthracenes and all of the binaphthalenes were symmetric, however, the ratio should be 1:2:1. Of course, neither extreme is the case; only about three quarters (by concentration) of the binaphthalenes, and half of the bianthracenes are symmetric.

Since concentrations of biaryl isomers are inversely proportional to their symmetry numbers at equilibrium, and their contribution to the total biaryl ratios must thus be discounted by that factor in determining consistency with the thermodynamic model, we find that symmetric isomers are only abundant enough to explain a ratio of approximately 3/4*1/2 + 1/4*1 : 1 : 0*1/4 + 1/2*1/2+1/2*1 = 1:1.6:1.17. It is unreasonable to assume the discrepancy between this equilibium based ratio and experiment is due to a systematic UV-spectrum response factor trend since such a trend could not simultaneously explain a raising of the response factor for the naphthyl-anthracenes and a lowering of the factor for the bianthracenes (both relative to the binaphthalenes), due to the unconjugated nature of the biaryl structure that results in distinct bands in the UV-Vis spectra that retain their respective arene's character (see Chapter 6). In other words, an enhancement of UV response in the naphthyl-anthracenes due to the anthracene component would require approximately double the enhancement to be observed in the bianthracenes, a trend that would make agreement with experiment even worse. The experimental results thus do not support the expected trend in free energies (except at the lowest temperature - an anomaly that is more reasonably explained by the kinetic model with enhanced anthracene radical formation, especially since the lowest temperature is the least likely place for equilibrium to be satisfied), and the concept of every biaryl being at equilibrium with respect to all others is therefore discounted. It is thus believed that kinetics, rather than equilibrium, determine the relative distribution of the biaryls.

Given that kinetics are probably controlling, the effect of radical populations on the product distribution will now be considered. At the lower temperatures, below 1280K, the bianthracenes are favored relative to the binaphthalenes. At the higher temperatures, above 1280K, the binaphthalenes are favored. This is consistent with what might be expected.

Fig. 4.3.6: Products of Pyrolysis of Naphthalene/ Anthracene Mixture at 1180K

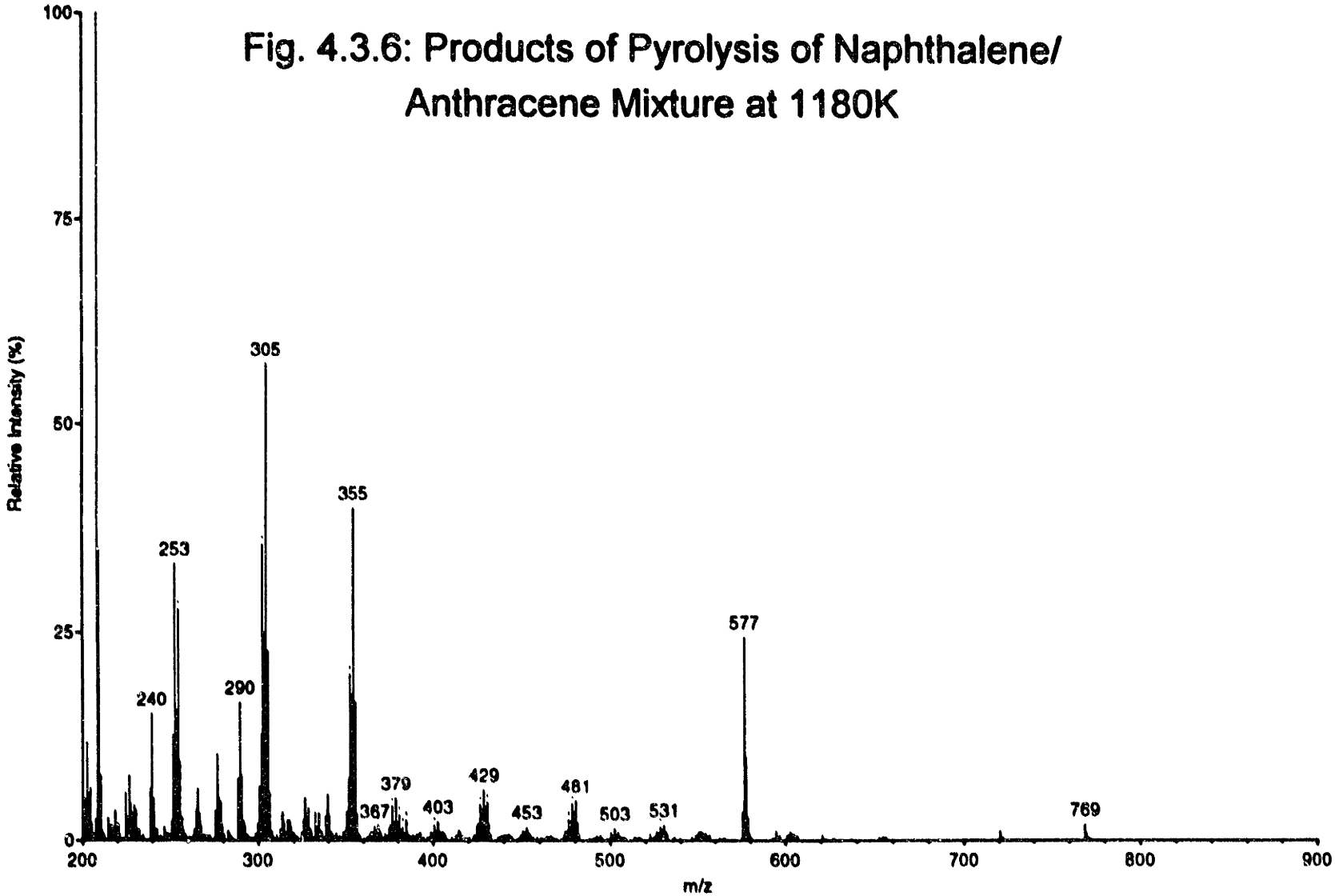

Total Ion Mass Spectra from LCMS

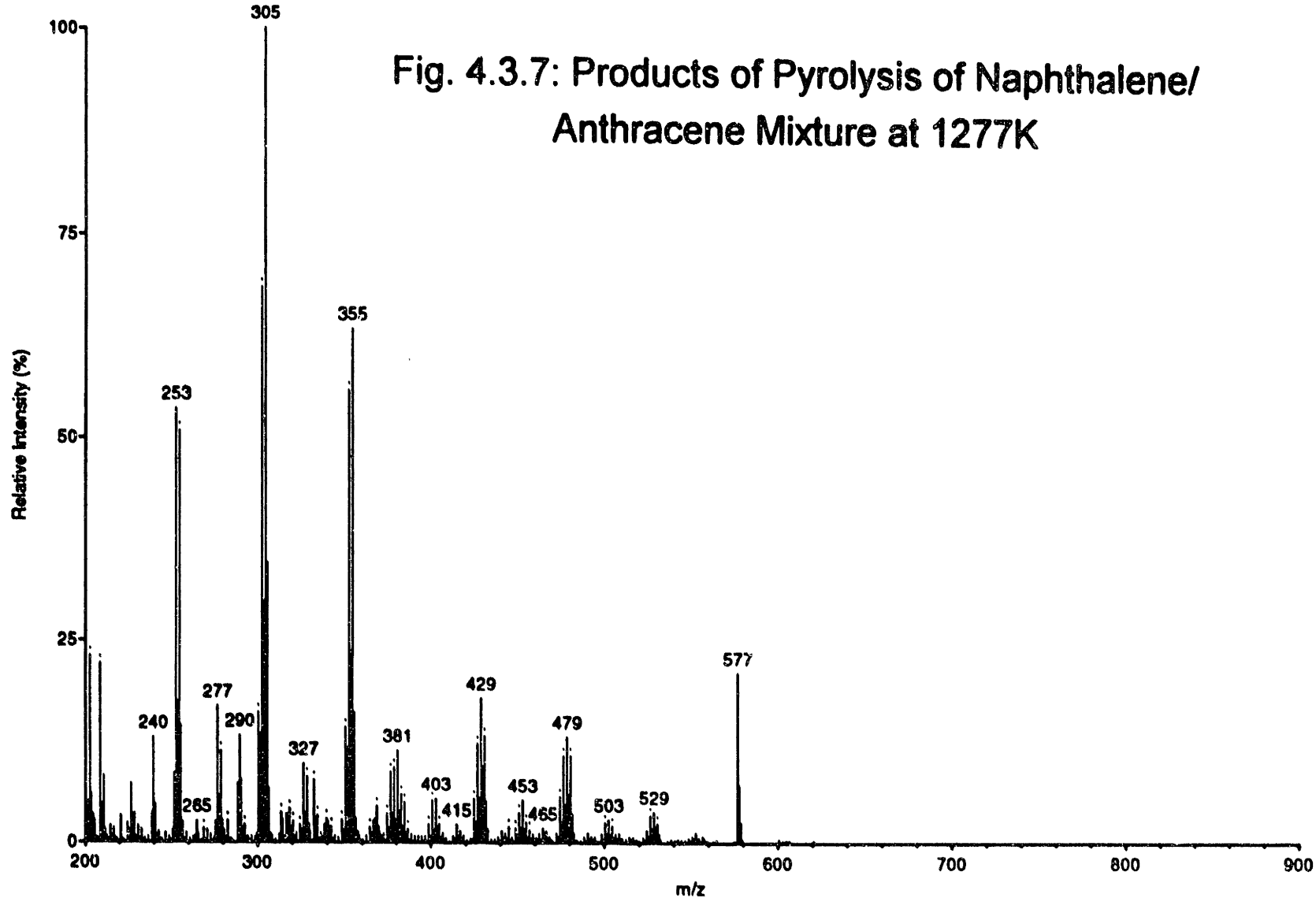

Fig. 4.3.7: Products of Pyrolysis of Naphthalene/ Anthracene Mixture at 1277K

Total Ion Mass Spectra from LCMS

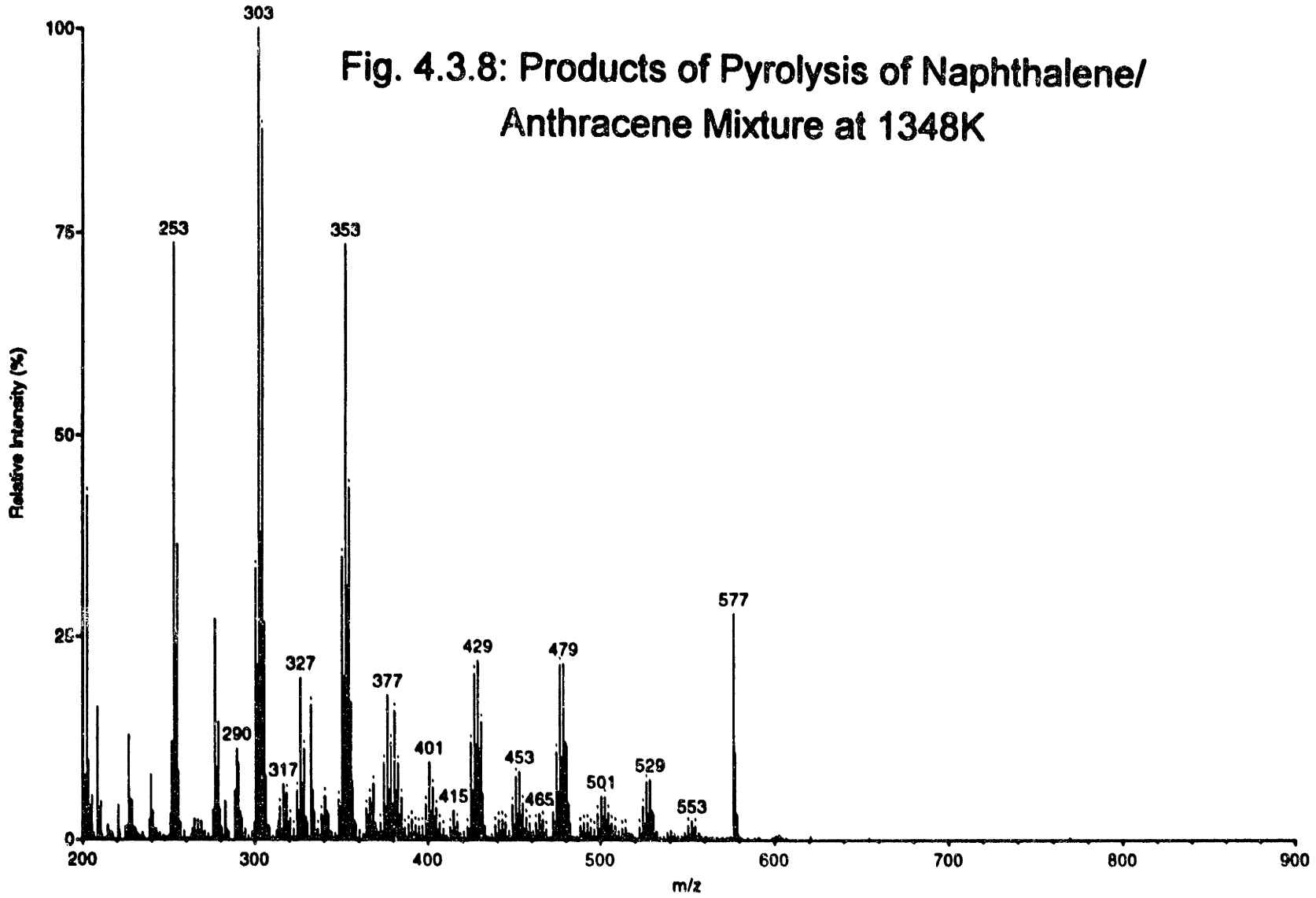

Fig. 4.3.8: Products of Pyrolysis of Naphthalene/ Anthracene Mixture at 1348K

Total Ion Mass Spectra from LCMS

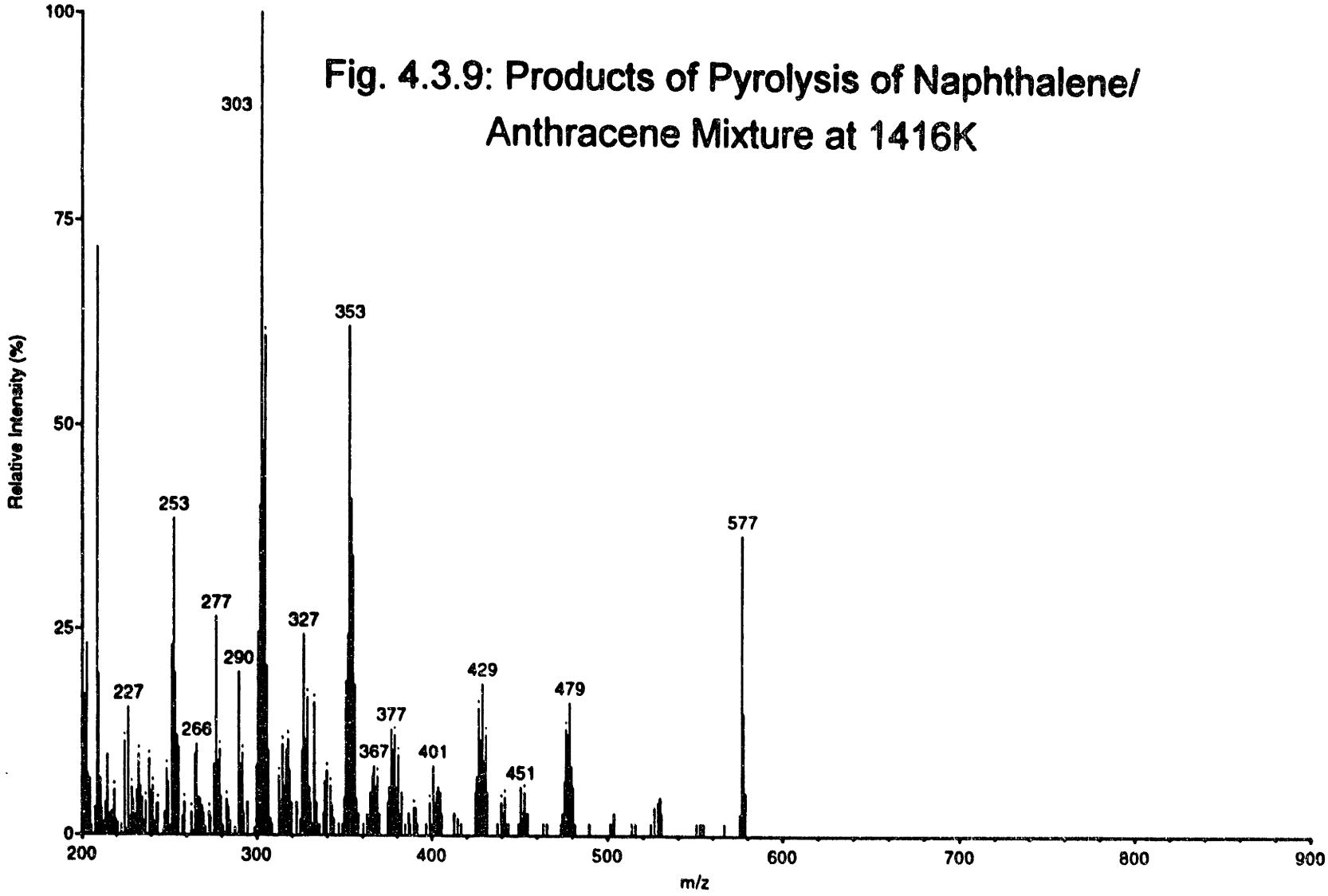

Fig. 4.3.9: Products of Pyrolysis of Naphthalene/ Anthracene Mixture at 1416K

Total Ion Mass Spectra from LCMS

Fig. 4.3.10: Products of Pyrolysis of Naphthalene/ Anthracene Mixture at 1496K

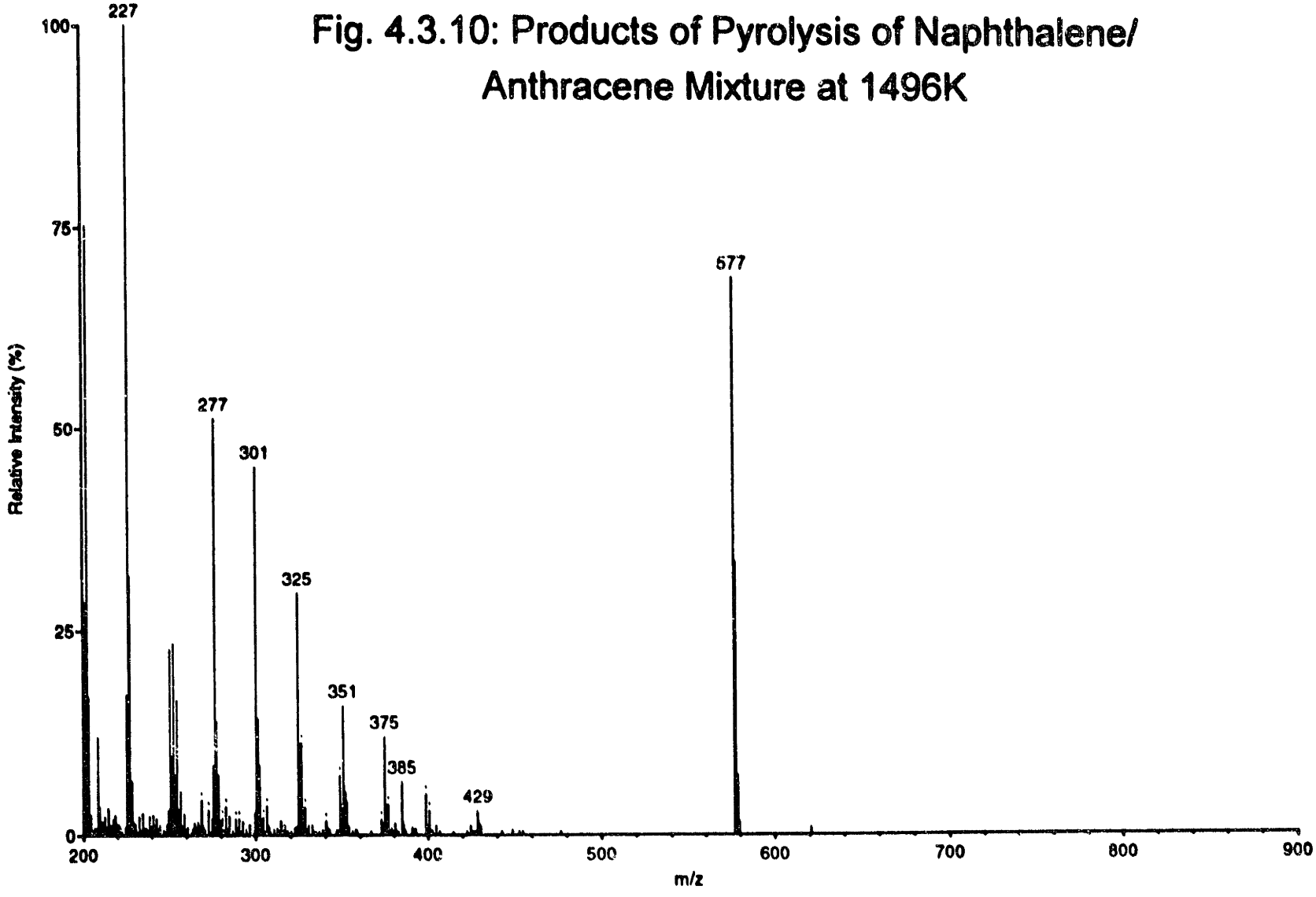

Total Ion Mass Spectra from LCMS

Anthracene, having a greater propensity for supporting sigma radicals by virtue of its more condensed nature (Howard, 1990), should form radicals more easily than does naphthalene, and will thus do so at lower temperatures. Products derived from the anthryl radical will thus exhibit a higher concentration relative to naphthyl products at the lower temperatures. At higher temperatures, however, the bianthracenes form quicker, as before, but they also are able to proceed to condensation products faster. Since the bianthracenes have had more time to overcome the delay for the onset of condensation, the condensation reactions will now have a larger relative influence on bianthracene concentrations than on the slower-forming binaphthalenes, which will still be more influenced by the biaryl formation reactions. The binaphthalenes will thus exhibit a higher concentration relative to the bianthracenes as the temperature increases. By similar reasoning, it is also possible to show that the naphthyl-anthracenes should peak in concentration at a temperature intermediate between those for the binaphthalenes and the bianthracenes. The data presented here show evidence of all of the trends mentioned in this paragraph (Fig.4.3.5), and therefore support a kinetic model for biaryl formation that is consistent with both the biaryl formation model of Badger and the concept that anthracene forms radicals more easily than does naphthalene.

Substantial evidence has been found for several varieties of polyaryls in all of these samples. In addition to the primary biaryl groups at molecular weight 254, 304 and 354, mass spectrometry shows strong evidence of the entire series of possible polyaryl structures up to at least molecular weight 750, after which the detection limit of the LCMS apparatus was reached (Figs.4.3.6-4.3.10). Corresponding late-eluting peaks on the HPLC also show evidence of numerous naphthyl and anthryl substituted compounds, as indicated by their UV spectra. In

the LCMS results, concentrations of the total polyaryls decrease by about a factor of 3-5 for each successive group in a series, and other comparable relative concentrations are consistent with an extension of the kinetic model described above. The mass spectra also show evidence of substantial condensation of these polymers, suggesting a possible pathway to the graphitic structural basis of some soots. This also suggests again that condensation may play a substantial role in contributing to biaryl product abundances, and no model, thermodynamic or kinetic, will be adequate at explaining them until condensation is taken fully into account.

4.4 - Conclusions

Interpretation of a number of trends involving the formation of biaryls in a pyrolysis environment suggest the following conclusions.

1. Biaryl concentration ratios appear to be governed by a kinetic model for the formation of these species, based on steric hindrance as well as probabilistic considerations that take into account the availability their aryl constituents and probabilities of collision.

2. The equilibrium model governing biaryl formation has been discounted on the basis of indications that the most likely mechanisms for the equilibration, most notably that of cleavage of the linking bond, are not significant participants in the reaction scheme. The cleavage mechanism has been eliminated based on the evidence that the naphthyl-anthracene concentrations are not close enough to being intermediate between those of the binaphthalenes and the bianthracenes, even when taking into account contributions from symmetric isomers.

3. The data support the concept of an anthracene radical that is easier to form than a naphthalene radical from their parent arenes, a result of anthracenes more condensed nature.

4. Support is found for the ability of naphthalene and anthracene to polymerize into polyaryl chains. Subsequent condensation of these species could result in the graphitic structural basis of soots.

Aside from the observed trends, pyrolysis of an arene mixture does not appear to significantly confound the kinetic modeling of such systems, and the results presented here could theoretically extend to many more complex mixtures.

Unfortunately, evidence for conclusions 1 and 2 above are more circumstantial than one would hope. A kinetic mechanism is the more favored conclusion, but doubts about artifacts and systematic trends in the analysis procedure remain. More experiments are needed to solidify the argument for kinetic control, and the results of the next chapter are capable of addressing some of these issues more effectively.

Chapter Five - Ortho-Terphenyl Pyrolysis

5.1 - Introduction

The naphthyl-anthracene pyrolysis experiments gave the first indications that molecular weight growth was possible, and furthermore, was kinetically controlled. The proof for kinetic control, however, is founded on evidence that is uncomfortably close to being circumstantial. Though the data still fit a simple kinetic model better than one based on thermodynamic equilibrium, the distinction is too small to make a decision one way or the other based on one set of experiments. In addition, the lack of ability to characterize many of the condensation products from the pyrolysis of a naphthalene/anthracene fuel mixture left open the question of whether toxic byproducts such as dibenzopyrenes could be produced in. Another experiment was thus devised to help answer some of the unresolved issues, and ortho-terphenyl (OTP) was chosen as the fuel to study for several reasons that are outlined in the following paragraphs.

Stein (1978) has suggested the use of a thermodynamic model to evaluate the relative importance of the polymerization pathway in the mechanism for molecular weight growth to soot. An important result of his work was the inferred existence of a critical barrier species in polymerization schemes that corresponds to the rate limiting step in the mechanism. Above a certain temperature, all polymerization/condensation pathways to molecular weight growth are limited by the formation of this critical compound. Though the analysis was from a thermodynamic viewpoint, Stein suggested that it may also have some relevance to kinetically controlled situations. At high temperatures, for example, the

diminished concentration of the critical species would tend to limit high molecular weight growth despite the thermodynamic stability of the larger compounds since the barrier to their formation has been raised. The bottleneck created by the critical species would also simultaneously result in the destruction of compounds that are smaller in molecular weight as a result of more time being available for ring rupture. Lower temperatures (suggested by Stein to be below about 1500K) present a different picture of molecular weight growth. The lack of a significant barrier via the thermodynamic route leads to substantial soot production, and more highly hydrogenated species become feasible intermediates in the reaction scheme. A closer inspection of the chemistry of large molecular weight compounds at these lower temperatures is of particular interest, since the previous studies on naphthalene and anthracene have already demonstrated the potential importance of polymerization as a growth pathway to high molecular weights at these temperatures, and many of the products of the relevant reaction pathways are known to be mutagenic.

Stein's work is further characterized by its calculations of thermodynamic properties for most of the important intermediates in the benzene polymerization pathway up to high molecular weight. Relative abundances of intermediates at equilibrium have thus already been calculated over a broad range of temperatures for a molecular weight growth pathway that is of interest to this thesis. OTP is an expected intermediate in the benzene polymerization pathway, and this is one of the reasons why it was chosen as the fuel to study. Stein also calculated that OTP was the critical species in the benzene polymerization scheme over a broad range of conditions. Starting with an abundance of

this compound should thus result in a very broad spectrum of observable large molecular weight products, as the barrier to their formation has been largely removed.

Several other reasons influenced the decision to used ortho-terphenyl as a starting fuel for a pyrolysis experiment. First, since benzene is the simplest arene, and it is relatively low in molecular weight, it will be possible to observe many generations in the polymerization scheme, and the product spectrum should have relatively few isomers to separate. Second, the benzene polymerization/condensation pathway is capable of directly forming total-resonant-sextet (TRS) compounds (Clar, 1964; Knop et al., 1987) - PAH consisting entirely of mutually exclusive six-membered rings (a formal definition is provided in the next section). This unusual p structure makes the TRS compounds very stable (indeed, evidence for them has been found in interstellar matter (Hendel et al., 1986)) relative to their same-molecular-weight counterparts (Clar, 1964), and inspection of their role in the product spectrum should provide important insights into the relevance of thermodynamic considerations in the prediction of polymerization products. Third, benzene polymerization/condensation is one of the few ways already mentioned in Chapter 4 of making the toxic dibenzopyrenes, and it is the only polymerization mechanism by which they can form directly without ring rearrangement, making the possibilty of observing such compounds much greater than in the previous naphthalene/anthracene study.

5.2 - Specific Experimental Methods

Solid ortho-terphenyl (Aldrich Cat. No. 84-15-1, 99% pure) is crushed and seived, fed into the furnace, and pyrolyzed in a flow of nitrogen for a residence time of approximately 2 seconds at 5 different temperatures: 1248, 1275, 1302, 1326 and 1352K, the temperature range at which a fundamental shift in product types is known to occur (Mukherjee, 1993). The filters containing the condensed phase products are then individually extracted with dichloromethane (DCM) and a portion of each is transferred into dimethylsulfoxide (DMSO) for analysis on the HPLC system. A portion of each sample that remains in DCM is analyzed on the LCMS system, and another portion of the highest and lowest temperature samples are used for analysis on the GCMS system.

An important feature of this study is the presence of TRS compounds, and a structural definition is needed. The most convenient strict definition is achieved using graph theory. To start, a molecular graph is constructed from the sigma-bond framework of a fully benzenoid PAH, where the hydrogens are ignored, the carbon atoms are represented by vertices on the graph, and the individual C-C sigma-bonds are represented by the edges of the graph. A ring is defined as any 6 vertices and 6 edges that completely define the boundaries of a face of this graph. If a subset of this graph (ie, using only existing edges and vertices) can be drawn that consists entirely of mutally exclusive rings while still spanning the entire vertex set (although not necessarily the edge set) of the graph, the PAH is said to be a total resonant sextet. A more intuitive definition is that of a fully-benzenoid PAH whose π resonance structure (represented by circles within hexagons) can be drawn properly and entirely with non-adjacent circles, with no need for

additional double bonds. A consequence of this definition is the requirement that a TRS compound must possess a multiple of 6 carbons, exactly the series that is obtained by polymerizing benzene.

5.3 - Results and Discussion

The total product mass spectra for the 5 temperatures in this study are shown in Figs. 5.3.1-5.3.5. Polymers (up to at least 9 phenyl units long) and their associated condensation products that are involved in the benzene polymerization pathway can be readily identified as the large clusters separated by roughly 76 in molecular weight. Several clear trends with temperature can be seen. Less condensed elements of the benzene polymerization pathway (primarily polyphenyls) dominate the product spectrum at the lower temperatures as predicted by Stein. Moderately condensed compounds become more prevalent in the intermediate temperatures and the shift continues on to favor the highly condensed TRS compounds as the temperature increases. Ring rupture that results in the creation of small aliphatic fragments is not in evidence at any of these temperatures, as indicated by the lack of acetylene-addition products. However, significant fragmentation of the fuel into its component phenyl groups is evidenced by the existence of clusters representing 4, 5, 7, and 8 membered polyphenyl chains and their condensation products. As in previous studies, dimer formation is in evidence as a dominant mechanism to molecular weight growth. This is most clearly indicated by the large magnitude of the hexa-phenyl component cluster (a direct dimerization product of ortho-terphenyl) relative to the surrounding clusters in the polymerization series. This is

Fig. 5.3.1:

Total Mass Spectra of Products from the Pyrolysis of *o*-terphenyl at 1248 K.

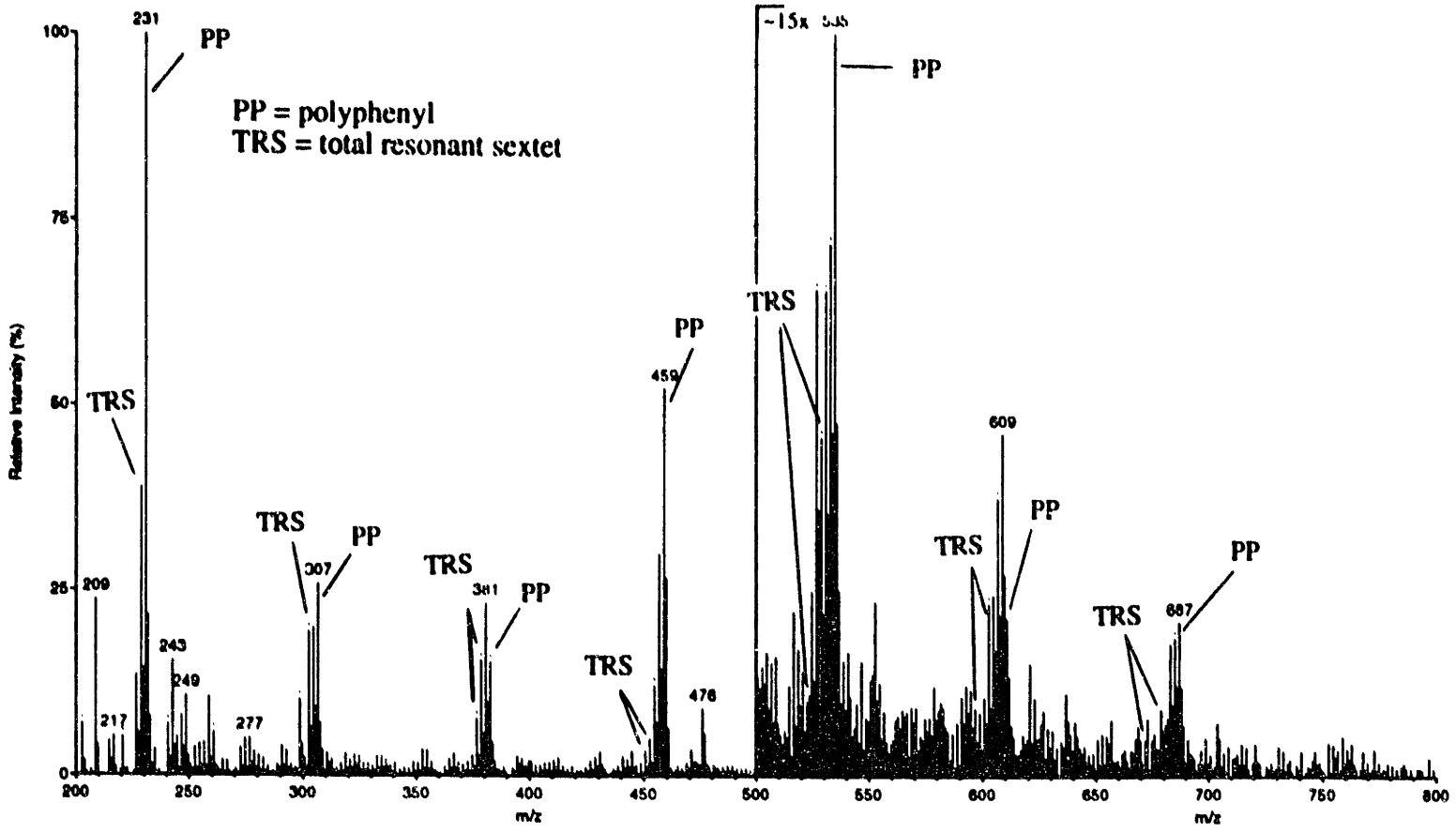

Fig. 5.3.2:

Total Mass Spectra of Products from the Pyrolysis of *o*-terphenyl at 1275 K.

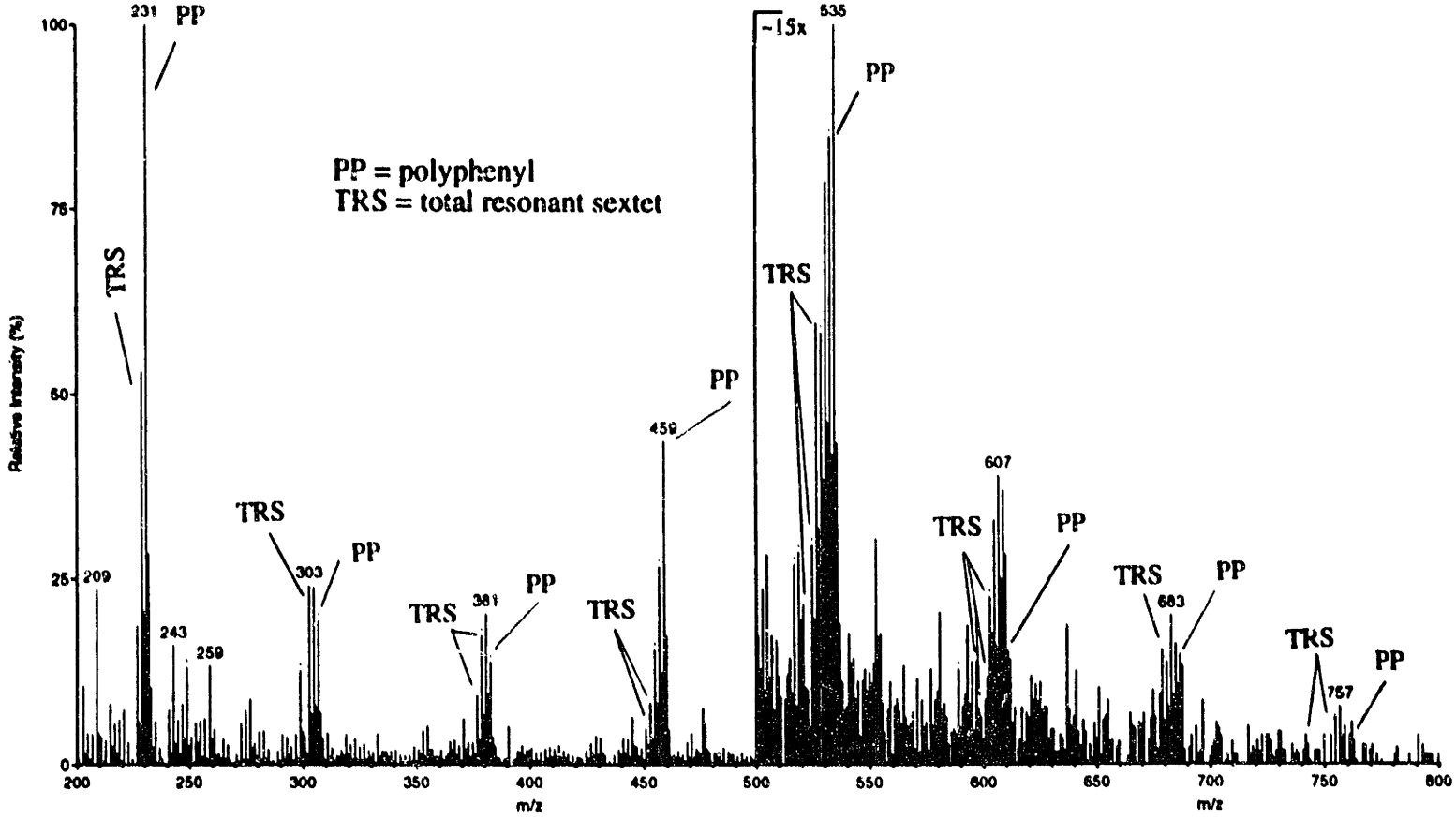

Fig. 5.3.3:

Total Mass Spectra of Products of the Pyrolysis of *o*-terphenyl at 1302 K.

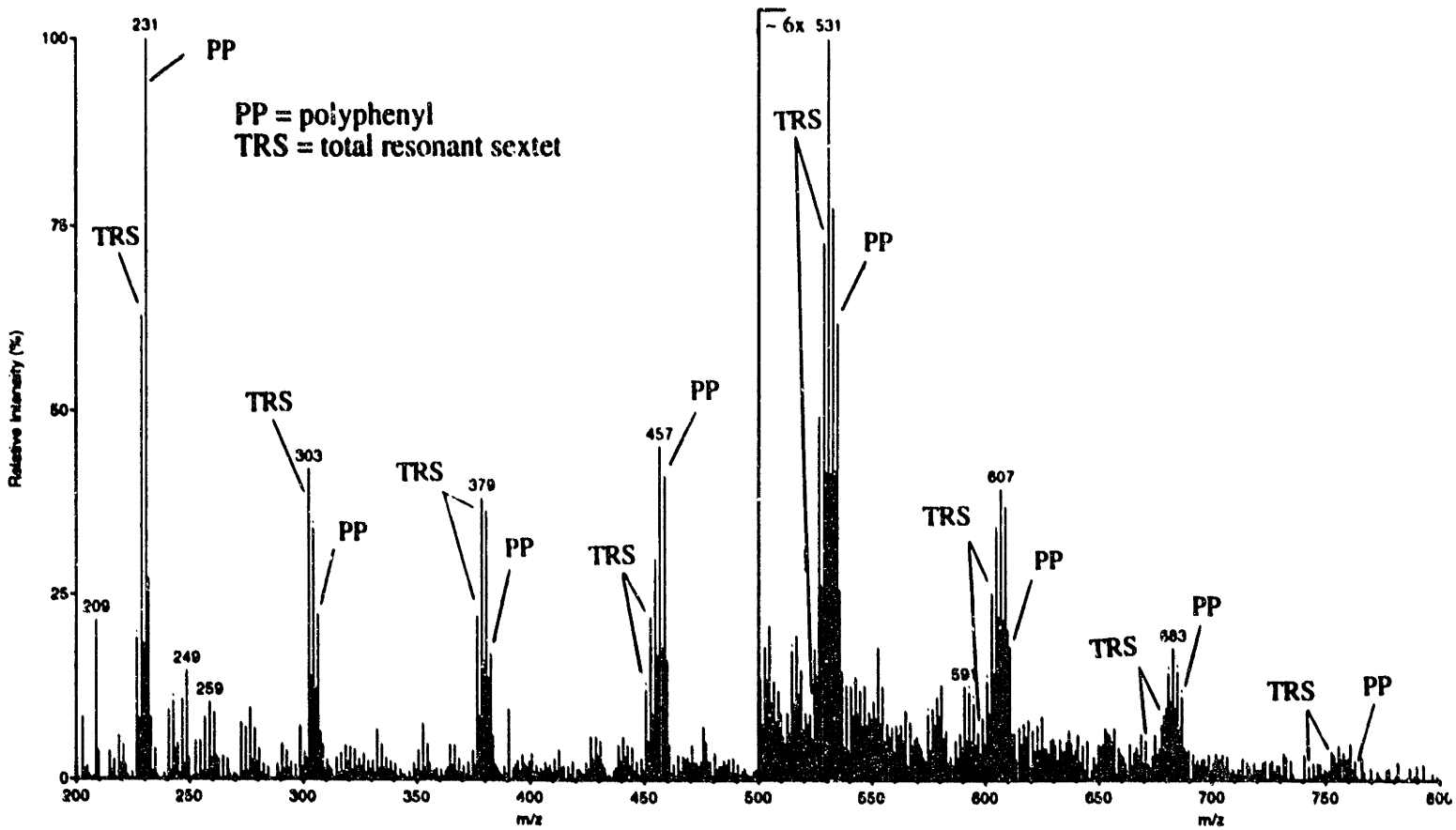

Fig. 5.3.4:

Total Mass Spectra of Products from the Pyrolysis of *o*-terphenyl at 1326 K.

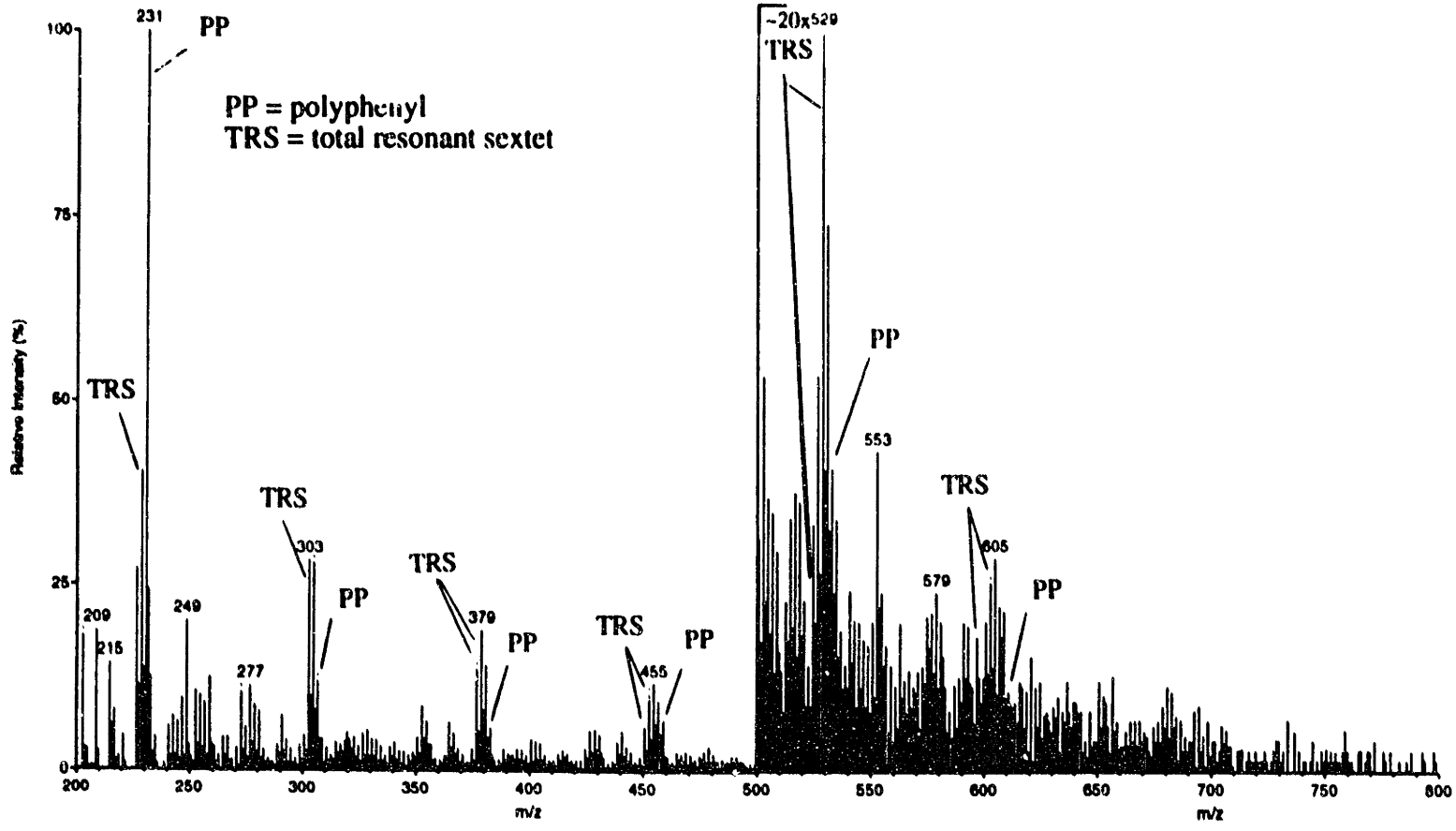

Fig. 5.3.5:

Total Mass Spectra of Products from the Pyrolysis of *o*-terphenyl at 1352 K.

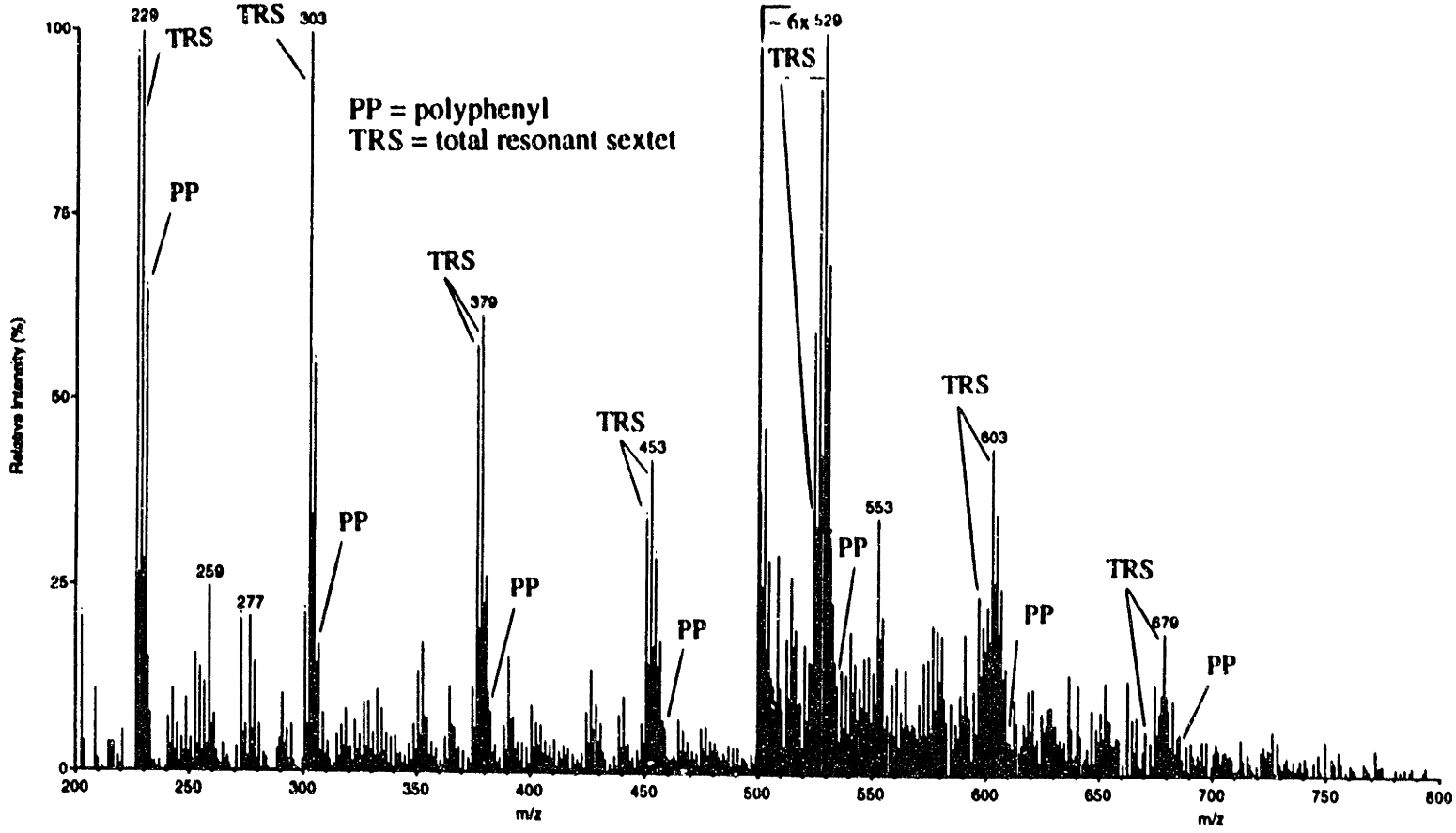

Fig. 5.3.6
Total Ion GC/MS Chromatogram from the Pyrolysis Products of *o*-terphenyl at 1352 K.

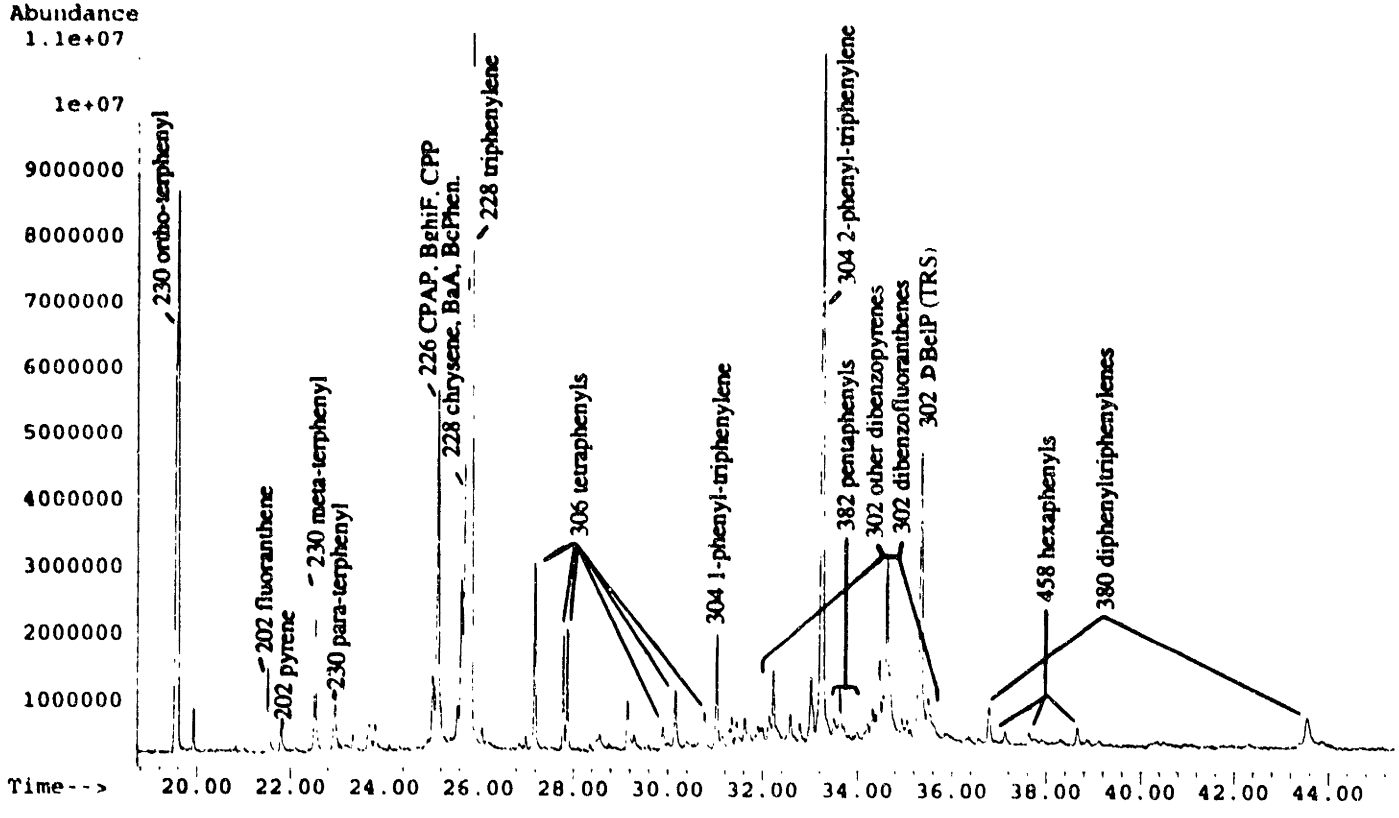

the first genuinely substantial argument for kinetic control that has been seen in these polymerization experiments. The abundance of the hexaphenyl series of isomers relative to the surrounding pentaphenyl and heptaphenyl groups cannot be a reflection of the expected monotonic increase in the free energy of such compound groups. Thus, equilibrium has not yet been established among the intermediates of the benzene polymerization pathway, and kinetic control is indicated.

Of immediate concern in correlating data with predictions is the lack of abundance of species corresponding to the molecular weights of the expected TRS compounds, especially at the lower temperatures. The highly stable products are apparently present in much lower quantities relative to their precursor counterparts than what was predicted by Stein based on his thermodynamic model of the benzene polymerization pathway. Only at the highest temperatures in this study do the ratios of TRS compounds to their precursors start to even pass unity, let alone the several orders of magnitude predicted by Stein. For example, at 1350, the equilibrium constant for the reaction:

1-phenyl-triphenylene <===> dibenzo(e,l)pyrene + H_2

is calculated to be 10^{49} atm. As the H partial pressure must be (far) less than 1 atm, this equilibrium constant requires that the concentration of DBelP be at least 5 orders of magnitude larger than 1PT at equilibrium. This is clearly not supported by the experiment. This observation points strongly to kinetic control of the reaction pathway at these temperatures, but further examination of the actual product types and number of isomers and their relative concentrations is warranted before making such a judgement.

A GCMS chromatogram is shown in Fig. 5.3.6 for the highest temperature sample (1352 K). Correlation and comparison of the peaks contained therein to HPLC/UV-Vis analysis performed on the same sample make possible some interesting observations. First, many non-TRS compounds are observed among the most condensed species in each stage of the polymeric sequence, as indicated by the abundance of "extra" compounds of the same molecular weight as TRS compounds but with different elution time and thus structure (e.g. there are at least 8 peaks representing MW 302 in the samples, whereas only one can be the TRS dibenzo(e,l)pyrene). This is puzzling since the second observation indicates that the direct precursors to the TRS compounds show a corresponding lack of diversity; only the expected isomers from the benzene polymerization pathway are observed (e.g. only the two phenyl-triphenylene isomers are present in any great abundance at MW 304). Third, the ratios of species directly involved in the polymerization scheme are closer (but still not the correct order of magnitude) to Stein's predictions than was previously indicated in the the LCMS analysis. Fourth, the few TRS compounds that can be identified are confirmed to fall off with molecular weight, counter to the prediction of Stein for thermodynamic control. A closer examination of these observations follow.

The thermodynamic model apparently fails to explain the existence of many non-TRS isomers of the most condensed species in each stage of the polymeric sequence. The easiest route to formation of the most condensed species should always lead to TRS compounds in the benzene polymerization pathway. Let us take the tetraphenyl cluster of compounds as an example, since GCMS data is available for these compounds and has

been found to be a superior technique to LCMS for separating the relavant isomers in this size range.

Four phenyls can combine in 9 ways (see App. D). Six peaks of molecular weight 306 are indeed observed in the GCMS spectra (Fig. 5.3.6), and identifications for four out of those six are corroborated with corresponding peaks on the HPLC/UV-Vis chromatogram that exhibit characteristics of their spectra that are consistent with polyphenyls (by comparison with known reference standards of ortho- meta- and para-terphenyl, Aldrich Chemical Co.). Those tetraphenyls that can condense without ring rupture must form the two isomers of phenyl-triphenylene (MW 304), both of which can be identified in the GCMS and HPLC chromatograms based on similarities with other published mass and UV spectra (Wornat et al., 1993; Masonjones et al., 1995, Chapter 6). The condensible isomer has only one option for condensation, and that is to a TRS compound, dibenzo(e,l)pyrene (DBelP). TRS compounds are known for their resistance to chemical transformation, and it would be extremely unlikely for them to change form once created. There should thus be an abundance of only one compound of MW 302.

The GCMS data, however, display an unexpected phenomena. In the transformation to the most condensed state, there suddenly appear at least 7 extra peaks that are discernible in the GCMS chromatogram. A similar phenomenon occurs in the triphenyl cluster where at least 3 extra peaks of MW 228 (confirmed to be chrysene, benzo(a)anthracene (BaA) and benzo(c)phenanthrene by matching UV-Vis spectra to known standards), and at least three MW 226 (confirmed by the same method to be cyclopenta(hi)acephenanthrylene (CPAP), benzo(ghi)fluoranthene (BghiF) and possibly

cyclopenta(cd)pyrene (CPP)) occur. UV spectra corresponding to the GCMS peaks show that there are a number of compounds in the MW 302 size range that match the general spectral characteristics of dibenzopyrenes and dibenzofluoranthenes (Clar, 1964, Schmidt et al., 1987, Wise et al., 1988), although definitive matches could only be made on a few compounds due to the abundance of overlapping and/or low signal peaks and also the lack of UV spectra information in the literature for these compounds. It should be noted that the lack of similar abundances of the same compounds in similar pyrolysis studies (Wornat, 1992, Masonjones, 1995) indicate that the particular MW 302/228/226 are characteristic of the benzene polymerization pathway, and are not products of, for example, acetylene addition to smaller, more universal, substituents. This supposed excess of isomers of the most condensed species in the benzene polymerization pathway is puzzling from a thermodynamic point of view, but as theory is allowed to shift to encompass kinetically controlled ring rupture and rearrangement reactions, a more reasonable explanation of the observations can be obtained.

While DBelP is the most abundant representative of the MW 302 group, (as expected, but not in large enough abundance to claim thermodynamic control) there are a number of compounds present of this molecular weight that are near one quarter to one third the abundance of DBelP (see Fig. 5.3.6). Likewise, the MW 228 group indicates a dominant TRS compound (triphenylene) with a number of other 228 isomers (chrysene, BaA and BcPHEN) and 226 isomers (CPAP, BghiF and CPP) that are present in significant relative concetrations despite very strained structure in some cases. By contrast, the only two MW 304 isomers that are observed correspond in MS and UV

spectra to the two possible isomers of phenyl-triphenylene, and the only three MW 230 isomers correspond to the three terphenyls. This apparent lack of selectivity in creating a TRS compound given only its direct precursors strongly indicates a kinetically controlled mechanism, perhaps featuring ring rupture as a key step. Indeed, many of the observed products at these molecular weights can be achieved by simple one-ring rupture and recombination mechanisms involving the phenyl-triphenylene and terphenyl isomers as starting points (Fig 5.3.7). Some of the fluoranthene isomers may be achieved via further 1,2 carbon shifts similar to those outlined by Scott and Roelofs (1987).

Possible route to benzo(ghi)fluoranthene:

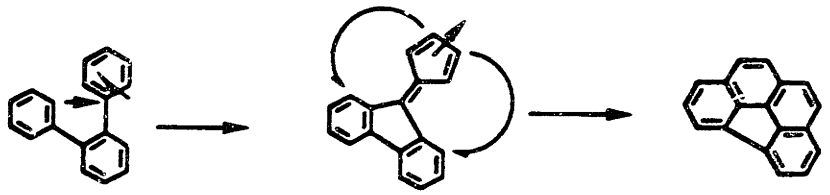

Possible route to cyclopenta(def)acephenanthrylene (CPAP):

Possible route to chrysene:

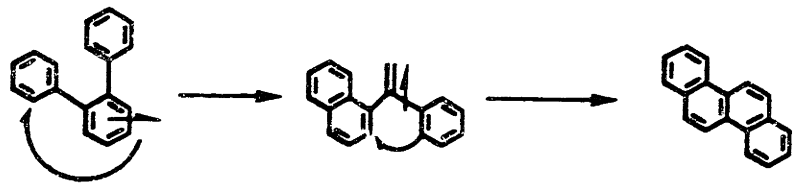

Fig. 5.3.7 Three examples of a ring rupture/recombination mechanism that can lead to the observed unusual products.

The last observation to be addressed is the evidence that the ratios of participants in the benzene polymerization scheme are not very close to what is predicted by Stein for a thermodynamically controlled pathway. Concentrations of three TRS compounds could be observed directly (triphenylene, benzo(e,l)pyrene, and tribenzo(fg,ij,rst)pentacene by comparison with published UV spectra. A significant falloff in concentration with molecular weight was observed. Correlation of known trends in spectra of non-planar biaryls also enabled identification of the condensible terphenyl, phenyl-triphenylene and biphenyl-triphenylene isomers, direct precursors to the TRS species. Their concentrations were found to be of the same order of magnitude as the TRS species at all temperatures with a trend towards a decreasing ratio of precursor to TRS at the higher temperatures. Thus two major features of Stein's prediction - a rise in concentration of the TRS compounds with molecular weight and the several orders of magnitude difference between the concentrations of TRS compounds and their partially condensed precursor intermediates - are both found to be unsubstantiated at all temperatures of the study (although there is a clear trend toward thermodynamic control as the temperature is raised, as might be expected). This again reinforces the concept of a kinetically controlled soot inception process at temperatures below 1400K and residense times of less than 2 seconds. That is, the characteristic time for equilibration of soot precursors formed via the reactive coagulation pathway is longer than the characteristic time for their formation.

5.4 - Conclusions

The feasibility of a kinetically controlled alternate route in the benzene polymerization pathway has been demonstrated via analysis of experimental data from the pyrolysis of ortho-terphenyl.

Many ring rupture products, in addition to the expected total resonant sextet compounds, are observed, indicating a competition between ring-rupture/recombination and condensation reactions.

As indicated by observations of a dominant dimer product, the lack of abundance of TRS compounds relative to their precursors, the lack of a critical species as defined by Stein's work, and the presence of highly strained PAH that could only arise from a competing alternate route to condensation, the theory proposed by Stein based on thermodynamic considerations appears not to be in effect except in the kinetically controlled limit that he describes.

However, the possibility outlined by Stein for a benzene polymerization scheme that leads to high molecular weight growth is not negated by this observation. This is shown by the sequence of benzene polymers and their correct molecular weight (if not the actual predicted compounds) condensation products that are in evidence to at least MW 700, with little corresponding evidence for the accompanying acetylene addition products. The dominance of the benzene polymerization series relative to acetylene addition products provide further evidence that the reactive coagulation pathways to soot growth are very relevant and should not be ignored.

Toxic byproducts such as dibenzopyrenes, dibenzofluoranthenes, CPAP, etc., are observed in abundance, and a pathway that can create them in a pyrolysis environment has been demonstrated. Similar pathways in the anthracene/naphthalene pyrolysis could not be confirmed in the naphthalene/anthracene pyrolysis products due to lack of identification procedures for the relevant compounds

Having established kinetic control for the molecular weight growth process via polymerization and condensation of aromatic compounds, a model must now be developed to test the theory This is the focus of Chapter 8 of this thesis

Chapter Six - Biaryl Isomer Identification

6.1 - Introduction

Before any attempt could be made to understand the high-temperature pyrolysis kinetics relevant to the experiments performed in Chapters 4 and 5 of this thesis, realization of a means of identifying individual compounds in at least the first generation biaryl products was necessary. By analogy to previous studies (Badger and coworkers, 1961-4, Wornat et al., 1992, Mukherjee et al., 1994, Mulholland et al., 1992), the primary products of the pyrolysis of a mixture of naphthalene and anthracene are expected to be the 3 binaphthalene, 6 bianthracene and 6 naphthyl-anthracene isomers. The individual compounds in the first two series of isomers have been previously identified and characterized (Wornat et al., 1993, Clar, 1964, Photoelectric Spectrometry Group, 1966, Heller, 1978, Thermodynamics Research Center, 1983), but the six naphthyl-anthracene isomers (see Appendix D for structures) have not been previously characterized in a manner that clearly differentiates individual isomers. Identification of the individual isomers is essential to understanding the kinetics of biaryl formation, and a means of obtaining this information must be explored before the research can proceed.

Whereas biaryl formation has been well documented in the literature (see references. in Chapter 2.1), identification of compounds has been restricted to classifying biaryls as groups of related molecules with a given molecular weight. It is becoming increasingly necessary to identify individual isomers in a given series in order to obtain a

deeper understanding of the chemistry underlying their formation. Recent attempts to gain insight on the mechanisms involved in biaryl formation (Mulholland et al., 1992, Takatsu and Yamamoto, 1993, Bermudez and Pfefferle, 1991) have focused on starting materials that lead to well-known products (e.g. biphenyl and binaphthalene derivatives). Selecting molecules like anthracene and pyrene (Wornat et al., 1992, Mukherjee et al., 1993, Stein, 1987) whose pyrolysis products are at least partially characterized (Clar, 1964, Photoelectric Spectrometry Group, 1966), can help in the task of product identification (Wornat, 1993), but successful product identification has been limited to simple symmetric biaryls. These shortcomings in product analysis have greatly curtailed the understanding of key mechanisms in biaryl formation, and an attempt is made here to extend the knowledge gained in previous studies to more complex product systems and improve our understanding of major reaction pathways in a pyrolysis environment.

6.2 - Naphthyl-Anthracene Identification

Figure 6.2.1 shows a total-absorbance (236-500 nm) HPLC chromatogram for the pyrolysis products of the anthracene+naphthalene mixture at 1348 K, the temperature at which the most concentrated products and thus most reliable spectra were obtained. Of the major unknown peaks in the correct size range, 5 exhibited remarkably similar UV-Vis spectra (Figs. 6.2.2-6). Furthermore, these spectra exhibited features characteristic of both naphthalene and anthracene, as indicated by the strong absorbances near 226 and 256 nm. The one remaining unidentified large peak possessed features in its spectra (Fig. 6.2.7), abundance and elution time that were also very similar to the corresponding peak

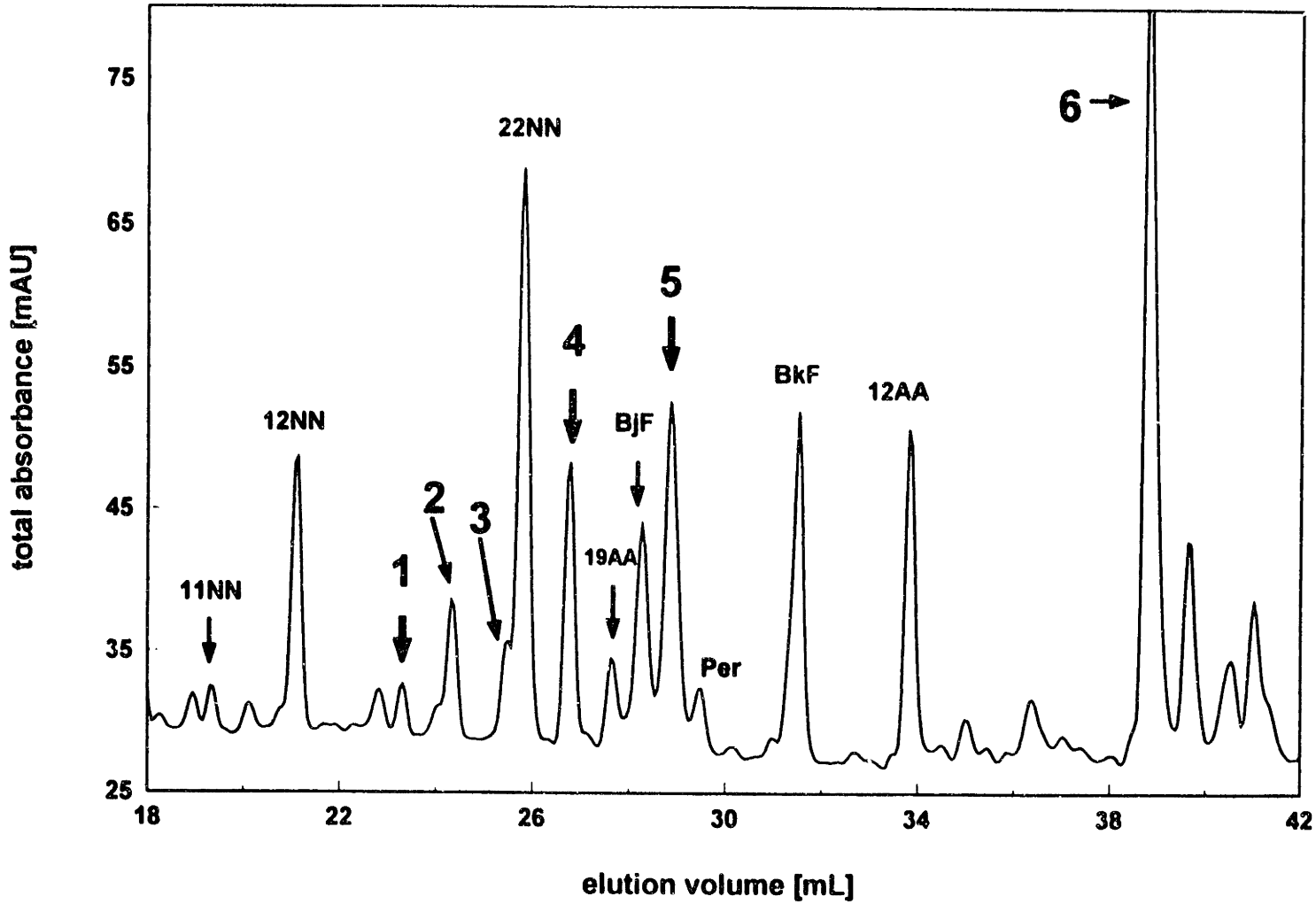

Fig. 6.2.1 HPLC Chromatogram of Biaryl Products

Fig 6.2.2 UV-Vis Spectrum of 91NA

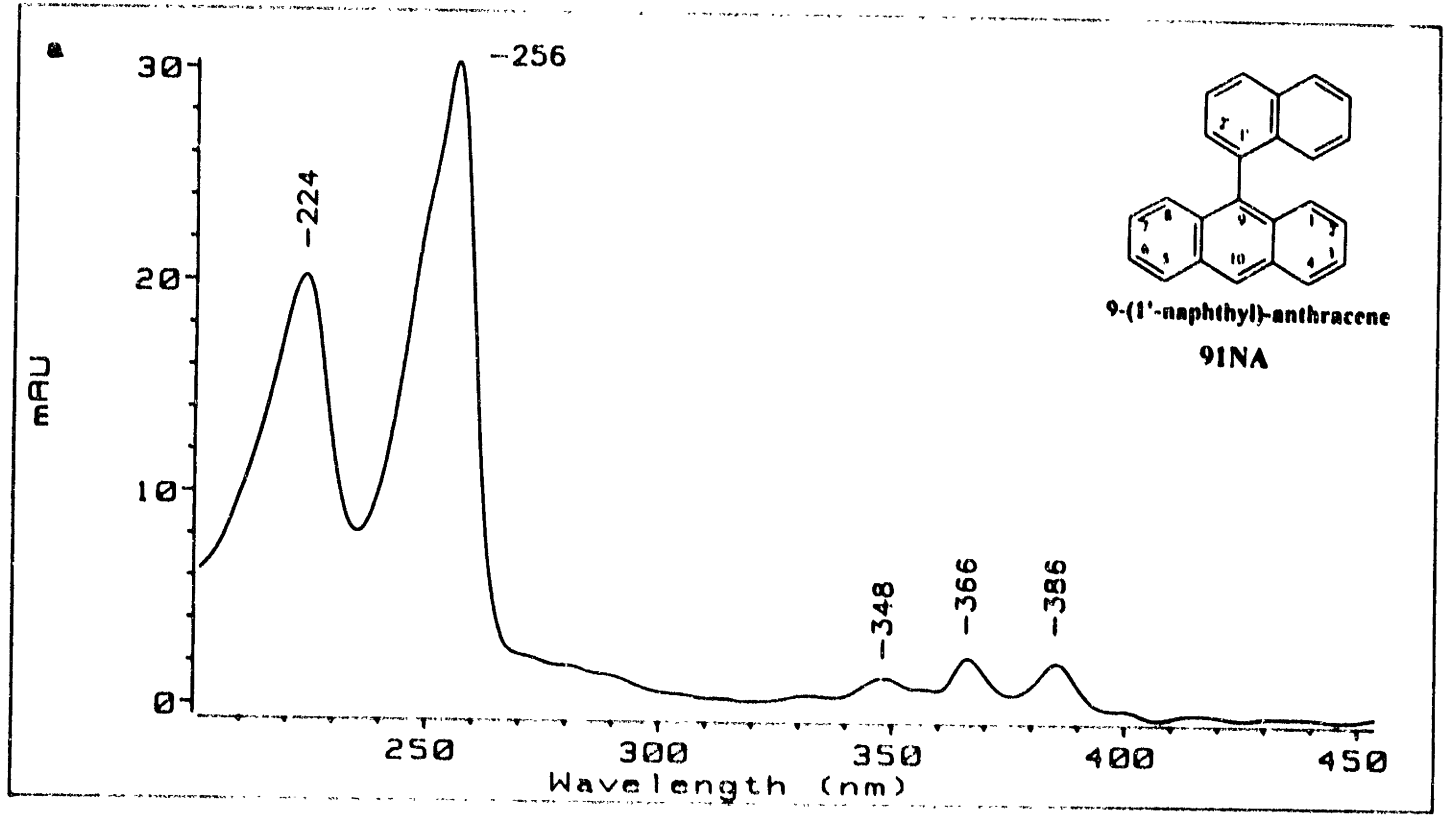

Fig 6.2.3 UV-Vis Spectrum of 92NA

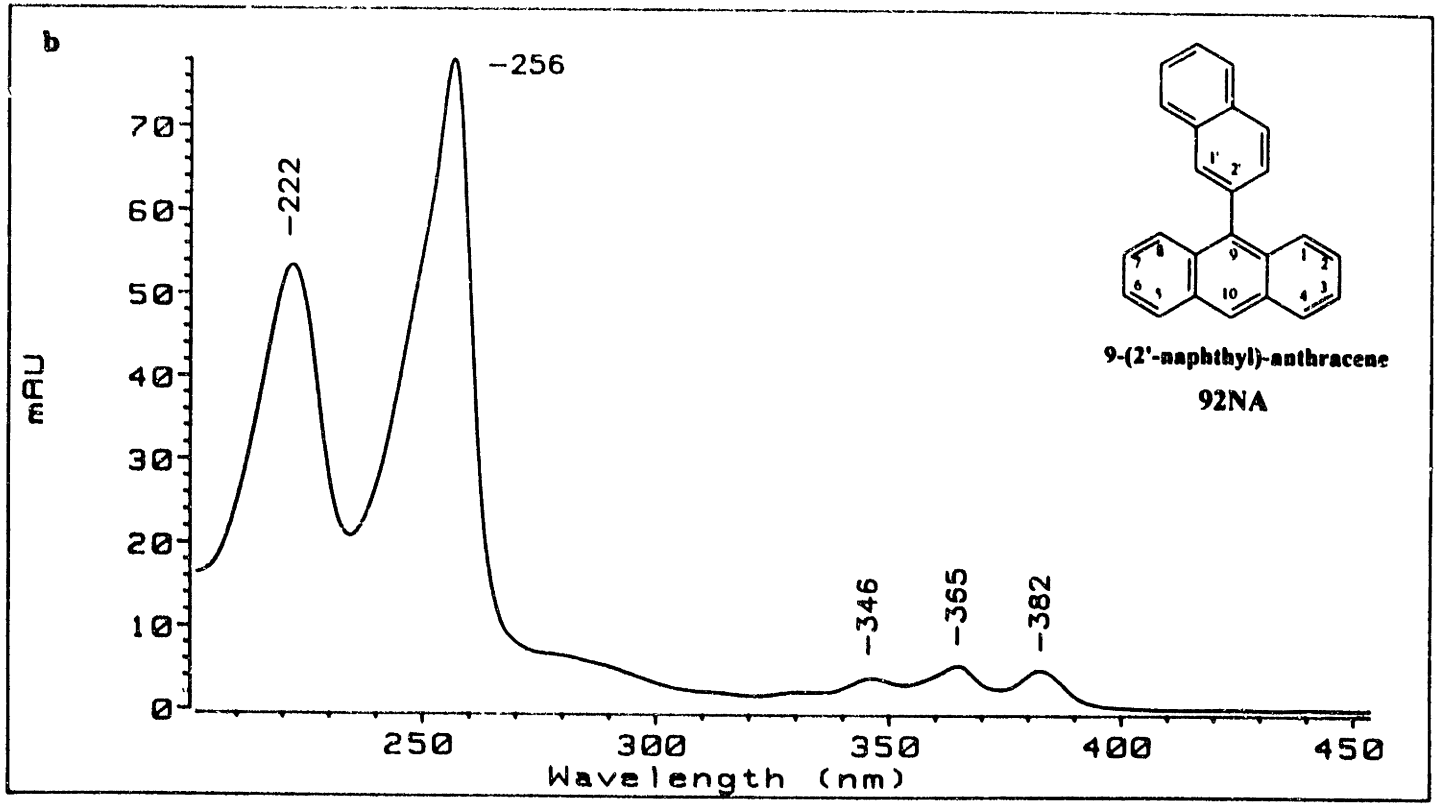

Fig 6.2.4 UV-Vis Spectrum of 11NA

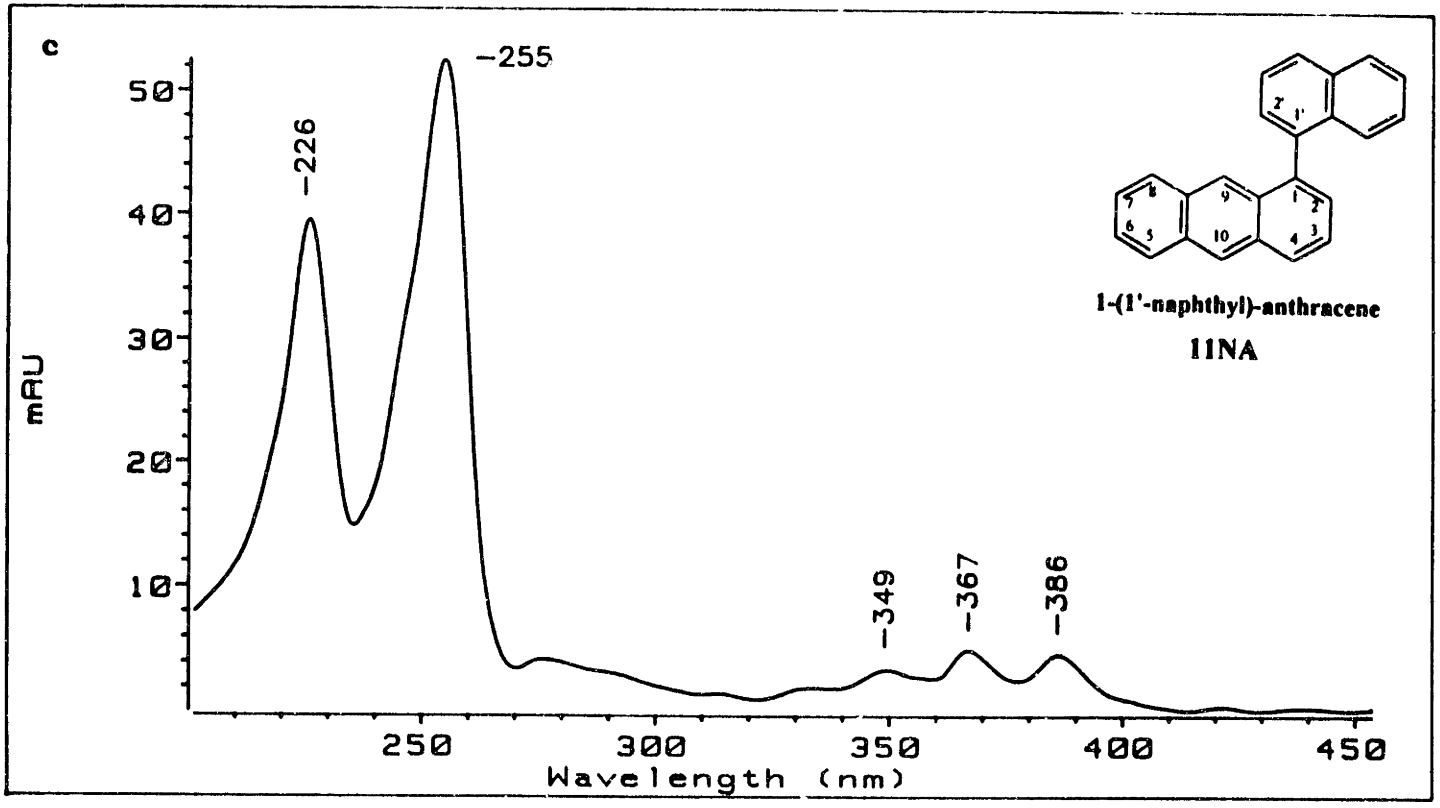

Fig 6.2.5 UV-Vis Spectrum of 21NA

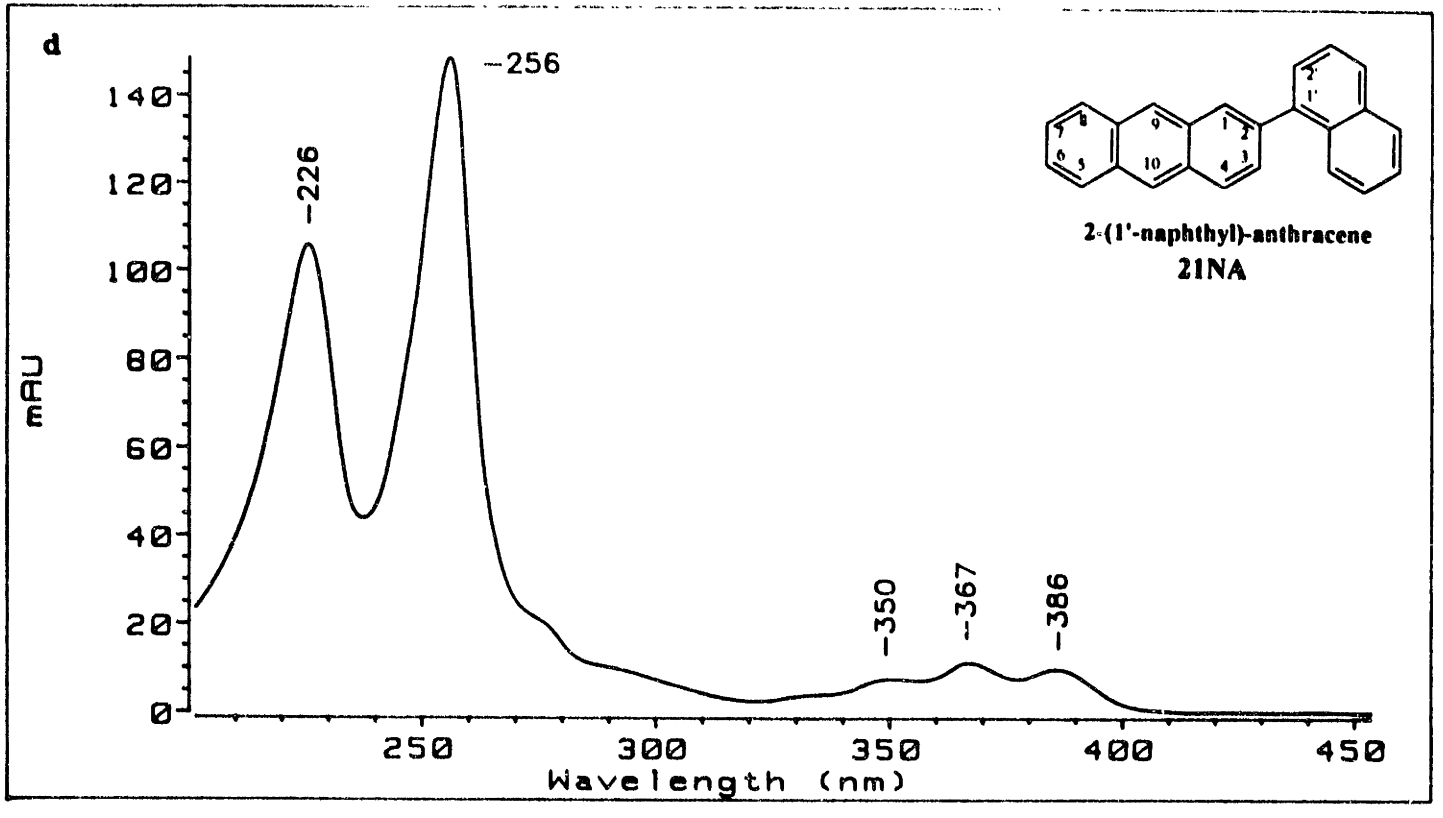

Fig 6.2.6 UV-Vis Spectrum of 12NA

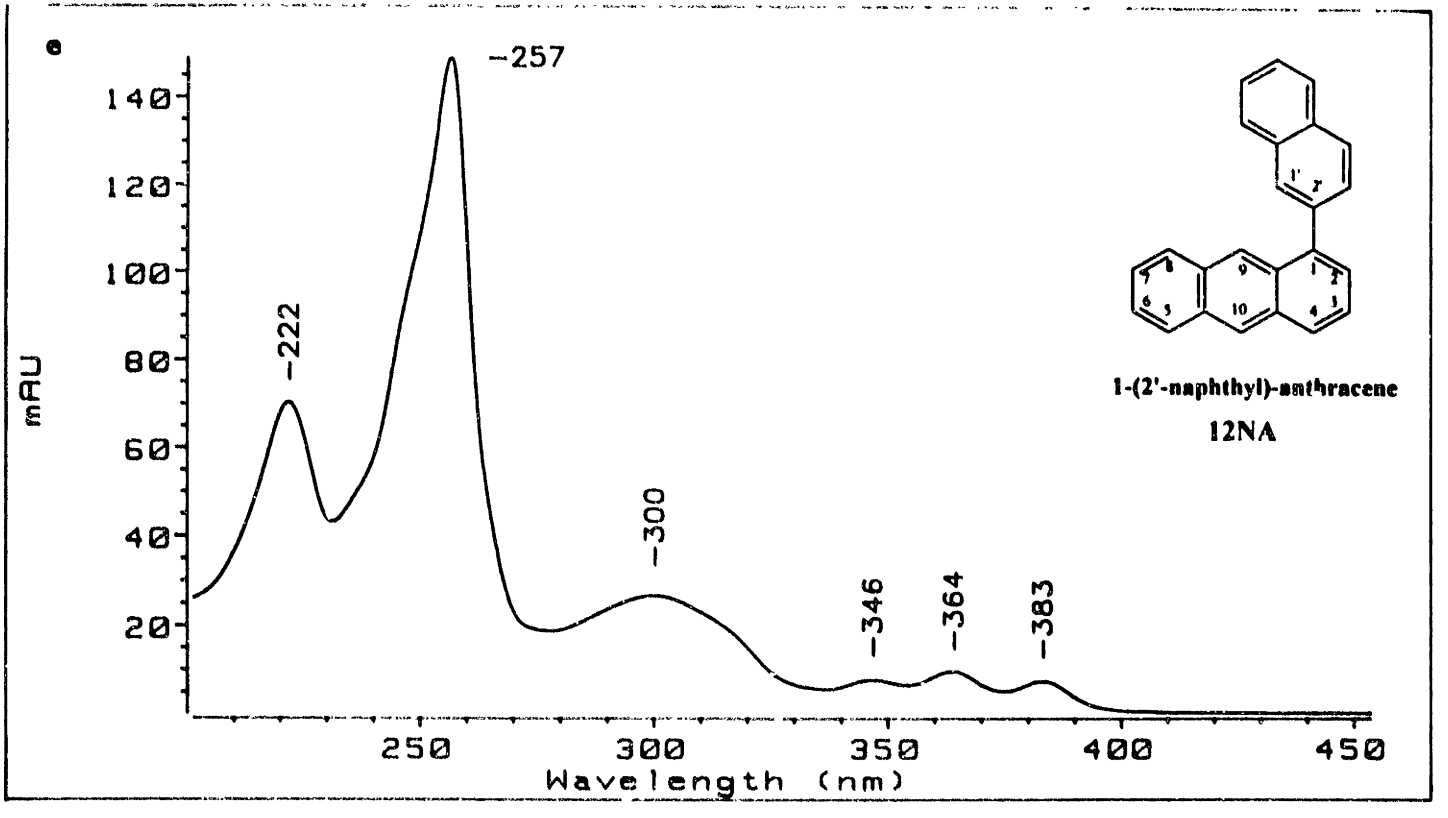

Fig 6.2.7 UV-Vis Spectrum of 22NA

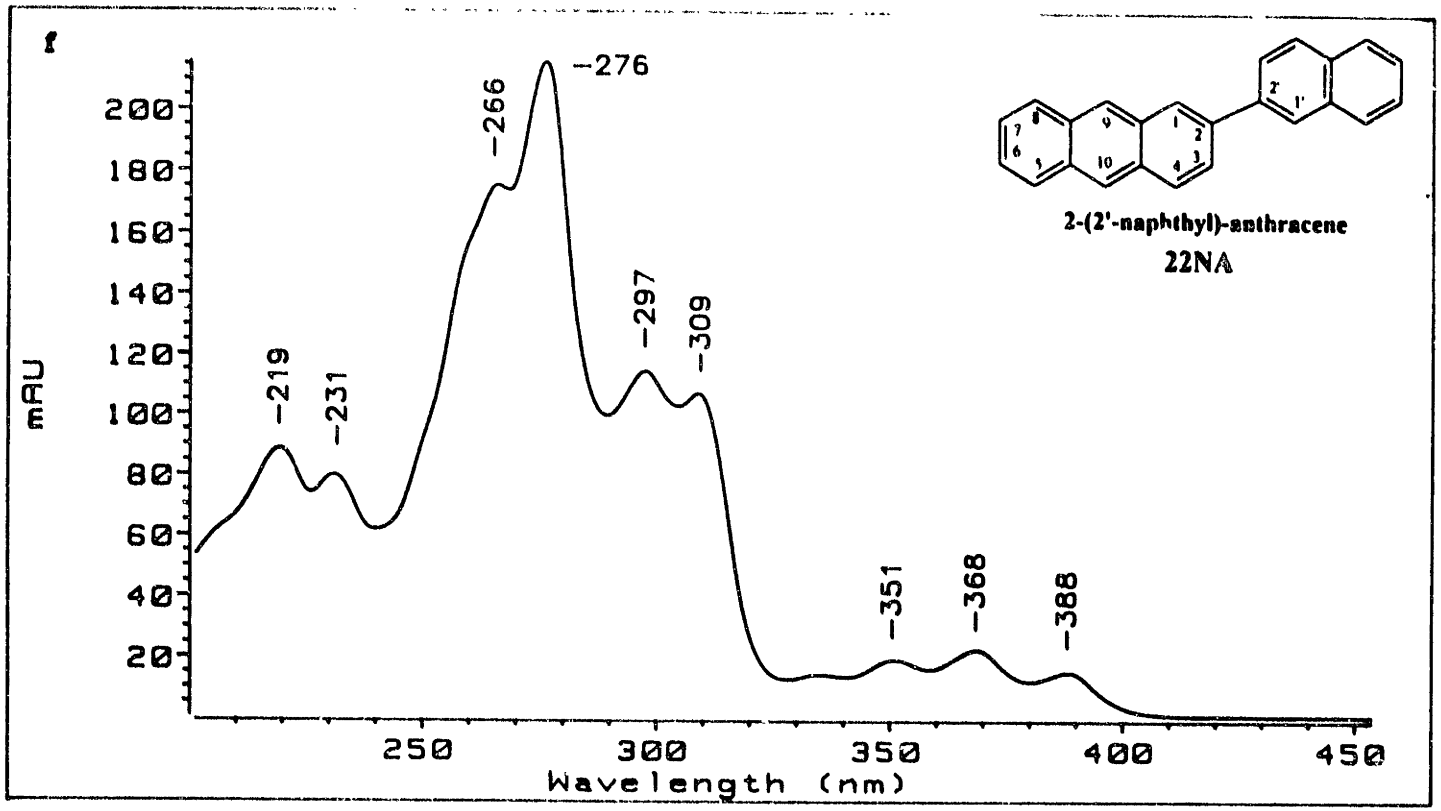

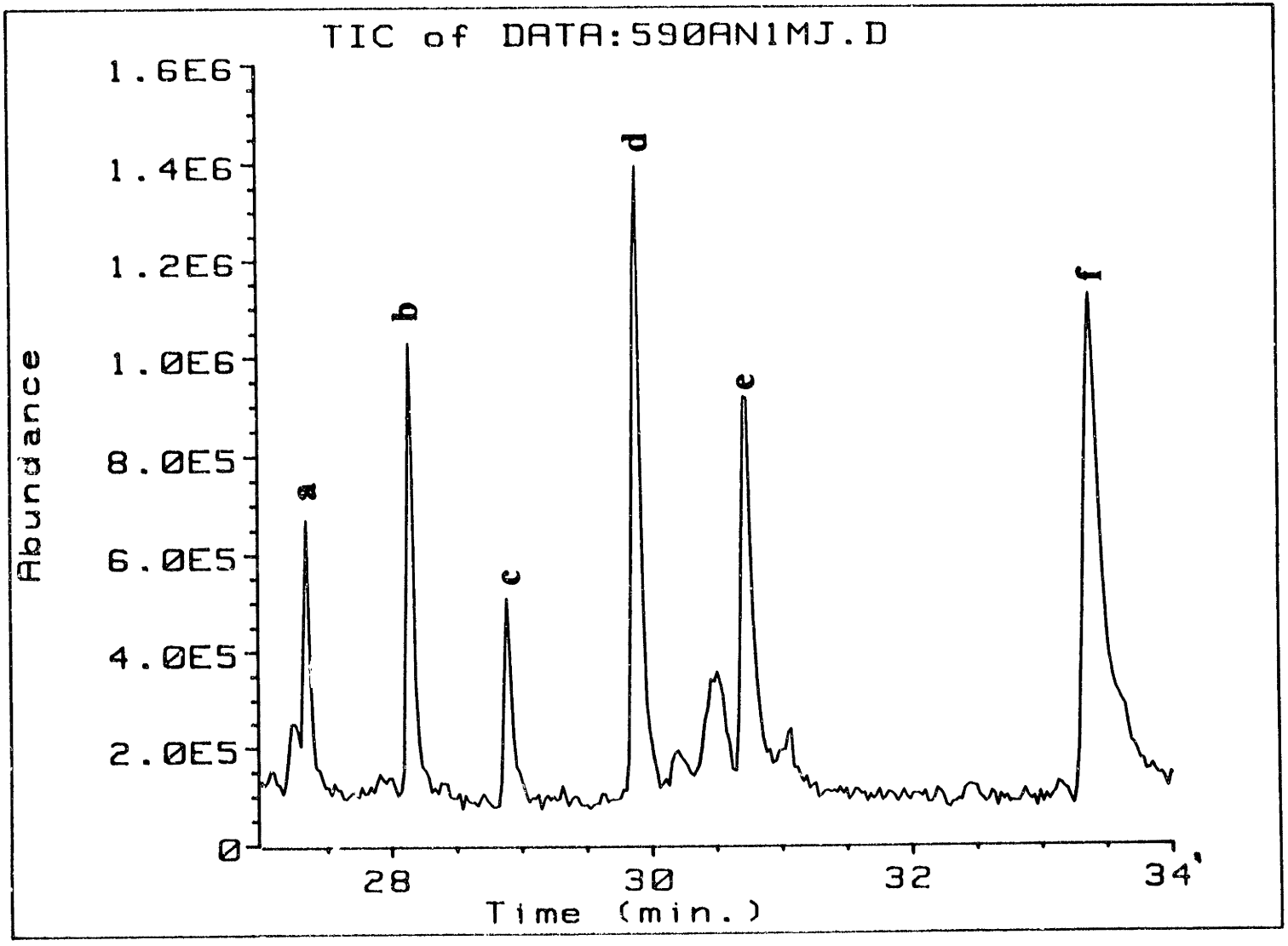

Fig. 6.2.8 GCMS Chromatogram of Naphthyl-Anthracenes

in the bianthryl series (Wornat et al., 1993). Thus, these 6 peaks were taken to be the 6 naphthyl-anthracenes. They are indicated in Fig. 6.2.1 by the numbers **1-6**, referring to the elution order of the compound. As a reference, the binaphthalenes and bianthracenes that have been identified as a consequence of previous studies are indicated by two numbers (indicating bonding sites of linking aryl-aryl bond) followed by NN or AA which indicate the aryl-aryl bond structure (e.g.: 11NN = 1,1'-binaphthalene and 29AA = 2,9'-bianthracene). For ease in discussion, specific naphthyl-anthracene isomers will also be referred to in this fashion, with the first number corresponding to the anthracene's connectivity and the second to naphthalene's (e.g. 92NA = 9-(2'-naphthyl)anthracene).

The GCMS total-ion chromatogram is shown in Fig. 6.2.8. The six unknown isomers (mass 304) are indicated by the letters **a-f**. The fact that there are exactly 6 peaks of MW 304, along with the fact that the compounds represented by these peaks are similar in abundance to the known binaphthalenes and bianthracenes produced in the same pyrolysis, strongly suggest that these are indeed the six naphthyl-anthracene isomers. Table 6.2.1 lists the prominent mass ion peaks and their normalized abundances for each of the unkown naphthyl-anthracene isomers. Corresponding binaphthyl data is included in Table 6.2.2 for comparison and later discussion. The reader is referred to Wornat et al. (1993) for detailed mass spectral information on the bianthracenes, performed on the same GCMS apparatus.

Table 6.2.1. Normalized Mass Ion Abundance for the Six Naphthyl-Anthracenes.

		NAPHTHYL-ANTHRACENES					
	M/z	91NA	92NA	11NA	21NA	12NA	22NA
M+2	306	2.70	2.97	3.42	2.95	3.25	3.20
M+1	305	26.05	24.17	24.72	22.90	24.19	24.64
M+	304	100.00	100.00	100.00	100.00	100.00	100.00
M-1	303	59.59	96.54	76.53	82.29	70.22	9.16
M-2	302	39.03	47.73	42.55	45.96	50.57	25.12
M-3	301	16.86	15.19	12.83	9.93	6.19	4.21
M-4	300	29.35	26.57	23.47	21.29	17.14	8.59
M-5	299	3.89	4.28	3.43	2.79	2.56	0.89
M-6	298	5.74	5.09	5.48	4.26	3.45	2.10
M-14	290	2.03	3.05	1.41	0.69	0.95	0.21
M-15	289	9.89	8.70	3.60	2.05	1.66	0.66
M-16	288	1.29	0.99	1.17	0.81	0.00	0.38
M-17	287	3.15	2.05	1.73	1.33	1.11	0.59
M-27	277	2.60	2.39	2.04	1.39	0.57	0.32
M-28	276	5.60	4.55	3.98	4.45	2.18	1.41
M-29	275	0.00	1.35	1.33	1.06	1.38	0.00
M-30	274	3.46	3.38	3.31	2.65	2.92	1.21
M++	152	2.69	3.05	2.29	2.45	0.00	4.44
(M-2)++	151	5.66	8.54	8.04	7.31	8.92	5.05
(M-4)++	150	8.37	6.79	5.55	5.58	5.33	2.75
(M-6)++	149	2.88	2.47	2.00	1.00	1.37	1.11
(M-16)++	144	3.51	3.15	3.29	2.75	3.19	0.59
(M-18)++	143	2.05	1.76	2.78	1.09	0.57	0.49
(M-28)++	138	3.85	3.43	3.49	2.74	3.26	1.44
(M-30)++	137	2.62	2.20	2.77	2.16	1.28	0.84

Table 6.2.2. Normalized Mass Ion Abundance for the three Binaphthalenes.

		BINAPHTHYLS		
	M/z	11NN	12NN	22NN
M+2	256	1.73	1.65	1.99
M+1	255	17.73	17.86	21.65
M+	254	78.36	88.04	100.00
M-1	253	100.00	100.00	16.78
M-2	252	76.26	59.94	32.45
M-3	251	8.37	6.34	2.99
M-4	250	22.04	18.25	8.90
M-5	249	2.71	2.09	1.07
M-6	248	3.32	2.15	1.09
M-14	240	4.95	0.89	0.10
M-15	239	19.98	3.94	1.02
M-16	238	0.00	0.36	0.25
M-17	237	1.45	0.95	0.53
M-27	227	1.59	0.68	0.48
M-28	226	3.90	3.22	1.94
M-29	225	2.27	1.93	0.90
M-30	224	3.50	2.59	1.33
M-31	223	0.90	0.71	0.35
(M+2)++	128	0.64	0.73	0.00
M++	127	0.00	3.15	2.64
(M-2)++	126	12.26	12.63	3.94
(M-4)++	125	5.66	4.46	1.68
(M-6)++	124	1.19	0.99	0.00
(M-16)++	119	1.58	1.85	0.89
(M-18)++	118	0.99	0.64	0.15
(M-28)++	113	4.99	4.48	2.10
(M-30)++	112	2.38	1.85	0.87

The 6 peaks with base peaks at M/z 304 in the GC/MS total-ion chromatogram (labeled **a-f** in Fig. 6.2.8) correspond roughly to the 6 peaks from the HPLC analysis (labeled **1-6** in Fig. 6.2.1) whose UV-Vis spectra show a very similar UV absorbance activity that in the bands corresponding to the strongest naphthalene and anthracene absorption. It should be noted that biarenes that are prevented from rotating about the

linking sigma-bond tend to have UV-Vis spectral characteristics that are representative of a linear combination of the component arenes (Jones, 1941). This is attributed to the steric-hindrance-induced non-planarity of the molecules, which contributes to the lack of π-structure conjugation between the two arene components. The two pieces of the biarene would thus show an independence of electronic response to incident radiation, and the biarene would exhibit a UV-Vis absorbance similar to a equimolar mixture of the two component halves. The effect dissapates as the biaryls become less hindered and more π-structure conjugation is allowed to occur. These observations are exactly what is seen here in the 6 peaks in the HPLC spectrum (Figs. 6.2.2-7), and it is strongly suggested that these peaks are the six naphthyl-anthracene isomers.

As a first step in the structural elucidation of the naphthyl-anthracene isomers, their UV spectra were examined for identifying features. Clar's notation (1964) for describing absorption bands of cata-condensed (ortho-fused) aromatic compounds was followed. Table 6.2.3 gives a summary correlating this notation with other researchers' (Platt, 1950). Two bands were discernible in our spectra, as expected (Worrat et al., 1993, Clar, 1964): the β-band, which refers to the lower wavelength (approx. 250± 40 nm) portion of the UV-Vis spectrum, and the ***para***-band or ***p***-band, which refers to the higher wavelength (approx. 370 ± 20 nm) structure. The β-band has been shown in previous studies Jones, 1945, Jones, 1947, House et al., 1972) to correspond to transitions which are polarized along the long axis of the anthracene molecule and the ***p***-band corresponds to those along the short axis. Consequently, substituents in the 9 position have the greatest effect on the ***p***-band whereas those in the 2 position have more effect on

Table 6.2.3. UV absorption bands of naphthalene and anthracene

transition	$^1L_b \leftarrow {}^1A$	$^1L_a \leftarrow {}^1A$	$^1B_b \leftarrow {}^1A$	$^1C_b \leftarrow {}^1A$
Clar notation	α	*para*	β	(none)
Platt classification	^1L_b	^1L_a	^1B	^1C_b
polarization	longitudinal	transverse	longitudinal	transverse
naphthalene				
λ_{max} [nm]	312	286-289	220-221	190
ε_{max}	280	9,300	133,000	10,000
notes	obscured			[<λcutoff)
anthracene				
λ_{max} [nm]		379 (onset)	256	221
ε_{max}		9,000	180,000	14,500
notes		(5+bands)		

Table 6.2.4. Summary of MOPAC calculations.

ISOMER	$\Delta H_{f,298}$ (kcal/mole)	Biaryl Angle (deg.)	Length (angstroms)
91NA	112.30	89.2	11.08
92NA	110.76	70.8	12.92
11NA	110.75	69.8	13.10
21NA	109.09	60.4	15.35
12NA	109.13	59.6	14.11
22NA	107.15	41.6	17.12
99AA	136.24	90.0	11.06
19AA	134.63	89.6	12.22
29AA	133.06	71.5	15.22
11AA	133.11	71.0	14.66
12AA	131.43	60.0	16.31
22AA	129.40	41.6	19.45
11NN	88.40	69.0	11.46
12NN	86.76	59.7	13.03
22NN	84.78	41.5	14.80

the β-band transitions, and those in the 1 position have an intermediate effect. Naphthalene has corresponding features in its spectrum (Clar, 1964, Photoelectric Spectrometry Group, 1966), but only its β-band can be recognized in the UV spectrum of thenaphthyl-anthracenes because its p-band is obscured by that of anthracene's.

This information alone is enough to identify unknown **f** as 2-(2'-naphthyl)-anthracene (22NA). The UV spectral features of unknown **f** shows a marked similarity to its late-eluting counterpart among the bianthracene isomers, 2, 2'-bianthracene (22AA) (Wornat et al., 1993). Their UV spectra are very similar in that they exhibit a unique broadening and splitting pattern in the β-band and a flattening in the p-band relative to the other isomers. Like 22AA, 22NA is the least strained of the naphthyl-anthracenes, and consequently, will be able to configure itself so that the angle between the planes of the naphthalene and anthracene components is smallest, enabling a conjugation of π-electrons across the arene-arene bond. This would have a marked effect on the UV spectrum (Jones, 1941), which is indeed what is observed for the **f** isomer and its bianthracene counterpart. As the 22NA isomer is the most capable of conjugation, and only one isomer shows evidence of this effect on its UV spectrum, it is strongly suggested that peak **f** represents the 22NA isomer.

Further support for the identification of unknown **f** as 22NA follows from the observation that for non-planar molecules, those isomers with the least planar configuration and smallest length-to-breadth ratio will elute first (Sander and Wise, 1986) under reversed-phase HPLC conditions. Conversely, the most planar species with the largest length-to-breadth ratio should elute last. A similar trend, with perhaps minor

modifications to order would also be expected for GC elution times, by analogy to previous experiments on the same equipment with similar isomer series (Wornat et al., 1993). Outcomes of certain calculations performed by the MOPAC program are summarized in Table 6.2.4. Included are the heats of formation, angle between planes of aryl constituents and lengths for the most stable configurations of each of the naphthyl-anthracenes. It is easy to see from this table that 22NA should elute last based on both planarity and aspect ratio (as approximated by length or excluded volume, since breadth data is rather ill-defined for non planar molecules), and unknown **f** clearly is the latest eluting NA isomer. . For comparison, the same calculations are performed on the binaphthalenes and bianthracenes.

In the GCMS analysis, the mass spectrum for 22AA was markedly different from the remaining isomers. A much larger M+/M-1 ratio was observed for this isomer (Wornat et al., 1993), suggesting a heightened resistance to fragmentation and thus a more stable compound. The 22AA isomer is the most stable isomer in the bianthracene series as a result of its reduced steric hindrance (Table 6.2.4). Likewise, 22NA is the most stable in the naphthyl-anthracene series, so it would also be expected to exhibit an intense M+ ion in its mass spectrum. Peak **6** is the only isomer peak that gives mass spectral data indicative of a less hindered biaryl (Table 6.2.1), and it is concluded that this unknown represents the 22NA isomer.

It is encouraging to note that there is some correspondence between the elution order and abundance of 22NA on the GCMS and HPLC apparatus. The molecule elutes last in both separation techniques, as expected by the size-exclusion principles mentioned

above, and also in agreement with the last eluting bianthracene isomer being 22AA on both apparatus. Peaks **6** and **f** are also the most abundant by far in their respective series, further corroborating the agreement of these two peaks in representing the 22NA isomer. Further correspondences can also be established in this manner. By 1) comparing abundances of individual compounds in the HPLC series **1-6** and in the GCMS series **a-f**, 2) noting the purity of the spectra corresponding to these peaks (indicating the unlikelihood of coeluting compounds) (Table 6.2.1 and Fig. 6.2.2-7) and 3) noting established trends in elution order that would be extremely unlikely to be violated (eg, 91NA must elute first, and 22NA must elute last), it is hypothesized that unknown **a** represents the same molcule as unknown **1**, unknown **b** = unknown **2**, unknown **c** = unknown **3**, and unknown **f** = unknown **6** (previously estabilshed). Only correspondence between unknowns **d**, **e** and unknowns **4**, **5** are uncertain.

Except for unknown **f**, all other naphthyl-anthracene isomers display the expected similarity in UV and mass spectra. However, some important differences can be discerned among the spectral data for the remaining isomers. As has already been mentioned, an important factor in distinguishing among isomers is the substituent-induced differences in the *β*- and *p*-bands of the UV spectra. Some elaboration is needed before the analysis can proceed further. A substituent in the 9 position of anthracene has been shown to lead to an enhancement of peak/valley ratios in the *p*-band of its UV spectrum relative to that of anthracene (Jones, 1947, Jones, 1945, House et al., 1972). More specifically, the UV peaks increase while valleys appear more pronounced.

However, the peaks in the *p*-band become much more flattened when substitutents are added to the 2 position. A substituent in the 1 position produces an effect intermediate between these two extremes. Substituents on anthracene also have an effect on the *β*-band structure, but it does not appear to be pronounced enough to be observed here and thus cannot be utilized. Another important trend that will be helpful is the fact that a substituent in the 1 position on naphthalene tends to create a shift in its *β*-band peak to a higher wavelength than one in the 2 position. This can be verified by comparing published UV spectra of isomeric substituted naphthalenes (Photoelectric Spectrometry Group, 1966).

Another important trend that will be useful for identifying the remaining 5 isomers involves the elution order. As mentioned previously, a rough estimate of elution time for a reverse phase HPLC run can be achieved using knowledge about relative nonplanarity and length to width ratio of the compounds. Based on these two considerations, and using the information from Table 6.2.4, the compounds should elute in the following order: 91NA < (92NA, 11NA) < (12NA, 21NA) < 22NA. By analogy to the corresponding compounds in the bianthracene series, it is also believed that 92NA will elute before 11NA. Differences in column or technique can make slight alterations to this order, but it must be stated that elution order for the compounds in the bianthracene and binaphthalene series were unaffected in translating from the technique of reverse phase HPLC to GCMS (Wornat et al., 1993). Consequently, a similar elution order is expected for the GCMS separation technique.

One last technique will be used to aid in the identification. It has not been noted in the literature before, but it does have a basis in theory, and the trend enjoys some

experimental support in published mass spectra for similar compounds (Wornat et al., 1993, Heller, 1978, Thermodynamics Research Center, 1983). The trend employed here makes use of the relative abundance of the minor fragments in a mass spectrum created by electron impact (all fragments mentioned in this paper are confirmed to coelute with their parent ions, and are thus thought to have come from the same compounds). There is a distinct trend in the ratio of the fragment group corresponding to a loss of one carbon relative to the parent ion group (Tables 6.2.1 and 6.2.2). In the binaphthalenes, the trend is (for the ratio of M/z 239 and its close companion ions to M/z 254 and its companions): 11NN >> 12NN >> 22NN (Heller, 1978, Thermodynamics Research Center, 1983, Table 6.2.2). A much greater than sign (>>) here indicates a difference strong enough to be very noticeable and thus distinct enough to be beyond the range of random noise. For the bianthracenes, the ordering is: 99AA >> 19AA > 29AA >> 11AA > 12AA >> 22AA (Wornat et al., 1993). That is, the 9-anthryl derivatives appear to fragment more readily by losing a carbon, whereas the 1 substituted anthracenes and naphthalenes hold together better under the strain of a charging by electron impact, and the 2 substituted compounds fare better still. While predicting or even explaining fragmentation trends is not often easy, it is suggested that the trend might be explained by the documented ability of an anthracene to support odd electrons or charges most effectively in the 9 position, followed by the 1, and then the 2 (Pullman and Pullman, 1958, Herndon, 1981, Chen et al., 1989). The naphthalene trend can then be shown to proceed in the exact same way. The ability for the charged intermediate to form may be crucial for the mechanism by which a carbon is lost. A mechanism similar to the one proposed by Johnstone (1966) for the loss of a

carbon in diphenylpropene, one in which a ring closing and rearrangement are precipitated by such a charging, may be responsible.

The fragment concept is based purely on empirical evidence, and while it is untested in any broad sense, it appears to apply quite well in this specific situation. For the naphthyl-anthracenes, we would then predict an ordering of: 91NA > (92NA > or < 11NA) > (12NA=21NA) > 22NA. Although the 92NA and 11NA are not directly comparable with the fragment concept, the ordering of the bianthracene isomers suggest that 92NA will exhibit the higher ratio, and in a noticeable way. That is, the presence of a 9-anthryl substituent is the dominant factor contributing to a carbon loss, with a 1-yl component of either type being of secondary importance.

With the above outlined trends, it is now possible to identify the remaining 5 naphthyl-anthracene ismoers. Correspondence of unknown **a** and unknown **1** has already been established above, and it is expected based on elution order that they represent the 91NA isomer. Mass spectra fragment data confirm that peak **a** is either 91NA or 92NA, but the *p*-band of unknown **1**'s UV spectrum is the most enhanced of any of the isomers, pointing again to unknown **a** (**1**) being the 91NA isomer.

Unknown **2** (**b**) and unknown **5** (**d** or **e**) are the only two isomers that exhibit any significant shift in wavelength of any band. Both the naphthalene β-band and the anthracene *p*-band shift to a lower wavelength. This similarity indicates that these two isomers possess a common component. The remaining unidentified isomers are 11NA, 12NA, 21NA and 92NA. Of the common components that appear exactly twice, only the 2-naphthyl would be expected to produce the β-band shift in wavelength. As mentioned

previously, substituents in the 2 position of naphthalene produce a shift in naphthalene's β-band to lower wavelength relative to the l-substituted species (Photoelectric Spectrometry Group., 1966). More corroborating evidence can be found in the literature for a shift in anthracene's *p*-band that is caused by the substituent (Wornat et al., 1993). In that study, bianthracene isomers containing a 2-anthryl component exhibited a slight shift to lower wavelength in the *p*-band peaks. While this shift was attributed not to the 2-anthryl component in a substituent position lowering the wavelength but to the 9-anthryl component raising it, the limited nature of the product spectrum prevented a thorough analysis of this trend. The data for the present study suggest that the 2-yl component, not the 9-yl component, is thus the cause of the *p*-band shift (although the 9-yl component would still be responsible for *p*-band enhancement, as previously described (Jones, 1947, Jones, 1945, House et al., 1972). This can be rationalized by again noting that isomers with a 2-yl component are much more planar than their counterparts, enabling greater conjugation between the pi structures of the two aryl components, which in turn creates features in the UV -Vis spectra that are unique to these isomers (Jones, 1941). This is reasonable considering the unusual UV spectrum for the 22NA isomer. It is thus concluded that peaks **2** (**b**) and **5** represent the 92NA and 12NA isomers, and from elution order and mass spectral cracking patterns that indicate a 9-anthryl component in unknown **b**, it is expected that unknown **2** (**b**) is 92NA and unknown **5** is the 12NA isomer. This is further corroborated by a relative enhancement of the *p*-band of anthracene for unknown **2** (**b**), corresponding to a 9-anthryl component being present in that species.

The remaining unidentified isomers are 11NA and 21NA. Elution order, mass specrtal cracking patterns, and *p*-band enhancement all strongly suggest that unknown **3** (**c**) is the 11NA and unknown **4** (**d** or **e**) is the 21NA isomer. The only remaining identification is that of matching 12NA and 21NA with unknown peaks **d** and **e**. While it is admittedly open to some speculation, since there is no corresponding pair in either the binaphthalene or bianthracene series to compare to, it is believed that unknown **d** represents the 21NA isomer and unknown **e** represents 12NA. This is based on expected correspondence of elution order (which has never failed in a similar series, but is nevertheless an uncertain identifying method for distiguishing this particular pairof isomers) and on the mass spectral cracking patterns. In the binaphthalene series, for example, replacing a 1-naphthyl with a 2-naphthyl on a given compound consistently reduces the loss-of-one-carbon mass group abundance 4- or 5-fold. A corresponding replacement in the bianthracene series using the same ionization technique results in only a factor of 1.5 to 2 loss in abundance. This is calculated roughly based on the limited bianthracenes available in the sampled used in this experiment, and it is corroborated by scrutinizing the relavant published mass spectra (Wornat et al., 1993). Thus, starting with 11NA, the smaller loss in the M-15 group abundance should correspond to the loss of a 1-anthryl conponent, making unkown **d** the 21NA isomer and unknown **e** the 12 NA isomer. The remaining losses of 1-yl components are consistent with this identification, and the respective factors of 4 to 5 and 1.5 to 2 observed in the previously characterized binaphthalene and bianthracene series are closely followed in the naphthyl-anthracene series, a trend that appears to support and corroborate this method of identification.

With all isomer assignments in place, it is now left to consider whether the isomer assignments are consistent with respect to each other relative to all known trends. It should be noted that 22NA has many unique characteristics, so it is not expected that all of the trends will extend to this species, and this isomer is not included in the following analysis.

Analogous to the bianthracene UV spectral features, *p*-band enhancements are all consistent with a trend that based on overall nearness to a maximum in the 9,1' isomer (9 > 1 > 2 enhancement): 91NA > 11NA > 92NA > (12NA, 21NA), with bond structure of the naphthyl components contributing to the shift of anthracene's *p*-band as well: (92NA, 12NA) > (91NA, 11NA, 21NA). *β*-band shift is consistent in that only the 2-naphthyl isomers exhibit the shift, and it is in the direction one would expect from comparisons with UV spectra of substituted naphthalenes.

Elution order is consistent with what is predicted by theory, with only fine adjustments and no changes in order occurring between reverse-phase HPLC and GCMS, as was also observed in the binaphthalene and bianthracene series.

Mass spectra fragmentation patterns also show a trend consistent with the one described earlier in this paper. 91NA and 92NA show a much greater tendency to lose one carbon upon electron impact than the other isomers, followed by 11NA > 21NA > 12NA > 22NA. This final ordering indicates that the 1-naphthyl component contributes more to the ability of a the compound to lose a carbon than the 1-anthryl component, consistent with calculations performed on the binaphthalene and bianthracene series present in these samples.

As a final indication of the accuracy of the identifications, the six isomers' relative concentrations are consistent with what one would predict from a kinetic model of the pyrolysis performed here based on probabilistic considerations (Chapter 4).

All six isomeric i-(j'-naphthyl)anthracenes (ijNA)are thus identified based on published trends in chromatography and spectroscopy. The compounds corresponding to unknowns **1-6** in Fig. 6.2.1 (**a-f** in Fig. 6.2.8) are: **1**=**a**=91NA; **2**=**b**=92NA; **3**=**c**=11NA; **4**=**d**=21NA; **5**=**e**=12NA; **6**=**f**=22NA.

6.3 - Phenyl-Triphenylene Identification

Though no new methods are employed in identifying the two previously unidentified key isomers in the benzene polymerization pathway - 1-phenyl-triphenylene and 2-phenyl-triphenylene (see Appendix D for structures) - a description of the process used is warranted. Identification of the two phenyl-triphenylenes proceeds along the same path to identification as the naphthyl-anthracenes (Chapter 6.2) and the bianthracenes (Wornat et al., 1993).

First, a GCMS spectra is used to confirm the existence of exactly two dominant isomers of molecular weight 304 (see Fig. 5.3.6). As with the previous three biaryl series that have been fully characterized, the compound whose rotor is least hindered is expected to elute last and be present in the largest concentration. MOPAC calculations are unnecessary - the choice of which of the two phenyl-triphenylenes is least hindered (2-phenyl-triphenylene) is readily made by inspection. The least hindered product should also show the greatest resistance to fracture by electron bombardment. It should therefore

Fig. 6.3.1 Mass Spectrum of 1-phenyl-triphenylene

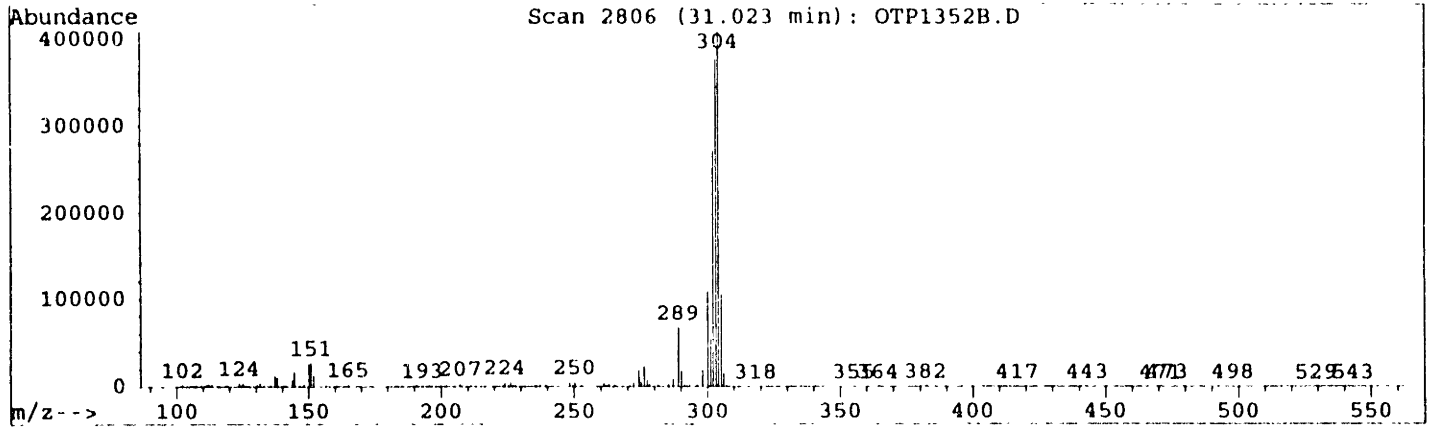

Fig. 6.3.2 Mass Spectrum of 2-phenyl-triphenylene

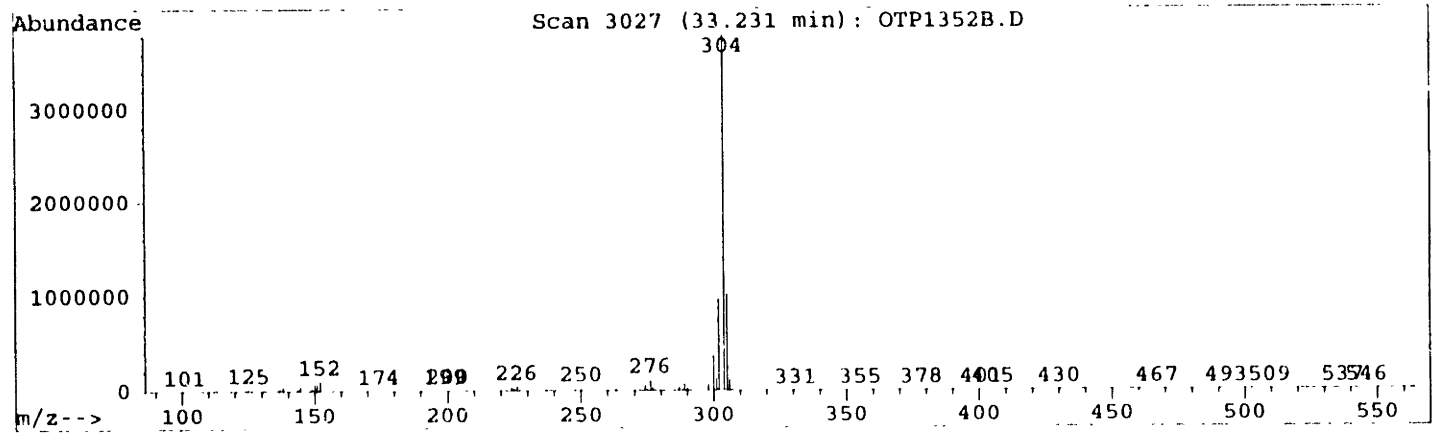

Fig. 6.3.3 HPLC Chromatogram of ortho-terphenyl pyrolysis products at 1352 K

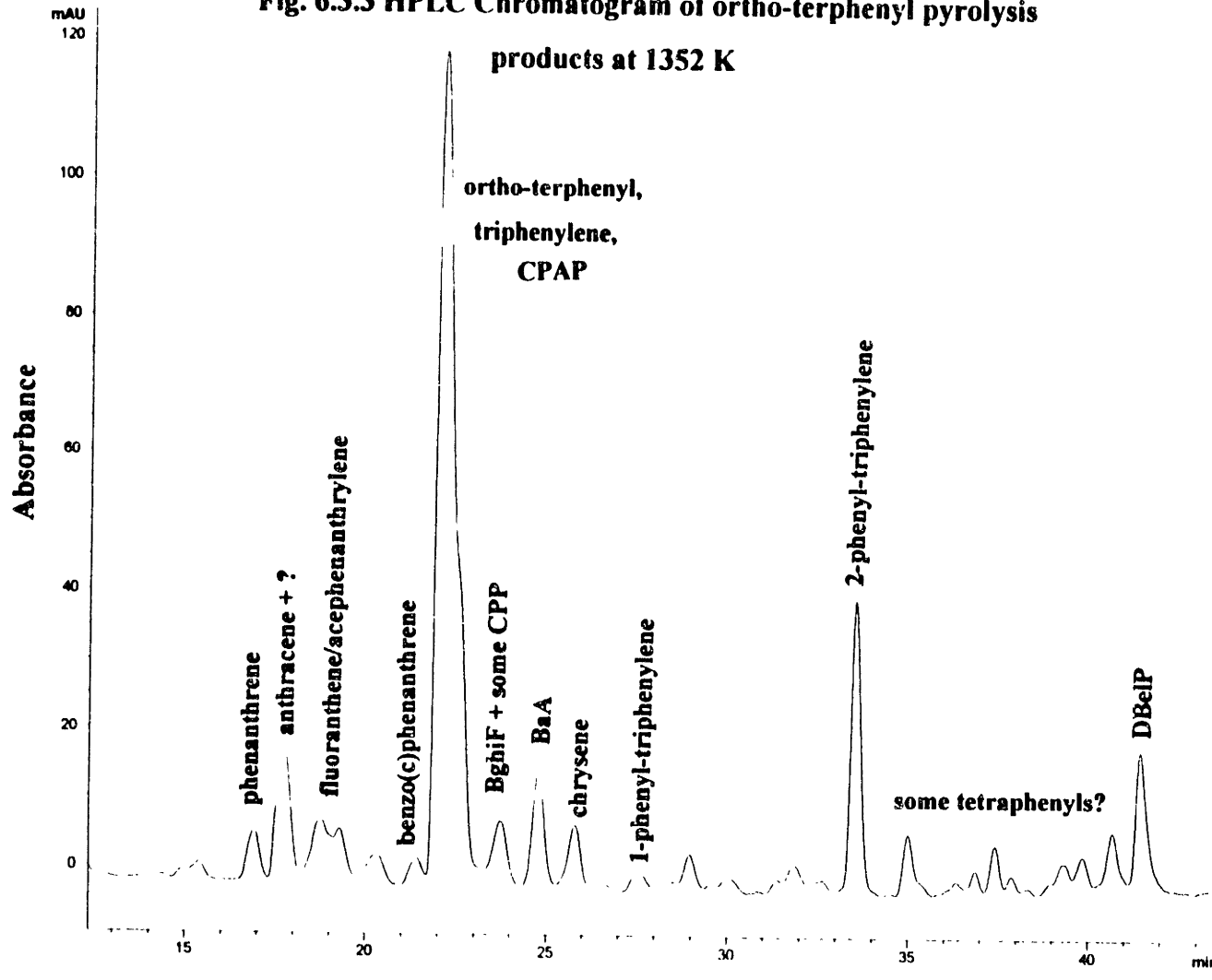

Fig. 6.3.4 UV-Vis Spectra of 1-phenyl-triphenylene

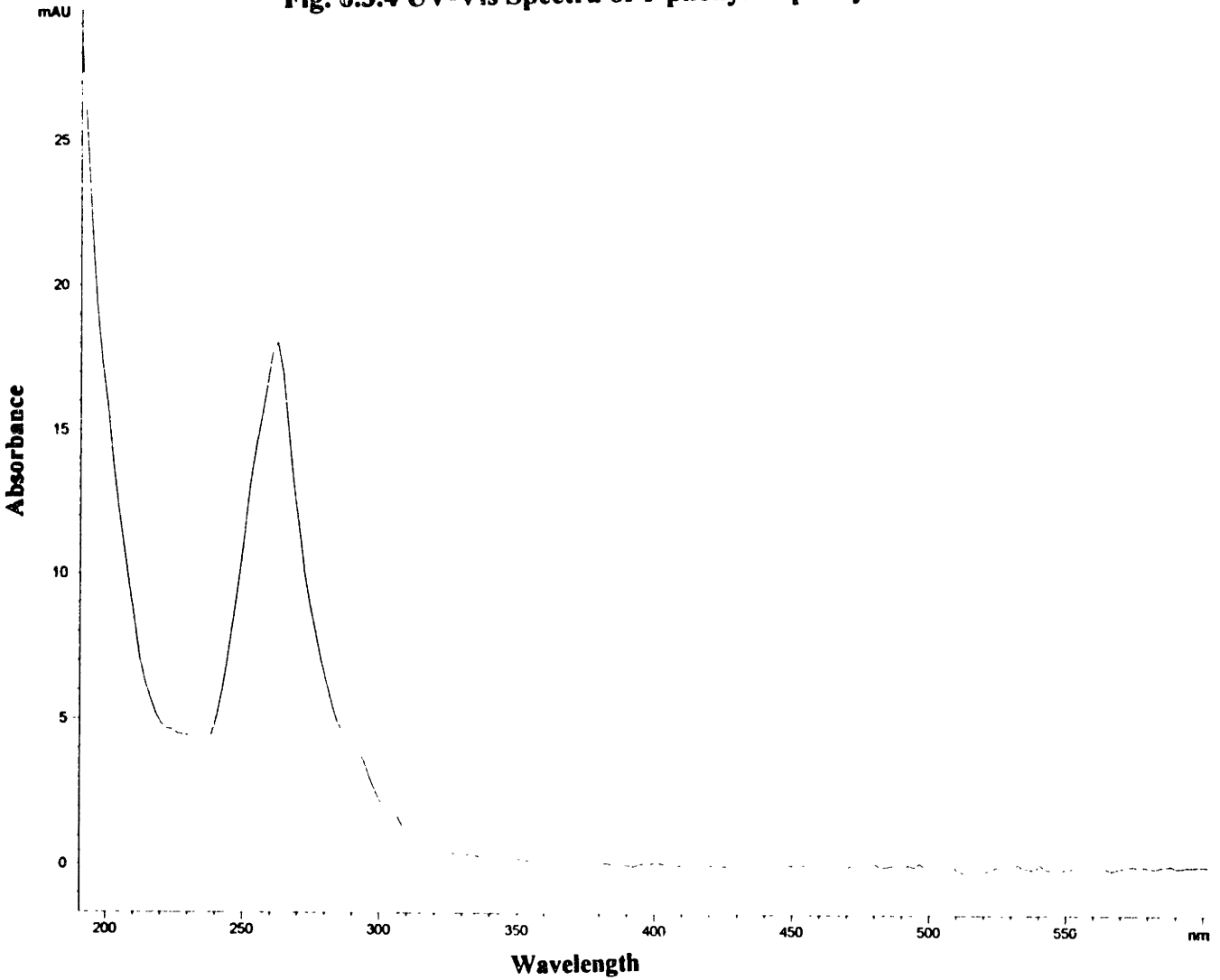

Fig. 6.3.5 UV-Vis Spectra of 2-phenyl-triphenylene

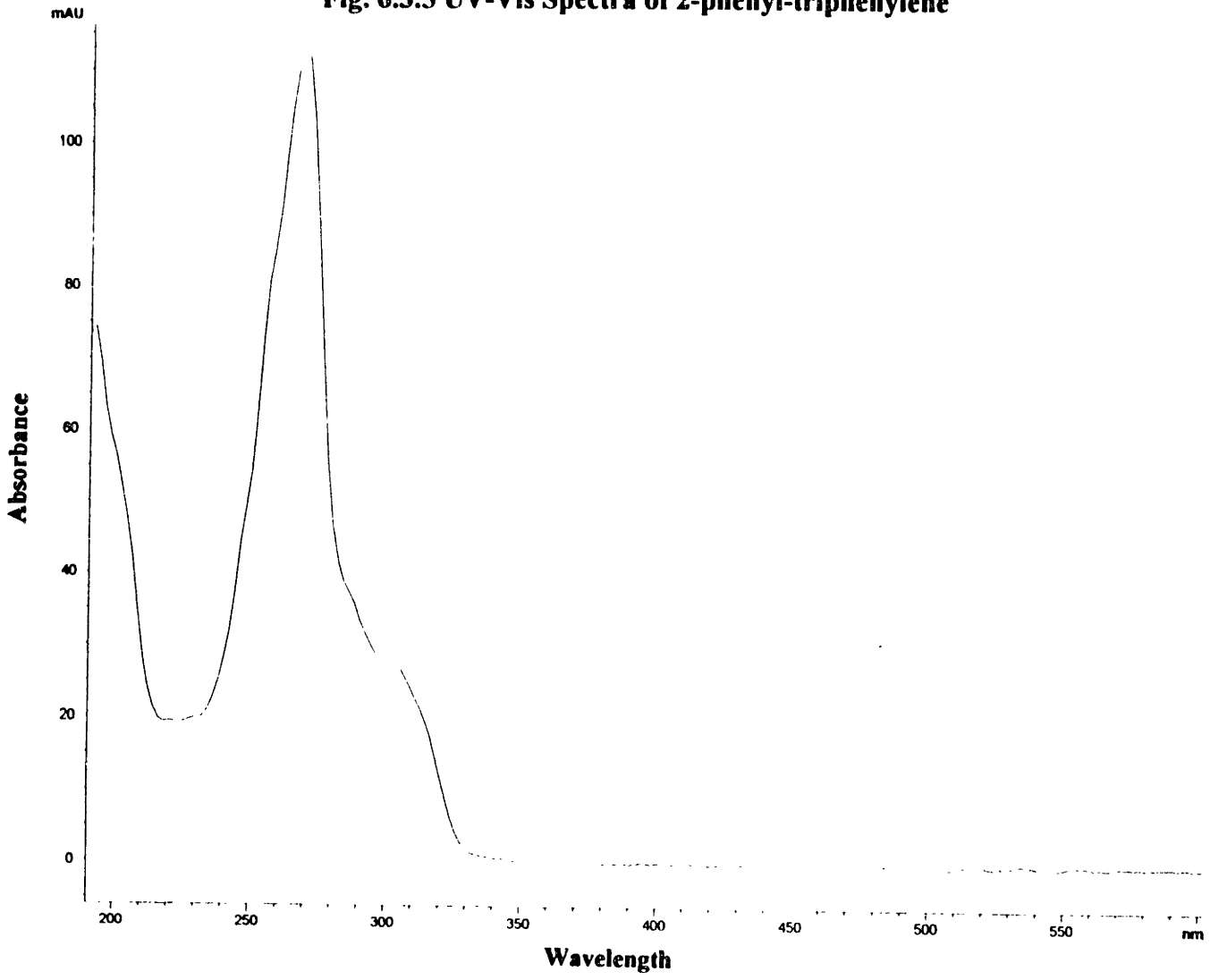

exhibit the larger base 304 peak relative to the 303 and 302 peaks and it should also have more difficulty than the hindered isomer in losing one carbon by a fracturing similar to the one described in section 6.2 for the other biaryl series. These observations can be easily confirmed by inspection of the abundances, elution times and mass spectra of the two unknown peaks of mass 304 (Fig. 5.3.6, Figs. 6.3.1-2).Second, a process of elimnation procedure is invoked to determine which peaks on the GCMS chromatogram correspond to which peaks on the HPLC chromatogram (Fig. 6.3.3). A rough correspondence is elution order is achieved between GCMS and reverse phase HPLC, and calculated relative concentrations are also roughly equivalent in poth processes. Only one pair of peaks in the HPLC chromatogram possess the correct relative elution order, correct concentrations relative to each other and to surrounding peaks, and similar activity in the band of their UV-Vis spectra (Fig. 6.3.4-5) that would correspond to a triphenylene component or a phenyl component being present in a biaryl. Those two peaks are labelled in Fig. 6.3.3. The lack of an apparent π-structure coupling effect on the UV spectrum of the 2-phenyl-triphenylene isomer is not worrisome, as the π-structures involved are more simple and symmetric than those of anthracene and naphthalene, and steric hindrance of that isomer is expected to be slightly more than the 2,2'-binaphthalene and 2-(2'-naphthyl)anthracene isomers due to the geometry of the triphenylene component, making pi-structure interaction less likely.

Identifications of both phenyl-triphenylene isomers are thus complete, and they are found to be consistent with previously described empirical rules for identifying individual isomers in a biaryl series.

6.4 - Conclusions

Both phenyl-triphenylenes and all six naphthyl-anthracenes, complete sets of two biaryl series, have been identified. Although no compound can ever be unequivocally identified without comparison to known standards, the identifications presented here are remarkably consistent with predicted elution order (based on molecular conformation and steric hindrance considerations) as well as with features of UV and mass spectra that are associated with substituents in various positions around the two arene components of these compounds. Knowledge of the identity of these first key intermediates in potentially important arene polymerization schemes has proved crucial to the argument for kinetic control that has been presented in Chapters 4 and 5 of this thesis. This knowledge will now enable the more critical testing of this hypothesis against experiment through a kinetic model of molecular weight growth via polymerization.

Chapter Seven - The Identification of the poly (ethylene terephthalate) Artifact (or: the Fullerene Fiasco)

7.1 - Introduction

A curious artifact was recognized in the naphthyl-anthracene experiments (see Figs 4.3.6-10) that became the cause for some excitement. At least one compound of molecular weight 576 was present that possessed several characteristics of a fullerene, a closed-cage carbon structure discovered for the first time in 1985 (Kroto et al.) that has been the subject of much combustion research in recent years (Gerhardt et al., 1987, Gerhardt et al., 1989, Howard et al., 1991, McKinnon et al., 1992, Pope, 1993). The presence of fullerenes in these pyrolysis samples would require taking into account their formation in the description of molecular weight growh kinetics, and proof for their existence or non-existence was needed before conclusions could be made in this thesis.

7.2 - The Mystery

As mentioned in the introduction, the first indication of an unusual compound in the chemical soups that are the pyrolysis samples was the presence of an apparently dominant product of molecular weight 576. The possibility of background noise was eliminated immediately by an inspection of the baseline mass spectrogram before and after the sample peak. The compound(s) was unusual in that it possessed many properties that were unlike any of the expected PAH products. Then again, some properties indicated a compound that was related to PAH. Each of these observations will be outlined in detail

below. Complicating the matter further was the newness of the LCMS apparatus to our lab and of the application of the LCMS technique to combustion samples. Nothing had yet been established for certain about expected trends in response factors, ionization or mass fracturing patterns of any compounds that were not plain PAH.

The concept that the mystery peak at 577(MW 576) might be a fullerene originated in the realization that 576 is a multiple of 12, the molecular weight of the carbon atom. MW 576 would thus correspond to a C_{48} fullerene. A companion peak at mass 768 was then noticed which could correspond to a C_{64} species. This was enough to start the investigation into the possibility of the guest molecule being a fullerene. The possibility of the 576/768 "series" representing an unfractured polymer with base unit mass 192 was ruled out at this point due to lack of evidence for a monomer or dimer and to the requirement that the polymer would have to be cyclic to avoid having capped ends that would make the base peaks at least MW 578/770. In other words, if the compounds in question were indeed a polymeric series, then it would almost certainly have to be cyclic with a minimum cycle of 3 (very unusual and unlikely) or fracturing in the mass spectrometer environment.

Next in the list of observations that put the mystery compounds into their own class of product type was the observation that both of the peak groupings near 576 and 768 possessed a peculiar cutoff that is uncharacteristic of high molecular weight PAH groupings. These groupings tend instead to be mixes of isomers at varying stages of condensation and hydrogen loss (see 4.3.6-10), resulting in broad clusters of peaks at least 10 amu wide in the total mass ion spectra. In ion exchange mode, the M+1 peak is

dominant, almost no M+ peak is present, and the M+2 peak is rather secondary. No fracturing is evident, indicating a resistance to such a process via ionization that is similar to PAH's. A comparison of the smaller (and more abundant) mystery molecule and a known standard C_{60} fullerene is shown in Fig 7.2.1. Though the distribution of peak heights due to isomer abundances (M+2 peak) and to lack of propensity for proton adsorption (M+ peak) appear to be unrepresentative of a fullerene, the resolution of the apparatus was not assumed to be good enough to make such a distinction. A better solution to the mystery was not forthcoming, and it seemed unwise to abandon the search for a potentially momentous find based on such flimsy evidence. Besides, if the molecule was a C_{48} fullerene, some unusual properties such as enhanced propensity for proton adsorption might be expected, given the different posibilities available for its structure.

To eliminate the possibility of the molecule being a flat PAH or biaryl, and to propose a structure for the fullerene series, some graph theory calculations were performed. For simplicity, the following discussion will center around the 576 molecule. The companion peak at 768 is assumed to be of the same type of structure as the 576 molecule, so they either both exist as PAH or both as fullerenes, etc. If the 768 molecule is of a different compound class than that of the 576 compound, then a more bizarre explanation than just a fullerene will be needed to describe the observations.

If the compound is a PAH, the compound must be $C_{46}H_{24}$; $C_{47}H_{12}$ and $C_{45}H_{36}$ have too few and too many hydrogens respectfully for any reasonable aromatic structure to be drawn. Furthermore, both of these compounds are odd carbon species, requiring the molecules not be fully aromatic, substantially reducing the likelihood that they would form in any great quantity relative to their even numbered cousins ($C_{48}H_{12}$, $C_{46}H_{10}$, $C_{46}H_{36}$, $C_{44}H_{34}$, plus or

Fig. 7.2.1: A Comparison of Mass Spectral Pattern of Mystery Compound with Known Fullerene

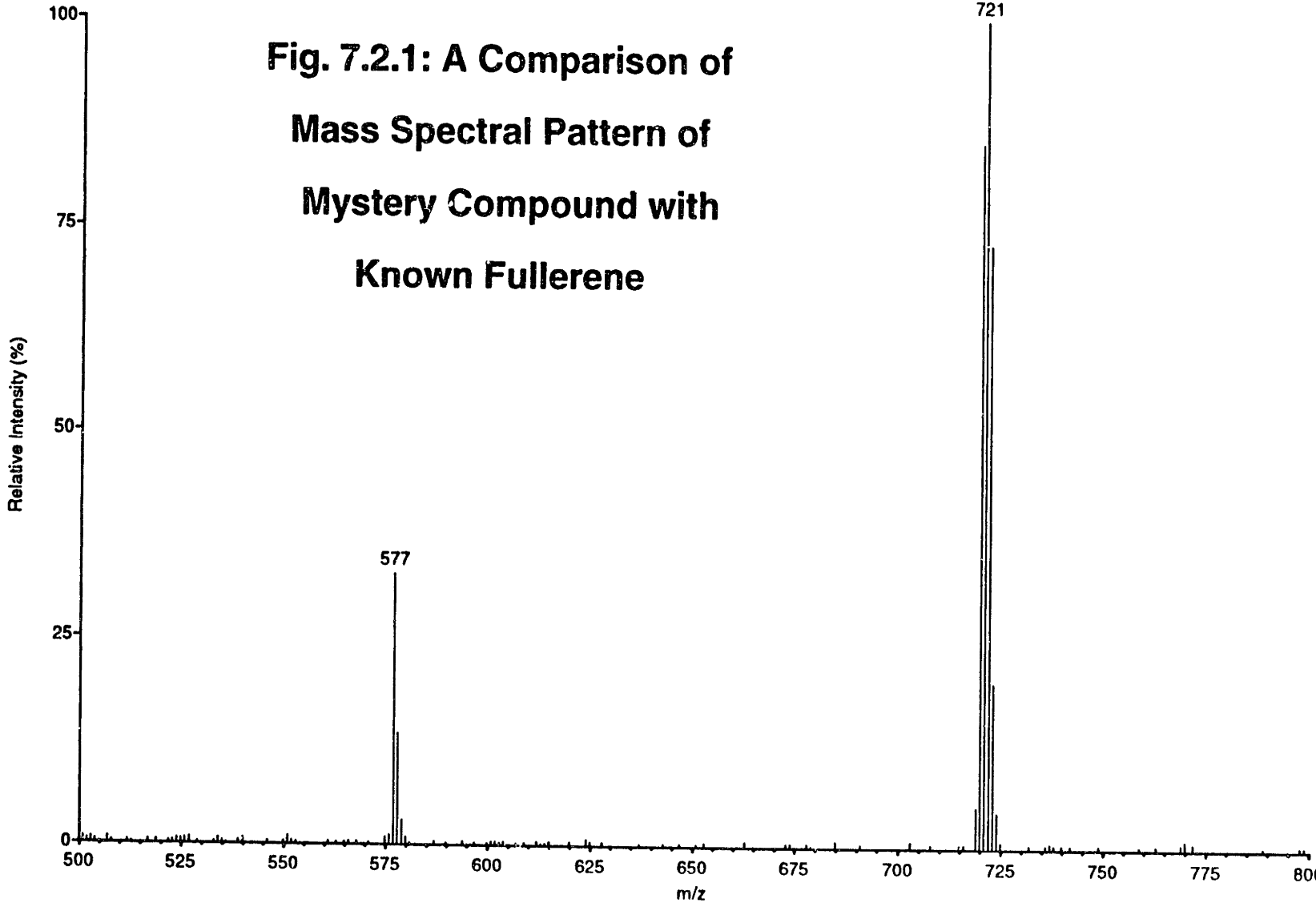

Total Ion Mass Spectra from LCMS

minus a couple of hydrogens), none of which are present..

Graph theory and stability constraints for a $C_{46}H_{24}$ PAH (see Appendix E) require that the molecule is not particularly condensed (no more than 4 carbons may be internal to the structure), which would result in a large number of isomers due to the extensive branching that becomes possible. None of the possible structures can be arrived at by mechanisms that would not also produce substantial amounts of related compounds (again, none of which are present in similar quantities). For example, it is very common to see series of PAHs sparated by mass units of 24 and 50 corresponding to ring forming additions of C_2 and C_4 species, respectively. Indeed, there is a series present in the product mixtures that goes 476, 526, 576, 626, etc, but it is very small compared to the molecule at 576 that is under investigation. In addition, no feature of any of the possible structures can explain why a 576 PAH in the series should be greater than an order of magnitude more abundant than the others in the series. More evidence against the 576 being part of a PAH series is that in every other case of series separated by 24 and 50 in this lab, there is aforementioned evidence of substantial "broadening" of the mass spec groupings due to successive losses of 2 hydrogens (the result of condensations in parallel pathways). This type of grouping is also characterized by alternating larger intensities for the even ions and lower intensities for the odd ions. These features are definitely not seen in the 576 grouping. Whereas most groupings in this size range broaden to 10-15 amu, the 576 peak belongs to a group whose width is no more than 5 amu.

Graph theory constraints also require that, if the molecule is a PAH, it must not contain an internal "hole" (a ring of larger than 6 carbons that is surrounded by other 5- and 6-membered rings). Nor can not be a dimer, or other combination of smaller PAHs connected

thru single bonds, because there are no combinations of constituent species present in the product mixture that could combine to form them. In addition, since no successive condensations are evident in the 576 mass grouping, the dimer (or trimer, etc) would have to be one in which there are no sites available for condensation. This would require the constituent monomers to be composed entirely of reactive sites that are in the beta position relative to any catacondensed carbon. This is impossible except for very simple constituents like benzene. Even for the case of polyphenyl or a variant thereof, there would still be many isomers that could condense as the 120 bond angles accumulated to enable ring formation involving several monomers.

From a graph theory point of view, it is evident that the molecule(s) in question cannot be "normal" PAH. However, the compound's UV spectrum looks like that for a PAH (or fullerene) (Fig. 7.2.2). This spectrum was obtained by using the LCMS to separate products using the same mobile phase and column as for the HPLC procedure, identifying the peak (and relative elution time) that was represented by the 576 molecule, performing the same run on the reverse phase HPLC, correlating the results with the LCMS run to identify which peak on the HPLC belonged to the molecule, and obtaining the UV-Vis spectra by the same means as for the biaryl products. This was possible only because the molecule eluted extremely early for a compound of it's molecular weight. With the methods of separation used, this indicates that the molecule is either very polar of very compact. The case of the latter would correspond to a fullerene, as the cross-sectional area of the expected C_{48} structure (Fig. 7.2.3) is approximate to that of anthracene, a compound with a similar elution time.

It should be noted that there is only one isomer of 576 that was detected in the HPLC/LCMS separation procedure. The fact that the peak occurs so far out of it natural

Fig. 7.2.2 UV-Vis Spectra of unknown MW 576 molecule

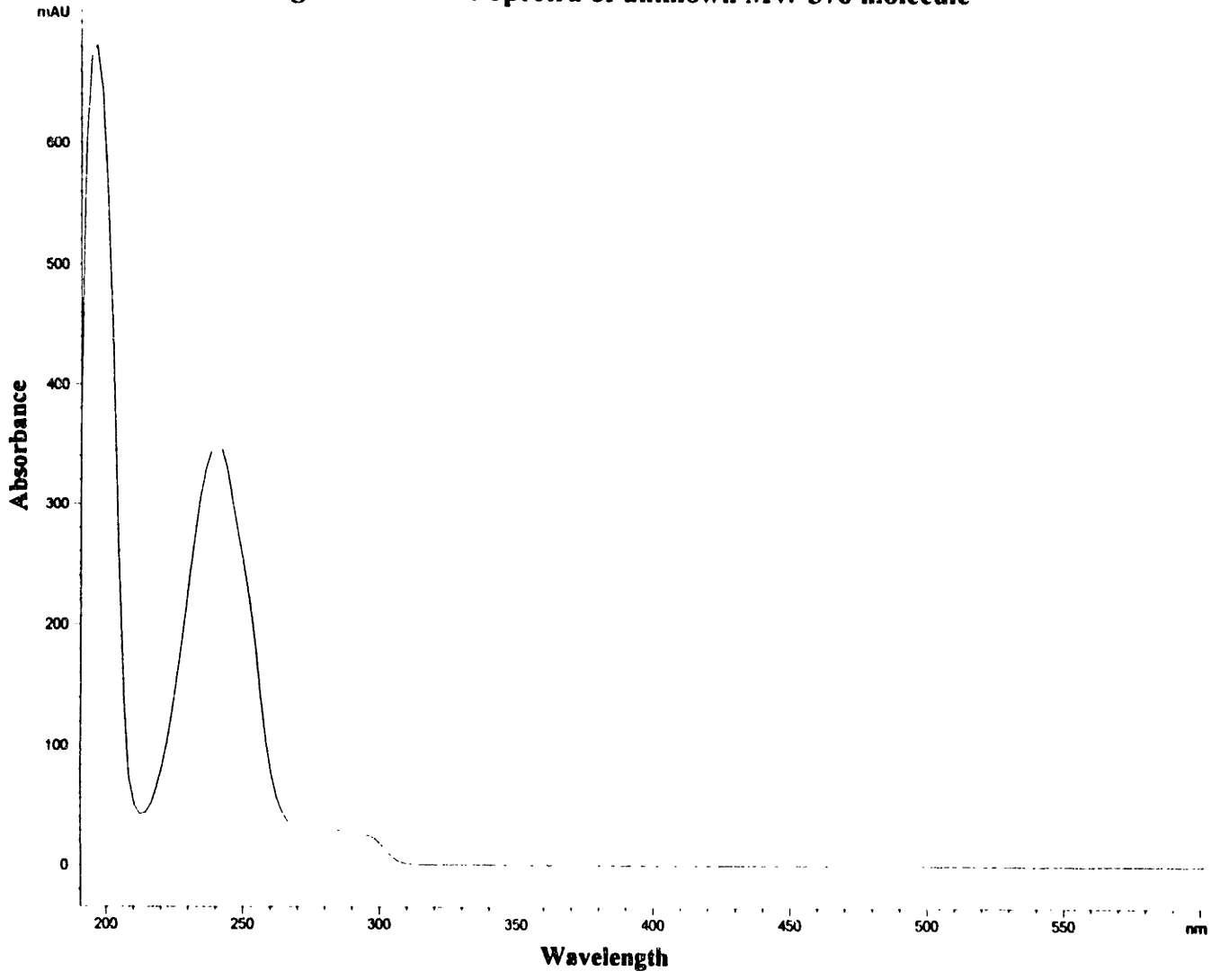

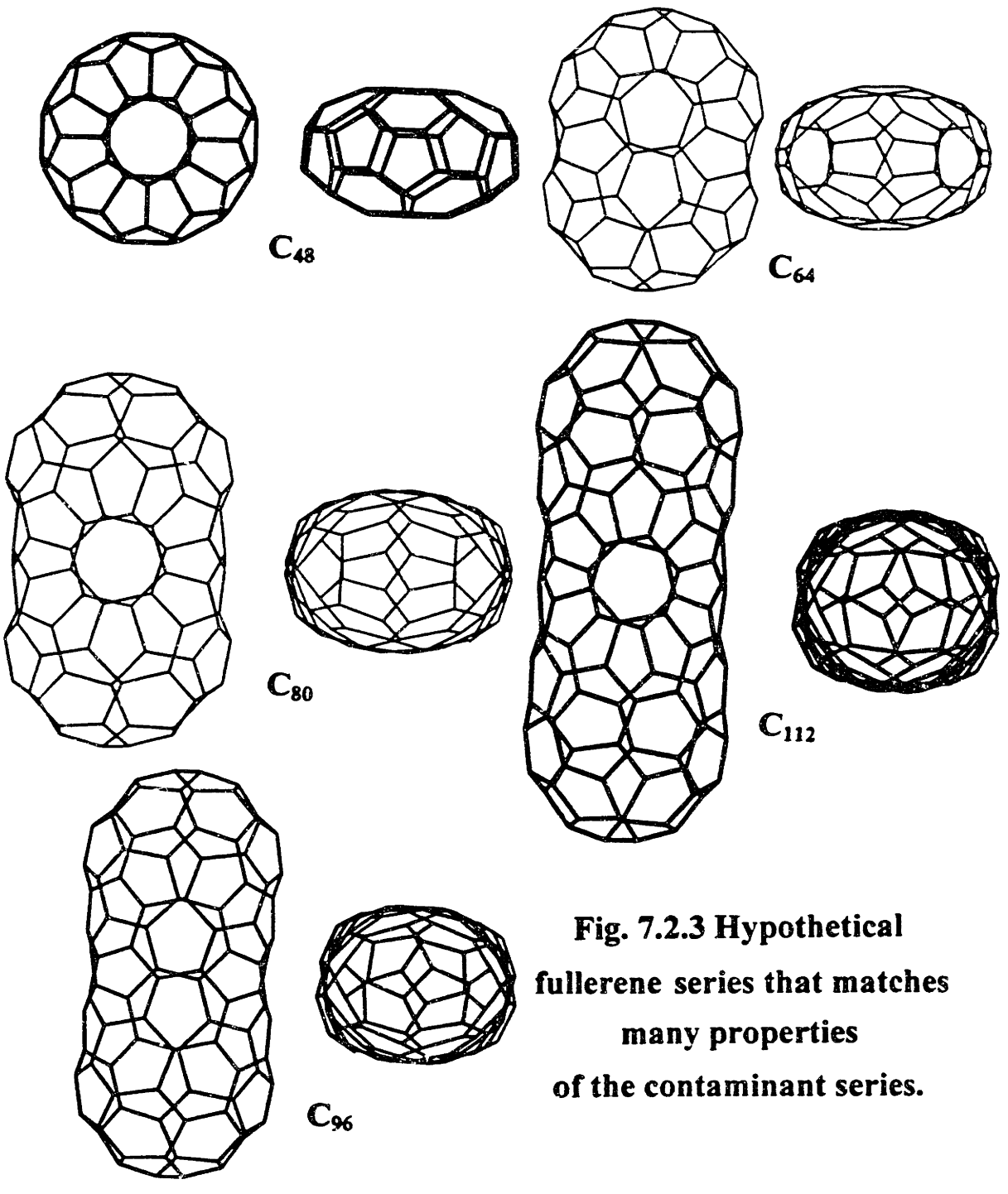

Fig. 7.2.3 Hypothetical fullerene series that matches many properties of the contaminant series.

position in PAH elution times, and that there is not evidence of the expected numerous isomers of the same molecular weight (which tend to elute at substantially different times, even for minor changes in geometry), strongly suggest that the molecule is not a plain PAH. Sensitivity to a certain MS run parameter (OR), for which PAHs in general are not very sensitive, provides further evidence that the molecule is not a PAH.

Another piece of circumstantial evidence that the molecule is not a PAH, is that, for a molecule this size and expected associated complexity, it's UV signal should have an associated complex pattern. Even small PAH that possess any degree of nonuniformity exhibit series of sharp peaks that shift higher in wavelength as you go higher in molecular weight. The UV spectrum for 576 is, however, smooth and almost featureless, and the majority of the obtainable spectrum falls below 270nm. This is not consistent with UV trends observed for PAHs.

With consideration of all of the above information, the likelihood of the mystery molecule being a PAH is virtually nonexistent. Only a highly polar compound or a fullerene would appear to fit the data available. As it's implications to pyrolysis chemistry would much more profound, and the analytical chemistry procedures needed would be easier to perform, the possibility of the molecule being a fullerene was investigated first.

As mentioned above, UV spectra and elution times of the 576 molecule are consistent with a fullerene. The response per mass in integrated UV signal (obtained by comparing relative abundances on HPLC chromatogram vs LCMS spectrum) is also similarly low - about a factor of 10 lower than that for PAHs - as is known to be the case for real fullerenes on the same equipment. The UV spectrum is also rather featureless and low in wavelength compared

to what would be expected for a corresponding weight PAH - just like the known fullerenes. But if the molecule is indeed a fullerene, what could its structure be?

The only known fullerenes that have been discovered obey the non-adjacent five-membered rings rule. Since every fullerene consisting of only five and six-membered rings must have exactly 12 five-membered rings (evident from simple graph theory calculations), this presents a problem for the existence of a fullerene smaller than C_{60}. If such a molecule were to exist, it must have a very special structure that would overcome instability due to neighboring five-membered rings. The proposed structure (Fig. 7.2.3), which amounts to two coronenes, stripped of their hydrogrens and joined together at the resulting dangling sigma bonds, fulfills the requirement quite nicely. A ring of 12 five-membered rings circumscribes the equator in this hypothetical fullerene, perhaps creating a special resonance structure that is able to offset any instabilities due to curvature. A ball and stick model indicates a curvature that is not as extensive as one might think.

The propsed structure has been modelled on MOPAC, and the heat of formation or geometry calculated did not indicate an unreasonable instability compared to other fullerenes. Only this isomer was tested - the possibility of other structures has not been exhaustively searched for, but it was deemed unnecessary for the following reason. All other possible isomers, if they even exist, would possess configurations of five membered rings would violate proximity principles in all cases. Only in the proposed structure do we have a unique feature that might explain its unusual stability despite the violation of the empirical "requirement" of non-neghboring 5 membered rings. The structure here is the most stable possible isomer that contains a circumscriptive ring of 5 membered rings.

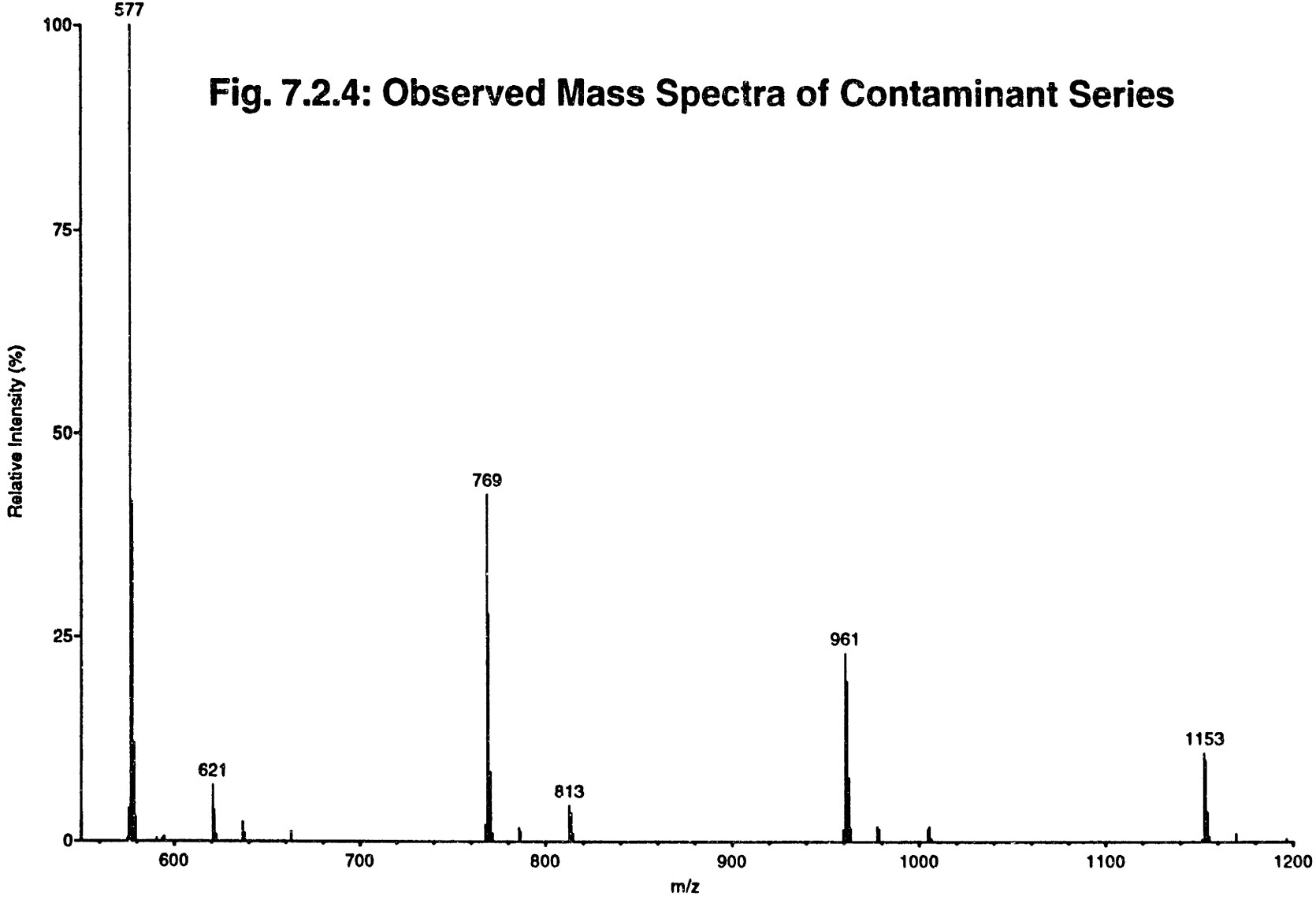

Fig. 7.2.4: Observed Mass Spectra of Contaminant Series

Total Ion Mass Spectra from LCMS

Since such a special structure does indeed exist for a hypothetical C_{48} fullerene species, the case for a fullerene is strengthened, but yet more evidence is found in the subsequent discovery of an entire series of compounds present in a highly concentrated version of the highest temperature naphthalene/anthracene pyrolysis sample, the sample that was found to contain the most of the mystery compound. Close inspection of this sample's total ion mass spectra revealed the presence of species that would correspond to C_{80} and C_{96} (Fig. 7.2.4). All of these compounds were present in very large quantities relative to the nearest molecular weight neighbors and to background noise. The small companion peaks are rationalized as being representative of weakly bound water or carbon dioxide adducts and/or molecules trapped in the cage structure -fullerene compound types that are known to occur with other molecules. Combined with C_{48} and C_{64} , these hypothetical fullerenes would form a series that 1) become tubes (perhaps even precursors to "buckytubes", the tube-like fullerene cousins that have been observed in laboratory experiments) at larger molecular weights (see Fig. 7.2.3), and 2) has a natural lower bound at 576, the exact cutoff for the experimentally observed series.

All of the above observations pointed strongly to the proposed fullerene series. Though the evidence was convincing as a whole, each individual piece was also uncomfortably circumstantial in nature. The mystery was fully-formed now, and all that remained was the answer to the dilemma of the true nature of the 576 compound.

7.3 - The Solution

The case for a fullerenic compound was becoming more convincing with every new piece of information that was obtained, but nothing was substantial enough to claim victory. An elemental analysis was needed, and the help of Steve McElvany and the Naval Research Lab's Tandem LCMS was called upon. The high resolution mass spectra for the 576 compound is shown in Fig. 7.3.1 and the mass fracture pattern of the 576 compound (as achieved with the tandem MS design by bombarding all ions of MW 576 that make it through the first mass spectrometer with Argon gas at 50 eV) is shown in Fig. 7.3.2. It is at this point that all theories of about a fullerene structure were abandoned. The high resolution spectrum indicates a shift of 0.1 to 0.2 amu of the base peak, and the ratio of the M+1 to M peaks, this time uninfluenced by the ability to adsorb a proton, are not consistent with natural ^{13}C abundances, both of which are consistent with the presence of atoms that are not carbon. A more detailed analysis of these two observations reveal a consistency with a molecule that contains 3-5 oxygens (no nitrogens or other heteroatoms are assumed due to the next observation) to every 10 carbons.

More damning is the observation that the fracture pattern clearly indicates the presence of water and carbon dioxide fragments, confirming the presence of oxygen in (and thus possible polarity of) the compounds, consistent with the early elution times observed in the HPLC and LCMS runs. No evidence of the usual fragments for molecules involving nitrogen or other atoms is found, and those atoms are thus assumed to not be present in the molecule. The mass spectral pattern also indicates a polymeric structure with a unit mass of 192, and a (loose) capping of ends with water, explaining both the

High Resolution Mass Spectrum of Contaminant 576

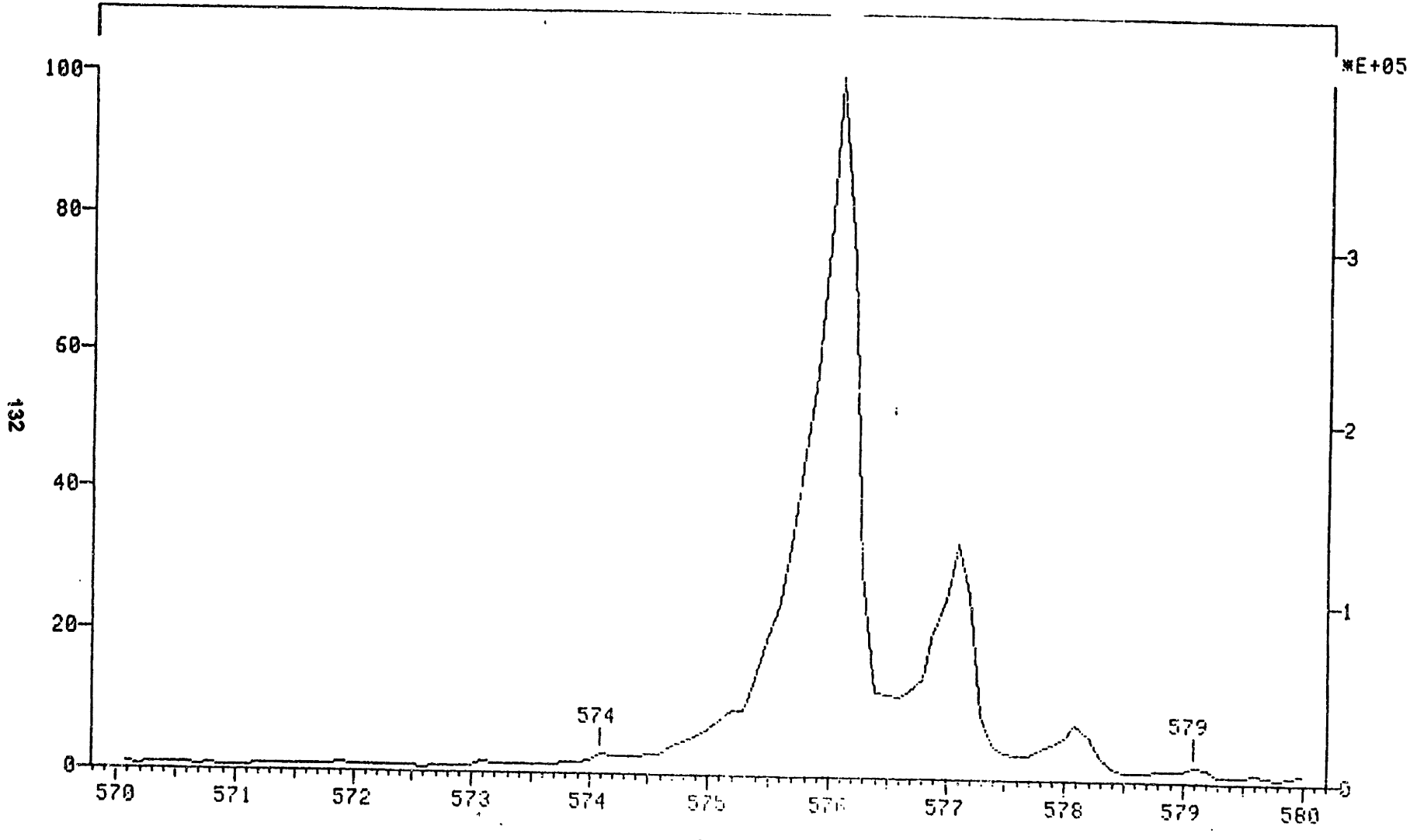

Fig. 7.3.1

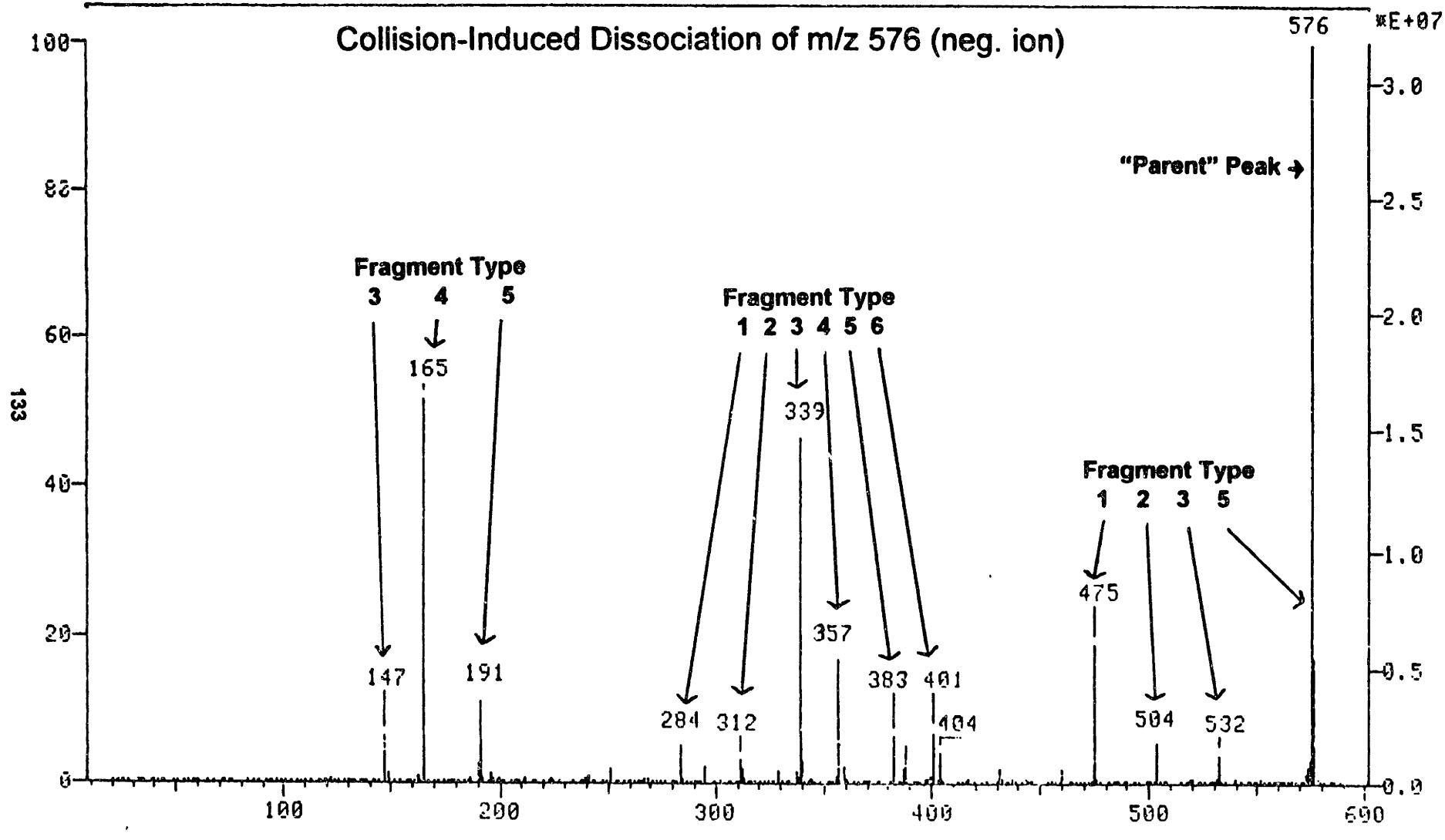
Collision-Induced Dissociation of m/z 576 (neg. ion)
*E+07
"Parent" Peak
576
Fragment Type
3 4 5
165
147
191
Fragment Type
1 2 3 4 5 6
339
284
312
357
383
401
404
Fragment Type
1 2 3 5
475
504
532
133
100
80
60
40
20
0
3.0
2.5
2.0
1.5
1.0
0.5
0.0
100
200
300
400
500
600

Fig. 7.3.2

observed series of base peaks separated by 192 that are also multiples of 192 in molecular weight, and the presence of small companion peaks to those base peaks that are 17-18 mass units higher than the base peak.

To be most consistent with the available data from the tandem mass spectrometer and knowledge about the PAH nature of the UV spectrum, the polymeric unit is thus believed to contain at least one ring and exactly 4 oxygens. By referring to McLafferty and Turecek (1993), the mass spectral fracturing pattern is also indicative of a phthalate that can cyclize to form a acid anhydride or lactone, consistent with the count of 4 oxygens per unit. That compound can only be one of the ethylene phthalate isomers.

A poly(ethylene terephthalate) (PET) standard (Aldrich Cat. No. 25038-59-9) is thus run on the LCMS apparatus and is found to produce the same series of mass fragments with their respective relative abundances as is observed in the samples (576, 768, 960, 1152, etc.). Note that the curious chopping off of the series at the trimer is also observed for the standard, indicating that such an observation is a characteristic of that molecule on this apparatus. Though PET should be unable to directly cyclize to the acid anhydride or lactone, it may be able to form comparable mass ions through a different mechanism. The fact that PET is a widely available plastic might also explain its abundance in the samples as a possible contaminant.

Cursory investigations were made into the source of the plastic contaminant, and a blank filter on which all procedures except using actual fuel were performed, turned up negative for the contaminant. The source of the contaminant is still a mystery, but it has since been found in other old samples from other researchers in the same lab on

completely unrelated sampling equipment, indicating a common source that does not involve the reactor or the fuel.

7.3 - Conclusions

A rather involved process of elimination has led to the identification of a contaminant that mimics many properties of a certain hypothetical series of fullerenes. Such an identification was crucial to this thesis, as the presence of fullerenes in the pyrolysis samples would greatly influence the conclusions made here and the methods used to model them. Previously unrecognized by this lab due to the unavailability of an analytical technique that could detect the compound, poly (ethylene terephthalate) has shown the vulnerability of samples to external contaminants, and recognition of this will (and should) influence the cautiousness of this and any lab in interpreting new results.

Chapter Eight - The Kinetic Model

8.1 - Introduction

The proof for kinetic control of the polymerization/condensation pathway to molecular weight growth is almost complete. A broader picture of the mechanism than only biaryl formation is needed, however, to fully investigate the implications of the proposed hypothesis. In the interest of gaining this insight, a kinetic model is developed to model the experimental observations. The naphthalene/anthracene experiment is chosen to model over the ortho-terphenyl in the interest of simplicity. The naphthalene/anthracene model requires a basis reaction set of approximately 2150 reactions to model growth to 700 MW. The ortho-terphenyl experiment, however, would require many more reactions, many of which would require the use of highly contested or unknown kinetic parameters and mechanisms, due to the abundance of ring rupture and rearrangement products. It is not suggested that such compounds don't exist in the naphthalene/anthracene pyrolysis experiments. Rather, the alternate pathway products are just present in smaller quantities in these samples and neglecting the importance of these mechanisms can more easily be justified.

8.2 - The Programs - THERM

Two computer programs are used in testing the kinetic model. The first is THERM, developed by Ritter and Bozelli (1991). It is used to calculate thermodynamic

properties of molecules, including heat and entropy of formation and heat capacities, using the estimation technique of group additivity described by Benson (1976), with several minor additions to encompass radical formation at different arene sites.

Radical estimation for this model uses those values for entropy and heat capacity that are provided for by the THERM program, with bond dissociation energies (BDEs - used by THERM to estimate heats of formation of the radical in question) replaced with literature values for anthracene and naphthalene radicals taken from Chen et al. (1989). It should be noted here that a key feature of this mechanism is that most of the compounds used are lumped. That is, one "compound" is used to represent the combined concentrations and thermodynamic properties of a multitude of closely related isomers - in some cases, up to 20,000. This substantially reduces the number of reactions needed for an already large mechanism. Consequently, most radical species in the mechanism carry lumped properties representative of their group type. A lumped BDE, taken as the weighted average over all isomers, each contributing equally, regardless of actual contribution in a reaction mixture, is thus used to approximate the BDE of that class of molecules in the mechanism. Although not strictly correct due to the exponential (not linear) nature of the contribution of BDEs to radical populations in a chemical mixture, the small differences in bond dissociation energies involved make the linear approximation a good one (within 0.2 kcal in the worst cases - close to the uncertainty in the BDE's themselves) and it's ease in application to the complex molecules involved far outweigh any shortcomings in the model due to the inaccuracies incurred.

Selection of group contributions is fairly straightforward for most of the compounds in the model; see Fig. 8.2.1 for group types and Table 8.2.1 for group

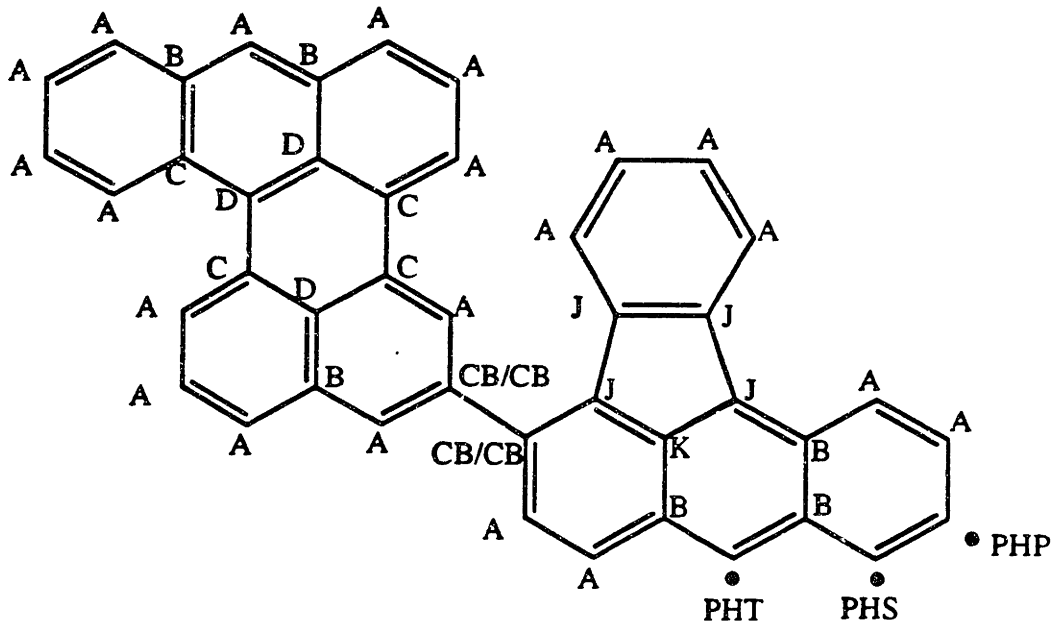

Fig. 8.2.1 Definition of Benson group types used to estimate thermodynamic properties with THERM.

contributions used to calculate molecular properties. As with the BDE calculations, some consideration for using an "average" or "typical" compound to represent an isomer group type must be taken into account in calculating properties of lumped compounds. For ease in utilizing the group additivity values available within the THERM program, a hypothetical "typical" compound is used that contains integer contributions of various group types that would be represented in such a compound, with consideration given to trends in numbers of each group type with growing molecular weight and condensation. For example, a replacement of a naphthalene component in a lumped condensed compound (such as C1NNN - see Appendix D for compound notation) with the equivalently condensed anthracene component (resulting in C1NNA) in a compound results in approximately 2 additional type A groups, 1 additional type B group, 1/2

Table 8.2.1 Benson Groups and BDEs Used in Model

Species	Description	BDE	Groups A	B	CB/C	C	D	J	K	Symmetry
N2	nitrogen		0	0	0	0	0	0	0	2.000E+00
h	H radical	52.1	0	0	0	0	0	0	0	1.000E+00
h2	hydrogen		0	0	0	0	0	0	0	2.000E+00
n	naphthalene		8	2	0	0	0	0	0	4.000E+00
a	anthracene		10	4	0	0	0	0	0	4.000E+00
n1-	1-naphthyl	107.7	8	2	0	0	0	0	0	1.000E+00
n2-	2-naphthyl	108.6	8	2	0	0	0	0	0	1.000E+00
a1-	1-anthryl	107.8	10	4	0	0	0	0	0	1.000E+00
a2-	2-anthryl	109.1	10	4	0	0	0	0	0	1.000E+00
a9-	9-anthryl	106.8	10	4	0	0	0	0	0	2.000E+00
n1n1	1,1'-binaphthalene		14	4	2	0	0	0	0	2.000E+00
n1n1-1	condensible 1' rad	107.7	14	4	2	0	0	0	0	1.000E+00
n1n1-2	condensible 2' rad	108.6	14	4	2	0	0	0	0	1.000E+00
n1n1-4	noncondens.rad.	108.2	14	4	2	0	0	0	0	2.000E-01
n1n2	1,2'-binaphthalene		14	4	2	0	0	0	0	1.000E+00
n1n2-1	condensible 1' rad	107.7	14	4	2	0	0	0	0	5.000E-01
n1n2-2	condensible 2' rad	108.6	14	4	2	0	0	0	0	1.000E+00
n1n2-4	noncondens.rad.	108.2	14	4	2	0	0	0	0	9.091E-02
n2n2	2,2'-binaphthalene		14	4	2	0	0	0	0	2.000E+00
n2n2-4	noncondens.rad.	108.1	14	4	2	0	0	0	0	1.429E-01
a1n1	1(1'naphthyl)anthr		16	6	2	0	0	0	0	1.000E+00
a1n1-1	condensible 1' rad	107.8	16	6	2	0	0	0	0	1.000E+00
a1n1-2	condensible 2' rad	108.8	16	6	2	0	0	0	0	5.000E-01
a1n1-3	condensible 9' rad	106.8	16	6	2	0	0	0	0	1.000E+00
a1n1-4	noncondens.rad.	108.2	16	6	2	0	0	0	0	8.333E-02
a1n2	1(2'naphthyl)anthr		16	6	2	0	0	0	0	1.000E+00
a1n2-1	condensible 1' rad	107.7	16	6	2	0	0	0	0	1.000E+00
a1n2-2	condensible 2' rad	108.6	16	6	2	0	0	0	0	1.000E+00
a1n2-3	condensible 9' rad	106.8	16	6	2	0	0	0	0	1.000E+00
a1n2-4	noncondens.rad.	108.2	16	6	2	0	0	0	0	7.692E-02
a2n1	2(1'naphthyl)anthr		16	6	2	0	0	0	0	1.000E+00
a2n1-1	condensible 1' rad	107.8	16	6	2	0	0	0	0	5.000E-01
a2n1-2	condensible 2' rad	109.1	16	6	2	0	0	0	0	1.000E+00
a2n1-4	noncondens.rad.	108.1	16	6	2	0	0	0	0	7.692E-02
a2n2	2(2'naphthyl)anthr		16	6	2	0	0	0	0	1.000E+00
a2n2-4	noncondens.rad.	108	16	6	2	0	0	0	0	6.250E-02
a9n1	9(1'naphthyl)anthr		16	6	2	0	0	0	0	1.000E+00
a9n1-1	condensible 1' rad	107.8	16	6	2	0	0	0	0	3.333E-01
a9n1-2	condensible 2' rad	108.6	16	6	2	0	0	0	0	1.000E+00
a9n1-4	noncondens.rad.	108.3	16	6	2	0	0	0	0	8.333E-02
a9n2	9(2'naphthyl)anthr		16	6	2	0	0	0	0	1.000E+00
a9n2-1	condensible 1' rad	107.8	16	6	2	0	0	0	0	3.333E-01
a9n2-2	condensible 2' rad	108.6	16	6	2	0	0	0	0	1.000E+00
a9n2-4	noncondens.rad.	108.3	16	6	2	0	0	0	0	8.333E-02
a1a1	1,1'-bianthracene		18	8	2	0	0	0	0	2.000E+00
a1a1-2	condensible 2' rad	109.1	18	8	2	0	0	0	0	1.000E+00
a1a1-3	condensible 9' rad	106.8	18	8	2	0	0	0	0	1.000E+00
a1a1-4	noncondens.rad.	108.2	18	8	2	0	0	0	0	1.429E-01
a1a2	1,2'-bianthracene		18	8	2	0	0	0	0	1.000E+00
a1a2-1	condensible 1' rad	107.8	18	8	2	0	0	0	0	1.000E+00
a1a2-2	condensible 2' rad	109.1	18	8	2	0	0	0	0	1.000E+00
a1a2-3	condensible 9' rad	106.8	18	8	2	0	0	0	0	1.000E+00
a1a2-4	noncondens.rad.	108.1	18	8	2	0	0	0	0	6.667E-02
a1a9	1,9'-bianthracene		18	8	2	0	0	0	0	1.000E+00
a1a9-1	condensible 1' rad	107.8	18	8	2	0	0	0	0	5.000E-01
a1a9-2	condensible 2' rad	109.1	18	8	2	0	0	0	0	1.000E+00
a1a9-3	condensible 9' rad	106.8	18	8	2	0	0	0	0	1.000E+00
a1a9-4	noncondens.rad.	108.3	18	8	2	0	0	0	0	7.143E-02
a2a2	2,2'-bianthracene		18	8	2	0	0	0	0	2.000E+00

a2a2-4	noncondens.rad.	108	18	8	2	0	0	0	0	1.111E-01
a2a9	2,9'-bianthracene		18	8	2	0	0	0	0	1.000E+00
a2a9-1	condensible 1' rad	107.8	18	8	2	0	0	0	0	3.333E-01
a2a9-2	condensible 2' rad	109.1	18	8	2	0	0	0	0	1.000E+00
a2a9-4	noncondens.rad.	108.1	18	8	2	0	0	0	0	7.143E-02
a9a9	9,9'-bianthracene		18	8	2	0	0	0	0	4.000E+00
a9a9-1	condensible 1' rad	107.8	18	8	2	0	0	0	0	1.000E+00
a9a9-4	noncondens.rad.	108.4	18	8	2	0	0	0	0	1.538E-01
BkF	benzo(k)fluoranthe		12	3	0	0	0	4	1	2.000E+00
BjF	benzo(j)fluoranthe		12	2	0	1	0	4	1	1.000E+00
Per	perylene		12	2	0	4	2	0	0	4.000E+00
DBajF	dibenzo(aj)fluoran		14	3	0	2	0	4	1	1.000E+00
DBakF	dibenzo(ak)fluoran		14	5	0	0	0	4	1	1.000E+00
DBalF	dibenzo(al)fluoran		14	3	0	2	0	4	1	1.000E+00
BaPer	benzo(a)perylene		14	3	0	5	2	0	0	1.000E+00
N23jF	naphtho(2,3-j)fluo		14	4	0	1	0	4	1	1.000E+00
N23kF	naphtho(2,3-k)fluo		14	5	0	0	0	4	1	2.000E+00
BaN23jF	B(a)N(2,3-j)fluora		16	5	0	2	0	4	1	1.000E+00
BaN23kF	B(a)N(2,3-k)fluora		16	6	0	1	0	4	1	1.000E+00
BaN23lF	B(a)N(2,3-l)fluora		16	5	0	2	0	4	1	1.000E+00
DBajPer	dibenzo(aj)perylen		16	4	0	6	2	0	0	2.000E+00
DBaoPer	dibenzo(ao)perylen		16	4	0	6	2	0	0	2.000E+00
BkF-	radical	108	12	3	0	0	0	4	1	1.667E-01
BjF-	radical	108.1	12	2	0	1	0	4	1	8.333E-02
Per-	radical	108.1	12	2	0	4	2	0	0	3.333E-01
DBajF-	radical	108.1	14	3	0	2	0	4	1	7.143E-02
DBakF-	radical	107.9	14	5	0	0	0	4	1	7.143E-02
DBalF-	radical	108.1	14	3	0	2	0	4	1	7.143E-02
BaPer-	radical	108.1	14	3	0	5	2	0	0	7.143E-02
N23jF-	radical	107.9	14	4	0	1	0	4	1	7.143E-02
N23kF-	radical	107.8	14	5	0	0	0	4	1	1.429E-01
BaN23jF-	radical	107.9	16	5	0	2	0	4	1	6.250E-02
BaN23kF-	radical	107.8	16	6	0	1	0	4	1	6.250E-02
BaN23lF-	radical	107.9	16	5	0	2	0	4	1	6.250E-02
DBajPer-	radical	108	16	4	0	6	2	0	0	1.250E-01
DBaoPer-	radical	108	16	4	0	6	2	0	0	1.250E-01
NNN	trinaphthyl		20	6	4	0	0	0	0	4.082E-02
NNA	binaphthyl-anthryl		22	8	4	0	0	0	0	8.889E-03
NAA	naphthyl-bianthryl		24	10	4	0	0	0	0	5.222E-03
AAA	trianthryl		26	12	4	0	0	0	0	1.130E-02
NNN-	radical	108.2	20	6	4	0	0	0	0	2.041E-03
NNA-	radical	108.1	22	8	4	0	0	0	0	4.040E-04
NAA-	radical	108.1	24	10	4	0	0	0	0	2.176E-04
AAA-	radical	108.1	26	12	4	0	0	0	0	4.346E-04
NNNN	tetranaphthyl		26	8	6	0	0	0	0	3.185E-03
NNNA	trinaphthyl-anthry		28	10	6	0	0	0	0	4.593E-04
NNAA	binaphthyl-bianthr		30	12	6	0	0	0	0	1.755E-04
NAAA	naphthyl-trianthry		32	14	6	0	0	0	0	1.548E-04
AAAA	tetraanthryl		34	16	6	0	0	0	0	3.993E-04
NNNN-	radical	108.2	26	8	6	0	0	0	0	1.225E-04
NNNA-	radical	108.1	28	10	6	0	0	0	0	1.641E-05
NNAA-	radical	108.1	30	12	6	0	0	0	0	5.850E-06
NAAA-	radical	108.1	32	14	6	0	0	0	0	4.839E-06
AAAA-	radical	108.1	34	16	6	0	0	0	0	1.174E-05
NNNNN	pentanaphthyl		32	10	8	0	0	0	0	1.629E-04
NNNNN-	radical	108.2	32	10	8	0	0	0	0	5.091E-06
C1NNN	NNN w/ one condens		18	5	2	1	1	2	1	2.381E-02
C1NNA	NNA w/ one condens		20	6	2	2	1	2	1	4.608E-03
C1NAA	NAA w/ one condens		22	7	2	2	1	3	1	2.786E-03
C1AAA	AAA w/ one condens		24	8	2	3	1	3	1	5.208E-03
C2NNN	NNN w/ two condens		16	4	0	2	2	4	2	7.692E-02
C2NNA	NNA w/ two condens		18	5	0	3	2	4	2	1.258E-02
C2NAA	NAA w/ two condens		20	6	0	3	2	5	2	7.812E-03
C2AAA	AAA w/ two condens		22	7	0	4	2	5	2	1.220E-02
C1NNN-	radical	108.1	18	5	2	1	1	2	1	1.323E-03
C1NNA-	radical	108	20	6	2	2	1	2	1	2.304E-04
C1NAA-	radical	108	22	7	2	2	1	3	1	1.266E-04

C1AAA-	radical	108	24	8	2	3	1	3	1	2.170E-04
C2NNN-	radical	107.9	16	4	0	2	2	4	2	4.808E-03
C2NNA-	radical	107.8	18	5	0	3	2	4	2	6.988E-04
C2NAA-	radical	107.8	20	6	0	3	2	5	2	3.906E-04
C2AAA-	radical	107.8	22	7	0	4	2	5	2	5.543E-04
C1NNNN	NNNN w/ one conden		24	7	4	1	1	2	1	1.129E-03
C1NNNA	NNNA w/ one conden		26	8	4	2	1	2	1	1.566E-04
C1NNAA	NNAA w/ one conden		28	9	4	2	1	3	1	6.215E-05
C1NAAA	NAAA w/ one conden		30	10	4	3	1	3	1	5.563E-05
C1AAAA	AAAA w/ one conden		32	11	4	3	1	4	1	1.335E-04
C2NNNN	NNNN w/ two conden		22	6	2	2	2	4	2	1.571E-03
C2NNNA	NNNA w/ two conden		24	7	2	3	2	4	2	1.960E-04
C2NNAA	NNAA w/ two conden		26	8	2	3	2	5	2	7.291E-05
C2NAAA	NAAA w/ two conden		28	9	2	4	2	5	2	6.177E-05
C2AAAA	AAAA w/ two conden		30	10	2	4	2	6	2	1.349E-04
C3NNNN	NNNN w/ three cond		20	5	0	2	3	8	2	7.326E-03
C3NNNA	NNNA w/ three cond		22	6	0	3	3	8	2	1.305E-03
C3NNAA	NNAA w/ three cond		24	7	0	4	3	8	2	3.217E-04
C3NAAA	NAAA w/ three cond		26	8	0	4	3	9	2	2.714E-04
C3AAAA	AAAA w/ three cond		28	9	0	5	3	9	2	3.888E-04
C1NNNN-	radical	108.1	24	7	4	1	1	2	1	4.705E-05
C1NNNA-	radical	108.1	26	8	4	2	1	2	1	6.021E-06
C1NNAA-	radical	108	28	9	4	2	1	3	1	2.220E-06
C1NAAA-	radical	108	30	10	4	3	1	3	1	1.854E-06
C1AAAA-	radical	108	32	11	4	3	1	4	1	4.171E-06
C2NNNN-	radical	108	22	6	2	2	2	4	2	7.141E-05
C2NNNA-	radical	108	24	7	2	3	2	4	2	8.165E-06
C2NNAA-	radical	107.9	26	8	2	3	2	5	2	2.804E-06
C2NAAA-	radical	107.9	28	9	2	4	2	5	2	2.206E-06
C2AAAA-	radical	107.9	30	10	2	4	2	6	2	4.496E-06
C3NNNN-	radical	107.9	20	5	0	2	3	8	2	3.663E-04
C3NNNA-	radical	107.9	22	6	0	3	3	8	2	5.930E-05
C3NNAA-	radical	107.8	24	7	0	4	3	8	2	1.340E-05
C3NAAA-	radical	107.8	26	8	0	4	3	9	2	1.044E-05
C3AAAA-	radical	107.8	28	9	0	5	3	9	2	1.389E-05
C1NNNNN	NNNNN w/ 1 cond.		30	9	6	1	1	2	1	4.878E-05
C2NNNNN	NNNNN w/ 2 cond.		28	8	4	2	2	4	2	4.232E-05
C3NNNNN	NNNNN w/ 3 cond.		26	7	2	3	2	8	2	1.018E-04
C4NNNNN	NNNNN w/ 4 cond.		24	6	0	4	3	10	3	1.718E-03
C1NNNNN-	radical	108.1	30	9	6	1	1	2	1	1.626E-06
C2NNNNN-	radical	108	28	8	4	2	2	4	2	1.511E-06
C3NNNNN-	radical	108	26	7	2	3	2	8	2	3.913E-06
C4NNNNN-	radical	107.9	24	6	0	4	3	10	3	7.159E-05

additional type C group, and 1/2 additional type J group, on average. Condensation, similarly, results in loss of 2 A groups, loss of 1 B group, loss of 2 CB/CB groups, gain of 1 C group, gain of 1 D group, gain of 2 J group, and gain of 1 K group, on average. Note that these approximations only affect the higher molecular weight condensed species; group contributions for polyaryls and for the first generation condensed species (BjF, BkF, etc) are quite straightforward and do not require these additional approximations.

In calculating thermodynamic properties for the biaryls, some additional information about steric hindrance is needed beyond that which THERM can provide. Without steric hindrance considerations, each biaryl of a given type (binaphthalenes, naphthyl/anthracenes, bianthracenes) will possess the exact same thermodynamic parameters as their counterparts in the same group since they all depend on the same group contributions. This is very undesirable since the testing of the kinetic model will include a check of the accuracy in predicting relative biaryl concentrations, expected to be quite sensitive to changes in thermodynamic parameters. Fortunately, a solution is readily obtainable. Since the CB/CB group contribution used in Benson's method is most likely strongly based on the simplest polyaryl available - biphenyl - and that compound is calculated (Mulholland et al., 1993a,b) to have steric hindrance properties that are similar to the least hindered biaryl products in each series (2,2'-binaphthalene, 2-(2'-naphthyl)anthracene, and 2,2'-bianthracene), as reflected by enthalpy of formation and angle of rotation of the internal rotor (see Table 4.3.1). The heat of formation for each of the biaryl products (and their respective radicals), as calculated by THERM, will therefore be modified by adding increases in enthalpy due to steric hindrance relative to the most stable isomer in each series, using values from the previous MOPAC calculations (Chapter 3, 4).

One more consideration must be in place before the thermodynamics as calculated by THERM are usable by CHEMKIN. That is the symmetry factor. As symmetry factors in the traditional strict sense (Benson, 1976, Nicholas, 1976) are no longer valid for lumped compounds, a new definition must be made for a lumped symmetry number that,

when applied to the kinetic model via the calcuated thermodynamic parameters, results in the correct rate constants for the back reactions. This will be done in the intuitive tradition of Laidler (1969), where real statistical factors are used to define a non-integral symmetry number rather than the more theoretically based (but more perilous) method of doing the reverse. The dilemma is as follows - consider the following reaction involving a lumped compound (NNN):

n2n2(2,2'-binap.) + n1-(1'-naphthyl) <===> NNN(trinaphthalene) + h(hydrogen radical)

Naphthalene has a symmetry number of 4, and n1- and h both have symmetry numbers of 1, by the formal definition. It is tempting to use a symmetry number of 1 for trinaphthalene also, since only a very small percentage of the isomers represented by this group possess any symmetry at all. Using such a symmetry number, however, is very unrealistic when we consider what is happening in the reverse reaction. Only a fraction of the reverse reaction actually goes back to the listed reactants. Many possibilities are available for decomposition of NNN other than to n2n2 and n1-. That fraction that does go back to these specific products is dependent on the fraction of NNN that can directly decompose into n2n2 and n1- (eg, a connectivity of 2, 2, and 1 - naphthalene is needed among the 4 connection sites, with the first two along the same linking bond), and the fraction collisions with hydrogen that occur at the correct site.

There are 29 isomers of NNN that do not violate the rules set forth in the next section, 9 of which have a symmetry number of 2. Only 7 (all symmetry number 1) of

these compounds can result in a reaction that goes back to n2n2 and n1-, and at only one site of hydrogen attack each. As the mole fraction of an individual isomer, at approximate equilibrium with the others in its group, can be expected to be inversely proportional to its symmetry number, a back reaction statistical factor of 7/(20+9/2) is thus needed to achieve the correct reverse rate constant. Note that the forward reaction requires the application of a statistical factor of 14 to the standard polymerization A factor to get a correct rate since there are 14 sites available for attack by the n1- radical on n2n2. Since the ratio of products of reactant symmetry numbers to product symmetry numbers must equal the ratio of forward to back statistical factors, an empirical symmetry number of 1/(20+9/2) is needed to describe the symmetry of the NNN lumped species.

The question now arises of how a symmetry number for a lumped compound might be defined in general. Since 1) the 7 arises due to the number of reactive sites on n2n2 being 14 and its symmetry number being 2, (ie, from known symmetry numbers and forward statistical factors already accounted for in previous kinetic theories), 2) the back reaction rate should be scaled inversely to the total number of isomers (discounted by symmetry number) and 3) the ratio of forward to reverse statistical factors should equal the ratio of reactant to product symmetry numbers, a natural definition of a lumped symmetry number becomes:

$$\sigma \equiv \frac{1}{\sum_{isomers} \frac{1}{\sigma}}$$

It is comforting to note that this reverts to the regular symmetry number for the case of a one compound group (a standard, well-defined molecule). The "resistance in parallel"-like

behavior of the symmetry number is also consistent with the notion that individual contributions of symmetry to the whole are dependent on the available parallel reaction pathways to formation of the lumped compound, the rates of which are hindered directly by symmetries of the products. Application of this definition for a lumped symmetry number to a number of other types of reactions confirms the reliability of this technique for use on the entire mechanism. Errors in back reaction statistical factors are all due to the artificial limitations about neighboring reactive sites that are imposed in the next section to keep the mechanism to a manageable size, and are never more than 10-15%. This method is considerably better than simply assuming a symmetry number of 1 for all lumped compounds. Indeed, in some cases, this can result in back reaction rates that are off by 3 or 4 orders of magnitude for the larger compounds used in this mechanism.

A detailed analysis of the isomer counting procedure is too straighforward and long to be appropriately included in this thesis document, so only the results are reported. The column labelled "Symmetry" in Table 8.2.1 lists the effective lumped symmetry numbers that are used as input into the THERM program. As THERM accepts only integer input of symmetry numbers, the factors were put in by hand by subtracting R ln σ from the value of entropy of formation calculated by THERM.

All of the considerations necessary to perform the THERM calculations are now complete. Results of the THERM calculations in the NASA format used as input for CHEMKIN are shown in Appendix F.

8.3 - The Programs - CHEMKIN

The second program that is used in testing the kinetic model is CHEMKIN (Kee et al., 1989). Considerations involving the theory and use of CHEMKIN are significantly less troublesome that those described above for the THERM program, due to the fact that most of the unusual treatments that are required when using lumped compounds are already implicit in the thermodynamic parameters as calculated by THERM, and the rest are noted in the section on the mechanism (Ch. 8.4).

The first consideration to be examined is what reactor code to use. Plug flow is assumed in modeling of the laminar flow drop tube reactor in an attempt to keep calculation time down. Though obviously not what one would ideally choose, the approximation is considered resonable enough considering the other approximations that have been made in the mechanism. Another advantage of assuming plug flow is in the availability of a standard reactor code known as SENKIN (Lutz et al., 1988), for use with CHEMKIN as a plug-flow simulator in an unmodified form.

The only other considerations required for CHEMKIN are the input parameters. Temperature for each simulation is taken to be that of the experimental run it is attempting to model. Pressure is taken to be 0.95 atm in all cases. Input mole fractions of anthracene, naphthalene, and nitrogen are calculated for each run based on gas flow rate (4.8 standard lpm), and the measured amount of fuel that was used over the approximate two minute sampling event. Residence times were calculated based on bulk gas flow rate, corrected for temperature-induced expansion. A list of the parameters used in each run can be found in Table 8.3.1. The input mechanism used by CHEMKIN is shown in

Table 8.3.1 A List of CHEMKIN Run Parameters

Temp. (K)	N_2	anthracene (mole percent)	naphthalene	Res. Time	Comments
1177	0.99855	0	0.00145	2.09	
1277	0.99666	0	0.00334	1.93	Pure
1350	0.99308	0	0.00692	1.82	Naphthalene
1415	0.99647	0	0.00353	1.74	Runs
1498	0.99517	0	0.000483	1.64	
1180	0.99885	0.000575	0.000575	2.09	
1277	0.998382	0.000809	0.000809	1.93	Naphthalene/
1348	0.998174	0.000913	0.000913	1.83	Anthracene
1416	0.99725	0.001375	0.001375	1.74	Runs
1496	0.999032	0.000484	0.000484	1.65	
1181	0.99776	0.00224	0	2.08	
1278	0.99025	0.000975	0	1.93	Pure
1350	0.99890	0.00110	0	1.82	Anthracene
1415	0.99877	0.00123	0	1.74	Runs
1496	0.99202	0.000798	0	1.65	
1180	0.99885	0.000575	0.000575	2000	Naphthalene/
1277	0.998382	0.000809	0.000809	2000	Anthracene
1348	0.998174	0.000913	0.000913	2000	Approximate
1416	0.99725	0.001375	0.001375	2000	Equilibrium
1496	0.999032	0.000484	0.000484	2000	
Sensitivity Analysis Runs					Perturbation in:
1348	0.998174	0.000913	0.000913	1.83	A Fact. Rxn 1
1348	0.998174	0.000913	0.000913	1.83	E_{act} Rxn 1
1348	0.998174	0.000913	0.000913	1.83	A Fact. Rxn 2
1348	0.998174	0.000913	0.000913	1.83	E_{act} Rxn 2
1348	0.998174	0.000913	0.000913	1.83	A Fact. Rxn 3
1348	0.998174	0.000913	0.000913	1.83	E_{act} Rxn 3
1348	0.998174	0.000913	0.000913	1.83	A Fact. Rxn 4
1348	0.998174	0.000913	0.000913	1.83	E_{act} Rxn 4
1348	0.998174	0.000913	0.000913	1.83	A Fact. Rxn 5
1348	0.998174	0.000913	0.000913	1.83	E_{act} Rxn 5
1349	0.998174	0.000913	0.000913	1.83	Temperature
1348	0.998174	0.000913	0.000913	1.84	Res. Time
1348	0.998174	0.000913	0.000913	1.83	Steric Hindrance
1348	0.998174	0.000913	0.000913	1.83	BDE

Appendix C. The thermodynamic data, in the NASA format required by CHEMKIN, is listed in Appendix F.

8.4 - The Kinetic Model

The reaction set discussed in this section is included in its entirety in Appendix C. Derivation of the kinetic rate parameters that are found there is included in this section.

The mechanism can be broken down into five main reaction types. The first is the rather trivial hydrogen balance that allows for direct conversion between hydrogen molecules and hydrogen radicals. For the reaction:

$$H + H <=> H_2 ,$$

and a rate constant of the form:

$$k = A\, T^b\, e^{-E/RT} ,$$

A is taken as 1.00 E18 cc/mol/sec, b as -1, and E as 0 kcal/mole (Miller and Bowman, 1989).

The second reaction type is that of radical-radical termination:

$$A^{\cdot} + B^{\cdot} <=> A\text{-}B$$

Note that the reverse of this reaction provides the intiation of radical population needed for the mechanism to proceed. Lack of agreement in the literature on back reaction rate parameters forces the use of the reaction in this form, rather than in reverse. Since radicals are assumed to recombine with almost 100% efficiency, a simple collison model can be used to estimate rate parameters (Benson, 1976, Nicholas, 1976). A collision diameter that is proportional to the square root of molecular weight, with a base distance

of 3 angstroms for the smallest molecular weight combinations, is assumed resulting in a base (without statistical factor included) pre-exponential factor of 3.1E12 cc/mol/sec for biaryl recombinations and 2.5E13 cc/mol/sec for hydrogen recombinations, a temperature exponent of 0.5 and an activation energy of 0 kcal/mol.

The third reaction type is that of hydrogen abstraction to form a radical:

$$A + H \Longleftrightarrow A^{\cdot} + H_2$$

A value of 4.17 E13 cc/mol/sec is assumed for the base pre-exponential factor (Kiefer et al., 1985) based on analogy to the case where A is taken to be benzene, a typical arene. The factor of 6 descrepancy between the value used here and the one in the literature is a result of the removal of the statistical factor that was present in the reported literature value. The appropriate statistical factor is put back in when actual rate parameters are calculated for the mechanism. A b value of 0 is used, along with an activation energy of 16 kcal/mol, as reported in the same reference.

The fourth reaction type is that of aryl-arene combination:

$$A^{\cdot} + B \Longleftrightarrow A\text{-}B + H$$

By analogy to the case where A and B are both benzene ($A^{\cdot}$ = phenyl radical), a base pre-exponential factor of 6.64 E10 cc/mol/sec is taken from the literature value reported by Fahr and Stein (1988), again stripped of its statistical factor. The temperature exponent is again taken to be 0, and the activation energy is taken as 4 kcal/mol, as reported in the same reference.

The last reaction type is that of a ring-closing condensation:

$$A^{\cdot} \Longleftrightarrow CA + H_2$$

A base pre-exponential factor of 4.0 E13 sec^{-1} is assumed, along with a temperature exponent of 0 and an activation energy of 10 kcal/mol, as a compromise between two reaction types as outlined by Pope (1993). Literature values for this type of reaction are largely unknown and uncertain, but this guess will serve as the starting point for modelling this mechanism.

In addition to the base pre-exponential factor assumptions above, forward statistical factors must be considered before final values can be calculated for use in the CHEMKIN input mechanism. There is only one main assumption used in calculating these statistical factors: only the bound condensing aryl, the hydrogen radical and the hydrogen molecule are assumed able to reach potential condensation sites in a compound. Anything larger and unbound to the radical compound would be too sterically hindered to reach the condensation sites, and consideration of such reactions would greatly increase the size of the reaction set. Consequently, only the fraction of a given radical type that can undergo a particular reaction are counted in the statistical factor. A table of the number of reachable (by large molecules) and total radical sites for all radicals in the mechanism is listed in Table 8.4.1.

For more accuracy in the biaryl products, the assumption of the last paragraph is applied as follows. Biaryl radicals are divided into four types (pictoral representations for the radicals considered for each compound type can be found in Appendix D). The first type - denoted by an ending of -1 on the compound identification - is a lumped compound representing all secondary radicals (equivalent to a 1' position on a naphthalene or anthracene molecule) on the biaryl isomer that are at sites that can undergo condensation

Table 8.4.1 Number of Reachable and Total Radical Sites on all Radicals in the Model

Compound	Rea.	Tot	Compound	Rea.	Tot	Compound	Rea.	Tot
n1n1-1	0	1	a1a2-4	14	14	C2NAA-	18	20
n1n1-2	0	1	a1a9-1	0	2	C2AAA-	19	22
n1n1-4	5	5	a1a9-2	0	1	C1NNNN-	18	24
n1n2-1	0	2	a1a9-3	0	1	C1NNNA-	19	26
n1n2-2	0	2	a1a9-4	14	14	C1NNAA-	20	28
n1n2-4	00	10	a2a2-4	9	9	C1NAAA-	21	30
n2n2-4	7	7	a2a9-1	0	3	C1AAAA-	22	32
a1n1-1	0	1	a2a9-2	0	1	C2NNNN-	19	22
a1n1-2	0	2	a2a9-4	14	14	C2NNNA-	20	24
a1n1-3	0	1	a9a9-1	0	1	C2NNAA-	21	26
a1n1-4	12	12	a9a9-4	4	4	C2NAAA-	22	28
a1n2-1	0	1	BkF-	12	12	C2AAAA-	23	30
a1n2-2	0	1	BjF-	12	12	C3NNNN-	20	20
a1n2-3	0	1	Per-	12	12	C3NNNA-	21	22
a1n2-4	13	13	DBajF-	14	14	C3NNAA-	22	24
a2n1-1	0	2	DBakF-	14	14	C3NAAA-	23	26
a2n1-2	0	1	DBalF-	12	14	C3AAAA-	24	28
a2n1-4	13	13	N23jF-	14	14	C1NNNNN-	21	30
a2n2-4	16	16	N23kF-	14	14	C2NNNNN-	22	28
a9n1-1	0	3	BaPer-	12	14	C3NNNNN-	23	26
a9n1-2	0	1	BaN23jF-	16	16	C4NNNNN-	24	24
a9n1-4	12	12	BaN23kF-	16	16	NNN-	14	20
a9n2-1	0	3	BaN23lF-	14	16	NNA-	16	22
a9n2-2	0	1	DBajPer-	12	16	NAA-	18	24
a9n2-4	12	12	DBaoPer-	14	16	AAA-	20	26
a1a1-2	0	1	C1NNN-	15	18	NNNN-	17	26
a1a1-3	0	1	C1NNA-	16	20	NNNA-	19	28
a1a1-4	7	7	C1NAA-	17	22	NNAA-	21	30
a1a2-1	0	1	C1AAA-	18	24	NAAA-	23	32
a1a2-2	0	1	C2NNN-	16	16	AAAA-	25	34
a1a2-3	0	1	C2NNA-	17	18	NNNNN-	20	32

reactions. The second type, denoted by an ending of -2, represents the same type of condensible lumped radical, but at the primary position (2' position of an anthracene on naphthalene). The third type (-3 ending) represents the same thing but for a tertiary

radical (equivalent to a 9' site of an anthracene). The fourth type (-4 ending) is used to represent all noncondensible site on the biaryls. These are the sites that can be reached by naphthalene and anthracene for polymerization. The BDE's for these radicals are considered in their weighted average composite form, as described in section 8.2.

With simplifications to keep mechanism size down and reasonable values for kinetic parameters in place, construction of the mechansim is straightforward, but cumbersome. 2,146 reactions are needed to adequately describe the kinetic mechanism with the listed compounds. Appendix C attempts to list the reaction set in a sensible order that proceeds generally from smallest to largest compounds in a given reaction category. Major reaction classes are indicated, along with their references and base parameters. A guide to compound identification is given in Appendix D.

8.5 - Results

Thirty-four simulations have been performed with CHEMKIN using the described mechanism. The pure naphthalene, pure anthracene, and naphthalene/anthracene pyrolysis runs have all been simulated at each of the five temperatures of the experiment. "Equilibrium" (long run time) counterpart runs have also been performed for the naphthalene/anthracene model . Sensitivity analyses of 14 different input parameters has also been performed at 1348 K for the naphthalene/anthracene mechanism, each requiring a different run, since this analysis was performed manually.

The calculated downstream mole fractions for all species present in the 5 pure naphthalene, 5 naphthalene/anthracene, 5 pure anthracene and 5 anthracene/naphthalene

equilibrium runs are listed in Appendix G. A composite total-ion mass spectrum is shown for each of these runs in Figs. 8.5.1-20. The corresponding experimental mass spectra for the 5 pure naphthalene, 5 naphthalene/anthracene runs, and the highest and lowest temperature pure anthracene runs are shown in Figs. 8.5.21-32. Calculated temperature profiles for the binaphthalene isomers, naphthyl-anthracene isomers, bianthracene isomers, total biaryls (by group), and total condensation products, are shown for the naphthyl-anthracene runs in Figs. 8.5.33-37, with corresponding experimental profiles shown in Figs. 8.5.38-42. The pure anthracene runs are used to generate Fig. 8.5.40 since data is not available for the complete bianthracene series from the naphthalene/anthracene pyrolysis - the relative abundances of bianthracene isomers within each series are expected to be very similar in both sets of runs. Attribution of condensation products to isomer groups is very uncertain due to lack of convincing compound identifications, but a rough idea of temperature profile and onset of condensation can still be discerned in this last figure.

The kinetic model seems to do an acceptable job at predicting relative concentrations of biaryl isomers within a series (Figs. 8.5.33-35, 8.5.38-40), if we first consider that a significant enhancement of all compounds possessing a 1-naphthyl component is evident. Similar enhancements can be seen in compounds containing a 1-anthryl component (though a slightly smaller effect) and a 9-anthryl component. This may be a consistent failing of MOPAC's calculated steric hindrance contributions to heat of formation, or it may be due to an overabundance of, for example, 1-naphthyl radicals due to an estimated bond dissociation energy that is too low. Both of these possibilities will be

Fig. 8.5.1: Pure Naphthalene Pyrolysis at 1177K, Calculated

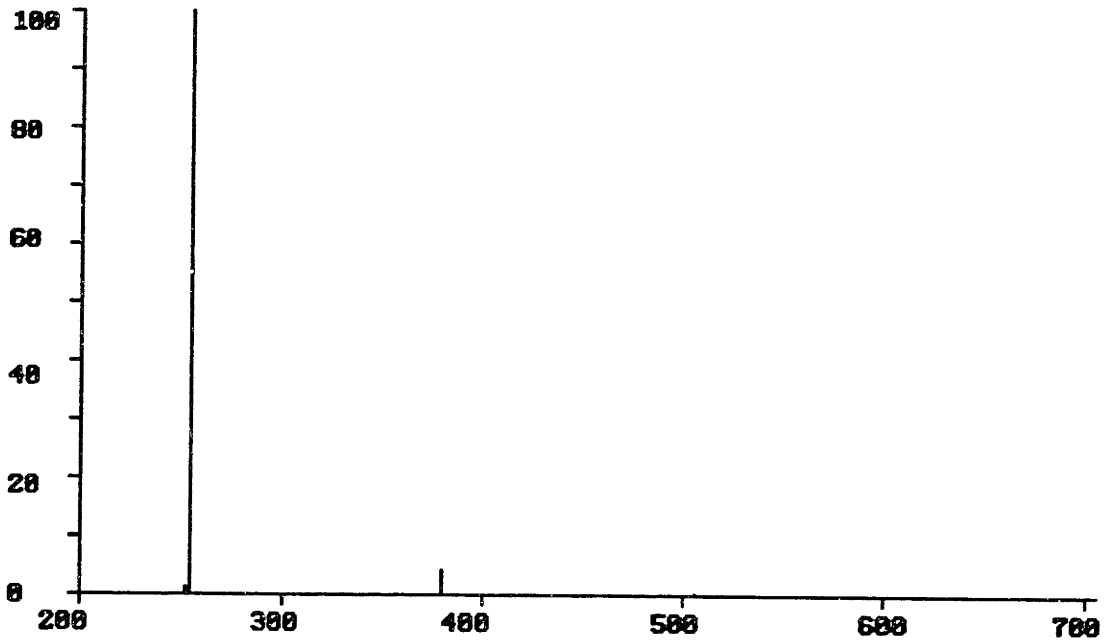

M/z Ratio as seen on Total Ion Mass Spectrum

Fig. 8.5.2: Pure Naphthalene Pyrolysis at 1277K, Calculated

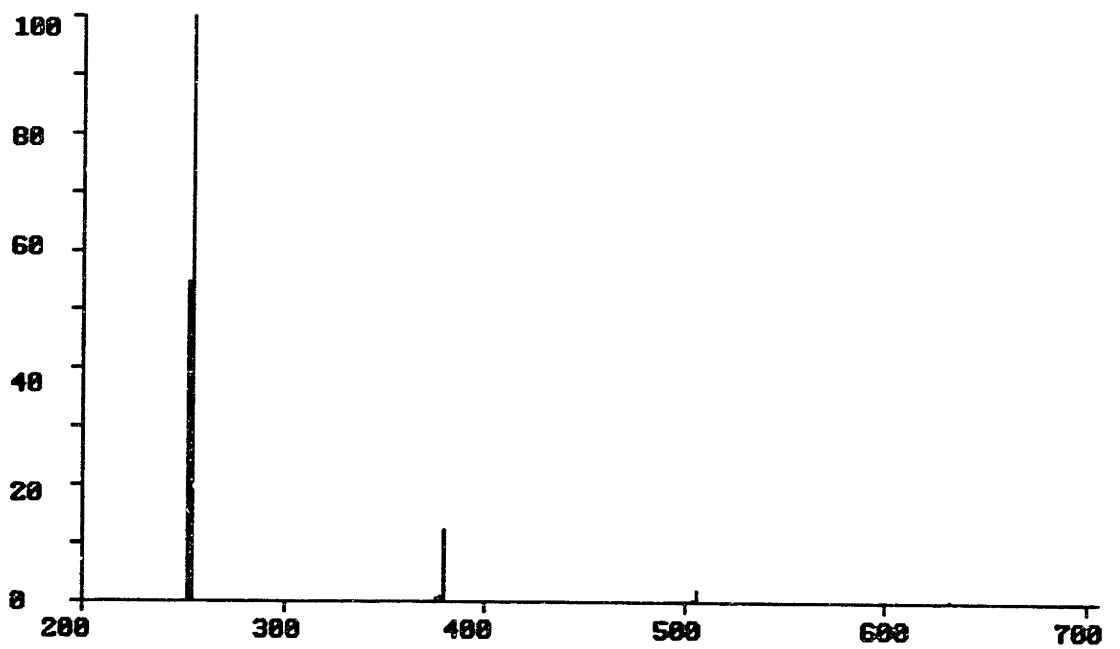

M/z Ratio as seen on Total Ion Mass Spectrum

Fig. 8.5.3: Pure Naphthalene Pyrolysis at 1350K, Calculated

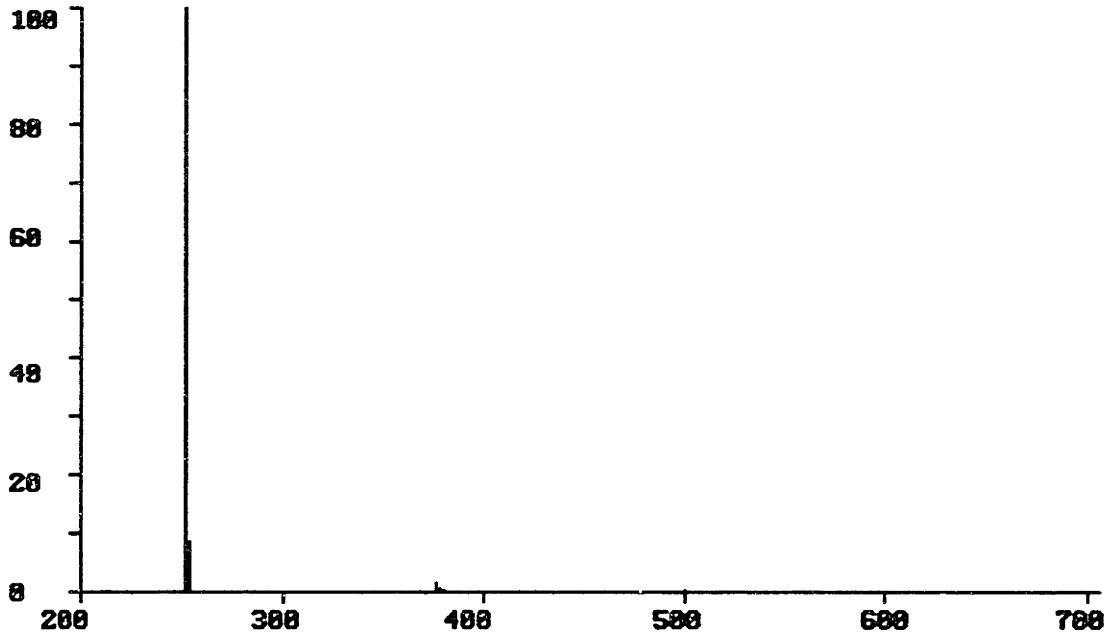

M/z Ratio as seen on Total Ion Mass Spectrum

Fig. 8.5.4: Pure Naphthalene Pyrolysis at 1415K, Calculated

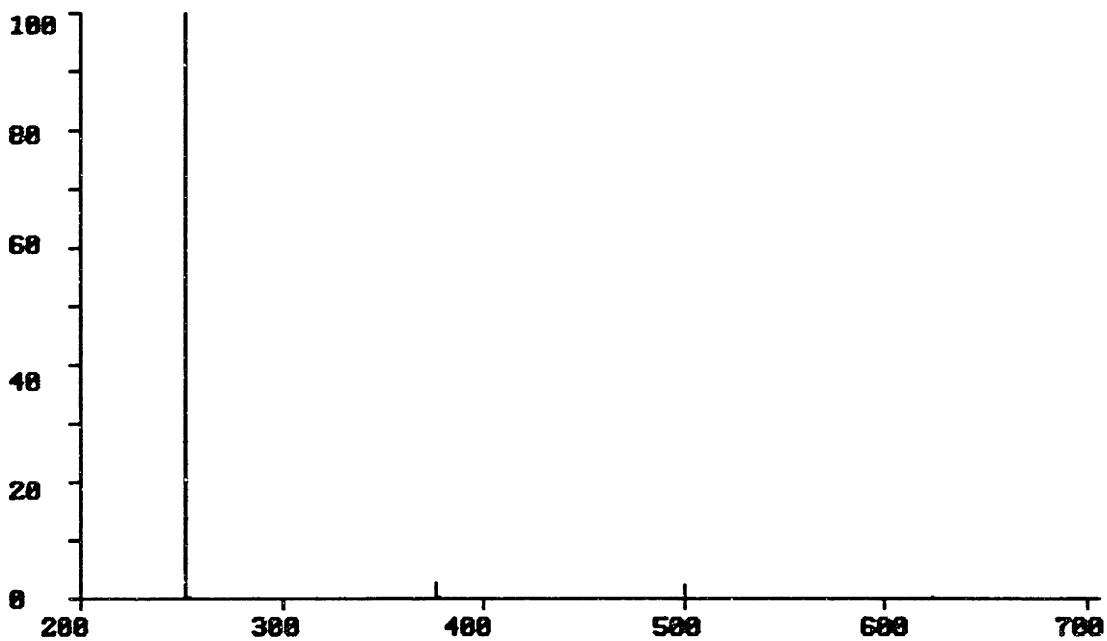

M/z Ratio as seen on Total Ion Mass Spectrum

Fig. 8.5.5: Pure Naphthalene Pyrolysis at 1498K, Calculated

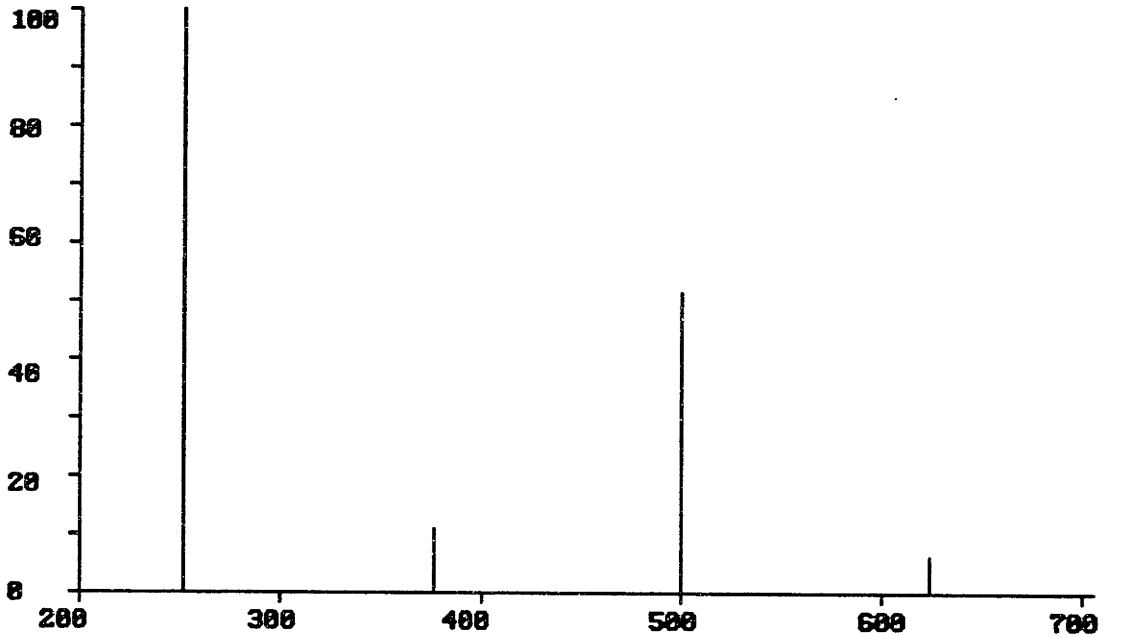

M/z Ratio as seen on Total Ion Mass Spectrum

Fig. 8.5.6: Naphthalene/Anthracene Mixture Pyrolysis at 1180K, Calculated

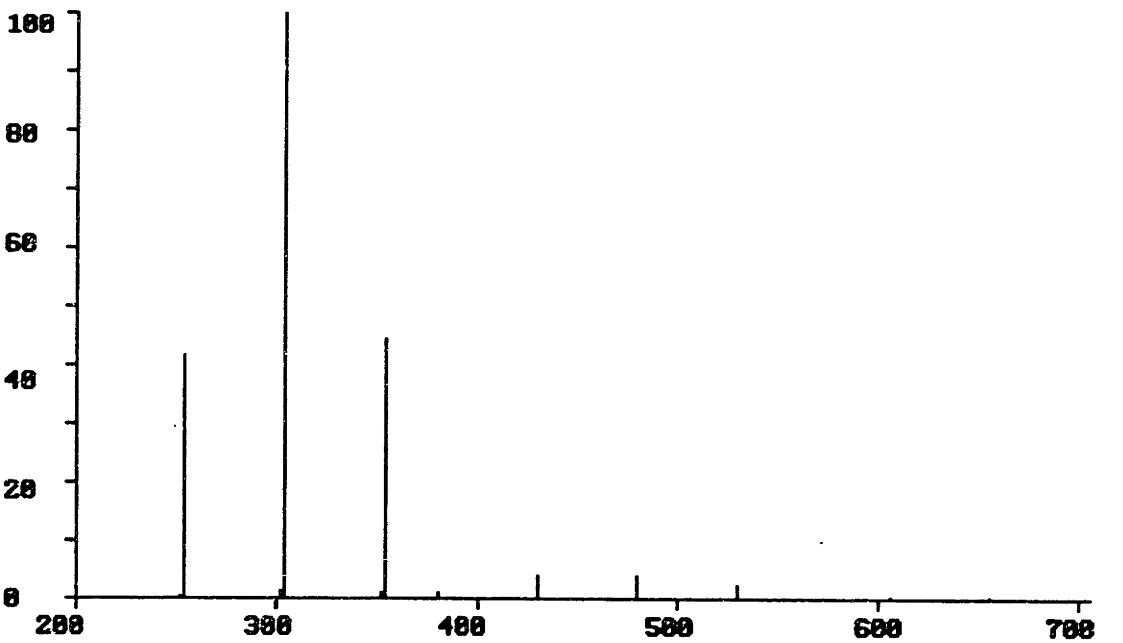

M/z Ratio as seen on Total Ion Mass Spectrum

Fig. 8.5.7: Naphthalene/Anthracene Mixture Pyrolysis at 1277K, Calculated

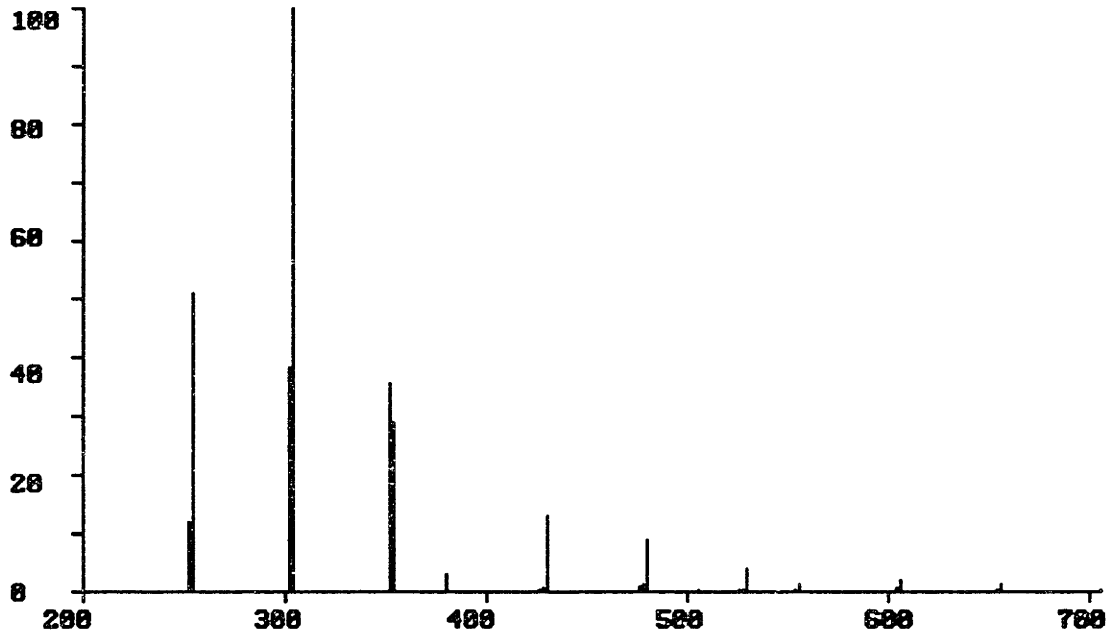

M/z Ratio as seen on Total Ion Mass Spectrum

Fig. 8.5.8: Naphthalene/Anthracene Mixture Pyrolysis at 1348K, Calculated

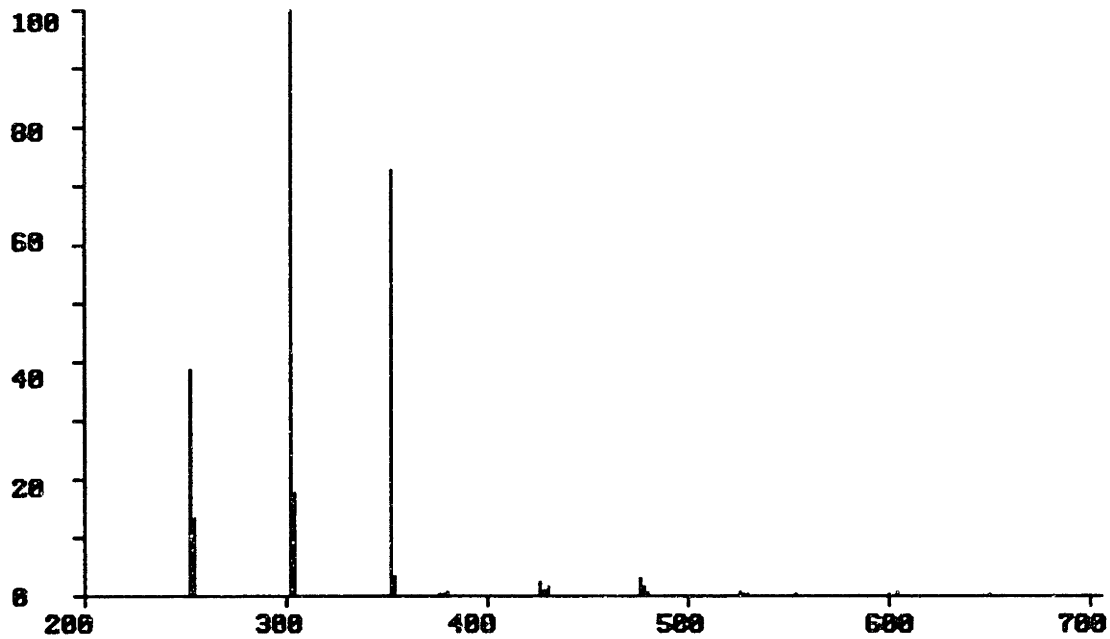

M/z Ratio as seen on Total Ion Mass Spectrum

Fig. 8.5.9: Naphthalene/Anthracene Mixture Pyrolysis at 1416K, Calculated

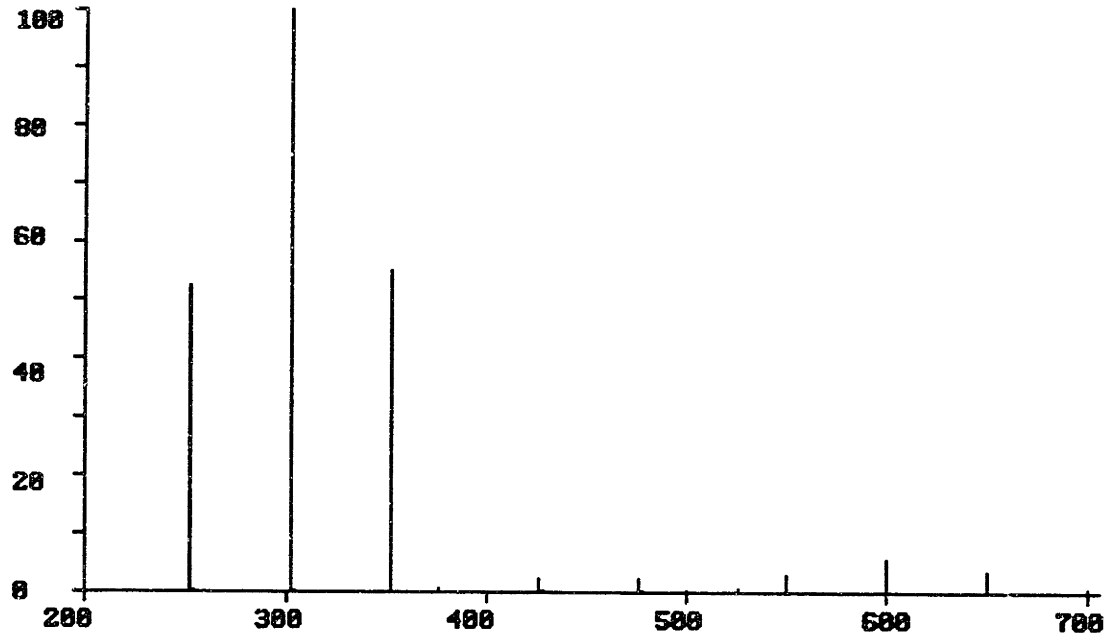

M/z Ratio as seen on Total Ion Mass Spectrum

Fig. 8.5.10: Naphthalene/Anthracene Mixture Pyrolysis at 1496K, Calculated

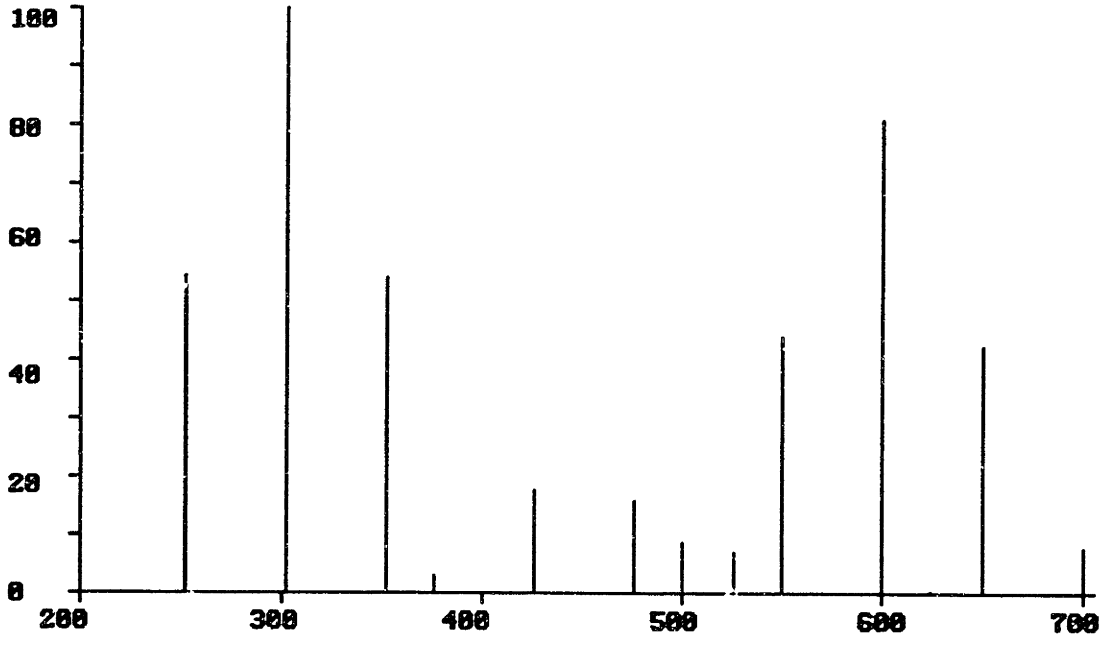

M/z Ratio as seen on Total Ion Mass Spectrum

Fig. 8.5.11: Pure Anthracene Pyrolysis at 1181K, Calculated

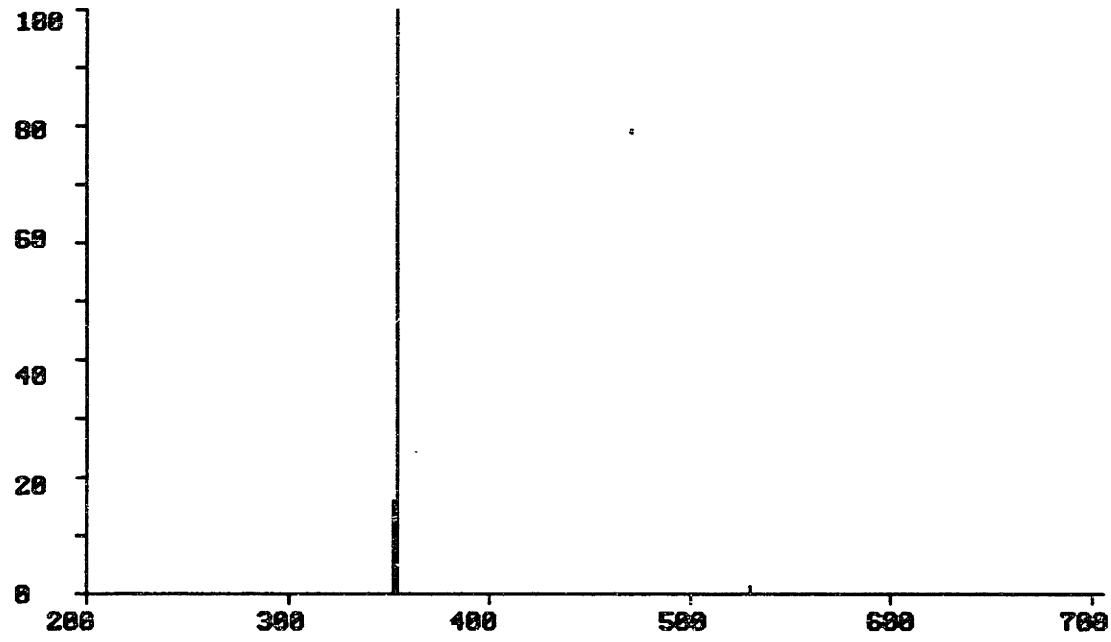

M/z Ratio as seen on Total Ion Mass Spectrum

Fig. 8.5.12: Pure Anthracene Pyrolysis at 1278K, Calculated

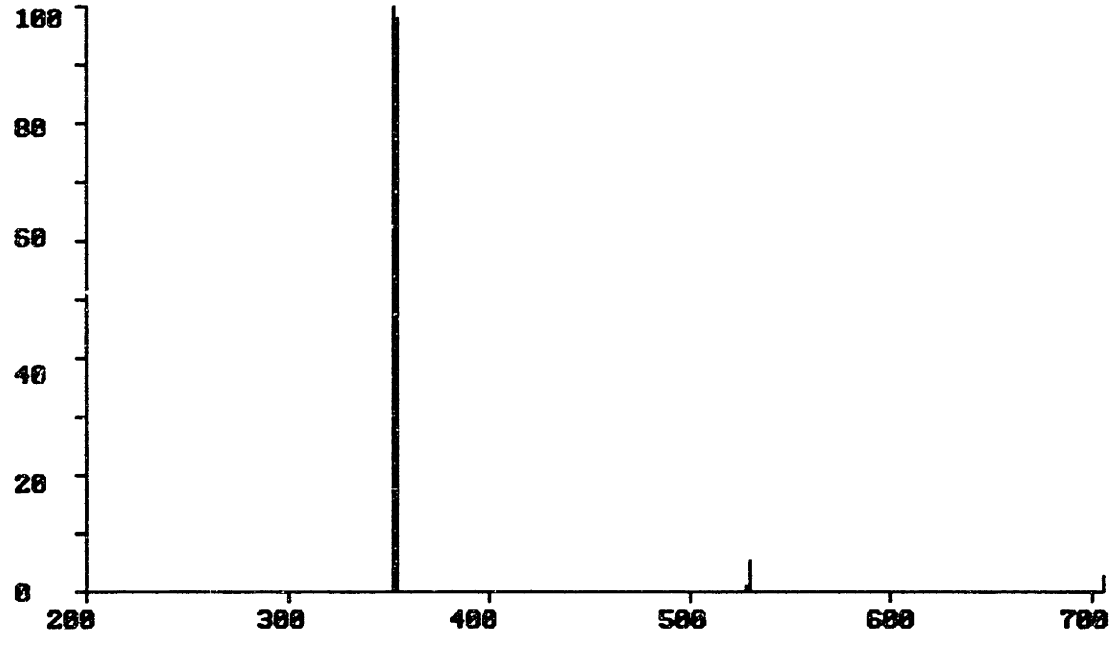

M/z Ratio as seen on Total Ion Mass Spectrum

Fig. 8.5.13: Pure Anthracene Pyrolysis at 1350K, Calculated

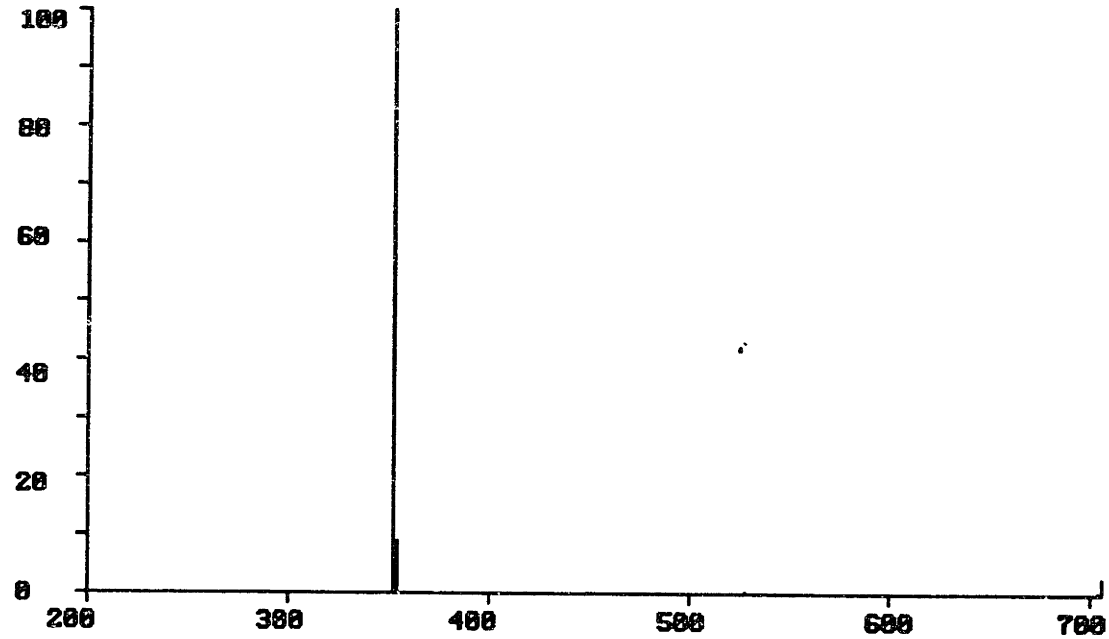

M/z Ratio as seen on Total Ion Mass Spectrum

Fig. 8.5.14: Pure Anthracene Pyrolysis at 1415K, Calculated

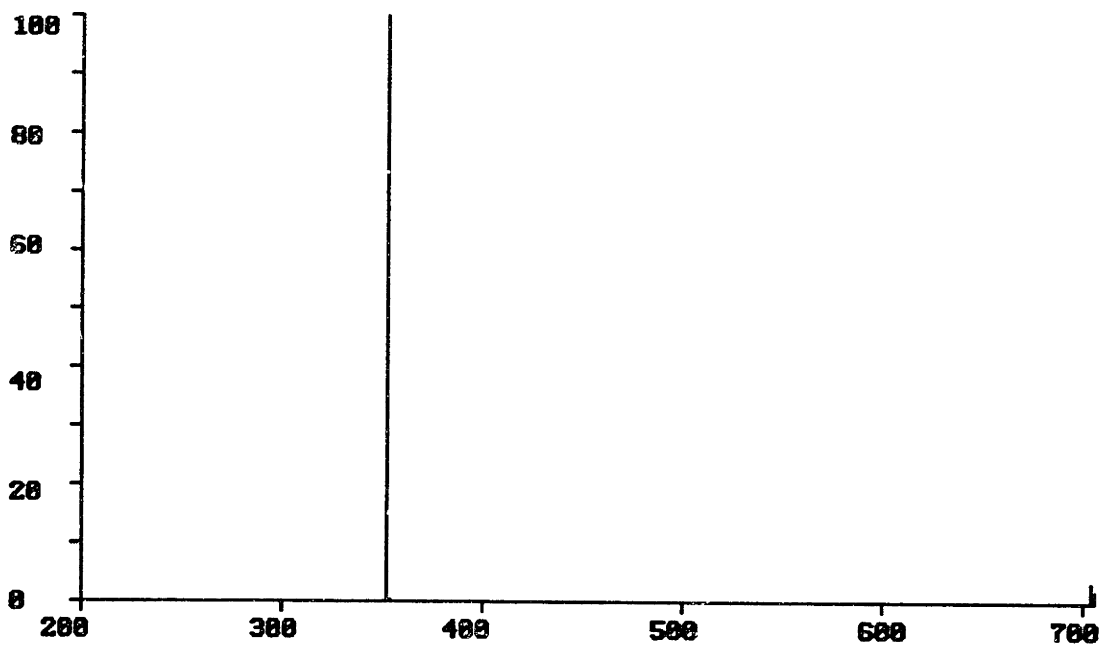

M/z Ratio as seen on Total Ion Mass Spectrum

Fig. 8.5.15: Pure Anthracene Pyrolysis at 1496K, Calculated

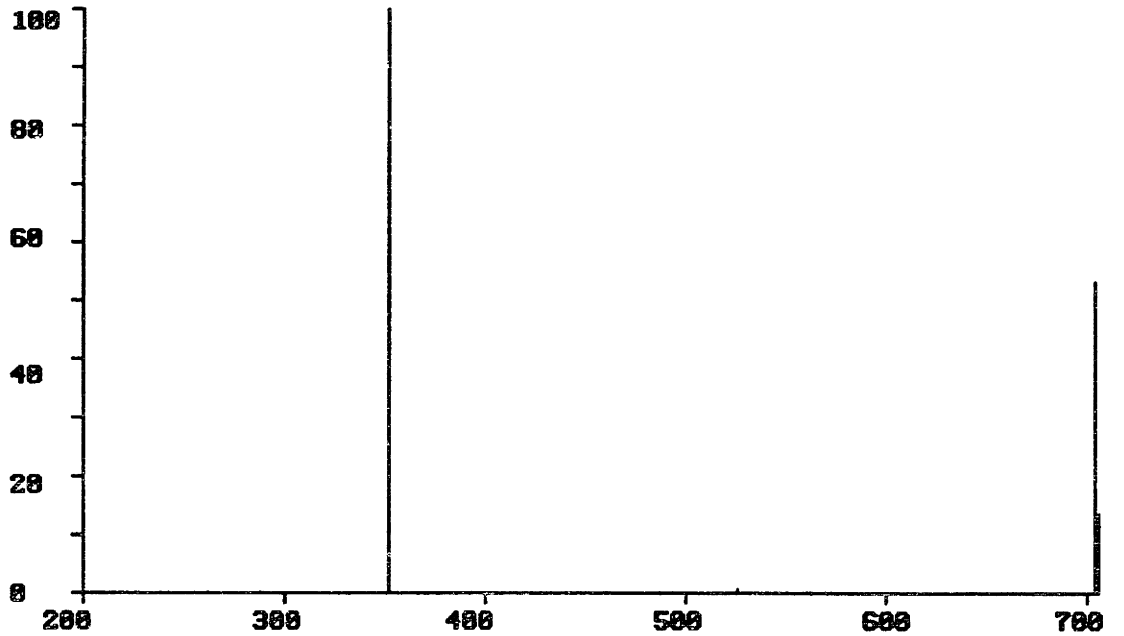

M/z Ratio as seen on Total Ion Mass Spectrum

Fig. 8.5.16: Naph./Anth. Mixture Pyrolysis at 1180K, Calculated Equil.

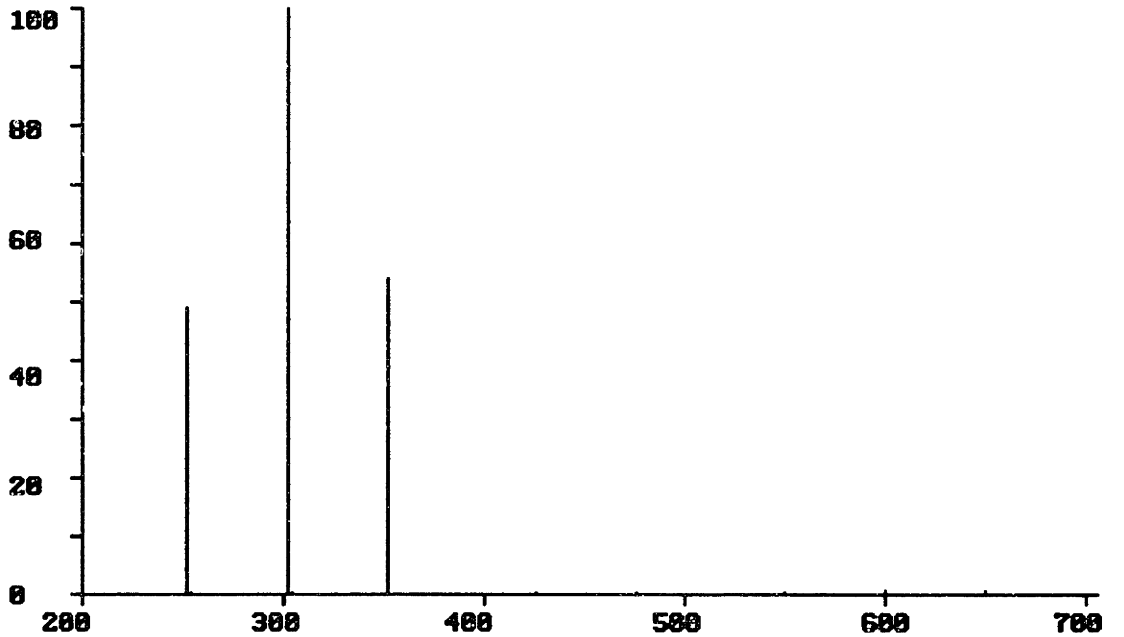

M/z Ratio as seen on Total Ion Mass Spectrum

Fig. 8.5.17: Naph./Anth. Mixture Pyrolysis at 1277K, Calculated Equil.

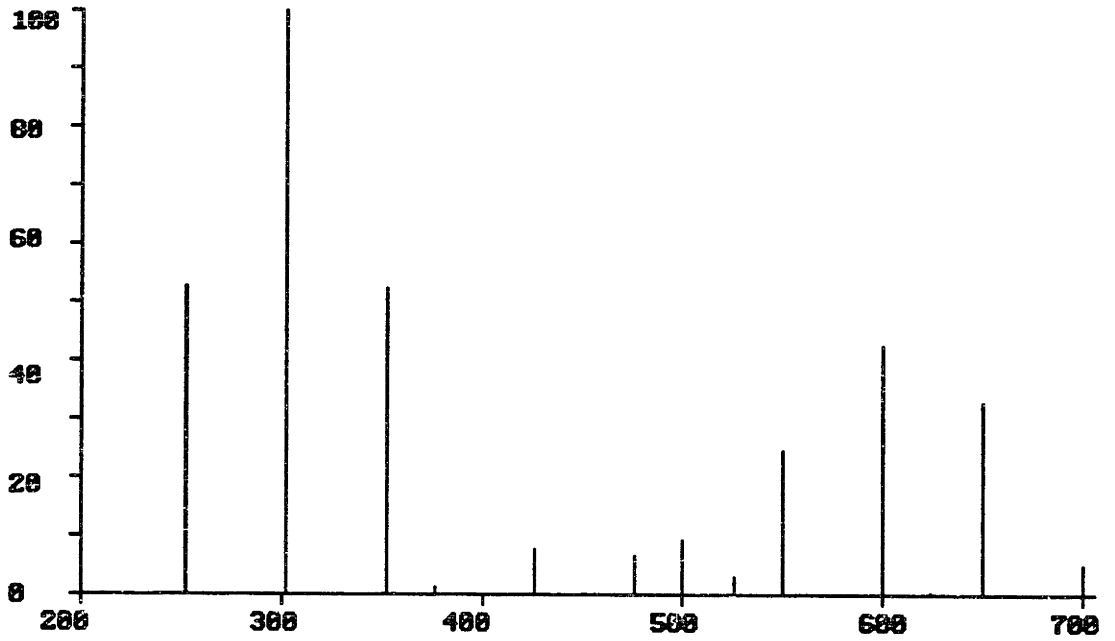

M/z Ratio as seen on Total Ion Mass Spectrum

Fig. 8.5.18: Naph./Anth. Mixture Pyrolysis at 1348K, Calculated Equil.

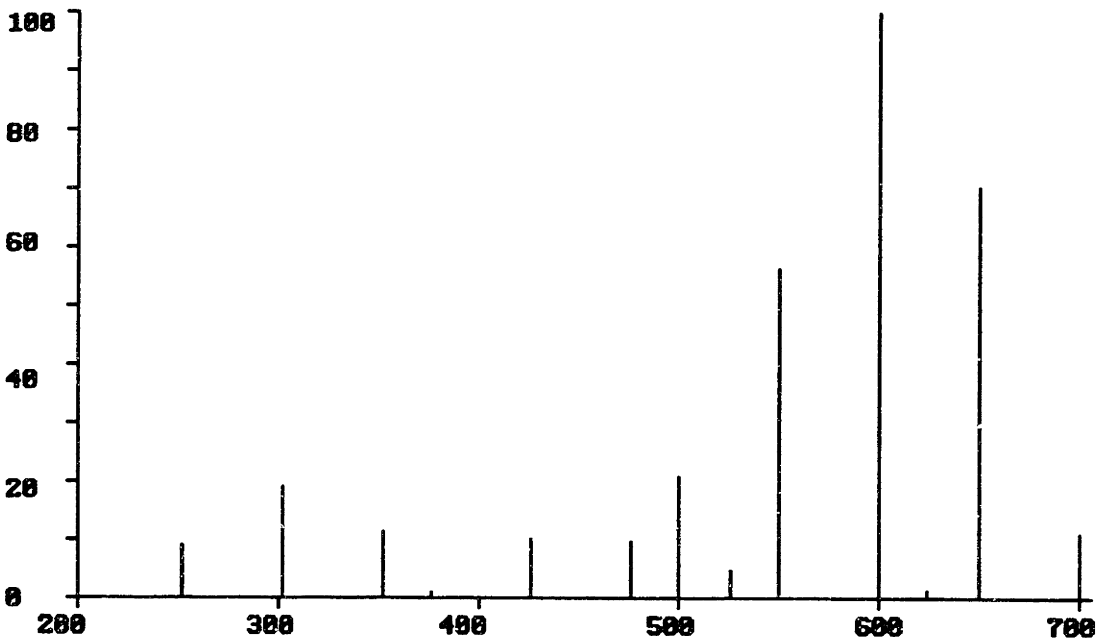

M/z Ratio as seen on Total Ion Mass Spectrum

Fig. 8.5.19: Naph./Anth. Mixture Pyrolysis at 1416K, Calculated Equil.

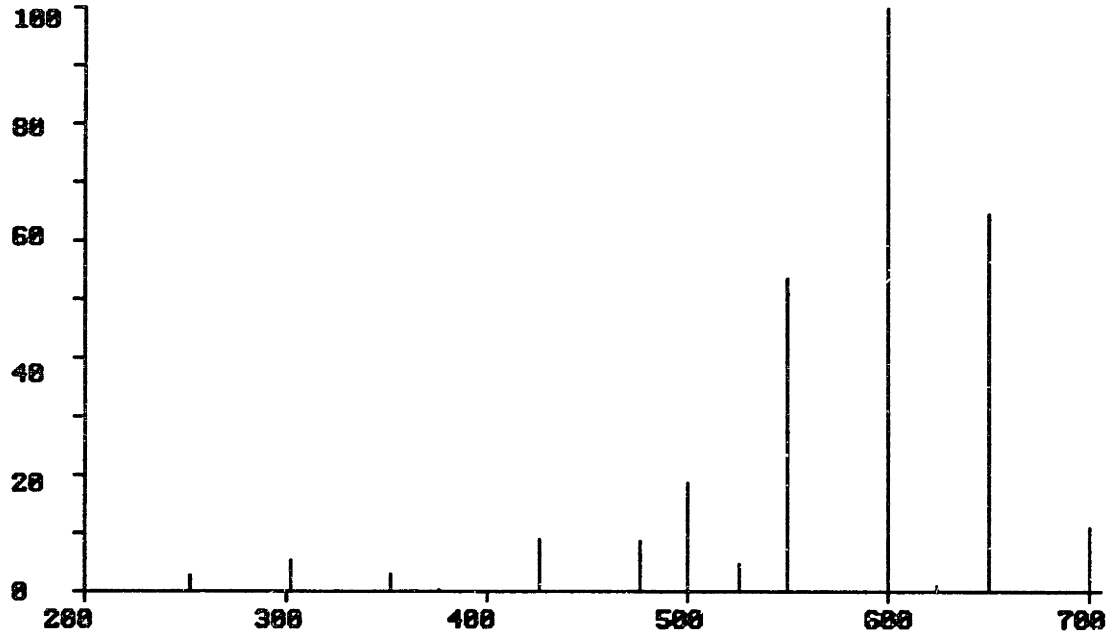

M/z Ratio as seen on Total Ion Mass Spectrum

Fig. 8.5.20: Naph./Anth. Mixture Pyrolysis at 1496K, Calculated Equil.

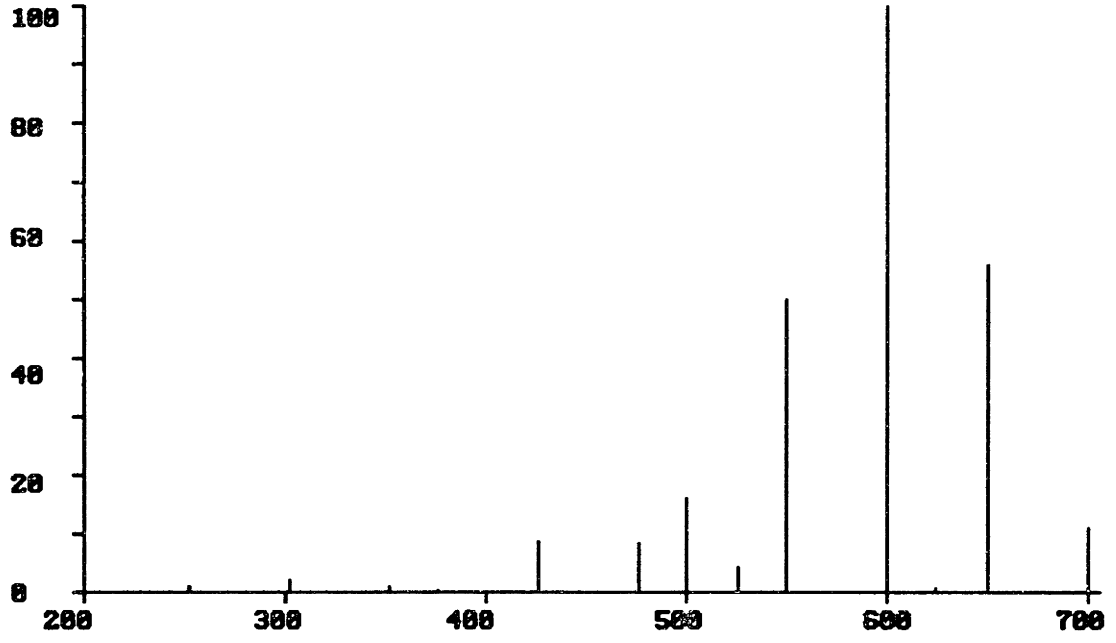

M/z Ratio as seen on Total Ion Mass Spectrum

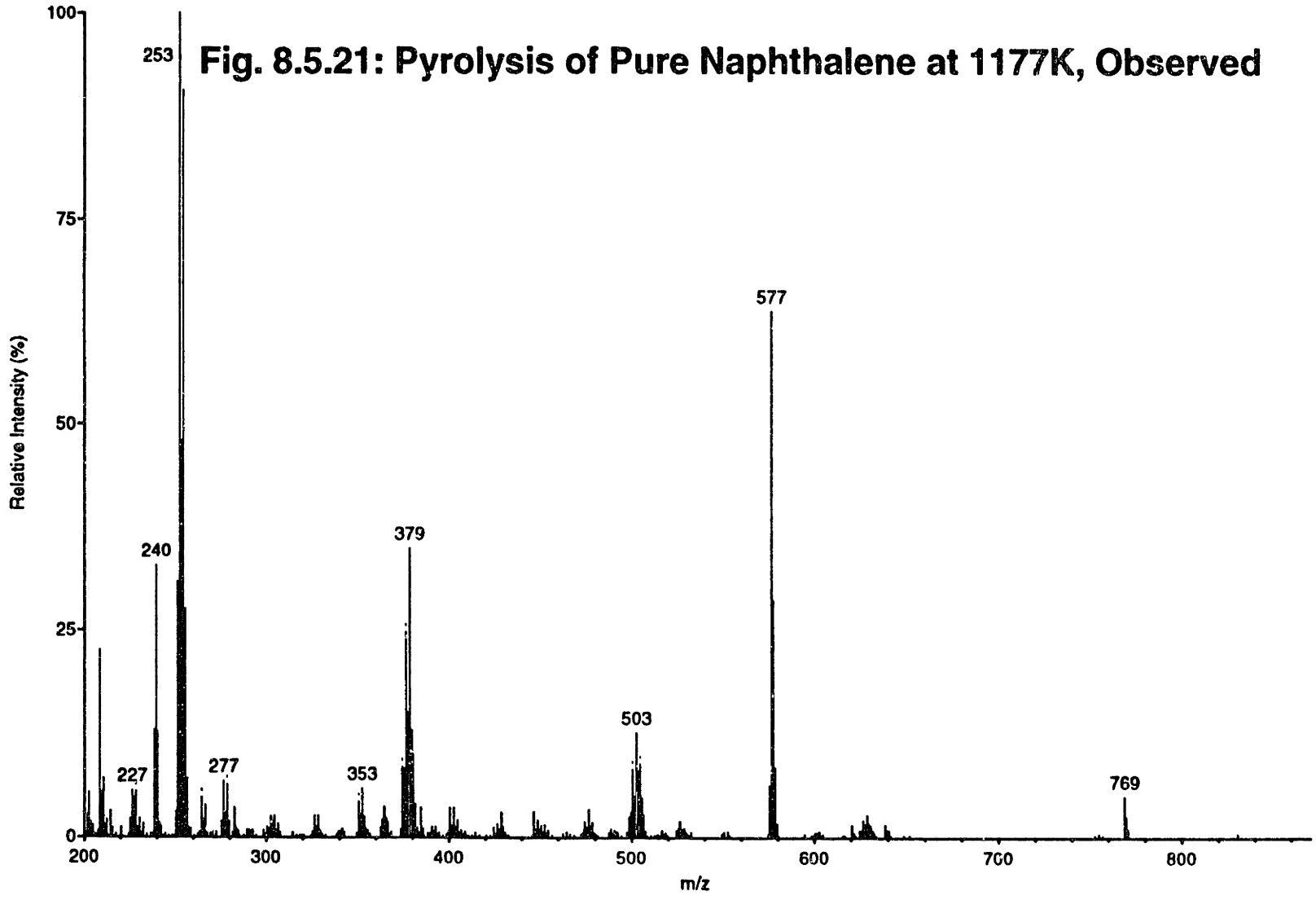

Fig. 8.5.21: Pyrolysis of Pure Naphthalene at 1177K, Observed Total Ion Mass Spectra from LCMS

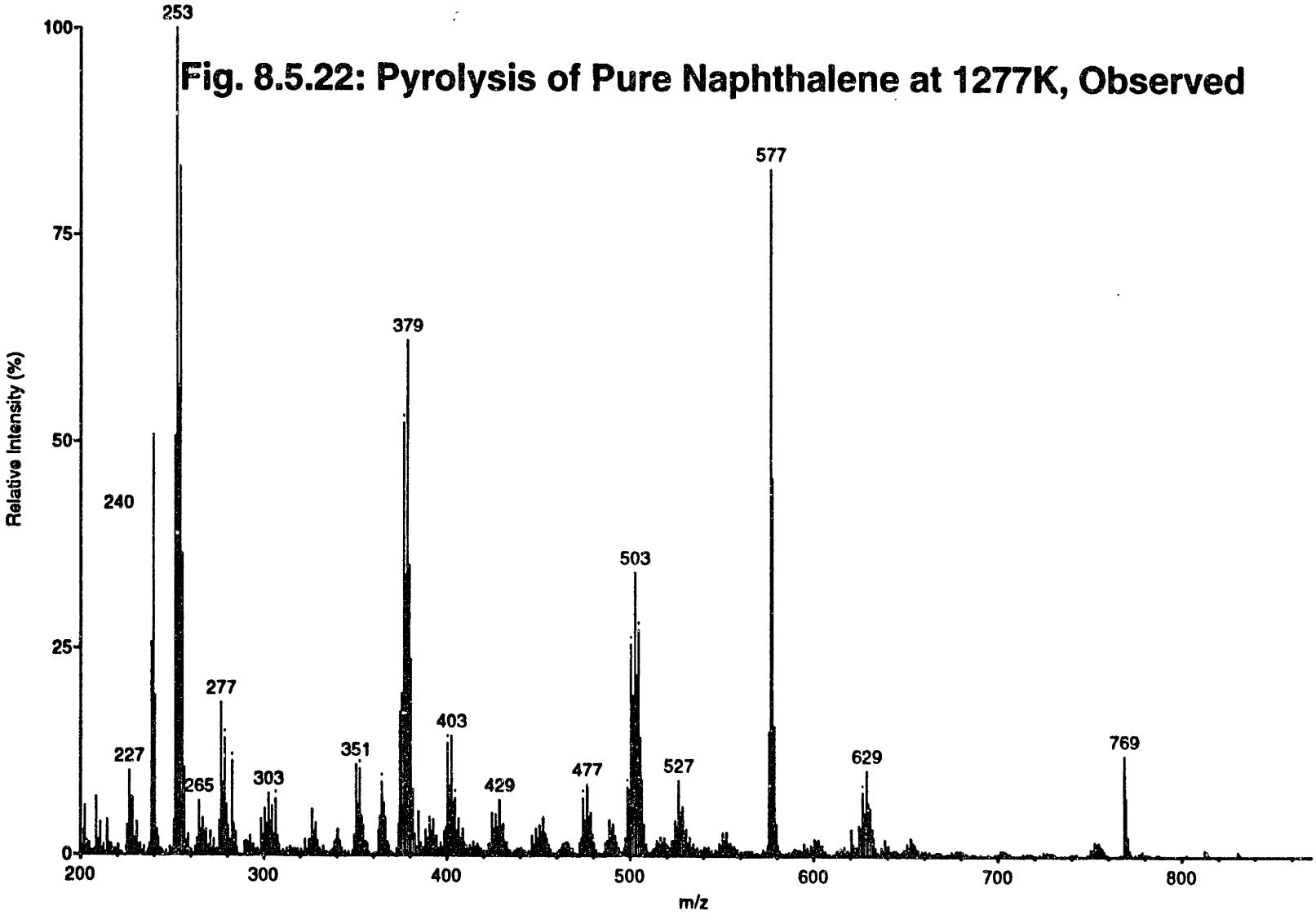

Fig. 8.5.22: Pyrolysis of Pure Naphthalene at 1277K, Observed Total Ion Mass Spectra from LCMS

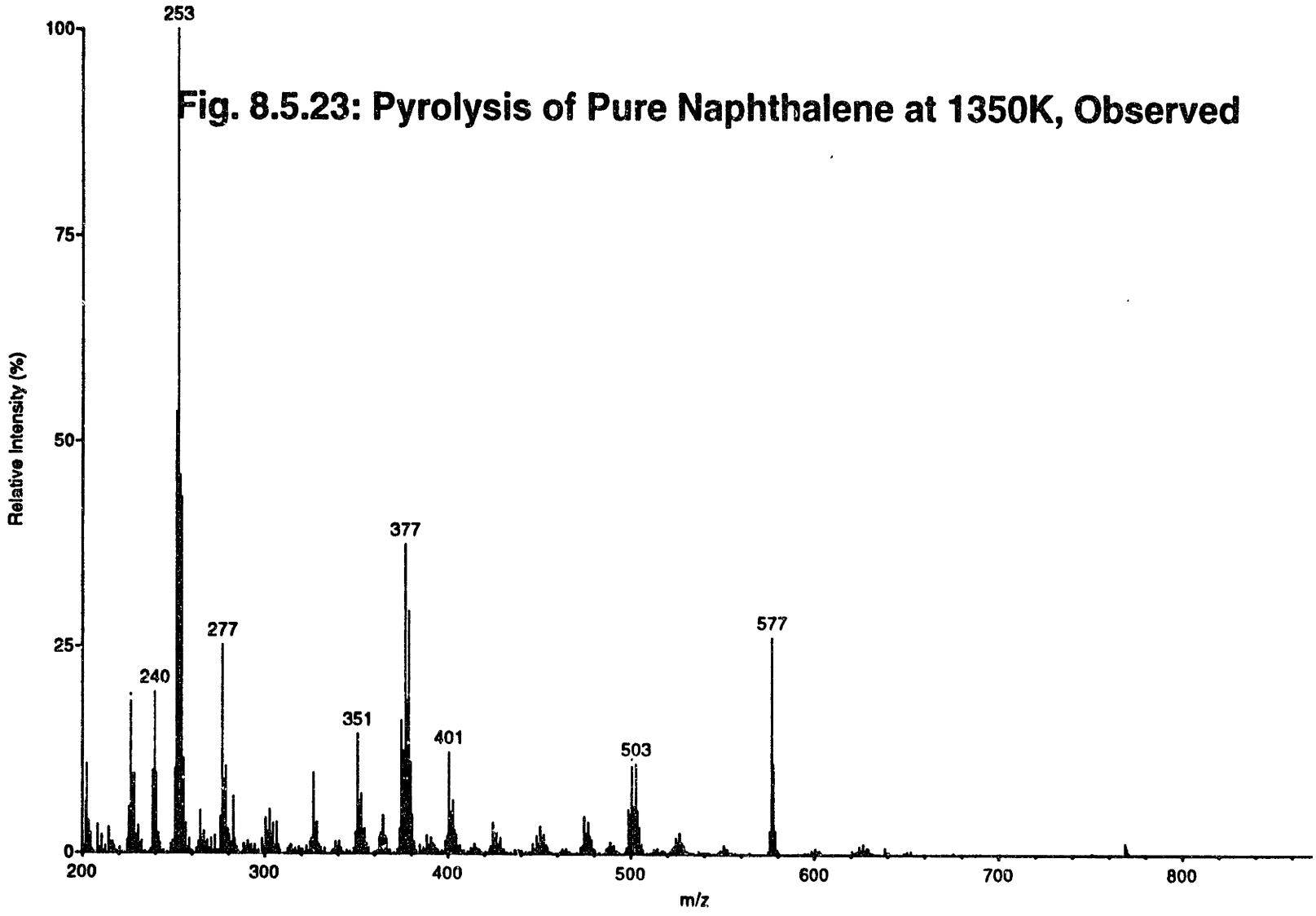

Fig. 8.5.23: Pyrolysis of Pure Naphthalene at 1350K, Observed Total Ion Mass Spectra from LCMS

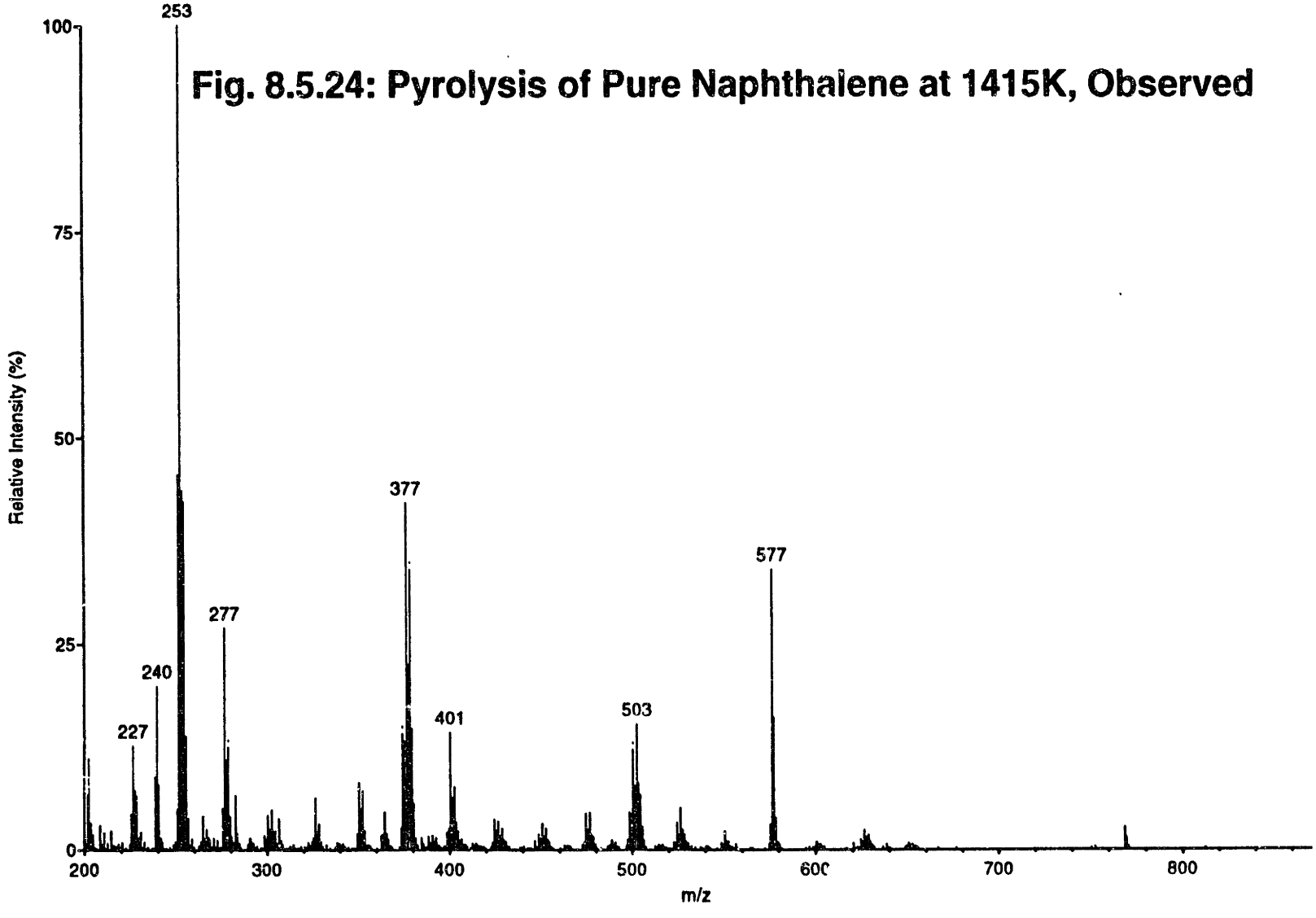

Fig. 8.5.24: Pyrolysis of Pure Naphthalene at 1415K, Observed

Total Ion Mass Spectra from LCMS

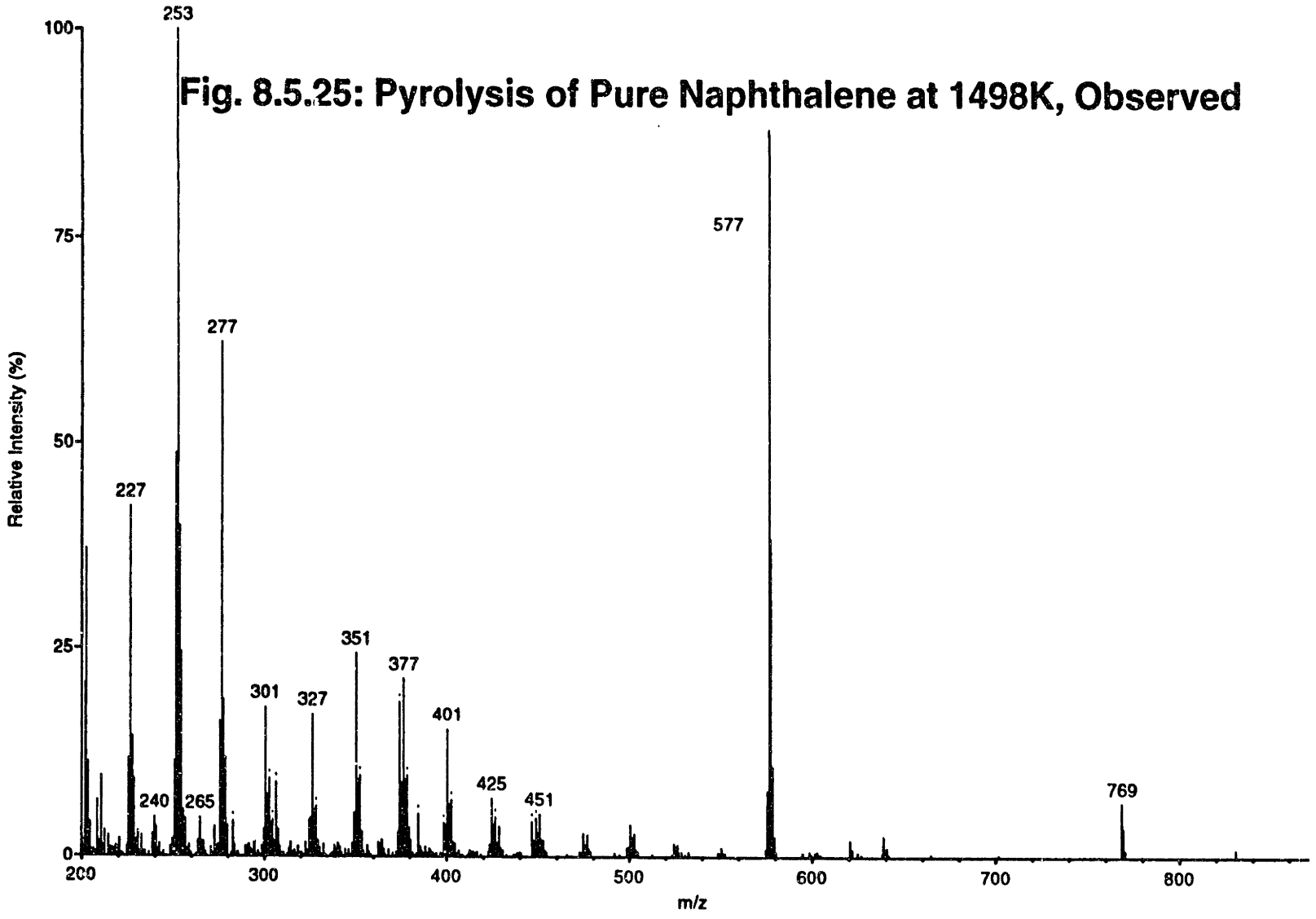

Fig. 8.5.25: Pyrolysis of Pure Naphthalene at 1498K, Observed

Total Ion Mass Spectra from LCMS

Fig. 8.5.26: Pyrolysis of a Naphthalene/Anthracene Mixture at 1180K, Observed

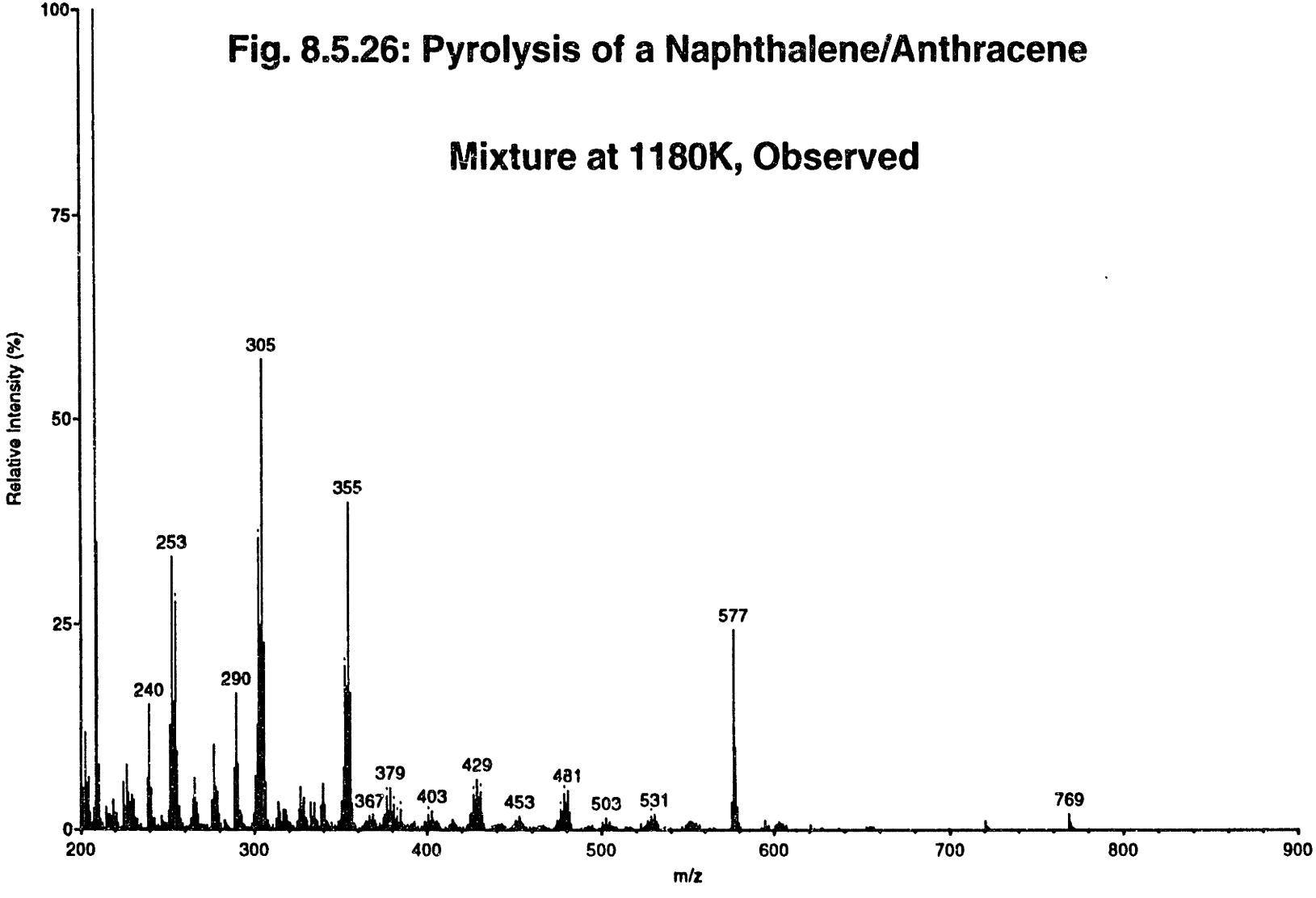

Total Ion Mass Spectra from LCMS

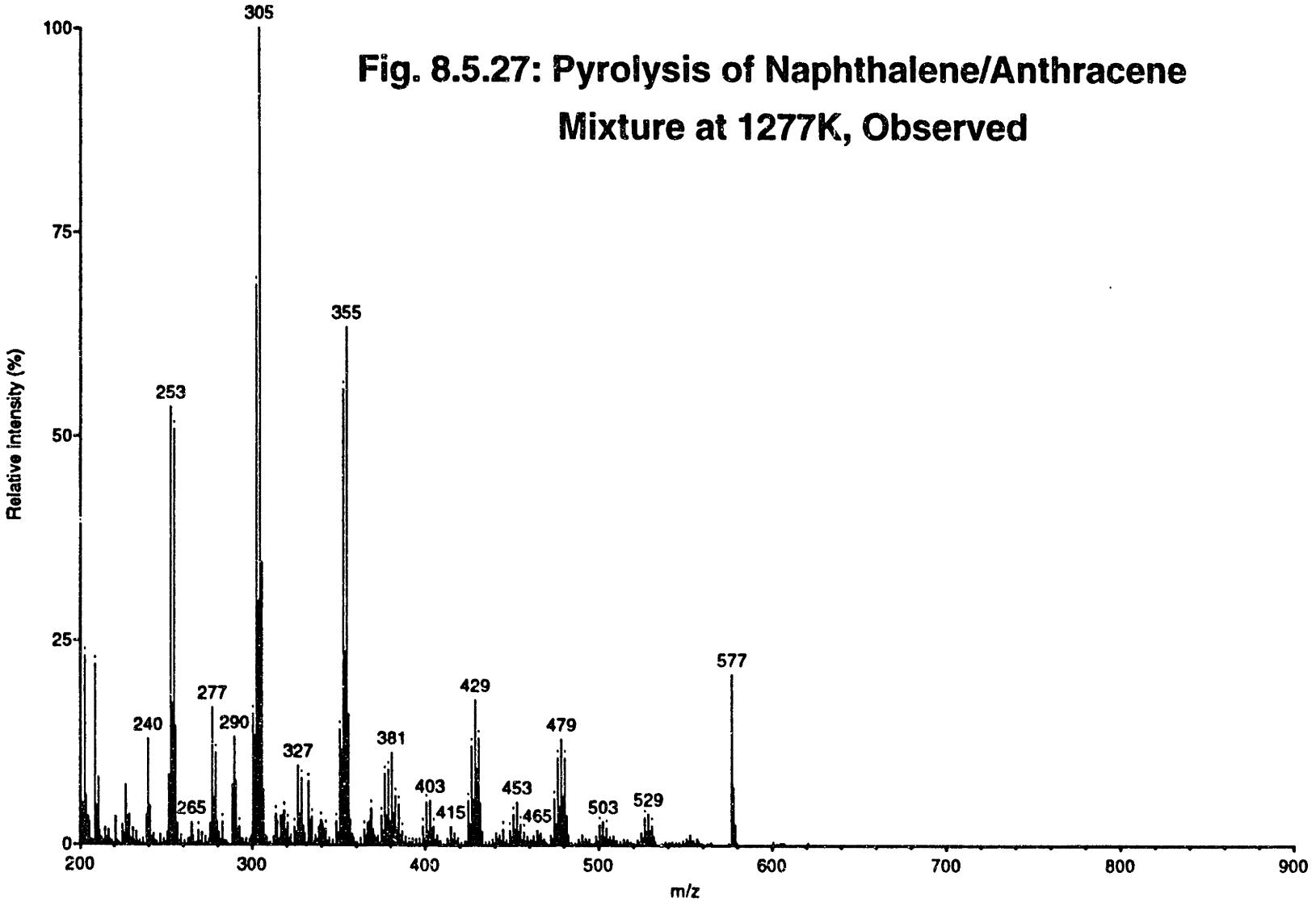

Fig. 8.5.27: Pyrolysis of Naphthalene/Anthracene Mixture at 1277K, Observed

Total Ion Mass Spectra from LCMS

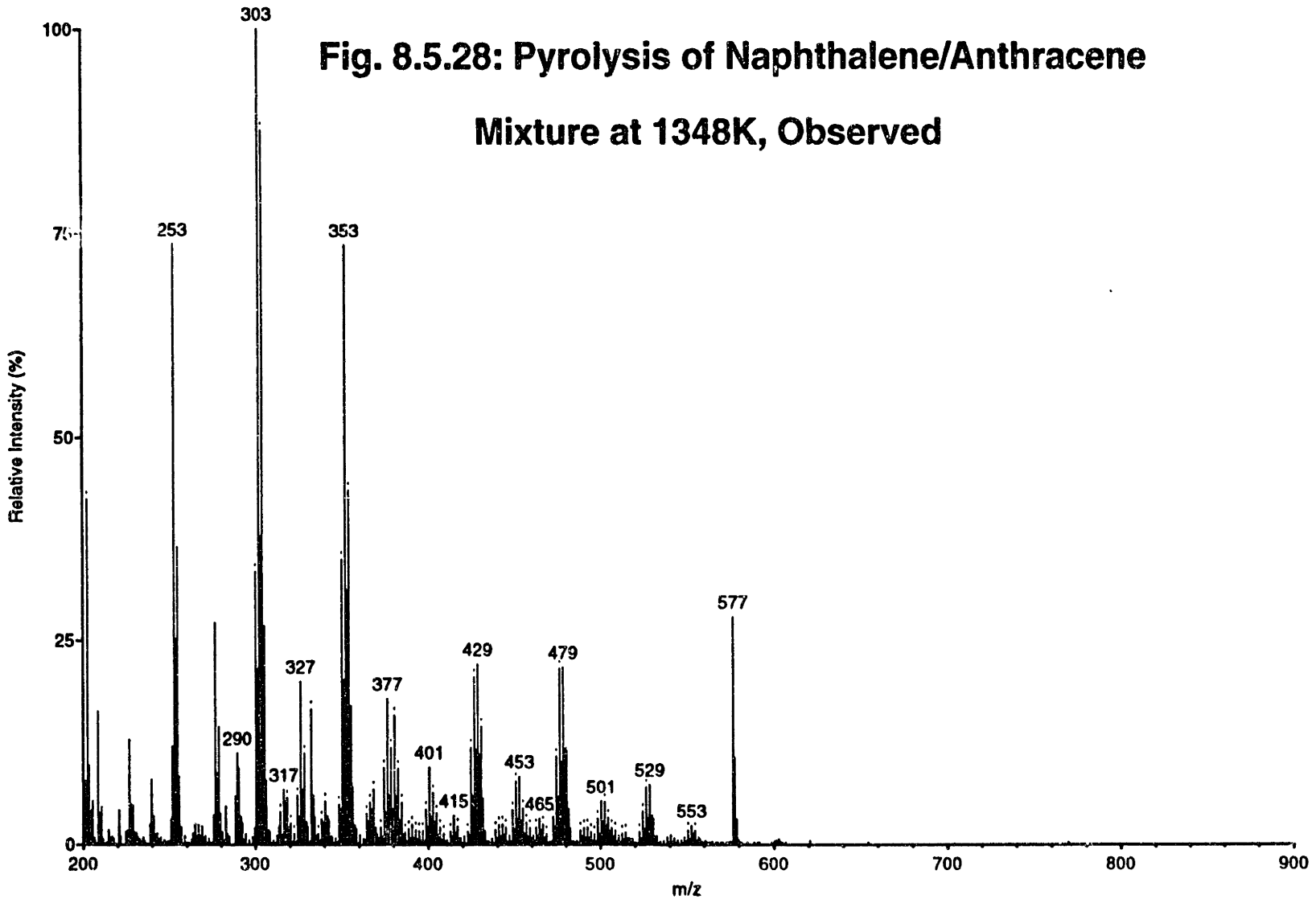

Fig. 8.5.28: Pyrolysis of Naphthalene/Anthracene Mixture at 1348K, Observed

Total Ion Mass Spectra from LCMS

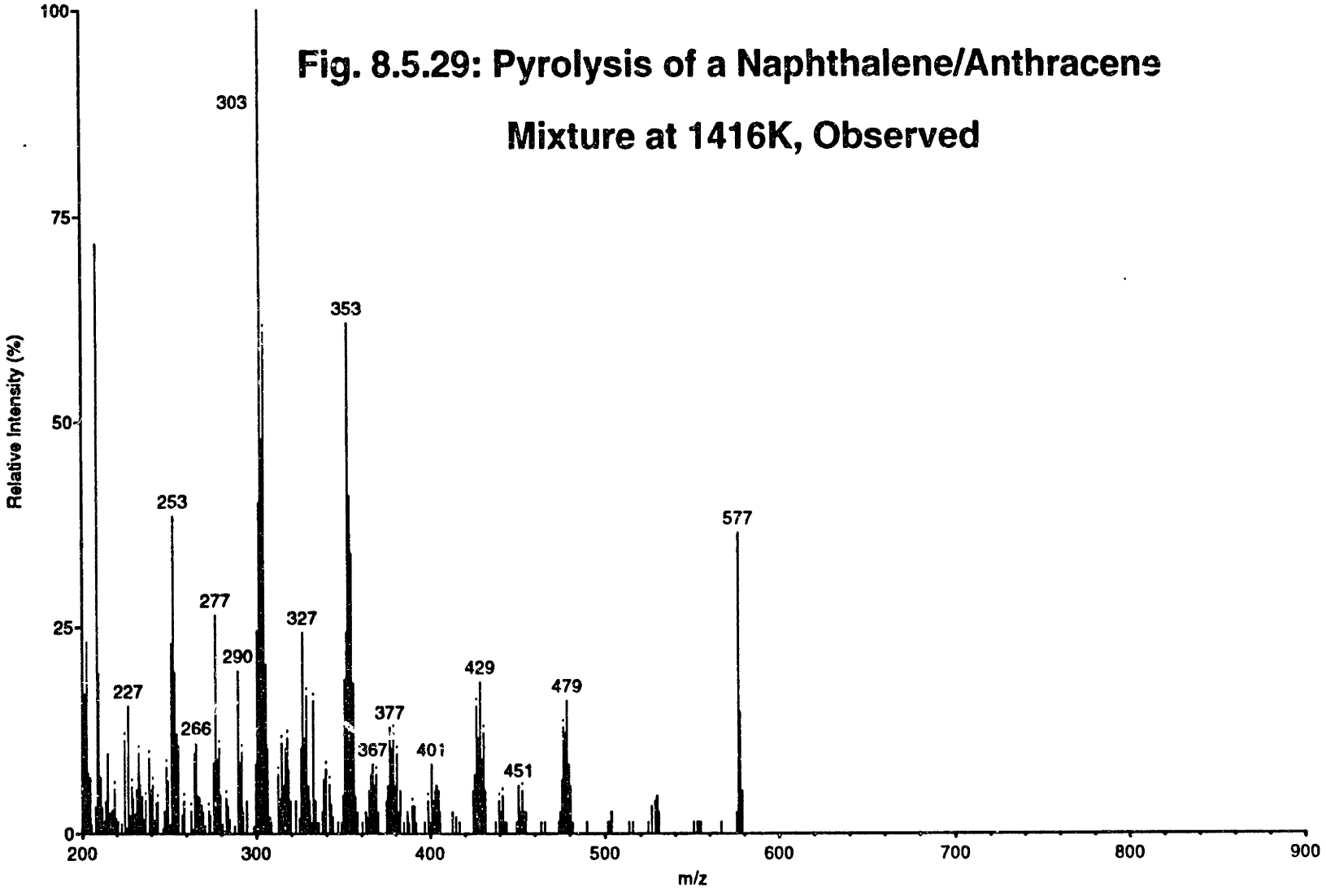

Fig. 8.5.29: Pyrolysis of a Naphthalene/Anthracene Mixture at 1416K, Observed Total Ion Mass Spectra from LCMS

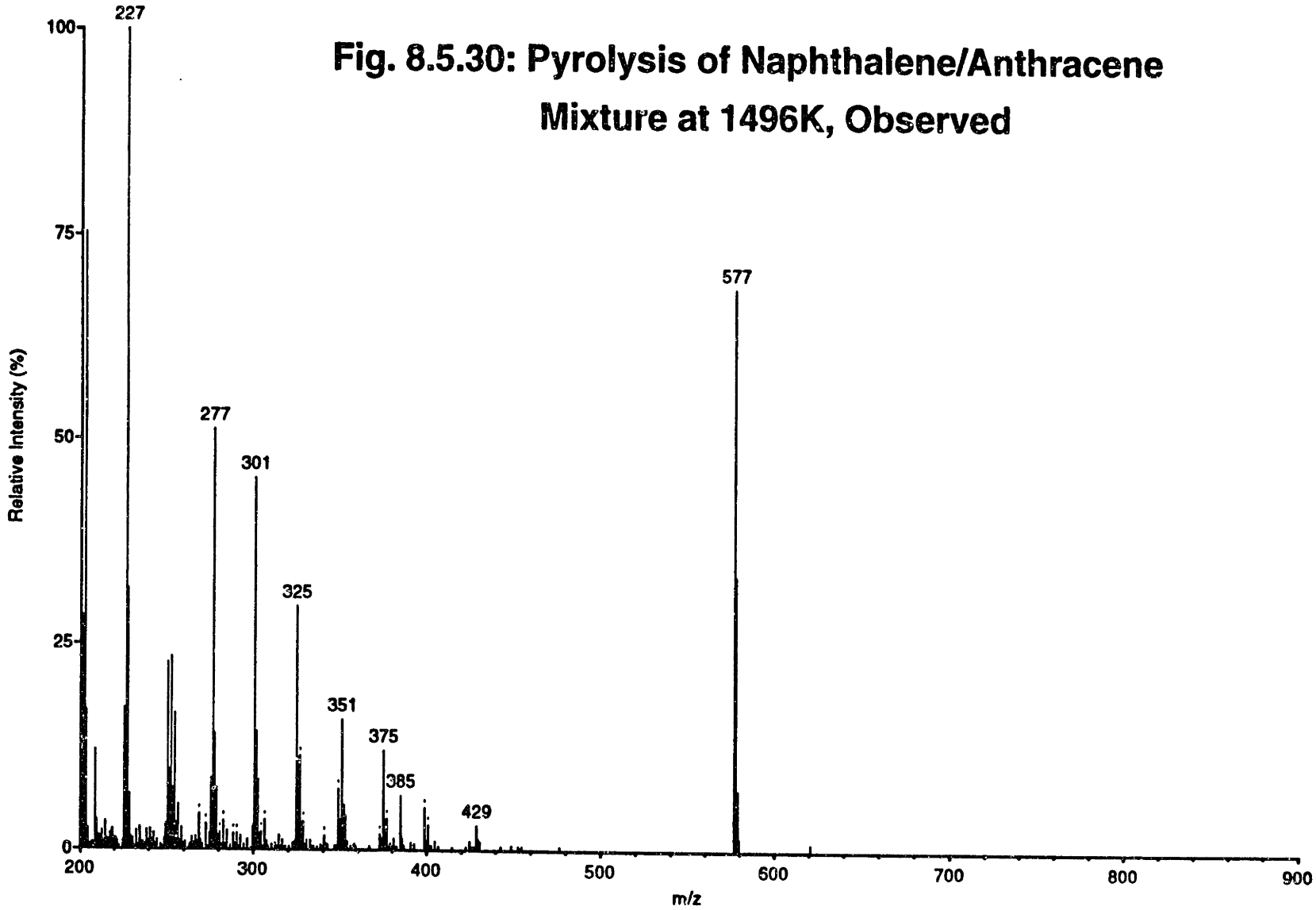

Fig. 8.5.30: Pyrolysis of Naphthalene/Anthracene Mixture at 1496K, Observed Total Ion Mass Spectra from LCMS

Fig. 8.5.31: Pyrolysis of Pure Anthracene at 1181K, Observed

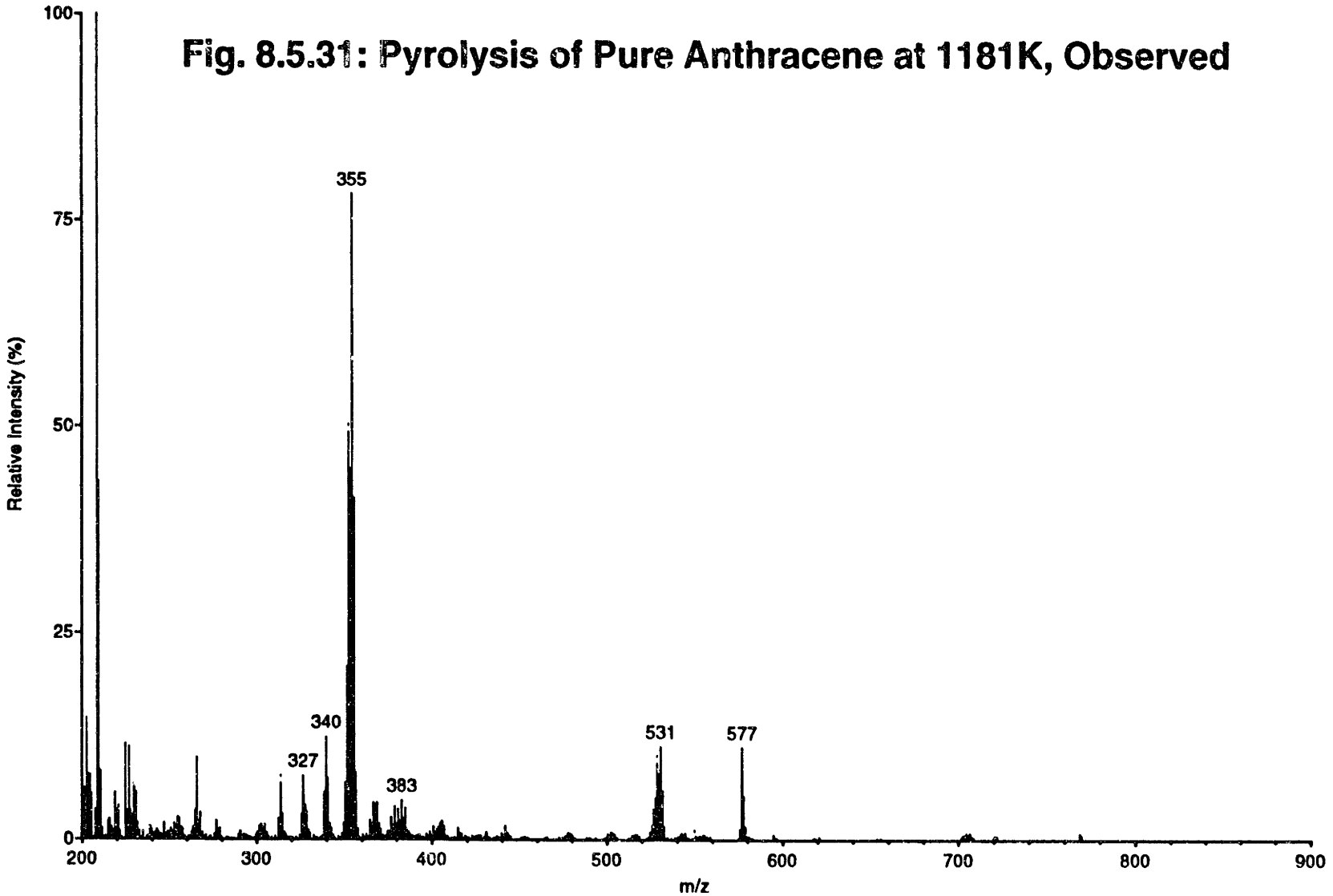

Total Ion Mass Spectra from LCMS

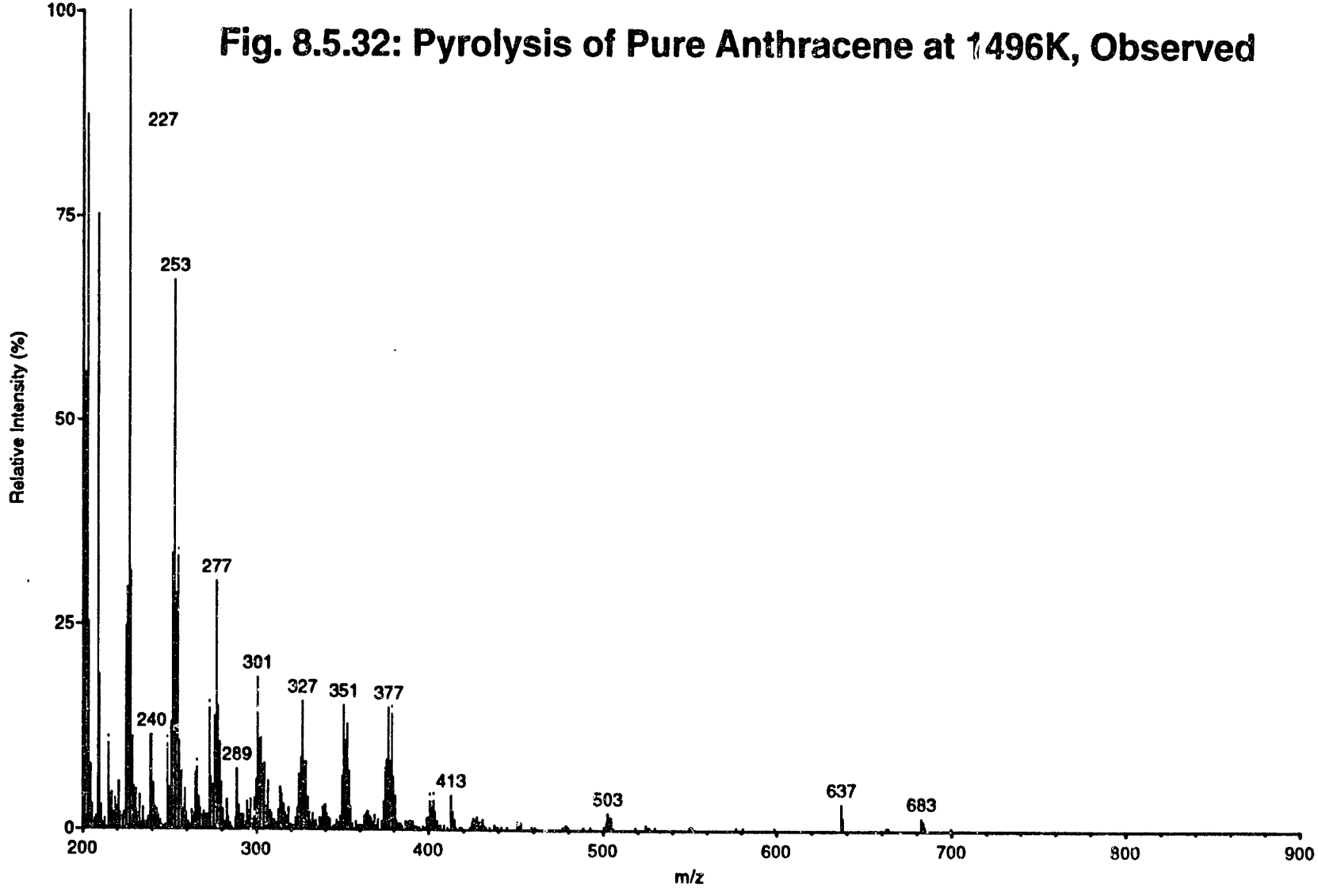

Fig. 8.5.32: Pyrolysis of Pure Anthracene at 1496K, Observed

Total Ion Mass Spectra from LCMS

Fig. 8.5.33
Chemkin Results–
Binaphthalenes

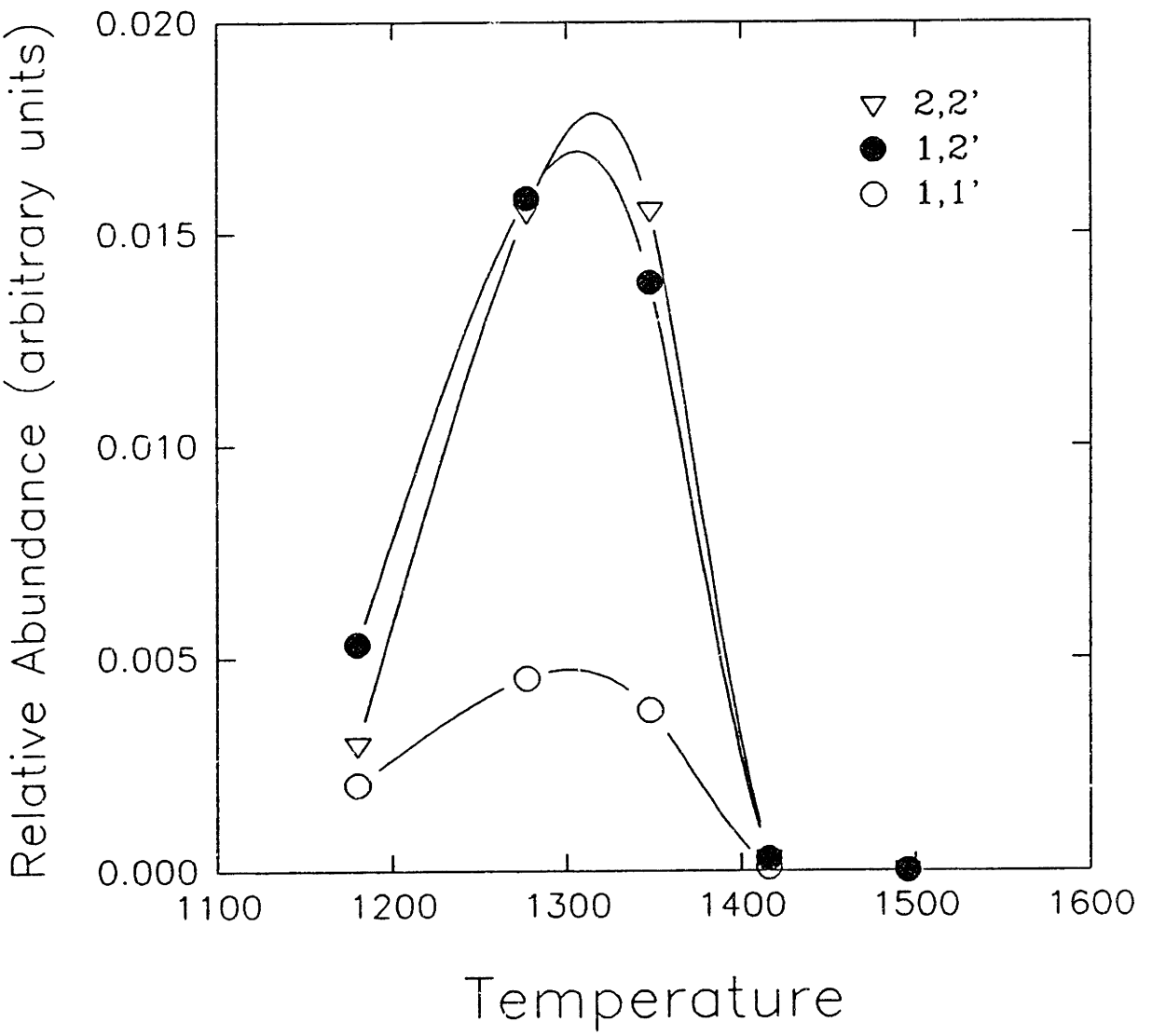

Fig. 8.5.34
Chemkin Results–
Naphthyl–Anthracenes

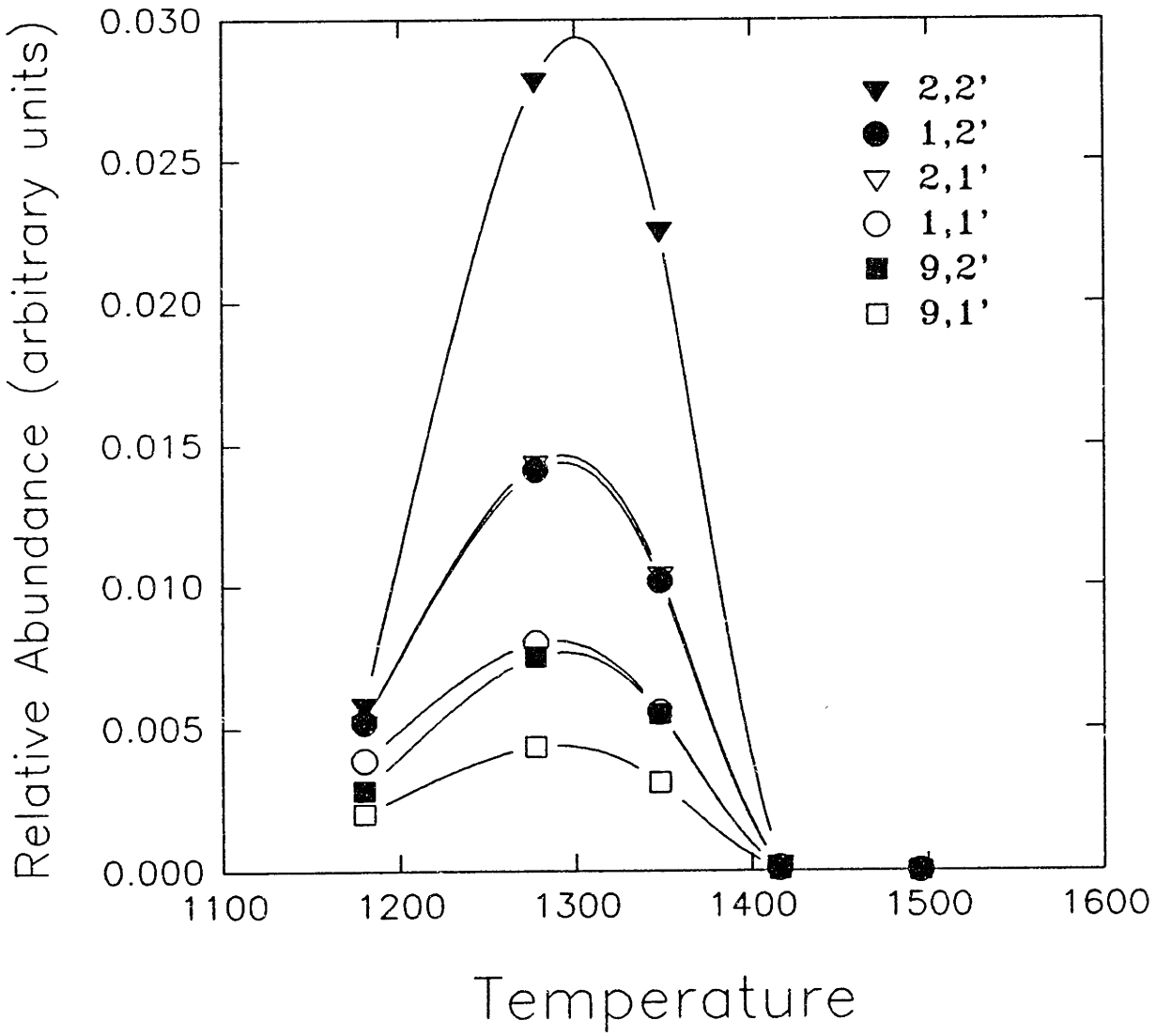

Fig. 8.5.35
Chemkin Results–
Bianthracenes

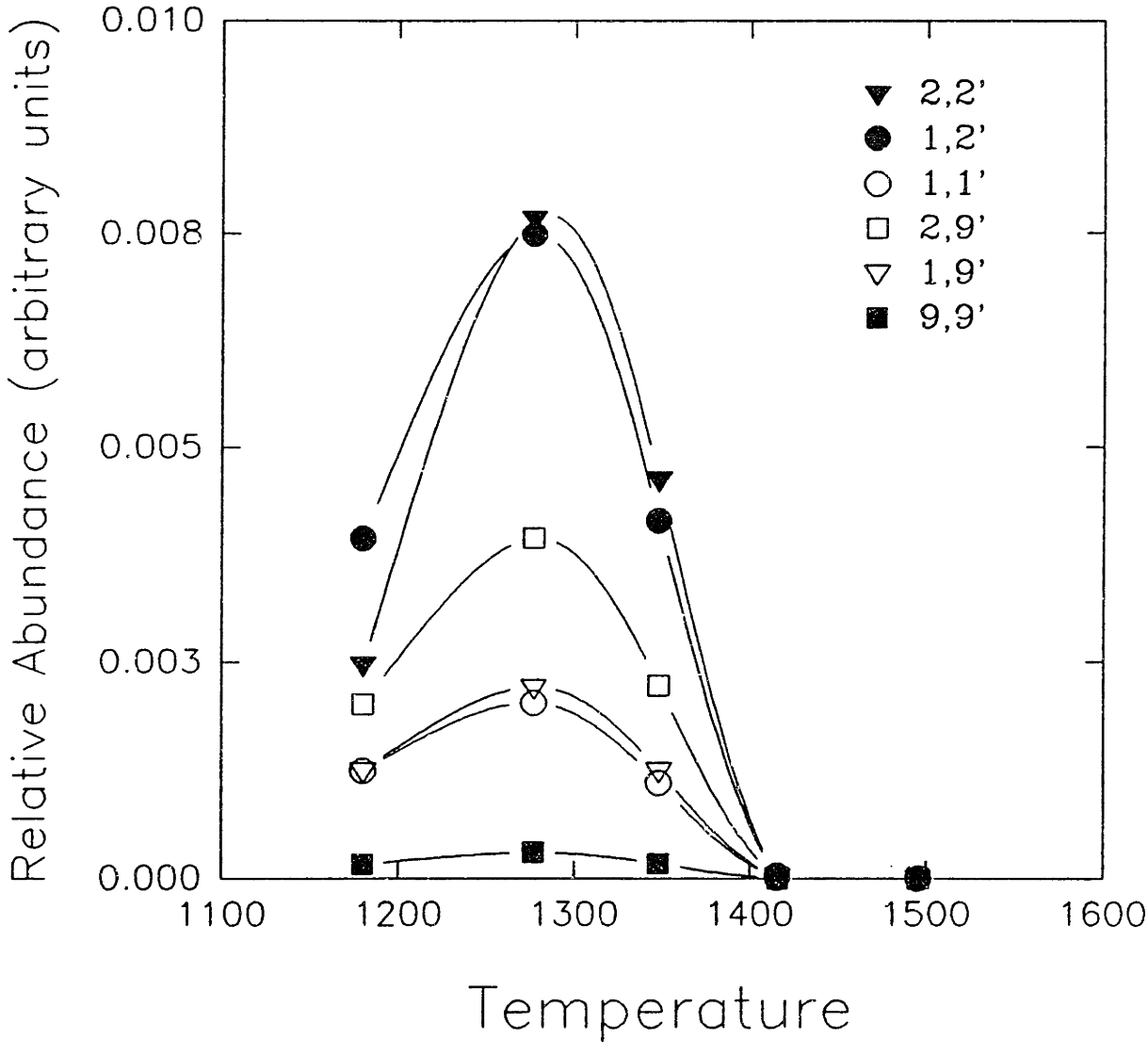

Fig. 8.5.36
Chemkin Results–
Total Biaryls

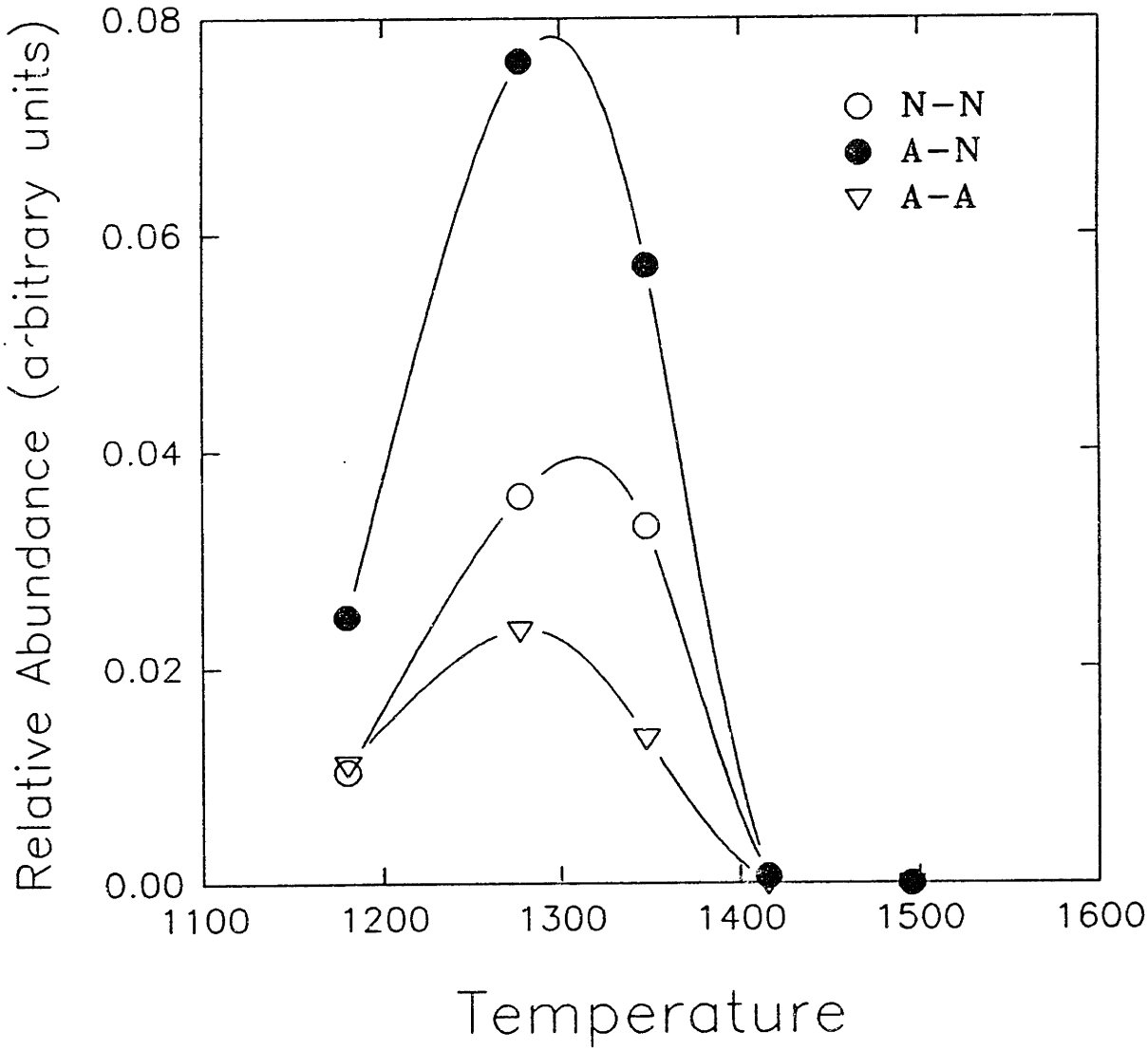

Fig. 8.5.37
Chemkin Results–
Total Condensation Products

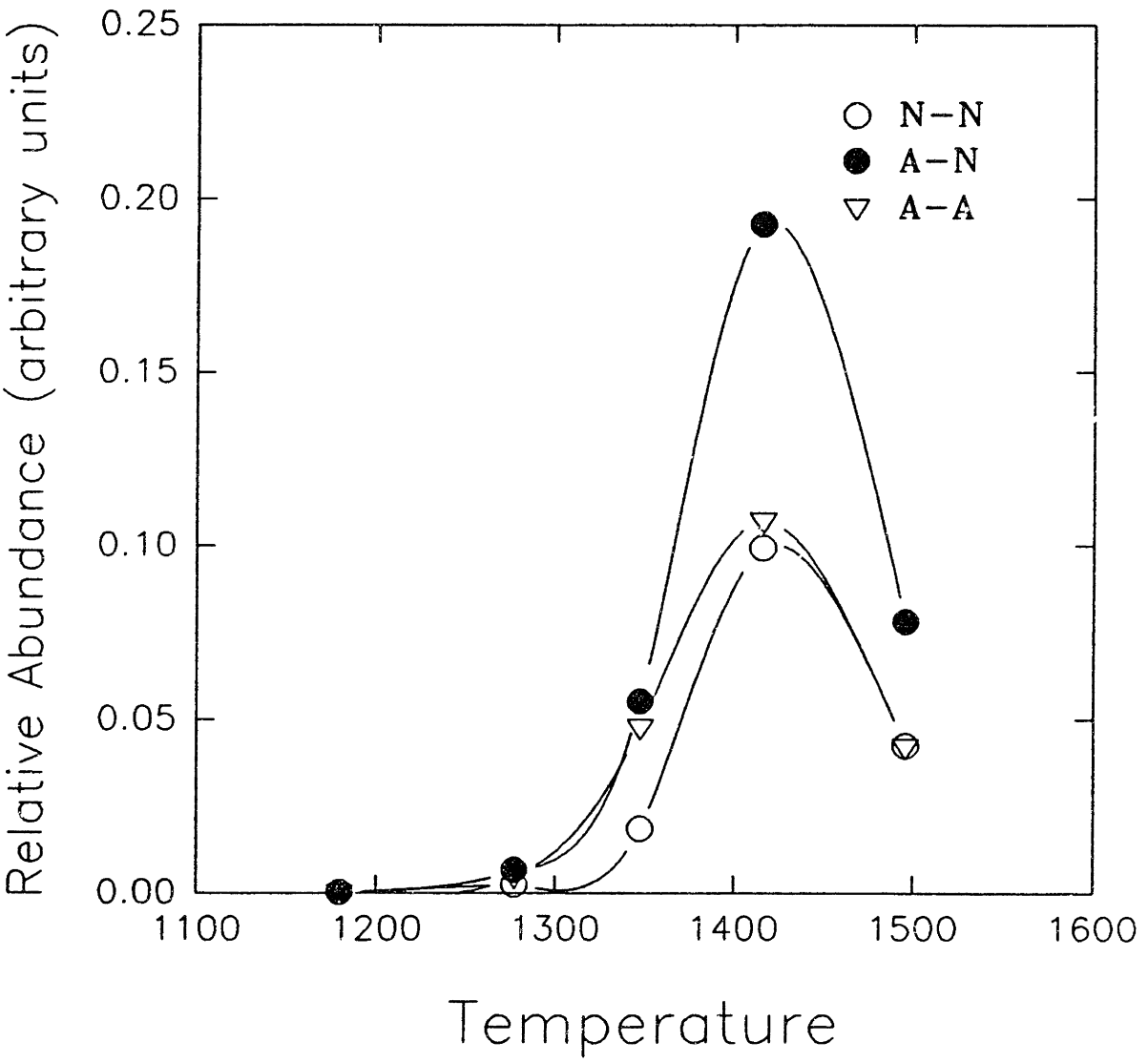

Fig. 8.5.38

BINAPHTHALENES

ANTHRACENE/NAPHTHALENE PYROLYSIS

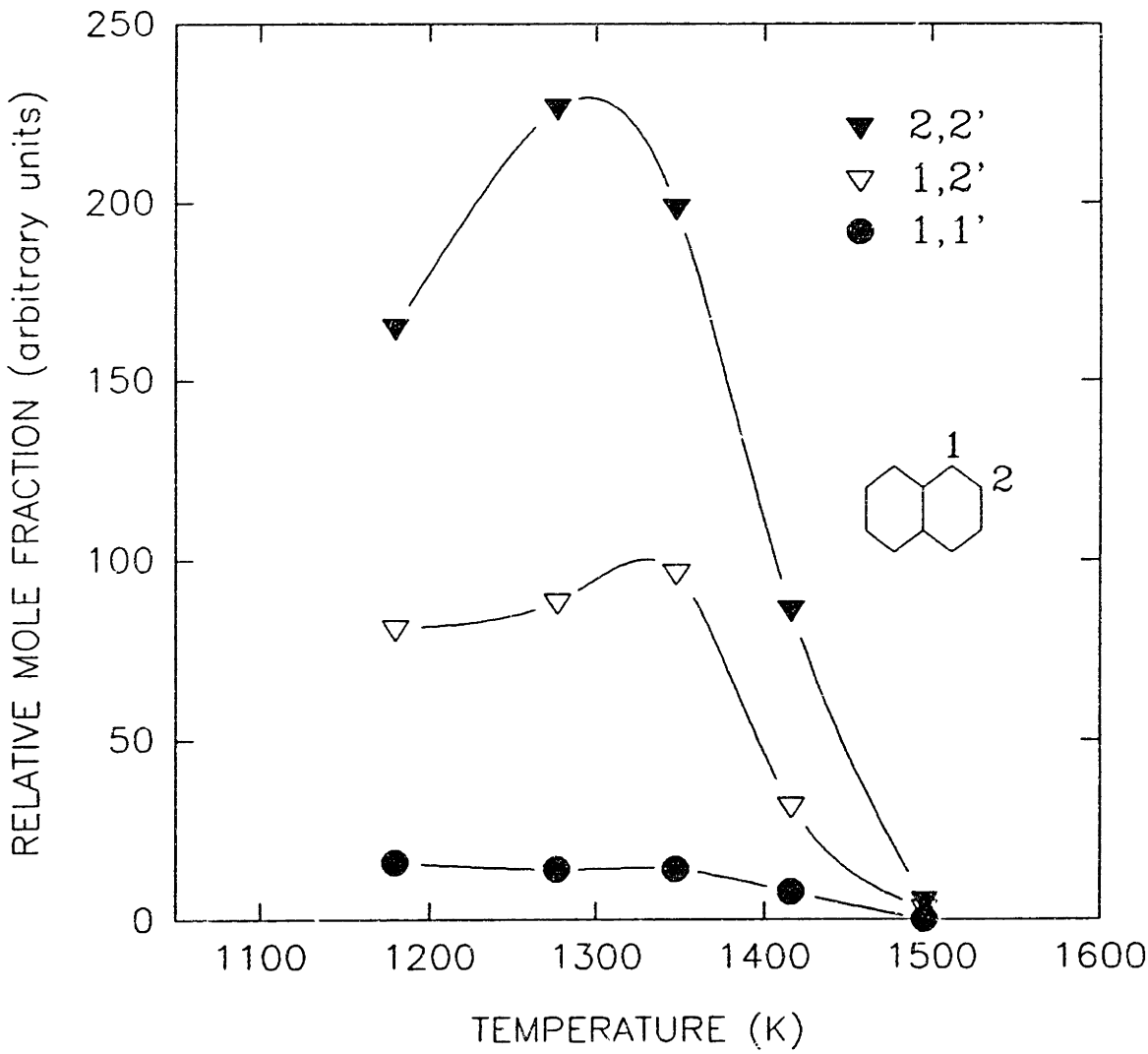

Fig. 8.5.39

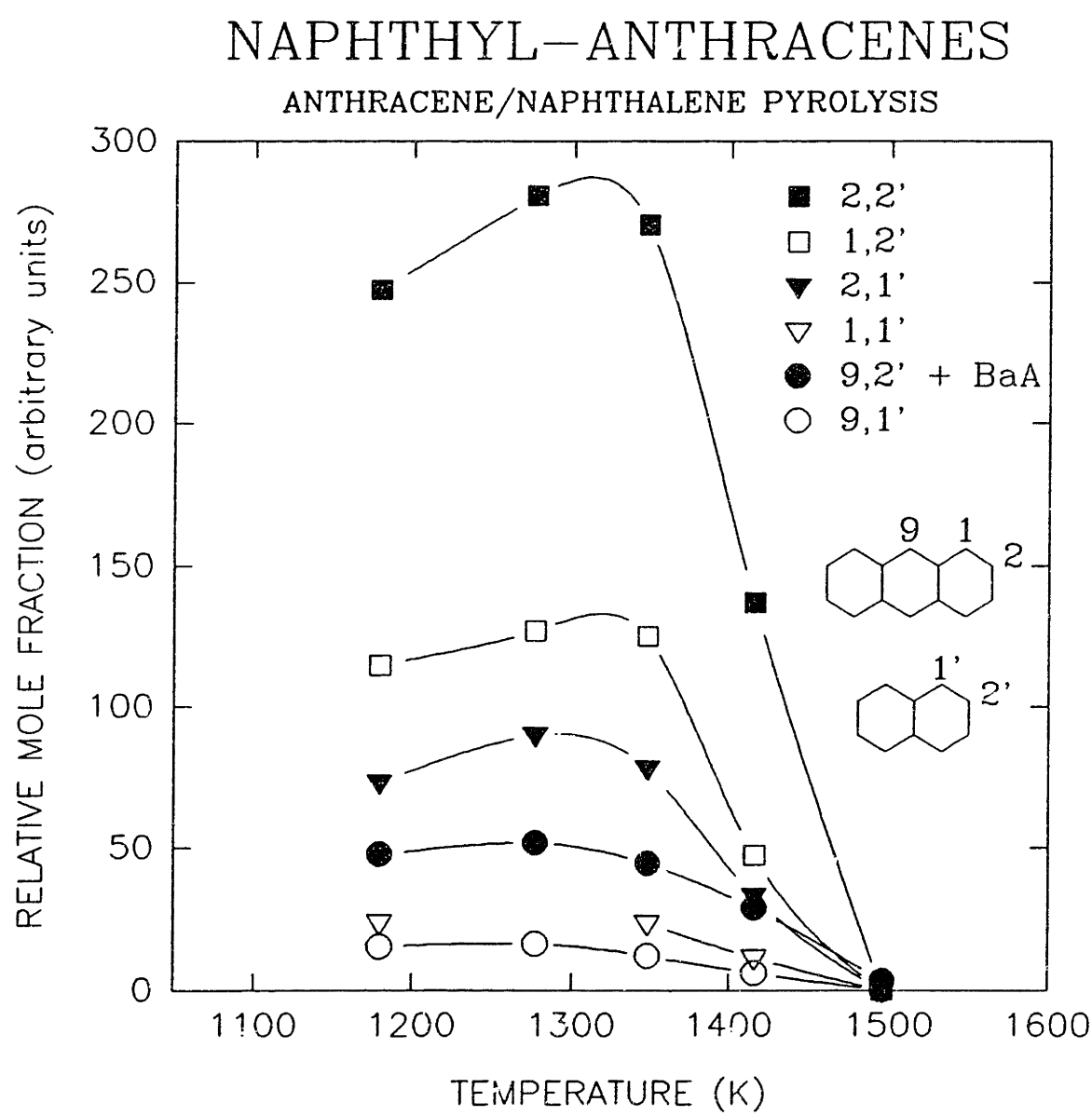
NAPHTHYL–ANTHRACENES
ANTHRACENE/NAPHTHALENE PYROLYSIS
RELATIVE MOLE FRACTION (arbitrary units)
300
250
200
150
100
50
0
1100
1200
1300
1400
1500
1600
TEMPERATURE (K)
2,2'
1,2'
2,1'
1,1'
9,2' + BaA
9,1'
9
1
2
1'
2'

Fig. 8.5.40

BIANTHRACENES

PURE ANTHRACENE PYROLYSIS

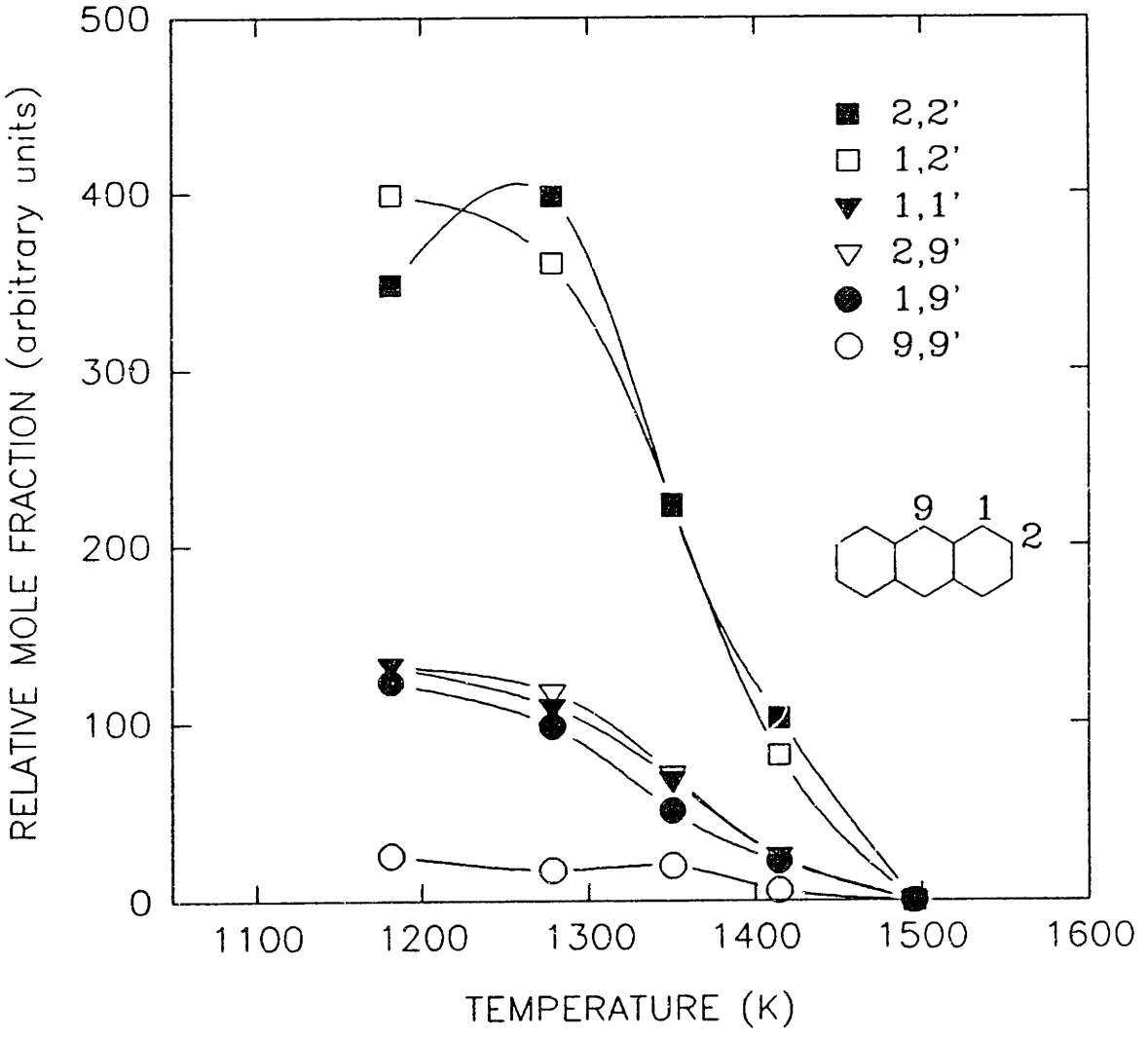

Fig. 8.5.41
TOTAL BIARYLS

(ANTHRACENE/NAPHTHALENE PYROLYSIS)

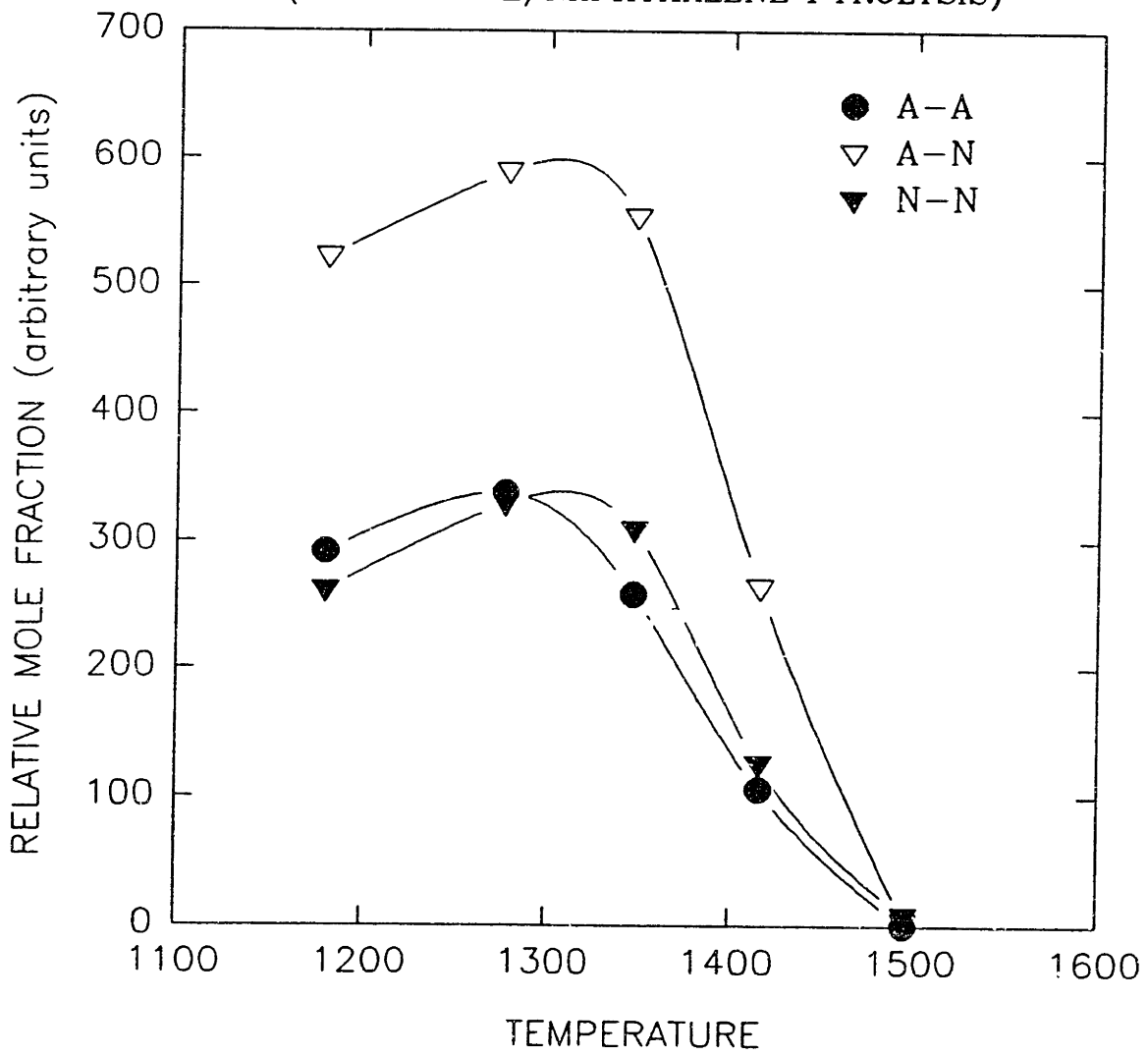

Fig. 8.5.42
TOTAL CONDENSATION PRODUCTS

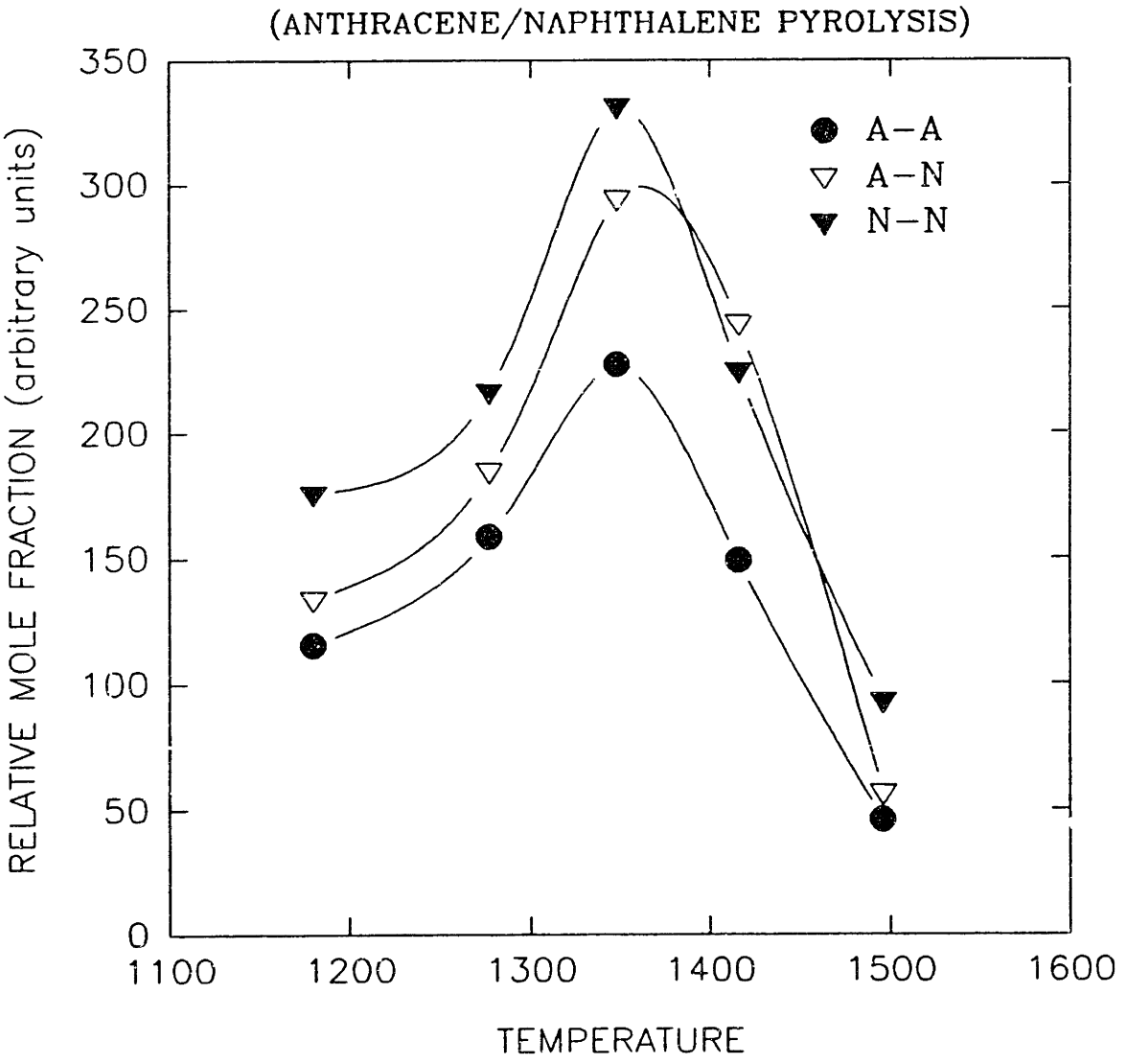

investigated in the sensitivity analysis. Even though, as a whole, relative abundances of the biaryl species are not predicted any more accurately with this model than with the previous simple theories described in chapter 4, it can be seen that trends in the errors of those predictions are much more consistent in this model. That is, discrepancies between experiment and the CHEMIN model appear attributable to one set of systematic errors in input parameters (BDEs or steric hindrance), whereas in the thermodynamic model of Chapter 4, a more complex set of input errors (no condensation taken into account, steric hindrance, radical populations) are needed to rationalize experiment with theory. It is thus very likely that, if the major inaccuracies caused by steric hindrance or BDE can be resolved, a very good match will be see between experiment and theory.

Temperature evolution of the total biaryls is consistent with experiment, with biaryl products dominating slightly over binaphthalenes at the lower temperatures, both approximately a factor of 2 below the naphthyl-anthracenes, bianthracenes peaking first in concentration, followed by naphthyl-anthracenes and then binaphthalenes. The experimental 1:2:1 ratio discussed in Chapter 4 would be approximated by the CHEMKIN calculations more nearly if the compounds with a 1-naphthyl component are appropriately discounted as proposed in the previous paragraph. This would have the effect of bringing both the binaphthalene concentration and the naphthyl-anthracene concentration down to levels that would make Fig. 8.5.36 look very similar to Fig. 8.5.41. The temperature peaks in the calculated runs occur 20 to 40 K lower and the profiles drop off 60-80 K sooner than in experiment, the discrepancy appearing to be due to a later but more excessive loss of biaryl due to condensation in the CHEMKIN simulation than in

experiment (see Figs.8.5.42 and 8.5.37). This possibility will be investigated in the sensitivity analysis.

Experimental conversions to higher molecular weight products (Figs. 8.5.21-32) appear slightly underestimated by the kinetic model (Figs. 8.5.1-15), but the mass spectra of some of the midrange naphthyl-anthracene experiments are quite closely predicted by the theory. Relative concentrations of polyaryl/condensed product groups are also predicted rather well by the model, especially in the MW 200-550 range. In contrast, thermodynamic model (Figs. 8.5.16-20) fares much worse at predicting experimental observations, tending to substantially overpredict conversion to condensed prodects and high molecular weight. Equilibrium populations of the larger products appear much more enhanced relative to the smaller products, (Figs. 8.5.16-20) indicating a thermodynamic tendency to the larger compounds, and experimental conversion (Figs. 8.5.21-32) that is intermediate between that which is calculated via kinetic and thermodynamic control. This demonstrates that high molecular weight growth with this mechanism should be possible given enough time, but the kinetic parameters chosen are not conducive to fast enough conversion of fuel to soot.

As the kinetic model underpredicts and the thermodynamic model overpredicts, a good match between experiment and theory may therefore be found somewhere between the short and long run times, and this observation may be an artifact of using a plug flow simulator to model a laminar flow pyrolysis environment. Some account must be taken for the distribution of residence times available to the compounds to adequately describe their chemistry with the kinetic model.

8.6 - Sensitivity Analysis

An analysis of the sensitivity to each of the 10 input kinetic parameters (5 basic reaction types, 2 parameters each), temperature, time, steric hindrance of biaryls, and BDE of the 1-naphthyl radical. All analyses are run separately at the median run temperature of 1348 K. The effects of small perturbations in input parameters on certain key results are measured by manually inserting the appropriate deviations into the input files. Pre-exponential factors are incremented by +10%, activation energies by +1 cal/mol, time by +0.01 sec, temperature by +1 K, BDE of 1-naphthyl by 0.5 kcal/mol and steric hindrance by 0.5 kcal/mol for 1-naphthyl components, 0.25 kcal/mol for 1-anthryl components, and 0.5 kcal/mol for 9-anthryl components. Results of the sensitivity analysis are shown in Table 8.6.1.

Pert. Type	Conversion to Polyaryl	Condensed Fraction	Total AA/ Total AN	Total NN/ Total AA	N1N2/N2N2
1 A:	2.15E-06	7.28E-06	-6.65E-05	1.77E-03	-7.55E-16
2 A:	-1.47E-04	4.96E-04	-2.30E-04	9.63E-03	-8.91E-05
3 A:	-1.01E-04	6.43E-04	-2.31E-04	9.77E-03	-8.98E-05
4 A:	-1.43E-04	2.16E-04	-1.16E-04	4.90E-03	-3.52E-05
5 A:	1.17E-07	-6.03E-07	-2.22E-15	-2.22E-14	-1.05E-13
1Eact:	0.00E+00	0.00E+00	0.00E+00	0.00E+00	0.00E+00
2Eact:	-2.87E-06	-1.86E-05	-4.65E-05	-1.24E-11	-7.55E-12
3Eact:	-1.81E-03	-1.66E-03	6.94E-13	-5.33E-12	0.00E+00
4Eact:	0.00E+00	0.00E+00	2.22E-13	-5.33E-12	0.00E+00
5Eact:	-3.20E-05	1.64E-04	-2.50E-13	-5.33E-12	0.00E+00
time:	-1.45E-02	4.68E-02	-5.64E-02	2.48E+00	-7.56E-01
temp:	-6.91E-04	3.70E-03	-1.82E-03	6.59E-02	-5.36E-04
s.hind:	4.66E-03	-3.53E-03	3.38E-03	-1.06E-01	-3.05E-01
BDE:	3.07E-03	-5.81E-03	8.03E-04	-6.36E-02	-1.35E-02

Table 8.6.1 Sensitivity of certain key represenative measuresof the kinetic model to changes in input parameters. Numbers indicate reaction type. A = pre-exponential factor was changed, Eact indicates activation energy was perturbed. See text for more details.

All of the major factors investigated in this thesis are represented in Table 8.6.1. Conversion to higher molecular weight products is approximated by taking the ratio of all triaryl compounds and higher to the biaryls. Condensation products of these compounds are also included here. A rough idea of the degree of condensation is obtained by adding all abundances of condensed products (C1 species count once, C2 species count twice, etc.)and dividing by amount of original fuel. Measures of the 1:2:1 ratio are accounted for by the ratios of total bianthracenes to naphthyl-anthracenes and total binaphthalenes to bianthracenes. The errors in relative isomer concentrations, since only one cause appears to dominate, can be adequately represented by looking at a single ratio, that of 1,2'-binaphthalene concentration to 2,2'-binaphthalene. The numbers in Table 8.6.1 represent a change in ratio caused by the perturbation divided by the magnitude of the perturbation. Units are thus fraction change per percent for the pre-exponential factor modifications, fraction change per kcal/mol for all results that represent response to energy perturbations, and fraction change per second and kelvin for the time and temperature perturbation analyses, respectively.

Inspection of Table 8.6.1 yields some interesting observations. Let us first consider sensitivity to activation energies. MW growth and Condensation are most sensitive to reaction type 3 (hydrogen abstraction) activation energies. The harder it is to make radicals, the harder it is to form the higher molecular weights and to condense. Thus a rate limiting effect is seen in radical fomation that is only approached by the secondary rate limiting effect of the condensation reactions. The former is intuitively the correct behavior for a pyrolysis environment, and the latter is consistent with the

experimental observations described in Chapters 4 and 5, where some rate-limiting behavior is seen at the condensation step. Of the biaryl ratios considered, only the total bianthracene to total naphthyl-anthracene ratio is affected to any great extent by an activation energy, and that sensitivity is to reaction type 2 (radical recombination). Specifically, bianthracene formation is disfavored relative to smaller biaryls when it is made more difficult for radicals to recombine. This makes sense when one considers that an enhancement of the radical popluation in general will help naphthalene to dimerize more than it will help anthracene, since anthracene is already nearer to a saturated radical population than is naphthalene.

Next to be investigated is the effect of time and temperature on the relevant ratios. Shifts from one product type to another (bianthracene to binaphthalene and naphthyl-anthracene, less stable to more stable biaryl isomers, non-condensed to condensed species at the expense of MW growth (see below)) that are represented in these sensitivites are all consistent with what one would expect given relative propensities of anthracene and naphthalene to form radicals and stability of condensed products relative to their polyaryl precursors. Nothing of significant interest is to be found in these numbers except to illustrate again that knowledge of the average residence time alone (used to approximate laminar flow with plug flow) of the laminar flow reactor is insufficent.

Next to be investigated is the effect of steric hindrance and the BDE of 1-naphthyl on the listed ratios. Ratios between and within the biaryl group types, as indicated by the latter three ratios listed in Table 8.6.1, are the most sensitive to changes in these parameters, especially that of steric hindrance. The directions of the sensitivities indicate

that contribution of steric hindrance to heat of formation is severely underestimated in the MOPAC calculations. Further evidence for the underestimation of steric hindrance can be found in the overabundance of perylene relative to the other binaphthalene condensation products as compared with experiment (see Fig.6.2.1 for a typical perylene abundance and Appendix G). MW growth and condensation are more sensitive to these parameters as they are to the activation energies of the rate limiting radical formation and condensation reactions. As might be expected, condensation is significantly adversely affected by how hard it is to get polyaryls into the correct rotation angle and by how hard it is to form the radicals necessary for condensation, and conversion to higher molecular weights is enhanced by the same factors. The first observation makes intuitive sense, but the second is harder to justify. A trade-off between the parallel reactions represented by MW growth and Condensation seems to be occuring; and one type is enhanced at the expense of the other. More evidence for this can be found in the analysis of the pre-exponential factors.

All of the important ratios are almost equally and significantly sensitive to changes in pre-exponential factor for reaction types 2, 3 and 4(molecular weight growth/propagation). A rate limitation involving these reaction types is thus indicated, and as the reactions are able to equilibrate faster, a shift in products similar to that seen for temperature and time dependence is evident. Condensation is enhanced with the faster rates, as might be expected if that process is kinetically limited. Naphthyl-anthracenes and binaphthalenes are also enhanced in favor of bianthracenes as the general radical population is enhanced by the faster reaction times for the rate-limiting step of radical formation. A shift from reactions favoring MW growth to ones leading to condensation is

also seen as overall rates are increased, indicating a competetion between the two reaction classes. This was also seen in the sensitivity of these ratios to steric hindrance and ease of radical formation, and it is consistent with expected trends at thermodynamic equilibrium (equivalent to much faster reaction rates). In other words, molecular weight growth can proceed by the mechanism described in this thesis only because the thermodynamically stabilizing condensation reactions are so rate-limited.

With the sensitivity analysis complete, a realization of the capacity for making some suggestions about how to improve the kinetic model becomes possible. Lowering pre-exponential factors on reaction types 2, 3, and 4 (and possibly 1) would shift the balance between condensation and MW growth in the right direction. A simultaneous reevaluation of the underestimated steric hindrances would also be appropriate to correct the relative biaryl ratios within and between the three group types. To do this properly, activation energies as well as thermodynamic properties would have to be modified, and obtaining reliable values for these parameters would require the latest technology in modeling molecular orbital structure, and the scope of such a project is beyond the range of this thesis.

Although the biaryl ratios are also moderately sensitive to BDEs of the arene radicals, modification of the BDE parameters would be inappropriate at this stage. The reasons for this are that the values for BDEs used have undergone much more scrutiny in the literature (and are thus assumed more reliable), and sensitivity to them is not as great as it is for the more unreliable steric hindrance values.

8.7 - Conclusions

A kinetic model for naphthalene/anthracene pyrolysis using 169 compounds and 2146 reactions has been developed and tested against the experimental results of Chapter 4. A working definition for a symmetry number for lumped compounds is also developed.

All of the major trends that were observed in the experiments were represented to some extent in the results of the model. Relative biaryl isomer concentrations and total biaryl abundances, as well as temperature trends of biaryls and their condensation products are all roughly predicted by the model, and errors in these predictions can be attributed primarily to systematic flaws in steric hindrance predictions made in the MOPAC calculations.

Conversion to high molecular weight compounds is underestimated at the same time that the competing reactions that lead to condensed products are overestimated. Errors in this portion of the prediction are attributable to reaction types 2 (radical recombination), 3 (hydrogen abstraction) and 4 (polymerization) being too fast and/or the use of a PFR code to model laminar flow.

Sensitivity analysis reveals that radical formation by hydrogen abstraction is the major rate limiting step, followed in importance by condensation reactions. Both of these observations are consistent with the experimental data presented in Chapters 4 and 5.

Chapter 9 - General Conclusions and Direction of Future Research

An investigation into the possibility of molecular weight growth and mutagen formation via a reactive polymerization/condensation pathway has been made. To this end, four solid fuels representative of small PAH (pure naphthalene, pure anthracene, a 1:1 mole ratio mixture, and pure ortho-terphenyl) have been pyrolyzed in a flow of nitrogen for a residence time of 2 seconds in a drop-tube furnace at temperatures in the range 1180 K to 1500 K. High molecular weight growth is indeed achieved in the form of polymers of benzene, naphthalene and anthracene in various stages of condensation.

Kinetic control of the polymerization route was first indicated by the existence of an approximately 1:2:1 total binaphthalene:naphthyl-anthracene:bianthracene ratio in the naphthalene/anthracene pyrolysis experiments. Relative abundances of biaryl isomers in each of these three series was explainable by a kinetic model that took steric hindrance of the biaryls into account by use of semi-empirical molecular orbital calculations in the computer program MOPAC. Deviations from expected trends in these series were thought due to condensation products which had not yet been taken into account. Though the data fit a kinetic model for biaryl formation better than a thermodynamic one, evidence against thermodynamic control was not strong enough in this experiment. More convincing evidence was found in the ortho-terphenyl pyrolysis.

Evidence for kinetic control was found in abundance in the benzene polymerization pathway, studied by pyrolyzing ortho-terphenyl. Investigation of the benzene polymerization pathway presented an advantage over the naphthalene/anthracene one in

that extensive thermodynamic calculations had already been performed. These previous calculations indicated the necessity of the presence of a critical species in thermodynamic control. This is a compound of relatively low molecular weight that is at a minimum concentration realtive to other intermediates in the pathway. For the benzene pathway, this critical species was expected to be ortho-terphenyl over a broad range of conditions. Ortho-terphenyl was observed, in fact, to be maximum in concentration among the intermediates, and species fell off in concentration monotonically with increase in size. This observation is exactly opposite of what was predicted in the thremodynamic theory, where concentrations were expected to go up with molecular weight at equilibrium.

More damning evidence against thermodynamic control was found in the analysis of the product spectrum. An abundance of high-energy ring-rupture products (among them CPAP, BghiF, BcPhen, chrysene, BaA, dibenzopyrenes, and dibenzofluoranthenes) was seen to compete with the highly stabilizing condensation reactions (all products of condensation in the straightforward benzene polymerization scheme are known to be the very stable total resonant sextet compounds). Furthermore, the dimer of ortho-terphenyl (hexaphenyl) was seen in unusual abundance compared the surrounding compound groups in the series (penta- and hepta-phenyl). Both of these observations strongly indicated a kinetically controlled growth pathway that is limited by condensation and polymerization bottleneck reactions.

A kinetic mechanism to test the hypothesis that had formed about the arene polymerization pathways to high molecular weight growth was then developed, with naphthalene/anthracene pyrolysis used as the test case. A reaction set consisting of 2146

reactions, 169 "lumped" compounds representing 5.5 million compounds up to molecular weight 700, and 5 major types of reactions (including radical recombination, hydrogen abstraction, polymerization, condensation, and a hydrogen balance) was used. Steric hindrance of biaryls, as well as differing propensities of different arene sites to form radicals, is taken into account, and a working definition of symmetry number for a lumped species was developed to account properly for parallel back reaction rates.

Results of the kinetic modeling conform roughly to those experimental observations that are most critical to an understanding of high molecular weight growth (conversion to high MW, conversion to condensed products, relative biaryl concentrations). The correct trends with temperature and time (within an order of magnitude) are seen, and the model makes a much better prediction about relative biaryl isomer concentrations than has been seen previously. Sensitivities to condensation and radical population are consistent in with what has been observed in the pyrolysis experiments, and a general corroboration of the conclusions (kinetic over thermodynamic control, radical formation followed in importance by condensation as rate-limiting steps, tradeoff between condensation and polymerization) made in the analysis of those studies is found. Molecular weight growth and steric hindrance considerations appear underestimated by the mechanism, but recommendations are made for correcting these shortfalls.

Eight new biaryl compounds, critical to the investigation of the viability of a kinetically controlled polymerization pathway, have been identified and characterized. These are the 6 naphthyl-anthracenes and the 2 phenyl-triphenylenes. Thes compounds

have been identified based on comparison with known trends in elution time, steric hindrance, and UV spectra; and a new hypothesis regarding a technique for indentifying biaryls in a series based on mass spectral cracking patterns is offered. A contaminant of unknown origin has also been identified as poly-(ethylene terephthalate).

Evidence for a pathway to mutagen formation has been found in the ortho-terphenyl pyrolysis experiments. The corresponding pathways in the naphthalene/anthracene pyrolysis could neither be confirmed nor disproved on the basis of a lack of ability to identify key products in those schemes. However, the similarity of reaction mechanisms involved strongly suggest that these toxic byproducts are formed, and the possibility should be investigated further.

Direction of Future Research

Taken as a whole, the results presented in this thesis demonstrate the relevance and importance of polymerization/condensation pathways to soot growth and mutagen formation, and they provide important insight into the mechanisms that control such schemes. More research is needed, however, and suggestions for the direction of future research can be made.

A more complete mechanism for describing naphthalene/anthracene pyrolysis is needed as a first step in furthering understanding of the polymerization/condensation pathway. More reactions are not recommended, but use of a more refined set of rate parameters and thermodynamic data is needed to more accurately predict product spectra. Steric hindrance data should be the easiest to obtain with a good enough molecular orbital

program. Such programs are becoming more advanced and available every day, and a reliable estimate of steric hindrance, or even all the thermodynamic parameters needed for a biaryl, should be close at hand. The lack of reliable or consistent rate parameters in the literature make the best route to their refinement a method of trial and error, guided by sensitivity analysis, and this is recommended as the best, however time consuming, route to the solution to this problem.

Armed with more reliable rate data to describe the naphthalene/anthracene pyrolysis, an attempt should be made to model the ortho-terphenyl pyrolysis, complete with ring-rupture and rearrangement mechanisms. As this would involve a much larger reaction set in order to effectively model high molecular weight growth, this analysis should not proceed until shortfalls in the naphthalene/anthracene mechanism are overcome.

Condensation product identification, including that of mutagenic rearrangement products, is also needed for further investigation into these rather important but largely unknown portions of the mechanism.

Last, a recommendation must be made to study larger compounds, and perhaps more complex mixtures, as fuels, in order to close the gap between the relatively clean laboratory experiments and practical combustion environments. Though arguably the predominant flame chemistry is a result of small fragment reactions, this thesis has demonstrated that reactions between large compounds may constitute a substantial part of the soot formation mechanism, and their contribution should be investigated further.

These recommendations for the direction of future research could easily take many investigators well into the next century, and caution should and will be exercised in planning their implementaion.

Appendix A: Sample MOPAC Input and Output

Sample MOPAC Input for 1,9'-bianthracene

```
AM1 GEO-OK EF NOINTER
1,9'-BIANTHRYL

  C     0.000000  0     0.000000  0     0.000000  0     0     0     0
  C     1.400000  1     0.000000  0     0.000000  0     1     0     0
  C     1.400000  1   120.000000  1     0.000000  0     2     1     0
  C     1.400000  1   120.000000  1     0.000000  1     3     2     1
  C     1.400000  1   120.000000  1     0.000000  1     4     3     2
  C     1.400000  1   120.000000  1   180.000000  1     5     4     3
  C     1.400000  1   120.000000  1   180.000000  1     6     5     4
  C     1.400000  1   120.000000  1   180.000000  1     7     6     5
  C     1.400000  1   120.000000  1   180.000000  1     8     7     6
  C     1.400000  1   120.000000  1     0.000000  1     9     8     7
  C     1.400000  1   120.000000  1     0.000000  1    10     9     8
  C     1.400000  1   120.000000  1     0.000000  1    11    10     9
  C     1.400000  1   120.000000  1   180.000000  1    12    11    10
  C     1.400000  1   120.000000  1   180.000000  1    13    12    11
  C     1.400000  1   120.000000  1   180.000000  1     1     2     3
  C     1.400000  1   120.000000  1   180.000000  1    15     1     2
  C     1.400000  1   120.000000  1     0.000000  1    16    15     1
  C     1.400000  1   120.000000  1   180.000000  1    17    16    15
  C     1.400000  1   120.000000  1     0.000000  1    18    17    16
  C     1.400000  1   120.000000  1     0.000000  1    19    18    17
  C     1.400000  1   120.000000  1     0.000000  1    20    19    18
  C     1.400000  1   120.000000  1   180.000000  1    21    20    19
  C     1.400000  1   120.000000  1   180.000000  1    22    21    20
  C     1.400000  1   120.000000  1   180.000000  1    23    22    21
  C     1.400000  1   120.000000  1   180.000000  1    24    23    22
  C     1.400000  1   120.000000  1     0.000000  1    25    24    23
  C     1.400000  1   120.000000  1     0.000000  1    26    25    24
  C     1.400000  1   120.000000  1     0.000000  1    27    26    25
  H     1.100000  1   120.000000  1   180.000000  1     2     3     4
  H     1.100000  1   120.000000  1   180.000000  1     3     4     5
  H     1.100000  1   120.000000  1     0.000000  1     4     5     6
  H     1.100000  1   120.000000  1     0.000000  1     6     7     8
  H     1.100000  1   120.000000  1   180.000000  1     8     9    10
  H     1.100000  1   120.000000  1   180.000000  1     9    10    11
  H     1.100000  1   120.000000  1   180.000000  1    10    11    12
  H     1.100000  1   120.000000  1     0.000000  1    11    12    13
  H     1.100000  1   120.000000  1     0.000000  1    13    14     1
  H     1.100000  1   120.000000  1   180.000000  1    17    18    19
  H     1.100000  1   120.000000  1   180.000000  1    18    19    20
  H     1.100000  1   120.000000  1   180.000000  1    19    20    21
  H     1.100000  1   120.000000  1     0.000000  1    20    21    22
  H     1.100000  1   120.000000  1     0.000000  1    22    23    24
```

```
H     1.100000  1   120.000000  1   180.000000  1    24    25    26
H     1.100000  1   120.000000  1   180.000000  1    25    26    27
H     1.100000  1   120.000000  1   180.000000  1    26    27    28
H     1.100000  1   120.000000  1     0.000000  1    27    28    15
0     0.000000  0     0.000000  0     0.000000  0     0     0     0
```

Abridged Sample Output for 1,9'-bianthracene

```
**********************************************************************
** FRANK J. SEILER RES. LAB., U.S. AIR FORCE ACADEMY, COLO. SPGS., CO. 80840 **
**********************************************************************

                          AM1 CALCULATION RESULTS

**********************************************************************
*          MOPAC:  VERSION  6.00              CALC'D. 08/17/93
*  GEO-OK    - OVERRIDE INTERATOMIC DISTANCE CHECK
*   T=       - A TIME OF  3600.0 SECONDS REQUESTED
*  DUMP=N    - RESTART FILE WRITTEN EVERY  3600.0 SECONDS
*  EF        - USE EF ROUTINE FOR MINIMUM SEARCH
*  AM1       - THE AM1 HAMILTONIAN TO BE USED
*  NOINTER   - INTERATOMIC DISTANCES NOT TO BE PRINTED
**********************************************************************100BY100
AM1 GEO-OK EF NOINTER
1,9'-BIANTHRYL
```

ATOM NUMBER (I)	CHEMICAL SYMBOL	BOND LENGTH (ANGSTROMS) NA:I		BOND ANGLE (DEGREES) NB:NA:I		TWIST ANGLE (DEGREES) NC:NB:NA:I		NA	NB	NC
1	C									
2	C	1.40000	*					1		
3	C	1.40000	*	120.00000	*			2	1	
4	C	1.40000	*	120.00000	*	0.00000	*	3	2	1
5	C	1.40000	*	120.00000	*	0.00000	*	4	3	2
6	C	1.40000	*	120.00000	*	180.00000	*	5	4	3
7	C	1.40000	*	120.00000	*	180.00000	*	6	5	4
8	C	1.40000	*	120.00000	*	180.00000	*	7	6	5
9	C	1.40000	*	120.00000	*	180.00000	*	8	7	6
10	C	1.40000	*	120.00000	*	0.00000	*	9	8	7
11	C	1.40000	*	120.00000	*	0.00000	*	10	9	8
12	C	1.40000	*	120.00000	*	0.00000	*	11	10	9
13	C	1.40000	*	120.00000	*	180.00000	*	12	11	10
14	C	1.40000	*	120.00000	*	180.00000	*	13	12	11
15	C	1.40000	*	120.00000	*	180.00000	*	1	2	3
16	C	1.40000	*	120.00000	*	180.00000	*	15	1	2
17	C	1.40000	*	120.00000	*	0.00000	*	16	15	1
18	C	1.40000	*	120.00000	*	180.00000	*	17	16	15
19	C	1.40000	*	120.00000	*	0.00000	*	18	17	16
20	C	1.40000	*	120.00000	*	0.00000	*	19	18	17
21	C	1.40000	*	120.00000	*	0.00000	*	20	19	18
22	C	1.40000	*	120.00000	*	180.00000	*	21	20	19
23	C	1.40000	*	120.00000	*	180.00000	*	22	21	20
24	C	1.40000	*	120.00000	*	180.00000	*	23	22	21
25	C	1.40000	*	120.00000	*	180.00000	*	24	23	22
26	C	1.40000	*	120.00000	*	0.00000	*	25	24	23
27	C	1.40000	*	120.00000	*	0.00000	*	26	25	24
28	C	1.40000	*	120.00000	*	0.00000	*	27	26	25
29	H	1.10000	*	120.00000	*	180.00000	*	2	3	4
30	H	1.10000	*	120.00000	*	180.00000	*	3	4	5
31	H	1.10000	*	120.00000	*	0.00000	*	4	5	6
32	H	1.10000	*	120.00000	*	0.00000	*	6	7	8
33	H	1.10000	*	120.00000	*	180.00000	*	8	9	10
34	H	1.10000	*	120.00000	*	180.00000	*	9	10	11
35	H	1.10000	*	120.00000	*	180.00000	*	10	11	12

36	H	1.10000	*	120.00000	*	0.00000	*	11	12	13
37	H	1.10000	*	120.00000	*	0.00000	*	13	14	1
38	H	1.10000	*	120.00000	*	180.00000	*	17	18	19
39	H	1.10000	*	120.00000	*	180.00000	*	18	19	20
40	H	1.10000	*	120.00000	*	180.00000	*	19	20	21
41	H	1.10000	*	120.00000	*	0.00000	*	20	21	22
42	H	1.10000	*	120.00000	*	0.00000	*	22	23	24
43	H	1.10000	*	120.00000	*	180.00000	*	24	25	26
44	H	1.10000	*	120.00000	*	180.00000	*	25	26	27
45	H	1.10000	*	120.00000	*	180.00000	*	26	27	28
46	H	1.10000	*	120.00000	*	0.00000	*	27	28	15

CARTESIAN COORDINATES

NO.	ATOM	X	Y	Z
1	C	0.0000	0.0000	0.0000
2	C	1.4000	0.0000	0.0000
3	C	2.1000	1.2124	0.0000
4	C	1.4000	2.4249	0.0000
5	C	0.0000	2.4249	0.0000
6	C	-0.7000	3.6373	0.0000
7	C	-2.1000	3.6373	0.0000
8	C	-2.8000	4.8497	0.0000
9	C	-4.2000	4.8497	0.0000
10	C	-4.9000	3.6373	0.0000
11	C	-4.2000	2.4249	0.0000
12	C	-2.8000	2.4249	0.0000
13	C	-2.1000	1.2124	0.0000
14	C	-0.7000	1.2124	0.0000
15	C	-0.7000	-1.2124	0.0000
16	C	-2.1000	-1.2124	0.0000
17	C	-2.8000	0.0000	0.0000
18	C	-4.2000	0.0000	0.0000
19	C	-4.9000	-1.2124	0.0000
20	C	-4.2000	-2.4249	0.0000
21	C	-2.8000	-2.4249	0.0000
22	C	-2.1000	-3.6373	0.0000
23	C	-0.7000	-3.6373	0.0000
24	C	0.0000	-4.8497	0.0000
25	C	1.4000	-4.8497	0.0000
26	C	2.1000	-3.6373	0.0000
27	C	1.4000	-2.4249	0.0000
28	C	0.0000	-2.4249	0.0000
29	H	1.9500	-0.9526	0.0000
30	H	3.2000	1.2124	0.0000
31	H	1.9500	3.3775	0.0000
32	H	-0.1500	4.5899	0.0000
33	H	-2.2500	5.8024	0.0000
34	H	-4.7500	5.8024	0.0000
35	H	-6.0000	3.6373	0.0000
36	H	-4.7500	1.4722	0.0000
37	H	-2.6500	0.2598	0.0000
38	H	-2.2500	0.9526	0.0000
39	H	-4.7500	0.9526	0.0000
40	H	-6.0000	-1.2124	0.0000
41	H	-4.7500	-3.3775	0.0000
42	H	-2.6500	-4.5899	0.0000
43	H	-0.5500	-5.8024	0.0000
44	H	1.9500	-5.8024	0.0000
45	H	3.2000	-3.6373	0.0000
46	H	1.9500	-1.4722	0.0000

H: (AM1): M.J.S. DEWAR ET AL, J. AM. CHEM. SOC. 107 3902-3909 (1985)
C: (AM1): M.J.S. DEWAR ET AL, J. AM. CHEM. SOC. 107 3902-3909 (1985)

RHF CALCULATION, NO. OF DOUBLY OCCUPIED LEVELS = 65

```
CYCLE:    1 TIME:    3.38 TIME LEFT:    3596.6 GRAD.: 64225.539 HEAT: 2391.853
CYCLE:    2 TIME:    0.01 TIME LEFT:    3596.6 GRAD.:124775.704 HEAT: 4988.407
CYCLE:    3 TIME:    2.49 TIME LEFT:    3594.1 GRAD.: 11749.449 HEAT: 633.2326
CYCLE:    4 TIME:    2.26 TIME LEFT:    3591.9 GRAD.: 12355.888 HEAT: 741.3060
CYCLE:    5 TIME:    2.39 TIME LEFT:    3589.5 GRAD.:  8441.346 HEAT: 538.3367
CYCLE:    6 TIME:    2.31 TIME LEFT:    3587.2 GRAD.:  5141.133 HEAT: 483.3787
```

```
                                   .
                                   .
CYCLE:  33 TIME:    2.49 TIME LEFT:    3522.6 GRAD.:     49.560 HEAT: 136.2844

ALL CONVERGERS ARE NOW FORCED ON
SHIFT=10, PULAY ON, CAMP-KING ON
AND ITERATION COUNTER RESET

CYCLE:  34 TIME:    2.48 TIME LEFT:    3520.1 GRAD.:     30.360 HEAT: 135.8986
                                   .
                                   .
                                   .
CYCLE:  67 TIME:    4.61 TIME LEFT:    3339.6 GRAD.:      0.352 HEAT: 134.6280

 ---------------------------------------------------------------------------
 AM1 GEO-OK EF NOINTER
 1,9'-BIANTHRYL


     GEOMETRY OPTIMISED USING EIGENVECTOR FOLLOWING (EF).
     SCF FIELD WAS ACHIEVED

                                AM1    CALCULATION
                                                VERSION  6.00
                                                          08/17/93



          FINAL HEAT OF FORMATION =         134.62814 KCAL


          TOTAL ENERGY            =       -3830.29733 EV
          ELECTRONIC ENERGY       =      -31837.51792 EV
          CORE-CORE REPULSION     =       28007.22059 EV

          IONIZATION POTENTIAL    =           8.08843
          NO. OF FILLED LEVELS    =          65
          MOLECULAR WEIGHT        =     354.450


          SCF CALCULATIONS  =                68
          COMPUTATION TIME =  4 MINUTES AND       27.6453 SECONDS
```

ATOM NUMBER (I)	CHEMICAL SYMBOL	BOND LENGTH (ANGSTROMS) NA:I		BOND ANGLE (DEGREES) NB:NA:I		TWIST ANGLE (DEGREES) NC:NB:NA:I		NA	NB	NC
1	C									
2	C	1.37198	*					1		
3	C	1.42348	*	120.88593	*			2	1	
4	C	1.36390	*	120.49809	*	0.07390	*	3	2	1
5	C	1.43222	*	120.63817	*	0.00235	*	4	3	2
6	C	1.39949	*	121.15265	*	179.97869	*	5	4	3
7	C	1.39856	*	121.09703	*	-179.95212	*	6	5	4
8	C	1.43269	*	121.83659	*	179.96937	*	7	6	5
9	C	1.36469	*	120.71674	*	-179.97238	*	8	7	6
10	C	1.42573	*	120.46380	*	-0.00852	*	9	8	7
11	C	1.36472	*	120.45944	*	0.00240	*	10	9	8
12	C	1.43283	*	120.72259	*	-0.00263	*	11	10	9
13	C	1.39904	*	121.63388	*	-179.99760	*	12	11	10
14	C	1.39990	*	121.21967	*	-179.96309	*	13	12	11
15	C	1.47143	*	120.10960	*	179.80210	*	1	2	3
16	C	1.40817	*	119.80530	*	-89.63603	*	15	1	2
17	C	1.43414	*	122.06708	*	-0.89349	*	16	15	1
18	C	1.36446	*	121.07075	*	179.90096	*	17	16	15
19	C	1.42505	*	120.49369	*	0.01509	*	18	17	16

20	C	1.36417	*	120.22796	*	0.02654	*	19	18	17
21	C	1.43327	*	120.85831	*	-0.06445	*	20	19	18
22	C	1.39797	*	121.18029	*	-179.82597	*	21	20	19
23	C	1.39807	*	120.89124	*	179.86576	*	22	21	20
24	C	1.43318	*	121.18043	*	-179.90894	*	23	22	21
25	C	1.36426	*	120.86042	*	179.84696	*	24	23	22
26	C	1.42509	*	120.22558	*	0.03603	*	25	24	23
27	C	1.36453	*	120.49181	*	-0.01223	*	26	25	24
28	C	1.43408	*	121.07320	*	0.01459	*	27	26	25
29	H	1.10089	*	118.58196	*	179.96386	*	2	3	4
30	H	1.10025	*	121.07901	*	-179.98472	*	3	4	5
31	H	1.10057	*	118.15443	*	-0.03519	*	4	5	6
32	H	1.10101	*	119.49054	*	-0.00581	*	6	7	8
33	H	1.10041	*	121.18731	*	179.98081	*	8	9	10
34	H	1.10001	*	118.56567	*	-179.99254	*	9	10	11
35	H	1.09997	*	120.96339	*	179.99375	*	10	11	12
36	H	1.10064	*	118.05422	*	-0.01526	*	11	12	13
37	H	1.10230	*	119.34805	*	0.00614	*	13	14	1
38	H	1.10179	*	120.96128	*	-179.88958	*	17	18	19
39	H	1.10012	*	118.64035	*	-179.91088	*	18	19	20
40	H	1.09988	*	121.05955	*	179.91144	*	19	20	21
41	H	1.10044	*	117.97220	*	0.13457	*	20	21	22
42	H	1.10105	*	119.55036	*	-0.00201	*	22	23	24
43	H	1.10042	*	121.16120	*	-179.99137	*	24	25	26
44	H	1.09988	*	118.71669	*	-179.96765	*	25	26	27
45	H	1.10015	*	120.85620	*	-179.94777	*	26	27	28
46	H	1.10176	*	117.95408	*	0.13270	*	27	28	15

Error opening SYBYL MOPAC output

EIGENVALUES

-41.58260	-40.65838	-38.84076	-38.74653	-35.75187	-35.16849	-34.67481	-33.12854
-31.69533	-31.32286	-30.63669	-30.63355	-29.03373	-28.16582	-25.35264	-24.95148
-23.80970	-23.80420	-23.44640	-22.53722	-22.36631	-21.03977	-19.80695	-19.55500
-18.00879	-17.83690	-17.45868	-16.96367	-16.41298	-16.32721	-15.85504	-15.79440
-15.52185	-15.46742	-15.40879	-14.77397	-14.68592	-14.47506	-14.19496	-14.15429
-14.01602	-14.00606	-13.97248	-13.43216	-13.24813	-13.13690	-13.05383	-13.03035
-12.99747	-12.25220	-11.98857	-11.90351	-11.88597	-11.66882	-11.31013	-11.23138
-11.19902	-11.01308	-10.94713	-9.81805	-9.78147	-9.20733	-9.18846	-8.10169
-8.08843	-0.88526	-0.85721	-0.05519	-0.03427	0.51429	0.61800	1.37769
1.42682	1.54123	1.55262	2.62433	2.70472	3.30504	3.34498	3.37496
3.57675	3.60698	3.77377	3.82146	3.84452	3.88171	3.89431	3.90440
3.92629	4.05911	4.14975	4.16671	4.21854	4.22780	4.26654	4.27440
4.29916	4.31214	4.37533	4.39200	4.51680	4.70747	4.75352	4.77029
4.88911	4.89729	4.95227	5.04475	5.07859	5.09119	5.11656	5.12208
5.27649	5.31857	5.42707	5.43371	5.46722	5.50709	5.55656	5.63203
5.63863	5.66105	5.77152	5.77891	5.81566	5.90961	5.99670	6.01969
6.10594	6.13187						

NET ATOMIC CHARGES AND DIPOLE CONTRIBUTIONS

ATOM NO.	TYPE	CHARGE	ATOM ELECTRON DENSITY
1	C	-0.0321	4.0321
2	C	-0.1151	4.1151
3	C	-0.1300	4.1300
4	C	-0.1159	4.1159
5	C	-0.0364	4.0364
6	C	-0.1102	4.1102
7	C	-0.0321	4.0321
8	C	-0.1199	4.1199
9	C	-0.1246	4.1246
10	C	-0.1289	4.1289
11	C	-0.1138	4.1138
12	C	-0.0350	4.0350
13	C	-0.0977	4.0977
14	C	-0.0271	4.0271
15	C	-0.0236	4.0236
16	C	-0.0216	4.0216
17	C	-0.1143	4.1143
18	C	-0.1281	4.1281
19	C	-0.1246	4.1246
20	C	-0.1216	4.1216
21	C	-0.0358	4.0358

22	C	-0.1057	4.1057
23	C	-0.0357	4.0357
24	C	-0.1217	4.1217
25	C	-0.1245	4.1245
26	C	-0.1281	4.1281
27	C	-0.1143	4.1143
28	C	-0.0217	4.0217
29	H	0.1414	0.8586
30	H	0.1346	0.8654
31	H	0.1331	0.8669
32	H	0.1339	0.8661
33	H	0.1317	0.8683
34	H	0.1319	0.8681
35	H	0.1324	0.8676
36	H	0.1353	0.8647
37	H	0.1473	0.8527
38	H	0.1441	0.8559
39	H	0.1336	0.8664
40	H	0.1324	0.8676
41	H	0.1318	0.8682
42	H	0.1349	0.8651
43	H	0.1318	0.8682
44	H	0.1324	0.8676
45	H	0.1336	0.8664
46	H	0.1440	0.8560

DIPOLE	X	Y	Z	TOTAL
POINT-CHG.	-0.096	0.128	-0.001	0.160
HYBRID	-0.001	-0.028	0.000	0.028
SUM	-0.097	0.099	-0.001	0.139

CARTESIAN COORDINATES

NO.	ATOM	X	Y	Z
1	C	0.0000	0.0000	0.0000
2	C	1.3720	0.0000	0.0000
3	C	2.1027	1.2216	0.0000
4	C	1.4495	2.4189	0.0015
5	C	0.0181	2.4695	0.0032
6	C	-0.6031	3.6919	0.0052
7	C	-2.0609	3.7399	0.0078
8	C	-2.7744	4.9823	0.0106
9	C	-4.1389	5.0024	0.0137
10	C	-4.8798	3.7844	0.0140
11	C	-4.2343	2.5820	0.0114
12	C	-2.8028	2.5196	0.0081
13	C	-2.1216	1.2977	0.0053
14	C	-0.7226	1.2469	0.0028
15	C	-0.7381	-1.2729	-0.0044
16	C	-1.0826	-1.8780	-1.2284
17	C	-0.7529	-1.2834	-2.4911
18	C	-1.0949	-1.8887	-3.6652
19	C	-1.7914	-3.1319	-3.6618
20	C	-2.1240	-3.7296	-2.4814
21	C	-1.7808	-3.1241	-1.2285
22	C	-2.1151	-3.7324	-0.0150
23	C	-1.7748	-3.1378	1.2037
24	C	-2.1128	-3.7569	2.4513
25	C	-1.7748	-3.1724	3.6368
26	C	-1.0773	-1.9298	3.6509
27	C	-0.7400	-1.3119	2.4819
28	C	-1.0762	-1.8919	1.2142
29	H	1.9312	-0.9482	-0.0019
30	H	3.2019	1.1743	-0.0010
31	H	2.0027	3.3703	0.0013
32	H	-0.0886	4.6311	0.0051
33	H	-2.1907	5.9151	0.0099
34	H	-4.6910	5.9539	0.0160
35	H	-5.9786	3.8368	0.0165
36	H	-4.7937	1.6341	0.0114
37	H	-2.6963	0.3571	0.0051
38	H	-0.2160	-0.3213	-2.4847
39	H	-0.8410	-1.4292	-4.6320
40	H	-2.0518	-3.5943	-4.6251

41	H	-2.6620	-4.6893	-2.4607
42	H	-2.6522	-4.6936	-0.0191
43	H	-2.6515	-4.7160	2.4225
44	H	-2.0327	-3.6446	4.5961
45	H	-0.8184	-1.4812	4.6214
46	H	-0.2022	-0.3503	2.4836

ATOMIC ORBITAL ELECTRON POPULATIONS

1.18564	0.92482	0.90706	1.01453	1.21910	0.92624	0.97780	0.99192
1.21699	0.99101	0.91821	1.00384	1.21798	0.92605	0.97486	0.99705
1.18495	0.92605	0.92088	1.00453	1.21613	0.92820	0.96342	1.00244
1.18493	0.92369	0.92515	0.99834	1.21740	0.93908	0.95983	1.00363
1.21774	0.93597	0.97376	0.99710	1.21771	0.99008	0.91960	1.00152
1.21805	0.92531	0.97489	0.99559	1.18523	0.92779	0.92066	1.00134
1.21824	0.92735	0.97019	0.98190	1.18472	0.92413	0.91074	1.00754
1.18470	0.99046	0.93487	0.91354	1.18541	0.97972	0.93602	0.92049
1.21943	0.99288	0.99501	0.90703	1.21777	0.98495	0.95110	0.97424
1.21774	0.98249	0.95245	0.97188	1.21741	1.00127	0.99148	0.91148
1.18469	0.98347	0.93952	0.92807	1.21674	0.99325	0.98928	0.90641
1.18472	0.98340	0.93958	0.92804	1.21741	1.00130	0.99134	0.91162
1.21777	0.98227	0.95304	0.97142	1.21779	0.98510	0.95056	0.97467
1.21943	0.99278	0.99514	0.90697	1.18536	0.97980	0.93586	0.92063
0.85864	0.86543	0.86698	0.86606	0.86830	0.86808	0.86756	0.86473
0.85275	0.85592	0.86641	0.86762	0.86817	0.86512	0.86817	0.86761
0.86641	0.85598						

TOTAL CPU TIME: 267.7064 SECONDS

== MOPAC DONE ==

Appendix B - Selected Programs

Program 1: Converts MOPAC output into rotatable 3-dim image of molecule on IBM PC

```
1 CLEAR : INPUT "file"; f$
2 c = 100: DIM x(c), y(c), z(c), mm$(c), xtemp(c), ytemp(c), ztemp(c), k(c, 3)
3 REM c= max number of atoms. This can be changed only if larger number of atoms is
needed
4 e = 20: cx = 200: cy = 200: angres = 5: SCREEN 9
5 REM e, cx and cy are size and location factors, angres is angle of revolution
6 g$ = "d:\programs\thesis\" + f$ + ".out"
7 REM make sure the path is right on line 5
10 OPEN g$ FOR INPUT AS #1
15 LINE INPUT #1, temp$
16 IF MID$(temp$, 11, 9) <> "CARTESIAN" GOTO 15
17 z = z + 1: ON z GOTO 15, 19
19 FOR i = 1 TO 3: LINE INPUT #1, temp$: NEXT i: i = 0
20 REM Now it's cued up to the cartesian coordinates, starts taking data
40 i = i + 1
41 LINE INPUT #1, temp$
42 mm$(i) = MID$(temp$, 16, 1): IF mm$(i) = "" THEN LET c = i - 1: GOTO 70
43 x(i) = VAL(MID$(temp$, 33, 8))
44 y(i) = VAL(MID$(temp$, 43, 8))
45 z(i) = VAL(MID$(temp$, 53, 8))
60 GOTO 40
70 CLS : PRINT c: FOR i = 1 TO c - 1: m = 1
72 FOR j = i + 1 TO c
75 dist = SQR((x(i) - x(j)) ^ 2 + (y(i) - y(j)) ^ 2 + (z(i) - z(j)) ^ 2)
80 IF dist < 1.5 THEN LINE (e * x(i) + cx, e * y(i) + cy)-(e * x(j) + cx, e * y(j) + cy)
82 IF dist < 1.5 THEN LET k(i, m) = j: m = m + 1
83 REM draws a line for all interatomic distances less than 1.5 angstroms
85 NEXT j
90 NEXT i
100 ON KEY(11) GOSUB 110
101 ON KEY(12) GOSUB 120
102 ON KEY(13) GOSUB 130
103 ON KEY(14) GOSUB 140
104 KEY(0) ON
107 REM takes input from cursor keys and calculates rotation matrix
109 GOTO 109
110 phiy = angres * 3.14159 / 180
```

```
112 a11 = 1: a12 = 0: a13 = 0: a21 = 0: a22 = COS(phi): a23 = SIN(-phiy)
113 a31 = 0: a32 = SIN(phiy): a33 = COS(phiy): GOSUB 215
120 phix = angres * 3.14159 / 180
122 a22 = 1: a21 = 0: a23 = 0: a12 = 0: a11 = COS(phix): a13 = SIN(-phix)
123 a32 = 0: a31 = SIN(phix): a33 = COS(phix): GOSUB 215
130 phix = -angres * 3.14159 / 180: GOTO 122
140 phiy = -angres * 3.14159 / 180: GOTO 112
145 RETURN
200 REM There's a bug due to the key statements gosub calling, but it's livable
215 FOR i = 1 TO c
220 xtemp(i) = x(i) * a11 + y(i) * a21 + z(i) * a31
221 ytemp(i) = x(i) * a12 + y(i) * a22 + z(i) * a32
222 ztemp(i) = x(i) * a13 + y(i) * a23 + z(i) * a33
223 x(i) = xtemp(i): y(i) = ytemp(i): z(i) = ztemp(i)
225 NEXT i
228 REM uses more efficient drawing routine after initial drawing
230 CLS : FOR i = 1 TO c
235 FOR m = 1 TO 3
240 IF k(i, m) <> 0 THEN LINE (e * x(i) + cx, e * y(i) + cy)-(e * x(k(i, m)) + cx, e *
y(k(i, m)) + cy)
250 NEXT m: NEXT i
255 RETURN 145
```

Program 2: Converts Lotus123 printfile output into format readable by CHEMKIN

```
10 CLEAR : DIM tmp AS STRING * 70, sp AS STRING
20 OPEN "d:\chemkin\mech.dat" FOR INPUT AS #1
30 OPEN "d:\chemkin\mech.out" FOR OUTPUT AS #2
35 OPEN "d:\chemkin\species.dat" FOR INPUT AS #3
36 IF EOF(3) THEN GOTO 40
37 LINE INPUT #3, tmp
38 PRINT #2, tmp
39 GOTO 36
40 IF EOF(1) THEN GOTO 150
50 LINE INPUT #1, tmp
60 aa$ = MID$(tmp, 5, 9): REM Reactant 1 in field A
61 ab$ = MID$(tmp, 14, 9): REM Reactant 2 in field B
62 ac$ = MID$(tmp, 23, 9): REM Product 1 in field C
63 ad$ = MID$(tmp, 32, 9): REM Product 2 in field D
64 ae$ = MID$(tmp, 42, 5): REM A-Factor in field E formatted to width of 10 in LOTUS
65 af$ = MID$(tmp, 48, 2): REM exponent of A factor
66 ag$ = MID$(tmp, 57, 2): REM b in field F
```

```
67 ah$ = MID$(tmp, 62, 6): REM acitivation energy in field G
70 FOR i = 1 TO 9
71 IF MID$(aa$, i, 1) = " " THEN LET aa$ = LEFT$(aa$, i - 1): i = 9
72 NEXT i
80 FOR i = 1 TO 9
81 IF MID$(ab$, i, 1) = " " THEN LET ab$ = LEFT$(ab$, i - 1): i = 9
82 NEXT i
90 FOR i = 1 TO 9
91 IF MID$(ac$, i, 1) = " " THEN LET ac$ = LEFT$(ac$, i - 1): i = 9
92 NEXT i
100 FOR i = 1 TO 9
101 IF MID$(ad$, i, 1) = " " THEN LET ad$ = LEFT$(ad$, i - 1): i = 9
102 NEXT i
110 IF ab$ <> "" THEN aa$ = aa$ + "+"
115 IF ad$ <> "" THEN ac$ = ac$ + "+"
125 z = 40 - LEN(aa$ + ab$ + ac$ + ad$) - 5: sp = ""
130 FOR i = 1 TO z: sp = sp + " ": NEXT i
140 tmp = "    " + aa$ + ab$ + "=" + ac$ + ad$ + sp$ + ae$ + af$ + "    " + ag$ + "    " +
ah$
145 PRINT #2, tmp: PRINT tmp
147 GOTO 40
150 PRINT #2, "END"
155 CLOSE #1: CLOSE #2
160 END
```

Program 3: Converts output from CHEMKIN into graph of total ion mass spectrum

```
CLEAR : SCREEN 9: DIM aa AS STRING * 90, x(169), m(169), t(706)
DIM b AS STRING * 12, f AS STRING * 40
x = 35: y = 300: INPUT "file?", b$
CLS : PRINT "100": PRINT : PRINT : PRINT
PRINT "80": PRINT : PRINT : PRINT
PRINT "60": PRINT : PRINT : PRINT : PRINT
PRINT "40": PRINT : PRINT : PRINT
PRINT "20": PRINT : PRINT : PRINT
PRINT "0"
PRINT "  200        300        400        500        600        700"
f$ = "d:\chemkin\tign\" + b$
OPEN f$ FOR INPUT AS #1
REM Load in MWs of Species
DATA 28,2,1,128,178,128,128,178,178,178
FOR i = 1 TO 10: READ m(i): NEXT i
```

```
FOR i = 11 TO 20: m(i) = 254: NEXT i
FOR i = 21 TO 44: m(i) = 304: NEXT i
FOR i = 45 TO 67: m(i) = 354: NEXT i
FOR j = 0 TO 1
FOR i = 68 + j * 14 TO 70 + j * 14: m(i) = 252: NEXT i
FOR i = 71 + j * 14 TO 76 + j * 14: m(i) = 302: NEXT i
FOR i = 77 + j * 14 TO 81 + j * 14: m(i) = 352: NEXT i
FOR i = 0 TO 3: m(96 + i + 4 * j) = 380 + 50 * i: NEXT i
FOR i = 0 TO 4: m(104 + i + 5 * j) = 506 + 50 * i: NEXT i
m(114 + j) = 632
FOR i = 0 TO 3: FOR k = 0 TO 1: m(116 + i + 8 * j + 4 * k) = 378 + 50 * i - 2 * k:
NEXT k: NEXT i
FOR i = 0 TO 4: FOR k = 0 TO 2: m(132 + i + 15 * j + 5 * k) = 504 + 50 * i - 2 * k:
NEXT k: NEXT i
FOR i = 0 TO 3: m(162 + i + 4 * j) = 630 - 2 * i: NEXT i
NEXT j
REM Read data from file
10 LINE INPUT #1, aa
IF MID$(aa, 2, 6) = "t(sec)" THEN LET z = z + 1
IF z <= 1 THEN GOTO 10
z = 4: FOR i = 0 TO 42
IF i = 42 THEN LET z = 1
LINE INPUT #1, aa
FOR j = 1 TO z
x(i * 4 + j) = VAL(MID$(aa, 22 * j - 8, 9))
NEXT j: NEXT i
REM Normalize data
FOR i = 1 TO 169: t(m(i)) = t(m(i)) + x(i): NEXT i
FOR i = 200 TO 706: IF t(i) > tmax THEN LET tmax = t(i)
NEXT i
FOR i = 200 TO 706: t(i) = t(i) / tmax * 300
REM Draw graph
LINE (x + i - 200, y)-(x + i - 200, y - t(i))
NEXT i
FOR i = 0 TO 10: LINE (x, y - i * 30)-(x - 5, y - i * 30): NEXT i
FOR i = 0 TO 5: LINE (x + i * 100, y)-(x + i * 100, y + 5): NEXT i
LINE (x, y - 300)-(x, y): LINE (x + 506, y)-(x, y)
STOP: REM To enable print screen
END
```

Program 4: Converts output from CHEMKIN for Sensitivity Analysis

```
CLEAR : OPEN "d:\chemkin\tign\sens.out" FOR OUTPUT AS #2
DIM bb AS STRING * 90, x(169) AS DOUBLE, t(15) AS STRING
DIM f AS STRING * 40, biaryl(15) AS DOUBLE, aa AS DOUBLE, nn AS DOUBLE,
an AS DOUBLE
DIM cnn AS DOUBLE, can AS DOUBLE, caa AS DOUBLE
DIM high AS DOUBLE, high0 AS DOUBLE, cond AS DOUBLE, cond0 AS DOUBLE
DIM ratioaa AS DOUBLE, raa0 AS DOUBLE, rationn AS DOUBLE, rnn0 AS
DOUBLE
DIM ratiobb AS DOUBLE, rbb0 AS DOUBLE, react AS DOUBLE
DIM normal AS DOUBLE, conv AS DOUBLE, param AS DOUBLE
DATA "-2","t0a","t1a","t2a","t3a","t4a","t0e","t1e","t2e","t3e","t4e","ttm","ttp"
DATA "mop", "1n"
FOR k = 1 TO 15: READ t(k)
f$ = "d:\chemkin\tign\z1348" + t(k) + ".dat"
OPEN f$ FOR INPUT AS #1: z = 0
110 LINE INPUT #1, bb
IF MID$(bb, 2, 6) = "t(sec)" THEN LET z = z + 1: IF z = 1 THEN LINE INPUT #1, bb:
normal = 2 * VAL(MID$(bb, 80, 9))
IF z <= 1 THEN GOTO 110
z = 4: FOR i = 0 TO 42
IF i = 42 THEN LET z = 1
LINE INPUT #1, bb
FOR j = 1 TO z
x(i * 4 + j) = VAL(MID$(bb, 22 * j - 8, 9))
NEXT j: NEXT i
CLOSE #1
ERASE biaryl: nn = 0: an = 0: aa = 0: cnn = 0: can = 0: caa = 0: react = 0
FOR i = 11 TO 14: biaryl(1) = biaryl(1) + x(i): NEXT i
FOR i = 15 TO 18: biaryl(2) = biaryl(2) + x(i): NEXT i
FOR i = 19 TO 20: biaryl(3) = biaryl(3) + x(i): NEXT i
FOR i = 21 TO 25: biaryl(4) = biaryl(4) + x(i): NEXT i
FOR i = 26 TO 30: biaryl(5) = biaryl(5) + x(i): NEXT i
FOR i = 31 TO 34: biaryl(6) = biaryl(6) + x(i): NEXT i
FOR i = 35 TO 36: biaryl(7) = biaryl(7) + x(i): NEXT i
FOR i = 37 TO 40: biaryl(8) = biaryl(8) + x(i): NEXT i
FOR i = 41 TO 44: biaryl(9) = biaryl(9) + x(i): NEXT i
FOR i = 45 TO 48: biaryl(10) = biaryl(10) + x(i): NEXT i
FOR i = 49 TO 53: biaryl(11) = biaryl(11) + x(i): NEXT i
FOR i = 54 TO 58: biaryl(12) = biaryl(12) + x(i): NEXT i
FOR i = 59 TO 60: biaryl(13) = biaryl(13) + x(i): NEXT i
```

```
FOR i = 61 TO 64: biaryl(14) = biaryl(14) + x(i): NEXT i
FOR i = 65 TO 67: biaryl(15) = biaryl(15) + x(i): NEXT i
FOR i = 1 TO 3: nn = nn + biaryl(i): NEXT i
FOR i = 4 TO 9: an = an + biaryl(i): NEXT i
FOR i = 10 TO 15: aa = aa + biaryl(i): NEXT i
FOR j = 0 TO 1
FOR i = 68 + j * 14 TO 70 + j * 14: cnn = cnn + x(i): NEXT i
FOR i = 71 + j * 14 TO 76 + j * 14: can = can + x(i): NEXT i
FOR i = 77 + j * 14 TO 81 + j * 14: caa = caa + x(i): NEXT i
NEXT j
FOR i = 96 TO 169: react = react + x(i): NEXT i
cond = cnn + can + caa
FOR q = 0 TO 1: FOR j = 0 TO 1: FOR i = 116 + 4 * j + 8 * q TO 119 + 4 * j + 8 * q
cond = cond + x(i) * (j + 1): NEXT i: NEXT j: NEXT q
FOR q = 0 TO 1: FOR j = 0 TO 2: FOR i = 132 + 5 * j + 15 * q TO 136 + 5 * j + 15 * q
cond = cond + x(i) * (j + 1): NEXT i: NEXT j: NEXT q
FOR q = 0 TO 1: FOR j = 0 TO 3: i = 162 + j + 4 * q
cond = cond + x(i) * (j + 1): NEXT j: NEXT q
conv = (react + nn + an + aa + cnn + can + caa) / normal
high = react / (nn + an + aa + cnn + can + caa)
cond = cond / normal
FOR i = 1 TO 15: biaryl(i) = biaryl(i) / normal: NEXT i
nn = nn / normal: an = an / normal: aa = aa / normal
cnn = cnn / normal: can = can / normal: caa = caa / normal
ratioaa = aa / an: rationn = nn / aa
ratiobb = biaryl(2) / biaryl(3)
SELECT CASE k
CASE 1: high0 = high: cond0 = cond: raa0 = ratioaa: rnn0 = rationn: rbb0 = ratiobb
CASE 2 TO 6: param = 10
CASE 7 TO 11: param = .001
CASE 12: param = .01
CASE 13: param = 1
CASE 14 TO 15: param = .5
END SELECT
IF k > 1 THEN
senshigh = (high - high0) / param: senscond = (cond - cond0) / param
sensaa = (ratioaa - raa0) / param: sensnn = (rationn - rnn0) / param
sensbb = (ratiobb - rbb0) / param
END IF
IF k = 1 THEN
CLS : PRINT , , "Sensitivity Analysis": PRINT
PRINT "Type  Conversion  Condensed  Total AA/  Total NN/  N1N2/N2N2"
PRINT "     to Polyaryl  Fraction  Total AN   Total AA"
ELSE
```

```
PRINT USING "&\ \##.##^^^^&##.##^^^^&##.##^^^^&##.##^^^^&##.##^^^^"; t(k); ":
"; senshigh; "   "; senscond; "   "; sensaa; "   "; sensnn; "   "; sensbb
END IF
IF k = 1 THEN
PRINT #2, , , "Sensitivity Analysis": PRINT #2,
PRINT #2, "Type  Conversion  Condensed   Total AA/  Total NN/  N1N2/N2N2"
PRINT #2, "     to Polyaryl  Fraction   Total AN   Total AA"
ELSE
PRINT #2, USING "&\ \##.##^^^^&##.##^^^^&##.##^^^^&##.##^^^^&##.##^^^^";
t(k); ": "; senshigh; "   "; senscond; "   "; sensaa; "   "; sensnn; "   "; sensbb
END IF
NEXT k
```

Appendix C - The Kinetic Mechanism

```
ELEMENTS
H     C     N
END
SPECIES
N2  h2  h  n  a  n1-  n2-  a1-  a2-  a9-
n1n1  n1n1-1  n1n1-2  n1n1-4
n1n2  n1n2-1  n1n2-2  n1n2-4
n2n2  n2n2-4
a1n1  a1n1-1  a1n1-2  a1n1-3  a1n1-4
a1n2  a1n2-1  a1n2-2  a1n2-3  a1n2-4
a2n1  a2n1-1  a2n1-2  a2n1-4
a2n2  a2n2-4
a9n1  a9n1-1  a9n1-2  a9n1-4
a9n2  a9n2-1  a9n2-2  a9n2-4
a1a1  a1a1-2  a1a1-3  a1a1-4
a1a2  a1a2-1  a1a2-2  a1a2-3  a1a2-4
a1a9  a1a9-1  a1a9-2  a1a9-3  a1a9-4
a2a2  a2a2-4
a2a9  a2a9-1  a2a9-2  a2a9-4
a9a9  a9a9-1  a9a9-4
BkF  BjF  Per
DBajF  DBakF  DBalF  BaPer  N23jF  N23kF
BaN23jF  BaN23kF  BaN23lF  DBajPer  DBaoPer
BkF-  BjF-  Per-
DBajF-  DBakF-  DBalF-  BaPer-  N23jF-  N23kF-
BaN23jF-  BaN23kF-  BaN23lF-  DBajPer-  DBaoPer-
NNN  NNA  NAA  AAA  NNN-  NNA-  NAA-  AAA-
NNNN  NNNA  NNAA  NAAA  AAAA  NNNN-  NNNA-  NNAA-  NAAA- AAAA-
NNNNN  NNNNN-
C1NNN  C1NNA  C1NAA  C1AAA  C2NNN  C2NNA  C2NAA  C2AAA
C1NNN-  C1NNA-  C1NAA-  C1AAA-  C2NNN-  C2NNA-  C2NAA-  C2AAA-
C1NNNN  C1NNNA  C1NNAA  C1NAAA  C1AAAA
C2NNNN  C2NNNA  C2NNAA  C2NAAA  C2AAAA
C3NNNN  C3NNNA  C3NNAA  C3NAAA  C3AAAA
C1NNNN-  C1NNNA-  C1NNAA-  C1NAAA-  C1AAAA-
C2NNNN-  C2NNNA-  C2NNAA-  C2NAAA-  C2AAAA-
C3NNNN-  C3NNNA-  C3NNAA-  C3NAAA-  C3AAAA-
C1NNNNN  C2NNNNN  C3NNNNN  C4NNNNN
C1NNNNN-  C2NNNNN-  C3NNNNN-  C4NNNNN-
END
```

REACTIONS	coefficents for forward reaction A (cc/mol/sec)	b	E (cal/mol)
Reaction Type 1 (hydrogen balance) $1E18/T*e^{-Q/RT}$ (Miller and Bowman, 1989)			
h+h=h2	1.00E18	-1	0
Reaction Type 2 (radical recombination) $2.5E13\ T^{0.5}\ e^{-Q/RT}$ (Benson, 1976)			
n1-+h=n	2.50E13	.5	0
n2-+h=n	2.50E13	.5	0
a1-+h=a	2.50E13	.5	0
a2-+h=a	2.50E13	.5	0
a9-+h=a	2.50E13	.5	0
n1n1-1+h=n1n1	2.50E13	.5	0

n1n1-2+h=n1n1	2.50E13	.5	0
n1n1-4+h=n1n1	2.50E13	.5	0
n1n2-1+h=n1n2	2.50E13	.5	0
n1n2-2+h=n1n2	2.50E13	.5	0
n1n2-4+h=n1n2	2.50E13	.5	0
n2n2-4+h=n2n2	2.50E13	.5	0
a1n1-1+h=a1n1	2.50E13	.5	0
a1n1-2+h=a1n1	2.50E13	.5	0
a1n1-3+h=a1n1	2.50E13	.5	0
a1n1-4+h=a1n1	2.50E13	.5	0
a1n2-1+h=a1n2	2.50E13	.5	0
a1n2-2+h=a1n2	2.50E13	.5	0
a1n2-3+h=a1n2	2.50E13	.5	0
a1n2-4+h=a1n2	2.50E13	.5	0
a2n1-1+h=a2n1	2.50E13	.5	0
a2n1-2+h=a2n1	2.50E13	.5	0
a2n1-4+h=a2n1	2.50E13	.5	0
a2n2-4+h=a2n2	2.50E13	.5	0
a9n1-1+h=a9n1	2.50E13	.5	0
a9n1-2+h=a9n1	2.50E13	.5	0
a9n1-4+h=a9n1	2.50E13	.5	0
a9n2-1+h=a9n2	2.50E13	.5	0
a9n2-2+h=a9n2	2.50E13	.5	0
a9n2-4+h=a9n2	2.50E13	.5	0
a1a1-2+h=a1a1	2.50E13	.5	0
a1a1-3+h=a1a1	2.50E13	.5	0
a1a1-4+h=a1a1	2.50E13	.5	0
a1a2-1+h=a1a2	2.50E13	.5	0
a1a2-2+h=a1a2	2.50E13	.5	0
a1a2-3+h=a1a2	2.50E13	.5	0
a1a2-4+h=a1a2	2.50E13	.5	0
a1a9-1+h=a1a9	2.50E13	.5	0
a1a9-2+h=a1a9	2.50E13	.5	0
a1a9-3+h=a1a9	2.50E13	.5	0
a1a9-4+h=a1a9	2.50E13	.5	0
a2a2-4+h=a2a2	2.50E13	.5	0
a2a9-1+h=a2a9	2.50E13	.5	0
a2a9-2+h=a2a9	2.50E13	.5	0
a2a9-4+h=a2a9	2.50E13	.5	0
a9a9-1+h=a9a9	2.50E13	.5	0
a9a9-4+h=a9a9	2.50E13	.5	0
BkF-+h=BkF	2.50E13	.5	0
BjF-+h=BjF	2.50E13	.5	0
Per-+h=Per	2.50E13	.5	0
DBajF-+h=DBajF	2.50E13	.5	0
DBakF-+h=DBakF	2.50E13	.5	0
DBalF-+h=DBalF	2.50E13	.5	0
BaPer-+h=BaPer	2.50E13	.5	0
N23jF-+h=N23jF	2.50E13	.5	0
N23kF-+h=N23kF	2.50E13	.5	0
BaN23jF-+h=BaN23jF	2.50E13	.5	0
BaN23kF-+h=BaN23kF	2.50E13	.5	0
BaN23lF-+h=BaN23lF	2.50E13	.5	0
DBajPer-+h=DBajPer	2.50E13	.5	0
DBaoPer-+h=DBaoPer	2.50E13	.5	0
NNN-+h=NNN	2.50E13	.5	0
NNA-+h=NNA	2.50E13	.5	0
NAA-+h=NAA	2.50E13	.5	0
AAA-+h=AAA	2.50E13	.5	0
NNNN-+h=NNNN	2.50E13	.5	0

NNNA-+h=NNNA	2.50E13	.5	0
NNAA-+h=NNAA	2.50E13	.5	0
NAAA-+h=NAAA	2.50E13	.5	0
AAAA-+h=AAAA	2.50E13	.5	0
NNNNN-+h=NNNNN	2.50E13	.5	0
C1NNN-+h=C1NNN	2.50E13	.5	0
C2NNN-+h=C2NNN	2.50E13	.5	0
C1NNA-+h=C1NNA	2.50E13	.5	0
C2NNA-+h=C2NNA	2.50E13	.5	0
C1NAA-+h=C1NAA	2.50E13	.5	0
C2NAA-+h=C2NAA	2.50E13	.5	0
C1AAA-+h=C1AAA	2.50E13	.5	0
C2AAA-+h=C2AAA	2.50E13	.5	0
C1NNNN-+h=C1NNNN	2.50E13	.5	0
C2NNNN-+h=C2NNNN	2.50E13	.5	0
C3NNNN-+h=C3NNNN	2.50E13	.5	0
C1NNNA-+h=C1NNNA	2.50E13	.5	0
C2NNNA-+h=C2NNNA	2.50E13	.5	0
C3NNNA-+h=C3NNNA	2.50E13	.5	0
C1NNAA-+h=C1NNAA	2.50E13	.5	0
C2NNAA-+h=C2NNAA	2.50E13	.5	0
C3NNAA-+h=C3NNAA	2.50E13	.5	0
C1NAAA-+h=C1NAAA	2.50E13	.5	0
C2NAAA-+h=C2NAAA	2.50E13	.5	0
C3NAAA-+h=C3NAAA	2.50E13	.5	0
C1AAAA-+h=C1AAAA	2.50E13	.5	0
C2AAAA-+h=C2AAAA	2.50E13	.5	0
C3AAAA-+h=C3AAAA	2.50E13	.5	0
C1NNNNN-+h=C1NNNNN	2.50E13	.5	0
C2NNNNN-+h=C2NNNNN	2.50E13	.5	0
C3NNNNN-+h=C3NNNNN	2.50E13	.5	0
C4NNNNN-+h=C4NNNNN	2.50E13	.5	0
n1-+n1-=n1n1	1.55E12	.5	0
n1-+n2-=n1n2	3.10E12	.5	0
n1-+a1-=a1n1	3.39E12	.5	0
n1-+a2-=a2n1	3.39E12	.5	0
n1-+a9-=a9n1	3.39E12	.5	0
n2-+n2-=n2n2	1.55E12	.5	0
n2-+a1-=a1n2	3.39E12	.5	0
n2-+a2-=a2n2	3.39E12	.5	0
n2-+a9-=a9n2	3.39E12	.5	0
a1-+a1-=a1a1	1.83E12	.5	0
a1-+a2-=a1a2	3.66E12	.5	0
a1-+a9-=a1a9	3.66E12	.5	0
a2-+a2-=a2a2	1.83E12	.5	0
a2-+a9-=a2a9	3.66E12	.5	0
a9-+a9-=a9a9	1.83E12	.5	0
n1-+n1n1-4=NNN	3.79E12	.5	0
n1-+n1n2-4=NNN	3.79E12	.5	0
n1-+n2n2-4=NNN	3.79E12	.5	0
n1-+a1n1-4=NNA	4.03E12	.5	0
n1-+a1n2-4=NNA	4.03E12	.5	0
n1-+a2n1-4=NNA	4.03E12	.5	0
n1-+a2n2-4=NNA	4.03E12	.5	0
n1-+a9n1-4=NNA	4.03E12	.5	0
n1-+a9n2-4=NNA	4.03E12	.5	0
n1-+a1a1-4=NAA	4.26E12	.5	0
n1-+a1a2-4=NAA	4.26E12	.5	0
n1-+a1a9-4=NAA	4.26E12	.5	0
n1-+a2a2-4=NAA	4.26E12	.5	0

n1-+a2a9-4=NAA	4.26E12	.5	0
n1-+a9a9-4=NAA	4.26E12	.5	0
n2-+n1n1-4=NNN	3.79E12	.5	0
n2-+n1n2-4=NNN	3.79E12	.5	0
n2-+n2n2-4=NNN	3.79E12	.5	0
n2-+a1n1-4=NNA	4.03E12	.5	0
n2-+a1n2-4=NNA	4.03E12	.5	0
n2-+a2n1-4=NNA	4.03E12	.5	0
n2-+a2n2-4=NNA	4.03E12	.5	0
n2-+a9n1-4=NNA	4.03E12	.5	0
n2-+a9n2-4=NNA	4.03E12	.5	0
n2-+a1a1-4=NAA	4.26E12	.5	0
n2-+a1a2-4=NAA	4.26E12	.5	0
n2-+a1a9-4=NAA	4.26E12	.5	0
n2-+a2a2-4=NAA	4.26E12	.5	0
n2-+a2a9-4=NAA	4.26E12	.5	0
n2-+a9a9-4=NAA	4.26E12	.5	0
a1-+n1n1-4=NNA	4.03E12	.5	0
a1-+n1n2-4=NNA	4.03E12	.5	0
a1-+n2n2-4=NNA	4.03E12	.5	0
a1-+a1n1-4=NAA	4.26E12	.5	0
a1-+a1n2-4=NAA	4.26E12	.5	0
a1-+a2n1-4=NAA	4.26E12	.5	0
a1-+a2n2-4=NAA	4.26E12	.5	0
a1-+a9n1-4=NAA	4.26E12	.5	0
a1-+a9n2-4=NAA	4.26E12	.5	0
a1-+a1a1-4=AAA	4.48E12	.5	0
a1-+a1a2-4=AAA	4.48E12	.5	0
a1-+a1a9-4=AAA	4.48E12	.5	0
a1-+a2a2-4=AAA	4.48E12	.5	0
a1-+a2a9-4=AAA	4.48E12	.5	0
a1-+a9a9-4=AAA	4.48E12	.5	0
a2-+n1n1-4=NNA	4.03E12	.5	0
a2-+n1n2-4=NNA	4.03E12	.5	0
a2-+n2n2-4=NNA	4.03E12	.5	0
a2-+a1n1-4=NAA	4.26E12	.5	0
a2-+a1n2-4=NAA	4.26E12	.5	0
a2-+a2n1-4=NAA	4.26E12	.5	0
a2-+a2n2-4=NAA	4.26E12	.5	0
a2-+a9n1-4=NAA	4.26E12	.5	0
a2-+a9n2-4=NAA	4.26E12	.5	0
a2-+a1a1-4=AAA	4.48E12	.5	0
a2-+a1a2-4=AAA	4.48E12	.5	0
a2-+a1a9-4=AAA	4.48E12	.5	0
a2-+a2a2-4=AAA	4.48E12	.5	0
a2-+a2a9-4=AAA	4.48E12	.5	0
a2-+a9a9-4=AAA	4.48E12	.5	0
a9-+n1n1-4=NNA	4.03E12	.5	0
a9-+n1n2-4=NNA	4.03E12	.5	0
a9-+n2n2-4=NNA	4.03E12	.5	0
a9-+a1n1-4=NAA	4.26E12	.5	0
a9-+a1n2-4=NAA	4.26E12	.5	0
a9-+a2n1-4=NAA	4.26E12	.5	0
a9-+a2n2-4=NAA	4.26E12	.5	0
a9-+a9n1-4=NAA	4.26E12	.5	0
a9-+a9n2-4=NAA	4.26E12	.5	0
a9-+a1a1-4=AAA	4.48E12	.5	0
a9-+a1a2-4=AAA	4.48E12	.5	0
a9-+a1a9-4=AAA	4.48E12	.5	0
a9-+a2a2-4=AAA	4.48E12	.5	0

a9-+a2a9-4=AAA	4.48E12	.5	0
a9-+a9a9-4=AAA	4.48E12	.5	0
n1-+BkF-=C1NNN	3.79E12	.5	0
n1-+BjF-=C1NNN	3.79E12	.5	0
n1-+Per-=C1NNN	3.79E12	.5	0
n1-+DBajF-=C1NNA	4.03E12	.5	0
n1-+DBakF-=C1NNA	4.03E12	.5	0
n1-+DBalF-=C1NNA	3.46E12	.5	0
n1-+BaPer-=C1NNA	3.46E12	.5	0
n1-+N23jF-=C1NNA	4.03E12	.5	0
n1-+N23kF-=C1NNA	4.03E12	.5	0
n1-+BaN23jF-=C1NAA	4.26E12	.5	0
n1-+BaN23kF-=C1NAA	4.26E12	.5	0
n1-+BaN23lF-=C1NAA	3.73E12	.5	0
n1-+DBajPer-=C1NAA	3.20E12	.5	0
n1-+DBaoPer-=C1NAA	3.73E12	.5	0
n2-+BkF-=C1NNN	3.79E12	.5	0
n2-+BjF-=C1NNN	3.79E12	.5	0
n2-+Per-=C1NNN	3.79E12	.5	0
n2-+DBajF-=C1NNA	4.03E12	.5	0
n2-+DBakF-=C1NNA	4.03E12	.5	0
n2-+DBalF-=C1NNA	3.46E12	.5	0
n2-+BaPer-=C1NNA	3.46E12	.5	0
n2-+N23jF-=C1NNA	4.03E12	.5	0
n2-+N23kF-=C1NNA	4.03E12	.5	0
n2-+BaN23jF-=C1NAA	4.26E12	.5	0
n2-+BaN23kF-=C1NAA	4.26E12	.5	0
n2-+BaN23lF-=C1NAA	3.73E12	.5	0
n2-+DBajPer-=C1NAA	3.20E12	.5	0
n2-+DBaoPer-=C1NAA	3.73E12	.5	0
a1-+BkF-=C1NNA	4.03E12	.5	0
a1-+BjF-=C1NNA	4.03E12	.5	0
a1-+Per-=C1NNA	4.03E12	.5	0
a1-+DBajF-=C1NAA	4.26E12	.5	0
a1-+DBakF-=C1NAA	4.26E12	.5	0
a1-+DBalF-=C1NAA	3.65E12	.5	0
a1-+BaPer-=C1NAA	3.65E12	.5	0
a1-+N23jF-=C1NAA	4.26E12	.5	0
a1-+N23kF-=C1NAA	4.26E12	.5	0
a1-+BaN23jF-=C1AAA	4.48E12	.5	0
a1-+BaN23kF-=C1AAA	4.48E12	.5	0
a1-+BaN23lF-=C1AAA	3.92E12	.5	0
a1-+DBajPer-=C1AAA	3.36E12	.5	0
a1-+DBaoPer-=C1AAA	3.92E12	.5	0
a2-+BkF-=C1NNA	4.03E12	.5	0
a2-+BjF-=C1NNA	4.03E12	.5	0
a2-+Per-=C1NNA	4.03E12	.5	0
a2-+DBajF-=C1NAA	4.26E12	.5	0
a2-+DBakF-=C1NAA	4.26E12	.5	0
a2-+DBalF-=C1NAA	3.65E12	.5	0
a2-+BaPer-=C1NAA	3.65E12	.5	0
a2-+N23jF-=C1NAA	4.26E12	.5	0
a2-+N23kF-=C1NAA	4.26E12	.5	0
a2-+BaN23jF-=C1AAA	4.48E12	.5	0
a2-+BaN23kF-=C1AAA	4.48E12	.5	0
a2-+BaN23lF-=C1AAA	3.92E12	.5	0
a2-+DBajPer-=C1AAA	3.36E12	.5	0
a2-+DBaoPer-=C1AAA	3.92E12	.5	0
a9-+BkF-=C1NNA	4.03E12	.5	0
a9-+BjF-=C1NNA	4.03E12	.5	0

a9-+Per-=C1NNA	4.03E12	.5	0
a9-+DBajF-=C1NAA	4.26E12	.5	0
a9-+DBakF-=C1NAA	4.26E12	.5	0
a9-+DBalF-=C1NAA	3.65E12	.5	0
a9-+BaPer-=C1NAA	3.65E12	.5	0
a9-+N23jF-=C1NAA	4.26E12	.5	0
a9-+N23kF-=C1NAA	4.26E12	.5	0
a9-+BaN23jF-=C1AAA	4.48E12	.5	0
a9-+BaN23kF-=C1AAA	4.48E12	.5	0
a9-+BaN23lF-=C1AAA	3.92E12	.5	0
a9-+DBajPer-=C1AAA	3.36E12	.5	0
a9-+DBaoPer-=C1AAA	3.92E12	.5	0
n1-+NNN-=NNNN	3.06E12	.5	0
n1-+NNA-=NNNA	3.34E12	.5	0
n1-+NAA-=NNAA	3.59E12	.5	0
n1-+AAA-=NAAA	3.83E12	.5	0
n1-+NNNN-=NNNNN	3.20E12	.5	0
n1-+C1NNN-=C1NNNN	3.65E12	.5	0
n1-+C1NNA-=C1NNNA	3.67E12	.5	0
n1-+C1NAA-=C1NNAA	3.70E12	.5	0
n1-+C1AAA-=C1NAAA	3.74E12	.5	0
n1-+C2NNN-=C2NNNN	4.38E12	.5	0
n1-+C2NNA-=C2NNNA	4.33E12	.5	0
n1-+C2NAA-=C2NNAA	4.31E12	.5	0
n1-+C2AAA-=C2NAAA	4.30E12	.5	0
n1-+C1NNNN-=C1NNNNN	3.67E12	.5	0
n1-+C2NNNN-=C2NNNNN	4.22E12	.5	0
n1-+C3NNNN-=C3NNNNN	4.89E12	.5	0
n2-+NNN-=NNNN	3.06E12	.5	0
n2-+NNA-=NNNA	3.34E12	.5	0
n2-+NAA-=NNAA	3.59E12	.5	0
n2-+AAA-=NAAA	3.83E12	.5	0
n2-+NNNN-=NNNNN	3.20E12	.5	0
n2-+C1NNN-=C1NNNN	3.65E12	.5	0
n2-+C1NNA-=C1NNNA	3.67E12	.5	0
n2-+C1NAA-=C1NNAA	3.70E12	.5	0
n2-+C1AAA-=C1NAAA	3.74E12	.5	0
n2-+C2NNN-=C2NNNN	4.38E12	.5	0
n2-+C2NNA-=C2NNNA	4.33E12	.5	0
n2-+C2NAA-=C2NNAA	4.31E12	.5	0
n2-+C2AAA-=C2NAAA	4.30E12	.5	0
n2-+C1NNNN-=C1NNNNN	3.67E12	.5	0
n2-+C2NNNN-=C2NNNNN	4.22E12	.5	0
n2-+C3NNNN-=C3NNNNN	4.89E12	.5	0
a1-+NNN-=NNNA	3.21E12	.5	0
a1-+NNA-=NNAA	3.48E12	.5	0
a1-+NAA-=NAAA	3.74E12	.5	0
a1-+AAA-=AAAA	3.98E12	.5	0
a1-+C1NNN-=C1NNNA	3.82E12	.5	0
a1-+C1NNA-=C1NNAA	3.83E12	.5	0
a1-+C1NAA-=C1NAAA	3.85E12	.5	0
a1-+C1AAA-=C1AAAA	3.88E12	.5	0
a1-+C2NNN-=C2NNNA	4.59E12	.5	0
a1-+C2NNA-=C2NNAA	4.52E12	.5	0
a1-+C2NAA-=C2NAAA	4.48E12	.5	0
a1-+C2AAA-=C2AAAA	4.46E12	.5	0
a2-+NNN-=NNNA	3.21E12	.5	0
a2-+NNA-=NNAA	3.48E12	.5	0
a2-+NAA-=NAAA	3.74E12	.5	0
a2-+AAA-=AAAA	3.98E12	.5	0

a2-+C1NNN-=C1NNNA	3.82E12	.5	0
a2-+C1NNA-=C1NNAA	3.83E12	.5	0
a2-+C1NAA-=C1NAAA	3.85E12	.5	0
a2-+C1AAA-=C1AAAA	3.88E12	.5	0
a2-+C2NNN-=C2NNNA	4.59E12	.5	0
a2-+C2NNA-=C2NNAA	4.52E12	.5	0
a2-+C2NAA-=C2NAAA	4.48E12	.5	0
a2-+C2AAA-=C2AAAA	4.46E12	.5	0
a9-+NNN-=NNNA	3.21E12	.5	0
a9-+NNA-=NNAA	3.48E12	.5	0
a9-+NAA-=NAAA	3.74E12	.5	0
a9-+AAA-=AAAA	3.98E12	.5	0
a9-+C1NNN-=C1NNNA	3.82E12	.5	0
a9-+C1NNA-=C1NNAA	3.83E12	.5	0
a9-+C1NAA-=C1NAAA	3.85E12	.5	0
a9-+C1AAA-=C1AAAA	3.88E12	.5	0
a9-+C2NNN-=C2NNNA	4.59E12	.5	0
a9-+C2NNA-=C2NNAA	4.52E12	.5	0
a9-+C2NAA-=C2NAAA	4.48E12	.5	0
a9-+C2AAA-=C2AAAA	4.46E12	.5	0
n1n1-4+n1n1-4=NNNN	2.19E12	.5	0
n1n1-4+n1n2-4=NNNN	4.38E12	.5	0
n1n1-4+n2n2-4=NNNN	4.38E12	.5	0
n1n1-4+a1n1-4=NNNA	4.59E12	.5	0
n1n1-4+a1n2-4=NNNA	4.59E12	.5	0
n1n1-4+a2n1-4=NNNA	4.59E12	.5	0
n1n1-4+a2n2-4=NNNA	4.59E12	.5	0
n1n1-4+a9n1-4=NNNA	4.59E12	.5	0
n1n1-4+a9n2-4=NNNA	4.59E12	.5	0
n1n1-4+a1a1-4=NNAA	4.79E12	.5	0
n1n1-4+a1a2-4=NNAA	4.79E12	.5	0
n1n1-4+a1a9-4=NNAA	4.79E12	.5	0
n1n1-4+a2a2-4=NNAA	4.79E12	.5	0
n1n1-4+a2a9-4=NNAA	4.79E12	.5	0
n1n1-4+a9a9-4=NNAA	4.79E12	.5	0
n1n2-4+n1n2-4=NNNN	2.19E12	.5	0
n1n2-4+n2n2-4=NNNN	4.38E12	.5	0
n1n2-4+a1n1-4=NNNA	4.59E12	.5	0
n1n2-4+a1n2-4=NNNA	4.59E12	.5	0
n1n2-4+a2n1-4=NNNA	4.59E12	.5	0
n1n2-4+a2n2-4=NNNA	4.59E12	.5	0
n1n2-4+a9n1-4=NNNA	4.59E12	.5	0
n1n2-4+a9n2-4=NNNA	4.59E12	.5	0
n1n2-4+a1a1-4=NNAA	4.79E12	.5	0
n1n2-4+a1a2-4=NNAA	4.79E12	.5	0
n1n2-4+a1a9-4=NNAA	4.79E12	.5	0
n1n2-4+a2a2-4=NNAA	4.79E12	.5	0
n1n2-4+a2a9-4=NNAA	4.79E12	.5	0
n1n2-4+a9a9-4=NNAA	4.79E12	.5	0
n2n2-4+n2n2-4=NNNN	2.19E12	.5	0
n2n2-4+a1n1-4=NNNA	4.59E12	.5	0
n2n2-4+a1n2-4=NNNA	4.59E12	.5	0
n2n2-4+a2n1-4=NNNA	4.59E12	.5	0
n2n2-4+a2n2-4=NNNA	4.59E12	.5	0
n2n2-4+a9n1-4=NNNA	4.59E12	.5	0
n2n2-4+a9n2-4=NNNA	4.59E12	.5	0
n2n2-4+a1a1-4=NNAA	4.79E12	.5	0
n2n2-4+a1a2-4=NNAA	4.79E12	.5	0
n2n2-4+a1a9-4=NNAA	4.79E12	.5	0
n2n2-4+a2a2-4=NNAA	4.79E12	.5	0

n2n2-4+a2a9-4=NNAA	4.79E12	.5	0
n2n2-4+a9a9-4=NNAA	4.79E12	.5	0
a1n1-4+a1n1-4=NNAA	2.39E12	.5	0
a1n1-4+a1n2-4=NNAA	4.79E12	.5	0
a1n1-4+a2n1-4=NNAA	4.79E12	.5	0
a1n1-4+a2n2-4=NNAA	4.79E12	.5	0
a1n1-4+a9n1-4=NNAA	4.79E12	.5	0
a1n1-4+a9n2-4=NNAA	4.79E12	.5	0
a1n1-4+a1a1-4=NAAA	4.98E12	.5	0
a1n1-4+a1a2-4=NAAA	4.98E12	.5	0
a1n1-4+a1a9-4=NAAA	4.98E12	.5	0
a1n1-4+a2a2-4=NAAA	4.98E12	.5	0
a1n1-4+a2a9-4=NAAA	4.98E12	.5	0
a1n1-4+a9a9-4=NAAA	4.98E12	.5	0
a1n2-4+a1n2-4=NNAA	2.39E12	.5	0
a1n2-4+a2n1-4=NNAA	4.79E12	.5	0
a1n2-4+a2n2-4=NNAA	4.79E12	.5	0
a1n2-4+a9n1-4=NNAA	4.79E12	.5	0
a1n2-4+a9n2-4=NNAA	4.79E12	.5	0
a1n2-4+a1a1-4=NAAA	4.98E12	.5	0
a1n2-4+a1a2-4=NAAA	4.98E12	.5	0
a1n2-4+a1a9-4=NAAA	4.98E12	.5	0
a1n2-4+a2a2-4=NAAA	4.98E12	.5	0
a1n2-4+a2a9-4=NAAA	4.98E12	.5	0
a1n2-4+a9a9-4=NAAA	4.98E12	.5	0
a2n1-4+a2n1-4=NNAA	2.39E12	.5	0
a2n1-4+a2n2-4=NNAA	4.79E12	.5	0
a2n1-4+a9n1-4=NNAA	4.79E12	.5	0
a2n1-4+a9n2-4=NNAA	4.79E12	.5	0
a2n1-4+a1a1-4=NAAA	4.98E12	.5	0
a2n1-4+a1a2-4=NAAA	4.98E12	.5	0
a2n1-4+a1a9-4=NAAA	4.98E12	.5	0
a2n1-4+a2a2-4=NAAA	4.98E12	.5	0
a2n1-4+a2a9-4=NAAA	4.98E12	.5	0
a2n1-4+a9a9-4=NAAA	4.98E12	.5	0
a2n2-4+a2n2-4=NNAA	2.39E12	.5	0
a2n2-4+a9n1-4=NNAA	4.79E12	.5	0
a2n2-4+a9n2-4=NNAA	4.79E12	.5	0
a2n2-4+a1a1-4=NAAA	4.98E12	.5	0
a2n2-4+a1a2-4=NAAA	4.98E12	.5	0
a2n2-4+a1a9-4=NAAA	4.98E12	.5	0
a2n2-4+a2a2-4=NAAA	4.98E12	.5	0
a2n2-4+a2a9-4=NAAA	4.98E12	.5	0
a2n2-4+a9a9-4=NAAA	4.98E12	.5	0
a9n1-4+a9n1-4=NNAA	2.39E12	.5	0
a9n1-4+a9n2-4=NNAA	4.79E12	.5	0
a9n1-4+a1a1-4=NAAA	4.98E12	.5	0
a9n1-4+a1a2-4=NAAA	4.98E12	.5	0
a9n1-4+a1a9-4=NAAA	4.98E12	.5	0
a9n1-4+a2a2-4=NAAA	4.98E12	.5	0
a9n1-4+a2a9-4=NAAA	4.98E12	.5	0
a9n1-4+a9a9-4=NAAA	4.98E12	.5	0
a9n2-4+a9n2-4=NNAA	2.39E12	.5	0
a9n2-4+a1a1-4=NAAA	4.98E12	.5	0
a9n2-4+a1a2-4=NAAA	4.98E12	.5	0
a9n2-4+a1a9-4=NAAA	4.98E12	.5	0
a9n2-4+a2a2-4=NAAA	4.98E12	.5	0
a9n2-4+a2a9-4=NAAA	4.98E12	.5	0
a9n2-4+a9a9-4=NAAA	4.98E12	.5	0
a1a1-4+a1a1-4=AAAA	2.58E12	.5	0

a1a1-4+a1a2-4=AAAA	5.17E12	.5	0
a1a1-4+a1a9-4=AAAA	5.17E12	.5	0
a1a1-4+a2a2-4=AAAA	5.17E12	.5	0
a1a1-4+a2a9-4=AAAA	5.17E12	.5	0
a1a1-4+a9a9-4=AAAA	5.17E12	.5	0
a1a2-4+a1a2-4=AAAA	2.58E12	.5	0
a1a2-4+a1a9-4=AAAA	5.17E12	.5	0
a1a2-4+a2a2-4=AAAA	5.17E12	.5	0
a1a2-4+a2a9-4=AAAA	5.17E12	.5	0
a1a2-4+a9a9-4=AAAA	5.17E12	.5	0
a1a9-4+a1a9-4=AAAA	2.58E12	.5	0
a1a9-4+a2a2-4=AAAA	5.17E12	.5	0
a1a9-4+a2a9-4=AAAA	5.17E12	.5	0
a1a9-4+a9a9-4=AAAA	5.17E12	.5	0
a2a2-4+a2a2-4=AAAA	2.58E12	.5	0
a2a2-4+a2a9-4=AAAA	5.17E12	.5	0
a2a2-4+a9a9-4=AAAA	5.17E12	.5	0
a2a9-4+a2a9-4=AAAA	2.58E12	.5	0
a2a9-4+a9a9-4=AAAA	5.17E12	.5	0
a9a9-4+a9a9-4=AAAA	2.58E12	.5	0
n1n1-4+BkF-=C1NNNN	4.38E12	.5	0
n1n1-4+BjF-=C1NNNN	4.38E12	.5	0
n1n1-4+Per-=C1NNNN	4.38E12	.5	0
n1n1-4+DBajF-=C1NNNA	4.59E12	.5	0
n1n1-4+DBakF-=C1NNNA	4.59E12	.5	0
n1n1-4+DBalF-=C1NNNA	3.93E12	.5	0
n1n1-4+BaPer-=C1NNNA	3.93E12	.5	0
n1n1-4+N23jF-=C1NNNA	4.59E12	.5	0
n1n1-4+N23kF-=C1NNNA	4.59E12	.5	0
n1n1-4+BaN23jF-=C1NNAA	4.79E12	.5	0
n1n1-4+BaN23kF-=C1NNAA	4.79E12	.5	0
n1n1-4+BaN23lF-=C1NNAA	4.19E12	.5	0
n1n1-4+DBajPer-=C1NNAA	3.59E12	.5	0
n1n1-4+DBaoPer-=C1NNAA	4.19E12	.5	0
n1n2-4+BkF-=C1NNNN	4.38E12	.5	0
n1n2-4+BjF-=C1NNNN	4.38E12	.5	0
n1n2-4+Per-=C1NNNN	4.38E12	.5	0
n1n2-4+DBajF-=C1NNNA	4.59E12	.5	0
n1n2-4+DBakF-=C1NNNA	4.59E12	.5	0
n1n2-4+DBalF-=C1NNNA	3.93E12	.5	0
n1n2-4+BaPer-=C1NNNA	3.93E12	.5	0
n1n2-4+N23jF-=C1NNNA	4.59E12	.5	0
n1n2-4+N23kF-=C1NNNA	4.59E12	.5	0
n1n2-4+BaN23jF-=C1NNAA	4.79E12	.5	0
n1n2-4+BaN23kF-=C1NNAA	4.79E12	.5	0
n1n2-4+BaN23lF-=C1NNAA	4.19E12	.5	0
n1n2-4+DBajPer-=C1NNAA	3.59E12	.5	0
n1n2-4+DBaoPer-=C1NNAA	4.19E12	.5	0
n2n2-4+BkF-=C1NNNN	4.38E12	.5	0
n2n2-4+BjF-=C1NNNN	4.38E12	.5	0
n2n2-4+Per-=C1NNNN	4.38E12	.5	0
n2n2-4+DBajF-=C1NNNA	4.59E12	.5	0
n2n2-4+DBakF-=C1NNNA	4.59E12	.5	0
n2n2-4+DBalF-=C1NNNA	3.93E12	.5	0
n2n2-4+BaPer-=C1NNNA	3.93E12	.5	0
n2n2-4+N23jF-=C1NNNA	4.59E12	.5	0
n2n2-4+N23kF-=C1NNNA	4.59E12	.5	0
n2n2-4+BaN23jF-=C1NNAA	4.79E12	.5	0
n2n2-4+BaN23kF-=C1NNAA	4.79E12	.5	0
n2n2-4+BaN23lF-=C1NNAA	4.19E12	.5	0

n2n2-4+DBajPer-=C1NNAA	3.59E12	.5	0
n2n2-4+DBaoPer-=C1NNAA	4.19E12	.5	0
a1n1-4+BkF-=C1NNNA	4.59E12	.5	0
a1n1-4+BjF-=C1NNNA	4.59E12	.5	0
a1n1-4+Per-=C1NNNA	4.59E12	.5	0
a1n1-4+DBajF-=C1NNAA	4.79E12	.5	0
a1n1-4+DBakF-=C1NNAA	4.79E12	.5	0
a1n1-4+DBalF-=C1NNAA	4.10E12	.5	0
a1n1-4+BaPer-=C1NNAA	4.10E12	.5	0
a1n1-4+N23jF-=C1NNAA	4.79E12	.5	0
a1n1-4+N23kF-=C1NNAA	4.79E12	.5	0
a1n1-4+BaN23jF-=C1NAAA	4.98E12	.5	0
a1n1-4+BaN23kF-=C1NAAA	4.98E12	.5	0
a1n1-4+BaN23lF-=C1NAAA	4.36E12	.5	0
a1n1-4+DBajPer-=C1NAAA	3.74E12	.5	0
a1n1-4+DBaoPer-=C1NAAA	4.36E12	.5	0
a1n2-4+BkF-=C1NNNA	4.59E12	.5	0
a1n2-4+BjF-=C1NNNA	4.59E12	.5	0
a1n2-4+Per-=C1NNNA	4.59E12	.5	0
a1n2-4+DBajF-=C1NNAA	4.79E12	.5	0
a1n2-4+DBakF-=C1NNAA	4.79E12	.5	0
a1n2-4+DBalF-=C1NNAA	4.10E12	.5	0
a1n2-4+BaPer-=C1NNAA	4.10E12	.5	0
a1n2-4+N23jF-=C1NNAA	4.79E12	.5	0
a1n2-4+N23kF-=C1NNAA	4.79E12	.5	0
a1n2-4+BaN23jF-=C1NAAA	4.98E12	.5	0
a1n2-4+BaN23kF-=C1NAAA	4.98E12	.5	0
a1n2-4+BaN23lF-=C1NAAA	4.36E12	.5	0
a1n2-4+DBajPer-=C1NAAA	3.74E12	.5	0
a1n2-4+DBaoPer-=C1NAAA	4.36E12	.5	0
a2n1-4+BkF-=C1NNNA	4.59E12	.5	0
a2n1-4+BjF-=C1NNNA	4.59E12	.5	0
a2n1-4+Per-=C1NNNA	4.59E12	.5	0
a2n1-4+DBajF-=C1NNAA	4.79E12	.5	0
a2n1-4+DBakF-=C1NNAA	4.79E12	.5	0
a2n1-4+DBalF-=C1NNAA	4.10E12	.5	0
a2n1-4+BaPer-=C1NNAA	4.10E12	.5	0
a2n1-4+N23jF-=C1NNAA	4.79E12	.5	0
a2n1-4+N23kF-=C1NNAA	4.79E12	.5	0
a2n1-4+BaN23jF-=C1NAAA	4.98E12	.5	0
a2n1-4+BaN23kF-=C1NAAA	4.98E12	.5	0
a2n1-4+BaN23lF-=C1NAAA	4.36E12	.5	0
a2n1-4+DBajPer-=C1NAAA	3.74E12	.5	0
a2n1-4+DBaoPer-=C1NAAA	4.36E12	.5	0
a2n2-4+BkF-=C1NNNA	4.59E12	.5	0
a2n2-4+BjF-=C1NNNA	4.59E12	.5	0
a2n2-4+Per-=C1NNNA	4.59E12	.5	0
a2n2-4+DBajF-=C1NNAA	4.79E12	.5	0
a2n2-4+DBakF-=C1NNAA	4.79E12	.5	0
a2n2-4+DBalF-=C1NNAA	4.10E12	.5	0
a2n2-4+BaPer-=C1NNAA	4.10E12	.5	0
a2n2-4+N23jF-=C1NNAA	4.79E12	.5	0
a2n2-4+N23kF-=C1NNAA	4.79E12	.5	0
a2n2-4+BaN23jF-=C1NAAA	4.98E12	.5	0
a2n2-4+BaN23kF-=C1NAAA	4.98E12	.5	0
a2n2-4+BaN23lF-=C1NAAA	4.36E12	.5	0
a2n2-4+DBajPer-=C1NAAA	3.74E12	.5	0
a2n2-4+DBaoPer-=C1NAAA	4.36E12	.5	0
a9n1-4+BkF-=C1NNNA	4.59E12	.5	0
a9n1-4+BjF-=C1NNNA	4.59E12	.5	0

a9n1-4+Per-=C1NNNA	4.59E12	.5	0
a9n1-4+DBajF-=C1NNAA	4.79E12	.5	0
a9n1-4+DBakF-=C1NNAA	4.79E12	.5	0
a9n1-4+DBalF-=C1NNAA	4.10E12	.5	0
a9n1-4+BaPer-=C1NNAA	4.10E12	.5	0
a9n1-4+N23jF-=C1NNAA	4.79E12	.5	0
a9n1-4+N23kF-=C1NNAA	4.79E12	.5	0
a9n1-4+BaN23jF-=C1NAAA	4.98E12	.5	0
a9n1-4+BaN23kF-=C1NAAA	4.98E12	.5	0
a9n1-4+BaN23lF-=C1NAAA	4.36E12	.5	0
a9n1-4+DBajPer-=C1NAAA	3.74E12	.5	0
a9n1-4+DBaoPer-=C1NAAA	4.36E12	.5	0
a9n2-4+BkF-=C1NNNA	4.59E12	.5	0
a9n2-4+BjF-=C1NNNA	4.59E12	.5	0
a9n2-4+Per-=C1NNNA	4.59E12	.5	0
a9n2-4+DBajF-=C1NNAA	4.79E12	.5	0
a9n2-4+DBakF-=C1NNAA	4.79E12	.5	0
a9n2-4+DBalF-=C1NNAA	4.10E12	.5	0
a9n2-4+BaPer-=C1NNAA	4.10E12	.5	0
a9n2-4+N23jF-=C1NNAA	4.79E12	.5	0
a9n2-4+N23kF-=C1NNAA	4.79E12	.5	0
a9n2-4+BaN23jF-=C1NAAA	4.98E12	.5	0
a9n2-4+BaN23kF-=C1NAAA	4.98E12	.5	0
a9n2-4+BaN23lF-=C1NAAA	4.36E12	.5	0
a9n2-4+DBajPer-=C1NAAA	3.74E12	.5	0
a9n2-4+DBaoPer-=C1NAAA	4.36E12	.5	0
a1a1-4+BkF-=C1NNAA	4.79E12	.5	0
a1a1-4+BjF-=C1NNAA	4.79E12	.5	0
a1a1-4+Per-=C1NNAA	4.79E12	.5	0
a1a1-4+DBajF-=C1NAAA	4.98E12	.5	0
a1a1-4+DBakF-=C1NAAA	4.98E12	.5	0
a1a1-4+DBalF-=C1NAAA	4.27E12	.5	0
a1a1-4+BaPer-=C1NAAA	4.27E12	.5	0
a1a1-4+N23jF-=C1NAAA	4.98E12	.5	0
a1a1-4+N23kF-=C1NAAA	4.98E12	.5	0
a1a1-4+BaN23jF-=C1AAAA	5.17E12	.5	0
a1a1-4+BaN23kF-=C1AAAA	5.17E12	.5	0
a1a1-4+BaN23lF-=C1AAAA	4.52E12	.5	0
a1a1-4+DBajPer-=C1AAAA	3.88E12	.5	0
a1a1-4+DBaoPer-=C1AAAA	4.52E12	.5	0
a1a2-4+BkF-=C1NNAA	4.79E12	.5	0
a1a2-4+BjF-=C1NNAA	4.79E12	.5	0
a1a2-4+Per-=C1NNAA	4.79E12	.5	0
a1a2-4+DBajF-=C1NAAA	4.98E12	.5	0
a1a2-4+DBakF-=C1NAAA	4.98E12	.5	0
a1a2-4+DBalF-=C1NAAA	4.27E12	.5	0
a1a2-4+BaPer-=C1NAAA	4.27E12	.5	0
a1a2-4+N23jF-=C1NAAA	4.98E12	.5	0
a1a2-4+N23kF-=C1NAAA	4.98E12	.5	0
a1a2-4+BaN23jF-=C1AAAA	5.17E12	.5	0
a1a2-4+BaN23kF-=C1AAAA	5.17E12	.5	0
a1a2-4+BaN23lF-=C1AAAA	4.52E12	.5	0
a1a2-4+DBajPer-=C1AAAA	3.88E12	.5	0
a1a2-4+DBaoPer-=C1AAAA	4.52E12	.5	0
a1a9-4+BkF-=C1NNAA	4.79E12	.5	0
a1a9-4+BjF-=C1NNAA	4.79E12	.5	0
a1a9-4+Per-=C1NNAA	4.79E12	.5	0
a1a9-4+DBajF-=C1NAAA	4.98E12	.5	0
a1a9-4+DBakF-=C1NAAA	4.98E12	.5	0
a1a9-4+DBalF-=C1NAAA	4.27E12	.5	0

a1a9-4+BaPer-=C1NAAA	4.27E12	.5	0
a1a9-4+N23jF-=C1NAAA	4.98E12	.5	0
a1a9-4+N23kF-=C1NAAA	4.98E12	.5	0
a1a9-4+BaN23jF-=C1AAAA	5.17E12	.5	0
a1a9-4+BaN23kF-=C1AAAA	5.17E12	.5	0
a1a9-4+BaN23lF-=C1AAAA	4.52E12	.5	0
a1a9-4+DBajPer-=C1AAAA	3.88E12	.5	0
a1a9-4+DBaoPer-=C1AAAA	4.52E12	.5	0
a2a2-4+BkF-=C1NNAA	4.79E12	.5	0
a2a2-4+BjF-=C1NNAA	4.79E12	.5	0
a2a2-4+Per-=C1NNAA	4.79E12	.5	0
a2a2-4+DBajF-=C1NAAA	4.98E12	.5	0
a2a2-4+DBakF-=C1NAAA	4.98E12	.5	0
a2a2-4+DBalF-=C1NAAA	4.27E12	.5	0
a2a2-4+BaPer-=C1NAAA	4.27E12	.5	0
a2a2-4+N23jF-=C1NAAA	4.98E12	.5	0
a2a2-4+N23kF-=C1NAAA	4.98E12	.5	0
a2a2-4+BaN23jF-=C1AAAA	5.17E12	.5	0
a2a2-4+BaN23kF-=C1AAAA	5.17E12	.5	0
a2a2-4+BaN23lF-=C1AAAA	4.52E12	.5	0
a2a2-4+DBajPer-=C1AAAA	3.88E12	.5	0
a2a2-4+DBaoPer-=C1AAAA	4.52E12	.5	0
a2a9-4+BkF-=C1NNAA	4.79E12	.5	0
a2a9-4+BjF-=C1NNAA	4.79E12	.5	0
a2a9-4+Per-=C1NNAA	4.79E12	.5	0
a2a9-4+DBajF-=C1NAAA	4.98E12	.5	0
a2a9-4+DBakF-=C1NAAA	4.98E12	.5	0
a2a9-4+DBalF-=C1NAAA	4.27E12	.5	0
a2a9-4+BaPer-=C1NAAA	4.27E12	.5	0
a2a9-4+N23jF-=C1NAAA	4.98E12	.5	0
a2a9-4+N23kF-=C1NAAA	4.98E12	.5	0
a2a9-4+BaN23jF-=C1AAAA	5.17E12	.5	0
a2a9-4+BaN23kF-=C1AAAA	5.17E12	.5	0
a2a9-4+BaN23lF-=C1AAAA	4.52E12	.5	0
a2a9-4+DBajPer-=C1AAAA	3.88E12	.5	0
a2a9-4+DBaoPer-=C1AAAA	4.52E12	.5	0
a9a9-4+BkF-=C1NNAA	4.79E12	.5	0
a9a9-4+BjF-=C1NNAA	4.79E12	.5	0
a9a9-4+Per-=C1NNAA	4.79E12	.5	0
a9a9-4+DBajF-=C1NAAA	4.98E12	.5	0
a9a9-4+DBakF-=C1NAAA	4.98E12	.5	0
a9a9-4+DBalF-=C1NAAA	4.27E12	.5	0
a9a9-4+BaPer-=C1NAAA	4.27E12	.5	0
a9a9-4+N23jF-=C1NAAA	4.98E12	.5	0
a9a9-4+N23kF-=C1NAAA	4.98E12	.5	0
a9a9-4+BaN23jF-=C1AAAA	5.17E12	.5	0
a9a9-4+BaN23kF-=C1AAAA	5.17E12	.5	0
a9a9-4+BaN23lF-=C1AAAA	4.52E12	.5	0
a9a9-4+DBajPer-=C1AAAA	3.88E12	.5	0
a9a9-4+DBaoPer-=C1AAAA	4.52E12	.5	0
n1n1-4+NNN-=NNNNN	3.42E12	.5	0
n1n1-4+C1NNN-=C1NNNNN	4.07E12	.5	0
n1n1-4+C2NNN-=C2NNNNN	4.89E12	.5	0
n1n2-4+NNN-=NNNNN	3.42E12	.5	0
n1n2-4+C1NNN-=C1NNNNN	4.07E12	.5	0
n1n2-4+C2NNN-=C2NNNNN	4.89E12	.5	0
n2n2-4+NNN-=NNNNN	3.42E12	.5	0
n2n2-4+C1NNN-=C1NNNNN	4.07E12	.5	0
n2n2-4+C2NNN-=C2NNNNN	4.89E12	.5	0
BkF-+BkF-=C2NNNN	2.19E12	.5	0

BkF-+BjF-=C2NNNN	4.38E12	.5	0
BkF-+Per-=C2NNNN	4.38E12	.5	0
BkF-+DBajF-=C2NNNA	4.59E12	.5	0
BkF-+DBakF-=C2NNNA	4.59E12	.5	0
BkF-+DBalF-=C2NNNA	3.93E12	.5	0
BkF-+BaPer-=C2NNNA	3.93E12	.5	0
BkF-+N23jF-=C2NNNA	4.59E12	.5	0
BkF-+N23kF-=C2NNNA	4.59E12	.5	0
BkF-+BaN23jF-=C2NNAA	4.79E12	.5	0
BkF-+BaN23kF-=C2NNAA	4.79E12	.5	0
BkF-+BaN23lF-=C2NNAA	4.19E12	.5	0
BkF-+DBajPer-=C2NNAA	3.59E12	.5	0
BkF-+DBaoPer-=C2NNAA	4.19E12	.5	0
BjF-+BjF-=C2NNNN	2.19E12	.5	0
BjF-+Per-=C2NNNN	4.38E12	.5	0
BjF-+DBajF-=C2NNNA	4.59E12	.5	0
BjF-+DBakF-=C2NNNA	4.59E12	.5	0
BjF-+DBalF-=C2NNNA	3.93E12	.5	0
BjF-+BaPer-=C2NNNA	3.93E12	.5	0
BjF-+N23jF-=C2NNNA	4.59E12	.5	0
BjF-+N23kF-=C2NNNA	4.59E12	.5	0
BjF-+BaN23jF-=C2NNAA	4.79E12	.5	0
BjF-+BaN23kF-=C2NNAA	4.79E12	.5	0
BjF-+BaN23lF-=C2NNAA	4.19E12	.5	0
BjF-+DBajPer-=C2NNAA	3.59E12	.5	0
BjF-+DBaoPer-=C2NNAA	4.19E12	.5	0
Per-+Per-=C2NNNN	2.19E12	.5	0
Per-+DBajF-=C2NNNA	4.59E12	.5	0
Per-+DBakF-=C2NNNA	4.59E12	.5	0
Per-+DBalF-=C2NNNA	3.93E12	.5	0
Per-+BaPer-=C2NNNA	3.93E12	.5	0
Per-+N23jF-=C2NNNA	4.59E12	.5	0
Per-+N23kF-=C2NNNA	4.59E12	.5	0
Per-+BaN23jF-=C2NNAA	4.79E12	.5	0
Per-+BaN23kF-=C2NNAA	4.79E12	.5	0
Per-+BaN23lF-=C2NNAA	4.19E12	.5	0
Per-+DBajPer-=C2NNAA	3.59E12	.5	0
Per-+DBaoPer-=C2NNAA	4.19E12	.5	0
DBajF-+DBajF-=C2NNAA	2.39E12	.5	0
DBajF-+DBakF-=C2NNAA	4.79E12	.5	0
DBajF-+DBalF-=C2NNAA	4.10E12	.5	0
DBajF-+BaPer-=C2NNAA	4.10E12	.5	0
DBajF-+N23jF-=C2NNAA	4.79E12	.5	0
DBajF-+N23kF-=C2NNAA	4.79E12	.5	0
DBajF-+BaN23jF-=C2NAAA	4.98E12	.5	0
DBajF-+BaN23kF-=C2NAAA	4.98E12	.5	0
DBajF-+BaN23lF-=C2NAAA	4.36E12	.5	0
DBajF-+DBajPer-=C2NAAA	3.74E12	.5	0
DBajF-+DBaoPer-=C2NAAA	4.36E12	.5	0
DBakF-+DBakF-=C2NNAA	2.39E12	.5	0
DBakF-+DBalF-=C2NNAA	4.10E12	.5	0
DBakF-+BaPer-=C2NNAA	4.10E12	.5	0
DBakF-+N23jF-=C2NNAA	4.79E12	.5	0
DBakF-+N23kF-=C2NNAA	4.79E12	.5	0
DBakF-+BaN23jF-=C2NAAA	4.98E12	.5	0
DBakF-+BaN23kF-=C2NAAA	4.98E12	.5	0
DBakF-+BaN23lF-=C2NAAA	4.36E12	.5	0
DBakF-+DBajPer-=C2NAAA	3.74E12	.5	0
DBakF-+DBaoPer-=C2NAAA	4.36E12	.5	0
DBalF-+DBalF-=C2NNAA	1.76E12	.5	0

DBalF-+BaPer-=C2NNAA	3.52E12	.5	0
DBalF-+N23jF-=C2NNAA	4.10E12	.5	0
DBalF-+N23kF-=C2NNAA	4.10E12	.5	0
DBalF-+BaN23jF-=C2NAAA	4.27E12	.5	0
DBalF-+BaN23kF-=C2NAAA	4.27E12	.5	0
DBalF-+BaN231F-=C2NAAA	3.74E12	.5	0
DBalF-+DBajPer-=C2NAAA	3.20E12	.5	0
DBalF-+DBaoPer-=C2NAAA	3.74E12	.5	0
BaPer-+BaPer-=C2NNAA	1.76E12	.5	0
BaPer-+N23jF-=C2NNAA	4.10E12	.5	0
BaPer-+N23kF-=C2NNAA	4.10E12	.5	0
BaPer-+BaN23jF-=C2NAAA	4.27E12	.5	0
BaPer-+BaN23kF-=C2NAAA	4.27E12	.5	0
BaPer-+BaN231F-=C2NAAA	3.74E12	.5	0
BaPer-+DBajPer-=C2NAAA	3.20E12	.5	0
BaPer-+DBaoPer-=C2NAAA	3.74E12	.5	0
N23jF-+N23jF-=C2NNAA	2.39E12	.5	0
N23jF-+N23kF-=C2NNAA	4.79E12	.5	0
N23jF-+BaN23jF-=C2NAAA	4.98E12	.5	0
N23jF-+BaN23kF-=C2NAAA	4.98E12	.5	0
N23jF-+BaN231F-=C2NAAA	4.36E12	.5	0
N23jF-+DBajPer-=C2NAAA	3.74E12	.5	0
N23jF-+DBaoPer-=C2NAAA	4.36E12	.5	0
N23kF-+N23kF-=C2NNAA	2.39E12	.5	0
N23kF-+BaN23jF-=C2NAAA	4.98E12	.5	0
N23kF-+BaN23kF-=C2NAAA	4.98E12	.5	0
N23kF-+BaN231F-=C2NAAA	4.36E12	.5	0
N23kF-+DBajPer-=C2NAAA	3.74E12	.5	0
N23kF-+DBaoPer-=C2NAAA	4.36E12	.5	0
BaN23jF-+BaN23jF-=C2AAAA	2.58E12	.5	0
BaN23jF-+BaN23kF-=C2AAAA	5.17E12	.5	0
BaN23jF-+BaN231F-=C2AAAA	4.52E12	.5	0
BaN23jF-+DBajPer-=C2AAAA	3.88E12	.5	0
BaN23jF-+DBaoPer-=C2AAAA	4.52E12	.5	0
BaN23kF-+BaN23kF-=C2AAAA	2.58E12	.5	0
BaN23kF-+BaN231F-=C2AAAA	4.52E12	.5	0
BaN23kF-+DBajPer-=C2AAAA	3.88E12	.5	0
BaN23kF-+DBaoPer-=C2AAAA	4.52E12	.5	0
BaN231F-+BaN231F-=C2AAAA	1.98E12	.5	0
BaN231F-+DBajPer-=C2AAAA	3.39E12	.5	0
BaN231F-+DBaoPer-=C2AAAA	3.96E12	.5	0
DBajPer-+DBajPer-=C2AAAA	1.45E12	.5	0
DBajPer-+DBaoPer-=C2AAAA	3.39E12	.5	0
DBaoPer-+DBaoPer-=C2AAAA	1.98E12	.5	0
BkF-+NNN-=C1NNNNN	3.42E12	.5	0
BkF-+C1NNN-=C2NNNNN	4.07E12	.5	0
BkF-+C2NNN-=C3NNNNN	4.89E12	.5	0
BjF-+NNN-=C1NNNNN	3.42E12	.5	0
BjF-+C1NNN-=C2NNNNN	4.07E12	.5	0
BjF-+C2NNN-=C3NNNNN	4.89E12	.5	0
Per-+NNN-=C1NNNNN	3.42E12	.5	0
Per-+C1NNN-=C2NNNNN	4.07E12	.5	0
Per-+C2NNN-=C3NNNNN	4.89E12	.5	0

Reaction Type 3 (hydrogen abstraction)	2.5E14 $e^{-16/RT}$			(Kiefer et al, 1985)
n+h=n1-+h2	1.67E14	0	16000	
n+h=n2-+h2	1.67E14	0	16000	
a+h=a1-+h2	1.67E14	0	16000	
a+h=a2-+h2	1.67E14	0	16000	

a+h=a9-+h2	8.33E13	0	16000
n1n1+h=n1n1-1+h2	8.33E13	0	16000
n1n1+h=n1n1-2+h2	8.33E13	0	16000
n1n1+h=n1n1-4+h2	4.17E14	0	16000
n1n2+h=n1n2-1+h2	8.33E13	0	16000
n1n2+h=n1n2-2+h2	4.17E13	0	16000
n1n2+h=n1n2-4+h2	4.58E14	0	16000
n2n2+h=n2n2-4+h2	5.83E14	0	16000
a1n1+h=a1n1-1+h2	4.17E13	0	16000
a1n1+h=a1n1-2+h2	8.33E13	0	16000
a1n1+h=a1n1-3+h2	4.17E13	0	16000
a1n1+h=a1n1-4+h2	5.00E14	0	16000
a1n2+h=a1n2-1+h2	4.17E13	0	16000
a1n2+h=a1n2-2+h2	4.17E13	0	16000
a1n2+h=a1n2-3+h2	4.17E13	0	16000
a1n2+h=a1n2-4+h2	5.42E14	0	16000
a2n1+h=a2n1-1+h2	8.33E13	0	16000
a2n1+h=a2n1-2+h2	4.17E13	0	16000
a2n1+h=a2n1-4+h2	5.42E14	0	16000
a2n2+h=a2n2-4+h2	6.67E14	0	16000
a9n1+h=a9n1-1+h2	1.25E14	0	16000
a9n1+h=a9n1-2+h2	4.17E13	0	16000
a9n1+h=a9n1-4+h2	5.00E14	0	16000
a9n2+h=a9n2-1+h2	1.25E14	0	16000
a9n2+h=a9n2-2+h2	4.17E13	0	16000
a9n2+h=a9n2-4+h2	5.00E14	0	16000
a1a1+h=a1a1-2+h2	8.33E13	0	16000
a1a1+h=a1a1-3+h2	8.33E13	0	16000
a1a1+h=a1a1-4+h2	5.83E14	0	16000
a1a2+h=a1a2-1+h2	4.17E13	0	16000
a1a2+h=a1a2-2+h2	4.17E13	0	16000
a1a2+h=a1a2-3+h2	4.17E13	0	16000
a1a2+h=a1a2-4+h2	6.25E14	0	16000
a1a9+h=a1a9-1+h2	8.33E13	0	16000
a1a9+h=a1a9-2+h2	4.17E13	0	16000
a1a9+h=a1a9-3+h2	4.17E13	0	16000
a1a9+h=a1a9-4+h2	5.83E14	0	16000
a2a2+h=a2a2-4+h2	7.50E14	0	16000
a2a9+h=a2a9-1+h2	1.25E14	0	16000
a2a9+h=a2a9-2+h2	4.17E13	0	16000
a2a9+h=a2a9-4+h2	5.83E14	0	16000
a9a9+h=a9a9-1+h2	1.67E14	0	16000
a9a9+h=a9a9-4+h2	5.83E14	0	16000
BkF+h=BkF-+h2	5.00E14	0	16000
BjF+h=BjF-+h2	5.00E14	0	16000
Per+h=Per-+h2	5.00E14	0	16000
DBajF+h=DBajF-+h2	5.83E14	0	16000
DBakF+h=DBakF-+h2	5.83E14	0	16000
DBalF+h=DBalF-+h2	5.83E14	0	16000
BaPer+h=BaPer-+h2	5.83E14	0	16000
N23jF+h=N23jF-+h2	5.83E14	0	16000
N23kF+h=N23kF-+h2	5.83E14	0	16000
BaN23jF+h=BaN23jF-+h2	6.67E14	0	16000
BaN23kF+h=BaN23kF-+h2	6.67E14	0	16000
BaN23lF+h=BaN23lF-+h2	6.67E14	0	16000
DBajPer+h=DBajPer-+h2	6.67E14	0	16000
DBaoPer+h=DBaoPer-+h2	6.67E14	0	16000
NNN+h=NNN-+h2	8.33E14	0	16000
NNA+h=NNA-+h2	9.17E14	0	16000
NAA+h=NAA-+h2	1.00E15	0	16000

AAA+h=AAA-+h2	1.08E15	0	16000
NNNN+h=NNNN-+h2	1.08E15	0	16000
NNNA+h=NNNA-+h2	1.17E15	0	16000
NNAA+h=NNAA-+h2	1.25E15	0	16000
NAAA+h=NAAA-+h2	1.33E15	0	16000
AAAA+h=AAAA-+h2	1.42E15	0	16000
NNNNN+h=NNNNN-+h2	1.33E15	0	16000
C1NNN+h=C1NNN-+h2	7.50E14	0	16000
C2NNN+h=C2NNN-+h2	6.67E14	0	16000
C1NNA+h=C1NNA-+h2	8.33E14	0	16000
C2NNA+h=C2NNA-+h2	7.50E14	0	16000
C1NAA+h=C1NAA-+h2	9.17E14	0	16000
C2NAA+h=C2NAA-+h2	8.33E14	0	16000
C1AAA+h=C1AAA-+h2	1.00E15	0	16000
C2AAA+h=C2AAA-+h2	9.17E14	0	16000
C1NNNN+h=C1NNNN-+h2	1.00E15	0	16000
C2NNNN+h=C2NNNN-+h2	9.17E14	0	16000
C3NNNN+h=C3NNNN-+h2	8.33E14	0	16000
C1NNNA+h=C1NNNA-+h2	1.08E15	0	16000
C2NNNA+h=C2NNNA-+h2	1.00E15	0	16000
C3NNNA+h=C3NNNA-+h2	9.17E14	0	16000
C1NNAA+h=C1NNAA-+h2	1.17E15	0	16000
C2NNAA+h=C2NNAA-+h2	1.08E15	0	16000
C3NNAA+h=C3NNAA-+h2	1.00E15	0	16000
C1NAAA+h=C1NAAA-+h2	1.25E15	0	16000
C2NAAA+h=C2NAAA-+h2	1.17E15	0	16000
C3NAAA+h=C3NAAA-+h2	1.08E15	0	16000
C1AAAA+h=C1AAAA-+h2	1.33E15	0	16000
C2AAAA+h=C2AAAA-+h2	1.25E15	0	16000
C3AAAA+h=C3AAAA-+h2	1.17E15	0	16000
C1NNNNN+h=C1NNNNN-+h2	1.25E15	0	16000
C2NNNNN+h=C2NNNNN-+h2	1.17E15	0	16000
C3NNNNN+h=C3NNNNN-+h2	1.08E15	0	16000
C4NNNNN+h=C4NNNNN-+h2	1.00E15	0	16000

Reaction Type 4 (polymerization) $6.64E10\ e^{-4/RT}$ (Fahr and Stein, 1988)

n+n1-=n1n1+h	2.65E11	0	4000
n+n1-=n1n2+h	2.65E11	0	4000
n+n2-=n1n2+h	2.65E11	0	4000
n+n2-=n2n2+h	2.65E11	0	4000
n+a1-=a1n1+h	2.65E11	0	4000
n+a1-=a1n2+h	2.65E11	0	4000
n+a2-=a2n1+h	2.65E11	0	4000
n+a2-=a2n2+h	2.65E11	0	4000
n+a9-=a9n1+h	2.65E11	0	4000
n+a9-=a9n2+h	2.65E11	0	4000
a+n1-=a1n1+h	2.65E11	0	4000
a+n1-=a2n1+h	2.65E11	0	4000
a+n1-=a9n1+h	1.33E11	0	4000
a+n2-=a1n2+h	2.65E11	0	4000
a+n2-=a2n2+h	2.65E11	0	4000
a+n2-=a9n2+h	1.33E11	0	4000
a+a1-=a1a1+h	2.65E11	0	4000
a+a1-=a1a2+h	2.65E11	0	4000
a+a1-=a1a9+h	1.33E11	0	4000
a+a2-=a1a2+h	2.65E11	0	4000
a+a2-=a2a2+h	2.65E11	0	4000
a+a2-=a2a9+h	1.33E11	0	4000
a+a9-=a1a9+h	2.65E11	0	4000

a+a9-=a2a9+h	2.65E11	0	4000
a+a9-=a9a9+h	1.33E11	0	4000
n1n1+n1-=NNN+h	6.63E11	0	4000
n1n1+n2-=NNN+h	6.63E11	0	4000
n1n1-4+n=NNN+h	5.31E11	0	4000
n1n2+n1-=NNN+h	7.30E11	0	4000
n1n2+n2-=NNN+h	7.30E11	0	4000
n1n2-4+n=NNN+h	5.31E11	0	4000
n2n2+n1-=NNN+h	9.29E11	0	4000
n2n2+n2-=NNN+h	9.29E11	0	4000
n2n2-4+n=NNN+h	5.31E11	0	4000
n1n1+a1-=NNA+h	6.63E11	0	4000
n1n1+a2-=NNA+h	6.63E11	0	4000
n1n1+a9-=NNA+h	6.63E11	0	4000
n1n1-4+a=NNA+h	6.63E11	0	4000
n1n2+a1-=NNA+h	7.30E11	0	4000
n1n2+a2-=NNA+h	7.30E11	0	4000
n1n2+a9-=NNA+h	7.30E11	0	4000
n1n2-4+a=NNA+h	6.63E11	0	4000
n2n2+a1-=NNA+h	9.29E11	0	4000
n2n2+a2-=NNA+h	9.29E11	0	4000
n2n2+a9-=NNA+h	9.29E11	0	4000
n2n2-4+a=NNA+h	6.63E11	0	4000
a1n1+n1-=NNA+h	7.96E11	0	4000
a1n1+n2-=NNA+h	7.96E11	0	4000
a1n1-4+n=NNA+h	5.31E11	0	4000
a1n2+n1-=NNA+h	8.62E11	0	4000
a1n2+n2-=NNA+h	8.62E11	0	4000
a1n2-4+n=NNA+h	5.31E11	0	4000
a2n1+n1-=NNA+h	8.62E11	0	4000
a2n1+n2-=NNA+h	8.62E11	0	4000
a2n1-4+n=NNA+h	5.31E11	0	4000
a2n2+n1-=NNA+h	1.06E12	0	4000
a2n2+n2-=NNA+h	1.06E12	0	4000
a2n2-4+n=NNA+h	5.31E11	0	4000
a9n1+n1-=NNA+h	7.96E11	0	4000
a9n1+n2-=NNA+h	7.96E11	0	4000
a9n1-4+n=NNA+h	5.31E11	0	4000
a9n2+n1-=NNA+h	7.96E11	0	4000
a9n2+n2-=NNA+h	7.96E11	0	4000
a9n2-4+n=NNA+h	5.31E11	0	4000
a1n1+a1-=NAA+h	7.96E11	0	4000
a1n1+a2-=NAA+h	7.96E11	0	4000
a1n1+a9-=NAA+h	7.96E11	0	4000
a1n1-4+a=NAA+h	6.63E11	0	4000
a1n2+a1-=NAA+h	8.62E11	0	4000
a1n2+a2-=NAA+h	8.62E11	0	4000
a1n2+a9-=NAA+h	8.62E11	0	4000
a1n2-4+a=NAA+h	6.63E11	0	4000
a2n1+a1-=NAA+h	8.62E11	0	4000
a2n1+a2-=NAA+h	8.62E11	0	4000
a2n1+a9-=NAA+h	8.62E11	0	4000
a2n1-4+a=NAA+h	6.63E11	0	4000
a2n2+a1-=NAA+h	1.06E12	0	4000
a2n2+a2-=NAA+h	1.06E12	0	4000
a2n2+a9-=NAA+h	1.06E12	0	4000
a2n2-4+a=NAA+h	6.63E11	0	4000
a9n1+a1-=NAA+h	7.96E11	0	4000
a9n1+a2-=NAA+h	7.96E11	0	4000
a9n1+a9-=NAA+h	7.96E11	0	4000

a9n1-4+a=NAA+h	6.63E11	0	4000
a9n2+a1-=NAA+h	7.96E11	0	4000
a9n2+a2-=NAA+h	7.96E11	0	4000
a9n2+a9-=NAA+h	7.96E11	0	4000
a9n2-4+a=NAA+h	6.63E11	0	4000
a1a1+n1-=NAA+h	9.29E11	0	4000
a1a1+n2-=NAA+h	9.29E11	0	4000
a1a1-4+n=NAA+h	5.31E11	0	4000
a1a2+n1-=NAA+h	9.95E11	0	4000
a1a2+n2-=NAA+h	9.95E11	0	4000
a1a2-4+n=NAA+h	5.31E11	0	4000
a1a9+n1-=NAA+h	9.29E11	0	4000
a1a9+n2-=NAA+h	9.29E11	0	4000
a1a9-4+n=NAA+h	5.31E11	0	4000
a2a2+n1-=NAA+h	1.19E12	0	4000
a2a2+n2-=NAA+h	1.19E12	0	4000
a2a2-4+n=NAA+h	5.31E11	0	4000
a2a9+n1-=NAA+h	9.29E11	0	4000
a2a9+n2-=NAA+h	9.29E11	0	4000
a2a9-4+n=NAA+h	5.31E11	0	4000
a9a9+n1-=NAA+h	9.29E11	0	4000
a9a9+n2-=NAA+h	9.29E11	0	4000
a9a9-4+n=NAA+h	5.31E11	0	4000
a1a1+a1-=AAA+h	9.29E11	0	4000
a1a1+a2-=AAA+h	9.29E11	0	4000
a1a1+a9-=AAA+h	9.29E11	0	4000
a1a1-4+a=AAA+h	6.63E11	0	4000
a1a2+a1-=AAA+h	9.95E11	0	4000
a1a2+a2-=AAA+h	9.95E11	0	4000
a1a2+a9-=AAA+h	9.95E11	0	4000
a1a2-4+a=AAA+h	6.63E11	0	4000
a1a9+a1-=AAA+h	9.29E11	0	4000
a1a9+a2-=AAA+h	9.29E11	0	4000
a1a9+a9-=AAA+h	9.29E11	0	4000
a1a9-4+a=AAA+h	6.63E11	0	4000
a2a2+a1-=AAA+h	1.19E12	0	4000
a2a2+a2-=AAA+h	1.19E12	0	4000
a2a2+a9-=AAA+h	1.19E12	0	4000
a2a2-4+a=AAA+h	6.63E11	0	4000
a2a9+a1-=AAA+h	9.29E11	0	4000
a2a9+a2-=AAA+h	9.29E11	0	4000
a2a9+a9-=AAA+h	9.29E11	0	4000
a2a9-4+a=AAA+h	6.63E11	0	4000
a9a9+a1-=AAA+h	9.29E11	0	4000
a9a9+a2-=AAA+h	9.29E11	0	4000
a9a9+a9-=AAA+h	9.29E11	0	4000
a9a9-4+a=AAA+h	6.63E11	0	4000
NNN+n1-=NNNN+h	9.29E11	0	4000
NNN+n2-=NNNN+h	9.29E11	0	4000
NNN+a1-=NNNA+h	9.29E11	0	4000
NNN+a2-=NNNA+h	9.29E11	0	4000
NNN+a9-=NNNA+h	9.29E11	0	4000
NNA+n1-=NNNA+h	1.06E12	0	4000
NNA+n2-=NNNA+h	1.06E12	0	4000
NNA+a1-=NNAA+h	1.06E12	0	4000
NNA+a2-=NNAA+h	1.06E12	0	4000
NNA+a9-=NNAA+h	1.06E12	0	4000
NAA+n1-=NNAA+h	1.19E12	0	4000
NAA+n2-=NNAA+h	1.19E12	0	4000
NAA+a1-=NAAA+h	1.19E12	0	4000

NAA+a2-=NAAA+h	1.19E12	0	4000
NAA+a9-=NAAA+h	1.19E12	0	4000
AAA+n1-=NAAA+h	1.33E12	0	4000
AAA+n2-=NAAA+h	1.33E12	0	4000
AAA+a1-=AAAA+h	1.33E12	0	4000
AAA+a2-=AAAA+h	1.33E12	0	4000
AAA+a9-=AAAA+h	1.33E12	0	4000
NNN-+n=NNNN+h	3.71E11	0	4000
NNA-+n=NNNA+h	3.86E11	0	4000
NAA-+n=NNAA+h	3.98E11	0	4000
AAA-+n=NAAA+h	4.08E11	0	4000
NNN-+a=NNNA+h	4.64E11	0	4000
NNA-+a=NNAA+h	4.82E11	0	4000
NAA-+a=NAAA+h	4.98E11	0	4000
AAA-+a=AAAA+h	5.10E11	0	4000
NNNN+n1-=NNNNN+h	1.13E12	0	4000
NNNN+n2-=NNNNN+h	1.13E12	0	4000
NNNN-+n=NNNNN+h	3.47E11	0	4000
n1n1-4+n1n1=NNNN+h	6.63E11	0	4000
n1n1-4+n1n2=NNNN+h	7.30E11	0	4000
n1n1-4+n2n2=NNNN+h	9.29E11	0	4000
n1n1-4+a1n1=NNNA+h	7.96E11	0	4000
n1n1-4+a1n2=NNNA+h	8.62E11	0	4000
n1n1-4+a2n1=NNNA+h	8.62E11	0	4000
n1n1-4+a2n2=NNNA+h	1.06E12	0	4000
n1n1-4+a9n1=NNNA+h	7.96E11	0	4000
n1n1-4+a9n2=NNNA+h	7.96E11	0	4000
n1n1-4+a1a1=NNAA+h	9.29E11	0	4000
n1n1-4+a1a2=NNAA+h	9.95E11	0	4000
n1n1-4+a1a9=NNAA+h	9.29E11	0	4000
n1n1-4+a2a2=NNAA+h	1.19E12	0	4000
n1n1-4+a2a9=NNAA+h	9.29E11	0	4000
n1n1-4+a9a9=NNAA+h	9.29E11	0	4000
n1n2-4+n1n1=NNNN+h	6.63E11	0	4000
n1n2-4+n1n2=NNNN+h	7.30E11	0	4000
n1n2-4+n2n2=NNNN+h	9.29E11	0	4000
n1n2-4+a1n1=NNNA+h	7.96E11	0	4000
n1n2-4+a1n2=NNNA+h	8.62E11	0	4000
n1n2-4+a2n1=NNNA+h	8.62E11	0	4000
n1n2-4+a2n2=NNNA+h	1.06E12	0	4000
n1n2-4+a9n1=NNNA+h	7.96E11	0	4000
n1n2-4+a9n2=NNNA+h	7.96E11	0	4000
n1n2-4+a1a1=NNAA+h	9.29E11	0	4000
n1n2-4+a1a2=NNAA+h	9.95E11	0	4000
n1n2-4+a1a9=NNAA+h	9.29E11	0	4000
n1n2-4+a2a2=NNAA+h	1.19E12	0	4000
n1n2-4+a2a9=NNAA+h	9.29E11	0	4000
n1n2-4+a9a9=NNAA+h	9.29E11	0	4000
n2n2-4+n1n1=NNNN+h	6.63E11	0	4000
n2n2-4+n1n2=NNNN+h	7.30E11	0	4000
n2n2-4+n2n2=NNNN+h	9.29E11	0	4000
n2n2-4+a1n1=NNNA+h	7.96E11	0	4000
n2n2-4+a1n2=NNNA+h	8.62E11	0	4000
n2n2-4+a2n1=NNNA+h	8.62E11	0	4000
n2n2-4+a2n2=NNNA+h	1.06E12	0	4000
n2n2-4+a9n1=NNNA+h	7.96E11	0	4000
n2n2-4+a9n2=NNNA+h	7.96E11	0	4000
n2n2-4+a1a1=NNAA+h	9.29E11	0	4000
n2n2-4+a1a2=NNAA+h	9.95E11	0	4000
n2n2-4+a1a9=NNAA+h	9.29E11	0	4000

n2n2-4+a2a2=NNAA+h	1.19E12	0	4000
n2n2-4+a2a9=NNAA+h	9.29E11	0	4000
n2n2-4+a9a9=NNAA+h	9.29E11	0	4000
a1n1-4+n1n1=NNNA+h	6.63E11	0	4000
a1n1-4+n1n2=NNNA+h	7.30E11	0	4000
a1n1-4+n2n2=NNNA+h	9.29E11	0	4000
a1n1-4+a1n1=NNAA+h	7.96E11	0	4000
a1n1-4+a1n2=NNAA+h	8.62E11	0	4000
a1n1-4+a2n1=NNAA+h	8.62E11	0	4000
a1n1-4+a2n2=NNAA+h	1.06E12	0	4000
a1n1-4+a9n1=NNAA+h	7.96E11	0	4000
a1n1-4+a9n2=NNAA+h	7.96E11	0	4000
a1n1-4+a1a1=NAAA+h	9.29E11	0	4000
a1n1-4+a1a2=NAAA+h	9.95E11	0	4000
a1n1-4+a1a9=NAAA+h	9.29E11	0	4000
a1n1-4+a2a2=NAAA+h	1.19E12	0	4000
a1n1-4+a2a9=NAAA+h	9.29E11	0	4000
a1n1-4+a9a9=NAAA+h	9.29E11	0	4000
a1n2-4+n1n1=NNNA+h	6.63E11	0	4000
a1n2-4+n1n2=NNNA+h	7.30E11	0	4000
a1n2-4+n2n2=NNNA+h	9.29E11	0	4000
a1n2-4+a1n1=NNAA+h	7.96E11	0	4000
a1n2-4+a1n2=NNAA+h	8.62E11	0	4000
a1n2-4+a2n1=NNAA+h	8.62E11	0	4000
a1n2-4+a2n2=NNAA+h	1.06E12	0	4000
a1n2-4+a9n1=NNAA+h	7.96E11	0	4000
a1n2-4+a9n2=NNAA+h	7.96E11	0	4000
a1n2-4+a1a1=NAAA+h	9.29E11	0	4000
a1n2-4+a1a2=NAAA+h	9.95E11	0	4000
a1n2-4+a1a9=NAAA+h	9.29E11	0	4000
a1n2-4+a2a2=NAAA+h	1.19E12	0	4000
a1n2-4+a2a9=NAAA+h	9.29E11	0	4000
a1n2-4+a9a9=NAAA+h	9.29E11	0	4000
a2n1-4+n1n1=NNNA+h	6.63E11	0	4000
a2n1-4+n1n2=NNNA+h	7.30E11	0	4000
a2n1-4+n2n2=NNNA+h	9.29E11	0	4000
a2n1-4+a1n1=NNAA+h	7.96E11	0	4000
a2n1-4+a1n2=NNAA+h	8.62E11	0	4000
a2n1-4+a2n1=NNAA+h	8.62E11	0	4000
a2n1-4+a2n2=NNAA+h	1.06E12	0	4000
a2n1-4+a9n1=NNAA+h	7.96E11	0	4000
a2n1-4+a9n2=NNAA+h	7.96E11	0	4000
a2n1-4+a1a1=NAAA+h	9.29E11	0	4000
a2n1-4+a1a2=NAAA+h	9.95E11	0	4000
a2n1-4+a1a9=NAAA+h	9.29E11	0	4000
a2n1-4+a2a2=NAAA+h	1.19E12	0	4000
a2n1-4+a2a9=NAAA+h	9.29E11	0	4000
a2n1-4+a9a9=NAAA+h	9.29E11	0	4000
a2n2-4+n1n1=NNNA+h	6.63E11	0	4000
a2n2-4+n1n2=NNNA+h	7.30E11	0	4000
a2n2-4+n2n2=NNNA+h	9.29E11	0	4000
a2n2-4+a1n1=NNAA+h	7.96E11	0	4000
a2n2-4+a1n2=NNAA+h	8.62E11	0	4000
a2n2-4+a2n1=NNAA+h	8.62E11	0	4000
a2n2-4+a2n2=NNAA+h	1.06E12	0	4000
a2n2-4+a9n1=NNAA+h	7.96E11	0	4000
a2n2-4+a9n2=NNAA+h	7.96E11	0	4000
a2n2-4+a1a1=NAAA+h	9.29E11	0	4000
a2n2-4+a1a2=NAAA+h	9.95E11	0	4000
a2n2-4+a1a9=NAAA+h	9.29E11	0	4000

a2n2-4+a2a2=NAAA+h	1.19E12	0	4000
a2n2-4+a2a9=NAAA+h	9.29E11	0	4000
a2n2-4+a9a9=NAAA+h	9.29E11	0	4000
a9n1-4+n1n1=NNNA+h	6.63E11	0	4000
a9n1-4+n1n2=NNNA+h	7.30E11	0	4000
a9n1-4+n2n2=NNNA+h	9.29E11	0	4000
a9n1-4+a1n1=NNAA+h	7.96E11	0	4000
a9n1-4+a1n2=NNAA+h	8.62E11	0	4000
a9n1-4+a2n1=NNAA+h	8.62E11	0	4000
a9n1-4+a2n2=NNAA+h	1.06E12	0	4000
a9n1-4+a9n1=NNAA+h	7.96E11	0	4000
a9n1-4+a9n2=NNAA+h	7.96E11	0	4000
a9n1-4+a1a1=NAAA+h	9.29E11	0	4000
a9n1-4+a1a2=NAAA+h	9.95E11	0	4000
a9n1-4+a1a9=NAAA+h	9.29E11	0	4000
a9n1-4+a2a2=NAAA+h	1.19E12	0	4000
a9n1-4+a2a9=NAAA+h	9.29E11	0	4000
a9n1-4+a9a9=NAAA+h	9.29E11	0	4000
a9n2-4+n1n1=NNNA+h	6.63E11	0	4000
a9n2-4+n1n2=NNNA+h	7.30E11	0	4000
a9n2-4+n2n2=NNNA+h	9.29E11	0	4000
a9n2-4+a1n1=NNAA+h	7.96E11	0	4000
a9n2-4+a1n2=NNAA+h	8.62E11	0	4000
a9n2-4+a2n1=NNAA+h	8.62E11	0	4000
a9n2-4+a2n2=NNAA+h	1.06E12	0	4000
a9n2-4+a9n1=NNAA+h	7.96E11	0	4000
a9n2-4+a9n2=NNAA+h	7.96E11	0	4000
a9n2-4+a1a1=NAAA+h	9.29E11	0	4000
a9n2-4+a1a2=NAAA+h	9.95E11	0	4000
a9n2-4+a1a9=NAAA+h	9.29E11	0	4000
a9n2-4+a2a2=NAAA+h	1.19E12	0	4000
a9n2-4+a2a9=NAAA+h	9.29E11	0	4000
a9n2-4+a9a9=NAAA+h	9.29E11	0	4000
a1a1-4+n1n1=NNAA+h	6.63E11	0	4000
a1a1-4+n1n2=NNAA+h	7.30E11	0	4000
a1a1-4+n2n2=NNAA+h	9.29E11	0	4000
a1a1-4+a1n1=NAAA+h	7.96E11	0	4000
a1a1-4+a1n2=NAAA+h	8.62E11	0	4000
a1a1-4+a2n1=NAAA+h	8.62E11	0	4000
a1a1-4+a2n2=NAAA+h	1.06E12	0	4000
a1a1-4+a9n1=NAAA+h	7.96E11	0	4000
a1a1-4+a9n2=NAAA+h	7.96E11	0	4000
a1a1-4+a1a1=AAAA+h	9.29E11	0	4000
a1a1-4+a1a2=AAAA+h	9.95E11	0	4000
a1a1-4+a1a9=AAAA+h	9.29E11	0	4000
a1a1-4+a2a2=AAAA+h	1.19E12	0	4000
a1a1-4+a2a9=AAAA+h	9.29E11	0	4000
a1a1-4+a9a9=AAAA+h	9.29E11	0	4000
a1a2-4+n1n1=NNAA+h	6.63E11	0	4000
a1a2-4+n1n2=NNAA+h	7.30E11	0	4000
a1a2-4+n2n2=NNAA+h	9.29E11	0	4000
a1a2-4+a1n1=NAAA+h	7.96E11	0	4000
a1a2-4+a1n2=NAAA+h	8.62E11	0	4000
a1a2-4+a2n1=NAAA+h	8.62E11	0	4000
a1a2-4+a2n2=NAAA+h	1.06E12	0	4000
a1a2-4+a9n1=NAAA+h	7.96E11	0	4000
a1a2-4+a9n2=NAAA+h	7.96E11	0	4000
a1a2-4+a1a1=AAAA+h	9.29E11	0	4000
a1a2-4+a1a2=AAAA+h	9.95E11	0	4000
a1a2-4+a1a9=AAAA+h	9.29E11	0	4000

a1a2-4+a2a2=AAAA+h	1.19E12	0	4000
a1a2-4+a2a9=AAAA+h	9.29E11	0	4000
a1a2-4+a9a9=AAAA+h	9.29E11	0	4000
a1a9-4+n1n1=NNAA+h	6.63E11	0	4000
a1a9-4+n1n2=NNAA+h	7.30E11	0	4000
a1a9-4+n2n2=NNAA+h	9.29E11	0	4000
a1a9-4+a1n1=NAAA+h	7.96E11	0	4000
a1a9-4+a1n2=NAAA+h	8.62E11	0	4000
a1a9-4+a2n1=NAAA+h	8.62E11	0	4000
a1a9-4+a2n2=NAAA+h	1.06E12	0	4000
a1a9-4+a9n1=NAAA+h	7.96E11	0	4000
a1a9-4+a9n2=NAAA+h	7.96E11	0	4000
a1a9-4+a1a1=AAAA+h	9.29E11	0	4000
a1a9-4+a1a2=AAAA+h	9.95E11	0	4000
a1a9-4+a1a9=AAAA+h	9.29E11	0	4000
a1a9-4+a2a2=AAAA+h	1.19E12	0	4000
a1a9-4+a2a9=AAAA+h	9.29E11	0	4000
a1a9-4+a9a9=AAAA+h	9.29E11	0	4000
a2a2-4+n1n1=NNAA+h	6.63E11	0	4000
a2a2-4+n1n2=NNAA+h	7.30E11	0	4000
a2a2-4+n2n2=NNAA+h	9.29E11	0	4000
a2a2-4+a1n1=NAAA+h	7.96E11	0	4000
a2a2-4+a1n2=NAAA+h	8.62E11	0	4000
a2a2-4+a2n1=NAAA+h	8.62E11	0	4000
a2a2-4+a2n2=NAAA+h	1.06E12	0	4000
a2a2-4+a9n1=NAAA+h	7.96E11	0	4000
a2a2-4+a9n2=NAAA+h	7.96E11	0	4000
a2a2-4+a1a1=AAAA+h	9.29E11	0	4000
a2a2-4+a1a2=AAAA+h	9.95E11	0	4000
a2a2-4+a1a9=AAAA+h	9.29E11	0	4000
a2a2-4+a2a2=AAAA+h	1.19E12	0	4000
a2a2-4+a2a9=AAAA+h	9.29E11	0	4000
a2a2-4+a9a9=AAAA+h	9.29E11	0	4000
a2a9-4+n1n1=NNAA+h	6.63E11	0	4000
a2a9-4+n1n2=NNAA+h	7.30E11	0	4000
a2a9-4+n2n2=NNAA+h	9.29E11	0	4000
a2a9-4+a1n1=NAAA+h	7.96E11	0	4000
a2a9-4+a1n2=NAAA+h	8.62E11	0	4000
a2a9-4+a2n1=NAAA+h	8.62E11	0	4000
a2a9-4+a2n2=NAAA+h	1.06E12	0	4000
a2a9-4+a9n1=NAAA+h	7.96E11	0	4000
a2a9-4+a9n2=NAAA+h	7.96E11	0	4000
a2a9-4+a1a1=AAAA+h	9.29E11	0	4000
a2a9-4+a1a2=AAAA+h	9.95E11	0	4000
a2a9-4+a1a9=AAAA+h	9.29E11	0	4000
a2a9-4+a2a2=AAAA+h	1.19E12	0	4000
a2a9-4+a2a9=AAAA+h	9.29E11	0	4000
a2a9-4+a9a9=AAAA+h	9.29E11	0	4000
a9a9-4+n1n1=NNAA+h	6.63E11	0	4000
a9a9-4+n1n2=NNAA+h	7.30E11	0	4000
a9a9-4+n2n2=NNAA+h	9.29E11	0	4000
a9a9-4+a1n1=NAAA+h	7.96E11	0	4000
a9a9-4+a1n2=NAAA+h	8.62E11	0	4000
a9a9-4+a2n1=NAAA+h	8.62E11	0	4000
a9a9-4+a2n2=NAAA+h	1.06E12	0	4000
a9a9-4+a9n1=NAAA+h	7.96E11	0	4000
a9a9-4+a9n2=NAAA+h	7.96E11	0	4000
a9a9-4+a1a1=AAAA+h	9.29E11	0	4000
a9a9-4+a1a2=AAAA+h	9.95E11	0	4000
a9a9-4+a1a9=AAAA+h	9.29E11	0	4000

a9a9-4+a2a2=AAAA+h	1.19E12	0	4000
a9a9-4+a2a9=AAAA+h	9.29E11	0	4000
a9a9-4+a9a9=AAAA+h	9.29E11	0	4000
n1n1-4+NNN=NNNNN+h	9.29E11	0	4000
n1n2-4+NNN=NNNNN+h	9.29E11	0	4000
n2n2-4+NNN=NNNNN+h	9.29E11	0	4000
n1n1+NNN-=NNNNN+h	6.63E11	0	4000
n1n2+NNN-=NNNNN+h	7.30E11	0	4000
n2n2+NNN-=NNNNN+h	9.29E11	0	4000
BkF+n1-=C1NNN+h	7.96E11	0	4000
BkF+n2-=C1NNN+h	7.96E11	0	4000
BkF+a1-=C1NNA+h	7.96E11	0	4000
BkF+a2-=C1NNA+h	7.96E11	0	4000
BkF+a9-=C1NNA+h	7.96E11	0	4000
BjF+n1-=C1NNN+h	7.96E11	0	4000
BjF+n2-=C1NNN+h	7.96E11	0	4000
BjF+a1-=C1NNA+h	7.96E11	0	4000
BjF+a2-=C1NNA+h	7.96E11	0	4000
BjF+a9-=C1NNA+h	7.96E11	0	4000
Per+n1-=C1NNN+h	7.96E11	0	4000
Per+n2-=C1NNN+h	7.96E11	0	4000
Per+a1-=C1NNA+h	7.96E11	0	4000
Per+a2-=C1NNA+h	7.96E11	0	4000
Per+a9-=C1NNA+h	7.96E11	0	4000
DBajF+n1-=C1NNA+h	9.29E11	0	4000
DBajF+n2-=C1NNA+h	9.29E11	0	4000
DBajF+a1-=C1NAA+h	9.29E11	0	4000
DBajF+a2-=C1NAA+h	9.29E11	0	4000
DBajF+a9-=C1NAA+h	9.29E11	0	4000
DBakF+n1-=C1NNA+h	9.29E11	0	4000
DBakF+n2-=C1NNA+h	9.29E11	0	4000
DBakF+a1-=C1NAA+h	9.29E11	0	4000
DBakF+a2-=C1NAA+h	9.29E11	0	4000
DBakF+a9-=C1NAA+h	9.29E11	0	4000
DBalF+n1-=C1NNA+h	7.96E11	0	4000
DBalF+n2-=C1NNA+h	7.96E11	0	4000
DBalF+a1-=C1NAA+h	7.96E11	0	4000
DBalF+a2-=C1NAA+h	7.96E11	0	4000
DBalF+a9-=C1NAA+h	7.96E11	0	4000
BaPer+n1-=C1NNA+h	7.96E11	0	4000
BaPer+n2-=C1NNA+h	7.96E11	0	4000
BaPer+a1-=C1NAA+h	7.96E11	0	4000
BaPer+a2-=C1NAA+h	7.96E11	0	4000
BaPer+a9-=C1NAA+h	7.96E11	0	4000
N23jF+n1-=C1NNA+h	9.29E11	0	4000
N23jF+n2-=C1NNA+h	9.29E11	0	4000
N23jF+a1-=C1NAA+h	9.29E11	0	4000
N23jF+a2-=C1NAA+h	9.29E11	0	4000
N23jF+a9-=C1NAA+h	9.29E11	0	4000
N23kF+n1-=C1NNA+h	9.29E11	0	4000
N23kF+n2-=C1NNA+h	9.29E11	0	4000
N23kF+a1-=C1NAA+h	9.29E11	0	4000
N23kF+a2-=C1NAA+h	9.29E11	0	4000
N23kF+a9-=C1NAA+h	9.29E11	0	4000
BaN23jF+n1-=C1NAA+h	1.06E12	0	4000
BaN23jF+n2-=C1NAA+h	1.06E12	0	4000
BaN23jF+a1-=C1AAA+h	1.06E12	0	4000
BaN23jF+a2-=C1AAA+h	1.06E12	0	4000
BaN23jF+a9-=C1AAA+h	1.06E12	0	4000
BaN23kF+n1-=C1NAA+h	1.06E12	0	4000

BaN23kF+n2-=C1NAA+h	1.06E12	0	4000
BaN23kF+a1-=C1AAA+h	1.06E12	0	4000
BaN23kF+a2-=C1AAA+h	1.06E12	0	4000
BaN23kF+a9-=C1AAA+h	1.06E12	0	4000
BaN23lF+n1-=C1NAA+h	9.29E11	0	4000
BaN23lF+n2-=C1NAA+h	9.29E11	0	4000
BaN23lF+a1-=C1AAA+h	9.29E11	0	4000
BaN23lF+a2-=C1AAA+h	9.29E11	0	4000
BaN23lF+a9-=C1AAA+h	9.29E11	0	4000
DBajPer+n1-=C1NAA+h	7.96E11	0	4000
DBajPer+n2-=C1NAA+h	7.96E11	0	4000
DBajPer+a1-=C1AAA+h	7.96E11	0	4000
DBajPer+a2-=C1AAA+h	7.96E11	0	4000
DBajPer+a9-=C1AAA+h	7.96E11	0	4000
DBaoPer+n1-=C1NAA+h	9.29E11	0	4000
DBaoPer+n2-=C1NAA+h	9.29E11	0	4000
DBaoPer+a1-=C1AAA+h	9.29E11	0	4000
DBaoPer+a2-=C1AAA+h	9.29E11	0	4000
DBaoPer+a9-=C1AAA+h	9.29E11	0	4000
BkF-+n=C1NNN+h	5.31E11	0	4000
BjF-+n=C1NNN+h	5.31E11	0	4000
Per-+n=C1NNN+h	5.31E11	0	4000
DBajF-+n=C1NNA+h	5.31E11	0	4000
DBakF-+n=C1NNA+h	5.31E11	0	4000
DBalF-+n=C1NNA+h	4.55E11	0	4000
BaPer-+n=C1NNA+h	4.55E11	0	4000
N23jF-+n=C1NNA+h	5.31E11	0	4000
N23kF-+n=C1NNA+h	5.31E11	0	4000
BaN23jF-+n=C1NAA+h	5.31E11	0	4000
BaN23kF-+n=C1NAA+h	5.31E11	0	4000
BaN23lF-+n=C1NAA+h	4.64E11	0	4000
DBajPer-+n=C1NAA+h	3.98E11	0	4000
DBaoPer-+n=C1NAA+h	4.64E11	0	4000
BkF-+a=C1NNA+h	6.63E11	0	4000
BjF-+a=C1NNA+h	6.63E11	0	4000
Per-+a=C1NNA+h	6.63E11	0	4000
DBajF-+a=C1NAA+h	6.63E11	0	4000
DBakF-+a=C1NAA+h	6.63E11	0	4000
DBalF-+a=C1NAA+h	5.69E11	0	4000
BaPer-+a=C1NAA+h	5.69E11	0	4000
N23jF-+a=C1NAA+h	6.63E11	0	4000
N23kF-+a=C1NAA+h	6.63E11	0	4000
BaN23jF-+a=C1AAA+h	6.63E11	0	4000
BaN23kF-+a=C1AAA+h	6.63E11	0	4000
BaN23lF-+a=C1AAA+h	5.80E11	0	4000
DBajPer-+a=C1AAA+h	4.98E11	0	4000
DBaoPer-+a=C1AAA+h	5.80E11	0	4000
BkF+n1n1-4=C1NNNN+h	7.96E11	0	4000
BkF+n1n2-4=C1NNNN+h	7.96E11	0	4000
BkF+n2n2-4=C1NNNN+h	7.96E11	0	4000
BkF+a1n1-4=C1NNNA+h	7.96E11	0	4000
BkF+a1n2-4=C1NNNA+h	7.96E11	0	4000
BkF+a2n1-4=C1NNNA+h	7.96E11	0	4000
BkF+a2n2-4=C1NNNA+h	7.96E11	0	4000
BkF+a9n1-4=C1NNNA+h	7.96E11	0	4000
BkF+a9n2-4=C1NNNA+h	7.96E11	0	4000
BkF+a1a1-4=C1NNAA+h	7.96E11	0	4000
BkF+a1a2-4=C1NNAA+h	7.96E11	0	4000
BkF+a1a9-4=C1NNAA+h	7.96E11	0	4000
BkF+a2a2-4=C1NNAA+h	7.96E11	0	4000

BkF+a2a9-4=C1NNAA+h	7.96E11	0	4000
BkF+a9a9-4=C1NNAA+h	7.96E11	0	4000
BjF+n1n1-4=C1NNNN+h	7.96E11	0	4000
BjF+n1n2-4=C1NNNN+h	7.96E11	0	4000
BjF+n2n2-4=C1NNNN+h	7.96E11	0	4000
BjF+a1n1-4=C1NNNA+h	7.96E11	0	4000
BjF+a1n2-4=C1NNNA+h	7.96E11	0	4000
BjF+a2n1-4=C1NNNA+h	7.96E11	0	4000
BjF+a2n2-4=C1NNNA+h	7.96E11	0	4000
BjF+a9n1-4=C1NNNA+h	7.96E11	0	4000
BjF+a9n2-4=C1NNNA+h	7.96E11	0	4000
BjF+a1a1-4=C1NNAA+h	7.96E11	0	4000
BjF+a1a2-4=C1NNAA+h	7.96E11	0	4000
BjF+a1a9-4=C1NNAA+h	7.96E11	0	4000
BjF+a2a2-4=C1NNAA+h	7.96E11	0	4000
BjF+a2a9-4=C1NNAA+h	7.96E11	0	4000
BjF+a9a9-4=C1NNAA+h	7.96E11	0	4000
Per+n1n1-4=C1NNNN+h	7.96E11	0	4000
Per+n1n2-4=C1NNNN+h	7.96E11	0	4000
Per+n2n2-4=C1NNNN+h	7.96E11	0	4000
Per+a1n1-4=C1NNNA+h	7.96E11	0	4000
Per+a1n2-4=C1NNNA+h	7.96E11	0	4000
Per+a2n1-4=C1NNNA+h	7.96E11	0	4000
Per+a2n2-4=C1NNNA+h	7.96E11	0	4000
Per+a9n1-4=C1NNNA+h	7.96E11	0	4000
Per+a9n2-4=C1NNNA+h	7.96E11	0	4000
Per+a1a1-4=C1NNAA+h	7.96E11	0	4000
Per+a1a2-4=C1NNAA+h	7.96E11	0	4000
Per+a1a9-4=C1NNAA+h	7.96E11	0	4000
Per+a2a2-4=C1NNAA+h	7.96E11	0	4000
Per+a2a9-4=C1NNAA+h	7.96E11	0	4000
Per+a9a9-4=C1NNAA+h	7.96E11	0	4000
DBajF+n1n1-4=C1NNNA+h	9.29E11	0	4000
DBajF+n1n2-4=C1NNNA+h	9.29E11	0	4000
DBajF+n2n2-4=C1NNNA+h	9.29E11	0	4000
DBajF+a1n1-4=C1NNAA+h	9.29E11	0	4000
DBajF+a1n2-4=C1NNAA+h	9.29E11	0	4000
DBajF+a2n1-4=C1NNAA+h	9.29E11	0	4000
DBajF+a2n2-4=C1NNAA+h	9.29E11	0	4000
DBajF+a9n1-4=C1NNAA+h	9.29E11	0	4000
DBajF+a9n2-4=C1NNAA+h	9.29E11	0	4000
DBajF+a1a1-4=C1NAAA+h	9.29E11	0	4000
DBajF+a1a2-4=C1NAAA+h	9.29E11	0	4000
DBajF+a1a9-4=C1NAAA+h	9.29E11	0	4000
DBajF+a2a2-4=C1NAAA+h	9.29E11	0	4000
DBajF+a2a9-4=C1NAAA+h	9.29E11	0	4000
DBajF+a9a9-4=C1NAAA+h	9.29E11	0	4000
DBakF+n1n1-4=C1NNNA+h	9.29E11	0	4000
DBakF+n1n2-4=C1NNNA+h	9.29E11	0	4000
DBakF+n2n2-4=C1NNNA+h	9.29E11	0	4000
DBakF+a1n1-4=C1NNAA+h	9.29E11	0	4000
DBakF+a1n2-4=C1NNAA+h	9.29E11	0	4000
DBakF+a2n1-4=C1NNAA+h	9.29E11	0	4000
DBakF+a2n2-4=C1NNAA+h	9.29E11	0	4000
DBakF+a9n1-4=C1NNAA+h	9.29E11	0	4000
DBakF+a9n2-4=C1NNAA+h	9.29E11	0	4000
DBakF+a1a1-4=C1NAAA+h	9.29E11	0	4000
DBakF+a1a2-4=C1NAAA+h	9.29E11	0	4000
DBakF+a1a9-4=C1NAAA+h	9.29E11	0	4000
DBakF+a2a2-4=C1NAAA+h	9.29E11	0	4000

DBakF+a2a9-4=C1NAAA+h	9.29E11	0	4000
DBakF+a9a9-4=C1NAAA+h	9.29E11	0	4000
DBalF+n1n1-4=C1NNNA+h	7.96E11	0	4000
DBalF+n1n2-4=C1NNNA+h	7.96E11	0	4000
DBalF+n2n2-4=C1NNNA+h	7.96E11	0	4000
DBalF+a1n1-4=C1NNAA+h	7.96E11	0	4000
DBalF+a1n2-4=C1NNAA+h	7.96E11	0	4000
DBalF+a2n1-4=C1NNAA+h	7.96E11	0	4000
DBalF+a2n2-4=C1NNAA+h	7.96E11	0	4000
DBalF+a9n1-4=C1NNAA+h	7.96E11	0	4000
DBalF+a9n2-4=C1NNAA+h	7.96E11	0	4000
DBalF+a1a1-4=C1NAAA+h	7.96E11	0	4000
DBalF+a1a2-4=C1NAAA+h	7.96E11	0	4000
DBalF+a1a9-4=C1NAAA+h	7.96E11	0	4000
DBalF+a2a2-4=C1NAAA+h	7.96E11	0	4000
DBalF+a2a9-4=C1NAAA+h	7.96E11	0	4000
DBalF+a9a9-4=C1NAAA+h	7.96E11	0	4000
BaPer+n1n1-4=C1NNNA+h	7.96E11	0	4000
BaPer+n1n2-4=C1NNNA+h	7.96E11	0	4000
BaPer+n2n2-4=C1NNNA+h	7.96E11	0	4000
BaPer+a1n1-4=C1NNAA+h	7.96E11	0	4000
BaPer+a1n2-4=C1NNAA+h	7.96E11	0	4000
BaPer+a2n1-4=C1NNAA+h	7.96E11	0	4000
BaPer+a2n2-4=C1NNAA+h	7.96E11	0	4000
BaPer+a9n1-4=C1NNAA+h	7.96E11	0	4000
BaPer+a9n2-4=C1NNAA+h	7.96E11	0	4000
BaPer+a1a1-4=C1NAAA+h	7.96E11	0	4000
BaPer+a1a2-4=C1NAAA+h	7.96E11	0	4000
BaPer+a1a9-4=C1NAAA+h	7.96E11	0	4000
BaPer+a2a2-4=C1NAAA+h	7.96E11	0	4000
BaPer+a2a9-4=C1NAAA+h	7.96E11	0	4000
BaPer+a9a9-4=C1NAAA+h	7.96E11	0	4000
N23jF+n1n1-4=C1NNNA+h	9.29E11	0	4000
N23jF+n1n2-4=C1NNNA+h	9.29E11	0	4000
N23jF+n2n2-4=C1NNNA+h	9.29E11	0	4000
N23jF+a1n1-4=C1NNAA+h	9.29E11	0	4000
N23jF+a1n2-4=C1NNAA+h	9.29E11	0	4000
N23jF+a2n1-4=C1NNAA+h	9.29E11	0	4000
N23jF+a2n2-4=C1NNAA+h	9.29E11	0	4000
N23jF+a9n1-4=C1NNAA+h	9.29E11	0	4000
N23jF+a9n2-4=C1NNAA+h	9.29E11	0	4000
N23jF+a1a1-4=C1NAAA+h	9.29E11	0	4000
N23jF+a1a2-4=C1NAAA+h	9.29E11	0	4000
N23jF+a1a9-4=C1NAAA+h	9.29E11	0	4000
N23jF+a2a2-4=C1NAAA+h	9.29E11	0	4000
N23jF+a2a9-4=C1NAAA+h	9.29E11	0	4000
N23jF+a9a9-4=C1NAAA+h	9.29E11	0	4000
N23kF+n1n1-4=C1NNNA+h	9.29E11	0	4000
N23kF+n1n2-4=C1NNNA+h	9.29E11	0	4000
N23kF+n2n2-4=C1NNNA+h	9.29E11	0	4000
N23kF+a1n1-4=C1NNAA+h	9.29E11	0	4000
N23kF+a1n2-4=C1NNAA+h	9.29E11	0	4000
N23kF+a2n1-4=C1NNAA+h	9.29E11	0	4000
N23kF+a2n2-4=C1NNAA+h	9.29E11	0	4000
N23kF+a9n1-4=C1NNAA+h	9.29E11	0	4000
N23kF+a9n2-4=C1NNAA+h	9.29E11	0	4000
N23kF+a1a1-4=C1NAAA+h	9.29E11	0	4000
N23kF+a1a2-4=C1NAAA+h	9.29E11	0	4000
N23kF+a1a9-4=C1NAAA+h	9.29E11	0	4000
N23kF+a2a2-4=C1NAAA+h	9.29E11	0	4000

N23kF+a2a9-4=C1NAAA+h	9.29E11	0	4000
N23kF+a9a9-4=C1NAAA+h	9.29E11	0	4000
BaN23jF+n1n1-4=C1NNAA+h	1.06E12	0	4000
BaN23jF+n1n2-4=C1NNAA+h	1.06E12	0	4000
BaN23jF+n2n2-4=C1NNAA+h	1.06E12	0	4000
BaN23jF+a1n1-4=C1NAAA+h	1.06E12	0	4000
BaN23jF+a1n2-4=C1NAAA+h	1.06E12	0	4000
BaN23jF+a2n1-4=C1NAAA+h	1.06E12	0	4000
BaN23jF+a2n2-4=C1NAAA+h	1.06E12	0	4000
BaN23jF+a9n1-4=C1NAAA+h	1.06E12	0	4000
BaN23jF+a9n2-4=C1NAAA+h	1.06E12	0	4000
BaN23jF+a1a1-4=C1AAAA+h	1.06E12	0	4000
BaN23jF+a1a2-4=C1AAAA+h	1.06E12	0	4000
BaN23jF+a1a9-4=C1AAAA+h	1.06E12	0	4000
BaN23jF+a2a2-4=C1AAAA+h	1.06E12	0	4000
BaN23jF+a2a9-4=C1AAAA+h	1.06E12	0	4000
BaN23jF+a9a9-4=C1AAAA+h	1.06E12	0	4000
BaN23kF+n1n1-4=C1NNAA+h	1.06E12	0	4000
BaN23kF+n1n2-4=C1NNAA+h	1.06E12	0	4000
BaN23kF+n2n2-4=C1NNAA+h	1.06E12	0	4000
BaN23kF+a1n1-4=C1NAAA+h	1.06E12	0	4000
BaN23kF+a1n2-4=C1NAAA+h	1.06E12	0	4000
BaN23kF+a2n1-4=C1NAAA+h	1.06E12	0	4000
BaN23kF+a2n2-4=C1NAAA+h	1.06E12	0	4000
BaN23kF+a9n1-4=C1NAAA+h	1.06E12	0	4000
BaN23kF+a9n2-4=C1NAAA+h	1.06E12	0	4000
BaN23kF+a1a1-4=C1AAAA+h	1.06E12	0	4000
BaN23kF+a1a2-4=C1AAAA+h	1.06E12	0	4000
BaN23kF+a1a9-4=C1AAAA+h	1.06E12	0	4000
BaN23kF+a2a2-4=C1AAAA+h	1.06E12	0	4000
BaN23kF+a2a9-4=C1AAAA+h	1.06E12	0	4000
BaN23kF+a9a9-4=C1AAAA+h	1.06E12	0	4000
BaN23lF+n1n1-4=C1NNAA+h	9.29E11	0	4000
BaN23lF+n1n2-4=C1NNAA+h	9.29E11	0	4000
BaN23lF+n2n2-4=C1NNAA+h	9.29E11	0	4000
BaN23lF+a1n1-4=C1NAAA+h	9.29E11	0	4000
BaN23lF+a1n2-4=C1NAAA+h	9.29E11	0	4000
BaN23lF+a2n1-4=C1NAAA+h	9.29E11	0	4000
BaN23lF+a2n2-4=C1NAAA+h	9.29E11	0	4000
BaN23lF+a9n1-4=C1NAAA+h	9.29E11	0	4000
BaN23lF+a9n2-4=C1NAAA+h	9.29E11	0	4000
BaN23lF+a1a1-4=C1AAAA+h	9.29E11	0	4000
BaN23lF+a1a2-4=C1AAAA+h	9.29E11	0	4000
BaN23lF+a1a9-4=C1AAAA+h	9.29E11	0	4000
BaN23lF+a2a2-4=C1AAAA+h	9.29E11	0	4000
BaN23lF+a2a9-4=C1AAAA+h	9.29E11	0	4000
BaN23lF+a9a9-4=C1AAAA+h	9.29E11	0	4000
DBajPer+n1n1-4=C1NNAA+h	7.96E11	0	4000
DBajPer+n1n2-4=C1NNAA+h	7.96E11	0	4000
DBajPer+n2n2-4=C1NNAA+h	7.96E11	0	4000
DBajPer+a1n1-4=C1NAAA+h	7.96E11	0	4000
DBajPer+a1n2-4=C1NAAA+h	7.96E11	0	4000
DBajPer+a2n1-4=C1NAAA+h	7.96E11	0	4000
DBajPer+a2n2-4=C1NAAA+h	7.96E11	0	4000
DBajPer+a9n1-4=C1NAAA+h	7.96E11	0	4000
DBajPer+a9n2-4=C1NAAA+h	7.96E11	0	4000
DBajPer+a1a1-4=C1AAAA+h	7.96E11	0	4000
DBajPer+a1a2-4=C1AAAA+h	7.96E11	0	4000
DBajPer+a1a9-4=C1AAAA+h	7.96E11	0	4000
DBajPer+a2a2-4=C1AAAA+h	7.96E11	0	4000

DBajPer+a2a9-4=C1AAAA+h	7.96E11	0	4000
DBajPer+a9a9-4=C1AAAA+h	7.96E11	0	4000
DBaoPer+n1n1-4=C1NNAA+h	9.29E11	0	4000
DBaoPer+n1n2-4=C1NNAA+h	9.29E11	0	4000
DBaoPer+n2n2-4=C1NNAA+h	9.29E11	0	4000
DBaoPer+a1n1-4=C1NAAA+h	9.29E11	0	4000
DBaoPer+a1n2-4=C1NAAA+h	9.29E11	0	4000
DBaoPer+a2n1-4=C1NAAA+h	9.29E11	0	4000
DBaoPer+a2n2-4=C1NAAA+h	9.29E11	0	4000
DBaoPer+a9n1-4=C1NAAA+h	9.29E11	0	4000
DBaoPer+a9n2-4=C1NAAA+h	9.29E11	0	4000
DBaoPer+a1a1-4=C1AAAA+h	9.29E11	0	4000
DBaoPer+a1a2-4=C1AAAA+h	9.29E11	0	4000
DBaoPer+a1a9-4=C1AAAA+h	9.29E11	0	4000
DBaoPer+a2a2-4=C1AAAA+h	9.29E11	0	4000
DBaoPer+a2a9-4=C1AAAA+h	9.29E11	0	4000
DBaoPer+a9a9-4=C1AAAA+h	9.29E11	0	4000
BkF-+n1n1=C1NNNN+h	6.63E11	0	4000
BkF-+n1n2=C1NNNN+h	7.30E11	0	4000
BkF-+n2n2=C1NNNN+h	9.29E11	0	4000
BkF-+a1n1=C1NNNA+h	7.96E11	0	4000
BkF-+a1n2=C1NNNA+h	8.62E11	0	4000
BkF-+a2n1=C1NNNA+h	8.62E11	0	4000
BkF-+a2n2=C1NNNA+h	1.06E12	0	4000
BkF-+a9n1=C1NNNA+h	7.96E11	0	4000
BkF-+a9n2=C1NNNA+h	7.96E11	0	4000
BkF-+a1a1=C1NNAA+h	9.29E11	0	4000
BkF-+a1a2=C1NNAA+h	9.95E11	0	4000
BkF-+a1a9=C1NNAA+h	9.29E11	0	4000
BkF-+a2a2=C1NNAA+h	1.19E12	0	4000
BkF-+a2a9=C1NNAA+h	9.29E11	0	4000
BkF-+a9a9=C1NNAA+h	9.29E11	0	4000
BjF-+n1n1=C1NNNN+h	6.63E11	0	4000
BjF-+n1n2=C1NNNN+h	7.30E11	0	4000
BjF-+n2n2=C1NNNN+h	9.29E11	0	4000
BjF-+a1n1=C1NNNA+h	7.96E11	0	4000
BjF-+a1n2=C1NNNA+h	8.62E11	0	4000
BjF-+a2n1=C1NNNA+h	8.62E11	0	4000
BjF-+a2n2=C1NNNA+h	1.06E12	0	4000
BjF-+a9n1=C1NNNA+h	7.96E11	0	4000
BjF-+a9n2=C1NNNA+h	7.96E11	0	4000
BjF-+a1a1=C1NNAA+h	9.29E11	0	4000
BjF-+a1a2=C1NNAA+h	9.95E11	0	4000
BjF-+a1a9=C1NNAA+h	9.29E11	0	4000
BjF-+a2a2=C1NNAA+h	1.19E12	0	4000
BjF-+a2a9=C1NNAA+h	9.29E11	0	4000
BjF-+a9a9=C1NNAA+h	9.29E11	0	4000
Per-+n1n1=C1NNNN+h	6.63E11	0	4000
Per-+n1n2=C1NNNN+h	7.30E11	0	4000
Per-+n2n2=C1NNNN+h	9.29E11	0	4000
Per-+a1n1=C1NNNA+h	7.96E11	0	4000
Per-+a1n2=C1NNNA+h	8.62E11	0	4000
Per-+a2n1=C1NNNA+h	8.62E11	0	4000
Per-+a2n2=C1NNNA+h	1.06E12	0	4000
Per-+a9n1=C1NNNA+h	7.96E11	0	4000
Per-+a9n2=C1NNNA+h	7.96E11	0	4000
Per-+a1a1=C1NNAA+h	9.29E11	0	4000
Per-+a1a2=C1NNAA+h	9.95E11	0	4000
Per-+a1a9=C1NNAA+h	9.29E11	0	4000
Per-+a2a2=C1NNAA+h	1.19E12	0	4000

Per-+a2a9=C1NNAA+h	9.29E11	0	4000
Per-+a9a9=C1NNAA+h	9.29E11	0	4000
DBajF-+n1n1=C1NNNA+h	6.63E11	0	4000
DBajF-+n1n2=C1NNNA+h	7.30E11	0	4000
DBajF-+n2n2=C1NNNA+h	9.29E11	0	4000
DBajF-+a1n1=C1NNAA+h	7.96E11	0	4000
DBajF-+a1n2=C1NNAA+h	8.62E11	0	4000
DBajF-+a2n1=C1NNAA+h	8.62E11	0	4000
DBajF-+a2n2=C1NNAA+h	1.06E12	0	4000
DBajF-+a9n1=C1NNAA+h	7.96E11	0	4000
DBajF-+a9n2=C1NNAA+h	7.96E11	0	4000
DBajF-+a1a1=C1NAAA+h	9.29E11	0	4000
DBajF-+a1a2=C1NAAA+h	9.95E11	0	4000
DBajF-+a1a9=C1NAAA+h	9.29E11	0	4000
DBajF-+a2a2=C1NAAA+h	1.19E12	0	4000
DBajF-+a2a9=C1NAAA+h	9.29E11	0	4000
DBajF-+a9a9=C1NAAA+h	9.29E11	0	4000
DBakF-+n1n1=C1NNNA+h	6.63E11	0	4000
DBakF-+n1n2=C1NNNA+h	7.30E11	0	4000
DBakF-+n2n2=C1NNNA+h	9.29E11	0	4000
DBakF-+a1n1=C1NNAA+h	7.96E11	0	4000
DBakF-+a1n2=C1NNAA+h	8.62E11	0	4000
DBakF-+a2n1=C1NNAA+h	8.62E11	0	4000
DBakF-+a2n2=C1NNAA+h	1.06E12	0	4000
DBakF-+a9n1=C1NNAA+h	7.96E11	0	4000
DBakF-+a9n2=C1NNAA+h	7.96E11	0	4000
DBakF-+a1a1=C1NAAA+h	9.29E11	0	4000
DBakF-+a1a2=C1NAAA+h	9.95E11	0	4000
DBakF-+a1a9=C1NAAA+h	9.29E11	0	4000
DBakF-+a2a2=C1NAAA+h	1.19E12	0	4000
DBakF-+a2a9=C1NAAA+h	9.29E11	0	4000
DBakF-+a9a9=C1NAAA+h	9.29E11	0	4000
DBalF-+n1n1=C1NNNA+h	5.69E11	0	4000
DBalF-+n1n2=C1NNNA+h	6.25E11	0	4000
DBalF-+n2n2=C1NNNA+h	7.96E11	0	4000
DBalF-+a1n1=C1NNAA+h	6.82E11	0	4000
DBalF-+a1n2=C1NNAA+h	7.39E11	0	4000
DBalF-+a2n1=C1NNAA+h	7.39E11	0	4000
DBalF-+a2n2=C1NNAA+h	9.10E11	0	4000
DBalF-+a9n1=C1NNAA+h	6.82E11	0	4000
DBalF-+a9n2=C1NNAA+h	6.82E11	0	4000
DBalF-+a1a1=C1NAAA+h	7.96E11	0	4000
DBalF-+a1a2=C1NAAA+h	8.53E11	0	4000
DBalF-+a1a9=C1NAAA+h	7.96E11	0	4000
DBalF-+a2a2=C1NAAA+h	1.02E12	0	4000
DBalF-+a2a9=C1NAAA+h	7.96E11	0	4000
DBalF-+a9a9=C1NAAA+h	7.96E11	0	4000
BaPer-+n1n1=C1NNNA+h	5.69E11	0	4000
BaPer-+n1n2=C1NNNA+h	6.25E11	0	4000
BaPer-+n2n2=C1NNNA+h	7.96E11	0	4000
BaPer-+a1n1=C1NNAA+h	6.82E11	0	4000
BaPer-+a1n2=C1NNAA+h	7.39E11	0	4000
BaPer-+a2n1=C1NNAA+h	7.39E11	0	4000
BaPer-+a2n2=C1NNAA+h	9.10E11	0	4000
BaPer-+a9n1=C1NNAA+h	6.82E11	0	4000
BaPer-+a9n2=C1NNAA+h	6.82E11	0	4000
BaPer-+a1a1=C1NAAA+h	7.96E11	0	4000
BaPer-+a1a2=C1NAAA+h	8.53E11	0	4000
BaPer-+a1a9=C1NAAA+h	7.96E11	0	4000
BaPer-+a2a2=C1NAAA+h	1.02E12	0	4000

BaPer-+a2a9=C1NAAA+h	7.96E11	0	4000
BaPer-+a9a9=C1NAAA+h	7.96E11	0	4000
N23jF-+n1n1=C1NNNA+h	6.63E11	0	4000
N23jF-+n1n2=C1NNNA+h	7.30E11	0	4000
N23jF-+n2n2=C1NNNA+h	9.29E11	0	4000
N23jF-+a1n1=C1NNAA+h	7.96E11	0	4000
N23jF-+a1n2=C1NNAA+h	8.62E11	0	4000
N23jF-+a2n1=C1NNAA+h	8.62E11	0	4000
N23jF-+a2n2=C1NNAA+h	1.06E12	0	4000
N23jF-+a9n1=C1NNAA+h	7.96E11	0	4000
N23jF-+a9n2=C1NNAA+h	7.96E11	0	4000
N23jF-+a1a1=C1NAAA+h	9.29E11	0	4000
N23jF-+a1a2=C1NAAA+h	9.95E11	0	4000
N23jF-+a1a9=C1NAAA+h	9.29E11	0	4000
N23jF-+a2a2=C1NAAA+h	1.19E12	0	4000
N23jF-+a2a9=C1NAAA+h	9.29E11	0	4000
N23jF-+a9a9=C1NAAA+h	9.29E11	0	4000
N23kF-+n1n1=C1NNNA+h	6.63E11	0	4000
N23kF-+n1n2=C1NNNA+h	7.30E11	0	4000
N23kF-+n2n2=C1NNNA+h	9.29E11	0	4000
N23kF-+a1n1=C1NNAA+h	7.96E11	0	4000
N23kF-+a1n2=C1NNAA+h	8.62E11	0	4000
N23kF-+a2n1=C1NNAA+h	8.62E11	0	4000
N23kF-+a2n2=C1NNAA+h	1.06E12	0	4000
N23kF-+a9n1=C1NNAA+h	7.96E11	0	4000
N23kF-+a9n2=C1NNAA+h	7.96E11	0	4000
N23kF-+a1a1=C1NAAA+h	9.29E11	0	4000
N23kF-+a1a2=C1NAAA+h	9.95E11	0	4000
N23kF-+a1a9=C1NAAA+h	9.29E11	0	4000
N23kF-+a2a2=C1NAAA+h	1.19E12	0	4000
N23kF-+a2a9=C1NAAA+h	9.29E11	0	4000
N23kF-+a9a9=C1NAAA+h	9.29E11	0	4000
BaN23jF-+n1n1=C1NNAA+h	6.63E11	0	4000
BaN23jF-+n1n2=C1NNAA+h	7.30E11	0	4000
BaN23jF-+n2n2=C1NNAA+h	9.29E11	0	4000
BaN23jF-+a1n1=C1NAAA+h	7.96E11	0	4000
BaN23jF-+a1n2=C1NAAA+h	8.62E11	0	4000
BaN23jF-+a2n1=C1NAAA+h	8.62E11	0	4000
BaN23jF-+a2n2=C1NAAA+h	1.06E12	0	4000
BaN23jF-+a9n1=C1NAAA+h	7.96E11	0	4000
BaN23jF-+a9n2=C1NAAA+h	7.96E11	0	4000
BaN23jF-+a1a1=C1AAAA+h	9.29E11	0	4000
BaN23jF-+a1a2=C1AAAA+h	9.95E11	0	4000
BaN23jF-+a1a9=C1AAAA+h	9.29E11	0	4000
BaN23jF-+a2a2=C1AAAA+h	1.19E12	0	4000
BaN23jF-+a2a9=C1AAAA+h	9.29E11	0	4000
BaN23jF-+a9a9=C1AAAA+h	9.29E11	0	4000
BaN23kF-+n1n1=C1NNAA+h	6.63E11	0	4000
BaN23kF-+n1n2=C1NNAA+h	7.30E11	0	4000
BaN23kF-+n2n2=C1NNAA+h	9.29E11	0	4000
BaN23kF-+a1n1=C1NAAA+h	7.96E11	0	4000
BaN23kF-+a1n2=C1NAAA+h	8.62E11	0	4000
BaN23kF-+a2n1=C1NAAA+h	8.62E11	0	4000
BaN23kF-+a2n2=C1NAAA+h	1.06E12	0	4000
BaN23kF-+a9n1=C1NAAA+h	7.96E11	0	4000
BaN23kF-+a9n2=C1NAAA+h	7.96E11	0	4000
BaN23kF-+a1a1=C1AAAA+h	9.29E11	0	4000
BaN23kF-+a1a2=C1AAAA+h	9.95E11	0	4000
BaN23kF-+a1a9=C1AAAA+h	9.29E11	0	4000
BaN23kF-+a2a2=C1AAAA+h	1.19E12	0	4000

BaN23kF-+a2a9=C1AAAA+h	9.29E11	0	4000
BaN23kF-+a9a9=C1AAAA+h	9.29E11	0	4000
BaN23lF-+n1n1=C1NNAA+h	5.80E11	0	4000
BaN23lF-+n1n2=C1NNAA+h	6.38E11	0	4000
BaN23lF-+n2n2=C1NNAA+h	8.13E11	0	4000
BaN23lF-+a1n1=C1NAAA+h	6.97E11	0	4000
BaN23lF-+a1n2=C1NAAA+h	7.55E11	0	4000
BaN23lF-+a2n1=C1NAAA+h	7.55E11	0	4000
BaN23lF-+a2n2=C1NAAA+h	9.29E11	0	4000
BaN23lF-+a9n1=C1NAAA+h	6.97E11	0	4000
BaN23lF-+a9n2=C1NAAA+h	6.97E11	0	4000
BaN23lF-+a1a1=C1AAAA+h	8.13E11	0	4000
BaN23lF-+a1a2=C1AAAA+h	8.71E11	0	4000
BaN23lF-+a1a9=C1AAAA+h	8.13E11	0	4000
BaN23lF-+a2a2=C1AAAA+h	1.04E12	0	4000
BaN23lF-+a2a9=C1AAAA+h	8.13E11	0	4000
BaN23lF-+a9a9=C1AAAA+h	8.13E11	0	4000
DBajPer-+n1n1=C1NNAA+h	4.98E11	0	4000
DBajPer-+n1n2=C1NNAA+h	5.47E11	0	4000
DBajPer-+n2n2=C1NNAA+h	6.97E11	0	4000
DBajPer-+a1n1=C1NAAA+h	5.97E11	0	4000
DBajPer-+a1n2=C1NAAA+h	6.47E11	0	4000
DBajPer-+a2n1=C1NAAA+h	6.47E11	0	4000
DBajPer-+a2n2=C1NAAA+h	7.96E11	0	4000
DBajPer-+a9n1=C1NAAA+h	5.97E11	0	4000
DBajPer-+a9n2=C1NAAA+h	5.97E11	0	4000
DBajPer-+a1a1=C1AAAA+h	6.97E11	0	4000
DBajPer-+a1a2=C1AAAA+h	7.46E11	0	4000
DBajPer-+a1a9=C1AAAA+h	6.97E11	0	4000
DBajPer-+a2a2=C1AAAA+h	8.96E11	0	4000
DBajPer-+a2a9=C1AAAA+h	6.97E11	0	4000
DBajPer-+a9a9=C1AAAA+h	6.97E11	0	4000
DBaoPer-+n1n1=C1NNAA+h	5.80E11	0	4000
DBaoPer-+n1n2=C1NNAA+h	6.38E11	0	4000
DBaoPer-+n2n2=C1NNAA+h	8.13E11	0	4000
DBaoPer-+a1n1=C1NAAA+h	6.97E11	0	4000
DBaoPer-+a1n2=C1NAAA+h	7.55E11	0	4000
DBaoPer-+a2n1=C1NAAA+h	7.55E11	0	4000
DBaoPer-+a2n2=C1NAAA+h	9.29E11	0	4000
DBaoPer-+a9n1=C1NAAA+h	6.97E11	0	4000
DBaoPer-+a9n2=C1NAAA+h	6.97E11	0	4000
DBaoPer-+a1a1=C1AAAA+h	8.13E11	0	4000
DBaoPer-+a1a2=C1AAAA+h	8.71E11	0	4000
DBaoPer-+a1a9=C1AAAA+h	8.13E11	0	4000
DBaoPer-+a2a2=C1AAAA+h	1.04E12	0	4000
DBaoPer-+a2a9=C1AAAA+h	8.13E11	0	4000
DBaoPer-+a9a9=C1AAAA+h	8.13E11	0	4000
BkF+BkF-=C2NNNN+h	7.96E11	0	4000
BkF+BjF-=C2NNNN+h	7.96E11	0	4000
BkF+Per-=C2NNNN+h	7.96E11	0	4000
BkF+DBajF-=C2NNNA+h	7.96E11	0	4000
BkF+DBakF-=C2NNNA+h	7.96E11	0	4000
BkF+DBalF-=C2NNNA+h	6.82E11	0	4000
BkF+BaPer-=C2NNNA+h	6.82E11	0	4000
BkF+N23jF-=C2NNNA+h	7.96E11	0	4000
BkF+N23kF-=C2NNNA+h	7.96E11	0	4000
BkF+BaN23jF-=C2NNAA+h	7.96E11	0	4000
BkF+BaN23kF-=C2NNAA+h	7.96E11	0	4000
BkF+BaN23lF-=C2NNAA+h	6.97E11	0	4000
BkF+DBajPer-=C2NNAA+h	5.97E11	0	4000

BkF+DBaoPer-=C2NNAA+h	6.97E11	0	4000
BjF+BkF-=C2NNNN+h	7.96E11	0	4000
BjF+BjF-=C2NNNN+h	7.96E11	0	4000
BjF+Per-=C2NNNN+h	7.96E11	0	4000
BjF+DBajF-=C2NNNA+h	7.96E11	0	4000
BjF+DBakF-=C2NNNA+h	7.96E11	0	4000
BjF+DBalF-=C2NNNA+h	6.82E11	0	4000
BjF+BaPer-=C2NNNA+h	6.82E11	0	4000
BjF+N23jF-=C2NNNA+h	7.96E11	0	4000
BjF+N23kF-=C2NNNA+h	7.96E11	0	4000
BjF+BaN23jF-=C2NNAA+h	7.96E11	0	4000
BjF+BaN23kF-=C2NNAA+h	7.96E11	0	4000
BjF+BaN23lF-=C2NNAA+h	6.97E11	0	4000
BjF+DBajPer-=C2NNAA+h	5.97E11	0	4000
BjF+DBaoPer-=C2NNAA+h	6.97E11	0	4000
Per+BkF-=C2NNNN+h	7.96E11	0	4000
Per+BjF-=C2NNNN+h	7.96E11	0	4000
Per+Per-=C2NNNN+h	7.96E11	0	4000
Per+DBajF-=C2NNNA+h	7.96E11	0	4000
Per+DBakF-=C2NNNA+h	7.96E11	0	4000
Per+DBalF-=C2NNNA+h	6.82E11	0	4000
Per+BaPer-=C2NNNA+h	6.82E11	0	4000
Per+N23jF-=C2NNNA+h	7.96E11	0	4000
Per+N23kF-=C2NNNA+h	7.96E11	0	4000
Per+BaN23jF-=C2NNAA+h	7.96E11	0	4000
Per+BaN23kF-=C2NNAA+h	7.96E11	0	4000
Per+BaN23lF-=C2NNAA+h	6.97E11	0	4000
Per+DBajPer-=C2NNAA+h	5.97E11	0	4000
Per+DBaoPer-=C2NNAA+h	6.97E11	0	4000
DBajF+BkF-=C2NNNA+h	9.29E11	0	4000
DBajF+BjF-=C2NNNA+h	9.29E11	0	4000
DBajF+Per-=C2NNNA+h	9.29E11	0	4000
DBajF+DBajF-=C2NNAA+h	9.29E11	0	4000
DBajF+DBakF-=C2NNAA+h	9.29E11	0	4000
DBajF+DBalF-=C2NNAA+h	7.96E11	0	4000
DBajF+BaPer-=C2NNAA+h	7.96E11	0	4000
DBajF+N23jF-=C2NNAA+h	9.29E11	0	4000
DBajF+N23kF-=C2NNAA+h	9.29E11	0	4000
DBajF+BaN23jF-=C2NAAA+h	9.29E11	0	4000
DBajF+BaN23kF-=C2NAAA+h	9.29E11	0	4000
DBajF+BaN23lF-=C2NAAA+h	8.13E11	0	4000
DBajF+DBajPer-=C2NAAA+h	6.97E11	0	4000
DBajF+DBaoPer-=C2NAAA+h	8.13E11	0	4000
DBakF+BkF-=C2NNNA+h	9.29E11	0	4000
DBakF+BjF-=C2NNNA+h	9.29E11	0	4000
DBakF+Per-=C2NNNA+h	9.29E11	0	4000
DBakF+DBajF-=C2NNAA+h	9.29E11	0	4000
DBakF+DBakF-=C2NNAA+h	9.29E11	0	4000
DBakF+DBalF-=C2NNAA+h	7.96E11	0	4000
DBakF+BaPer-=C2NNAA+h	7.96E11	0	4000
DBakF+N23jF-=C2NNAA+h	9.29E11	0	4000
DBakF+N23kF-=C2NNAA+h	9.29E11	0	4000
DBakF+BaN23jF-=C2NAAA+h	9.29E11	0	4000
DBakF+BaN23kF-=C2NAAA+h	9.29E11	0	4000
DBakF+BaN23lF-=C2NAAA+h	8.13E11	0	4000
DBakF+DBajPer-=C2NAAA+h	6.97E11	0	4000
DBakF+DBaoPer-=C2NAAA+h	8.13E11	0	4000
DBalF+BkF-=C2NNNA+h	7.96E11	0	4000
DBalF+BjF-=C2NNNA+h	7.96E11	0	4000
DBalF+Per-=C2NNNA+h	7.96E11	0	4000

DBalF+DBajF-=C2NNAA+h	7.96E11	0	4000
DBalF+DBakF-=C2NNAA+h	7.96E11	0	4000
DBalF+DBalF-=C2NNAA+h	6.82E11	0	4000
DBalF+BaPer-=C2NNAA+h	6.82E11	0	4000
DBalF+N23jF-=C2NNAA+h	7.96E11	0	4000
DBalF+N23kF-=C2NNAA+h	7.96E11	0	4000
DBalF+BaN23jF-=C2NAAA+h	7.96E11	0	4000
DBalF+BaN23kF-=C2NAAA+h	7.96E11	0	4000
DBalF+BaN23lF-=C2NAAA+h	6.97E11	0	4000
DBalF+DBajPer-=C2NAAA+h	5.97E11	0	4000
DBalF+DBaoPer-=C2NAAA+h	6.97E11	0	4000
BaPer+BkF-=C2NNNA+h	7.96E11	0	4000
BaPer+BjF-=C2NNNA+h	7.96E11	0	4000
BaPer+Per-=C2NNNA+h	7.96E11	0	4000
BaPer+DBajF-=C2NNAA+h	7.96E11	0	4000
BaPer+DBakF-=C2NNAA+h	7.96E11	0	4000
BaPer+DBalF-=C2NNAA+h	6.82E11	0	4000
BaPer+BaPer-=C2NNAA+h	6.82E11	0	4000
BaPer+N23jF-=C2NNAA+h	7.96E11	0	4000
BaPer+N23kF-=C2NNAA+h	7.96E11	0	4000
BaPer+BaN23jF-=C2NAAA+h	7.96E11	0	4000
BaPer+BaN23kF-=C2NAAA+h	7.96E11	0	4000
BaPer+BaN23lF-=C2NAAA+h	6.97E11	0	4000
BaPer+DBajPer-=C2NAAA+h	5.97E11	0	4000
BaPer+DBaoPer-=C2NAAA+h	6.97E11	0	4000
N23jF+BkF-=C2NNNA+h	9.29E11	0	4000
N23jF+BjF-=C2NNNA+h	9.29E11	0	4000
N23jF+Per-=C2NNNA+h	9.29E11	0	4000
N23jF+DBajF-=C2NNAA+h	9.29E11	0	4000
N23jF+DBakF-=C2NNAA+h	9.29E11	0	4000
N23jF+DBalF-=C2NNAA+h	7.96E11	0	4000
N23jF+BaPer-=C2NNAA+h	7.96E11	0	4000
N23jF+N23jF-=C2NNAA+h	9.29E11	0	4000
N23jF+N23kF-=C2NNAA+h	9.29E11	0	4000
N23jF+BaN23jF-=C2NAAA+h	9.29E11	0	4000
N23jF+BaN23kF-=C2NAAA+h	9.29E11	0	4000
N23jF+BaN23lF-=C2NAAA+h	8.13E11	0	4000
N23jF+DBajPer-=C2NAAA+h	6.97E11	0	4000
N23jF+DBaoPer-=C2NAAA+h	8.13E11	0	4000
N23kF+BkF-=C2NNNA+h	9.29E11	0	4000
N23kF+BjF-=C2NNNA+h	9.29E11	0	4000
N23kF+Per-=C2NNNA+h	9.29E11	0	4000
N23kF+DBajF-=C2NNAA+h	9.29E11	0	4000
N23kF+DBakF-=C2NNAA+h	9.29E11	0	4000
N23kF+DBalF-=C2NNAA+h	7.96E11	0	4000
N23kF+BaPer-=C2NNAA+h	7.96E11	0	4000
N23kF+N23jF-=C2NNAA+h	9.29E11	0	4000
N23kF+N23kF-=C2NNAA+h	9.29E11	0	4000
N23kF+BaN23jF-=C2NAAA+h	9.29E11	0	4000
N23kF+BaN23kF-=C2NAAA+h	9.29E11	0	4000
N23kF+BaN23lF-=C2NAAA+h	8.13E11	0	4000
N23kF+DBajPer-=C2NAAA+h	6.97E11	0	4000
N23kF+DBaoPer-=C2NAAA+h	8.13E11	0	4000
BaN23jF+BkF-=C2NNAA+h	1.06E12	0	4000
BaN23jF+BjF-=C2NNAA+h	1.06E12	0	4000
BaN23jF+Per-=C2NNAA+h	1.06E12	0	4000
BaN23jF+DBajF-=C2NAAA+h	1.06E12	0	4000
BaN23jF+DBakF-=C2NAAA+h	1.06E12	0	4000
BaN23jF+DBalF-=C2NAAA+h	9.10E11	0	4000
BaN23jF+BaPer-=C2NAAA+h	9.10E11	0	4000

BaN23jF+N23jF-=C2NAAA+h	1.06E12	0	4000
BaN23jF+N23kF-=C2NAAA+h	1.06E12	0	4000
BaN23jF+BaN23jF-=C2AAAA+h	1.06E12	0	4000
BaN23jF+BaN23kF-=C2AAAA+h	1.06E12	0	4000
BaN23jF+BaN23lF-=C2AAAA+h	9.29E11	0	4000
BaN23jF+DBajPer-=C2AAAA+h	7.96E11	0	4000
BaN23jF+DBaoPer-=C2AAAA+h	9.29E11	0	4000
BaN23kF+BkF-=C2NNAA+h	1.06E12	0	4000
BaN23kF+BjF-=C2NNAA+h	1.06E12	0	4000
BaN23kF+Per-=C2NNAA+h	1.06E12	0	4000
BaN23kF+DBajF-=C2NAAA+h	1.06E12	0	4000
BaN23kF+DBakF-=C2NAAA+h	1.06E12	0	4000
BaN23kF+DBalF-=C2NAAA+h	9.10E11	0	4000
BaN23kF+BaPer-=C2NAAA+h	9.10E11	0	4000
BaN23kF+N23jF-=C2NAAA+h	1.06E12	0	4000
BaN23kF+N23kF-=C2NAAA+h	1.06E12	0	4000
BaN23kF+BaN23jF-=C2AAAA+h	1.06E12	0	4000
BaN23kF+BaN23kF-=C2AAAA+h	1.06E12	0	4000
BaN23kF+BaN23lF-=C2AAAA+h	9.29E11	0	4000
BaN23kF+DBajPer-=C2AAAA+h	7.96E11	0	4000
BaN23kF+DBaoPer-=C2AAAA+h	9.29E11	0	4000
BaN23lF+BkF-=C2NNAA+h	9.29E11	0	4000
BaN23lF+BjF-=C2NNAA+h	9.29E11	0	4000
BaN23lF+Per-=C2NNAA+h	9.29E11	0	4000
BaN23lF+DBajF-=C2NAAA+h	9.29E11	0	4000
BaN23lF+DBakF-=C2NAAA+h	9.29E11	0	4000
BaN23lF+DBalF-=C2NAAA+h	7.96E11	0	4000
BaN23lF+BaPer-=C2NAAA+h	7.96E11	0	4000
BaN23lF+N23jF-=C2NAAA+h	9.29E11	0	4000
BaN23lF+N23kF-=C2NAAA+h	9.29E11	0	4000
BaN23lF+BaN23jF-=C2AAAA+h	9.29E11	0	4000
BaN23lF+BaN23kF-=C2AAAA+h	9.29E11	0	4000
BaN23lF+BaN23lF-=C2AAAA+h	8.13E11	0	4000
BaN23lF+DBajPer-=C2AAAA+h	6.97E11	0	4000
BaN23lF+DBaoPer-=C2AAAA+h	8.13E11	0	4000
DBajPer+BkF-=C2NNAA+h	7.96E11	0	4000
DBajPer+BjF-=C2NNAA+h	7.96E11	0	4000
DBajPer+Per-=C2NNAA+h	7.96E11	0	4000
DBajPer+DBajF-=C2NAAA+h	7.96E11	0	4000
DBajPer+DBakF-=C2NAAA+h	7.96E11	0	4000
DBajPer+DBalF-=C2NAAA+h	6.82E11	0	4000
DBajPer+BaPer-=C2NAAA+h	6.82E11	0	4000
DBajPer+N23jF-=C2NAAA+h	7.96E11	0	4000
DBajPer+N23kF-=C2NAAA+h	7.96E11	0	4000
DBajPer+BaN23jF-=C2AAAA+h	7.96E11	0	4000
DBajPer+BaN23kF-=C2AAAA+h	7.96E11	0	4000
DBajPer+BaN23lF-=C2AAAA+h	6.97E11	0	4000
DBajPer+DBajPer-=C2AAAA+h	5.97E11	0	4000
DBajPer+DBaoPer-=C2AAAA+h	6.97E11	0	4000
DBaoPer+BkF-=C2NNAA+h	9.29E11	0	4000
DBaoPer+BjF-=C2NNAA+h	9.29E11	0	4000
DBaoPer+Per-=C2NNAA+h	9.29E11	0	4000
DBaoPer+DBajF-=C2NAAA+h	9.29E11	0	4000
DBaoPer+DBakF-=C2NAAA+h	9.29E11	0	4000
DBaoPer+DBalF-=C2NAAA+h	7.96E11	0	4000
DBaoPer+BaPer-=C2NAAA+h	7.96E11	0	4000
DBaoPer+N23jF-=C2NAAA+h	9.29E11	0	4000
DBaoPer+N23kF-=C2NAAA+h	9.29E11	0	4000
DBaoPer+BaN23jF-=C2AAAA+h	9.29E11	0	4000
DBaoPer+BaN23kF-=C2AAAA+h	9.29E11	0	4000

DBaoPer+BaN23lF-=C2AAAA+h	8.13E11	0	4000
DBaoPer+DBajPer-=C2AAAA+h	6.97E11	0	4000
DBaoPer+DBaoPer-=C2AAAA+h	8.13E11	0	4000
BkF+NNN-=C1NNNNN+h	5.57E11	0	4000
BjF+NNN-=C1NNNNN+h	5.57E11	0	4000
Per+NNN-=C1NNNNN+h	5.57E11	0	4000
BkF-+NNN=C1NNNNN+h	9.29E11	0	4000
BjF-+NNN=C1NNNNN+h	9.29E11	0	4000
Per-+NNN=C1NNNNN+h	9.29E11	0	4000
C1NNN+n1-=C1NNNN+h	9.95E11	0	4000
C1NNN+n2-=C1NNNN+h	9.95E11	0	4000
C1NNN+a1-=C1NNNA+h	9.95E11	0	4000
C1NNN+a2-=C1NNNA+h	9.95E11	0	4000
C1NNN+a9-=C1NNNA+h	9.95E11	0	4000
C1NNN-+n=C1NNNN+h	4.42E11	0	4000
C1NNN-+a=C1NNNA+h	5.53E11	0	4000
C1NNA+n1-=C1NNNA+h	1.06E12	0	4000
C1NNA+n2-=C1NNNA+h	1.06E12	0	4000
C1NNA+a1-=C1NNAA+h	1.06E12	0	4000
C1NNA+a2-=C1NNAA+h	1.06E12	0	4000
C1NNA+a9-=C1NNAA+h	1.06E12	0	4000
C1NNA-+n=C1NNNA+h	4.25E11	0	4000
C1NNA-+a=C1NNAA+h	5.31E11	0	4000
C1NAA+n1-=C1NNAA+h	1.13E12	0	4000
C1NAA+n2-=C1NNAA+h	1.13E12	0	4000
C1NAA+a1-=C1NAAA+h	1.13E12	0	4000
C1NAA+a2-=C1NAAA+h	1.13E12	0	4000
C1NAA+a9-=C1NAAA+h	1.13E12	0	4000
C1NAA-+n=C1NNAA+h	4.10E11	0	4000
C1NAA-+a=C1NAAA+h	5.13E11	0	4000
C1AAA+n1-=C1NAAA+h	1.19E12	0	4000
C1AAA+n2-=C1NAAA+h	1.19E12	0	4000
C1AAA+a1-=C1AAAA+h	1.19E12	0	4000
C1AAA+a2-=C1AAAA+h	1.19E12	0	4000
C1AAA+a9-=C1AAAA+h	1.19E12	0	4000
C1AAA-+n=C1NAAA+h	3.98E11	0	4000
C1AAA-+a=C1AAAA+h	4.42E11	0	4000
C2NNN+n1-=C2NNNN+h	1.06E12	0	4000
C2NNN+n2-=C2NNNN+h	1.06E12	0	4000
C2NNN+a1-=C2NNNA+h	1.06E12	0	4000
C2NNN+a2-=C2NNNA+h	1.06E12	0	4000
C2NNN+a9-=C2NNNA+h	1.06E12	0	4000
C2NNN-+n=C2NNNN+h	5.31E11	0	4000
C2NNN-+a=C2NNNA+h	6.63E11	0	4000
C2NNA+n1-=C2NNNA+h	1.13E12	0	4000
C2NNA+n2-=C2NNNA+h	1.13E12	0	4000
C2NNA+a1-=C2NNAA+h	1.13E12	0	4000
C2NNA+a2-=C2NNAA+h	1.13E12	0	4000
C2NNA+a9-=C2NNAA+h	1.13E12	0	4000
C2NNA-+n=C2NNNA+h	5.01E11	0	4000
C2NNA-+a=C2NNAA+h	6.26E11	0	4000
C2NAA+n1-=C2NNAA+h	1.19E12	0	4000
C2NAA+n2-=C2NNAA+h	1.19E12	0	4000
C2NAA+a1-=C2NAAA+h	1.19E12	0	4000
C2NAA+a2-=C2NAAA+h	1.19E12	0	4000
C2NAA+a9-=C2NAAA+h	1.19E12	0	4000
C2NAA-+n=C2NNAA+h	4.78E11	0	4000
C2NAA-+a=C2NAAA+h	5.97E11	0	4000
C2AAA+n1-=C2NAAA+h	1.26E12	0	4000
C2AAA+n2-=C2NAAA+h	1.26E12	0	4000

C2AAA+a1-=C2AAAA+h	1.26E12	0	4000
C2AAA+a2-=C2AAAA+h	1.26E12	0	4000
C2AAA+a9-=C2AAAA+h	1.26E12	0	4000
C2AAA-+n=C2NAAA+h	4.58E11	0	4000
C2AAA-+a=C2AAAA+h	5.73E11	0	4000
C1NNN+n1n1-4=C1NNNNN+h	9.95E11	0	4000
C1NNN+n1n2-4=C1NNNNN+h	9.95E11	0	4000
C1NNN+n2n2-4=C1NNNNN+h	9.95E11	0	4000
C1NNN-+n1n1=C1NNNNN+h	5.53E11	0	4000
C1NNN-+n1n2=C1NNNNN+h	6.08E11	0	4000
C1NNN-+n2n2=C1NNNNN+h	7.74E11	0	4000
C1NNN+BjF-=C2NNNNN+h	9.95E11	0	4000
C1NNN+BkF-=C2NNNNN+h	9.95E11	0	4000
C1NNN+Per-=C2NNNNN+h	9.95E11	0	4000
C1NNN-+BjF=C2NNNNN+h	6.63E11	0	4000
C1NNN-+BkF=C2NNNNN+h	6.63E11	0	4000
C1NNN-+Per=C2NNNNN+h	6.63E11	0	4000
C2NNN+n1n1-4=C2NNNNN+h	1.06E12	0	4000
C2NNN+n1n2-4=C2NNNNN+h	1.06E12	0	4000
C2NNN+n2n2-4=C2NNNNN+h	1.06E12	0	4000
C2NNN-+n1n1=C2NNNNN+h	6.63E11	0	4000
C2NNN-+n1n2=C2NNNNN+h	7.30E11	0	4000
C2NNN-+n2n2=C2NNNNN+h	9.29E11	0	4000
C2NNN+BjF-=C3NNNNN+h	1.06E12	0	4000
C2NNN+BkF-=C3NNNNN+h	1.06E12	0	4000
C2NNN+Per-=C3NNNNN+h	1.06E12	0	4000
C2NNN-+BjF=C3NNNNN+h	7.96E11	0	4000
C2NNN-+BkF=C3NNNNN+h	7.96E11	0	4000
C2NNN-+Per=C3NNNNN+h	7.96E11	0	4000
C1NNNN+n1-=C1NNNNN+h	1.19E12	0	4000
C1NNNN+n2-=C1NNNNN+h	1.19E12	0	4000
C1NNNN-+n=C1NNNNN+h	3.98E11	0	4000
C2NNNN+n1-=C2NNNNN+h	1.26E12	0	4000
C2NNNN+n2-=C2NNNNN+h	1.26E12	0	4000
C2NNNN-+n=C2NNNNN+h	4.58E11	0	4000
C3NNNN+n1-=C3NNNNN+h	1.33E12	0	4000
C3NNNN+n2-=C3NNNNN+h	1.33E12	0	4000
C3NNNN-+n=C3NNNNN+h	5.31E11	0	4000

Reaction Type 5 (condensation) $4E13e^{-10/RT}$ (Pope, 1993)

n1n1-1=Per+h	4.00E13	0	10000
n1n1-1=BjF+h	4.00E13	0	10000
n1n1-2=BjF+h	4.00E13	0	10000
n1n2-1=BjF+h	2.00E13	0	10000
n1n2-1=BkF+h	2.00E13	0	10000
n1n2-2=BkF+h	4.00E13	0	10000
a1n1-1=N23jF+h	4.00E13	0	10000
a1n1-1=BaPer+h	4.00E13	0	10000
a1n1-2=N23jF+h	2.00E13	0	10000
a1n1-2=DBajF+h	2.00E13	0	10000
a1n1-3=BaPer+h	4.00E13	0	10000
a1n1-3=DBajF+h	4.00E13	0	10000
a1n2-1=DBalF+h	4.00E13	0	10000
a1n2-2=DBakF+h	4.00E13	0	10000
a1n2-3=DBakF+h	2.00E13	0	10000
a1n2-3=DBalF+h	2.00E13	0	10000
a2n1-1=N23jF+h	4.00E13	0	10000
a2n1-1=N23kF+h	2.00E13	0	10000
a2n1-2=N23kF+h	4.00E13	0	10000

```
    a9n1-1=BaPer+h                  5.33E13     0     10000
    a9n1-1=DBalF+h                  2.67E13     0     10000
    a9n1-2=DBalF+h                  8.00E13     0     10000
    a9n2-1=DBajF+h                  5.33E13     0     10000
    a9n2-1=DBakF+h                  2.67E13     0     10000
    a9n2-2=DBakF+h                  8.00E13     0     10000
    a1a1-2=BaN23jF+h                4.00E13     0     10000
    a1a1-3=BaN23jF+h                4.00E13     0     10000
    a1a1-3=DBaoPer+h                4.00E13     0     10000
    a1a2-1=BaN23lF+h                4.00E13     0     10000
    a1a2-2=BaN23kF+h                4.00E13     0     10000
    a1a2-3=BaN23kF+h                4.00E13     0     10000
    a1a2-3=BaN23lF+h                4.00E13     0     10000
    a1a9-1=DBajPer+h                4.00E13     0     10000
    a1a9-1=BaN23lF+h                4.00E13     0     10000
    a1a9-2=BaN23lF+h                8.00E13     0     10000
    a1a9-3=DBajPer+h                8.00E13     0     10000
    a2a9-1=BaN23jF+h                5.33E13     0     10000
    a2a9-1=BaN23kF+h                2.67E13     0     10000
    a2a9-2=BaN23kF+h                8.00E13     0     10000
    a9a9-1=DBaoPer+h                8.00E13     0     10000
    NNN-=C1NNN+h                    1.80E13     0     10000
    NNA-=C1NNA+h                    1.64E13     0     10000
    NAA-=C1NAA+h                    1.50E13     0     10000
    AAA-=C1AAA+h                    1.38E13     0     10000
    C1NNN-=C2NNN+h                  1.00E13     0     10000
    C1NNA-=C2NNA+h                  1.20E13     0     10000
    C1NAA-=C2NAA+h                  1.36E13     0     10000
    C1AAA-=C2AAA+h                  1.50E13     0     10000
    NNNN-=C1NNNN+h                  2.08E13     0     10000
    NNNA-=C1NNNA+h                  1.93E13     0     10000
    NNAA-=C1NNAA+h                  1.80E13     0     10000
    NAAA-=C1NAAA+h                  1.69E13     0     10000
    AAAA-=C1AAAA+h                  1.59E13     0     10000
    C1NNNN-=C2NNNN+h                1.50E13     0     10000
    C1NNNA-=C2NNNA+h                1.62E13     0     10000
    C1NNAA-=C2NNAA+h                1.71E13     0     10000
    C1NAAA-=C2NAAA+h                1.80E13     0     10000
    C1AAAA-=C2AAAA+h                1.88E13     0     10000
    C2NNNN-=C3NNNN+h                8.18E12     0     10000
    C2NNNA-=C3NNNA+h                1.00E13     0     10000
    C2NNAA-=C3NNAA+h                1.15E13     0     10000
    C2NAAA-=C3NAAA+h                1.29E13     0     10000
    C2AAAA-=C3AAAA+h                1.40E13     0     10000
    NNNNN-=C1NNNNN+h                2.25E13     0     10000
    C1NNNNN-=C2NNNNN+h              1.80E13     0     10000
    C2NNNNN-=C3NNNNN+h              1.29E13     0     10000
    C3NNNNN-=C4NNNNN+h              6.92E12     0     10000
END
```

Appendix D: Relevant Compounds

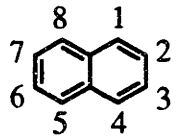

naphthalene (n)

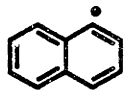

1-naphthyl (n1-)

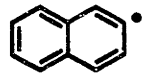

2-naphthyl (n2-)

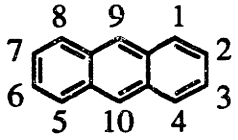

anthracene (a)

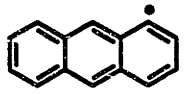

1-anthryl (a1-)

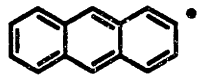

2-anthryl (a2-)

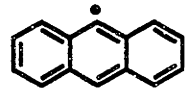

9-anthryl (a9-)

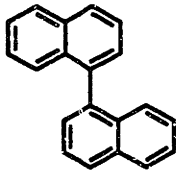

1,1'-binaphthalene
(11NN, n1n1)

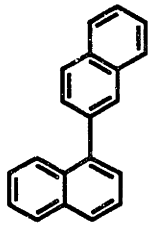

1,2'-binaphthalene
(12NN, n1n2)

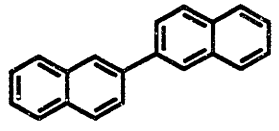

2,2'-binaphthalene
(22NN, n2n2)

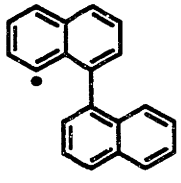

condensible type 1-yl monoradical (all sites shown) of 1,1'-binaphthalene (n1n1-1)

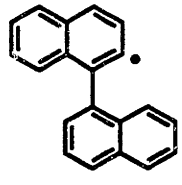

condensible type 2-yl monoradical (all sites shown) of 1,1'-binaphthalene (n1n1-2)

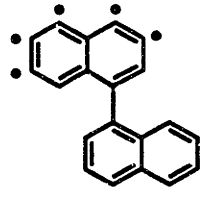

noncondensible monoradical (all sites shown) of 1,1'-binaphthalene (n1n1-4)

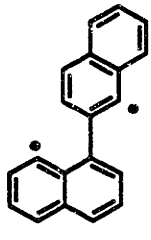

condensible type 1-yl monoradical (all sites shown) of 1,2'-binaphthalene (n1n2-1)

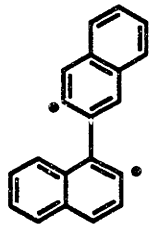

condensible type 2-yl monoradical (all sites shown) of 1,2'-binaphthalene (n1n2-2)

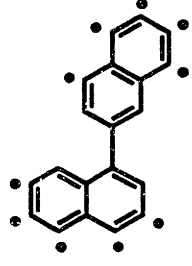

noncondensible monoradical (all sites shown) of 1,2'-binaphthalene (n1n2-4)

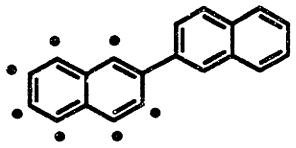

noncondensible monoradical (all sites shown) of 2,2'-binaphthalene (n2n2-4)

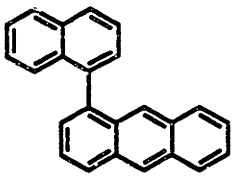

1-(1'-naphthyl) anthracene (11NA, a1n1)

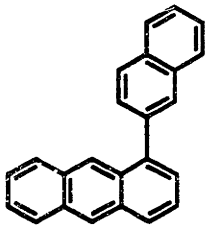

1-(2'-naphthyl) anthracene (12NA, a1n2)

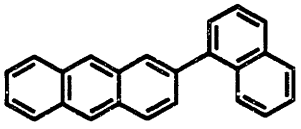

2-(1'-naphthyl) anthracene (21NA, a2n1)

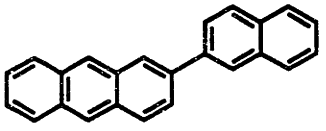

2-(2'-naphthyl) anthracene (22NA, a2n2)

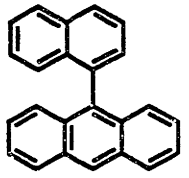

9-(1'-naphthyl) anthracene (91NA, a9n1)

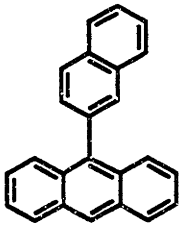

9-(2'-naphthyl) anthracene (92NA, a9n2)

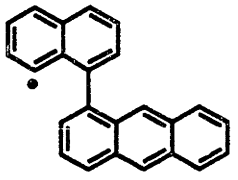

condensible 1-yl monoradical (all sites shown) of 1-(1'-naphthyl) anthracene (a1n1-1)

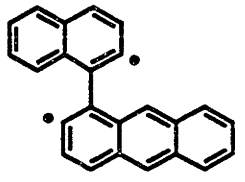

condensible 2-yl monoradical (all sites shown) of 1-(1'-naphthyl) anthracene (a1n1-2)

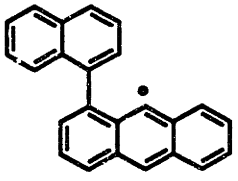

condensible 9-yl monoradical (all sites shown) of 1-(1'-naphthyl) anthracene (a1n1-3)

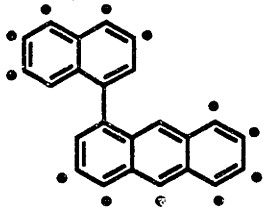

noncondensible monoradical (all sites shown) of 1-(1'-naphthyl) anthracene (a1n1-4)

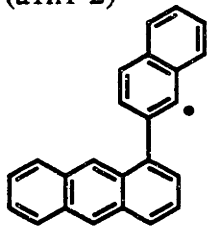

condensible 1-yl monoradical (all sites shown) of 1-(2'-naphthyl) anthracene (a1n2-1)

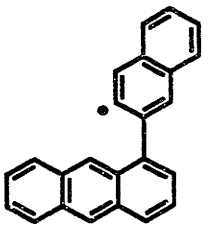

condensible 2-yl monoradical (all sites shown) of 1-(2'-naphthyl) anthracene (a1n2-2)

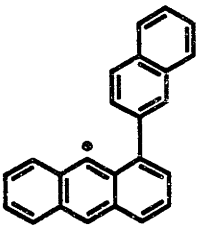

condensible 9-yl monoradical (all sites shown) of 1-(2'-naphthyl) anthracene (a1n2-3)

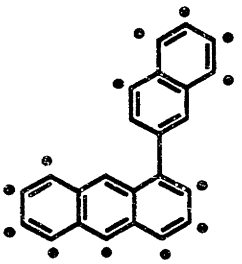

noncondensible monoradical (all sites shown) of 1-(2'-naphthyl) anthracene (a1n2-4)

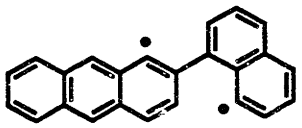

condensible 1-yl monoradical (all sites shown) of 2-(1'-naphthyl) anthracene (a2n1-1)

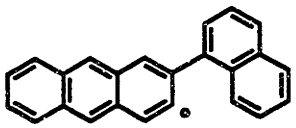

condensible 2-yl monoradical (all sites shown) of 2-(1'-naphthyl) anthracene (a2n1-2)

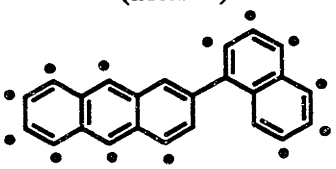

noncondensible monoradical (all sites shown) of 2-(1'-naphthyl) anthracene (a2n1-4)

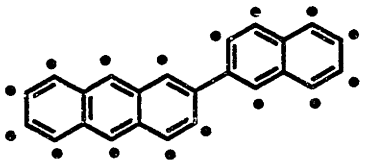

noncondensible 2-(2'-naphthyl) anthracene (a2n2-4)

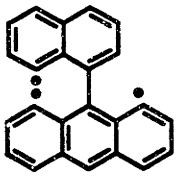

condensible 1-yl monoradical (all sites shown) of 9-(1'-naphthyl) anthracene (a9n1-1)

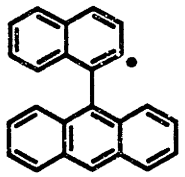

condensible 2-yl monoradical (all sites shown) of 9-(1'-naphthyl) anthracene (a9n1-2)

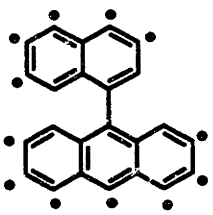

noncondensible monoradical (all sites shown) of 9-(1'-naphthyl) anthracene (a9n1-4)

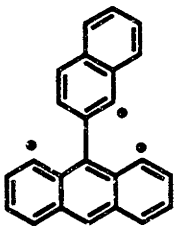

condensible 1-yl monoradical (all sites shown) of 9-(2'-naphthyl) anthracene (a9n2-1)

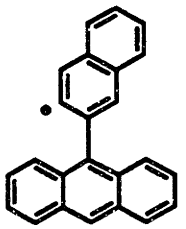

condensible 2-yl monoradical (all sites shown) of 9-(2'-naphthyl) anthracene (a9n2-2)

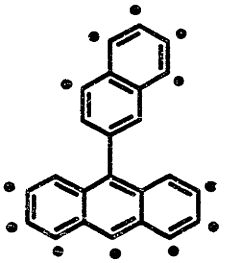

noncondensible monoradical (all sites shown) of 9-(2'-naphthyl) anthracene (a9n2-4)

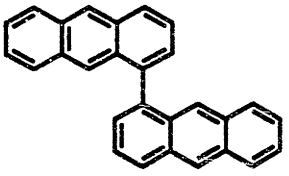

1,1'-bianthracene (11AA, a1a1)

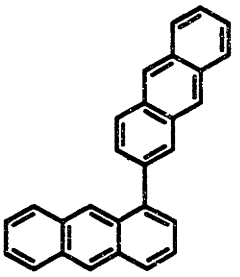

1,2'-bianthracene (12AA, a1a2)

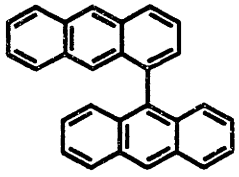

1,9'-anthracene (19AA, a1a9)

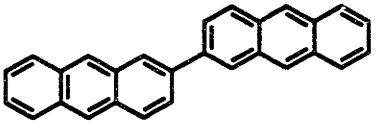

2,2'-bianthracene (22AA, a2a2)

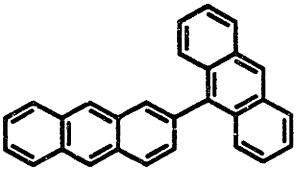

2,9'-bianthracene (29AA, a2a9)

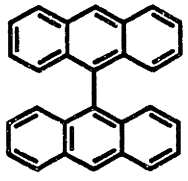

9,9'-bianthracene (99AA, a9a9)

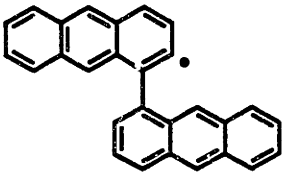

condensible 2-yl monoradical (all sites shown) of 1,1'-bianthracene (a1a1-2)

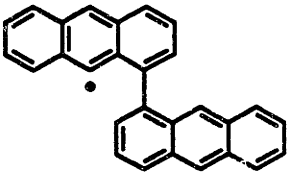

condensible 9-yl monoradical (all sites shown) of 1,1'-bianthracene (a1a1-3)

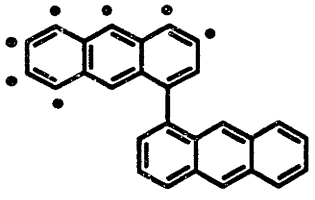

noncondensible monoradical (all sites shown) of 1,1'-bianthracene (a1a1-4)

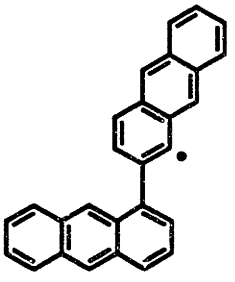

condensible 1-yl monoradical (all sites shown) of 1,2'-bianthracene (a1a2-1)

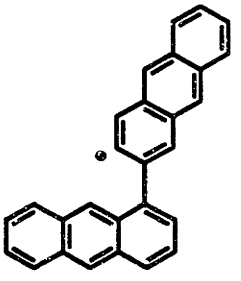

condensible 2-yl monoradical (all sites shown) of 1,2'-bianthracene (a1a2-2)

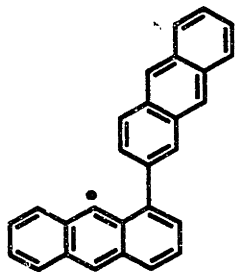

condensible 9-yl monoradical (all sites shown) of 1,2'-bianthracene (a1a2-3)

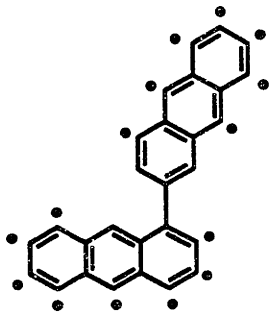

noncondensible monoradical (all sites shown) of 1,2'-bianthracene (a1a2-4)

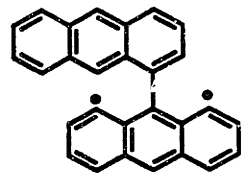

condensible 1-yl monoradical (all sites shown) of 1,9'-anthracene (a1a9-1)

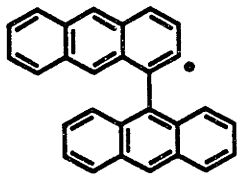

condensible 2-yl monoradical (all sites shown) of 1,9'-anthracene (a1a9-2)

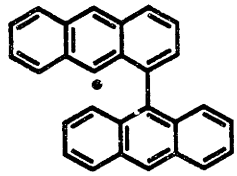

condensible 9-yl monoradical (all sites shown) of 1,9'-anthracene (a1a9-3)

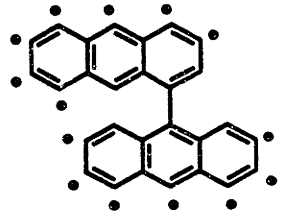

noncondensible monoradical (all sites shown) of 1,9'-anthracene (a1a9-4)

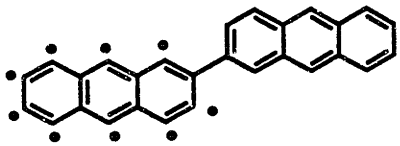

noncondensible monoradical (all sites shown) of 2,2'-bianthracene (a2a2-4)

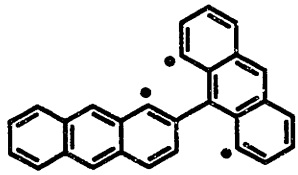

condensible 1-yl monoradical (all sites shown) of 2,9'-bianthracene (a2a9-1)

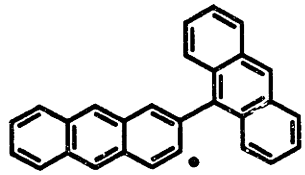

condensible 2-yl monoradical (all sites shown) of 2,9'-bianthracene (a2a9-2)

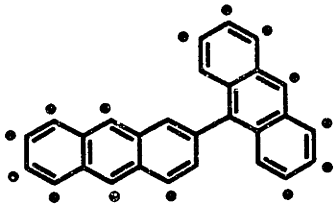

noncondensible monoradical (all sites shown) of 2,9'-bianthracene (a2a9-4)

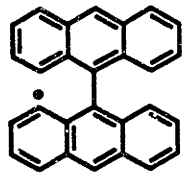

condensible 1-yl monoradical (all sites shown) of 9,9'-bianthracene (a9a9-1)

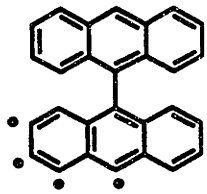

noncondensible monoradical (all sites shown) of 9,9'-bianthracene (a9a9-4)

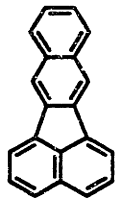

benzo(j)fluorathene
(BjF, BjF- radical)

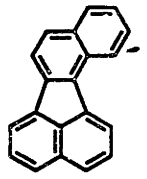

benzo(k)fluorathene
(BkF, BkF- radical)

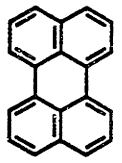

perylene
(Per, Per- radical)

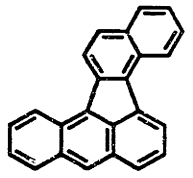

dibenzo(a,j)fluorathene
(DBajF, DBajF- radical)

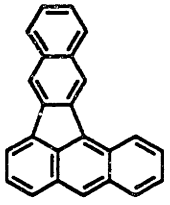

dibenzo(a,j)fluorathene
(DBajF, DBajF- radical)

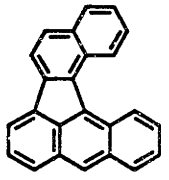

dibenzo(a,j)fluorathene
(DBajF, DBajF- radical)

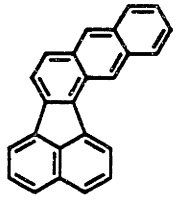

naphtho(2,3-j)-
fluoranthene
(N23jF, N23jF-)

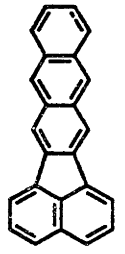

naphtho(2,3-j)-
fluoranthene
(N23jF, N23jF-)

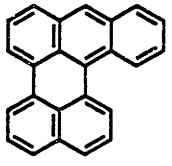

benzo(a)perylene
(BaPer, BaPer- radical)

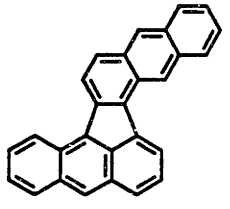

benzo(a)naphtho(2,3-j)
fluoranthene
(BaN23jF,
BaN23jF- radical)

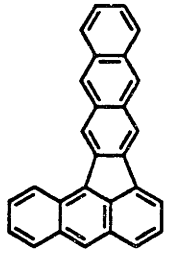

benzo(a)naphtho(2,3-k)
fluoranthene
(BaN23kF,
BaN23kF- radical)

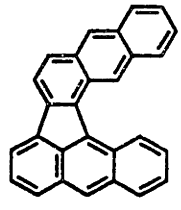

benzo(a)naphtho(2,3-l
fluoranthene
(BaN23lF,
BaN23lF- radical)

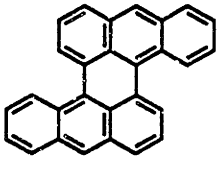

dibenzo(a,j)perylene
(DBajPer, DBajPer- radical)

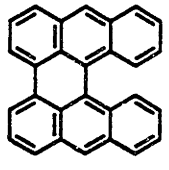

dibenzo(a,o)perylene
(DBaoPer, DBaoPer- radical)

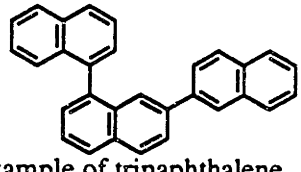

example of trinaphthalene
29 isomers, MW 380
(NNN, NNN- radical)

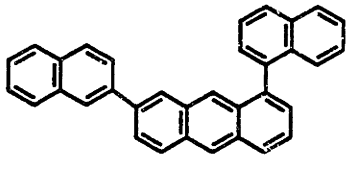

example of triaryl consisting of
2 naphthalenes and 1 anthracene
119 isomers, MW 430
(NNA, NNA- radical)

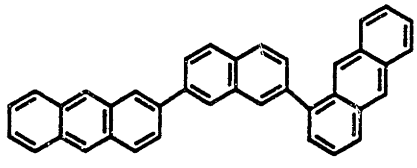

example of triaryl consisting of
1 naphthalene and 2 anthracenes
198 isomers, MW 530
(NAA, NAA- radical)

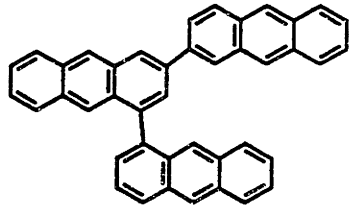

example of trianthracene
98 isomers, MW 580
(AAA, AAA- radical)

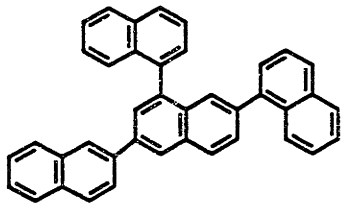

example of tetranaphthalene
326 isomers, MW 506
(NNNN, NNNN- radical)

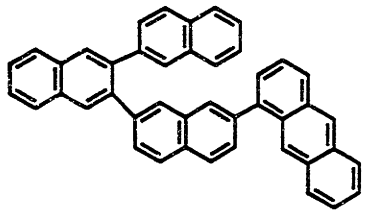

example of tetraaryl consisting of
3 naphthalenes and 1 anthracene
2177 isomers, MW 556
(NNNA, NNNA- radical)

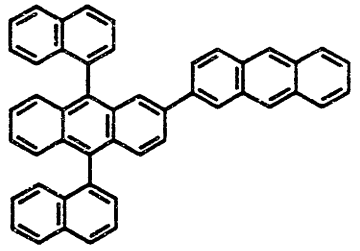

example of tetraaryl consisting of
2 naphthalenes and 2 anthracenes
5721 isomers, MW 606
(NNAA, NNAA- radical)

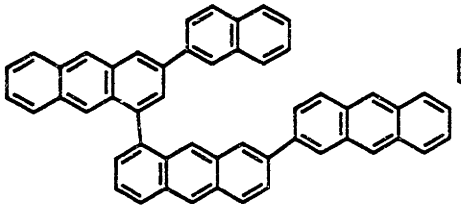

example of tetraaryl consisting of
1 naphthalene and 3 anthracenes
6458 isomers, MW 656
(NAAA, NAAA- radical)

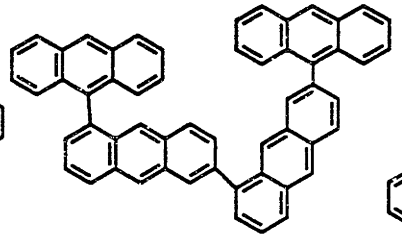

example of tetraanthracene
2539 isomers, MW 706
(AAAA, AAAA- radical)

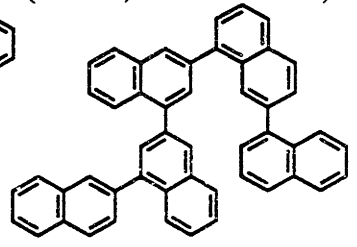

example of pentanaphthalene
6163 isomers, MW 632
(NNNNN, NNNNN- radical)

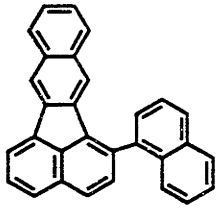

example of singly
condensed NNN
42 isomers, MW 378
(C1NNN, C1NNN- radical)

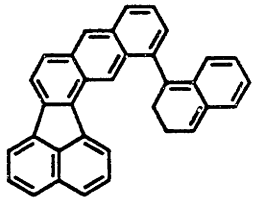

example of singly
condensed NNA
217 isomers, MW 428
(C1NNA, C1NNA- radical)

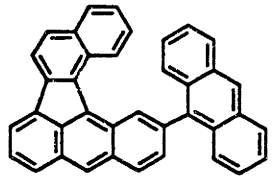

example of singly
condensed NAA
359 isomers, MW 478
(C1NAA, C1NAA- radical)

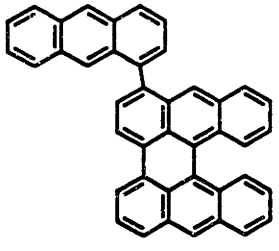

example of singly
condensed AAA
192 isomers, MW 578
(C1AAA, C1AAA- radical)

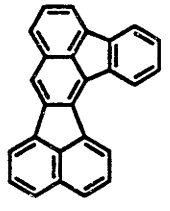

example of doubly
condensed NNN
16 isomers, MW 376
(C2NNN, C2NNN- radical)

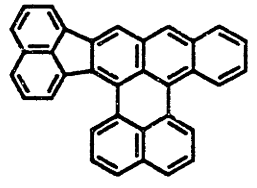

example of doubly
condensed NNA
84 isomers, MW 426
(C2NNA, C2NNA- radical)

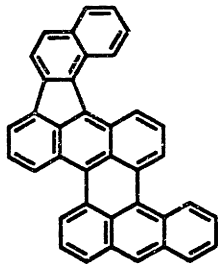

example of doubly
condensed NAA
132 isomers, MW 476
(C2NAA, C2NAA- radical)

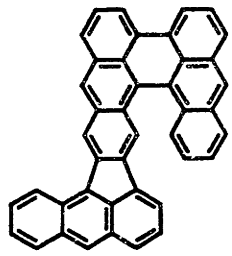

example of doubly
condensed AAA
89 isomers, MW 526
(C2AAA, C2AAA- radical)

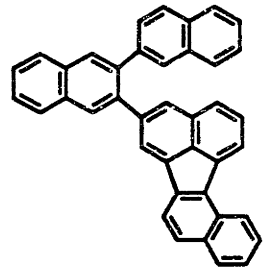

example of singly
condensed NNNN
899 isomers, MW 504
(C1NNNN, C1NNNN- radical)

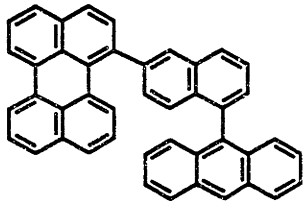

example of singly
condensed NNNA
6393 isomers, MW 554
(C1NNNA, C1NNNA- radical)

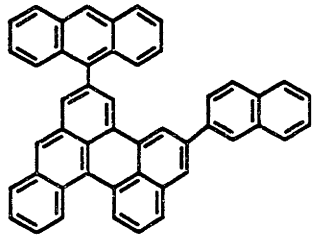

example of singly
condensed NNAA
16128 isomers, MW 604
(C1NNAA, C1NNAA- radical)

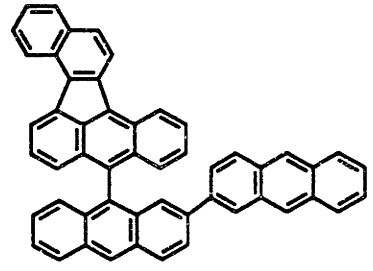

example of singly
condensed NAAA
17985 isomers, MW 654
(C1NAAA, C1NAAA- radical)

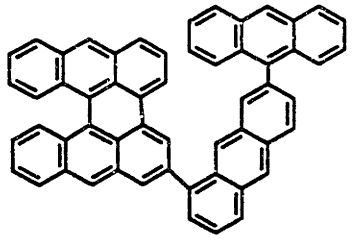

example of singly
condensed AAAA
7516 isomers, MW 504
(C1AAAA, C1AAAA- radical)

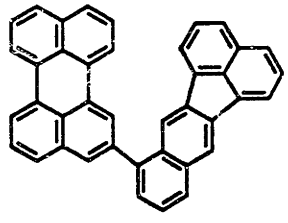

example of doubly
condensed NNNN
647 isomers, MW 502
(C2NNNN, C2NNNN- radical)

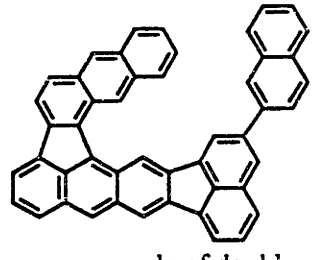

example of doubly
condensed NNNA
5103 isomers, MW 502
(C2NNNA, C2NNNA- radical)

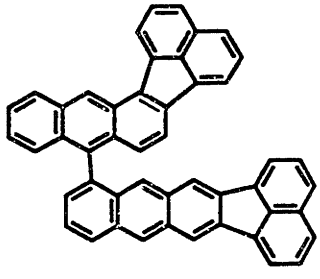

example of doubly
condensed NNAA
2997 isomers, MW 602
(C2NNAA, C2NNAA- radical)

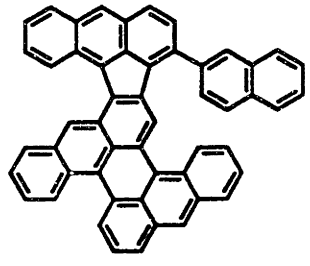

example of doubly
condensed NAAA
16188 isomers, MW 652
(C2NAAA, C2NAAA- radical)

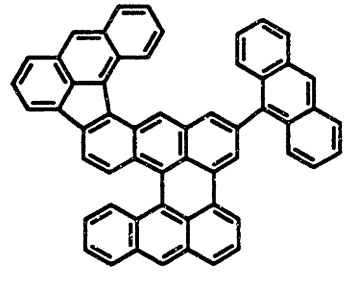

example of doubly
condensed AAAA
7450 isomers, MW 702
(C2AAAA, C2AAAA- radical)

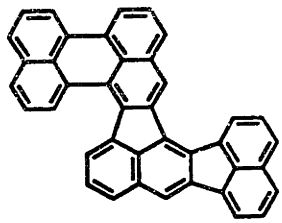

example of triply
condensed NNNN
144 isomers, MW 500
(C3NNNN, C3NNNN- radical)

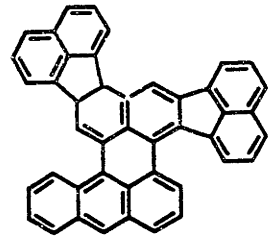

example of triply
condensed NNNA
769 isomers, MW 550
(C3NNNA, C3NNNA- radical)

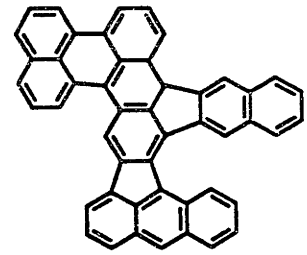

example of triply
condensed NNAA
3136 isomers, MW 600
(C3NNAA, C3NNAA- radical)

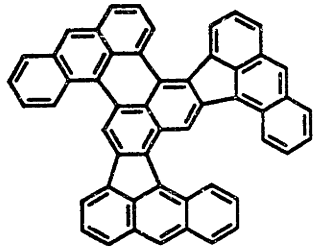

example of triply
condensed NAAA
3728 isomers, MW 650
(C3NAAA, C3NAAA- radical)

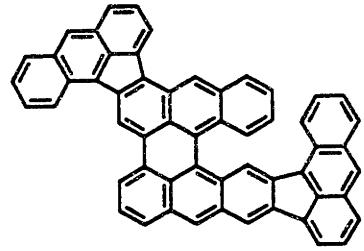

example of triply
condensed AAAA
2592 isomers, MW 700
(C3AAAA, C3AAAA- radical)

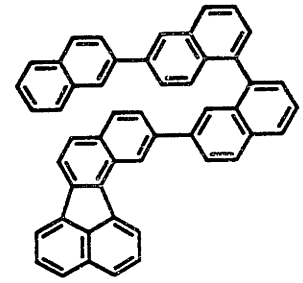

example of singly
condensed NNNNN
20500 isomers, MW 630
(C1NNNNN, C1NNNNN- radical)

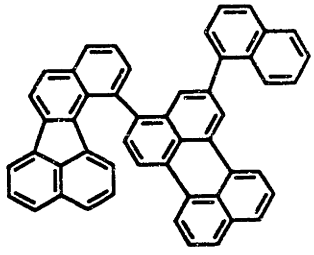

example of doubly
condensed NNNNN
23720 isomers, MW 628
(C2NNNNN, C2NNNNN- radical)

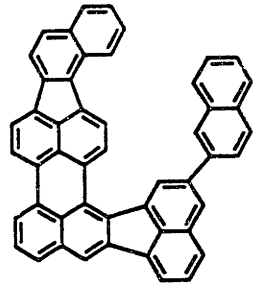

example of triply
condensed NNNNN
9828 isomers, MW 626
(C3NNNNN, C3NNNNN- radical)

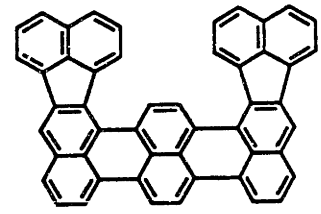

example of quadruply
condensed NNNNN
599 isomers, MW 624
(C4NNNNN, C4NNNNN- radical)

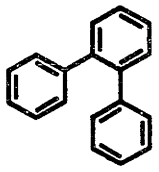

ortho-terphenyl

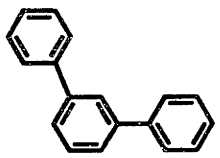

meta-terphenyl

para-terphenyl

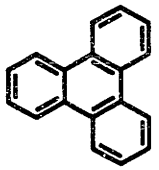

triphenylene,
a TRS compound

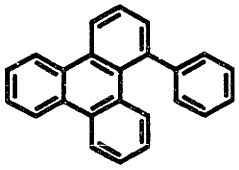

1-phenyl-triphenylene

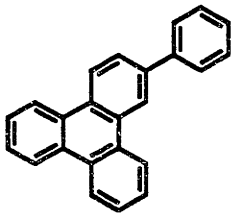

2-phenyl-triphenylene

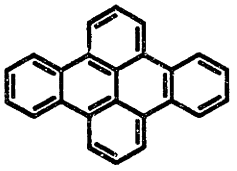

dibenzo(e,l)pyrene
(DBelP), a TRS compound

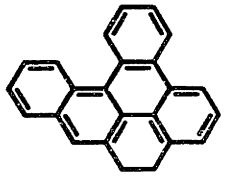

dibenzo(a,l)pyrene
DBalP

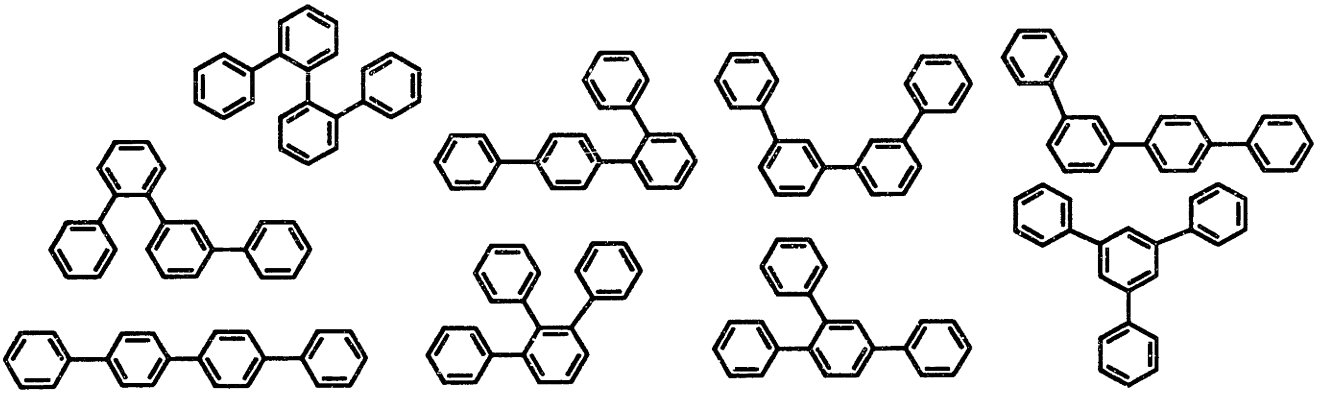

the set of 9 isomers of tetraphenyl

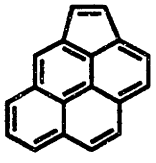

cyclopenta(cd)pyrene
(CPP)

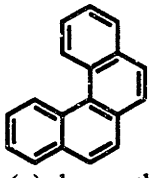

benzo(c)phenanthrene
(BcPhen)

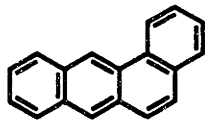

benzo(a)anthracene
(BaA)

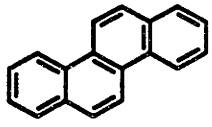

chrysene

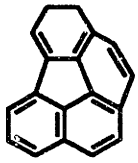

benzo(ghi)fluoranthene
(BghiF)

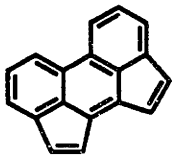

cyclopenta(def)
acephenanthrylene
(CPAP)

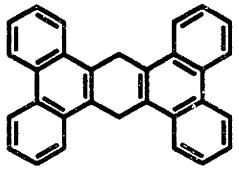

tetrabenzo(a,c,h,j)
anthracene, a TRS
compound

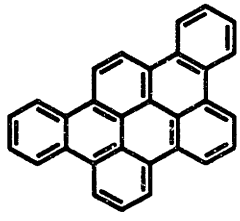

tribenzo(fg,ij,rst)
pentaphene, a TRS
compound

Appendix E - Graph Theory Considerations Used in Identification of Poly (ethylene terephthalate)

The purpose of this appendix is to give an outline of the process involved in eliminating the likelihood of the mystery MW576 compound described in chapter 7 being a PAH, opening the door to the possibility of that compound being a fullerene or a contaminant.

For the purposes of this discussion, a graph is taken to be a diagram made up of dots and non-intersecting lines (vertices and edges) enclosing regions (faces) in 2-dimensional space. The connective relationship between the vertices, as indicated by the edges, defines the nature of the graph. Graphs are especially well suited to investigating possible PAH structures because of this connectivity property. This binary linking relationship is analagous to the sigma bond skeleton of a PAH, making the vertices analagous to the atoms, and the faces analagous to rings in the PAH structure. Naphthalene would thus be represented as follows:

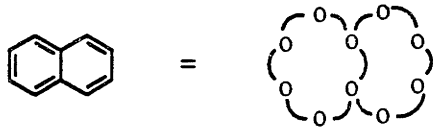

Hydrogens and double bonds are ignored since they provide no new information in a fully aromatic structure. It is a well known fact (attributed to Euler) that the sum of the vertices and the faces must equal 2 more than the number of edges in a 2-dimensional graph:

$$V + F = E + 2$$

This can be verified in the naphthalene example. 10 vertices plus 2 six-sided faces plus one ten-sided face (the infinite face) equals 11 edges plus 2.

Fully aromatic compounds possess some additional special properties relating faces and vertices. First, since PAH generally consist exclusively of five and six-membered rings, only five and six-sided faces need to be considered in the analysis. The external (infinite) face can, of course, be composed of a larger number of edges, but there will only be one face of that type. The possibility of "holes" (faces with more 10 edges, internal rings containing more than 10 carbon atoms) can also not be eliminated at this point, and they will be considered in the analysis.

By taking a simple inventory of edges, counting them two different ways, we find that:

$$5 F_5 + 6 F_6 + \text{sum}\ (i F_i\ (i>6) = 2 E = 3\ (\#\ \text{Carbons} - \#\ \text{Hydrogens}) + 2\ (\#\ \text{Hydrogens}),$$

where F_i = number of i-sided faces.

We must also have:

carbons = sum ($i F_i$) + I, where I = number of carbons "internal" to the structure, i.e. not on an outer edge (infinite face) or hole.

and: # Carbons = V = 46, # Hydrogens = 24 (see Ch. 7).

This forces E to be 57 and F to be 13. Plug-in and rearrangement results in two contraints on fully aromatic PAH conformation for a molecular weight 576 compound. These are:

$$F_5 + F_6 + i = 13 \text{ and } 5F_5 + 6F_6 - I = 68,$$

where i = # of additional faces (holes plus infinite face).

Note that a "flat" PAH must have $i > 0$, and a fullerene will have $i = 0$.

If $i > 1$, the maximum of $5F_5 + 6F_6 - I$ will be 66, violating the second constraint, so no holes are possible in the structure. This leaves only $i = 1$ as a possiblity for the 576 compound being a PAH. Only 5 sets of F_5 and F_6 are thus found to satisfy the constraints, given that I must also be greater than zero. These are: $F_5 = 4$ and $F_6 = 8$ (I=0), $F_5 = 3$ and $F_6 = 9$ (I=1), $F_5 = 2$ and $F_6 = 10$ (I=2), $F_5 = 1$ and $F_6 = 11$ (I=3), and $F_5 = 0$ and $F_6 = 12$ (I=4).

The first two can be immediately eliminated as possible structures for a reasonable PAH, since they would result in five-membered rings that are not internal to the structure, a requirement for stability.

ex. for I = 0

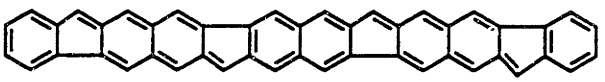

ex. for I = 1

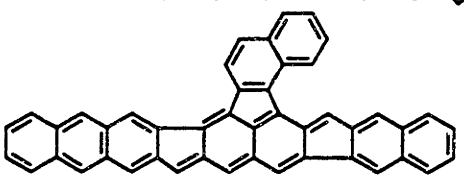

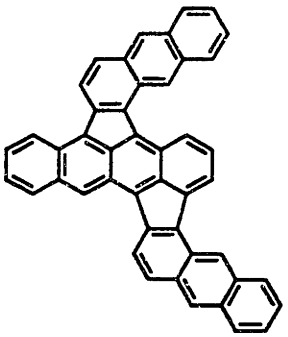

ex. for I = 2

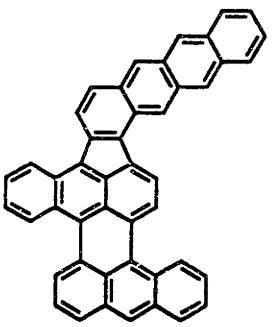

ex. for I = 3

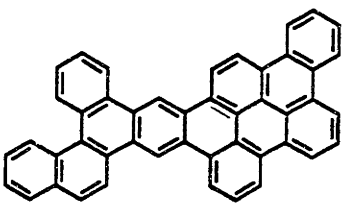

ex. for I = 4

The last three look very reasonable for PAH structures until one realizes the number of isomers that would be possible for each of them, none of which would be particularly favored over another in any reaction scheme. Numerous peaks would be evident on both the HPLC and LCMS, given that even slight changes in conformation for similar compounds result in substantial differences in elution times on these apparatus, and this is definitely not indicated in these samples.

Furthermore, such compounds could only arise from polymerization/condensation schemes involving compounds that aren't present in large enough abundance to explain the heightened amounts of the mystery compound that are present.

Though the possibility of the mystery compound being a PAH is eliminated with the application of graph theory constraints, the possibility of fullerenes, however, is not. In fact, graph theory strengthens the case for fullerenes. Since, with fullerenes, the number of hydrogens and holes are both zero, and I = # of Carbons, we must have $F_5 = 12$ and $F_6 = 14$. There is exactly one "special" structure that fits these constraints, matching the single isomer observation. See Chapter 7 for more details.

Appendix F: NASA Formatted Thermodynamic Parameters Used By CHEMKIN

Format is as follows:

Compound ID, Date	Elemental Composition	Tmin	Tmax	Tmidpt
a1	a2	a3	a4	a5
a6	a7	a8	a9	a10
a11	a12	a13	a14	

Where:

$$Cp(T) = R\,(a1 + a2\,T + a3\,T^2 + a4\,T^3 + a5\,T^4) \qquad T > Tmid.$$
$$= R\,(a8 + a9\,T + a10\,T^2 + a11\,T^3 + a12\,T^4) \qquad T < Tmid.$$
$$H(T) = R\,(a1\,T + a2\,T^2/2 + a3\,T^3/3 + a4\,T^4/4 + a5\,T^5/5 + a6) \qquad T > Tmid$$
$$= R\,(a8\,T + a9\,T^2/2 + a10\,T^3/3 + a11\,T^4/4 + a12\,T^5/5 + a13) \qquad T < Tmid$$
$$S(T) = R\,(a1\,\ln(T) + a2\,T + a3\,T^2/2 + a4\,T^3/3 + a5\,T^4/4 + a7) \qquad T > Tmid$$
$$= R\,(a8\,\ln(T) + a9\,T + a10\,T^2/2 + a11\,T^3/3 + a12\,T^4/4 + a14) \qquad T < Tmid$$

```
THERMO
   300.000  1500.000  5000.000
n         11/ 2/94      C  10H   8    0    0G   300.000  5000.000 1385.000    01
 2.28022962E+01 2.55027973E-02-8.96455035E-06 1.41766947E-09-8.33192985E-14    2
 6.38915120E+03-1.05196936E+02-3.88583278E+00 8.37196007E-02-5.56640841E-05    3
 1.76533869E-08-2.12050845E-12 1.60131563E+04 3.95062577E+01                   4
a         11/ 2/94      C  14H  10    0    0G   300.000  5000.000 1384.000    01
 3.26767918E+01 3.26895905E-02-1.15123181E-05 1.82295643E-09-1.07239467E-13    2
 9.90219343E+03-1.59859731E+02-3.57337687E+00 1.10683703E-01-7.20505269E-05    3
 2.14825826E-08-2.24765199E-12 2.30117882E+04 3.69541313E+01                   4
n1-       11/ 2/94      C  10H   7    0    0G   300.000  5000.000 1379.000    01
 2.22380553E+01 2.35872467E-02-8.33863288E-06 1.32367120E-09-7.79981744E-14    2
 3.47524176E+04-9.91887914E+01-2.56171206E+00 7.58027748E-02-4.78602931E-05    3
 1.37735979E-08-1.37699108E-12 4.38905004E+04 3.59559677E+01                   4
n2-       11/ 2/94      C  10H   7    0    0G   300.000  5000.000 1379.000    01
 2.22380553E+01 2.35872467E-02-8.33863288E-06 1.32367120E-09-7.79981744E-14    2
 3.52053618E+04-9.91887914E+01-2.56171206E+00 7.58027748E-02-4.78602931E-05    3
 1.37735979E-08-1.37699108E-12 4.43434445E+04 3.59559677E+01                   4
a1-       11/ 2/94      C  14H   9    0    0G   300.000  5000.000 1366.000    01
 3.07610958E+01 3.19900926E-02-1.13204921E-05 1.79819861E-09-1.06008629E-13    2
 3.88079889E+04-1.46100998E+02 1.05262245E+00 8.69815885E-02-4.26010819E-05    3
 5.43132760E-09 9.55970819E-13 5.04882650E+04 1.84380434E+01                   4
a2-       11/ 2/94      C  14H   9    0    0G   300.000  5000.000 1366.000    01
 3.07610958E+01 3.19900926E-02-1.13204921E-05 1.79819861E-09-1.06008629E-13    2
 3.94622416E+04-1.46100998E+02 1.05262245E+00 8.69815885E-02-4.26010819E-05    3
 5.43132760E-09 9.55970819E-13 5.11425177E+04 1.84380434E+01                   4
a9-       11/ 2/94      C  14H   9    0    0G   300.000  5000.000 1366.000    01
 3.07610958E+01 3.19900926E-02-1.13204921E-05 1.79819861E-09-1.06008629E-13    2
 3.83047177E+04-1.46795513E+02 1.05262245E+00 8.69815885E-02-4.26010819E-05    3
 5.43132760E-09 9.55970819E-13 4.99849938E+04 1.77435290E+01                   4
n1n1      11/ 2/94      C  20H  14    0    0G   300.000  5000.000 1394.000    11
 4.59817626E+01 4.63474171E-02-1.62060248E-05 2.55410685E-09-1.49761615E-13    2
 1.69035524E+04-2.28433728E+02-7.51507854E+00 1.69779869E-01-1.23090739E-04    3
 4.37809761E-08-6.11973559E-12 3.54265398E+04 5.90758843E+01                   4
n1n1-1    11/ 2/94      C  20H  13    0    0G   300.000  5000.000 1391.000    11
 4.65278749E+01 4.36554177E-02-1.53505856E-05 2.42838888E-09-1.42763442E-13    2
 4.47663147E+04-2.29667045E+02-6.66639861E+00 1.64280558E-01-1.16837230E-04    3
 3.98747541E-08-5.22174926E-12 6.33518614E+04 5.68930336E+01                   4
n1n1-2    11/ 2/94      C  20H  13    0    0G   300.000  5000.000 1391.000    11
 4.65278749E+01 4.36554177E-02-1.53505856E-05 2.42838888E-09-1.42763442E-13    2
 4.52192588E+04-2.29667045E+02-6.66639861E+00 1.64280558E-01-1.16837230E-04    3
 3.98747541E-08-5.22174926E-12 6.38048055E+04 5.68930336E+01                   4
n1n1-4    11/ 2/94      C  20H  13    0    0G   300.000  5000.000 1391.000    11
 4.65278749E+01 4.36554177E-02-1.53505856E-05 2.42838888E-09-1.42763442E-13    2
 4.50179503E+04-2.28056577E+02-6.66639861E+00 1.64280558E-01-1.16837230E-04    3
```

```
 3.98747541E-08-5.22174926E-12 6.36034971E+04 5.85035016E+01                4
n1n2      11/ 2/94      C  20H  14    0    0G   300.000  5000.000 1394.000   11
 4.59817626E+01 4.63474171E-02-1.62060248E-05 2.55410685E-09-1.49761615E-13   2
 1.60882530E+04-2.27739213E+02-7.51507854E+00 1.69779869E-01-1.23090739E-04   3
 4.37809761E-08-6.11973559E-12 3.46112404E+04 5.97703986E+01                4
n1n2-1    11/ 2/94      C  20H  13    0    0G   300.000  5000.000 1391.000   11
 4.65278749E+01 4.36554177E-02-1.53505856E-05 2.42838888E-09-1.42763442E-13   2
 4.39510152E+04-2.28972530E+02-6.66639861E+00 1.64280558E-01-1.16837230E-04   3
 3.98747541E-08-5.22174926E-12 6.25365620E+04 5.75875479E+01                4
n1n2-2    11/ 2/94      C  20H  13    0    0G   300.000  5000.000 1391.000   11
 4.65278749E+01 4.36554177E-02-1.53505856E-05 2.42838888E-09-1.42763442E-13   2
 4.44039594E+04-2.29667045E+02-6.66639861E+00 1.64280558E-01-1.16837230E-04   3
 3.98747541E-08-5.22174926E-12 6.29895061E+04 5.68930336E+01                4
n1n2-4    11/ 2/94      C  20H  13    0    0G   300.000  5000.000 1391.000   11
 4.65278749E+01 4.36554177E-02-1.53505856E-05 2.42838888E-09-1.42763442E-13   2
 4.42026509E+04-2.27271473E+02-6.66639861E+00 1.64280558E-01-1.16837230E-04   3
 3.98747541E-08-5.22174926E-12 6.27881976E+04 5.92886048E+01                4
n2n2      11/ 2/94      C  20H  14    0    0G   300.000  5000.000 1394.000   11
 4.59817626E+01 4.63474171E-02-1.62060248E-05 2.55410685E-09-1.49761615E-13   2
 1.50817104E+04-2.28433728E+02-7.51507854E+00 1.69779869E-01-1.23090739E-04   3
 4.37809761E-08-6.11973559E-12 3.36046978E+04 5.90758843E+01                4
n2n2-4    11/ 2/94      C  20H  13    0    0G   300.000  5000.000 1391.000   11
 4.65278749E+01 4.36554177E-02-1.53505856E-05 2.42838888E-09-1.42763442E-13   2
 4.31457812E+04-2.27719385E+02-6.66639861E+00 1.64280558E-01-1.16837230E-04   3
 3.98747541E-08-5.22174926E-12 6.17313280E+04 5.88406934E+01                4
a1n1      11/ 2/94      C  24H  16    0    0G   300.000  5000.000 1379.000   11
 5.49007367E+01 5.47773291E-02-1.92799141E-05 3.05179413E-09-1.79482166E-13   2
 2.05937108E+04-2.77240282E+02-1.42687967E+00 1.69414353E-01-9.94470208E-05   3
 2.38536408E-08-1.24613864E-12 4.16037404E+04 3.08795333E+01                4
a1n1-1    11/ 2/94      C  24H  15    0    0G   300.000  5000.000 1376.000   11
 5.40213335E+01 5.30733215E-02-1.87134545E-05 2.96558235E-09-1.74551213E-13   2
 4.91822344E+04-2.70689694E+02 8.66512572E-02 1.61033063E-01-9.18331085E-05   3
 2.04511778E-08-6.56980888E-13 6.94963901E+04 2.50090719E+01                4
a1n1-2    11/ 2/94      C  24H  15    0    0G   300.000  5000.000 1376.000   11
 5.40213335E+01 5.30733215E-02-1.87134545E-05 2.96558235E-09-1.74551213E-13   2
 4.96855056E+04-2.69995180E+02 8.66512572E-02 1.61033063E-01-9.18331085E-05   3
 2.04511778E-08-6.56980888E-13 6.99996614E+04 2.57035863E+01                4
a1n1-3    11/ 2/94      C  24H  15    0    0G   300.000  5000.000 1376.000   11
 5.40213335E+01 5.30733215E-02-1.87134545E-05 2.96558235E-09-1.74551213E-13   2
 4.86789631E+04-2.70689694E+02 8.66512572E-02 1.61033063E-01-9.18331085E-05   3
 2.04511778E-08-6.56980888E-13 6.89931189E+04 2.50090719E+01                4
a1n1-4    11/ 2/94      C  24H  15    0    0G   300.000  5000.000 1376.000   11
 5.40213335E+01 5.30733215E-02-1.87134545E-05 2.96558235E-09-1.74551213E-13   2
 4.93835429E+04-2.68203534E+02 8.66512572E-02 1.61033063E-01-9.18331085E-05   3
 2.04511778E-08-6.56980888E-13 6.96976986E+04 2.74952320E+01                4
a1n2      11/ 2/94      C  24H  16    0    0G   300.000  5000.000 1379.000   11
 5.49007367E+01 5.47773291E-02-1.92799141E-05 3.05179413E-09-1.79482166E-13   2
 1.97733786E+04-2.77240282E+02-1.42687967E+00 1.69414353E-01-9.94470208E-05   3
 2.38536408E-08-1.24613864E-12 4.07834082E+04 3.08795333E+01                4
a1n2-1    11/ 2/94      C  24H  15    0    0G   300.000  5000.000 1376.000   11
 5.40213335E+01 5.30733215E-02-1.87134545E-05 2.96558235E-09-1.74551213E-13   2
 4.83115751E+04-2.70689694E+02 8.66512572E-02 1.61033063E-01-9.18331085E-05   3
 2.04511778E-08-6.56980888E-13 6.86257308E+04 2.50090719E+01                4
a1n2-2    11/ 2/94      C  24H  15    0    0G   300.000  5000.000 1376.000   11
 5.40213335E+01 5.30733215E-02-1.87134545E-05 2.96558235E-09-1.74551213E-13   2
 4.87645192E+04-2.70689694E+02 8.66512572E-02 1.61033063E-01-9.18331085E-05   3
 2.04511778E-08-6.56980888E-13 6.90786750E+04 2.50090719E+01                4
a1n2-3    11/ 2/94      C  24H  15    0    0G   300.000  5000.000 1376.000   11
 5.40213335E+01 5.30733215E-02-1.87134545E-05 2.96558235E-09-1.74551213E-13   2
 4.78586310E+04 2.70689694E+02 8.66512572E-02 1.61033063E-01-9.18331085E-05   3
 2.04511778E-08-6.56980888E-13 6.81727867E+04 2.50090719E+01                4
a1n2-4    11/ 2/94      C  24H  15    0    0G   300.000  5000.000 1376.000   11
 5.40213335E+01 5.30733215E-02-1.87134545E-05 2.96558235E-09-1.74551213E-13   2
 4.85632107E+04-2.68123011E+02 8.66512572E-02 1.61033063E-01-9.18331085E-05   3
 2.04511778E-08-6.56980888E-13 6.88773665E+04 2.75757554E+01                4
a2n1      11/ 2/94      C  24H  16    0    0G   300.000  5000.000 1379.000   11
 5.49007367E+01 5.47773291E-02-1.92799141E-05 3.05179413E-09-1.79482166E-13   2
 1.97532478E+04-2.77240282E+02-1.42687967E+00 1.69414353E-01-9.94470208E-05   3
 2.38536408E-08-1.24613864E-12 4.07632773E+04 3.08795333E+01                4
```

```
a2n1-1     11/ 2/94       C  24H  15     0     0G   300.000  5000.000 1376.000    11
 5.40213335E+01 5.30733215E-02-1.87134545E-05 2.96558235E-09-1.74551213E-13    2
 4.83417714E+04-2.69995180E+02 8.66512572E-02 1.61033063E-01-9.18331085E-05    3
 2.04511778E-08-6.56980888E-13 6.86559271E+04 2.57035863E+01                   4
a2n1-2     11/ 2/94       C  24H  15     0     0G   300.000  5000.000 1376.000    11
 5.40213335E+01 5.30733215E-02-1.87134545E-05 2.96558235E-09-1.74551213E-13    2
 4.89960240E+04-2.70689694E+02 8.66512572E-02 1.61033063E-01-9.18331085E-05    3
 2.04511778E-08-6.56980888E-13 6.93101798E+04 2.50090719E+01                   4
a2n1-4     11/ 2/94       C  24H  15     0     0G   300.000  5000.000 1376.000    11
 5.40213335E+01 5.30733215E-02-1.87134545E-05 2.96558235E-09-1.74551213E-13    2
 4.84927527E+04-2.68123011E+02 8.66512572E-02 1.61033063E-01-9.18331085E-05    3
 2.04511778E-08-6.56980888E-13 6.88069085E+04 2.75757554E+01                   4
a2n2       11/ 2/94       C  24H  16     0     0G   300.000  5000.000 1379.000    11
 5.49007367E+01 5.47773291E-02-1.92799141E-05 3.05179413E-09-1.79482166E-13    2
 1.87769015E+04-2.77240282E+02-1.42687967E+00 1.69414353E-01-9.94470208E-05    3
 2.38536408E-08-1.24613864E-12 3.97869311E+04 3.08795333E+01                   4
a2n2-4     11/ 2/94       C  24H  15     0     0G   300.000  5000.000 1376.000    11
 5.40213335E+01 5.30733215E-02-1.87134545E-05 2.96558235E-09-1.74551213E-13    2
 4.74660794E+04-2.67916670E+02 8.66512572E-02 1.61033063E-01-9.18331085E-05    3
 2.04511778E-08-6.56980888E-13 6.77802351E+04 2.77820966E+01                   4
a9n1       11/ 2/94       C  24H  16     0     0G   300.000  5000.000 1379.000    11
 5.49007367E+01 5.47773291E-02-1.92799141E-05 3.05179413E-09-1.79482166E-13    2
 2.13737813E+04-2.77240282E+02-1.42687967E+00 1.69414353E-01-9.94470208E-05    3
 2.38536408E-08-1.24613864E-12 4.23838108E+04 3.08795333E+01                   4
a9n1-1     11/ 2/94       C  24H  15     0     0G   300.000  5000.000 1376.000    11
 5.40213335E+01 5.30733215E-02-1.87134545E-05 2.96558235E-09-1.74551213E-13    2
 4.99623048E+04-2.69592563E+02 8.66512572E-02 1.61033063E-01-9.18331085E-05    3
 2.04511778E-08-6.56980888E-13 7.02764606E+04 2.61062033E+01                   4
a9n1-2     11/ 2/94       C  24H  15     0     0G   300.000  5000.000 1376.000    11
 5.40213335E+01 5.30733215E-02-1.87134545E-05 2.96558235E-09-1.74551213E-13    2
 5.03649219E+04-2.70689694E+02 8.66512572E-02 1.61033063E-01-9.18331085E-05    3
 2.04511778E-08-6.56980888E-13 7.06790776E+04 2.50090719E+01                   4
a9n1-4     11/ 2/94       C  24H  15     0     0G   300.000  5000.000 1376.000    11
 5.40213335E+01 5.30733215E-02-1.87134545E-05 2.96558235E-09-1.74551213E-13    2
 5.02139405E+04-2.68203534E+02 8.66512572E-02 1.61033063E-01-9.18331085E-05    3
 2.04511778E-08-6.56980888E-13 7.05280962E+04 2.74952320E+01                   4
a9n2       11/ 2/94       C  24H  16     0     0G   300.000  5000.000 1379.000    11
 5.49007367E+01 5.47773291E-02-1.92799141E-05 3.05179413E-09-1.79482166E-13    2
 2.05937108E+04-2.77240282E+02-1.42687967E+00 1.69414353E-01-9.94470208E-05    3
 2.38536408E-08-1.24613864E-12 4.16037404E+04 3.08795333E+01                   4
a9n2-1     11/ 2/94       C  24H  15     0     0G   300.000  5000.000 1376.000    11
 5.40213335E+01 5.30733215E-02-1.87134545E-05 2.96558235E-09-1.74551213E-13    2
 4.91822344E+04-2.69592563E+02 8.66512572E-02 1.61033063E-01-9.18331085E-05    3
 2.04511778E-08-6.56980888E-13 6.94963901E+04 2.61062033E+01                   4
a9n2-2     11/ 2/94       C  24H  15     0     0G   300.000  5000.000 1376.000    11
 5.40213335E+01 5.30733215E-02-1.87134545E-05 2.96558235E-09-1.74551213E-13    2
 4.95848514E+04-2.70689694E+02 8.66512572E-02 1.61033063E-01-9.18331085E-05    3
 2.04511778E-08-6.56980888E-13 6.98990071E+04 2.50090719E+01                   4
a9n2-4     11/ 2/94       C  24H  15     0     0G   300.000  5000.000 1376.000    11
 5.40213335E+01 5.30733215E-02-1.87134545E-05 2.96558235E-09-1.74551213E-13    2
 4.94338700E+04-2.68203534E+02 8.66512572E-02 1.61033063E-01-9.18331085E-05    3
 2.04511778E-08-6.56980888E-13 6.97480258E+04 2.74952320E+01                   4
a1a1       11/ 2/94       C  28H  18     0     0G   300.000  5000.000 1676.000    11
 5.27356992E+01 7.67300744E-02-2.82157293E-05 4.61303525E-09-2.77800080E-13    2
 3.02735307E+04-2.62357383E+02 4.13656342E+00 1.70975905E-01-8.49797254E-05    3
 1.39442405E-08 5.03261878E-13 4.79648231E+04 4.03497532E+00                   4
a1a1-2     11/ 2/94       C  28H  17     0     0G   300.000  5000.000 1382.000    11
 6.40840923E+01 6.01156749E-02-2.12156268E-05 3.36425905E-09-1.98109142E-13    2
 5.30622616E+04-3.27053797E+02-3.29128481E+00 1.99058107E-01-1.19902970E-04    3
 2.95534917E-08-1.64673292E-12 7.78964437E+04 4.06598988E+01                   4
a1a1-3     11/ 2/94       C  28H  17     0     0G   300.000  5000.000 1382.000    11
 6.40840923E+01 6.01156749E-02-2.12156268E-05 3.36425905E-09-1.98109142E-13    2
 5.19047377E+04-3.27053797E+02-3.29128481E+00 1.99058107E-01-1.19902970E-04    3
 2.95534917E-08-1.64673292E-12 7.67389198E+04 4.06598988E+01                   4
a1a1-4     11/ 2/94       C  28H  17     0     0G   300.000  5000.000 1382.000    11
 6.40840923E+01 6.01156749E-02-2.12156268E-05 3.36425905E-09-1.98109142E-13    2
 5.26093175E+04-3.25106137E+02-3.29128481E+00 1.99058107E-01-1.19902970E-04    3
 2.95534917E-08-1.64673292E-12 7.74434996E+04 4.26075586E+01                   4
a1a2       11/ 2/94       C  28H  18     0     0G   300.000  5000.000 1676.000    11
```

```
 5.27356992E+01 7.67300744E-02-2.82157293E-05 4.61303525E-09-2.77800080E-13    2
 2.94280350E+04-2.61662869E+02 4.13656342E+00 1.70975905E-01-8.49797254E-05    3
 1.39442405E-08 5.03261878E-13 4.71193273E+04 4.72948966E+00                   4
a1a2-1     11/ 2/94       C  28H  17    0    0G   300.000  5000.000 1382.000   11
 6.40840923E+01 6.01156749E-02-2.12156268E-05 3.36425905E-09-1.98109142E-13    2
 5.15625133E+04-3.27053797E+02-3.29128481E+00 1.99058107E-01-1.19902970E-04    3
 2.95534917E-08-1.64673292E-12 7.63966954E+04 4.06598988E+01                   4
a1a2-2     11/ 2/94       C  28H  17    0    0G   300.000  5000.000 1382.000   11
 6.40840923E+01 6.01156749E-02-2.12156268E-05 3.36425905E-09-1.98109142E-13    2
 5.22167659E+04-3.27053797E+02-3.29128481E+00 1.99058107E-01-1.19902970E-04    3
 2.95534917E-08-1.64673292E-12 7.70509480E+04 4.06598988E+01                   4
a1a2-3     11/ 2/94       C  28H  17    0    0G   300.000  5000.000 1382.000   11
 6.40840923E+01 6.01156749E-02-2.12156268E-05 3.36425905E-09-1.98109142E-13    2
 5.10592420E+04-3.27053797E+02-3.29128481E+00 1.99058107E-01-1.19902970E-04    3
 2.95534917E-08-1.64673292E-12 7.58934241E+04 4.06598988E+01                   4
a1a2-4     11/ 2/94       C  28H  17    0    0G   300.000  5000.000 1382.000   11
 6.40840923E+01 6.01156749E-02-2.12156268E-05 3.36425905E-09-1.98109142E-13    2
 5.17134947E+04-3.24346197E+02-3.29128481E+00 1.99058107E-01-1.19902970E-04    3
 2.95534917E-08-1.64673292E-12 7.65476767E+04 4.33674982E+01                   4
a1a9       11/ 2/94       C  28H  18    0    0G   300.000  5000.000 1676.000   11
 5.27356992E+01 7.67300744E-02-2.82157293E-05 4.61303525E-09-2.77800080E-13    2
 3.10435357E+04-2.61662869E+02 4.13656342E+00 1.70975905E-01-8.49797254E-05    3
 1.39442405E-08 5.03261878E-13 4.87348281E+04 4.72948966E+00                   4
a1a9-1     11/ 2/94       C  28H  17    0    0G   300.000  5000.000 1382.000   11
 6.40840923E+01 6.01156749E-02-2.12156268E-05 3.36425905E-09-1.98109142E-13    2
 5.31780140E+04-3.26359282E+02-3.29128481E+00 1.99058107E-01-1.19902970E-04    3
 2.95534917E-08-1.64673292E-12 7.80121961E+04 4.13544132E+01                   4
a1a9-2     11/ 2/94       C  28H  17    0    0G   300.000  5000.000 1382.000   11
 6.40840923E+01 6.01156749E-02-2.12156268E-05 3.36425905E-09-1.98109142E-13    2
 5.38322667E+04-3.27053797E+02-3.29128481E+00 1.99058107E-01-1.19902970E-04    3
 2.95534917E-08-1.64673292E-12 7.86664488E+04 4.06598988E+01                   4
a1a9-3     11/ 2/94       C  28H  17    0    0G   300.000  5000.000 1382.000   11
 6.40840923E 01 6.01156749E-02-2.12156268E-05 3.36425905E-09-1.98109142E-13    2
 5.26747428E+04-3.27053797E+02-3.29128481E+00 1.99058107E-01-1.19902970E-04    3
 2.95534917E-08-1.64673292E-12 7.75089249E+04 4.06598988E+01                   4
a1a9-4     11/ 2/94       C  28H  17    0    0G   300.000  5000.000 1382.000   11
 6.40840923E+01 6.01156749E-02-2.12156268E-05 3.36425905E-09-1.98109142E-13    2
 5.34296497E+04-3.24416655E+02-3.29128481E+00 1.99058107E-01-1.19902970E-04    3
 2.95534917E-08-1.64673292E-12 7.82638318E+04 4.32970403E+01                   4
a2a2       11/ 2/94       C  28H  18    0    0G   300.000  5000.000 1676.000   11
 5.27356992E+01 7.67300744E-02-2.82157293E-05 4.61303525E-09-2.77800080E-13    2
 2.84114270E+04-2.62357383E+02 4.13656342E+00 1.70975905E-01-8.49797254E-05    3
 1.39442405E-08 5.03261878E-13 4.61027194E+04 4.03497532E+00                   4
a2a2-4     11/ 2/94       C  28H  17    0    0G   300.000  5000.000 1382.000   11
 6.40840923E+01 6.01156749E-02-2.12156268E-05 3.36425905E-09-1.98109142E-13    2
 5.06465596E+04-3.24854501E+02-3.29128481E+00 1.99058107E-01-1.19902970E-04    3
 2.95534917E-08-1.64673292E-12 7.54807417E+04 4.28591943E+01                   4
a2a9       11/ 2/94       C  28H  18    0    0G   300.000  5000.000 1676.000   11
 5.27356992E+01 7.67300744E-02-2.82157293E-05 4.61303525E-09-2.77800080E-13    2
 3.02533998E+04-2.61662869E+02 4.13656342E+00 1.70975905E-01-8.49797254E-05    3
 1.39442405E-08 5.03261878E-13 4.79446922E+04 4.72948966E+00                   4
a2a9-1     11/ 2/94       C  28H  17    0    0G   300.000  5000.000 1382.000   11
 6.40840923E+01 6.01156749E-02-2.12156268E-05 3.36425905E-09-1.98109142E-13    2
 5.23878782E+04-3.25956665E+02-3.29128481E+00 1.99058107E-01-1.19902970E-04    3
 2.95534917E-08-1.64673292E-12 7.72220602E+04 4.17570302E+01                   4
a2a9-2     11/ 2/94       C  28H  17    0    0G   300.000  5000.000 1382.000   11
 6.40840923E+01 6.01156749E-02-2.12156268E-05 3.36425905E-09-1.98109142E-13    2
 5.30421308E+04-3.27053797E+02-3.29128481E+00 1.99058107E-01-1.19902970E-04    3
 2.95534917E-08-1.64673292E-12 7.78763129E+04 4.06598988E+01                   4
a2a9-4     11/ 2/94       C  28H  17    0    0G   300.000  5000.000 1382.000   11
 6.40840923E+01 6.01156749E-02-2.12156268E-05 3.36425905E-09-1.98109142E-13    2
 5.25388595E+04-3.24416655E+02-3.29128481E+00 1.99058107E-01-1.19902970E-04    3
 2.95534917E-08-1.64673292E-12 7.73730416E+04 4.32970403E+01                   4
a9a9       11/ 2/94       C  28H  18    0    0G   300.000  5000.000 1676.000   11
 5.27356992E+01 7.67300744E-02-2.82157293E-05 4.61303525E-09-2.77800080E-13    2
 3.18538025E+04-2.63046865E+02 4.13656342E+00 1.70975905E-01-8.49797254E-05    3
 1.39442405E-08 5.03261878E-13 4.95450948E+04 3.34549368E+00                   4
a9a9-1     11/ 2/94       C  28H  17    0    0G   300.000  5000.000 1382.000   11
 6.40840923E+01 6.01156749E-02-2.12156268E-05 3.36425905E-09-1.98109142E-13    2
```

```
 5.39882808E+04-3.27053797E+02-3.29128481E+00 1.99058107E-01-1.19902970E-04    3
 2.95534917E-08-1.64673292E-12 7.88224629E+04 4.06598988E+01                   4
a9a9-4     11/ 2/94       C  28H  17     0     0G   300.000  5000.000 1382.000    11
 6.40840923E+01 6.01156749E-02-2.12156268E-05 3.36425905E-09-1.98109142E-13    2
 5.42902435E+04-3.25181628E+02-3.29128481E+00 1.99058107E-01-1.19902970E-04    3
 2.95534917E-08-1.64673292E-12 7.91244256E+04 4.25320679E+01                   4
BkF        11/ 2/94       C  20H  12     0     0G   300.000  5000.000 1387.000    01
 4.39402663E+01 4.40017872E-02-1.55309526E-05 2.46293848E-09-1.45035585E-13    2
 2.22817604E+04-2.23264581E+02-8.86969640E+00 1.62847270E-01-1.14954783E-04    3
 3.90780181E-08-5.13272887E-12 4.08867720E+04 6.16541359E+01                   4
BjF        11/ 2/94       C  20H  12     0     0G   300.000  5000.000 1387.000    01
 4.39402663E+01 4.40017872E-02-1.55309526E-05 2.46293848E-09-1.45035585E-13    2
 2.17281620E+04-2.22570067E+02-8.86969640E+00 1.62847270E-01-1.14954783E-04    3
 3.90780181E-08-5.13272887E-12 4.03331736E+04 6.23486502E+01                   4
Per        11/ 2/94       C  20H  12     0     0G   300.000  5000.000 1373.000    01
 4.46587811E+01 4.38683433E-02-1.55934247E-05 2.48422256E-09-1.46748672E-13    2
 1.13533763E+04-2.26866190E+02-2.08146408E+00 1.40317388E-01-8.64400516E-05    3
 2.37333999E-08-2.15247872E-12 2.88209026E+04 2.86225243E+01                   4
DBajF      11/ 2/94       C  24H  14     0     0G   300.000  5000.000 1385.000    01
 5.40272243E+01 5.11076408E-02-1.80741314E-05 2.87004391E-09-1.69167514E-13    2
 2.44943247E+04-2.78691283E+02-8.33582172E+00 1.87396149E-01-1.26179877E-04    3
 3.91592026E-08-4.36415972E-12 4.67809240E+04 5.90570054E+01                   4
DBakF      11/ 2/94       C  24H  14     0     0G   300.000  5000.000 1385.000    01
 5.40272243E+01 5.11076408E-02-1.80741314E-05 2.87004391E-09-1.69167514E-13    2
 2.56015215E+04-2.78691283E+02-8.33582172E+00 1.87396149E-01-1.26179877E-04    3
 3.91592026E-08-4.36415972E-12 4.78881208E+04 5.90570054E+01                   4
DBalF      11/ 2/94       C  24H  14     0     0G   300.000  5000.000 1385.000    01
 5.40272243E+01 5.11076408E-02-1.80741314E-05 2.87004391E-09-1.69167514E-13    2
 2.44943247E+04-2.78691283E+02-8.33582172E+00 1.87396149E-01-1.26179877E-04    3
 3.91592026E-08-4.36415972E-12 4.67809240E+04 5.90570054E+01                   4
BaPer      11/ 2/94       C  24H  14     0     0G   300.000  5000.000 2036.000    01
 4.47023441E+01 6.28973846E-02-2.32419330E-05 3.81167632E-09-2.30022041E-13    2
 1.95343087E+04-2.22311639E+02 2.16343420E+00 1.49688051E-01-8.21114695E-05    3
 1.82752022E-08-9.40372566E-13 3.47101578E+04 9.45309640E+00                   4
N23jF      11/ 2/94       C  24H  14     0     0G   300.000  5000.000 1385.000    01
 5.40272243E+01 5.11076408E-02-1.80741314E-05 2.87004391E-09-1.69167514E-13    2
 2.50479231E+04-2.78691283E+02-8.33582172E+00 1.87396149E-01-1.26179877E-04    3
 3.91592026E-08-4.36415972E-12 4.73345224E+04 5.90570054E+01                   4
N23kF      11/ 2/94       C  24H  14     0     0G   300.000  5000.000 1385.000    01
 5.40272243E+01 5.11076408E-02-1.80741314E-05 2.87004391E-09-1.69167514E-13    2
 2.56015215E+04-2.79385798E+02-8.33582172E+00 1.87396149E-01-1.26179877E-04    3
 3.91592026E-08-4.36415972E-12 4.78881208E+04 5.83624910E+01                   4
BaN23jF    11/ 2/94       C  28H  16     0     0G   300.000  5000.000 1370.000    01
 6.11052490E+01 6.07970860E-02-2.15122214E-05 3.41702079E-09-2.01444544E-13    2
 2.90640271E+04-3.17230097E+02-9.63532291E-01 1.81400123E-01-9.79201523E-05    3
 1.81084736E-08 5.01314037E-13 5.27920061E+04 2.43334209E+01                   4
BaN23kF    11/ 2/94       C  28H  16     0     0G   300.000  5000.000 1370.000    01
 6.11052490E+01 6.07970860E-02-2.15122214E-05 3.41702079E-09-2.01444544E-13    2
 2.96176255E+04-3.17230097E+02-9.63532291E-01 1.81400123E-01-9.79201523E-05    3
 1.81084736E-08 5.01314037E-13 5.33456045E+04 2.43334209E+01                   4
BaN23lF    11/ 2/94       C  28H  16     0     0G   300.000  5000.000 1370.000    01
 6.11052490E+01 6.07970860E-02-2.15122214E-05 3.41702079E-09-2.01444544E-13    2
 2.90640271E+04-3.17230097E+02-9.63532291E-01 1.81400123E-01-9.79201523E-05    3
 1.81084736E-08 5.01314037E-13 5.27920061E+04 2.43334209E+01                   4
DBajPer    11/ 2/94       C  28H  16     0     0G   300.000  5000.000 1368.000    01
 6.22794977E+01 6.01275919E-02-2.13557174E-05 3.40049113E-09-2.00806231E-13    2
 1.78844392E+04-3.23697439E+02 9.96072532E-01 1.77668987E-01-9.41041823E-05    3
 1.63727933E-08 7.75754089E-13 4.15228417E+04 1.41863979E+01                   4
DBaoPer    11/ 2/94       C  28H  16     0     0G   300.000  5000.000 1368.000    01
 6.22794977E+01 6.01275919E-02-2.13557174E-05 3.40049113E-09-2.00806231E-13    2
 1.78844392E+04-3.23697439E+02 9.96072532E-01 1.77668987E-01-9.41041823E-05    3
 1.63727933E-08 7.75754089E-13 4.15228417E+04 1.41863979E+01                   4
BkF-       11/ 2/94       C  20H  11     0     0G   300.000  5000.000 1384.000    01
 4.33832736E+01 4.20967861E-02-1.49124799E-05 2.37050720E-09-1.39822351E-13    2
 5.07793579E+04-2.16228383E+02-7.75759002E+00 1.55731875E-01-1.08243350E-04    3
 3.58490005E-08-4.53057470E-12 6.89511201E+04 6.02181172E+01                   4
BjF-       11/ 2/94       C  20H  11     0     0G   300.000  5000.000 1384.000    01
 4.33832736E+01 4.20967861E-02-1.49124799E-05 2.37050720E-09-1.39822351E-13    2
 5.02760866E+04-2.15533869E+02-7.75759002E+00 1.55731875E-01-1.08243350E-04    3
```

```
 3.58490005E-08-4.53057470E-12 6.84478488E+04 6.09126316E+01                4
Per-       11/ 2/94       C  20H  11     0     0G   300.000  5000.000 1367.000    01
 4.42864852E+01 4.17445643E-02-1.48863371E-05 2.37663494E-09-1.40600809E-13    2
 3.98396153E+04-2.20862019E+02-3.62587203E-01 1.30524557E-01-7.53627823E-05    3
 1.75825498E-08-8.69471980E-13 5.68405536E+04 2.43530378E+01                4
DBajF-     11/ 2/94       C  24H  13     0     0G   300.000  5000.000 1382.000    01
 5.30908086E+01 4.94634499E-02-1.75308952E-05 2.78773163E-09-1.64474858E-13    2
 5.32675151E+04-2.69147316E+02-6.70780061E+00 1.78849558E-01-1.18760357E-04    3
 3.60830974E-08-3.88054240E-12 7.47988893E+04 5.52266161E+01                4
DBakF-     11/ 2/94       C  24H  13     0     0G   300.000  5000.000 1382.000    01
 5.30908086E+01 4.94634499E-02-1.75308952E-05 2.78773163E-09-1.64474858E-13    2
 5.42740577E+04-2.69147316E+02-6.70780061E+00 1.78849558E-01-1.18760357E-04    3
 3.60830974E-08-3.88054240E-12 7.58054318E+04 5.52266161E+01                4
DBalF-     11/ 2/94       C  24H  13     0     0G   300.000  5000.000 1382.000    01
 5.30908086E+01 4.94634499E-02-1.75308952E-05 2.78773163E-09-1.64474858E-13    2
 5.32675151E+04-2.69147316E+02-6.70780061E+00 1.78849558E-01-1.18760357E-04    3
 3.60830974E-08-3.88054240E-12 7.47988893E+04 5.52266161E+01                4
BaPer-     11/ 2/94       C  24H  13     0     0G   300.000  5000.000 1371.000    01
 5.28508412E+01 4.99688409E-02-1.77727688E-05 2.83257786E-09-1.67374676E-13    2
 4.33589994E+04-2.66343208E+02-1.75902352E-01 1.57555916E-01-9.40931825E-05    3
 2.39968353E-08-1.74112777E-12 6.33360481E+04 2.41202757E+01                4
N23jF-     11/ 2/94       C  24H  13     0     0G   300.000  5000.000 1382.000    01
 5.30908086E+01 4.94634499E-02-1.75308952E-05 2.78773163E-09-1.64474858E-13    2
 5.37204593E+04-2.69147316E+02-6.70780061E+00 1.78849558E-01-1.18760357E-04    3
 3.60830974E-08-3.88054240E-12 7.52518334E+04 5.52266161E+01                4
N23kF-     11/ 2/94       C  24H  13     0     0G   300.000  5000.000 1382.000    01
 5.30908086E+01 4.94634499E-02-1.75308952E-05 2.78773163E-09-1.64474858E-13    2
 5.42237305E+04-2.69836797E+02-6.70780061E+00 1.78849558E-01-1.18760357E-04    3
 3.60830974E-08-3.88054240E-12 7.57551047E+04 5.45371345E+01                4
BaN23jF-   11/ 2/94       C  28H  15     0     0G   300.000  5000.000 2021.000    01
 5.06474108E+01 7.12313103E-02-2.62951724E-05 4.30984767E-09-2.59987288E-13    2
 6.29709759E+04-2.51478101E+02 9.01483331E-01 1.72778511E-01-9.48363652E-05    3
 2.07802751E-08-9.48409449E-13 8.06698518E+04 1.94567316E+01                4
BaN23kF-   11/ 2/94       C  28H  15     0     0G   300.000  5000.000 2021.000    01
 5.06474108E+01 7.12313103E-02-2.62951724E-05 4.30984767E-09-2.59987288E-13    2
 6.34742471E+04-2.51478101E+02 9.01483331E-01 1.72778511E-01-9.48363652E-05    3
 2.07802751E-08-9.48409449E-13 8.11731231E+04 1.94567316E+01                4
BaN23lF-   11/ 2/94       C  28H  15     0     0G   300.000  5000.000 2021.000    01
 5.06474108E+01 7.12313103E-02-2.62951724E-05 4.30984767E-09-2.59987288E-13    2
 6.29709759E+04-2.51478101E+02 9.01483331E-01 1.72778511E-01-9.48363652E-05    3
 2.07802751E-08-9.48409449E-13 8.06698518E+04 1.94567316E+01                4
DBajPer-   11/ 2/94       C  28H  15     0     0G   300.000  5000.000 2031.000    01
 5.28919024E+01 6.97577965E-02-2.58923494E-05 4.25884220E-09-2.57529154E-13    2
 5.14126993E+04-2.64182745E+02 1.23660519E+00 1.76633990E-01-1.00097723E-04    3
 2.34226730E-08-1.42502561E-12 6.96700529E+04 1.66696712E+01                4
DBaoPer-   11/ 2/94       C  28H  15     0     0G   300.000  5000.000 2031.000    01
 5.28919024E+01 6.97577965E-02-2.58923494E-05 4.25884220E-09-2.57529154E-13    2
 5.14126993E+04-2.64182745E+02 1.23660519E+00 1.76633990E-01-1.00097723E-04    3
 2.34226730E-08-1.42502561E-12 6.96700529E+04 1.66696712E+01                4
NNN        11/ 2/94       C  30H  20     0     0G   300.000  5000.000 1397.000    21
 6.91953148E+01 6.71633073E-02-2.34383223E-05 3.68924162E-09-2.16135000E-13    2
 2.67607887E+04-3.48706402E+02-1.13407736E+01 2.56481537E-01-1.91291985E-04    3
 7.03318125E-08-1.02062963E-11 5.42519784E+04 8.28052330E+01                4
NNA        11/ 2/94       C  34H  22     0     0G   300.000  5000.000 1381.000    21
 7.84528009E+01 7.56137813E-02-2.65891563E-05 4.20634881E-09-2.47290348E-13    2
 3.02114721E+04-3.98844786E+02-2.44453552E+00 2.43473478E-01-1.47979472E-04    3
 3.81165090E-08-2.64430336E-12 6.00081580E+04 4.24386130E+01                4
NAA        11/ 2/94       C  38H  24     0     0G   300.000  5000.000 1676.000    21
 7.23604985E+01 1.02697241E-01-3.77939460E-05 6.18220832E-09-3.72431951E-13    2
 4.18120748E+04-3.59926441E+02 5.78133522E+00 2.32832990E-01-1.17579056E-04    3
 2.02560392E-08 4.29610228E-13 6.59468058E+04 4.65008844E+00                4
AAA        11/ 2/94       C  42H  26     0     0G   300.000  5000.000 1392.000    21
 9.60644156E+01 9.12565557E-02-3.19959594E-05 5.05187811E-09-2.96600234E-13    2
 3.81127972E+04-4.96101380E+02-8.17579551E+00 3.21163107E-01-2.16703802E-04    3
 6.82115190E-08-7.81922394E-12 7.51200060E+04 6.76376847E+01                4
NNN-       11/ 2/94       C  30H  19     0     0G   300.000  5000.000 1395.000    21
 6.85514805E+01 6.53827769E-02-2.28729774E-05 3.60608368E-09-2.11498865E-13    2
 5.54003230E+04-3.40649124E+02-1.01272814E+01 2.49101655E-01-1.84423941E-04    3
 6.71243875E-08-9.62785046E-12 8.23970931E+04 8.13766476E+01                4
```

```
NNA-      11/ 2/94      C  34H  21    0    0G   300.000  5000.000 1371.000    21
 7.65233920E+01 7.50625724E-02-2.64784562E-05 4.19735457E-09-2.47102135E-13    2
 5.92631404E+04-3.83318297E+02 2.77532687E+00 2.17681379E-01-1.15884199E-04    3
 2.07128948E-08 8.02318795E-13 8.75306315E+04 2.27670532E+01                   4
NAA-      11/ 2/94      C  38H  23    0    0G   300.000  5000.000 1390.000    21
 8.65485349E+01 8.16981177E-02-2.87387703E-05 4.54735196E-09-2.67372413E-13    2
 6.26749673E+04-4.38481454E+02-8.01347247E+00 2.89988621E-01-1.96145184E-04    3
 6.20018761E-08-7.18305550E-12 9.63177509E+04 7.30889666E+01                   4
AAA-      11/ 2/94      C  42H  25    0    0G   300.000  5000.000 1385.000    21
 9.83363888E+01 8.77471935E-02-3.10095034E-05 4.92202366E-09-2.90040114E-13    2
 6.48697057E+04-5.06089267E+02-7.72514039E+00 3.09943787E-01-1.92528241E-04    3
 4.97405899E-08-3.25837960E-12 1.03488257E+05 7.13145507E+01                   4
NNNN      11/ 2/94      C  40H  26    0    0G   300.000  5000.000 1823.000    31
 8.10932244E+01 1.02693803E-01-3.72297284E-05 6.03179313E-09-3.61033053E-13    2
 4.34075956E+04-4.03471544E+02-1.54795278E+01 3.44122759E-01-2.60225279E-04    3
 9.69938022E-08-1.42640454E-11 7.34472579E+04 1.06730935E+02                   4
NNNA      11/ 2/94      C  44H  28    0    0G   300.000  5000.000 1374.000    31
 1.00751639E+02 9.79451866E-02-3.45101597E-05 5.46646240E-09-3.21654055E-13    2
 4.04643911E+04-5.15278947E+02 1.44476759E+00 2.94474702E-01-1.63836528E-04    3
 3.36157371E-08-2.06785209E-13 7.80279981E+04 2.98639925E+01                   4
NNAA      11/ 2/94      C  48H  30    0    0G   300.000  5000.000 1397.000    31
 1.10265340E+02 1.04213973E-01-3.64627241E-05 5.74923281E-09-3.37223647E-13    2
 4.44239061E+04-5.66433450E+02-1.24680807E+01 3.82043623E-01-2.68659371E-04    3
 9.01732265E-08-1.14721103E-11 8.72565960E+04 9.47407149E+01                   4
NAAA      11/ 2/94      C  52H  32    0    0G   300.000  5000.000 1394.000    31
 1.19368015E+02 1.12255073E-01-3.93494934E-05 6.21207561E-09-3.64683637E-13    2
 4.80344011E+04-6.16969694E+02-1.20364745E+01 4.05103979E-01-2.78168912E-04    3
 8.97444422E-08-1.06989001E-11 9.43404453E+04 9.25296212E+01                   4
AAAA      11/ 2/94      C  56H  34    0    0G   300.000  5000.000 1391.000    31
 1.30000768E+02 1.19092869E-01-4.18462451E-05 6.61695078E-09-3.88895690E-13    2
 5.10033711E+04-6.77440915E+02-8.65907333E+00 4.15777704E-01-2.66533223E-04    3
 7.49052320E-08-6.55348083E-12 1.00936622E+05 7.53364931E+01                   4
NNNN-     11/ 2/94      C  40H  25    0    0G   300.000  5000.000 1819.000    31
 8.04874040E+01 1.00858344E-01-3.66385976E-05 5.94378477E-09-3.56090021E-13    2
 7.20215092E+04-3.95381436E+02-1.43280454E+01 3.37056305E-01-2.53934730E-04    3
 9.42090976E-08-1.37910836E-11 1.01601246E+05 1.05846051E+02                   4
NNNA-     11/ 2/94      C  44H  27    0    0G   300.000  5000.000 2035.000    31
 8.56017226E+01 1.14728707E-01-4.21620694E-05 6.89064015E-09-4.14866953E-13    2
 7.71493250E+04-4.21306551E+02 2.04329924E+00 2.92406849E-01-1.71567728E-04    3
 4.38273888E-08-3.52846028E-12 1.06174339E+05 3.12256239E+01                   4
NNAA-     11/ 2/94      C  48H  29    0    0G   300.000  5000.000 1395.000    31
 1.09638892E+02 1.02293583E-01-3.58212469E-05 5.65126960E-09-3.31606686E-13    2
 7.31244979E+04-5.57801858E+02-1.06441229E+01 3.73732664E-01-2.61839042E-04    3
 8.74645256E-08-1.10621955E-11 1.15210272E+05 9.05122082E+01                   4
NAAA-     11/ 2/94      C  52H  31    0    0G   300.000  5000.000 1393.000    31
 1.18644178E+02 1.10277411E-01-3.86564157E-05 6.10267189E-09-3.58261333E-13    2
 7.68967025E+04-6.07436797E+02-9.81835821E+00 3.96583486E-01-2.72422563E-04    3
 8.81361837E-08-1.05808496E-11 1.22193368E+05 8.62218456E+01                   4
AAAA-     11/ 2/94      C  56H  33    0    0G   300.000  5000.000 1387.000    31
 1.31631691E+02 1.15925734E-01-4.09302440E-05 6.49290948E-09-3.82457103E-13    2
 7.81871443E+04-6.83105285E+02-1.00343455E+01 4.14641365E-01-2.60354491E-04    3
 6.86881703E-08-4.83664200E-12 1.29537243E+05 8.73795428E+01                   4
NNNNN     11/ 2/94      C  50H  32    0    0G   300.000  5000.000 1825.000    41
 1.01715390E+02 1.26899892E-01-4.59776999E-05 7.44640300E-09-4.45600948E-13    2
 5.50627573E+04-5.09352266E+02-1.91469217E+01 4.29938984E-01-3.26769625E-04    3
 1.22352017E-07-1.80613430E-11 9.25644640E+04 1.28842709E+02                   4
NNNNN-    11/ 2/94      C  50H  31    0    0G   300.000  5000.000 1805.000    41
 1.02481371E+02 1.24320283E-01-4.52333457E-05 7.34618981E-09-4.40443135E-13    2
 8.30322768E+04-5.09236363E+02-1.80488551E+01 4.23676415E-01-3.19308496E-04    3
 1.17938204E-07-1.71366354E-11 1.20691312E+05 1.28190301E+02                   4
C1NNN     11/ 2/94      C  30H  18    0    0G   300.000  5000.000 1390.000    11
 6.73507816E+01 6.50147983E-02-2.29131313E-05 3.63009699E-09-2.13625894E-13    2
 3.06517864E+04-3.41445927E+02-1.30766726E+01 2.48912518E-01-1.80029183E-04    3
 6.31061629E-08-8.61326208E-12 5.86535955E+04 9.13720695E+01                   4
C1NNA     11/ 2/94      C  34H  20    0    0G   300.000  5000.000 1388.000    11
 7.70718170E+01 7.23003153E-02-2.54881862E-05 4.03895678E-09-2.37726906E-13    2
 3.36847827E+04-3.93531572E+02-1.11535492E+01 2.68672931E-01-1.85890693E-04    3
 6.05449263E-08-7.35515379E-12 6.48575776E+04 8.30173742E+01                   4
C1NAA     11/ 2/94      C  38H  22    0    0G   300.000  5000.000 1388.000    11
```

```
 8.63922125E+01 7.99452584E-02-2.81905091E-05 4.46794748E-09-2.63008364E-13    2
 3.70357180E+04-4.44429731E+02-1.12804674E+01 2.96867853E-01-2.04713700E-04    3
 6.62600962E-08-7.96071652E-12 7.15881732E+04 8.33082274E+01                   4
C1AAA     11/ 2/94      C  42H  24    0    0G   300.000  5000.000 2031.000    11
 7.78202640E+01 1.09229356E-01-4.01967235E-05 6.57508971E-09-3.96092568E-13    2
 4.93397113E+04-3.91773847E+02 8.46198733E-01 2.70075629E-01-1.53831822E-04    3
 3.70512361E-08-2.52869358E-12 7.63684557E+04 2.61379255E+01                   4
C2NNN     11/ 2/94      C  30H  16    0    0G   300.000  5000.000 1383.000    01
 6.33528270E+01 6.42018881E-02-2.27367601E-05 3.61352599E-09-2.13108186E-13    2
 3.56516428E+04-3.22868116E+02-1.29839493E+01 2.34540488E-01-1.64171027E-04    3
 5.54413844E-08-7.27069249E-12 6.27727680E+04 8.96374747E+01                   4
C2NNA     11/ 2/94      C  34H  18    0    0G   300.000  5000.000 1381.000    01
 7.28420385E+01 7.17851121E-02-2.54368518E-05 4.04423233E-09-2.38575544E-13    2
 3.86914027E+04-3.73646954E+02-1.18556347E+01 2.56651280E-01-1.73135727E-04    3
 5.47928873E-08-6.44623586E-12 6.91330966E+04 8.53984792E+01                   4
C2NAA     11/ 2/94      C  38H  20    0    0G   300.000  5000.000 1753.000    01
 7.03676519E+01 9.47315557E-02-3.49544529E-05 5.72770090E-09-3.45467742E-13    2
 4.87522610E+04-3.54955866E+02-1.32310478E+01 2.90607035E-01-2.01743776E-04    3
 6.74815741E-08-8.80563807E-12 7.60533773E+04 9.14367661E+01                   4
C2AAA     11/ 2/94      C  42H  22    0    0G   300.000  5000.000 1380.000    01
 9.15192803E+01 8.70428370E-02-3.08301649E-05 4.90042240E-09-2.89033340E-13    2
 4.52273619E+04-4.76627163E+02-1.01833405E+01 3.05152666E-01-1.99363940E-04    3
 5.92803257E-08-6.14781228E-12 8.20915186E+04 7.58266508E+01                   4
C1NNN-    11/ 2/94      C  30H  17    0    0G   300.000  5000.000 1387.000    11
 6.65158140E+01 6.32916009E-02-2.23443266E-05 3.54397755E-09-2.08719275E-13    2
 5.93859217E+04-3.32230009E+02-1.10886266E+01 2.38830782E-01-1.70125058E-04    3
 5.83913510E-08-7.75301419E-12 8.66135610E+04 8.61030434E+01                   4
C1NNA-    11/ 2/94      C  34H  19    0    0G   300.000  5000.000 1386.000    11
 7.60986020E+01 7.07019460E-02-2.49636394E-05 3.95983514E-09-2.33230242E-13    2
 6.24250237E+04-3.83416107E+02-9.61965599E+00 2.60607656E-01-1.79292681E-04    3
 5.80257470E-08-7.00146750E-12 9.28381057E+04 7.99689561E+01                   4
C1NAA-    11/ 2/94      C  38H  21    0    0G   300.000  5000.000 1386.000    11
 8.53821001E+01 7.83798613E-02-2.76776464E-05 4.39067777E-09-2.58620538E-13    2
 6.57889367E+04-4.34009711E+02-9.77510467E+00 2.88889161E-01-1.98291996E-04    3
 6.38798199E-08-7.64272506E-12 9.95746594E+04 8.04988507E+01                   4
C1AAA-    11/ 2/94      C  42H  23    0    0G   300.000  5000.000 1684.000    11
 7.62344184E+01 1.08181687E-01-3.98692827E-05 6.52753282E-09-3.93469138E-13    2
 7.83531594E+04-3.77960676E+02 4.95483042E+00 2.50051078E-01-1.30767888E-04    3
 2.53755257E-08-3.76341406E-13 1.03984649E+05 1.15120058E+01                   4
C2NNN-    11/ 2/94      C  30H  15    0    0G   300.000  5000.000 1381.000    01
 6.29158893E+01 6.21992483E-02-2.20859537E-05 3.51621867E-09-2.07618919E-13    2
 6.40496180E+04-3.16244733E+02-1.25065928E+01 2.30490470E-01-1.62093248E-04    3
 5.50944084E-08-7.30566879E-12 9.08753365E+04 9.13726750E+01                   4
C2NNA-    11/ 2/94      C  34H  17    0    0G   300.000  5000.000 1379.000    01
 7.21259056E+01 6.99611181E-02-2.48339348E-05 3.95290662E-09-2.33372144E-13    2
 6.72021380E+04-3.65168044E+02-1.03847216E+01 2.48579409E-01-1.65839496E-04    3
 5.15314008E-08-5.88305107E-12 9.70272405E+04 8.25853187E+01                   4
C2NAA-    11/ 2/94      C  38H  19    0    0G   300.000  5000.000 1748.000    01
 6.97438288E+01 9.27740392E-02-3.42899337E-05 5.62489686E-09-3.39[illegible]751E-13    2
 7.72253722E+04-3.46879108E+02-1.13554713E+01 2.81131408E-01-1.92784015E-04    3
 6.34006029E-08-8.09989555E-12 1.03876118E+05 8.67702013E+01                   4
C2AAA-    11/ 2/94      C  42H  21    0    0G   300.000  5000.000 1378.000    01
 9.06779287E+01 8.53313741E-02-3.02671732E-05 4.81542315E-09-2.84201460E-13    2
 7.37954059E+04-4.67211522E+02-8.50755841E+00 2.96265073E-01-1.91171090E-04    3
 5.56226536E-08-5.52287703E-12 1.09953669E+05 7.22492397E+01                   4
C1NNNN    11/ 2/94      C  40H  24    0    0G   300.000  5000.000 1393.000    21
 9.18296438E+01 8.48882560E-02-2.98515964E-05 4.72278381E-09-2.77671092E-13    2
 4.02686940E+04-4.69971167E+02-1.61774472E+01 3.32741567E-01-2.41549984E-04    3
 8.43527359E-08-1.13539320E-11 7.76534315E+04 1.10729367E+02                   4
C1NNNA    11/ 2/94      C  44H  26    0    0G   300.000  5000.000 1392.000    21
 1.01684825E+02 9.20722334E-02-3.23946751E-05 5.12699416E-09-3.01515965E-13    2
 4.32359886E+04-5.22527732E+02-1.49151914E+01 3.55418116E-01-2.51527009E-04    3
 8.42257573E-08-1.06143132E-11 8.39566326E+04 1.05770214E+02                   4
C1NNAA    11/ 2/94      C  48H  28    0    0G   300.000  5000.000 1391.000    21
 1.10993655E+02 9.97301672E-02-3.51021101E-05 5.55684298E-09-3.26849650E-13    2
 4.65881327E+04-5.72945645E+02-1.51395442E+01 3.83977038E-01-2.70857240E-04    3
 9.02433942E-08-1.12847742E-11 9.07040140E+04 1.06950433E+02                   4
C1NAAA    11/ 2/94      C  52H  30    0    0G   300.000  5000.000 2025.000    21
 9.72001952E+01 1.35307599E-01-4.97889844E-05 8.14367369E-09-4.90569080E-13    2
```

```
 6.13552246E+04-4.89228958E+02 2.87008272E+00 3.30701687E-01-1.85484704E-04    3
 4.31135373E-08-2.58925057E-12 9.46365365E+04 2.35109932E+01                   4
C1AAAA    11/ 2/94       C  56H  32    0    0G   300.000  5000.000 1389.000   21
 1.25409647E+02 1.18437411E-01-4.16415671E-05 6.58688114E-09-3.87209638E-13    2
 5.47976771E+04-6.52145615E+02-1.05380402E+01 4.15214281E-01-2.76350007E-04    3
 8.48247984E-08-9.28275854E-12 1.03392005E+05 8.41987787E+01                   4
C2NNNN    11/ 2/94       C  40H  22    0    0G   300.000  5000.000 1791.000   11
 7.52695574E+01 1.00331136E-01-3.68979107E-05 6.03330783E-09-3.63377649E-13    2
 5.23245635E+04-3.76550738E+02-1.82639020E+01 3.27238292E-01-2.39273355E-04    3
 8.54798217E-08-1.20375141E-11 8.21317116E+04 1.20142112E+02                   4
C2NNNA    11/ 2/94       C  44H  24    0    0G   300.000  5000.000 1763.000   11
 8.36930478E+01 1.09261001E-01-4.01962099E-05 6.57432610E-09-3.96038415E-13    2
 5.60370855E+04-4.20631001E+02-1.70068191E+01 3.49896191E-01-2.50321784E-04    3
 8.68224551E-08-1.17998595E-11 8.84440827E+04 1.15354276E+02                   4
C2NNAA    11/ 2/94       C  48H  26    0    0G   300.000  5000.000 1758.000   11
 9.18937249E+01 1.18365390E-01-4.35500180E-05 7.12338719E-09-4.29137510E-13    2
 6.00258574E+04-4.64429574E+02-1.71051267E+01 3.78069942E-01-2.69366884E-04    3
 9.28712515E-08-1.25262349E-11 9.51684490E+04 1.15983765E+02                   4
C2NAAA    11/ 2/94       C  52H  28    0    0G   300.000  5000.000 1385.000   11
 1.15870429E+02 1.07060345E-01-3.78248485E-05 6.00245806E-09-3.53642756E-13    2
 5.49009831E+04-6.02184775E+02-1.42165351E+01 3.93198041E-01-2.67434265E-04    3
 8.46939145E-08-9.82066615E-12 1.01232023E+05 1.01735095E+02                   4
C2AAAA    11/ 2/94       C  56H  30    0    0G   300.000  5000.000 1374.000   11
 1.21147485E+02 1.18441243E-01-4.18818378E-05 6.64969786E-09-3.91904613E-13    2
 5.97344390E+04-6.31136764E+02-2.63210243E+00 3.66911343E-01-2.11435166E-04    3
 4.81724556E-08-1.85944623E-12 1.06310793E+05 4.72853336E+01                   4
C3NNNN    11/ 2/94       C  40H  20    0    0G   300.000  5000.000 1797.000   01
 7.36515585E+01 9.78497166E-02-3.62357280E-05 5.95134320E-09-3.59513644E-13    2
 4.98193985E+04-3.76799153E+02-1.61596368E+01 3.13294550E-01-2.26335811E-04    3
 7.98918953E-08-1.11517294E-11 7.87491398E+04 1.01128517E+02                   4
C3NNNA    11/ 2/94       C  44H  22    0    0G   300.000  5000.000 1782.000   01
 8.16473174E+01 1.07190894E-01-3.96863205E-05 6.51718536E-09-3.93660334E-13    2
 5.37020329E+04-4.18780591E+02-1.53287122E+01 3.37551359E-01-2.40162764E-04    3
 8.31100949E-08-1.13348276E-11 8.51385437E+04 9.80475123E+01                   4
C3NNAA    11/ 2/94       C  48H  24    0    0G   300.000  5000.000 1760.000   01
 8.96381667E+01 1.16495321E-01-4.31144541E-05 7.07844119E-09-4.27494375E-13    2
 5.76084441E+04-4.60994049E+02-1.34241824E+01 3.57434797E-01-2.47987963E-04    3
 8.29251106E-08-1.08364011E-11 9.13556133E+04 8.95882934E+01                   4
C3NAAA    11/ 2/94       C  52H  26    0    0G   300.000  5000.000 1755.000   01
 9.76582167E+01 1.25766330E-01-4.65284966E-05 7.63717253E-09-4.61166377E-13    2
 6.16737409E+04-5.04561171E+02-1.32721051E+01 3.84483461E-01-2.65685331E-04    3
 8.83208428E-08-1.14493782E-11 9.80446639E+04 8.82519459E+01                   4
C3AAAA    11/ 2/94       C  56H  28    0    0G   300.000  5000.000 1744.000   01
 1.05813345E+02 1.34907461E-01-4.98941343E-05 8.18795460E-09-4.94359259E-13    2
 6.55411138E+04-5.49429754E+02-1.18318037E+01 4.06935084E-01-2.77338675E-04    3
 9.03670787E-08-1.14018846E-11 1.04315620E+05 8.00618868E+01                   4
C1NNNN-   11/ 2/94       C  40H  23    0    0G   300.000  5000.000 1391.000   21
 9.08650647E+01 8.32975578E-02-2.93328398E-05 4.64487982E-09-2.73257608E-13    2
 6.90429265E+04-4.59752593E+02-1.48875280E+01 3.25551208E-01-2.36056841E-04    3
 8.24405040E-08-1.11226039E-11 1.05726760E+05 1.09040356E+02                   4
C1NNNA-   11/ 2/94       C  44H  25    0    0G   300.000  5000.000 1390.000   21
 1.00620016E+02 9.05580660E-02-3.19000199E-05 5.05258140E-09-2.97293813E-13    2
 7.20687995E+04-5.11614394E+02-1.34865818E+01 3.47835405E-01-2.45808806E-04    3
 8.23245985E-08-1.04070441E-11 1.12004051E+05 1.03473419E+02                   4
C1NNAA-   11/ 2/94       C  48H  27    0    0G   300.000  5000.000 1379.000   21
 1.06292752E+02 1.01670896E-01-3.58789861E-05 5.68909956E-09-3.34988857E-13    2
 7.67206188E+04-5.41033874E+02-3.24129623E+00 3.28542833E-01-2.00268839E-04    3
 5.21848642E-08-3.83030434E-12 1.17201341E+05 5.67661223E+01                   4
C1NAAA-   11/ 2/94       C  52H  29    0    0G   300.000  5000.000 1388.000   21
 1.15750973E+02 1.08721175E-01-3.82670217E-05 6.05739030E-09-3.56256378E-13    2
 7.99209626E+04-5.93050651E+02-8.85661070E+00 3.79192082E-01-2.50178669E-04    3
 7.55560601E-08-8.00583497E-12 1.24620477E+05 8.24278169E+01                   4
C1AAAA-   11/ 2/94       C  56H  31    0    0G   300.000  5000.000 1387.000   21
 1.24815376E+02 1.16593429E-01-4.10501992E-05 6.49927666E-09-3.82300472E-13    2
 8.33177556E+04-6.43902771E+02-9.16396383E+00 4.07136785E-01-2.68391683E-04    3
 8.09127581E-08-8.54463405E-12 1.31411279E+05 8.24837029E+01                   4
C2NNNN-   11/ 2/94       C  40H  21    0    0G   300.000  5000.000 1792.000   11
 7.45682777E+01 9.84652999E-02-3.62708266E-05 5.93695706E-09-3.57826013E-13    2
 8.09051026E+04-3.67997900E+02-1.70603633E+01 3.20188376E-01-2.33507673E-04    3
```

```
 8.31730272E-08-1.16824361E-11 1.10172539E+05 1.18803928E+02                4
C2NNNA-   11/ 2/94       C  44H  23     0     0G   300.000  5000.000 1761.000    11
 8.29451611E+01 1.07411975E-01-3.95690279E-05 6.47726973E-09-3.90415214E-13    2
 8.46662159E+04-4.11643278E+02-1.52434433E+01 3.40884170E-01-2.42196462E-04    3
 8.33034034E-08-1.12188493E-11 1.16386645E+05 1.11407342E+02                4
C2NNAA-   11/ 2/94       C  48H  25     0     0G   300.000  5000.000 1758.000    11
 9.10684511E+01 1.16589186E-01-4.29495409E-05 7.03066367E-09-4.23773067E-13    2
 8.86267916E+04-4.54943080E+02-1.55427989E+01 3.69711146E-01-2.62135261E-04    3
 8.98729021E-08-1.20520994E-11 1.23098510E+05 1.13098386E+02                4
C2NAAA-   11/ 2/94       C  52H  27     0     0G   300.000  5000.000 1374.000    11
 1.11489887E+02 1.08575800E-01-3.84226584E-05 6.10351454E-09-3.59837674E-13    2
 8.48549717E+04-5.72109412E+02-2.23552570E+00 3.36782653E-01-1.94248403E-04    3
 4.44214567E-08-1.77523742E-12 1.27679106E+05 5.12747254E+01                4
C2AAAA-   11/ 2/94       C  56H  29     0     0G   300.000  5000.000 1367.000    11
 1.18833807E+02 1.18072850E-01-4.18024924E-05 6.64229982E-09-3.91676021E-13    2
 8.89034919E+04-6.12917146E+02 4.22786509E+00 3.34178859E-01-1.70040770E-04    3
 2.54508269E-08 2.69553114E-12 1.33479922E+05 2.02718318E+01                4
C3NNNN-   11/ 2/94       C  40H  19     0     0G   300.000  5000.000 1806.000    01
 7.35196374E+01 9.54789687E-02-3.54303542E-05 5.82679999E-09-3.52309025E-13    2
 7.81316276E+04-3.71612181E+02-1.59072049E+01 3.11024192E-01-2.26981351E-04    3
 8.10460569E-08-1.14592197E-11 1.06860922E+05 1.03944399E+02                4
C3NNNA-   11/ 2/94       C  44H  21     0     0G   300.000  5000.000 1775.000    01
 8.12758610E+01 1.05019548E-01-3.89491923E-05 6.40326625E-09-3.87073776E-13    2
 8.20917710E+04-4.12138818E+02-1.38825094E+01 3.29549609E-01-2.32600606E-04    3
 7.95486959E-08-1.06943220E-11 1.13085472E+05 9.55411878E+01                4
C3NNAA-   11/ 2/94       C  48H  23     0     0G   300.000  5000.000 1753.000    01
 8.92116298E+01 1.14373811E-01-4.23950099E-05 6.96731573E-09-4.21071102E-13    2
 8.59873218E+04-4.53907628E+02-1.16158503E+01 3.48154446E-01-2.38906296E-04    3
 7.86009516E-08-1.00573910E-11 1.19189093E+05 8.54244009E+01                4
C3NAAA-   11/ 2/94       C  52H  25     0     0G   300.000  5000.000 1750.000    01
 9.71725004E+01 1.23704735E-01-4.58320367E-05 7.52989027E-09-4.54977560E-13    2
 9.00626615E+04-4.97087687E+02-1.17400595E+01 3.76114392E-01-2.57782822E-04    3
 8.46514921E-08-1.08002798E-11 1.25929200E+05 8.55179288E+01                4
C3AAAA-   11/ 2/94       C  56H  27     0     0G   300.000  5000.000 1365.000    01
 1.17864368E+02 1.14550696E-01-4.06615181E-05 6.47205347E-09-3.82085270E-13    2
 8.61060299E+04-6.16108044E+02 6.05124892E+00 3.23770597E-01-1.63042242E-04    3
 2.33547514E-08 2.87683319E-12 1.29828286E+05 2.34599024E+00                4
C1NNNNN   11/ 2/94       C  50H  30     0     0G   300.000  5000.000 1777.000    31
 1.01785358E+02 1.23677231E-01-4.52296735E-05 7.37025286E-09-4.42904825E-13    2
 5.81671154E+04-5.12679769E+02-2.15105185E+01 4.26444114E-01-3.18285409E-04    3
 1.15529357E-07-1.64284137E-11 9.69958791E+04 1.40550352E+02                4
C2NNNNN   11/ 2/94       C  50H  28     0     0G   300.000  5000.000 1791.000    21
 9.67381126E+01 1.24025567E-01-4.55184573E-05 7.43344615E-09-4.47333162E-13    2
 6.35825415E+04-4.86842724E+02-2.24740813E+01 4.15460421E-01-3.07577507E-04    3
 1.11149094E-07-1.58019901E-11 1.01318732E+05 1.45343697E+02                4
C3NNNNN   11/ 2/94       C  50H  26     0     0G   300.000  5000.000 1777.000    11
 9.56966075E+01 1.20975440E-01-4.46373329E-05 7.31448952E-09-4.41187538E-13    2
 6.21148878E+04-4.92787550E+02-1.78141750E+01 3.93506583E-01-2.84425719E-04    3
 9.98870545E-08-1.37837673E-11 9.85578525E+04 1.10993275E+02                4
C4NNNNN   11/ 2/94       C  50H  24     0     0G   300.000  5000.000 1778.000    01
 9.20408088E+01 1.20048423E-01-4.44721108E-05 7.30596085E-09-4.41428298E-13    2
 6.69228978E+04-4.78043514E+02-1.93090710E+01 3.85116381E-01-2.75544182E-04    3
 9.56700136E-08-1.30623296E-11 1.02939618E+05 1.15140873E+02                4
C1NNNNN-  11/ 2/94       C  50H  29     0     0G   300.000  5000.000 1777.000    31
 1.01011278E+02 1.21870527E-01-4.46205403E-05 7.27628773E-09-4.37469749E-13    2
 8.68574082E+04-5.03327206E+02-1.99569245E+01 4.18307143E-01-3.11371811E-04    3
 1.12698336E-07-1.59845717E-11 1.25021833E+05 1.37807264E+02                4
C2NNNNN-  11/ 2/94       C  50H  27     0     0G   300.000  5000.000 1784.000    21
 9.60729964E+01 1.22108482E-01-4.48682903E-05 7.33285581E-09-4.41506600E-13    2
 9.21839433E+04-4.78165564E+02-2.03792049E+01 4.05183767E-01-2.97622087E-04    3
 1.06544273E-07-1.49966609E-11 1.29204538E+05 1.39963846E+02                4
C3NNNNN-  11/ 2/94       C  50H  25     0     0G   300.000  5000.000 1772.000    11
 9.50459087E+01 1.19045812E-01-4.39835362E-05 7.21347179E-09-4.35343975E-13    2
 9.06943375E+04-4.84307189E+02-1.60443184E+01 3.84378904E-01-2.75917073E-04    3
 9.60568763E-08-1.31277562E-11 1.26500816E+05 1.07104953E+02                4
C4NNNNN-  11/ 2/94       C  50H  23     0     0G   300.000  5000.000 1773.000    01
 9.16300870E+01 1.17907985E-01-4.37449076E-05 7.19349578E-09-4.34921872E-13    2
 9.53312868E+04-4.71083660E+02-1.78918572E+01 3.77251000E-01-2.68252370E-04    3
 9.22976019E-08-1.24645630E-11 1.30891163E+05 1.12855045E+02                4
```

```
N2                      N   2    0    0    0G   300.000  5000.000 1361.000    01
 2.97194844E+00 1.24625792E-03-3.69731751E-07 4.93199963E-11-2.45610942E-15    2
-8.97416330E+02 5.84774887E+00 3.28917809E+00 4.95014977E-04 3.03204911E-07    3
-2.22444279E-10 3.94658465E-14-1.00492804E+03 4.15023583E+00                   4
h2                      H   2    0    0    0G   300.000  5000.000 1374.000    01
 2.81960206E+00 1.02640406E-03-2.61659739E-07 2.82559656E-11-1.04235129E-15    2
-7.56554725E+02-3.98138546E-01 3.56735260E+00-4.35937503E-04 7.58733449E-07    3
-2.67813045E-10 2.78894714E-14-1.05041729E+03-4.52471044E+00                   4
h                       H   1    0    0    0G   300.000  5000.000 1000.000    01
 2.51614107E+00 0.00000000E+00 0.00000000E+00 0.00000000E+00 0.00000000E+00    2
 2.54702455E+04-5.46324347E-01 2.51614107E+00 0.00000000E+00 0.00000000E+00    3
 0.00000000E+00 0.00000000E+00 2.54702455E+04-5.46324347E-01                   4
END
```

Appendix G: Selected Full Output from CHEMKIN Calculations

(units are mole fraction)

Pure naphthalene pyrolysis at 1177K

t(sec)= 0.0000E+00 P(atm)= 9.5000E-01 T(K)= 1.1770E+03

N2	= 9.99E-01	h2	= 0.00E+00	h	= 0.00E+00	n	= 1.45E-03

t(sec)= 2.0900E+00 P(atm)= 9.5000E-01 T(K)= 1.1770E+03

N2	= 9.99E-01	h2	= 7.50E-05	h	= 6.10E-09	n	= 1.31E-03
n1-	= 3.15E-08	n2-	= 1.95E-08	n1n1	= 1.26E-05	n1n1-1	= 8.38E-19
n1n1-2	= 1.17E-18	n1n1-4	= 6.03E-10	n1n2	= 3.44E-05	n1n2-1	= 7.23E-18
n1n2-2	= 2.76E-18	n1n2-4	= 2.28E-09	n2n2	= 1.99E-05	n2n2-4	= 2.94E-09
BkF	= 6.92E-09	BjF	= 1.78E-08	Per	= 8.30E-07	BkF-	= 1.83E-13
BjF-	= 4.75E-13	Per-	= 3.05E-10	NNN	= 2.97E-06	NNN-	= 1.42E-18
NNNN	= 1.28E-07	NNNN-	= 6.14E-20	NNNNN	= 7.47E-09	NNNNN-	= 4.01E-21
C1NNN	= 1.18E-08	C2NNN	= 7.22E-10	C1NNN-	= 9.55E-20	C2NNN-	= 2.39E-14
C1NNNN	= 8.57E-10	C2NNNN	= 3.26E-13	C3NNNN	= 1.37E-13	C1NNNN-	= 6.72E-22
C2NNNN-	= 9.30E-24	C3NNNN-	= 1.93E-17	C1NNNNN	= 1.38E-10	C2NNNNN	= 7.27E-13
C3NNNNN	= 1.34E-15	C4NNNNN	= 3.98E-17	C1NNNNN-	= 9.66E-23	C2NNNNN-	= 2.89E-24
		C3NNNNN-	= 3.93E-26	C4NNNNN-	= 4.25E-20		

Pure naphthalene pyrolysis at 1277K

t(sec)= 0.0000E+00 P(atm)= 9.5000E-01 T(K)= 1.2770E+03

N2	= 9.97E-01	h2	= 0.00E+00	h	= 0.00E+00	n	= 3.34E-03

t(sec)= 1.9300E+00 P(atm)= 9.5000E-01 T(K)= 1.2770E+03

N2	= 9.96E-01	h2	= 1.07E-03	h	= 3.48E-08	n	= 1.78E-03
n1-	= 3.60E-07	n2-	= 2.48E-07	n1n1	= 5.39E-05	n1n1-1	= 6.75E-17
n1n1-2	= 7.60E-17	n1n1-4	= 2.31E-08	n1n2	= 1.90E-04	n1n2-1	= 4.42E-16
n1n2-2	= 1.70E-16	n1n2-4	= 9.47E-08	n2n2	= 1.87E-04	n2n2-4	= 1.36E-07
BkF	= 9.49E-08	BjF	= 2.45E-07	Per	= 2.35E-04	BkF-	= 2.26E-11
BjF-	= 6.33E-11	Per-	= 1.70E-07	NNN	= 5.26E-05	NNN-	= 6.50E-16
NNNN	= 8.86E-06	NNNN-	= 1.12E-16	NNNNN	= 1.43E-06	NNNNN-	= 2.66E-17
C1NNN	= 3.76E-06	C2NNN	= 3.22E-06	C1NNN-	= 2.08E-15	C2NNN-	= 6.02E-10
C1NNNN	= 1.47E-06	C2NNNN	= 2.30E-08	C3NNNN	= 4.07E-08	C1NNNN-	= 1.81E-17
C2NNNN-	= 1.54E-17	C3NNNN-	= 3.20E-11	C1NNNNN	= 3.80E-07	C2NNNNN	= 2.99E-08
C3NNNNN	= 8.92E-10	C4NNNNN	= 4.01E-10	C1NNNNN-	= 1.14E-17	C2NNNNN-	= 1.17E-17
		C3NNNNN-	= 1.99E-18	C4NNNNN-	= 6.33E-13		

Pure naphthalene pyrolysis at 1350K

t(sec)= 0.0000E+00 P(atm)= 9.5000E-01 T(K)= 1.3500E+03

N2	= 9.93E-01	h2	= 0.00E+00	h	= 0.00E+00	n	= 6.92E-03

t(sec)= 1.8200E+00 P(atm)= 9.5000E-01 T(K)= 1.3500E+03

N2	= 9.91E-01	h2	= 4.94E-03	h	= 1.83E-07	n	= 1.81E-03
n1-	= 6.88E-07	n2-	= 4.92E-07	n1n1	= 2.39E-05	n1n1-1	= 1.99E-15
n1n1-2	= 1.51E-15	n1n1-4	= 2.20E-08	n1n2	= 8.45E-05	n1n2-1	= 7.85E-15
n1n2-2	= 2.85E-15	n1n2-4	= 8.76E-08	n2n2	= 8.78E-05	n2n2-4	= 1.22E-07
BkF	= 3.68E-07	BjF	= 1.08E-06	Per	= 2.23E-03	BkF-	= 3.57E-10
BjF-	= 1.03E-09	Per-	= 2.40E-06	NNN	= 1.07E-05	NNN-	= 6.99E-15
NNNN	= 8.21E-07	NNNN-	= 8.15E-16	NNNNN	= 4.95E-08	NNNNN-	= 7.97E-17
C1NNN	= 1.61E-05	C2NNN	= 3.74E-05	C1NNN-	= 1.17E-13	C2NNN-	= 3.44E-08
C1NNNN	= 3.33E-06	C2NNNN	= 1.21E-06	C3NNNN	= 4.70E-06	C1NNNN-	= 2.51E-15
C2NNNN-	= 1.07E-14	C3NNNN-	= 8.36E-09	C1NNNNN	= 2.82E-07	C2NNNNN	= 2.38E-07
C3NNNNN	= 5.61E-08	C4NNNNN	= 4.12E-07	C1NNNNN-	= 4.12E-16	C2NNNNN-	= 4.27E-15
		C3NNNNN-	= 9.96E-15	C4NNNNN-	= 9.70E-10		

Pure naphthalene pyrolysis at 1415K

t(sec)= 0.0000E+00 P(atm)= 9.5000E-01 T(K)= 1.4150E+03

N2	= 9.96E-01	h2	= 0.00E+00	h	= 0.00E+00	n	= 3.53E-03

t(sec)= 1.7400E+00 P(atm)= 9.5000E-01 T(K)= 1.4150E+03

N2	= 9.95E-01	h2	= 3.45E-03	h	= 3.69E-07	n	= 1.94E-04
n1-	= 2.32E-07	n2-	= 1.68E-07	n1n1	= 4.70E-07	n1n1-1	= 3.27E-15
n1n1-2	= 2.38E-15	n1n1-4	= 1.37E-09	n1n2	= 1.59E-06	n1n2-1	= 1.17E-14
n1n2-2	= 4.24E-15	n1n2-4	= 5.27E-09	n2n2	= 1.61E-06	n2n2-4	= 7.10E-09
BkF	= 3.08E-07	BjF	= 9.11E-07	Per	= 1.51E-03	BkF-	= 1.04E-09
BjF-	= 2.97E-09	Per-	= 5.14E-06	NNN	= 3.72E-08	NNN-	= 2.11E-15
NNNN	= 4.77E-10	NNNN-	= 4.40E-17	NNNNN	= 3.26E-12	NNNNN-	= 4.78E-19
C1NNN	= 2.69E-06	C2NNN	= 3.87E-05	C1NNN-	= 2.31E-13	C2NNN-	= 1.75E-07
C1NNNN	= 9.93E-08	C2NNNN	= 1.70E-06	C3NNNN	= 3.35E-05	C1NNNN-	= 6.59E-15
C2NNNN-	= 1.75E-13	C3NNNN-	= 2.20E-07	C1NNNNN	= 9.25E-10	C2NNNNN	= 2.82E-08
C3NNNNN	= 1.03E-07	C4NNNNN	= 3.72E-06	C1NNNNN-	= 9.39E-17	C2NNNNN-	= 1.73E-14
		C3NNNNN-	= 1.72E-13	C4NNNNN-	= 2.72E-08		

Pure naphthalene pyrolysis at 1498K

t(sec)= 0.0000E+00 P(atm)= 9.5000E-01 T(K)= 1.4980E+03

N2	= 1.00E+00	h2	= 0.00E+00	h	= 0.00E+00	n	= 4.83E-04

t(sec)= 1.6400E+00 P(atm)= 9.5000E-01 T(K)= 1.4980E+03

N2	= 9.99E-01	h2	= 6.19E-04	h	= 4.47E-07	n	= 2.46E-06
n1-	= 2.20E-08	n2-	= 1.62E-08	n1n1	= 5.32E-10	n1n1-1	= 3.41E-16
n1n1-2	= 2.52E-16	n1n1-4	= 1.06E-11	n1n2	= 1.66E-09	n1n2-1	= 1.18E-15
n1n2-2	= 4.35E-16	n1n2-4	= 3.78E-11	n2n2	= 1.55E-09	n2n2-4	= 4.76E-11
BkF	= 2.98E-08	BjF	= 8.63E-08	Per	= 9.92E-05	BkF-	= 7.20E-10
BjF-	= 2.02E-09	Per-	= 2.41E-06	NNN	= 3.22E-12	NNN-	= 1.91E-17
NNNN	= 2.80E-15	NNNN-	= 2.86E-20	NNNNN	= 3.91E-19	NNNNN-	= 6.24E-24
C1NNN	= 2.20E-08	C2NNN	= 1.07E-05	C1NNN-	= 7.32E-14	C2NNN-	= 3.67E-07
C1NNNN	= 5.94E-11	C2NNNN	= 9.51E-08	C3NNNN	= 5.03E-05	C1NNNN-	= 4.25E-16
C2NNNN-	= 3.72E-13	C3NNNN-	= 2.39E-06	C1NNNNN	= 1.10E-14	C2NNNNN	= 3.78E-11
C3NNNNN	= 1.59E-08	C4NNNNN	= 6.14E-06	C1NNNNN-	= 1.46E-19	C2NNNNN-	= 3.56E-15
		C3NNNNN-	= 3.23E-13	C4NNNNN-	= 3.20E-07		

Anthracene/naphthalene pyrolysis at 1180K

t(sec)= 0.0000E+00 P(atm)= 9.5000E-01 T(K)= 1.1800E+03

N2	= 9.99E-01	h2	= 0.00E+00	h	= 0.00E+00	n	= 5.75E-04
a	= 5.75E-04	n1-	= 0.00E+00	n2-	= 0.00E+00	a1-	= 0.00E+00

t(sec)= 2.0900E+00 P(atm)= 9.5000E-01 T(K)= 1.1800E+03

N2	= 9.99E-01	h2	= 6.21E-05	h	= 5.56E-09	n	= 5.17E-04
a	= 5.14E-04	n1-	= 1.39E-08	n2-	= 8.46E-09	a1-	= 1.31E-08
a2-	= 7.53E-09	a9-	= 9.07E-09	n1n1	= 2.33E-06	n1n1-1	= 1.42E-19
n1n1-2	= 1.98E-19	n1n1-4	= 1.21E-10	n1n2	= 6.14E-06	n1n2-1	= 1.22E-18
n1n2-2	= 4.65E-19	n1n2-4	= 4.53E-10	n2n2	= 3.41E-06	n2n2-4	= 5.83E-10
a1n1	= 4.45E-06	a1n1-1	= 1.14E-19	a1n1-2	= 2.80E-19	a1n1-3	= 1.34E-19
a1n1-4	= 2.50E-10	a1n2	= 5.99E-06	a1n2-1	= 3.36E-19	a1n2-2	= 3.00E-19
a1n2-3	= 5.48E-19	a1n2-4	= 4.63E-10	a2n1	= 5.96E-06	a2n1-1	= 9.25E-19
a2n1-2	= 3.10E-19	a2n1-4	= 4.81E-10	a2n2	= 6.65E-06	a2n2-4	= 1.16E-09
a9n1	= 2.31E-06	a9n1-1	= 9.37E-20	a9n1-2	= 5.92E-20	a9n1-4	= 1.26E-10
a9n2	= 3.24E-06	a9n2-1	= 5.29E-19	a9n2-2	= 1.43E-19	a9n2-4	= 2.13E-10
a1a1	= 1.43E-06	a1a1-2	= 7.76E-20	a1a1-3	= 9.33E-20	a1a1-4	= 1.08E-10
a1a2	= 4.53E-06	a1a2-1	= 2.88E-19	a1a2-2	= 1.87E-19	a1a2-3	= 4.35E-19
a1a2-4	= 4.42E-10	a1a9	= 1.43E-06	a1a9-1	= 7.50E-20	a1a9-2	= 4.21E-20
a1a9-3	= 4.40E-21	a1a9-4	= 1.07E-10	a2a2	= 2.83E-06	a2a2-4	= 5.47E-10
a2a9	= 2.31E-06	a2a9-1	= 3.86E-19	a2a9-2	= 8.75E-20	a2a9-4	= 2.07E-10
a9a9	= 1.86E-07	a9a9-1	= 2.07E-21	a9a9-4	= 2.06E-11	BkF	= 1.29E-09
BjF	= 3.32E-09	Per	= 1.28E-07	DBajF	= 4.81E-09	DBakF	= 2.26E-09
DBalF	= 4.45E-09	BaPer	= 3.81E-07	N23jF	= 3.91E-09	N23kF	= 1.43E-09
BaN23jF	= 3.13E-09	BaN23kF	= 2.48E-09	BaN231F	= 3.64E-09	DBajPer	= 1.32E-07
DBaoPer	= 1.52E-07	BkF-	= 3.55E-14	BjF-	= 9.20E-14	Per-	= 4.93E-11
DBajF-	= 1.54E-13	DBakF-	= 7.26E-14	DBalF-	= 1.64E-13	BaPer-	= 2.36E-10
N23jF-	= 1.25E-13	N23kF-	= 4.57E-14	BaN23jF-	= 1.11E-13	BaN23kF-	= 8.76E-14
BaN231F-	= 1.45E-13	DBajPer-	= 1.29E-10	DBaoPer-	= 1.30E-10	NNN	= 2.49E-07
NNA	= 1.18E-06	NAA	= 1.19E-06	AAA	= 6.40E-07	NNN-	= 1.10E-19
NNA-	= 5.78E-19	NAA-	= 7.98E-19	AAA-	= 4.54E-19	NNNN	= 4.91E-09
NNNA	= 3.36E-08	NNAA	= 6.68E-08	NAAA	= 6.10E-08	AAAA	= 2.55E-08
NNNN-	= 1.78E-21	NNNA-	= 1.11E-20	NNAA-	= 2.59E-20	NAAA-	= 2.70E-20
AAAA-	= 1.23E-20	NNNNN	= 1.31E-10	NNNNN-	= 6.29E-23	C1NNN	= 9.33E-10

C1NNA	= 6.64E-09	C1NAA	= 1.15E-08	C1AAA	= 3.67E-09	C2NNN	= 4.88E-11
C2NNA	= 3.90E-10	C2NAA	= 7.97E-10	C2AAA	= 2.74E-10	C1NNN-	= 5.91E-21
C1NNA-	= 4.99E-20	C1NAA-	= 1.19E-19	C1AAA-	= 1.45E-20	C2NNN-	= 1.79E-15
C2NNA-	= 1.72E-14	C2NAA-	= 4.09E-14	C2AAA-	= 1.60E-14	C1NNNN	= 2.80E-11
C1NNNA	= 3.05E-10	C1NNAA	= 9.63E-10	C1NAAA	= 5.36E-10	C1AAAA	= 4.38E-10
C2NNNN	= 9.36E-15	C2NNNA	= 9.23E-14	C2NNAA	= 2.65E-13	C2NAAA	= 3.37E-13
C2AAAA	= 7.96E-14	C3NNNN	= 2.08E-15	C3NNNA	= 3.07E-15	C3NNAA	= 9.57E-15
C3NAAA	= 1.22E-14	C3AAAA	= 3.22E-15	C1NNNN-	= 1.49E-23	C1NNNA-	= 1.05E-22
C1NNAA-	= 3.14E-22	C1NAAA-	= 2.02E-22	C1AAAA-	= 1.55E-22	C2NNNN-	= 1.33E-25
C2NNNA-	= 2.82E-25	C2NNAA-	= 6.22E-25	C2NAAA-	= 6.46E-25	C2AAAA-	= 9.25E-26
C3NNNN-	= 5.65E-19	C3NNNA-	= 3.21E-18	C3NNAA-	= 1.11E-17	C3NAAA-	= 1.52E-17
C3AAAA-	= 3.61E-18	C1NNNNN	= 2.21E-12	C2NNNNN	= 1.13E-14	C3NNNNN	= 1.67E-17
C4NNNNN	= 4.67E-19	C1NNNNN-	= 1.41E-24	C2NNNNN-	= 3.41E-26	C3NNNNN-	= 4.20E-28
			C4NNNNN- = 5.26E-22				

Anthracene/naphthalene pyrolysis at 1277K

t(sec)= 0.0000E+00 P(atm)= 9.5000E-01 T(K)= 1.2770E+03

N2	= 9.98E-01	h2	= 0.00E+00	h	= 0.00E+00	n	= 8.09E-04
a	= 8.09E-04	n1-	= 0.00E+00	n2-	= 0.00E+00	a1-	= 0.00E+00

t(sec)= 1.9300E+00 P(atm)= 9.5000E-01 T(K)= 1.2770E+03

N2	= 9.98E-01	h2	= 4.60E-04	h	= 2.51E-08	n	= 4.71E-04
a	= 4.65E-04	n1-	= 1.31E-07	n2-	= 8.80E-08	a1-	= 9.38E-08
a2-	= 5.56E-08	a9-	= 6.82E-08	n1n1	= 7.04E-06	n1n1-1	= 5.21E-18
n1n1-2	= 6.66E-18	n1n1-4	= 4.03E-09	n1n2	= 2.38E-05	n1n2-1	= 3.92E-17
n1n2-2	= 1.52E-17	n1n2-4	= 1.64E-08	n2n2	= 2.19E-05	n2n2-4	= 2.32E-08
a1n1	= 1.15E-05	a1n1-1	= 3.13E-18	a1n1-2	= 7.25E-18	a1n1-3	= 3.82E-18
a1n1-4	= 6.03E-09	a1n2	= 1.94E-05	a1n2-1	= 8.50E-18	a1n2-2	= 7.71E-18
a1n2-3	= 1.36E-17	a1n2-4	= 1.21E-08	a2n1	= 2.00E-05	a2n1-1	= 2.27E-17
a2n1-2	= 7.82E-18	a2n1-4	= 1.28E-08	a2n2	= 3.58E-05	a2n2-4	= 3.38E-08
a9n1	= 6.25E-06	a9n1-1	= 3.04E-18	a9n1-2	= 1.66E-18	a9n1-4	= 3.16E-09
a9n2	= 1.05E-05	a9n2-1	= 1.42E-17	a9n2-2	= 3.88E-18	a9n2-4	= 5.69E-09
a1a1	= 2.71E-06	a1a1-2	= 1.59E-18	a1a1-3	= 2.10E-18	a1a1-4	= 2.16E-09
a1a2	= 9.67E-06	a1a2-1	= 5.51E-18	a1a2-2	= 3.66E-18	a1a2-3	= 8.12E-18
a1a2-4	= 9.16E-09	a1a9	= 2.96E-06	a1a9-1	= 1.72E-18	a1a9-2	= 9.10E-19

a1a9-3 = 3.09E-19	a1a9-4 = 2.28E-09	a2a2 = 9.11E-06	a2a2-4 = 1.23E-08
a2a9 = 5.15E-06	a2a9-1 = 7.96E-18	a2a9-2 = 1.82E-18	a2a9-4 = 4.49E-09
a9a9 = 4.01E-07	a9a9-1 = 1.22E-19	a9a9-4 = 5.24E-10	BkF = 1.18E-08
BjF = 2.94E-08	Per = 1.23E-05	DBajF = 3.46E-08	DBakF = 1.72E-08
DBalF = 3.16E-08	BaPer = 3.94E-05	N23jF = 2.78E-08	N23kF = 1.05E-08
BaN23jF = 1.65E-08	BaN23kF = 1.31E-08	BaN23lF = 1.85E-08	DBajPer = 1.79E-05
DBaoPer = 1.89E-05	BkF- = 2.59E-12	BjF- = 6.90E-12	Per- = 1.31E-08
DBajF- = 9.45E-12	DBakF- = 4.60E-12	DBalF- = 9.57E-12	BaPer- = 5.81E-08
N23jF- = 7.29E-12	N23kF- = 2.66E-12	BaN23jF- = 4.89E-12	BaN23kF- = 3.64E-12
BaN23lF- = 5.52E-12	DBajPer- = 2.92E-08	DBaoPer- = 2.95E-08	NNN = 3.27E-06
NNA = 1.34E-05	NAA = 9.30E-06	AAA = 4.30E-06	NNN- = 2.09E-17
NNA- = 7.87E-17	NAA- = 8.70E-17	AAA- = 3.86E-17	NNNN = 2.57E-07
NNNA = 1.39E-06	NNAA = 2.03E-06	NAAA = 1.36E-06	AAAA = 4.56E-07
NNNN- = 1.39E-18	NNNA- = 6.33E-18	NNAA- = 1.22E-17	NAAA- = 1.00E-17
AAAA- = 3.41E-18	NNNNN = 1.90E-08	NNNNN- = 1.57E-19	C1NNN = 1.19E-07
C1NNA = 7.56E-07	C1NAA = 1.29E-06	C1AAA = 3.39E-07	C2NNN = 7.44E-08
C2NNA = 5.07E-07	C2NAA = 9.66E-07	C2AAA = 2.44E-07	C1NNN- = 3.46E-17
C1NNA- = 2.53E-16	C1NAA- = 5.70E-16	C1AAA- = 4.24E-17	C2NNN- = 1.75E-11
C2NNA- = 1.46E-10	C2NAA- = 3.21E-10	C2AAA- = 9.10E-11	C1NNNN = 1.99E-08
C1NNNA = 1.88E-07	C1NNAA = 5.21E-07	C1NAAA = 2.04E-07	C1AAAA = 1.33E-07
C2NNNN = 1.44E-10	C2NNNA = 1.35E-09	C2NNAA = 3.75E-09	C2NAAA = 5.39E-09
C2AAAA = 1.19E-09	C3NNNN = 1.83E-10	C3NNNA = 5.24E-10	C3NNAA = 1.59E-09
C3NAAA = 2.00E-09	C3AAAA = 5.32E-10	C1NNNN- = 1.15E-19	C1NNNA- = 8.63E-19
C1NNAA- = 1.70E-18	C1NAAA- = 1.32E-18	C1AAAA- = 6.21E-19	C2NNNN- = 5.04E-20
C2NNNA- = 2.45E-19	C2NNAA- = 5.11E-19	C2NAAA- = 4.71E-19	C2AAAA- = 5.55E-20
C3NNNN- = 2.27E-13	C3NNNA- = 1.09E-12	C3NNAA- = 3.76E-12	C3NAAA- = 4.90E-12
C3AAAA- = 8.65E-13	C1NNNNN = 2.61E-09	C2NNNNN = 1.40E-10	C3NNNNN = 2.10E-12
C4NNNNN = 7.21E-13	C1NNNNN- = 4.12E-20	C2NNNNN- = 2.02E-20	C3NNNNN- = 2.57E-21
		C4NNNNN- = 1.62E-15	

Anthracene/naphthalene pyrolysis at 1348K

t(sec)= 0.0000E+00 P(atm)= 9.5000E-01 T(K)= 1.3480E+03

N2 = 9.98E-01	h2 = 0.00E+00	h = 0.00E+00	n = 9.13E-04
a = 9.13E-04	n1- = 0.00E+00	n2- = 0.00E+00	a1- = 0.00E+00

t(sec)= 1.8300E+00 P(atm)= 9.5000E-01 T(K)= 1.3480E+03

N2	= 9.98E-01	h2	= 1.14E-03	h	= 8.95E-08	n	= 3.61E-04
a	= 2.52E-04	n1-	= 2.65E-07	n2-	= 1.89E-07	a1-	= 1.30E-07
a2-	= 8.01E-08	a9-	= 9.36E-08	n1n1	= 3.69E-06	n1n1-1	= 4.85E-17
n1n1-2	= 4.40E-17	n1n1-4	= 6.30E-09	n1n2	= 1.29E-05	n1n2-1	= 2.37E-16
n1n2-2	= 8.92E-17	n1n2-4	= 2.50E-08	n2n2	= 1.32E-05	n2n2-4	= 3.47E-08
a1n1	= 4.16E-06	a1n1-1	= 1.93E-17	a1n1-2	= 3.28E-17	a1n1-3	= 2.66E-17
a1n1-4	= 6.26E-09	a1n2	= 7.25E-06	a1n2-1	= 4.14E-17	a1n2-2	= 3.32E-17
a1n2-3	= 6.11E-17	a1n2-4	= 1.23E-08	a2n1	= 7.40E-06	a2n1-1	= 9.28E-17
a2n1-2	= 3.04E-17	a2n1-4	= 1.30E-08	a2n2	= 1.46E-05	a2n2-4	= 3.37E-08
a9n1	= 2.34E-06	a9n1-1	= 2.82E-17	a9n1-2	= 8.90E-18	a9n1-4	= 3.39E-09
a9n2	= 3.97E-06	a9n2-1	= 6.82E-17	a9n2-2	= 1.77E-17	a9n2-4	= 5.97E-09
a1a1	= 6.45E-07	a1a1-2	= 5.95E-18	a1a1-3	= 1.15E-17	a1a1-4	= 1.60E-09
a1a2	= 2.30E-06	a1a2-1	= 1.86E-17	a1a2-2	= 1.19E-17	a1a2-3	= 2.70E-17
a1a2-4	= 6.57E-09	a1a9	= 7.31E-07	a1a9-1	= 9.17E-18	a1a9-2	= 3.40E-18
a1a9-3	= 5.28E-18	a1a9-4	= 1.74E-09	a2a2	= 2.30E-06	a2a2-4	= 8.59E-09
a2a9	= 1.26E-06	a2a9-1	= 2.93E-17	a2a9-2	= 6.34E-18	a2a9-4	= 3.32E-09
a9a9	= 1.02E-07	a9a9-1	= 2.01E-18	a9a9-4	= 4.23E-10	BkF	= 2.29E-08
BjF	= 6.22E-08	Per	= 8.72E-05	DBajF	= 5.54E-08	DBakF	= 2.61E-08
DBa1F	= 5.30E-08	BaPer	= 2.25E-04	N23jF	= 3.98E-08	N23kF	= 1.42E-08
BaN23jF	= 1.99E-08	BaN23kF	= 1.42E-08	BaN231F	= 2.06E-08	DBajPer	= 8.15E-05
DBaoPer	= 8.21E-05	BkF-	= 3.13E-11	BjF-	= 8.84E-11	Per-	= 1.89E-07
DBajF-	= 9.45E-11	DBakF-	= 4.55E-11	DBa1F-	= 9.44E-11	BaPer-	= 6.49E-07
N23jF-	= 6.89E-11	N23kF-	= 2.43E-11	BaN23jF-	= 3.57E-11	BaN23kF-	= 2.50E-11
BaN231F-	= 3.65E-11	DBajPer-	= 2.43E-07	DBaoPer-	= 2.43E-07	NNN	= 1.26E-06
NNA	= 3.56E-06	NAA	= 1.58E-06	AAA	= 5.15E-07	NNN-	= 1.25E-16
NNA-	= 3.14E-16	NAA-	= 2.56E-16	AAA-	= 8.02E-17	NNNN	= 6.90E-08
NNNA	= 2.44E-07	NNAA	= 2.32E-07	NAAA	= 1.01E-07	AAAA	= 2.23E-08
NNNN-	= 9.97E-18	NNNA-	= 3.51E-17	NNAA-	= 5.17E-17	NAAA-	= 3.10E-17
AAAA-	= 7.59E-18	NNNNN	= 2.55E-09	NNNNN-	= 5.96E-19	C1NNN	= 5.17E-07
C1NNA	= 2.62E-06	C1NAA	= 3.55E-06	C1AAA	= 6.38E-07	C2NNN	= 9.69E-07
C2NNA	= 4.92E-06	C2NAA	= 6.84E-06	C2AAA	= 1.19E-06	C1NNN-	= 1.49E-15
C1NNA-	= 8.18E-15	C1NAA-	= 1.35E-14	C1AAA-	= 6.24E-16	C2NNN-	= 1.17E-09
C2NNA-	= 6.87E-09	C2NAA-	= 1.09E-08	C2AAA-	= 2.18E-09	C1NNNN	= 7.77E-08
C1NNNA	= 5.55E-07	C1NNAA	= 1.13E-06	C1NAAA	= 2.82E-07	C1AAAA	= 1.34E-07
C2NNNN	= 7.85E-09	C2NNNA	= 5.77E-08	C2NNAA	= 1.26E-07	C2NAAA	= 1.47E-07

C2AAAA	= 2.41E-08	C3NNNN	= 2.24E-08	C3NNNA	= 2.13E-07	C3NNAA	= 5.41E-07
C3NAAA	= 5.12E-07	C3AAAA	= 1.17E-07	C1NNNN-	= 8.90E-18	C1NNNA-	= 6.76E-17
C1NNAA-	= 8.21E-17	C1NAAA-	= 6.46E-17	C1AAAA-	= 2.06E-17	C2NNNN-	= 2.50E-17
C2NNNA-	= 4.16E-16	C2NNAA-	= 7.24E-16	C2NAAA-	= 4.77E-16	C2AAAA-	= 4.57E-17
C3NNNN-	= 7.39E-11	C3NNNA-	= 9.07E-10	C3NNAA-	= 2.64E-09	C3NAAA-	= 2.62E-09
C3AAAA-	= 3.36E-10	C1NNNNN	= 4.08E-09	C2NNNNN	= 1.58E-09	C3NNNNN	= 1.77E-10
C4NNNNN	= 6.32E-10	C1NNNNN-	= 1.38E-18	C2NNNNN-	= 6.62E-18	C3NNNNN-	= 7.50E-18
			C4NNNNN- = 2.90E-12				

Anthracene/naphthalene pyrolysis at 1416K

t(sec)= 0.0000E+00 P(atm)= 9.5000E-01 T(K)= 1.4160E+03

N2	= 9.97E-01	h2	= 0.00E+00	h	= 0.00E+00	n	= 1.38E-03
a	= 1.38E-03	n1-	= 0.00E+00	n2-	= 0.00E+00	a1-	= 0.00E+00

t(sec)= 1.7400E+00 P(atm)= 9.5000E-01 T(K)= 1.4160E+03

N2	= 9.96E-01	h2	= 2.79E-03	h	= 3.36E-07	n	= 8.78E-05
a	= 4.51E-05	n1-	= 1.18E-07	n2-	= 8.56E-08	a1-	= 4.27E-08
a2-	= 2.70E-08	a9-	= 3.03E-08	n1n1	= 1.18E-07	n1n1-1	= 5.52E-16
n1n1-2	= 4.02E-16	n1n1-4	= 3.88E-10	n1n2	= 4.01E-07	n1n2-1	= 1.97E-15
n1n2-2	= 7.17E-16	n1n2-4	= 1.49E-09	n2n2	= 4.06E-07	n2n2-4	= 2.00E-09
a1n1	= 9.92E-08	a1n1-1	= 1.64E-16	a1n1-2	= 2.31E-16	a1n1-3	= 2.34E-16
a1n1-4	= 2.85E-10	a1n2	= 1.68E-07	a1n2-1	= 3.04E-16	a1n2-2	= 2.21E-16
a1n2-3	= 4.19E-16	a1n2-4	= 5.41E-10	a2n1	= 1.71E-07	a2n1-1	= 5.97E-16
a2n1-2	= 1.88E-16	a2n1-4	= 3.69E-10	a2n2	= 3.34E-07	a2n2-4	= 1.43E-09
a9n1	= 5.75E-08	a9n1-1	= 2.83E-16	a9n1-2	= 7.13E-17	a9n1-4	= 1.59E-10
a9n2	= 9.44E-08	a9n2-1	= 4.93E-16	a9n2-2	= 1.24E-16	a9n2-4	= 2.71E-10
a1a1	= 1.11E-08	a1a1-2	= 3.56E-17	a1a1-3	= 8.05E-17	a1a1-4	= 5.64E-11
a1a2	= 3.82E-08	a1a2-1	= 1.03E-16	a1a2-2	= 6.48E-17	a1a2-3	= 1.47E-16
a1a2-4	= 2.23E-10	a1a9	= 1.29E-08	a1a9-1	= 6.56E-17	a1a9-2	= 2.07E-17
a1a9-3	= 4.66E-17	a1a9-4	= 6.31E-11	a2a2	= 3.78E-08	a2a2-4	= 2.82E-10
a2a9	= 2.15E-08	a2a9-1	= 1.72E-16	a2a9-2	= 3.62E-17	a2a9-4	= 1.16E-10
a9a9	= 1.87E-09	a9a9-1	= 1.84E-17	a9a9-4	= 1.60E-11	BkF	= 5.72E-08
BjF	= 1.69E-07	Per	= 2.78E-04	DBajF	= 1.23E-07	DBakF	= 5.64E-08
DBalF	= 1.23E-07	BaPer	= 5.32E-04	N23jF	= 8.34E-08	N23kF	= 2.82E-08
BaN23jF	= 3.46E-08	BaN23kF	= 2.35E-08	BaN23lF	= 3.47E-08	DBajPer	= 1.46E-04

DBaoPer	= 1.46E-04	BkF-	= 2.17E-10	BjF-	= 6.20E-10	Per-	= 1.07E-06
DBajF-	= 5.18E-10	DBakF-	= 2.55E-10	DBalF-	= 5.18E-10	BaPer-	= 2.77E-06
N23jF-	= 3.76E-10	N23kF-	= 1.32E-10	BaN23jF-	= 1.46E-10	BaN23kF-	= 1.03E-10
BaN231F-	= 1.47E-10	DBajPer-	= 7.77E-07	DBaoPer-	= 7.77E-07	NNN	= 5.30E-09
NNA	= 1.12E-08	NAA	= 3.57E-09	AAA	= 8.90E-10	NNN-	= 1.99E-16
NNA-	= 3.75E-16	NAA-	= 2.37E-16	AAA-	= 5.80E-17	NNNN	= 3.68E-11
NNNA	= 9.46E-11	NNAA	= 6.56E-11	NAAA	= 2.11E-11	AAAA	= 3.46E-12
NNNN-	= 2.29E-18	NNNA-	= 6.06E-18	NNAA-	= 6.88E-18	NAAA-	= 3.17E-18
AAAA-	= 6.23E-19	NNNNN	= 1.33E-13	NNNNN-	= 1.31E-20	C1NNN	= 2.80E-07
C1NNA	= 1.08E-06	C1NAA	= 1.11E-06	C1AAA	= 1.40E-07	C2NNN	= 3.38E-06
C2NNA	= 1.24E-05	C2NAA	= 1.24E-05	C2AAA	= 3.01E-06	C1NNN-	= 1.84E-14
C1NNA-	= 7.30E-14	C1NAA-	= 8.73E-14	C1AAA-	= 5.13E-15	C2NNN-	= 1.70E-08
C2NNA-	= 7.17E-08	C2NAA-	= 8.14E-08	C2AAA-	= 2.20E-08	C1NNNN	= 5.69E-09
C1NNNA	= 3.04E-08	C1NNAA	= 4.67E-08	C1NAAA	= 8.00E-09	C1AAAA	= 2.96E-09
C2NNNN	= 7.22E-08	C2NNNA	= 4.03E-07	C2NNAA	= 6.77E-07	C2NAAA	= 6.06E-07
C2AAAA	= 7.27E-08	C3NNNN	= 1.30E-06	C3NNNA	= 1.53E-05	C3NNAA	= 2.99E-05
C3NAAA	= 2.03E-05	C3AAAA	= 3.66E-06	C1NNNN-	= 2.55E-16	C1NNNA-	= 1.52E-15
C1NNAA-	= 1.31E-15	C1NAAA-	= 8.34E-16	C1AAAA-	= 2.02E-16	C2NNNN-	= 6.22E-15
C2NNNA-	= 1.29E-13	C2NNAA-	= 1.74E-13	C2NAAA-	= 7.87E-14	C2AAAA-	= 5.77E-15
C3NNNN-	= 9.58E-09	C3NNNA-	= 1.16E-07	C3NNAA-	= 2.61E-07	C3NAAA-	= 1.86E-07
C3AAAA-	= 1.72E-08	C1NNNNN	= 2.79E-11	C2NNNNN	= 6.46E-10	C3NNNNN	= 2.06E-09
C4NNNNN	= 6.90E-08	C1NNNNN-	= 1.96E-18	C2NNNNN-	= 3.16E-16	C3NNNNN-	= 2.90E-15
				C4NNNNN-	= 5.69E-10		

Anthracene/naphthalene pyrolysis at 1496K

t(sec)= 0.0000E+00 P(atm)= 9.5000E-01 T(K)= 1.4960E+03

N2	= 9.99E-01	h2	= 0.00E+00	h	= 0.00E+00	n	= 4.84E-04
a	= 4.84E-04	n1-	= 0.00E+00	n2-	= 0.00E+00	a1-	= 0.00E+00

t(sec)= 1.6500E+00 P(atm)= 9.5000E-01 T(K)= 1.4960E+03

N2	= 9.98E-01	h2	= 1.28E-03	h	= 6.26E-07	n	= 1.35E-06
a	= 6.95E-07	n1-	= 8.17E-09	n2-	= 6.04E-09	a1-	= 2.90E-09
a2-	= 1.87E-09	a9-	= 2.02E-09	n1n1	= 7.89E-11	n1n1-1	= 1.91E-16
n1n1-2	= 1.41E-16	n1n1-4	= 1.20E-12	n1n2	= 2.52E-10	n1n2-1	= 6.59E-16
n1n2-2	= 2.43E-16	n1n2-4	= 4.31E-12	n2n2	= 2.51E-10	n2n2-4	= 5.64E-12

a1n1	= 6.58E-11	a1n1-1	= 5.56E-17	a1n1-2	= 7.95E-17	a1n1-3	= 7.78E-17
a1n1-4	= 8.62E-13	a1n2	= 1.06E-10	a1n2-1	= 9.95E-17	a1n2-2	= 7.35E-17
a1n2-3	= 1.35E-16	a1n2-4	= 1.54E-12	a2n1	= 1.07E-10	a2n1-1	= 1.95E-16
a2n1-2	= 6.30E-17	a2n1-4	= 1.62E-12	a2n2	= 2.06E-10	a2n2-4	= 3.95E-12
a9n1	= 3.95E-11	a9n1-1	= 9.89E-17	a9n1-2	= 2.52E-17	a9n1-4	= 4.99E-13
a9n2	= 6.15E-11	a9n2-1	= 1.67E-16	a9n2-2	= 4.25E-17	a9n2-4	= 7.99E-13
a1a1	= 7.00E-12	a1a1-2	= 1.25E-17	a1a1-3	= 2.71E-17	a1a1-4	= 1.72E-13
a1a2	= 2.28E-11	a1a2-1	= 3.40E-17	a1a2-2	= 2.20E-17	a1a2-3	= 4.77E-17
a1a2-4	= 6.38E-13	a1a9	= 8.47E-12	a1a9-1	= 2.32E-17	a1a9-2	= 7.47E-18
a1a9-3	= 1.62E-17	a1a9-4	= 1.99E-13	a2a2	= 2.22E-11	a2a2-4	= 7.78E-13
a2a9	= 1.32E-11	a2a9-1	= 5.87E-17	a2a9-2	= 1.27E-17	a2a9-4	= 3.44E-13
a9a9	= 1.28E-12	a9a9-1	= 6.72E-18	a9a9-4	= 5.31E-14	BkF	= 1.19E-08
BjF	= 3.44E-08	Per	= 3.99E-05	DBajF	= 2.50E-08	DBakF	= 1.19E-08
DBalF	= 2.50E-08	BaPer	= 7.32E-05	N23jF	= 1.72E-08	N23kF	= 5.95E-09
BaN23jF	= 6.85E-09	BaN23kF	= 4.73E-09	BaN23lF	= 6.85E-09	DBajPer	= 1.98E-05
DBaoPer	= 1.98E-05	BkF-	= 1.95E-10	BjF-	= 5.47E-10	Per-	= 6.60E-07
DBajF-	= 4.54E-10	DBakF-	= 2.31E-10	DBalF-	= 4.54E-10	BaPer-	= 1.67E-06
N23jF-	= 3.35E-10	N23kF-	= 1.20E-10	BaN23jF-	= 1.23E-10	BaN23kF-	= 8.79E-11
BaN23lF-	= 1.23E-10	DBajPer-	= 4.57E-07	DBaoPer-	= 4.57E-07	NNN	= 1.46E-13
NNA	= 3.04E-13	NAA	= 9.14E-14	AAA	= 2.29E-14	NNN-	= 2.84E-18
NNA-	= 5.24E-18	NAA-	= 3.31E-18	AAA-	= 8.41E-19	NNNN	= 3.95E-17
NNNA	= 9.71E-17	NNAA	= 6.48E-17	NAAA	= 2.04E-17	AAAA	= 3.29E-18
NNNN-	= 1.32E-21	NNNA-	= 3.38E-21	NNAA-	= 3.85E-21	NAAA-	= 1.77E-21
AAAA-	= 3.72E-22	NNNNN	= 2.09E-21	NNNNN-	= 1.09E-25	C1NNN	= 2.33E-09
C1NNA	= 8.36E-09	C1NAA	= 8.94E-09	C1AAA	= 1.04E-09	C2NNN	= 2.28E-06
C2NNA	= 1.30E-05	C2NAA	= 1.24E-05	C2AAA	= 5.11E-06	C1NNN-	= 2.19E-14
C1NNA-	= 1.36E-13	C1NAA-	= 1.54E-13	C1AAA-	= 1.41E-14	C2NNN-	= 5.33E-08
C2NNA-	= 3.49E-07	C2NAA-	= 3.76E-07	C2AAA-	= 1.64E-07	C1NNNN	= 1.96E-12
C1NNNA	= 1.02E-11	C1NNAA	= 1.54E-11	C1NAAA	= 2.36E-12	C1AAAA	= 9.04E-13
C2NNNN	= 7.33E-09	C2NNNA	= 4.05E-08	C2NNAA	= 6.76E-08	C2NAAA	= 6.02E-08
C2AAAA	= 6.76E-09	C3NNNN	= 6.33E-06	C3NNNA	= 3.19E-05	C3NNAA	= 5.84E-05
C3NAAA	= 3.05E-05	C3AAAA	= 5.57E-06	C1NNNN-	= 4.59E-17	C1NNNA-	= 2.71E-16
C1NNAA-	= 2.19E-16	C1NAAA-	= 1.38E-16	C1AAAA-	= 3.30E-17	C2NNNN-	= 6.52E-14
C2NNNA-	= 5.84E-13	C2NNAA-	= 7.43E-13	C2NAAA-	= 2.45E-13	C2AAAA-	= 1.78E-14
C3NNNN-	= 2.04E-07	C3NNNA-	= 1.05E-06	C3NNAA-	= 2.20E-06	C3NAAA-	= 1.20E-06
C3AAAA-	= 1.05E-07	C1NNNNN	= 1.37E-16	C2NNNNN	= 9.57E-13	C3NNNNN	= 6.48E-10

C4NNNNN	= 2.91E-07	C1NNNNN-	= 5.17E-21	C2NNNNN-	= 2.03E-16	C3NNNNN-	= 2.14E-14	
				C4NNNNN-	= 1.03E-08			

Pure anthracene pyrolysis at 1181K

	t(sec)= 0.0000E+00		P(atm)= 9.5000E-01		T(K)= 1.1810E+03		
N2	= 9.98E-01	h2	= 0.00E+00	h	= 0.00E+00	a	= 2.24E-03

	t(sec)= 2.0800E+00		P(atm)= 9.5000E-01		T(K)= 1.1810E+03		
N2	= 9.98E-01	h2	= 1.68E-04	h	= 6.92E-09	a	= 1.93E-03
a1-	= 4.05E-08	a2-	= 2.21E-08	a9-	= 2.93E-08	a1a1	= 1.36E-05
a1a1-2	= 9.13E-19	a1a1-3	= 1.10E-18	a1a1-4	= 7.77E-10	a1a2	= 4.34E-05
a1a2-1	= 3.38E-18	a1a2-2	= 2.20E-18	a1a2-3	= 5.11E-18	a1a2-4	= 3.28E-09
a1a9	= 1.40E-05	a1a9-1	= 8.83E-19	a1a9-2	= 4.96E-19	a1a9-3	= 5.26E-20
a1a9-4	= 7.80E-10	a2a2	= 2.77E-05	a2a2-4	= 4.26E-09	a2a9	= 2.28E-05
a2a9-1	= 4.55E-18	a2a9-2	= 1.03E-18	a2a9-4	= 1.54E-09	a9a9	= 1.83E-06
a9a9-1	= 2.51E-20	a9a9-4	= 1.56E-10	BaN23jF	= 2.96E-08	BaN23kF	= 2.35E-08
BaN23lF	= 3.44E-08	DBajPer	= 1.92E-06	DBaoPer	= 2.20E-06	BaN23jF-	= 6.43E-13
BaN23kF-	= 5.03E-13	BaN23lF-	= 8.31E-13	DBajPer-	= 1.18E-09	DBaoPer-	= 1.18E-09
AAA	= 1.56E-05	AAA-	= 1.65E-17	AAAA	= 1.65E-06	AAAA-	= 9.84E-19
C1AAA	= 1.06E-07	C2AAA	= 1.06E-08	C1AAA-	= 6.80E-19	C2AAA-	= 3.71E-13
C1AAAA	= 3.13E-08	C2AAAA	= 7.23E-12	C3AAAA	= 3.47E-13	C1AAAA-	= 1.36E-20
		C2AAAA-	= 1.16E-23	C3AAAA-	= 2.90E-16		

Pure anthracene pyrolysis at 1278K

	t(sec)= 0.0000E+00		P(atm)= 9.5000E-01		T(K)= 1.2780E+03		
N2	= 9.99E-01	h2	= 0.00E+00	h	= 0.00E+00	a	= 9.75E-04

	t(sec)= 1.9300E+00		P(atm)= 9.5000E-01		T(K)= 1.2780E+03		
N2	= 9.99E-01	h2	= 2.58E-04	h	= 2.07E-08	a	= 6.15E-04
a1-	= 1.58E-07	a2-	= 9.23E-08	a9-	= 1.15E-07	a1a1	= 7.24E-06
a1a1-2	= 3.68E-18	a1a1-3	= 4.63E-18	a1a1-4	= 6.71E-09	a1a2	= 2.51E-05
a1a2-1	= 1.28E-17	a1a2-2	= 8.49E-18	a1a2-3	= 1.88E-17	a1a2-4	= 2.81E-08
a1a9	= 7.96E-06	a1a9-1	= 3.85E-18	a1a9-2	= 2.11E-18	a1a9-3	= 5.09E-19

a1a9-4	= 7.06E-09	a2a2	= 2.23E-05	a2a2-4	= 3.74E-08	a2a9	= 1.35E-05
a2a9-1	= 1.84E-17	a2a9-2	= 4.24E-18	a2a9-4	= 1.38E-08	a9a9	= 1.09E-06
a9a9-1	= 2.04E-19	a9a9-4	= 1.63E-09	BaN23jF	= 4.59E-08	BaN23kF	= 3.68E-08
BaN231F	= 5.19E-08	DBajPer	= 2.79E-05	DBaoPer	= 2.97E-05	BaN23jF-	= 1.37E-11
BaN23kF-	= 1.05E-11	BaN231F-	= 1.60E-11	DBajPer-	= 6.05E-08	DBaoPer-	= 6.11E-08
AAA	= 2.11E-05	AAA-	= 1.52E-16	AAAA	= 4.19E-06	AAAA-	= 2.27E-17
C1AAA	= 1.20E-06	C2AAA	= 7.94E-07	C1AAA-	= 1.14E-16	C2AAA-	= 3.49E-10
C1AAAA	= 8.57E-07	C2AAAA	= 5.16E-09	C3AAAA	= 2.12E-09	C1AAAA-	= 3.01E-18
		C2AAAA-	= 1.85E-19	C3AAAA-	= 4.44E-12		

Pure anthracene pyrolysis at 1350K

t(sec)= 0.0000E+00 P(atm)= 9.5000E-01 T(K)= 1.3500E+03

N2	= 9.99E-01	h2	= 0.00E+00	h	= 0.00E+00	a	= 1.10E-03

t(sec)= 1.8200E+00 P(atm)= 9.5000E-01 T(K)= 1.3500E+03

N2	= 9.99E-01	h2	= 6.82E-04	h	= 7.21E-08	a	= 3.92E-04
a1-	= 2.68E-07	a2-	= 1.64E-07	a9-	= 1.94E-07	a1a1	= 2.53E-06
a1a1-2	= 1.36E-17	a1a1-3	= 2.26E-17	a1a1-4	= 7.58E-09	a1a2	= 8.76E-06
a1a2-1	= 4.30E-17	a1a2-2	= 2.83E-17	a1a2-3	= 6.24E-17	a1a2-4	= 3.08E-08
a1a9	= 2.89E-06	a1a9-1	= 1.84E-17	a1a9-2	= 7.84E-18	a1a9-3	= 8.19E-18
a1a9-4	= 8.25E-09	a2a2	= 8.39E-06	a2a2-4	= 3.99E-08	a2a9	= 4.84E-06
a2a9-1	= 6.67E-17	a2a9-2	= 1.49E-17	a2a9-4	= 1.57E-08	a9a9	= 4.07E-07
a9a9-1	= 3.14E-18	a9a9-4	= 2.01E-09	BaN23jF	= 5.45E-08	BaN23kF	= 4.09E-08
BaN231F	= 5.80E-08	DBajPer	= 1.49E-04	DBaoPer	= 1.50E-04	BaN23jF-	= 9.79E-11
BaN23kF-	= 7.02E-11	BaN231F-	= 1.02E-10	DBajPer-	= 5.90E-07	DBaoPer-	= 5.91E-07
AAA	= 4.66E-06	AAA-	= 3.67E-16	AAAA	= 4.62E-07	AAAA-	= 7.17E-17
C1AAA	= 3.07E-06	C2AAA	= 5.33E-06	C1AAA-	= 2.26E-15	C2AAA-	= 1.17E-08
C1AAAA	= 1.47E-06	C2AAAA	= 1.39E-07	C3AAAA	= 5.88E-07	C1AAAA-	= 1.07E-16
		C2AAAA-	= 1.86E-16	C3AAAA-	= 2.22E-09		

Pure anthracene pyrolysis at 1415K

t(sec)= 0.0000E+00 P(atm)= 9.5000E-01 T(K)= 1.4150E+03

N2	= 9.99E-01	h2	= 0.00E+00	h	= 0.00E+00	a	= 1.23E-03

t(sec)= 1.7400E+00 P(atm)= 9.5000E-01 T(K)= 1.4150E+03

N2	= 9.98E-01	h2	= 1.17E-03	h	= 2.16E-07	a	= 1.03E-04
a1-	= 1.49E-07	a2-	= 9.38E-08	a9-	= 1.06E-07	a1a1	= 1.35E-07
a1a1-2	= 4.15E-17	a1a1-3	= 9.16E-17	a1a1-4	= 9.59E-10	a1a2	= 4.54E-07
a1a2-1	= 1.20E-16	a1a2-2	= 7.61E-17	a1a2-3	= 1.71E-16	a1a2-4	= 3.77E-09
a1a9	= 1.58E-07	a1a9-1	= 7.47E-17	a1a9-2	= 2.41E-17	a1a9-3	= 5.19E-17
a1a9-4	= 1.07E-09	a2a2	= 4.34E-07	a2a2-4	= 4.72E-09	a2a9	= 2.57E-07
a2a9-1	= 2.00E-16	a2a9-2	= 4.23E-17	a2a9-4	= 1.97E-09	a9a9	= 2.30E-08
a9a9-1	= 2.05E-17	a9a9-4	= 2.72E-10	BaN23jF	= 6.24E-08	BaN23kF	= 4.26E-08
BaN231F	= 6.27E-08	DBajPer	= 2.53E-04	DBaoPer	= 2.53E-04	BaN23jF-	= 3.89E-10
BaN23kF-	= 2.73E-10	BaN231F-	= 3.90E-10	DBajPer-	= 2.06E-06	DBaoPer-	= 2.06E-06
AAA	= 5.30E-08	AAA-	= 3.53E-16	AAAA	= 9.80E-10	AAAA-	= 1.83E-17
C1AAA	= 1.32E-06	C2AAA	= 8.38E-06	C1AAA-	= 9.25E-15	C2AAA-	= 8.23E-08
C1AAAA	= 1.35E-07	C2AAAA	= 5.18E-07	C3AAAA	= 1.72E-05	C1AAAA-	= 9.32E-16
		C2AAAA-	= 1.74E-14	C3AAAA-	= 1.23E-07		

Pure anthracene pyrolysis at 1496K

t(sec)= 0.0000E+00 P(atm)= 9.5000E-01 T(K)= 1.4960E+03

N2	= 9.99E-01	h2	= 0.00E+00	h	= 0.00E+00	a	= 7.98E-04

t(sec)= 1.6500E+00 P(atm)= 9.5000E-01 T(K)= 1.4960E+03

N2	= 9.99E-01	h2	= 1.01E-03	h	= 5.56E-07	a	= 3.02E-06
a1-	= 1.42E-08	a2-	= 9.14E-09	a9-	= 9.89E-09	a1a1	= 1.65E-10
a1a1-2	= 4.77E-17	a1a1-3	= 1.03E-16	a1a1-4	= 4.31E-12	a1a2	= 5.32E-10
a1a2-1	= 1.30E-16	a1a2-2	= 8.39E-17	a1a2-3	= 1.82E-16	a1a2-4	= 1.60E-11
a1a9	= 2.00E-10	a1a9-1	= 8.83E-17	a1a9-2	= 2.85E-17	a1a9-3	= 6.17E-17
a1a9-4	= 5.00E-12	a2a2	= 5.04E-10	a2a2-4	= 1.93E-11	a2a9	= 3.10E-10
a2a9-1	= 2.24E-16	a2a9-2	= 4.83E-17	a2a9-4	= 8.64E-12	a9a9	= 3.02E-11
a9a9-1	= 2.57E-17	a9a9-4	= 1.33E-12	BaN23jF	= 2.94E-08	BaN23kF	= 2.03E-08
BaN231F	= 2.94E-08	DBajPer	= 8.50E-05	DBaoPer	= 8.49E-05	BaN23jF-	= 5.95E-10
BaN23kF-	= 4.25E-10	BaN231F-	= 5.95E-10	DBajPer-	= 2.21E-06	DBaoPer-	= 2.21E-06
AAA	= 2.80E-12	AAA-	= 1.76E-17	AAAA	= 2.06E-15	AAAA-	= 4.00E-20
C1AAA	= 2.46E-08	C2AAA	= 2.36E-05	C1AAA-	= 5.81E-14	C2AAA-	= 8.52E-07
C1AAAA	= 1.09E-10	C2AAAA	= 1.58E-07	C3AAAA	= 9.10E-05	C1AAAA-	= 6.86E-16

C2AAAA- = 2.58E-13 C3AAAA- = 1.93E-06

Approximate equilibrium anthracene/naphthalene pyrolysis at 1180K

t(sec)= 0.0000E+00 P(atm)= 9.5000E-01 T(K)= 1.1800E+03

N2	= 9.99E-01	h2	= 0.00E+00	h	= 0.00E+00	n	= 5.75E-04
a	= 5.75E-04	n1-	= 0.00E+00	n2-	= 0.00E+00	a1-	= 0.00E+00

t(sec)= 2.0000E+03 P(atm)= 9.5000E-01 T(K)= 1.1800E+03

N2	= 9.98E-01	h2	= 1.08E-03	h	= 4.61E-09	n	= 5.09E-05
a	= 2.34E-05	n1-	= 2.17E-09	n2-	= 1.48E-09	a1-	= 7.46E-10
a2-	= 4.29E-10	a9-	= 5.70E-10	n1n1	= 5.69E-08	n1n1-1	= 1.27E-18
n1n1-2	= 8.67E-19	n1n1-4	= 5.92E-12	n1n2	= 2.25E-07	n1n2-1	= 5.09E-18
n1n2-2	= 1.73E-18	n1n2-4	= 2.59E-11	n2n2	= 2.65E-07	n2n2-4	= 4.05E-11
a1n1	= 4.43E-08	a1n1-1	= 3.75E-19	a1n1-2	= 4.92E-19	a1n1-3	= 5.75E-19
a1n1-4	= 4.38E-12	a1n2	= 8.78E-08	a1n2-1	= 7.86E-19	a1n2-2	= 5.37E-19
a1n2-3	= 1.16E-18	a1n2-4	= 9.49E-12	a2n1	= 8.93E-08	a2n1-1	= 1.54E-18
a2n1-2	= 4.42E-19	a2n1-4	= 1.01E-11	a2n2	= 2.04E-07	a2n2-4	= 2.96E-11
a9n1	= 2.29E-08	a9n1-1	= 5.80E-19	a9n1-2	= 1.38E-19	a9n1-4	= 2.17E-12
a9n2	= 4.39E-08	a9n2-1	= 1.13E-18	a9n2-2	= 2.68E-19	a9n2-4	= 4.19E-12
a1a1	= 5.10E-09	a1a1-2	= 6.72E-20	a1a1-3	= 1.79E-19	a1a1-4	= 7.94E-13
a1a2	= 2.07E-08	a1a2-1	= 2.40E-19	a1a2-2	= 1.38E-19	a1a2-3	= 3.67E-19
a1a2-4	= 3.62E-12	a1a9	= 5.33E-09	a1a9-1	= 1.22E-19	a1a9-2	= 3.50E-20
a1a9-3	= 9.29E-20	a1a9-4	= 7.90E-13	a2a2	= 2.44E-08	a2a2-4	= 5.37E-12
a2a9	= 1.03E-08	a2a9-1	= 3.56E-19	a2a9-2	= 6.84E-20	a2a9-4	= 1.68E-12
a9a9	= 6.74E-10	a9a9-1	= 3.05E-20	a9a9-4	= 1.77E-13	BkF	= 6.20E-09
BjF	= 1.98E-08	Per	= 1.27E-04	DBajF	= 1.38E-08	DBakF	= 5.42E-09
DBalF	= 1.38E-08	BaPer	= 2.59E-04	N23jF	= 8.66E-09	N23kF	= 2.71E-09
BaN23jF	= 3.98E-09	BaN23kF	= 2.49E-09	BaN23lF	= 3.98E-09	DBajPer	= 7.00E-05
DBaoPer	= 7.00E-05	BkF-	= 6.94E-13	BjF-	= 2.13E-12	Per-	= 1.41E-08
DBajF-	= 1.73E-12	DBakF-	= 7.36E-13	DBalF-	= 1.73E-12	BaPer-	= 3.77E-08
N23jF-	= 1.18E-12	N23kF-	= 3.85E-13	BaN23jF-	= 5.29E-13	BaN23kF-	= 3.45E-13
BaN23lF-	= 5.29E-13	DBajPer-	= 1.10E-08	DBaoPer-	= 1.10E-08	NNN	= 2.54E-09
NNA	= 4.96E-09	NAA	= 1.75E-09	AAA	= 3.88E-10	NNN-	= 3.88E-19
NNA-	= 7.17E-19	NAA-	= 4.16E-19	AAA-	= 8.45E-20	NNNN	= 1.90E-11
NNNA	= 4.86E-11	NNAA	= 3.46E-11	NAAA	= 1.15E-11	AAAA	= 1.83E-12

NNNN-	= 4.45E-21	NNNA-	= 1.19E-20	NNAA-	= 1.24E-20	NAAA-	= 5.35E-21
AAAA-	= 8.51E-22	NNNNN	= 1.36E-13	NNNNN-	= 5.03E-23	C1NNN	= 2.95E-08
C1NNA	= 1.11E-07	C1NAA	= 1.11E-07	C1AAA	= 1.74E-08	C2NNN	= 1.41E-07
C2NNA	= 4.76E-07	C2NAA	= 4.67E-07	C2AAA	= 1.22E-07	C1NNN-	= 1.29E-17
C1NNA-	= 4.69E-17	C1NAA-	= 5.45E-17	C1AAA-	= 4.59E-18	C2NNN-	= 1.96E-11
C2NNA-	= 7.49E-11	C2NAA-	= 8.29E-11	C2AAA-	= 2.49E-11	C1NNNN	= 5.59E-10
C1NNNA	= 2.97E-09	C1NNAA	= 4.46E-09	C1NAAA	= 1.06E-09	C1AAAA	= 3.41E-10
C2NNNN	= 1.76E-09	C2NNNA	= 9.64E-09	C2NNAA	= 1.56E-08	C2NAAA	= 1.36E-08
C2AAAA	= 1.94E-09	C3NNNN	= 2.83E-08	C3NNNA	= 8.50E-07	C3NNAA	= 1.60E-06
C3NAAA	= 1.52E-06	C3AAAA	= 2.62E-07	C1NNNN-	= 1.03E-19	C1NNNA-	= 5.93E-19
C1NNAA-	= 5.91E-19	C1NAAA-	= 3.79E-19	C1AAAA-	= 9.05E-20	C2NNNN-	= 1.05E-18
C2NNNA-	= 5.46E-17	C2NNAA-	= 6.95E-17	C2NAAA-	= 5.21E-17	C2AAAA-	= 3.96E-18
C3NNNN-	= 5.95E-12	C3NNNA-	= 1.91E-10	C3NNAA-	= 4.16E-10	C3NAAA-	= 4.16E-10
C3AAAA-	= 4.52E-11	C1NNNNN	= 5.53E-12	C2NNNNN	= 2.74E-11	C3NNNNN	= 2.63E-11
C4NNNNN	= 2.25E-09	C1NNNNN-	= 1.34E-21	C2NNNNN-	= 3.80E-20	C3NNNNN-	= 1.63E-18
				C4NNNNN-	= 5.47E-13		

Approximate equilibrium anthracene/naphthalene pyrolysis at 1277K

t(sec)= 0.0000E+00 P(atm)= 9.5000E-01 T(K)= 1.2770E+03

N2	= 9.98E-01	h2	= 0.00E+00	h	= 0.00E+00	n	= 8.09E-04
a	= 8.09E-04	n1-	= 0.00E+00	n2-	= 0.00E+00	a1-	= 0.00E+00

t(sec)= 2.0000E+03 P(atm)= 9.5000E-01 T(K)= 1.2770E+03

N2	= 9.97E-01	h2	= 2.05E-03	h	= 3.58E-08	n	= 1.03E-06
a	= 4.78E-07	n1-	= 1.98E-10	n2-	= 1.39E-10	a1-	= 6.68E-11
a2-	= 4.00E-11	a9-	= 4.94E-11	n1n1	= 1.74E-11	n1n1-1	= 1.12E-17
n1n1-2	= 7.85E-18	n1n1-4	= 8.41E-15	n1n2	= 6.46E-11	n1n2-1	= 4.24E-17
n1n2-2	= 1.49E-17	n1n2-4	= 3.46E-14	n2n2	= 7.20E-11	n2n2-4	= 5.09E-14
a1n1	= 1.33E-11	a1n1-1	= 3.19E-18	a1n1-2	= 4.31E-18	a1n1-3	= 4.74E-18
a1n1-4	= 5.98E-15	a1n2	= 2.49E-11	a1n2-1	= 6.32E-18	a1n2-2	= 4.43E-18
a1n2-3	= 9.01E-18	a1n2-4	= 1.22E-14	a2n1	= 2.53E-11	a2n1-1	= 1.24E-17
a2n1-2	= 3.70E-18	a2n1-4	= 1.29E-14	a2n2	= 5.49E-11	a2n2-4	= 3.56E-14
a9n1	= 7.27E-12	a9n1-1	= 5.19E-18	a9n1-2	= 1.27E-18	a9n1-4	= 3.13E-15
a9n2	= 1.31E-11	a9n2-1	= 9.57E-18	a9n2-2	= 2.33E-18	a9n2-4	= 5.69E-15
a1a1	= 1.45E-12	a1a1-2	= 5.99E-19	a1a1-3	= 1.48E-18	a1a1-4	= 1.09E-15

a1a2	= 5.55E-12	a1a2-1	= 1.94E-18	a1a2-2	= 1.16E-18	a1a2-3	= 2.87E-18
a1a2-4	= 4.64E-15	a1a9	= 1.59E-12	a1a9-1	= 1.10E-18	a1a9-2	= 3.28E-19
a1a9-3	= 8.11E-19	a1a9-4	= 1.14E-15	a2a2	= 6.17E-12	a2a2-4	= 6.45E-15
a2a9	= 2.91E-12	a2a9-1	= 3.04E-18	a2a9-2	= 6.08E-19	a2a9-4	= 2.27E-15
a9a9	= 2.14E-13	a9a9-1	= 2.90E-19	a9a9-4	= 2.70E-16	BkF	= 8.54E-09
BjF	= 2.64E-08	Per	= 9.14E-05	DBajF	= 1.81E-08	DBakF	= 7.59E-09
DBalF	= 1.81E-08	BaPer	= 1.74E-04	N23jF	= 1.17E-08	N23kF	= 3.79E-09
BaN23jF	= 4.97E-09	BaN23kF	= 3.22E-09	BaN23lF	= 4.97E-09	DBajPer	= 4.55E-05
DBaoPer	= 4.55E-05	BkF-	= 4.34E-12	BjF-	= 1.29E-11	Per-	= 4.62E-08
DBajF-	= 1.02E-11	DBakF-	= 4.64E-12	DBalF-	= 1.02E-11	BaPer-	= 1.17E-07
N23jF-	= 7.16E-12	N23kF-	= 2.42E-12	BaN23jF-	= 2.91E-12	BaN23kF-	= 1.96E-12
BaN23lF-	= 2.91E-12	DBajPer-	= 3.23E-08	DBaoPer-	= 3.23E-08	NNN	= 1.10E-14
NNA	= 2.13E-14	NAA	= 6.95E-15	AAA	= 1.57E-15	NNN-	= 4.93E-20
NNA-	= 8.83E-20	NAA-	= 5.13E-20	AAA-	= 1.08E-20	NNNN	= 1.16E-18
NNNA	= 2.87E-18	NNAA	= 1.97E-18	NAAA	= 6.25E-19	AAAA	= 9.73E-20
NNNN-	= 8.19E-24	NNNA-	= 2.10E-23	NNAA-	= 2.19E-23	NAAA-	= 9.40E-24
AAAA-	= 1.57E-24	NNNNN	= 1.07E-22	NNNNN-	= 1.19E-27	C1NNN	= 5.52E-10
C1NNA	= 2.03E-09	C1NAA	= 1.97E-09	C1AAA	= 2.67E-10	C2NNN	= 2.32E-06
C2NNA	= 1.31E-05	C2NAA	= 1.17E-05	C2AAA	= 5.15E-06	C1NNN-	= 1.50E-15
C1NNA-	= 9.13E-15	C1NAA-	= 9.71E-15	C1AAA-	= 1.22E-15	C2NNN-	= 1.67E-09
C2NNA-	= 1.10E-08	C2NAA-	= 1.11E-08	C2AAA-	= 5.19E-09	C1NNNN	= 1.56E-13
C1NNNA	= 8.02E-13	C1NNAA	= 1.17E-12	C1NAAA	= 2.32E-13	C1AAAA	= 7.64E-14
C2NNNN	= 1.99E-09	C2NNNA	= 1.06E-08	C2NNAA	= 1.68E-08	C2NAAA	= 1.43E-08
C2AAAA	= 1.81E-09	C3NNNN	= 1.64E-05	C3NNNA	= 4.31E-05	C3NNAA	= 7.42E-05
C3NAAA	= 5.74E-05	C3AAAA	= 8.65E-06	C1NNNN-	= 8.28E-19	C1NNNA-	= 4.66E-18
C1NNAA-	= 4.19E-18	C1NAAA-	= 2.59E-18	C1AAAA-	= 5.98E-19	C2NNNN-	= 6.11E-15
C2NNNA-	= 2.82E-14	C2NNAA-	= 3.31E-14	C2NAAA-	= 1.87E-14	C2AAAA-	= 1.21E-15
C3NNNN-	= 1.61E-08	C3NNNA-	= 4.37E-08	C3NNAA-	= 8.67E-08	C3NAAA-	= 7.03E-08
C3AAAA-	= 6.12E-09	C1NNNNN	= 1.97E-17	C2NNNNN	= 3.83E-13	C3NNNNN	= 3.20E-10
C4NNNNN	= 7.36E-07	C1NNNNN-	= 1.35E-22	C2NNNNN-	= 4.28E-18	C3NNNNN-	= 3.73E-15
				C4NNNNN-	= 8.07E-10		

Approximate equilibrium anthracene/naphthalene pyrolysis at 1348K

t(sec)= 0.0000E+00 P(atm)= 9.5000E-01 T(K)= 1.3480E+03

N2	= 9.98E-01	h2	= 0.00E+00	h	= 0.00E+00	n	= 9.13E-04

a	= 9.13E-04	n1-	= 0.00E+00	n2-	= 0.00E+00	a1-	= 0.00E+00

t(sec)= 2.0000E+03 P(atm)= 9.5000E-01 T(K)= 1.3480E+03

N2	= 9.97E-01	h2	= 2.66E-03	h	= 1.24E-07	n	= 4.91E-08
a	= 2.57E-08	n1-	= 2.65E-11	n2-	= 1.89E-11	a1-	= 9.89E-12
a2-	= 6.08E-12	a9-	= 7.17E-12	n1n1	= 3.81E-14	n1n1-1	= 7.67E-18
n1n1-2	= 5.48E-18	n1n1-4	= 5.49E-17	n1n2	= 1.38E-13	n1n2-1	= 2.81E-17
n1n2-2	= 1.00E-17	n1n2-4	= 2.18E-16	n2n2	= 1.49E-13	n2n2-4	= 3.11E-16
a1n1	= 3.27E-14	a1n1-1	= 2.49E-18	a1n1-2	= 3.43E-18	a1n1-3	= 3.62E-18
a1n1-4	= 4.26E-17	a1n2	= 5.94E-14	a1n2-1	= 4.75E-18	a1n2-2	= 3.39E-18
a1n2-3	= 6.64E-18	a1n2-4	= 8.40E-17	a2n1	= 6.03E-14	a2n1-1	= 9.30E-18
a2n1-2	= 2.86E-18	a2n1-4	= 8.86E-17	a2n2	= 1.27E-13	a2n2-4	= 2.37E-16
a9n1	= 1.83E-14	a9n1-1	= 4.18E-18	a9n1-2	= 1.04E-18	a9n1-4	= 2.30E-17
a9n2	= 3.23E-14	a9n2-1	= 7.46E-18	a9n2-2	= 1.85E-18	a9n2-4	= 4.06E-17
a1a1	= 3.82E-15	a1a1-2	= 5.61E-19	a1a1-3	= 1.32E-18	a1a1-4	= 8.73E-18
a1a2	= 1.42E-14	a1a2-1	= 1.71E-18	a1a2-2	= 1.05E-18	a1a2-3	= 2.48E-18
a1a2-4	= 3.60E-17	a1a9	= 4.33E-15	a1a9-1	= 1.03E-18	a1a9-2	= 3.17E-19
a1a9-3	= 7.48E-19	a1a9-4	= 9.47E-18	a2a2	= 1.54E-14	a2a2-4	= 4.85E-17
a2a9	= 7.71E-15	a2a9-1	= 2.77E-18	a2a9-2	= 5.69E-19	a2a9-4	= 1.82E-17
a9a9	= 5.98E-16	a9a9-1	= 2.82E-19	a9a9-4	= 2.34E-18	BkF	= 1.92E-09
BjF	= 5.80E-09	Per	= 1.35E-05	DBajF	= 4.57E-09	DBakF	= 2.01E-09
DBa1F	= 4.57E-09	BaPer	= 2.87E-05	N23jF	= 3.03E-09	N23kF	= 1.00E-09
BaN23jF	= 1.42E-09	BaN23kF	= 9.39E-10	BaN231F	= 1.42E-09	DBajPer	= 8.56E-06
DBaoPer	= 8.56E-06	BkF-	= 2.76E-12	BjF-	= 8.03E-12	Per-	= 1.94E-08
DBajF-	= 7.28E-12	DBakF-	= 3.45E-12	DBa1F-	= 7.28E-12	BaPer-	= 5.57E-08
N23jF-	= 5.20E-12	N23kF-	= 1.80E-12	BaN23jF-	= 2.30E-12	BaN23kF-	= 1.58E-12
BaN231F-	= 2.30E-12	DBajPer-	= 1.72E-08	DBaoPer-	= 1.72E-08	NNN	= 1.12E-18
NNA	= 2.45E-18	NAA	= 8.53E-19	AAA	= 2.26E-19	NNN-	= 1.49E-21
NNA-	= 3.04E-21	NAA-	= 2.04E-21	AAA-	= 5.00E-22	NNNN	= 6.21E-24
NNNA	= 1.78E-23	NNAA	= 1.46E-23	NAAA	= 5.75E-24	AAAA	= 1.16E-24
NNNN-	= 1.15E-26	NNNA-	= 3.39E-26	NNAA-	= 4.10E-26	NAAA-	= 1.99E-26
AAAA-	= 3.92E-27	NNNNN	= 4.46E-29	NNNNN-	= 1.31E-31	C1NNN	= 5.26E-12
C1NNA	= 2.20E-11	C1NAA	= 2.43E-11	C1AAA	= 3.43E-12	C2NNN	= 1.28E-06
C2NNA	= 1.53E-05	C2NAA	= 1.49E-05	C2AAA	= 7.33E-06	C1NNN-	= 2.70E-15
C1NNA-	= 3.50E-14	C1NAA-	= 4.05E-14	C1AAA-	= 5.20E-15	C2NNN-	= 2.61E-09
C2NNA-	= 3.62E-08	C2NAA-	= 3.99E-08	C2AAA-	= 2.07E-08	C1NNNN	= 7.07E-17

C1NNNA	= 4.19E-16	C1NNAA	= 6.95E-16	C1NAAA	= 1.39E-16	C1AAAA	= 5.27E-17
C2NNNN	= 8.31E-11	C2NNNA	= 5.04E-10	C2NNAA	= 9.19E-10	C2NAAA	= 8.94E-10
C2AAAA	= 1.23E-10	C3NNNN	= 3.12E-05	C3NNNA	= 8.59E-05	C3NNAA	= 1.52E-04
C3NAAA	= 1.07E-04	C3AAAA	= 1.69E-05	C1NNNN-	= 1.13E-19	C1NNNA-	= 7.31E-19
C1NNAA-	= 7.15E-19	C1NAAA-	= 5.01E-19	C1AAAA-	= 1.32E-19	C2NNNN-	= 4.76E-14
C2NNNA-	= 2.31E-13	C2NNAA-	= 2.81E-13	C2NAAA-	= 1.37E-13	C2AAAA-	= 9.01E-15
C3NNNN-	= 8.70E-08	C3NNNA-	= 2.46E-07	C3NNAA-	= 5.02E-07	C3NAAA-	= 3.69E-07
C3AAAA-	= 3.15E-08	C1NNNNN	= 6.93E-22	C2NNNNN	= 8.40E-16	C3NNNNN	= 2.99E-11
C4NNNNN	= 1.92E-06	C1NNNNN-	= 9.76E-25	C2NNNNN-	= 1.54E-18	C3NNNNN-	= 3.15E-14
			C4NNNNN- = 5.94E-09				

Approximate equilibrium anthracene/naphthalene pyrolysis at 1416K

	t(sec)= 0.0000E+00		P(atm)= 9.5000E-01		T(K)= 1.4160E+03		
N2	= 9.97E-01	h2	= 0.00E+00	h	= 0.00E+00	n	= 1.38E-03
a	= 1.38E-03	n1-	= 0.00E+00	n2-	= 0.00E+00	a1-	= 0.00E+00
	t(sec)= 2.0000E+03		P(atm)= 9.5000E-01		T(K)= 1.4160E+03		
N2	= 9.95E-01	h2	= 4.06E-03	h	= 4.00E-07	n	= 1.50E-08
a	= 7.61E-09	n1-	= 1.79E-11	n2-	= 1.30E-11	a1-	= 6.36E-12
a2-	= 4.01E-12	a9-	= 4.53E-12	n1n1	= 3.88E-15	n1n1-1	= 1.60E-17
n1n1-2	= 1.17E-17	n1n1-4	= 1.30E-17	n1n2	= 1.62E-14	n1n2-1	= 5.72E-17
n1n2-2	= 2.07E-17	n1n2-4	= 5.88E-17	n2n2	= 1.11E-14	n2n2-4	= 5.46E-17
a1n1	= 3.11E-15	a1n1-1	= 4.97E-18	a1n1-2	= 6.98E-18	a1n1-3	= 7.09E-18
a1n1-4	= 9.20E-18	a1n2	= 6.58E-15	a1n2-1	= 9.20E-18	a1n2-2	= 6.68E-18
a1n2-3	= 1.27E-17	a1n2-4	= 2.09E-17	a2n1	= 6.56E-15	a2n1-1	= 1.80E-17
a2n1-2	= 5.67E-18	a2n1-4	= 2.16E-17	a2n2	= 9.02E-15	a2n2-4	= 3.87E-17
a9n1	= 1.74E-15	a9n1-1	= 8.59E-18	a9n1-2	= 2.16E-18	a9n1-4	= 4.98E-18
a9n2	= 3.74E-15	a9n2-1	= 1.49E-17	a9n2-2	= 3.74E-18	a9n2-4	= 1.06E-17
a1a1	= 3.24E-16	a1a1-2	= 1.12E-18	a1a1-3	= 2.54E-18	a1a1-4	= 1.75E-18
a1a2	= 1.38E-15	a1a2-1	= 3.24E-18	a1a2-2	= 2.04E-18	a1a2-3	= 4.62E-18
a1a2-4	= 8.18E-18	a1a9	= 3.67E-16	a1a9-1	= 2.07E-18	a1a9-2	= 6.51E-19
a1a9-3	= 1.48E-18	a1a9-4	= 1.91E-18	a2a2	= 1.01E-15	a2a2-4	= 7.68E-18
a2a9	= 7.77E-16	a2a9-1	= 5.41E-18	a2a9-2	= 1.14E-18	a2a9-4	= 4.28E-18
a9a9	= 4.64E-17	a9a9-1	= 5.83E-19	a9a9-4	= 4.39E-19	BkF	= 1.39E-09
BjF	= 4.11E-09	Per	= 6.82E-06	DBajF	= 3.13E-09	DBakF	= 1.43E-09

DBalF	= 3.13E-09	BaPer	= 1.36E-05	N23jF	= 2.11E-09	N23kF	= 7.14E-10
BaN23jF	= 9.16E-10	BaN23kF	= 6.20E-10	BaN23lF	= 9.16E-10	DBajPer	= 3.87E-06
DBaoPer	= 3.87E-06	BkF-	= 4.43E-12	BjF-	= 1.27E-11	Per-	= 2.18E-08
DBajF-	= 1.10E-11	DBakF-	= 5.42E-12	DBalF-	= 1.10E-11	BaPer-	= 5.92E-08
N23jF-	= 8.02E-12	N23kF-	= 2.82E-12	BaN23jF-	= 3.25E-12	BaN23kF-	= 2.28E-12
BaN23lF-	= 3.25E-12	DBajPer-	= 1.73E-08	DBaoPer-	= 1.73E-08	NNN	= 3.66E-20
NNA	= 9.15E-20	NAA	= 3.11E-20	AAA	= 9.51E-21	NNN-	= 7.45E-22
NNA-	= 1.67E-21	NAA-	= 1.13E-21	AAA-	= 2.51E-22	NNNN	= 1.13E-25
NNNA	= 4.14E-25	NNAA	= 4.15E-25	NAAA	= 1.87E-25	AAAA	= 4.22E-26
NNNN-	= 2.04E-27	NNNA-	= 7.54E-27	NNAA-	= 9.78E-27	NAAA-	= 4.50E-27
AAAA-	= 8.65E-28	NNNNN	= 8.67E-31	NNNNN-	= 3.46E-32	C1NNN	= 8.80E-13
C1NNA	= 4.05E-12	C1NAA	= 4.45E-12	C1AAA	= 5.11E-13	C2NNN	= 1.06E-06
C2NNA	= 2.26E-05	C2NAA	= 2.21E-05	C2AAA	= 1.15E-05	C1NNN-	= 6.85E-15
C1NNA-	= 1.58E-13	C1NAA-	= 1.85E-13	C1AAA-	= 2.33E-14	C2NNN-	= 4.78E-09
C2NNA-	= 1.18E-07	C2NAA-	= 1.31E-07	C2AAA-	= 7.16E-08	C1NNNN	= 4.24E-18
C1NNNA	= 3.18E-17	C1NNAA	= 5.58E-17	C1NAAA	= 9.54E-18	C1AAAA	= 3.45E-18
C2NNNN	= 3.01E-11	C2NNNA	= 1.76E-10	C2NNAA	= 3.08E-10	C2NAAA	= 2.88E-10
C2AAAA	= 3.60E-11	C3NNNN	= 4.66E-05	C3NNNA	= 1.35E-04	C3NNAA	= 2.51E-04
C3NAAA	= 1.62E-04	C3AAAA	= 2.75E-05	C1NNNN-	= 1.27E-19	C1NNNA-	= 7.89E-19
C1NNAA-	= 7.07E-19	C1NAAA-	= 4.71E-19	C1AAAA-	= 1.19E-19	C2NNNN-	= 2.65E-13
C2NNNA-	= 1.36E-12	C2NNAA-	= 1.74E-12	C2NAAA-	= 7.47E-13	C2AAAA-	= 5.16E-14
C3NNNN-	= 2.90E-07	C3NNNA-	= 8.55E-07	C3NNAA-	= 1.83E-06	C3NAAA-	= 1.24E-06
C3AAAA-	= 1.07E-07	C1NNNNN	= 6.17E-23	C2NNNNN	= 2.45E-16	C3NNNNN	= 1.15E-11
C4NNNNN	= 2.24E-06	C1NNNNN-	= 8.82E-25	C2NNNNN-	= 2.10E-18	C3NNNNN-	= 1.12E-13
				C4NNNNN-	= 1.54E-08		

Approximate equilibrium anthracene/naphthalene pyrolysis at 1496K

t(sec)= 0.0000E+00 P(atm)= 9.5000E-01 T(K)= 1.4960E+03

N2	= 9.99E-01	h2	= 0.00E+00	h	= 0.00E+00	n	= 4.84E-04
a	= 4.84E-04	n1-	= 0.00E+00	n2-	= 0.00E+00	a1-	= 0.00E+00

t(sec)= 2.0000E+03 P(atm)= 9.5000E-01 T(K)= 1.4960E+03

N2	= 9.98E-01	h2	= 1.44E-03	h	= 6.62E-07	n	= 1.69E-09
a	= 8.67E-10	n1-	= 9.80E-12	n2-	= 7.24E-12	a1-	= 3.46E-12
a2-	= 2.23E-12	a9-	= 2.42E-12	n1n1	= 2.22E-16	n1n1-1	= 5.06E-18

n1n1-2	= 3.74E-18	n1n1-4	= 3.71E-18	n1n2	= 9.91E-16	n1n2-1	= 1.75E-17
n1n2-2	= 6.44E-18	n1n2-4	= 1.79E-17	n2n2	= 4.62E-16	n2n2-4	= 1.14E-17
a1n1	= 1.74E-16	a1n1-1	= 1.55E-18	a1n1-2	= 2.21E-18	a1n1-3	= 2.16E-18
a1n1-4	= 2.51E-18	a1n2	= 3.96E-16	a1n2-1	= 2.77E-18	a1n2-2	= 2.04E-18
a1n2-3	= 3.75E-18	a1n2-4	= 6.14E-18	a2n1	= 3.93E-16	a2n1-1	= 5.43E-18
a2n1-2	= 1.75E-18	a2n1-4	= 6.30E-18	a2n2	= 3.76E-16	a2n2-4	= 7.89E-18
a9n1	= 9.79E-17	a9n1-1	= 2.75E-18	a9n1-2	= 7.01E-19	a9n1-4	= 1.37E-18
a9n2	= 2.31E-16	a9n2-1	= 4.63E-18	a9n2-2	= 1.18E-18	a9n2-4	= 3.19E-18
a1a1	= 1.80E-17	a1a1-2	= 3.63E-19	a1a1-3	= 7.87E-19	a1a1-4	= 4.91E-19
a1a2	= 8.44E-17	a1a2-1	= 9.89E-19	a1a2-2	= 6.39E-19	a1a2-3	= 1.38E-18
a1a2-4	= 2.51E-18	a1a9	= 2.05E-17	a1a9-1	= 6.73E-19	a1a9-2	= 2.17E-19
a1a9-3	= 4.70E-19	a1a9-4	= 5.39E-19	a2a2	= 4.15E-17	a2a2-4	= 1.59E-18
a2a9	= 4.90E-17	a2a9-1	= 1.71E-18	a2a9-2	= 3.68E-19	a2a9-4	= 1.36E-18
a9a9	= 2.38E-18	a9a9-1	= 1.95E-19	a9a9-4	= 1.14E-19	BkF	= 2.98E-10
BjF	= 8.63E-10	Per	= 1.00E-06	DBajF	= 6.57E-10	DBakF	= 3.13E-10
DBalF	= 6.57E-10	BaPer	= 1.93E-06	N23jF	= 4.54E-10	N23kF	= 1.57E-10
BaN23jF	= 1.88E-10	BaN23kF	= 1.30E-10	BaN23lF	= 1.88E-10	DBajPer	= 5.44E-07
DBaoPer	= 5.44E-07	BkF-	= 4.64E-12	BjF-	= 1.30E-11	Per-	= 1.57E-08
DBajF-	= 1.13E-11	DBakF-	= 5.77E-12	DBalF-	= 1.13E-11	BaPer-	= 4.17E-08
N23jF-	= 8.36E-12	N23kF-	= 3.00E-12	BaN23jF-	= 3.21E-12	BaN23kF-	= 2.29E-12
BaN23lF-	= 3.21E-12	DBajPer-	= 1.19E-08	DBaoPer-	= 1.19E-08	NNN	= 8.66E-22
NNA	= 2.54E-21	NAA	= 9.36E-22	AAA	= 2.78E-22	NNN-	= 8.88E-23
NNA-	= 2.43E-22	NAA-	= 1.74E-22	AAA-	= 3.55E-23	NNNN	= 1.24E-27
NNNA	= 5.49E-27	NNAA	= 5.88E-27	NAAA	= 2.61E-27	AAAA	= 5.81E-28
NNNN-	= 1.24E-28	NNNA-	= 5.42E-28	NNAA-	= 7.21E-28	NAAA-	= 3.38E-28
AAAA-	= 6.69E-29	NNNNN	= 5.18E-33	NNNNN-	= 9.96E-34	C1NNN	= 6.90E-14
C1NNA	= 3.89E-13	C1NAA	= 4.45E-13	C1AAA	= 4.16E-14	C2NNN	= 2.37E-07
C2NNA	= 7.96E-06	C2NAA	= 7.79E-06	C2AAA	= 4.12E-06	C1NNN-	= 2.40E-15
C1NNA-	= 8.75E-14	C1NAA-	= 1.02E-13	C1AAA-	= 1.21E-14	C2NNN-	= 5.24E-09
C2NNA-	= 2.02E-07	C2NAA-	= 2.24E-07	C2AAA-	= 1.25E-07	C1NNNN	= 1.73E-19
C1NNNA	= 1.54E-18	C1NNAA	= 2.73E-18	C1NAAA	= 4.27E-19	C1AAAA	= 1.54E-19
C2NNNN	= 4.16E-12	C2NNNA	= 2.42E-11	C2NNAA	= 4.22E-11	C2NAAA	= 3.92E-11
C2AAAA	= 4.59E-12	C3NNNN	= 1.50E-05	C3NNNA	= 4.65E-05	C3NNAA	= 9.27E-05
C3NAAA	= 5.17E-05	C3AAAA	= 1.03E-05	C1NNNN-	= 2.75E-20	C1NNNA-	= 1.71E-19
C1NNAA-	= 1.45E-19	C1NAAA-	= 9.50E-20	C1AAAA-	= 2.37E-20	C2NNNN-	= 1.63E-13
C2NNNA-	= 9.02E-13	C2NNAA-	= 1.25E-12	C2NAAA-	= 4.38E-13	C2AAAA-	= 3.46E-14

C3NNNN-	= 4.57E-07	C3NNNA-	= 1.44E-06	C3NNAA-	= 3.29E-06	C3NAAA-	= 1.92E-06
C3AAAA-	= 1.83E-07	C1NNNNN	= 1.19E-24	C2NNNNN	= 1.28E-17	C3NNNNN	= 1.53E-12
C4NNNNN	= 6.54E-07	C1NNNNN-	= 7.30E-26	C2NNNNN-	= 5.07E-19	C3NNNNN-	= 5.09E-14
				C4NNNNN-	= 2.19E-08		

References

Badger, G.M. and Kimber, R.W.K., J.Chem Soc. 3400 (1961).

Badger, G.M. and Novotny, J., J.Chem Soc. 3407 (1961).

Badger, G.M., Donnelly, J.K., and Spotswood, T.M., Aust. J. Chem. 17:1138 (1964).

Badger, G.M., Donnelly, J.K., and Spotswood, T.M. Aust J. Chem. 17:1147 (1964).

Badger, G.M., Jolad, S.D., and Spotswood, T.M., Aust J. Chem. 17:771 (1964).

Badger, G.M., Progr. Phys. Org. Chem. 3:1 (1965).

Bauer, S.H., and Jeffers, P.M., Energy and Fuels 2:446 (1988).

Bell, F., and Waring, D.H., J. Chem. Soc. 267:2689 (1949).

Benson, S.W., Thermochemical Kinetics, John Wiley and Sons, New York (1976).

Bermudez, G. and Pfefferle, L.D., "Mechanisms and Models of Soot Formation International Workshop", Heidelberg (1991).

Bittner, J.D., and Howard, J.B., 18th Symposium (Int.) on Combustion, The Combustion Institute, Pittsburgh, 1105 (1981).

Calcote, C., "Mechanisms and Models of Soot Formation International Workshop", Heidelberg (1991).

Cavalieri, E.L., Higginbotham, S., RamaKrishna, N.V.S., Devanesan, P.D., Todorovic, R., Rogan, E.G., and Salmasi, S., Carcinogenesis12:1939 (1991).

Chen, R.H., Kafafi, S.A., and Stein, S.E., J. Am. Chem. Soc. 111:1418 (1989).

Coolidge, M.B., and Stewart, J.J.P., MOPAC, Version 6.00, Quantum Chemistry Program Exchange (1990).

Clar, E.J., Polycyclic Hydrocarbons, Academic Press, New York (1964).

Clar, E.J., The Aromatic Sextet, John Wiley & Sons, New York (1972).

Craig, D.P., and Hobbins, P.C., J. Chem. Soc. 1955:539 (1955).

Craig, D.P., and Hobbins, P.C., J. Chem. Soc. 1955:2309 (1955).

Dworkin, A.S., Poutsma, M.L., Brynestad, J., Brown, L.L., Gilpatrick, L.O., and Smith, G.P., J. Am. Chem. Soc. 101:5299 (1979).

Evans, M.G., and Polanyi, M., Trans. Faraday Soc. 34:11 (1938).

Fahr, A., and Stein, S.E., Twenty-second Symposium (International) on Combustion, The Combustion Institute, Pittsburgh, p.1023 (1988).

Frenklach, M., Clary, D.W., Gardiner, W.C.,Jr., Stein, S.E., Twentieth Symposium (International) on Combustion, The Combustion Institute, Pittsburgh, p.887, (1984).

Frenklach, M., and Warnatz, J., Combustion Science and Technology 51:265 (1987).

Frenklach, M., and Wang, H., Twenty-third Symposium (International) on Combustion, The Combustion Institute, Pittsburgh, p. 1559 (1990).

Gerhardt, P., Loeffler, S., and Homann, K.H., Chem. Phys. Lett. 137:306 (1987).

Gerhardt, P., Loeffler, S., and Homann, K.H., Twenty-second Symposium (International) on Combustion, The Combustion Institute, Pittsburgh, p.395 (1989).

Grinter, R., and Mason, S.F., Trans. Faraday Soc. 60:274 (1964).

Harris, S.J., and Weiner, A.M., Comb. Sci. Tech. 31:155 (1983).

Heller, S.R., EPA/NIH Mass Spectral Data Base NSRDS-NBS63 2:1801, U.S. Government Printing Office, Washington (1978).

Hendel, W., Khan, Z.H., and Schmidt, W., Tetrahedron 42, 4, 1127 (1986).

Hepp, H., Siegmann, K., and Sattler, K., submitted to Chem. Phys. Lett. (1994).

Herndon, W.C., J. Org. Chem. 46:2119 (1981).

Higginbotham, S., RamaKrishna, N.V.S., Johansson, S.L., Rogan, E.G., and Cavalieri, E.L., Carcinogenesis 14:875 (1993).

Hippler, H., Reihs, C., and Troe, J., Z. Phys. Chem. 167:1 (1990).

Homann, K.H., and Wagner, H.G., Eleventh Symposium (International) on Combustion, The Combustion Institute, Pittsburgh, p.371 (1967).

House, H.O., Koepsell, D.G., and Campbell, W.J., J. Org. Chem. 37:1003 (1972).

Howard, J.B., Twenty-Third Symposium (International) on Combustion, The Combustion Institute, Pittsburgh, p.1107 (1990).

Howard, J.B., McKinnon, J.T., Makarovsky, Y., Lafleur, A., Johnson, M.E., Nature 352:139 (1991).

Johnstone, R.A.W., and Millard, B.J., J. Chem. Soc. (C), p. 1955 (1966).

Jones, R.N., J. Amer. Chem. Soc. 63:1658 (1941).

Jones, R.N., J. Amer. Chem. Soc. 67:2127 (1945).

Jones, R.N., Chem. Reviews 41:353 (1947).

Kee, R.J., Rupley, F.M., and Miller, J.A., Chemkin-II: A Fortran Chemical Kinetics Package for the Analysis of Gas-Phase Chemical Kinetics, Rep. SAND89-8009, Sandia National Laboratory, Livermore, CA (1990).

Kern, R.D., Singh, H.J., Esslinger, M.A., and Winkeler, P.W., Nineteenth Symposium (International) on Combustion, The Combustion Institute, Pittsburgh, p. 1351 (1982).

Kiefer, J.H., Mizerka, L.J., Patel, M.R., and Wei, H.C., J. Phys Chem. 89:2013 (1985).

Kinney, C.R., Proceedings of the First and Second Conference on Carbon, Waverly Press, Baltimore, p.83 (1956).

Kroto, H.W., Heath, J.R., O'Brien, S.C., Curl, R.F., and Smalley, R.E. Nature 318:162 (1985).

Knop, J.V., Muller, W.R., Szymanski, K., and Trinajstic, N., J. Comput. Chem. 7:547 (1987).

Laidler, K.J., Theories of Chemical Reaction Rates, McGraw-Hill (1969).

Lang, K.F., Buffleb, H., and Kalowy, J., Chem. Ber. 90:2888 (1957).

Lang, K.F., and Buffleb, H., Chem. Ber. 90:2894 (1957).

Lang, K.F., Buffleb, H., and Kalowy, J., Chem. Ber. 93:303 (1960).

Lang, K.F., and Buffleb, H., Chem. Ber. 94:1075 (1961).

Lutz, A.E., Kee, R.J., Miller, J.A., SENKIN: A Fortran Program for Predicting Homogeneous Gas Phase Chemical Kinetics with Sensitivity Analysis, Rep. SAND87-8248, Sandia National Laboratory, Livermore, CA (1988).

Masonjones, M.C., Lafleur, A.F., and Sarofim, A.L., "Biaryl Formation during Pyrolysis of a Mixture of Anthracene and Naphthalene", submitted to Comb. Sci. Tech., 1994.

Masonjones, M.C., Lafleur, A.F., and Sarofim, A.L., "Identification of Isomeric Naphthyl-Anthracenes Generated from the Pyrolysis of an Anthracene/Naphthalene Mixture", in preparation, (1995).

McKinnon, J.T., and Howard, J.B., Combustion Science and Technology 74:175 (1990).

McKinnon, J.T., Bell, W.L., and Barkley, R.B., Combustion and Flame 88:102 (1992).

McLafferty, F.W., and Turecek, F., Interpretation of Mass Spectra, 4th ed., Univ. Sci. Books, Mill Valley, CA (1993).

Miller, J.A., and Bowman, C.T., Prog. in Energy and Comb. Sci 15:287 (1989).

Miller, , J.H., Smyth, K.C., and Mallard, W.G., Twentieth Symposium (International) on Combustion, The Combustion Institute, Pittsburgh, p. 1139 (1984).

Miller, J.H., Twenty-third Symposium (International) on Combustion, The Combustion Institute, Pittsburgh, p.91 (1990).

Mukherjee, J., Doctoral Thesis, Dept. of Chem. Eng., M.I.T. (1993).

Mukherjee, J., Sarofim, A F., and Longwell, J.P. Combustion and Flame 96:191 (1994).

Mulholland, J.A., Sarofim, A.F., Beer, J.M., and Lafleur, A.L., Twenty-Fourth Symposium (International) on Combustion, The Combustion Institute, Pittsburgh, 1091 (1992).

Mulholland, J.M., Doctoral Thesis, Dept. of Chem. Eng., M.I.T. (1992).

Mulholland, J.M., Sarofim, A.F., and Rutledge, G.C., J. Phys. Chem. 97:6890 (1993).

Mulholland, J.M., Mukherjee, J., Wornat, M.J., Sarofim, A.F., and Rutledge, G.C., Combustion and Flame 94: 233 (1993).

Nicholas, J., Chemical Kinetics, John Wiley & Sons, New York (1976).

Photoelectric Spectrometry Group, London, and Institut fur Spektrochemie und Angegandte Spektroskopie, Dortmund, UV Atlas of Organic Compounds, Plenum Press, New York (1966).

Platt, J.R., J. Chem. Phys. 18:1168 (1950).

Pope, C., Doctoral Thesis, Dept. of Chem. Eng., M.I.T., (1993).

Pullman, B., and Pullman, A., Progress in Organic Chemistry, (J.W.Cook, ed.) V.4, Ch.2, Butterworths (1958).

Ralston, S.L., Lau, H.H.S., Seidel, A., Luch, A., Platt, K.L., and Baird, W.M., Cancer Research 54:887 (1994).

Ritter, E. and Bozelli, J.W., "THERM: Thermodynamic Property Estimation of Radicals and Molecules", Int.J.Chem.Kin. (1991).

Robaugh, D. and Tsang, W., J. Phys. Chem. 90:4159 (1986).

Sander, L.C., and Wise, S.A., Advances in Chromatography 25:139 (1986).

Schmidt, W., Grimmer, G., Jacob, J., Dettbarn, G., and Naujack, K.W., Fresenius Z. Anal. Chem. 326:401 (1987).

Scott, L.T. and Roelofs, N.H., J. Am. Chem. Soc. 109:5461 (1987).

Stein, S.E., Griffith, L.L., Billmers, R., and Chen, R.H., J. Org. Chem. 52:1582 (1987).

Stein, S.E., J. Phys. Chem. 82,5:566 (1978).

Stewart, J.J.P., J. Computer-Aided Molecular Design 4:1 (1990).

Takatsu, M., and Yamamoto, T., J. Anal. App. Pyrolysis 26:53 (1993).

Thermodynamics Research Center Mass Spectral Data (Hydrocarbon Project), API Research Project 44, Texas A&M Univ. College Station, TX (1983).

Wagner, H.G., "Particulate Carbon Formation During Combustion," ed. D.C.Seigla, and G.W.Smith, Plenum Press (1981).

Wise, S.A., Benner, B.A., Liu, H., and Byrd, G.D., Anal. Chem. 60:630 (1988).

Wornat, M.J., Sarofim, A.F., and Longwell, J.P., Energy and Fuels 1:431 (1987).

Wornat, M.J., Sarofim, A.F., and Lafleur, A.L., Twenty-Fourth Symposium (International) on Combustion, The Combustion Institute, Pittsburgh, p.955 (1992).

Wornat, M.J., Lafleur, A.L., and Sarofim, A.F., Polycyclic Aromatic Compounds 3:149 (1993).